

## Cross-Electrophile Coupling: Principles, Methods, and Applications in Synthesis

Lauren E. Ehehalt,<sup>‡</sup> Omar M. Beleh,<sup>‡</sup> Isabella C. Priest, Julianna M. Mouat, Alyssa K. Olszewski, Benjamin N. Ahern, Alejandro R. Cruz, Benjamin K. Chi, Anthony J. Castro, Kai Kang, Jiang Wang, and Daniel J. Weix\*



Cite This: *Chem. Rev.* 2024, 124, 13397–13569



Read Online

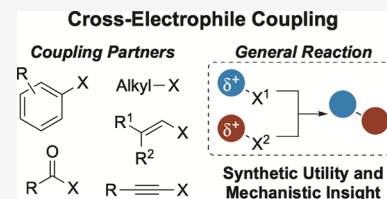
ACCESS |

Metrics & More

Article Recommendations

Supporting Information

**ABSTRACT:** Cross-electrophile coupling (XEC), defined by us as the cross-coupling of two different  $\sigma$ -electrophiles that is driven by catalyst reduction, has seen rapid progression in recent years. As such, this review aims to summarize the field from its beginnings up until mid-2023 and to provide comprehensive coverage on synthetic methods and current state of mechanistic understanding. Chapters are split by type of bond formed, which include  $C(sp^3)-C(sp^3)$ ,  $C(sp^2)-C(sp^2)$ ,  $C(sp^2)-C(sp^3)$ , and  $C(sp^2)-C(sp)$  bond formation. Additional chapters include alkene difunctionalization, alkyne difunctionalization, and formation of carbon-heteroatom bonds. Each chapter is generally organized with an initial summary of mechanisms followed by detailed figures and notes on methodological developments and ending with application notes in synthesis. While XEC is becoming an increasingly utilized approach in synthesis, its early stage of development means that optimal catalysts, ligands, additives, and reductants are still in flux. This review has collected data on these and various other aspects of the reactions to capture the state of the field. Finally, the data collected on the papers in this review is offered as Supporting Information for readers.



### CONTENTS

1. Introduction	13398
2. Global Trends	13399
2.1. Ligands	13400
2.2. Solvents	13401
2.3. Additives	13401
2.4. Reductants	13402
2.5. Photochemical Approaches	13402
2.6. Electrochemical Approaches	13403
2.7. Catalysts Used in XEC	13403
3. $C(sp^2)-C(sp^2)$ Bond Formation	13404
3.1. Overview	13404
3.2. Biaryls	13405
3.2.1. XEC of Aryl Halides	13405
3.2.2. XEC of Aryl Halides and Aryl Pseudohalides with Aryl Pseudohalides	13412
3.2.3. XEC of Aryl Halides with Other Coupling Partners	13414
3.2.4. XEC of Aryl Carboxylic Acid Esters, Aryl Ethers, and Anilines	13415
3.3. Vinyl Arenes	13416
3.3.1. XEC of Vinyl Halides with Aryl Halides	13416
3.3.2. XEC of Aryl Halides with Vinyl Acetates	13418
3.4. Synthesis of 1,3-Dienes	13419
3.4.1. Coupling of Vinyl Halides with Vinyl Halides and Pseudo Halides	13419
3.5. Ketones	13420
3.5.1. XEC with Acid Halides	13420

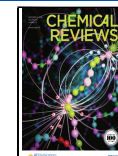
3.5.2. Carbonylative XEC to Form Ketones	13421
3.5.3. XEC of Aryl Halides with Other Activated Acids	13421
3.6. C–C Bond Activation XEC	13422
3.7. Synthetic Applications of $C(sp^2)-C(sp^2)$ XEC	13423
4. $C(sp^2)-C(sp^3)$ Bond Formation	13424
4.1. Overview	13424
4.2. Alkylated Arenes	13426
4.2.1. Alkyl Bromides as Electrophiles	13426
4.2.2. Alkyl Chlorides as Electrophiles	13445
4.2.3. Alkyl Iodides as Electrophiles	13448
4.2.4. Alkyl Amines as Electrophiles	13451
4.2.5. Alkyl Alcohols as Electrophiles	13454
4.2.6. Carboxylic Acids as Electrophiles	13461
4.2.7. Fluoroalkylation	13464
4.2.8. Other Alkyl Precursors	13467
4.2.9. Stereocontrolled XEC of Aryl–X with Alkyl–X	13468
4.2.10. Synthetic Applications of $C(sp^2)-C(sp^3)$ Aryl–Alkyl XEC	13472
4.3. Alkylated Alkenes	13474

Received: July 15, 2024

Revised: October 11, 2024

Accepted: October 16, 2024

Published: November 26, 2024



4.3.1. Overview	13474	9.7. Ask Your Own Questions About the Field	13549
4.3.2. XEC of Vinyl Halides with Alkyl Electrophiles	13475	Associated Content	13549
4.3.3. XEC of Vinyl Triflates and Acetates with Alkyl Electrophiles	13481	Supporting Information	13549
4.3.4. Stereocontrolled XEC of Vinyl-X with Alkyl-X	13483	Author Information	13549
4.3.5. Synthetic Applications of C(sp <sup>2</sup> )–C(sp <sup>3</sup> ) Vinyl–Alkyl XEC	13486	Corresponding Author	13549
4.4. Ketones	13488	Authors	13549
4.4.1. Overview	13488	Author Contributions	13549
4.4.2. Acid Halides as Electrophiles	13488	Notes	13549
4.4.3. Acid Esters as Electrophiles	13491	Biographies	13549
4.4.4. Acyl Imide Derivatives as Electrophiles	13492	Acknowledgments	13550
4.4.5. Mixed Anhydrides as Electrophiles	13494	Abbreviations	13550
4.4.6. XEC with Exogenous CO Source	13496	References	13551
4.4.7. Stereocontrolled XEC of Acyl-X with Alkyl-X	13498		
4.4.8. Synthetic Applications of C(sp <sup>2</sup> )–C(sp <sup>3</sup> ) Acyl–Alkyl XEC	13498		
5. Alkylated Alkynes	13500		
6. C(sp <sup>3</sup> )–C(sp <sup>3</sup> ) Bond Formation	13502		
6.1. Overview	13502		
6.1.1. Substrates and Organization	13502		
6.1.2. Catalysts and Ligands	13502		
6.1.3. Mechanisms	13502		
6.2. Intramolecular C(sp <sup>3</sup> )–C(sp <sup>3</sup> ) XEC	13502		
6.2.1. Ring-Forming Reactions	13502		
6.2.2. Ring-Contracting Reactions	13504		
6.3. Intermolecular C(sp <sup>3</sup> )–C(sp <sup>3</sup> ) XEC	13505		
6.3.1. Allyl–Alkyl Bond Formation	13505		
6.3.2. Benzyl–Alkyl Bond Formation	13507		
6.3.3. Alkyl–Alkyl Bond Formation	13507		
6.4. Enantioselective C(sp <sup>3</sup> )–C(sp <sup>3</sup> ) XEC	13512		
6.5. Synthetic Applications of C(sp <sup>3</sup> )–C(sp <sup>3</sup> ) XEC	13513		
7. Difunctionalization of Alkenes and Alkynes with Two Electrophiles	13513		
7.1. Alkene Difunctionalization	13513		
7.1.1. Intermolecular, Three-Component Difunctionalizations	13514	C–H Functionalization	
7.1.2. Cyclizations	13523	+ Skip R-[M]	
7.1.3. Synthetic Applications of Cross-Electrophile Difunctionalizations	13533	– Limited by C–H selectivity	
7.2. Alkyne Difunctionalization	13534		
7.2.1. Intermolecular, Three-Component Difunctionalization of Alkynes	13534	Cross-Coupling	
7.2.2. Cyclization Reactions	13537	+ Established, general	
8. Carbon–Heteroatom XEC	13538	– Limited by R-[M] stability / availability	
8.1. Group 14 (Si/Ge)	13538		
8.1.1. C–Si Bond Forming Reactions	13538	Cross-Electrophile Coupling	
8.1.2. C–Ge Bond Forming Reactions	13540	+ Skip R-[M], avoid C–H selectivity	
8.2. Group 15 (N/P/Sb)	13541	– Cross-selectivity challenges	
8.2.1. C–N Coupling	13541	Least developed approach	
8.2.2. C–P Coupling	13542		
8.3. Group 16 (S/Se)	13544		
9. Outlook and Challenges for the Field	13547		
9.1. Scope and Selectivity	13547		
9.2. Ligand Design and Discovery	13547		
9.3. Reductants, Photochemistry, and Electrochemistry	13548		
9.4. Stereocontrol	13548		
9.5. Mechanistic Understanding	13548		
9.6. No More Nucleophiles?	13548		

## 1. INTRODUCTION

C–C bond formation is central to organic synthesis and metal-catalyzed methods to form new C–C  $\sigma$ -bonds have revolutionized the way molecules are made.<sup>1–8</sup> For example, Pd-catalyzed cross-coupling reactions are the most-used C–C bond-forming reactions in medicinal chemistry and process chemistry.<sup>9–12</sup> The importance of this class of reactions was acknowledged in the awarding of the 2010 Nobel Prize in Chemistry<sup>13</sup> to Richard Heck, Ei-ichi Negishi, and Akira Suzuki “for palladium-catalyzed cross-couplings in organic synthesis.” Despite major advances in the synthesis and application of organometallic reagents, it is still the case that preformed carbon nucleophiles can be limiting for scope and substrate availability. The field of C–H functionalization addresses these shortcomings by utilizing the ubiquitous C–H bond as a carbon-nucleophile equivalent, in principle broadening the potential substrate scope to all possible molecules.<sup>14</sup> This field is still in its early stages, but challenges relating to reactivity and selectivity for one C–H bond out of many remain.<sup>14</sup> An approach that allows access to a broad substrate pool while also avoiding issues of site-selectivity could offer a fruitful middle ground for synthesis (Figure 1).

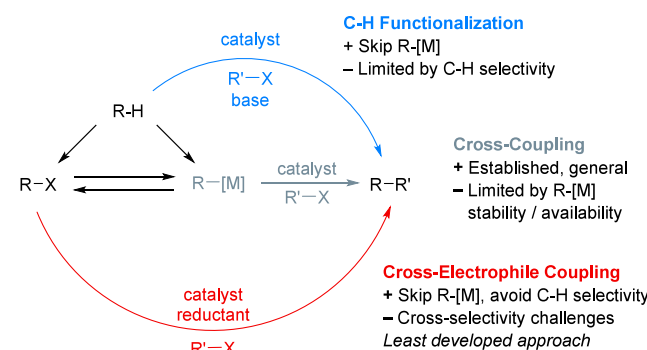


**Figure 1.** Cross-Coupling vs C–H Arylation/Akylation vs Cross-Electrophile Coupling.

Cross-electrophile coupling (XEC or sometimes CEC), the cross-coupling of two different  $\sigma$ -electrophiles that is driven by catalyst reduction, can address both of these outstanding challenges (Figure 2).<sup>15</sup> In this work, we differentiate ‘cross-electrophile coupling’ from the broader field of reductive coupling, which includes a wide variety of net-reductive reactions, including those that use nucleophilic hydride sources, homodimerize electrophiles, and hydrofunctionalize  $\pi$ -electrophiles. A key consideration was avoiding renaming reaction classes that already have developed nomenclature.

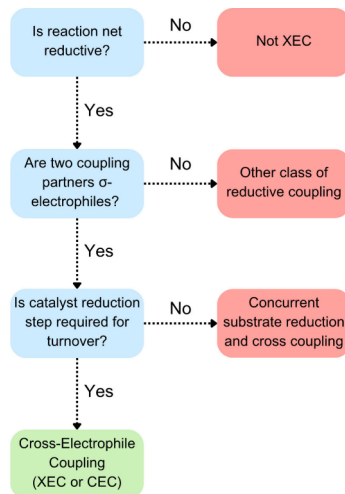


**Figure 2.** Definition and key attributes of cross-electrophile coupling.

This rules out processes where two known, distinct reactions are happening concurrently, such as direct insertion of Zn metal into Ar–X to form Ar–ZnX with concurrent Negishi coupling.<sup>16</sup> It also rules out reactions that do not involve a metal catalyst, such as reduction of one electrophile to form a nucleophile that reacts with a second electrophile.<sup>17–19</sup> In contrast, XEC reactions could involve organometallic intermediates (e.g., ZnX<sub>2</sub> mediated transfer of aryl groups from Ni to Pd).<sup>20</sup> For reactions that start with two electrophiles, but do not fit the mechanistic definition of XEC, we propose the term “formal XEC” in analogy to its use in “formal [4 + 2] reaction.” Formal XEC reactions are just as useful as XEC reactions, but are not covered in this review. We also include here reactions that add the two electrophiles across a  $\pi$ -system, even if it is the same electrophile added twice. These reactions figure prominently in the field, for both mechanistic and synthetic reasons, and there is a high degree of overlap in conditions and catalysts.

A key attraction for XEC is the broader commercial availability of electrophiles compared to carbon nucleophiles (Figure 3). Over the years, analysis of both compounds reported in the published literature and compounds listed for sale have shown the same trends depicted in these figures, even if the exact numbers change. The key takeaway is that even organic iodides, the least available carbon  $\sigma$ -electrophile class in the table, are more abundant than organoboron reagents, the most abundant carbon nucleophile class. It is interesting to note that aldehydes, a key electrophile for Grignard reactions and aldol chemistry, are only on the level of organic iodides with respect to availability. The broader commercial availability of electrophiles increases the chemical space that is accessible in a given number of steps and the mild reductive conditions are compatible with many sensitive functional groups. A broad goal for the field of XEC is finding approaches to accomplish general couplings with the largest substrate pools. As such, each subsection was organized by coupling partner.

Initial reports on cross-electrophile coupling built upon reductive homodimerization reactions of aryl, alkyl, and allylic electrophiles, the development of methods to turnover catalysts with terminal reductants, and stoichiometric organometallic reactions.<sup>21–30</sup> These seminal studies were concurrent with the major developments in cross-coupling of carbon-based nucleophiles with electrophiles, but XEC chemistry was

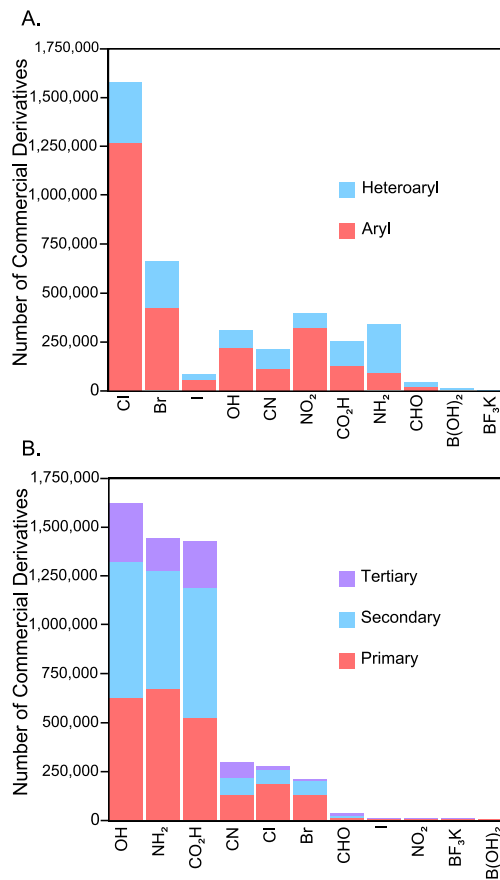


**Figure 3.** Chart of electrophile substrate availability for (A) Ar–X coupling partners, and (B) alkyl–X coupling partners utilizing data gathered from REAXYS and eMolecules on April 8, 2019.

slower to develop. In our view this was due to the challenges in studying first-row metals (that are most common for XEC) and in achieving cross-selective reactions.<sup>25,26,28</sup>

In the past 15 years, however, the field has rapidly progressed: 75% of all publications in this Review were reported only in the past six years (Figure 4). The cross-electrophile coupling concept can be applied to a wide array of potential bond-formations and many new methods take advantage of the unique features of XEC. These numbers have also included an increasing number of applications to complex molecules and drug candidates as well as a continued refinement of our understanding of the mechanisms of these reactions.

This review aims to summarize the field up until May 1, 2023 in a comprehensive manner to facilitate further uptake and expansion. Considerable effort was put into collating data that could be useful to both the novice and the expert, including surveys on ligands, solvents, classes of reactions, and mechanisms. This data was used to discuss trends throughout the manuscript and is supplied as a Supporting Information file to this review.

## 2. GLOBAL TRENDS

We sought to quantify trends in the field of XEC, both as a way of highlighting similarities between approaches and to determine areas for further improvement in the field. Taking inspiration from an excellent recent review by Louie and co-

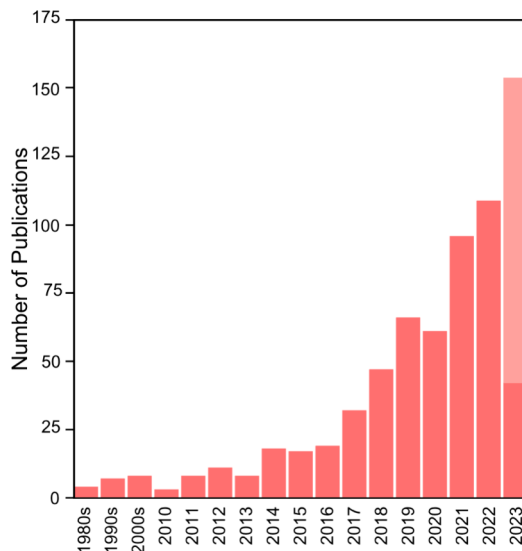


**Figure 4.** Distribution of publications covered in this review by year of publication showing the recent surge of activity. Note: publications in this review range until mid-2023. Light pink section denotes publications in 2023 not covered in this review.

workers on bidentate phosphines in nickel catalysis,<sup>31</sup> we elected to generate a number of charts with this data. We hope that this data will serve as a starting point for researchers attempting to quickly survey potential reaction conditions for a desired XEC transformation, as well as for researchers wishing to look at unexplored areas. For example, as can be seen in Figure 5, 55% of this review is comprised of C(sp<sup>2</sup>)–C(sp<sup>3</sup>)

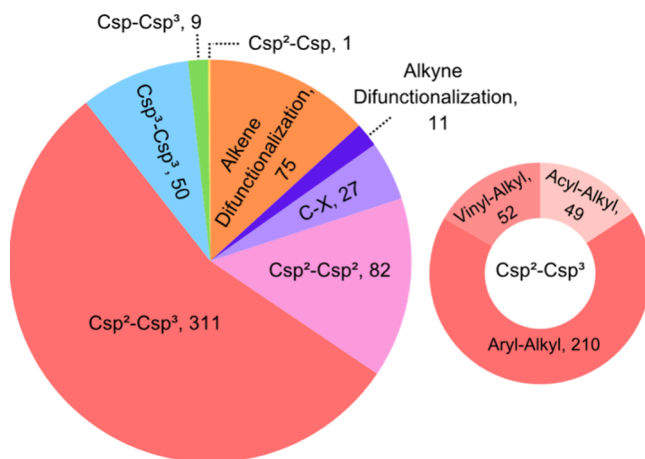


**Figure 5.** XEC reactions covered in this review categorized by type of bond formation.

bond forming reaction reports, in stark contrast to C(sp<sup>n</sup>)–C(sp) bond forming reactions, which are only 1.8%. While this data highlights the wide array of bonds that can be formed via XEC, as well as highlights further areas to be explored, it is by no means comprehensive because the field continues to develop rapidly. Indeed, the data collected from sections with fewer reports (e.g., C–X, C(sp<sup>2</sup>)–C(sp)) could be misleading because the charts arise from a small number of reports. Thus, while the data here is a good starting point, the absence of a reagent, catalyst, or condition should not be viewed as disqualifying.

## 2.1. Ligands

While there have been a variety of ligand classes explored in XEC reactions, undoubtedly the most utilized are bipyridines, representing around one-third of all ligands used, and N-bound ligands comprise approximately 85% of all ligands employed (Figure 6, Figure 7, and Figure 8). Bidentate phosphines have

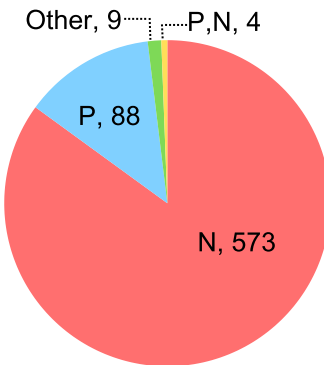


**Figure 6.** Distribution of ligand classes in this review. Total = 674 reports. Other = ligand classes with <10 reports, such as C(NHC) or O (acetate). There are some mixed ligand systems or reports where two different ligands are employed, and some reports are “ligandless” where the ligand is either solvent or the substrate.

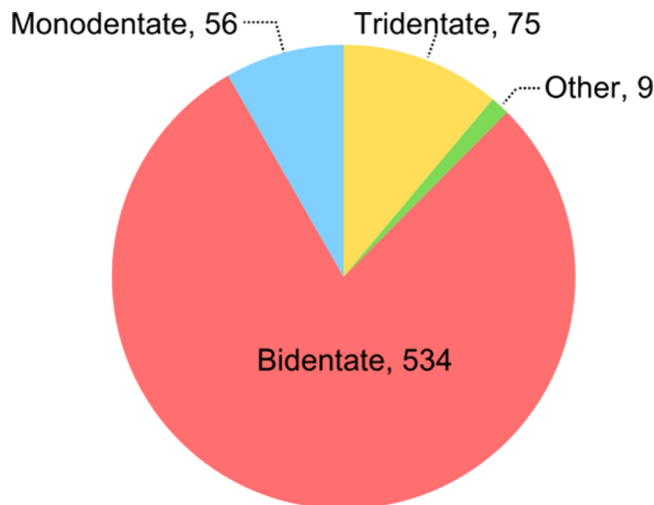


**Figure 7.** Denticity of ligands reported in this review. Other = tetradentate,  $\eta$ -binding.

been shown in several examples as successful ligands in Ni-catalyzed XEC but are most frequently seen bound to other transition metal precatalysts, either in multimetallic XEC or non-Ni-catalyzed XEC. Cobalt catalysts seem to work equally well with phosphine and nitrogen ligands, although this data is from a small number of papers.

Bidentate ligands are the most used, representing 79% of all ligands used, but this hides trends for certain pairs of coupling partners. For example, monodentate ligands (pyridine) and tridentate ligands (terpyridine, bpp) work better for tertiary alkyl coupling with aryl halides than bidentate ligands. Tridentate ligands seem to be superior for C(sp<sup>3</sup>)–C(sp<sup>3</sup>) bond forming reactions. These localized trends are evident in each subsection.

When ligand substructures are examined, the reliance of XEC on just a few classes can be seen clearly: bipyridine,

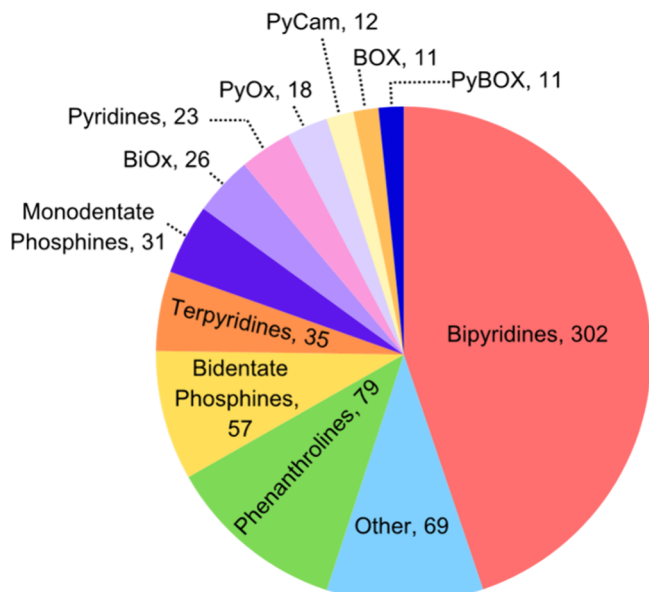


**Figure 8.** Ligand structures reported in this review. Total = 674 reports.

phenanthroline, and terpyridine classes represent 62% of all ligands used in XEC, and the structural diversity in these classes is relatively low, compared to phosphines. Newer ligands, such as carboxamidines (PyCam, PyBCam)<sup>32,33</sup> are becoming more common and are now commercially available, but more new classes of ligands would be a great benefit to the field. Finally, enantioselective reactions are dominated by BiOx, PyOx, and BOX ligands with a few bidentate phosphine examples. Here, too, additional classes of ligands would be advantageous.

## 2.2. Solvents

Currently, amide solvents predominate reported XEC reactions, with DMA and DMF accounting for approximately 50% of all reaction solvents (Figure 9). Although these solvents are useful on very small scales because of their high boiling points and general ability to solubilize molecules and metal salts, on large scale these solvents are problematic for health and safety reasons. Advances have been made in recent years to develop XEC reactions in nonamide solvents.<sup>34–36</sup> XEC reactions have also been reported with a variety of mixed-solvent systems; however, similar to their single solvent system analogues, mixed solvent systems with amides dominate heavily, representing 75% of all mixed solvent systems. Among these, unsurprisingly, amide/ether solvent systems represent 39% of all mixed solvent systems, paralleling the two largest solvent classes under single solvent conditions.

## 2.3. Additives

XEC reactions often benefit from the addition of additives. Both inorganic (Figure 10, Figure 11) and organic (Figure 12) additives can serve a variety of purposes: substrate activation, reductant activation, halide exchange, or simply to serve as a base. Many additives, however, can serve multiple proposed roles in the reaction (e.g., pyridine may act as a Brønsted base and as a ligand for the catalyst) or have a role that is not yet understood. As a result, it was difficult to separate additives by use type. Thus, we have tracked the number of reports of the most commonly used organic and inorganic additives to provide readers with a palette to choose from.

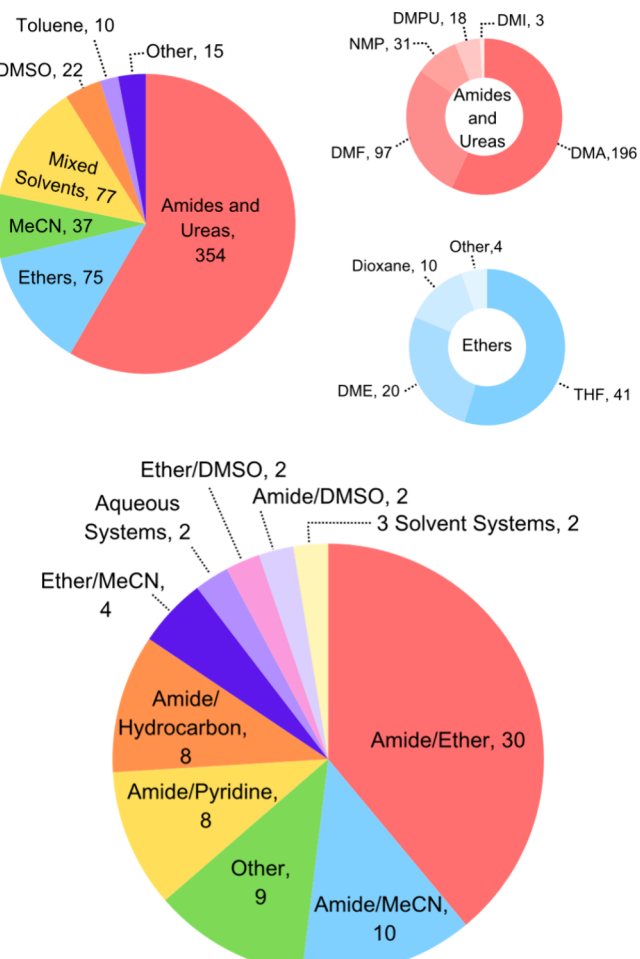


**Figure 9.** Distribution of solvent types used in XEC. Other = solvents with <10 reports.

Inorganic additives are more frequently used than organic additives and most commonly are thought to accelerate the reduction step ( $\text{MgCl}_2$ ,  $\text{LiCl}$ ,  $\text{LiBr}$ ), induce halide exchange on alkyls to increase reactivity ( $\text{NaI}$ ), or both ( $\text{NaI}$ ).<sup>37,38</sup> In some cases, the additive can serve as a suitable electrolyte for electrochemical XEC (for example,  $\text{KPF}_6$  is often,<sup>39</sup> but is not always,<sup>40</sup> used as an electrolyte). In organizing inorganic additives by cation, alkali and alkaline earth metal salts predominate by one to two orders of magnitude over other salt additives, such as transition metal salts, owing, at least in part, to their relative abundance (Figure 10).<sup>37,38</sup>

Organic additives play many similar roles to inorganic additives (Figure 12). For example, TBAI and TBAB add halides to the reaction mixture and play a similar role to inorganic halide additives. Silane reagents (e.g.,  $\text{TMSCl}$ ,  $\text{TESCl}$ ,  $\text{TMSBr}$ ) can activate metal powder reductants (by stripping the oxide layer from metallic surfaces) or by playing a direct role in the reaction mechanism (e.g.,  $(\text{TMS})_3\text{Si}\bullet$  mediated XAT or  $\text{R}_2\text{Si}^+$  activation of NHP esters).<sup>41–43</sup> Various pyridines (pyridine, DMAP, 4-ethylpyridine) are often employed to minimize unwanted side products, such as  $\beta$ -hydride elimination or product isomerization, presumably by occupying coordination sites on the metal to block these processes.<sup>44,45</sup> More hindered amines appear to play the role of base (2,6-lutidine, DIPEA). Notably, XEC reactions tolerate acid additives, such as TFA and  $\text{Et}_3\text{N}\bullet\text{HCl}$ .

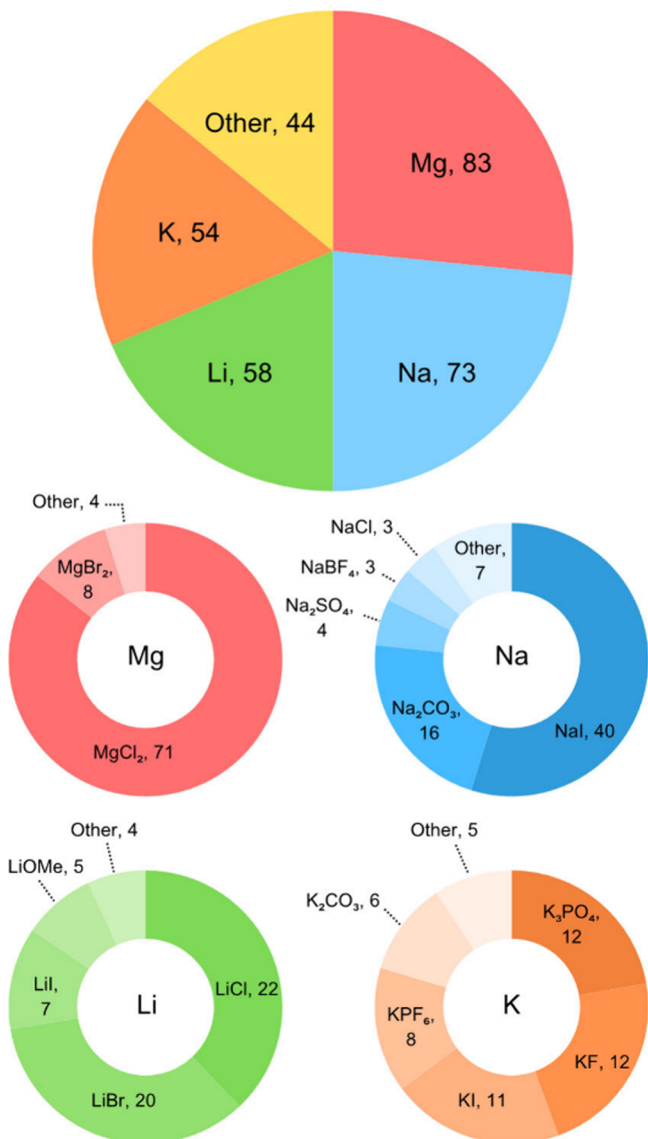


**Figure 10.** Common inorganic salt additives. Total = 312 reports. “Other” = reports with uncommon salt additives ( $\leq 2$  reports) “Other Cations” = reports with uncommon cations ( $\leq 10$  reports across entire cation).

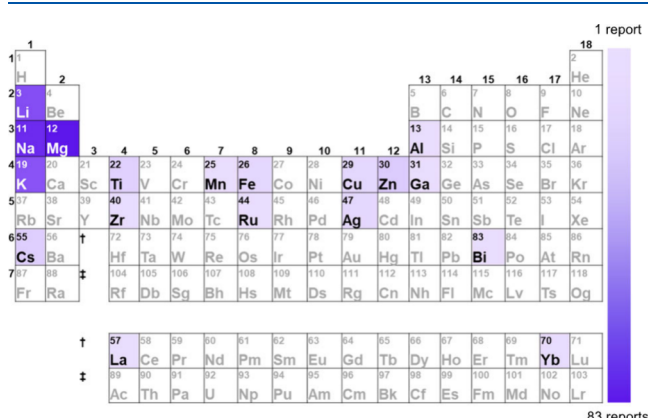


**Figure 11.** Element of cation for inorganic salt additives.

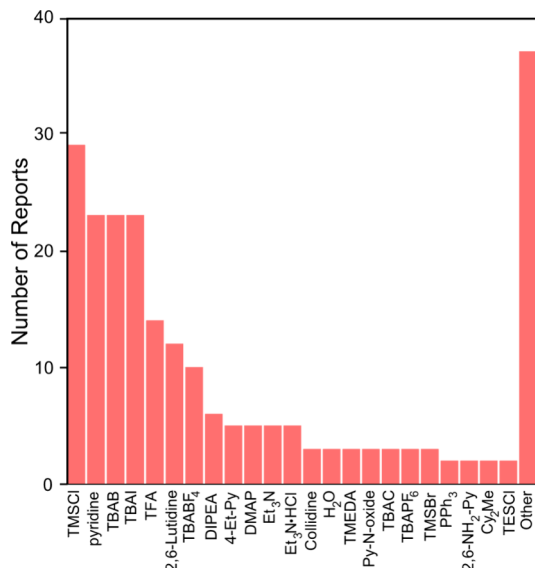


**Figure 12.** Organic additives by number of reports. Total number of additives: 243. Other = additives with 1 report.

#### 2.4. Reductants

The beginnings of XEC trace themselves to reactions that were stoichiometric in metal, such as the Ullman coupling (stoichiometric copper)<sup>29</sup> or nickel-mediated biaryl synthesis.<sup>24,25</sup> XEC is defined, in part, as reactions where a catalyst is reduced as part of the catalytic cycle. Stoichiometric metal reductants were among the first explored for XEC.<sup>26</sup> As Zn, Mn, Ni, and Co cost about the same, the main advantage is the freedom to utilize more complex ancillary ligands to modulate the catalyst reactivity and selectivity. Metallic reductants, such as Mn<sup>0</sup> and Zn<sup>0</sup> account for approximately 2/3 of all reductants studied in XEC reactions (Figure 13). However, difficulties with heterogeneous reactions, particularly on an industrial scale,<sup>46–49</sup> have provided motivation to explore alternative reductant pathways, such as homogeneous reductants (e.g., tetrakis(amino)ethylenes<sup>34,50,51</sup> and

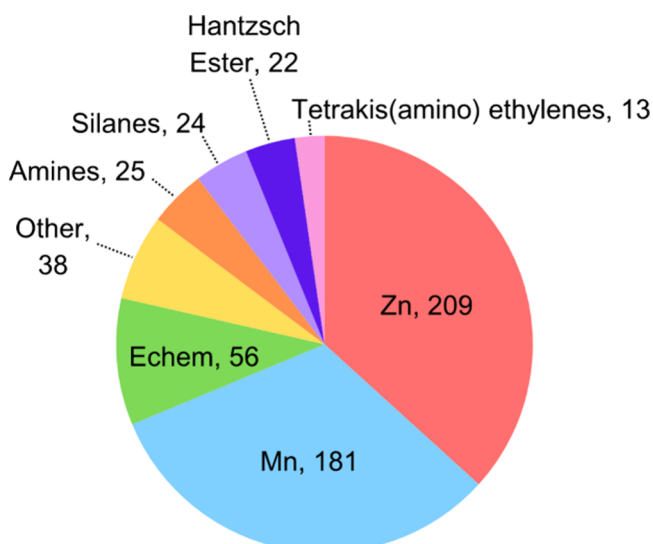


**Figure 13.** Reductants used in XEC. Total = 569 reports. Other = reductant categories w/ < 10 reports. “Echem” is discussed in further depth below and in a separate review.<sup>55</sup>

$\text{B}_2\text{pin}_2$ <sup>52–54</sup>) and photochemical and electrochemical XEC reactions (which are discussed in greater depth below).

Amines (such as DIPEA, TEOA, and  $\text{Et}_3\text{N}$ ), silanes, and Hantzsch ester are most commonly used as terminal reductants in electrochemical and photochemical reactions. Although these reductants are not capable of reducing nickel on their own, the applied potential or the energy of the photons makes up the difference. Amine reductants, once oxidized, can decompose to form secondary amines, iminiums, alkyl radicals, and aldehydes, so managing these intermediates is sometimes key to finding the best amine. Most of these terminal reductants require added base in addition to the electron source. Finally, the organic waste produced can sometimes be difficult to separate from the products. In electrochemistry, there is an opportunity to separate the cathodic and anodic compartments and avoid most of these problems, but divided cells have their own complications.<sup>55</sup>

## 2.5. Photochemical Approaches

Photochemically driven XEC generally uses a dye cocatalyst along with a terminal reductant (Figure 14). As with most photoredox chemistry reports,  $[(\text{Ir}(\text{bpy})(\text{ppy}))_2]X$  derivatives are the most-used cocatalysts and their properties can be varied by modifying the substitution on the bipyridine or phenylpyridine ligands. Cyanoarene-based donor–acceptor photocatalysts are also prevalent in XEC reactions, most frequently 4CzIPN. “No catalyst” reactions involve direct excitation of the substrate and terminal reductant, such as an EDA complex of Hantzsch ester with NHP esters.<sup>56</sup>

## 2.6. Electrochemical Approaches

Electrochemical XEC (eXEC) reactions, as in all electrochemical reactions, use an applied potential to drive paired reduction (cathodic) and oxidation (anodic) reactions. The XEC reaction is a cathodic reaction and must be paired with an oxidation at the anode. Most commonly, a sacrificial anode is used. In this case, the oxidation reaction is the oxidation of the metal anode itself and this releases salts into the reaction medium (i.e., a Zn anode releases  $\text{Zn}^{2+}$ ).<sup>55</sup> These metal salts may be noninnocent, and can either improve or hinder the reaction efficacy (dependent upon the identity of the metal salt, as well as reaction conditions), but are often ignored.<sup>57</sup> This anode corrosion can be problematic on scale-up, and the metal salt can be difficult to remove. Among the common anodes, Zn, Fe, Mg, stainless steel, Al, and Co are all sacrificial anodes (Figure 15). Carbon and platinum are not sacrificial anodes and are usually paired with the oxidation of a terminal reductant, such as an amine (vide supra). Under an applied potential, the amine can be oxidized to provide the electrons for the cathodic reaction. To prevent the oxidized form of the sacrificial reductant from interfering with the cathodic process, these reactions are often run in a divided electrochemical cell.<sup>49,55</sup>

Cathodes used in XEC reactions are less diverse than their anode counterparts (Figure 16). The most common cathodes are nickel (usually foam) and reticulated vitreous carbon (RVC, a kind of high-surface area glassy carbon).

## 2.7. Catalysts Used in XEC

XEC catalysis is dominated by the 3d transition metals (Ni, Co, Cu, Fe, Cr, Ti) with only a small number of reports with Pd and Rh (22 total) (Figure 17). Of these, nickel is far and away the most-used catalyst (88% of reports) and no other metal is more than 3%. This is likely for two reasons. First, as

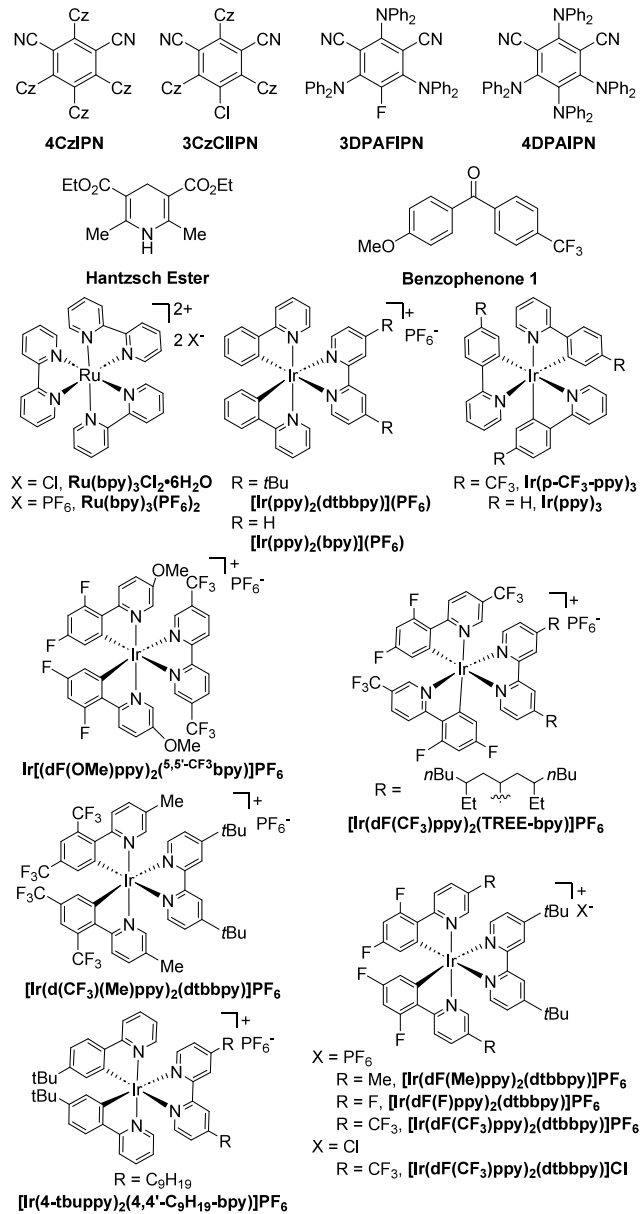


Figure 14. Photoredox catalysts utilized in XEC reactions.

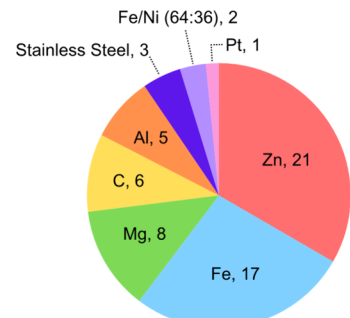
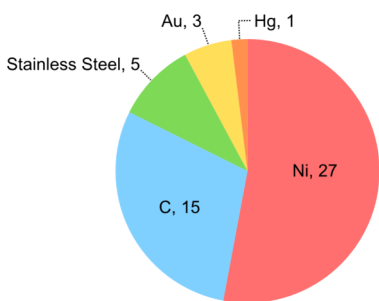
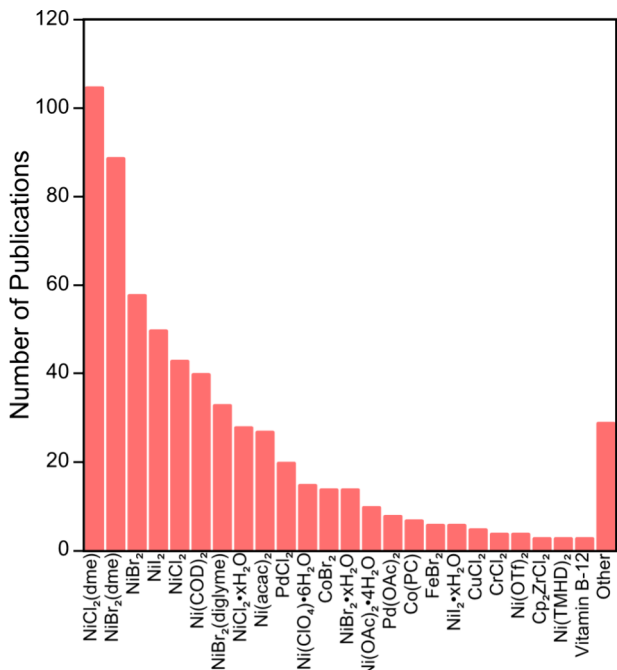


Figure 15. Anodes used in eXEC. Total count = 63. Multiple reports use multiple anodes dependent upon the conditions necessary for productive coupling.

will be noted later, the mechanisms of these reactions usually require single-electron oxidation and reduction events, and these are usually easier with the 3d metals. Second,



**Figure 16.** Cathodes used in eEXEC. Total count = 51.



**Figure 17.** Precatalysts used in XEC. Other = number of precursors with  $\leq 2$  reports. NiCl<sub>2</sub>(dme) = 102 reports.

development of XEC coincided with a general resurgence of interest in the 3d metals due to their lower cost, greater security of supply, and smaller environmental footprint. Somewhat confusingly, transition metals are also often used as terminal reductants for XEC (Zn, Mn, Fe, *vide supra*).

As XEC reactions include catalyst reduction as part of the catalytic cycle, the use of air stable precatalysts is common (Figure 17). Rather than Ni(cod)<sub>2</sub>, which is air-sensitive, various nickel halide salts are used. The same trend is observed for other metals. When differences are observed between precatalysts, they can usually be attributed to solubility in organic solvents (anhydrous NiX<sub>2</sub> salts have poor solubility, but NiX<sub>2</sub>(dme) precatalysts are very soluble), water content, and the influence of the counterion (e.g., iodide in NiI<sub>2</sub> might play a role like NaI). CoBr<sub>2</sub> is the most frequently reported monometallic non-nickel metal source in XEC and is most commonly seen in C(sp<sup>2</sup>)–C(sp<sup>2</sup>) coupling. However, approximately half of all coupling reactions using CoBr<sub>2</sub> have been reported over 10 years ago, representing an interesting area for future research. Pd precatalysts are most commonly reported under multimetallic conditions<sup>58,59</sup> either in concert with Ni or Cu. Under these conditions, each metal serves a distinct purpose, most frequently with each metal selectively activating one coupling partner. In XEC reactions, multi-

metallic systems are most frequently observed in biaryl syntheses (Chapter 3) and for cogeneration of radicals in C(sp<sup>2</sup>)–C(sp<sup>3</sup>) bond-forming reactions (section 4).

### 3. C(sp<sup>2</sup>)–C(sp<sup>2</sup>) BOND FORMATION

#### 3.1. Overview

C(sp<sup>2</sup>)–C(sp<sup>2</sup>) bond formation has a rich history in the synthesis of pharmaceuticals, agrochemicals, dyes, materials, ligands, and natural products.<sup>29</sup> In particular, the formation of symmetrical biaryls has long been accomplished using transition metals under reductive conditions, originally with copper (*i.e.*, Ullmann coupling).<sup>60–62</sup> Several important contributions in the field were later made, accomplishing symmetrical biaryl synthesis under both chemical and electrochemical conditions using stoichiometric nickel (including but not limited to the references cited herein).<sup>24,26,63–65</sup> Soon thereafter methods using catalytic nickel were reported, as well as methods using palladium catalysts.<sup>29,66–68</sup>

The translation of the reductive homocoupling chemistry to cross-selective coupling provided fast access to these useful products, but high cross-selectivity was usually difficult to achieve<sup>29,60,62,68</sup> except for when one “activated” component (usually an iodide) was coupled to an “unactivated” component (usually a bromide or chloride). For reactions with stoichiometric copper, high cross-selectivity could sometimes be achieved when the first aryl was reacted with copper (presumably to form an arylcopper species) followed by the second aryl halide.<sup>69</sup> Nickel catalysis using stoichiometric amounts of the metal was also developed followed by the first forays into what is now called cross-electrophile coupling using a nickel or palladium catalyst and stoichiometric reducing agent (initially electrochemical conditions or metal powders). This review will not cover uses of stoichiometric copper or nickel, but will cover the catalytic reactions.

The nascent state of XEC for C(sp<sup>2</sup>)–C(sp<sup>2</sup>) bond formation contrasts with the ubiquity of cross-coupling of aryl nucleophiles (Ar–M, M = ZnX, MgX, BR<sub>2</sub>, SiR<sub>2</sub>OH, etc.) with aryl electrophiles.<sup>7,9,12,29</sup> C(sp<sup>2</sup>)–C(sp<sup>2</sup>) cross-electrophile coupling (XEC), although challenging, offers several advantages including higher commercial availability and stability<sup>70</sup> of Ar–X vs organometallic reagents. Furthermore, the functional-group compatibility of XEC approaches can decrease reliance on protecting groups and increase flexibility in synthetic routes.

As might be surmised, the selective coupling of two different C(sp<sup>2</sup>) electrophiles is a challenge because the two substrates and any potential intermediates are very alike in reactivity. This challenge can be addressed with some combination of three strategies: (1) using an excess of one coupling partner to maximize the cross-product yield with respect to the limiting reagent (at the cost of large amounts of dimeric products), (2) utilizing substrates that are better differentiated by arene electronics and substitution (substrate control), and (3) finding approaches that differentiate the substrates based upon the leaving group regardless of electronics, such as multimetallic systems.

A variety of couplings involving (hetero)aryl and vinyl halides will be discussed, including pseudohalides such as sulfonate esters. Also included are couplings with acyl donors. Expansion to many other classes of electrophiles have also been recently reported and will be examined as well. One broad report, while largely C(sp<sup>2</sup>)–C(sp<sup>3</sup>) XEC (discussed in

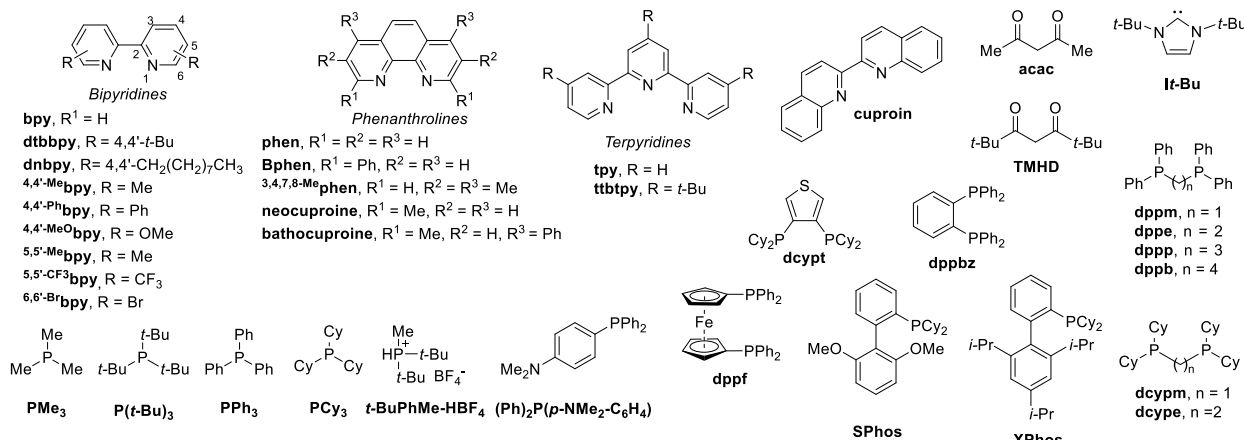


Figure 18. Ligands reported in C(sp<sup>2</sup>)–C(sp<sup>2</sup>) XEC reactions.

section 4.2.3.3, Scheme 163), also coupled aryl halides with alkynyl, alkenyl, and aryl electrophiles.<sup>71</sup>

We elected not to cover reactions that start with two electrophiles but proceed by in situ formation of an organometallic reagent by direct insertion (e.g., Mg<sup>0</sup> reacting with Ar–Br to form ArMgBr followed by Kumada coupling).<sup>72–76</sup> We chose to cover reactions where an arylmetal intermediate accumulates in the reaction mixture via transmetalation from the catalyst to an intermediate shuttling metal.<sup>77</sup> We realize that this distinction is subtle, but (as in other sections) we chose to focus on reactions where the catalyst is reduced as an essential part of the catalytic cycle.

A diverse array of ligands has been utilized in XEC for C(sp<sup>2</sup>)–C(sp<sup>2</sup>) bond formation, including bi- and tridentate nitrogenous ligands, mono- and bidentate phosphine ligands, and carbene ligands (Figure 18).

Ligands used in C(sp<sup>2</sup>)–C(sp<sup>2</sup>) bond formation represent a much broader array of scaffolds than are seen in other sections, owing to the greater diversity of metals used in this coupling type (Figure 19). The greatest difference is the increased portion of phosphine-based ligands (both monodentate and bidentate), which are not commonly employed in Ni-catalyzed XEC reactions. That being said, ligands on nickel in the reactions in this section largely follow trends observed in all XEC reactions, with bipyridine ligands dominating (Figure 19). Similarly, apart from acac, all ligands on palladium are unsurprisingly phosphine-based (Figure 20). Nickel and palladium, both in monometallic and bimetallic-catalyzed reactions, represent the greatest portion of metal precatalysts employed in this section.

Mechanistic proposals for C(sp<sup>2</sup>)–C(sp<sup>2</sup>) XEC reactions fall into two categories: (1) sequential oxidative additions at a single metal center (Figure 21A) or (2) transmetalation between two species (Figure 21B,C).<sup>78–82</sup> The transmetalation category can be between two different catalytic intermediates (Figure 21B, usually differentiated by metal identity, oxidation state, or ligand sphere), or involve an additional organometallic intermediate (Figure 21C, usually derived from the reductant, e.g., ArZnX from Zn<sup>0</sup> reductant). Both mechanisms require differentiation of the two electrophiles in oxidative addition, but the transmetalation mechanism requires additional selectivity in the aryl transfer step (Figure 21B,C). Additional mechanistic details will be discussed as they arise.

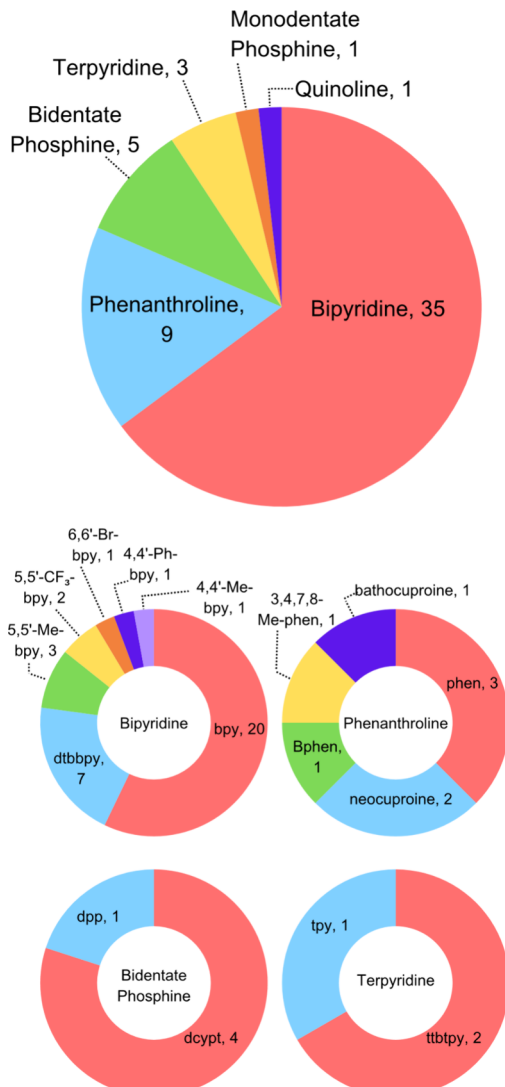
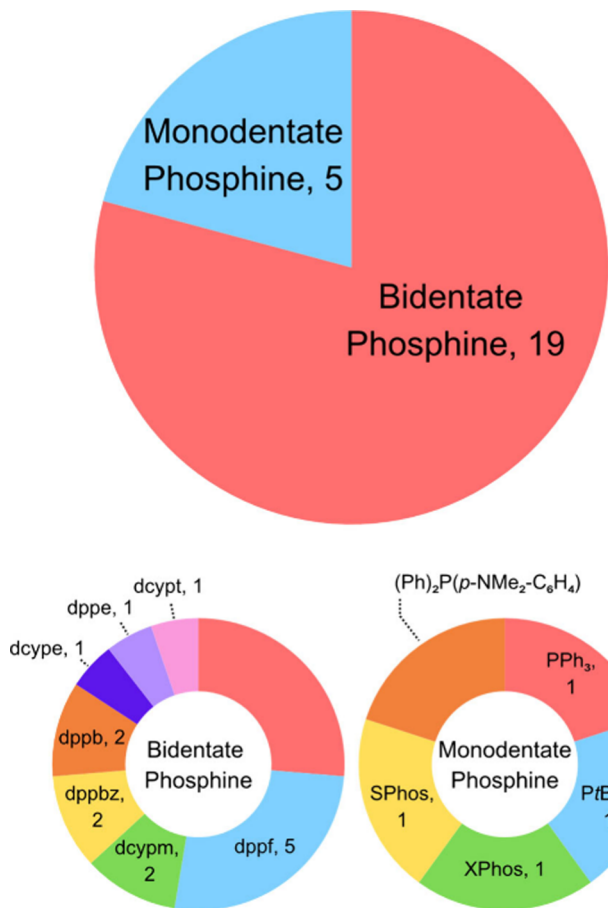


Figure 19. Common ligands on nickel in C(sp<sup>2</sup>)–C(sp<sup>2</sup>) XEC reactions.

### 3.2. Biaryls

**3.2.1. XEC of Aryl Halides.** **3.2.1.1. Ni-Catalyzed Systems.** Gosmini and co-workers developed two methods to couple aryl halides with 2-halopyridines.<sup>83</sup> In the presence

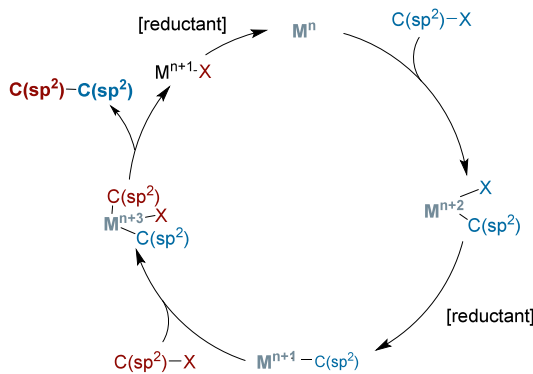


**Figure 20.** Common ligands on palladium in  $\text{C}(\text{sp}^2)\text{-C}(\text{sp}^2)$  XEC reactions.

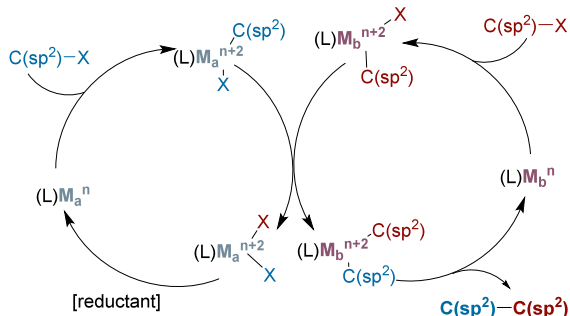
of  $\text{ZnBr}_2$ , formation of an arylzinc reagent through an electrochemical process and sequential coupling with 2-halopyridine are all catalyzed by the same nickel complex. The authors also propose a nonorganozinc mediated coupling of aryl halides and 2-halopyridines (**Scheme 1**) by a sequential oxidative addition mechanism (**Figure 21A**). They found that aryl bromides were more reactive than 2-chloropyridine, resulting in oxidative addition of the aryl bromide to the nickel(0) precatalyst to form an arylnickel(II) complex. The authors found that the use of more activated aryl bromides results in increased homocoupling yields as the reduced arylnickel(I) complex reacts faster with the aryl bromide than the 2-chloropyridine, thus limiting the scope to include only aryl bromides with electron-donating groups. However, if the 2-chloropyridine is swapped with the more reactive 2-bromopyridine, activated aryl bromides could be successfully cross-coupled in this protocol.

Previous work from Gosmini and co-workers attempting to couple aryl halides with 2-arylpyrimidines and 2-arylpyrazines under previously established conditions was found to be unsuccessful most likely due to the strong ligation of pyrimidine or pyrazine to the nickel catalyst.<sup>83</sup> The authors reported a new set of electrochemical conditions capable of coupling aryl halides with chloropyrimidines and 2-chloropyrazines.<sup>84</sup> The authors found that the introduction of iron salts at the beginning of electrolysis resulted in good yields of the cross-coupled product. The proposed mechanism follows **Figure 21A** with initial oxidative addition of the aryl bromide

### A) Sequential Oxidative Additions at a Single Metal Center



### B) Direct Transmetalation via two Catalytic Intermediates



### C) Transmetalation via Organometallic Intermediate Shuttle

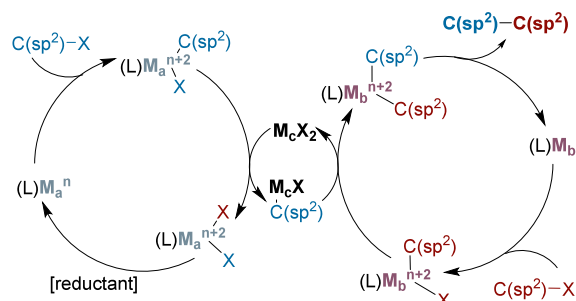
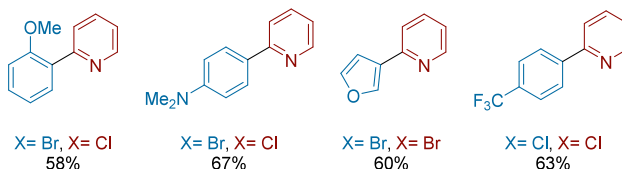


**Figure 21.** (A) Sequential oxidative addition mechanism, (B) Direct multimetallic transmetalation mechanism. (C) Multimetallic transmetalation via an organometallic intermediate shuttle.  $M_a$  may equal  $M_b$ .

### Scheme 1. Ni-Catalyzed Electrochemical XEC of Aryl Halides with 2-Halopyridines (1998)

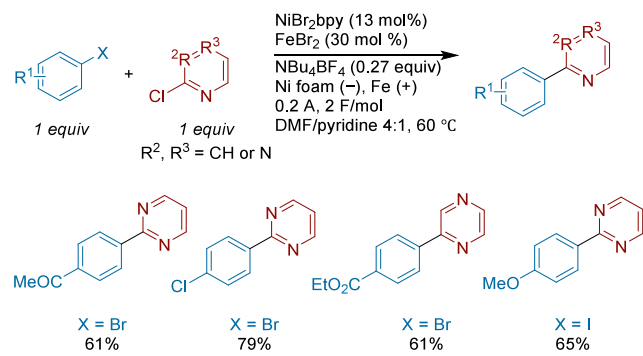


#### Selected Examples



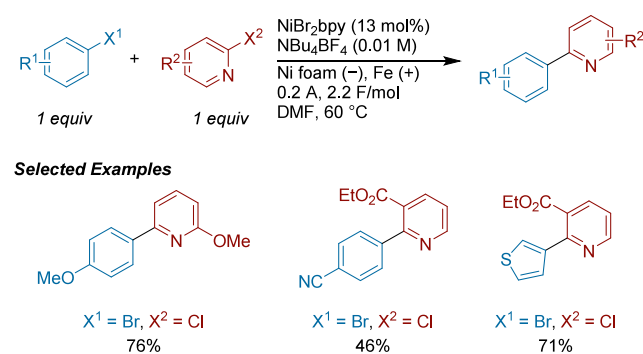
followed by the aryl chloride. The authors were able to couple aryl halides with both electron withdrawing and electron donating groups by changing the halide to better match the reactivity of the chloropyrimidine or 2-chloropyrazine (**Scheme 2**). The aryl bromide is paired with more activating electron withdrawing groups while the aryl iodide is paired with electron donating groups.

**Scheme 2. Ni-Catalyzed Electrochemical XEC of Aryl Halides with Chloropyrimidines and 2-Chloropyrazines (2000)**



Following their previous reports of the beneficial effect of iron salts in heteroaryl couplings, Gosmini and co-workers applied their same system to various substituted 2- and 3-halopyridines.<sup>85</sup> The authors report a ~20% improvement in yield by switching their previous zinc anode with an iron anode. A range of electron-donating and electron-withdrawing aryl halides and heteroaromatic halides were successfully coupled (**Scheme 3**).

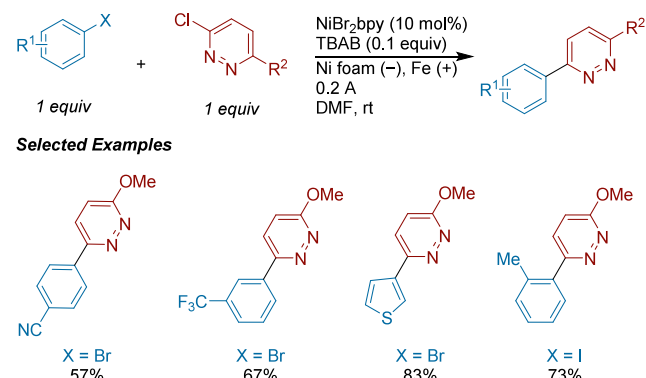
**Scheme 3. Ni-Catalyzed Electrochemical XEC of Aryl Halides with Halopyridines (2000)**



In 2007, Léonel and co-workers reported an electrochemical Ni-catalyzed coupling of aryl halides with 2-chloropyridazines.<sup>86</sup> The authors found aryl substitution and halogen identity to play a significant role in the yields. Unactivated aryls required the aryl iodide for efficient reactivity, but aryl bromides were sufficient for nearly all electron-withdrawing substituents except those in the *ortho*-position, which also required aryl iodides. (**Scheme 4**). The authors proposed a sequential oxidative addition catalytic cycle (**Figure 21A**).

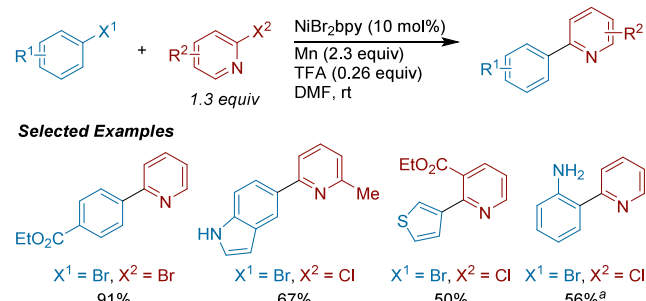
In 2009, the Gosmini group also reported translation of electrochemical conditions to chemical conditions (Mn reductant) for the Ni-catalyzed cross-electrophile coupling of

**Scheme 4. Ni-Catalyzed Electrochemical XEC of Aryl Halides with 2-Chloropyridazines (2007)**



aryl halides with 2-halopyridines to form functionalized 2-arylpyridines.<sup>87</sup> Both electron-donating and electron-withdrawing substituents were tolerated, but differing halogen identities (iodide and bromide, respectively) were required (**Scheme 5**). For example, when coupling with 2-chloropyr-

**Scheme 5. Ni-Catalyzed Cross-Electrophile Coupling of Aryl Bromides with 2-Halopyridines (2009)<sup>a</sup>**



<sup>a</sup> at 60 °C.

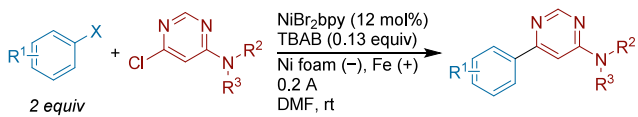
idine an aryl chloride is best for electron-poor aryls and an aryl bromide is best for electron-rich aryls. The cross-coupling is efficient at room temperature for unhindered substrates, but *ortho*-substitution requires heating to 60 °C (presumably due to slow reductive elimination). Functionalized 2-halopyridines were also tolerated but required further matching the reactivity of each coupling partner.

In 2011, Le Gall and Léonel reported an electrochemical Ni-catalyzed XEC of aryl halides with 6-chloropyrimidines (**Scheme 6**).<sup>88</sup> A decrease in yields was noted when using 2-chloropyrimidines with NHAr substitution at the 4-position due to competing dimerization. The authors hypothesized a sequential oxidative addition mechanism with the pyrimidine reacting first (**Figure 21A**).

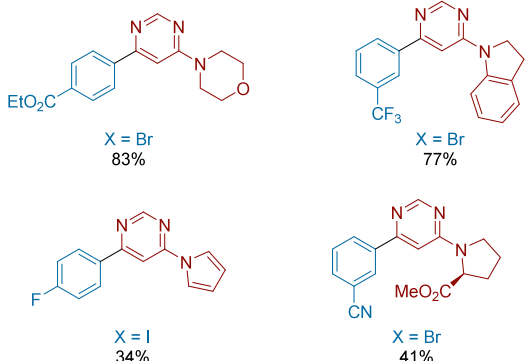
In 2012, Navarro and co-workers reported a Ni-catalyzed XEC of 2-halopyridines to form 2,2'-bipyridines (**Scheme 7**).<sup>89</sup> The authors report that using an iron anode provided higher yields than their previously used zinc anode. They indicate that trapping of free 2,2'-bipyridine is facilitated by the iron salts formed during oxidation. The authors propose a sequential oxidative addition mechanism (**Figure 21A**).

Léonel and co-workers reported an electrochemical Ni-catalyzed XEC of aryl halides with 3-amino-6-chloropyridazines (**Scheme 8**).<sup>90</sup> Using previous electrochemical methods developed by the group, only moderate yields were obtained.

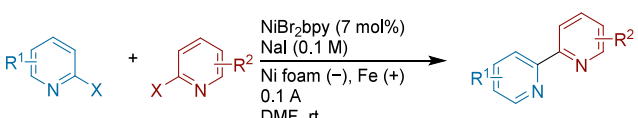
**Scheme 6. Ni-Catalyzed Electrochemical XEC of Aryl Halides with 2-Chloropyrimidines (2011)**



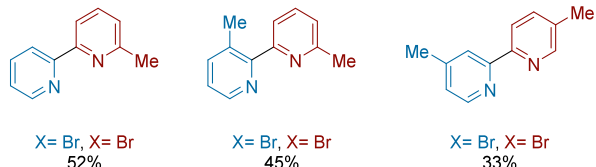
**Selected Examples**



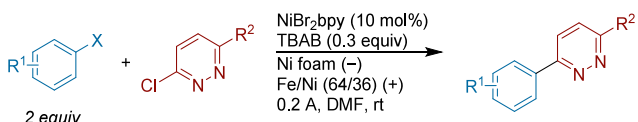
**Scheme 7. Ni-Catalyzed Electrochemical XEC of Various 2-Halopyridines to Form Nonsymmetrical 2,2'-Bipyridines (2012)**



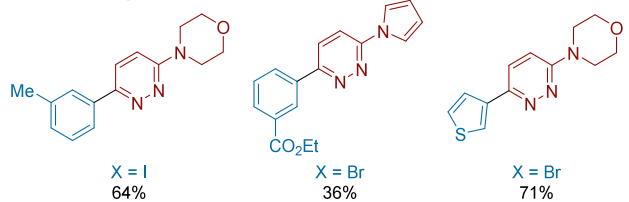
**Selected Examples**



**Scheme 8. Ni-Catalyzed Electrochemical XEC of Aryl Halides with 3-Amino-6-Chloropyridazines (2013)**



**Selected Examples**

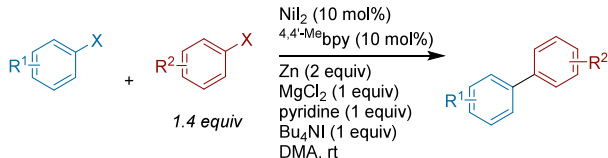


However, the authors saw an increase in yields by switching the anode from iron to an iron/nickel anode. They hypothesize that nickel salts generated by the anode may allow for the regeneration of the active organonickel species. Aryl iodides are best for electron-rich aryls and require an additional equivalent added to the reaction in the middle of electrolysis. For electron-poor (hetero)aryls, aryl bromides were best. Electrochemical studies were consistent with a sequential oxidative addition mechanism (Figure 21A) with initial

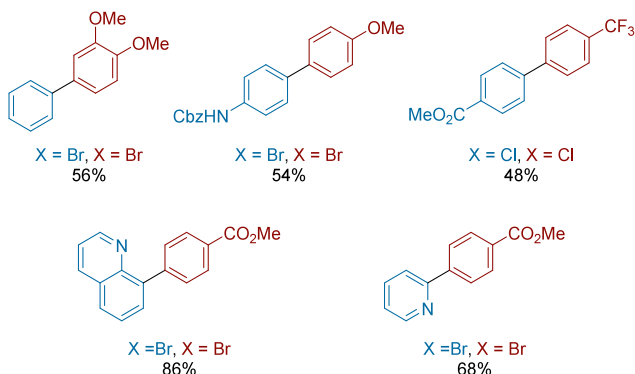
oxidative addition of the chloropyridazine. A variation on these conditions was later utilized to synthesize a variety of heteroaryl small molecules for biological evaluations as antitumor agents.<sup>91</sup>

Kunhua Lin, Qun Qian, and co-workers reported on the XEC of aryl halides to form unsymmetrical biaryls (Scheme 9).<sup>92</sup> The authors found the addition of MgCl<sub>2</sub> and Bu<sub>4</sub>NI to

**Scheme 9. Ni-Catalyzed XEC of Aryl Halides to Form Biaryls (2013)**



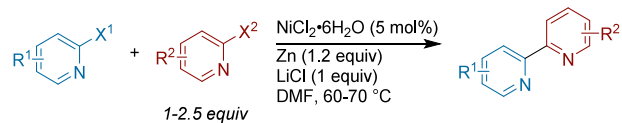
**Selected Examples**



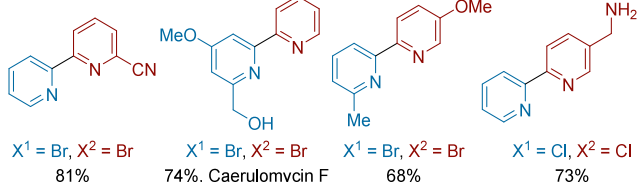
be necessary for coupling and attributed this to these reagents facilitating removal of salts from the zinc surface. Control tests were performed to rule out the intermediacy of an arylzinc species (Figure 21C). The authors favored a sequential oxidative addition process instead (Figure 21A).

Xin-Fang Duan and co-workers reported an external-ligand free Ni-catalyzed XEC of two different 2-halopyridines to form nonsymmetrical 2,2'-bipyridines (Scheme 10).<sup>93</sup> Instead of

**Scheme 10. Ni-Catalyzed XEC of 2-Halopyridines to Form Unsymmetrical 2,2'-Bipyridines (2014)**



**Selected Examples**

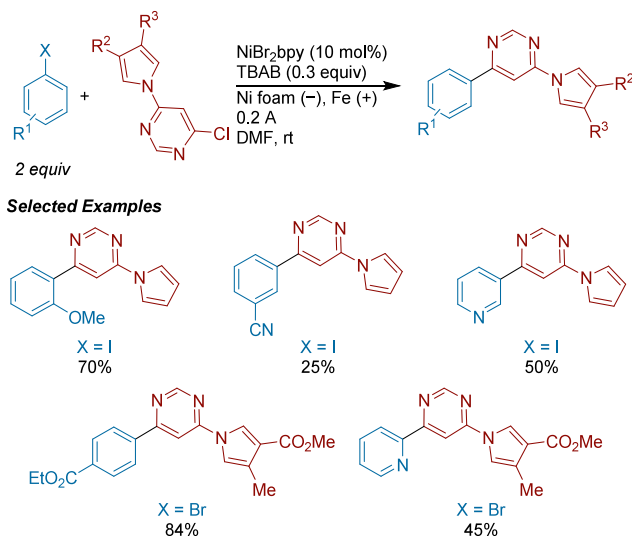


electrochemical conditions utilized previously (Scheme 7), zinc metal powder is the terminal reductant. The authors proposed that the 2,2'-bipyridines formed in the reaction coordinate to nickel and catalyze further turnovers. This was supported by strong evidence: the coupling of 3-bromopyridines resulted in 0% yield of 3,3'-bipyridine, but with 2,2'-bipyridine added the yield of 3,3'-bipyridine was 83%. A range

of 2,2'-bipyridines were synthesized, including the natural product caerulomycin F.

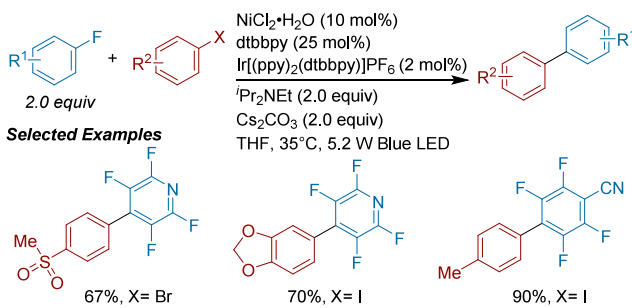
In 2016, Léonel, Le Gall, and co-workers reported a method for the electrochemical XEC of aryl halides with 4-chloro-6-pyrrolylpyrimidines (**Scheme 11**).<sup>94</sup> These conditions are very close to those they utilized for 3-amino-6-chloropyrimidines (**Scheme 8**).

**Scheme 11. Ni-Catalyzed Electrochemical Cross-Electrophile Coupling of Aryl Halides and 4-Chloro-6-Pyrrolylpyrimidines (2016)**



Rueping reported a method for the photochemical XEC of polyfluorinated arenes with aryl bromides and aryl iodides (**Scheme 12**).<sup>95</sup> The system uses an iridium dye photoredox

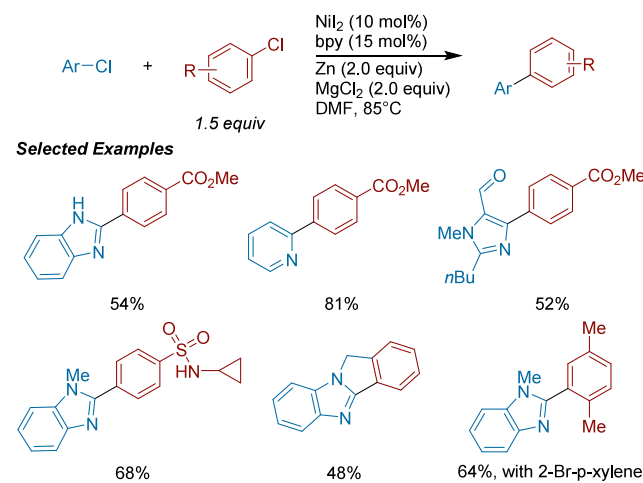
**Scheme 12. Nickel and Iridium Photochemical XEC of Polyfluorinated Arenes with Aryl Bromides (2020)**



catalyst, a tertiary amine as a terminal reductant, and Cs<sub>2</sub>CO<sub>3</sub> to sequester the HX formed under these conditions. The authors propose a variation on sequential oxidative addition (**Figure 21A**) where an intermediate arynickel(II) reacts with the perfluoroaryl radical anion to generate the diarylnickel(III) species that can reductively eliminate to form the desired product. The difference between this mechanism and **Figure 21A** is that the perfluoroaryl species is reduced instead of the nickel species. As evidence for the reduction step, the authors found that reactions without Cs<sub>2</sub>CO<sub>3</sub> formed the hydrodefluorinated product (presumably by H atom abstraction of the radical anion from i-Pr<sub>2</sub>NEt<sup>•+</sup>). This proposed mechanism, although unusual for C(sp<sup>2</sup>)–C(sp<sup>2</sup>) XEC, is familiar for C(sp<sup>2</sup>)–C(sp<sup>3</sup>) XEC.<sup>96</sup>

In 2021, Lautens reported a Ni-catalyzed XEC between aryl and heteroaryl chlorides (**Scheme 13**).<sup>97</sup> The presence of

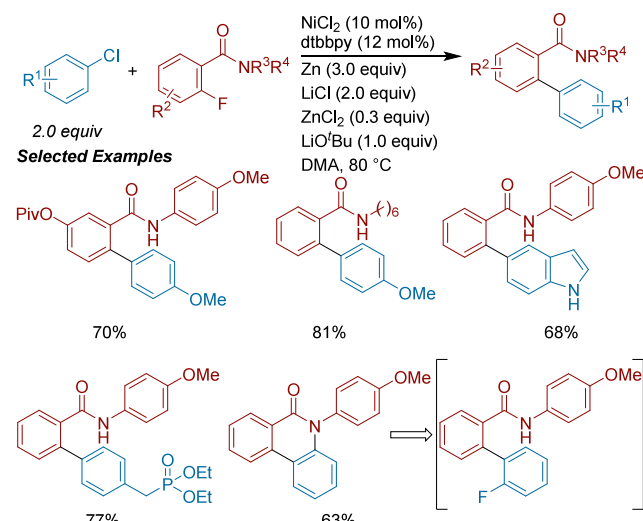
**Scheme 13. Ni-Catalyzed XEC Between Aryl Chlorides (2021)**



MgCl<sub>2</sub> and iodide were both essential and they were proposed to expedite reduction of Ni(II). Some degree of substrate-matching was required: heteroaryl chlorides could be coupled with activated aryl chlorides, but less activated aryl chlorides were not selective. In this case, electron-neutral or electron-rich aryl bromides could be used. Intriguingly, an intra-molecular XEC reaction proceeded in 48% yield, suggesting a mechanism as in **Figure 21A**.

In 2021, Naoto Chatani reported a method for the cross-electrophile coupling of *ortho*-fluoro aryl amides with aryl chlorides (**Scheme 14**).<sup>98</sup> LiCl and ZnCl<sub>2</sub> were effective

**Scheme 14. Ni-Catalyzed XEC of Aryl Fluorides with Aryl Chlorides by Use of a Directing Group (2021)**

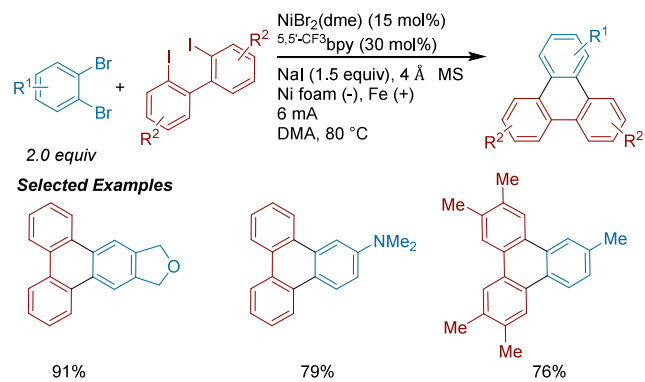


additives to facilitate reduction of Ni(II) to Ni(0) and promote a key transmetalation step, respectively. Lithium *tert*-butoxide was crucial as a base to deprotonate the –NH of the amide, which could then coordinate to Ni(0) and promote aryl C–F oxidative addition. A variety of functional groups were tolerated such as a phosphonate and a primary aryl amine.

An aryl triflate or aryl tosylate could also be used in place of an aryl chloride.

In 2022, Tian-Sheng Mei reported a Ni-catalyzed electrochemical XEC of 1,2-dibromobenzene derivatives with 2,2'-diiodo-biphenyl derivatives for the synthesis of triphenylenes (**Scheme 15**).<sup>99</sup> The reaction setup was carried out in an

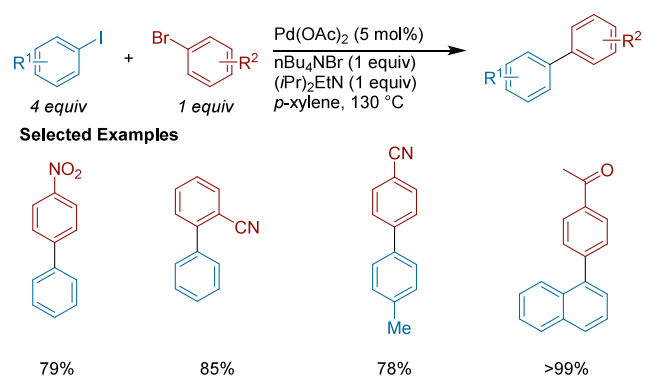
**Scheme 15. Ni-Catalyzed Electrochemical XEC Between Dihalobenzene Derivatives (2022)**



undivided cell with a sacrificial Fe anode, Ni foam cathode, and NaI as the electrolyte. A series of CV and electrolysis experiments were run with an (L)Ni<sup>II</sup>(Ar)<sup>-</sup>Br complex and in part led the authors to believe that the reaction starts with Ni(0) and the mechanism involves benzyne intermediates.

**3.2.1.2. Pd-Catalyzed Systems.** In 2000, Lemaire and co-workers reported the synthesis of unsymmetrical biaryls through the use of a Pd-catalyzed coupling reaction.<sup>100</sup> (**Scheme 16**) Notably, the authors reported biaryls bearing

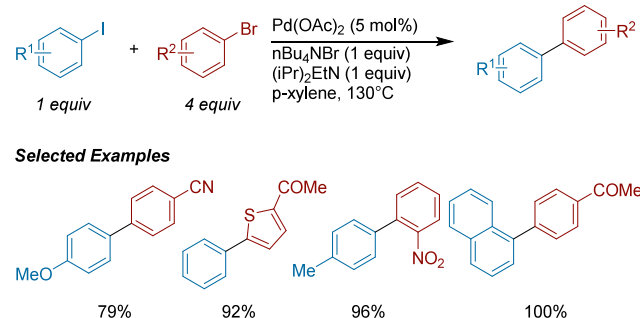
**Scheme 16. Pd-Catalyzed Coupling of Iodo- and Bromoarenes (2000)**



both electron-donating and electron-withdrawing functional groups. The authors found that an excess of one coupling partner and high temperatures are needed to promote the unsymmetrical coupling and reduce the competitive homocoupling. The XEC is proposed to proceed through the oxidative addition of the aryl iodide to the Pd(0) center, followed by either a second oxidative addition or a nucleophilic substitution.

In 2001, Lemaire and co-workers reported a Pd-catalyzed XEC of aryl iodides with an excess of aryl bromides (**Scheme 17**).<sup>101</sup> Compared to nickel systems, where explicit, strong reductants are required, palladium systems can utilize relatively mild reductants (proposed to be  $\text{Bu}_4\text{NBr}$ ). The mechanism of

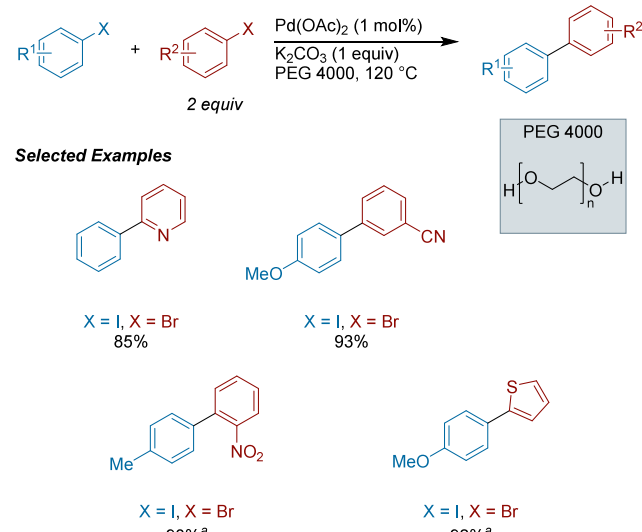
**Scheme 17. Pd-Catalyzed XEC of Iodoarenes with Bromoarenes (2001)**



this coupling is unclear, but was proposed to involve Pd(IV) as the penultimate intermediate. Reductive elimination from  $[\text{Pd}^{\text{IV}}]\text{Ar}^1\text{Ar}^2$  then results in the formation of the unsymmetrical biaryl. Separation of the unsymmetrical biaryl from the side products of the excess aryl bromide made product isolation difficult, but the high yields obtained are notable.

In 2006, Yuhong Zhang, Yanguang Wang, and co-workers reported a Pd-catalyzed coupling of aryl halides to form unsymmetrical biaryls (**Scheme 18**).<sup>102</sup> As observed by

**Scheme 18. Pd-Catalyzed XEC of Aryl Halides (2006)<sup>a</sup>**



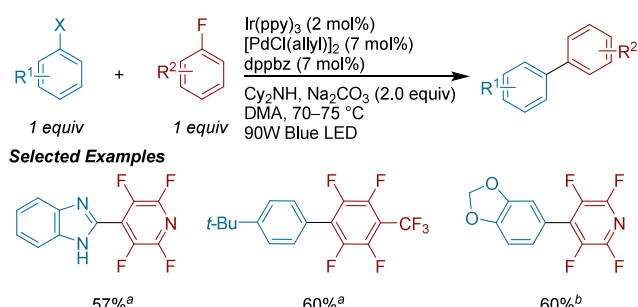
<sup>a</sup>With  $\text{Pd}(\text{OAc})_2$  (5 mol%).

Lemaire (**Scheme 17**), a conventional reductant was not required. The authors used polyethylene glycol (PEG) in place of organic solvents and were able to control selectivity by adjusting the amount of PEG. They found that larger chain length PEGs were selective toward the biaryl product and lowered the yield of hydrodehalogenation, the major side product. Although the authors noted that they could recycle the PEG 4000, which is inconsistent with it being the terminal reductant, we think it is likely that oxidation and partial degradation of the PEG is the most-likely source of electrons. As PEG 4000 is an affordable, relatively safe solvent/reductant, this system is especially attractive. Substrates with electron-withdrawing and electron-donating groups were well tolerated, but aryl halides with hydroxyl or amino substituents yielded no

product due to the interference with oxidative addition of the aryl halides to palladium.

Lingling Chu disclosed a complementary photoredox method for the synthesis of perfluoroarenes, catalyzed by Pd instead of Ni (Scheme 19).<sup>103</sup> Similar to work by the Rueping

**Scheme 19. Palladium and Iridium Photochemical XEC Between Aryl Bromides/Triflates and Polyfluoroarenes (2021)<sup>a</sup>**

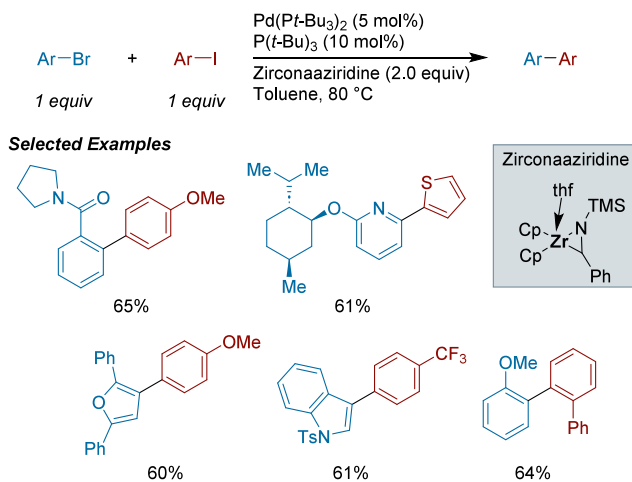


<sup>a</sup>(a) With X= Br (2.0 equiv) and Cy<sub>2</sub>NH (0.5 equiv). (b) With X = OTf (1.5 equiv), Cy<sub>2</sub>NH (0.8 equiv), LiI (0.3 equiv), and 1,4-dicyanobenzene (5 mol%).

lab (Scheme 12),<sup>95</sup> a radical anion from the aryl fluoride is proposed to be key in a sequential addition-type mechanism. A broad set of aryl bromides and electron-neutral and electron-deficient aryl triflates could be coupled with polyfluoroarenes, however aryl iodides could not be used in this system.

In 2021, Peng Liu, Toste, and Baihua Ye reported a method for the Pd-catalyzed XEC of aryl bromides with aryl iodides mediated by zirconiaaziridine as both a reductant and aryl group shuttle (Scheme 20).<sup>104</sup> The mechanism is proposed to

**Scheme 20. Pd-Catalyzed XEC of Aryl Halides Mediated by Zirconiaaziridine as a Reductant and Shuttle Agent (2021)**

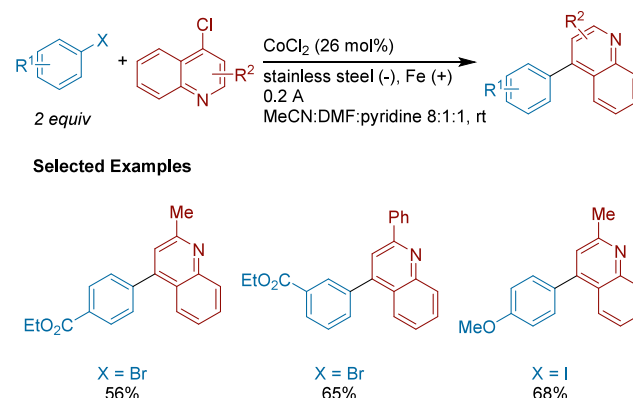


proceed by initial reaction of palladium with the aryl iodide to form (L)Pd<sup>II</sup>(Ar)(I), redox transmetalation of (L)Pd<sup>II</sup>(Ar)(I) with the zirconiaaziridine to form a pool of arylzirconocene, and subsequent Pd-catalyzed cross-coupling of this arylzirconocene with the remaining aryl bromide. The authors proposed a key redox transmetalation step of zirconiaaziridine with (L)Pd<sup>II</sup>(Ar)(I) that was supported by DFT calculations and experimental data. Direct activation of the aryl iodide by the zirconiaaziridine was proposed to be a minor pathway. This

mechanism is an extreme case of Figure 21C, where the intermediate species accumulates to a large extent. Perhaps as a result of this separation of the two stages, an impressive range of biaryl products were accessible, including aryl–aryl, heteroaryl–aryl, and heteroaryl–heteroaryl substrates (furan, pyrazole, etc.).

**3.2.1.3. Cobalt-Catalyzed Systems.** As an expansion of their previous work showing effective and efficient biaryl synthesis through cobalt-catalyzed electrochemical XEC, Gosmini and co-workers adapted their system for 4-chloroquinolines.<sup>105</sup> Pyridine was again found to be essential as a ligand for cobalt, allowing for both electron-donating and electron-withdrawing groups to be coupled in moderate yields (Scheme 21).

**Scheme 21. Cobalt-Catalyzed Electrochemical XEC of Aryl Halides and 4-Chloroquinolines (2001)**

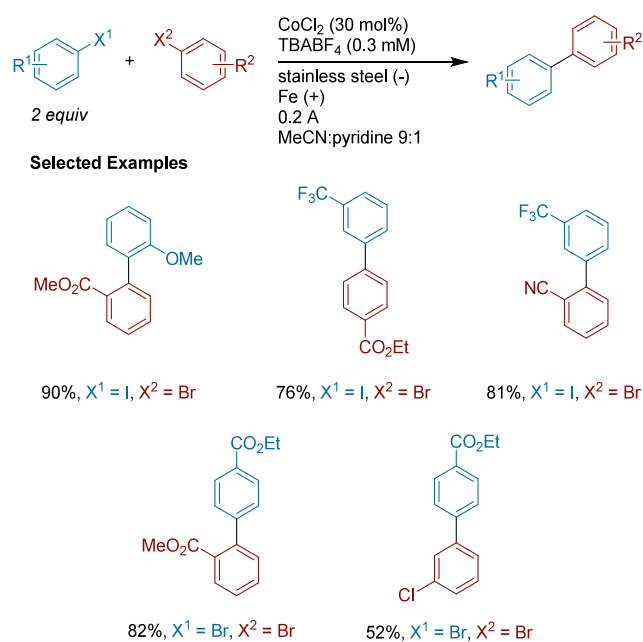


Gosmini and co-workers reported a new method that effectively couples two aryl halides both bearing electron-withdrawing substituents using cobalt catalysis instead of nickel catalysis.<sup>106</sup> Their work showed that selectivity toward the cross-product increases with higher cobalt catalyst loading, and that pyridine is necessary as a cosolvent (presumably it acts as a ligand for cobalt). Aryl halides bearing electron-withdrawing groups in the *ortho*-, *meta*-, and *para*- positions were all well-tolerated (Scheme 22). Aryl bromides and aryl chlorides also afforded moderate yields, but aryl chlorides exhibited lower rates of reactivity. The scope and yields reported are in many cases superior to the analogous Ni-catalyzed method.

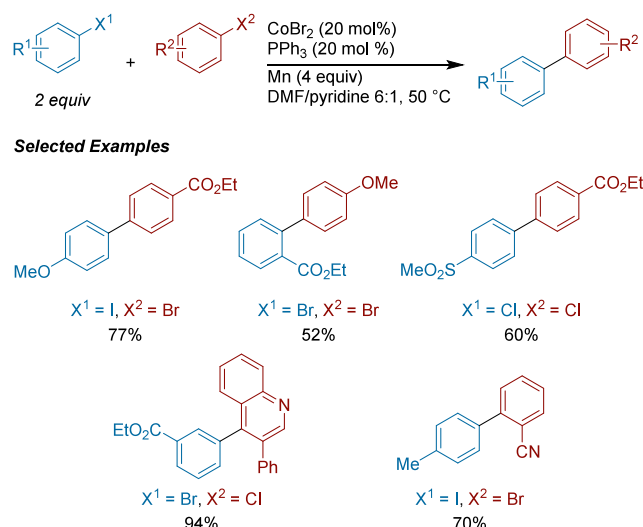
In a major advance for the field, Gosmini and co-workers reported a cobalt-catalyzed cross-electrophile coupling of aryl halides to form unsymmetrical biaryls in 2008 (Scheme 23).<sup>107</sup> Compared to their previous electrochemical conditions, these conditions utilized Mn powder reductant in place of an iron anode and an explicit ligand (triphenylphosphine) in addition to pyridine as a cosolvent. This coupling exhibited high functional group and steric tolerance. Heteroaryl halides could be coupled, but 3-bromothiophene and 2-chloropyridines only gave moderate yields due to their ability to act as a ligand for cobalt. The authors synthesized 2-(4-tolyl)benzonitrile, a key intermediate of the syntheses of sartan derivatives, in 70% yield. The authors proposed a sequential oxidative addition mechanism (Figure 21A).

**3.2.1.4. Rh-Catalyzed Systems.** In 2021, Krische disclosed an XEC of aryl bromides with aryl iodides with formate as the reductant (Scheme 24).<sup>108</sup> 2-pyridyl bromides were coupled in

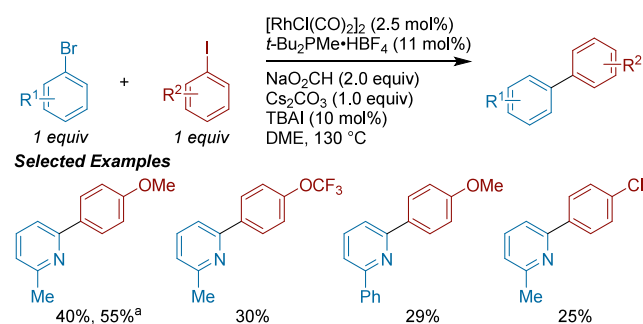
**Scheme 22. Cobalt-Catalyzed Electrochemical XEC of Aryl Halides (2002)**



**Scheme 23. Cobalt-Catalyzed XEC of Aryl Halides to Form Unsymmetrical Biaryls (2008)**



**Scheme 24. Rh-Catalyzed XEC of Aryl Bromides with Aryl Iodides (2021)<sup>a</sup>**



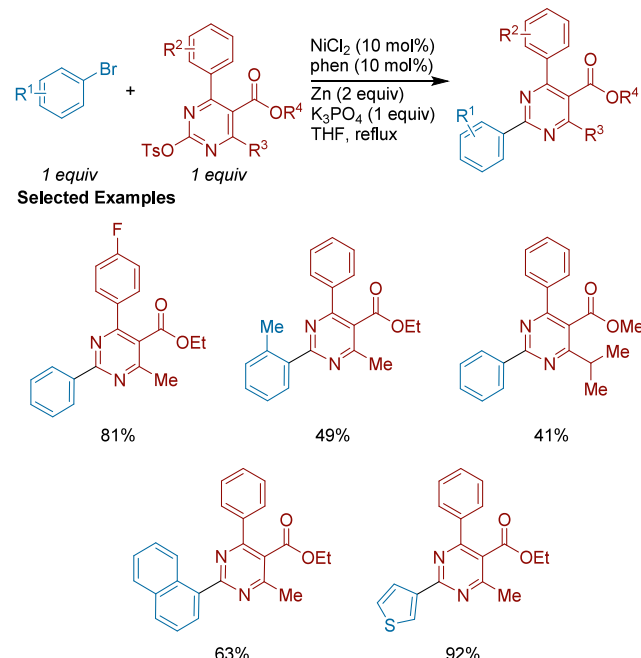
<sup>a</sup>With Pd metal (1 mol%), 3.0 equiv NaO2CH, 2.0 equiv TBAI in dioxane at 130 °C.

modest yields, with the major side product resulting from hydrodehalogenation. The authors also demonstrated an alternative method with Pd metal instead of Rh, which provided a higher yield. In both cases, TBAI was an effective additive, as the authors propose that it forms a more active catalyst to engage in oxidative addition. This is a particularly exciting and rare case of the use of an organic, green reductant (formic acid), but it remains to be seen if this success can be translated to other coupling partners.

**3.2.2. XEC of Aryl Halides and Aryl Pseudohalides with Aryl Pseudohalides.** In addition to aryl halides as coupling partners, there have been several reports in the literature to form biaryls using activated phenol derivatives, including tosylates and/or triflates. As phenols constitute a distinct substrate pool from aryl halides,<sup>109</sup> these reactions complement couplings of two different aryl halides.

**3.2.2.1. Ni-Catalyzed Systems.** Xicun Wang, Zhengjun Quan, and co-workers reported on the synthesis of tetrasubstituted pyrimidines using Ni-catalyzed cross-electrophile coupling (**Scheme 25**).<sup>110</sup> The authors noted some

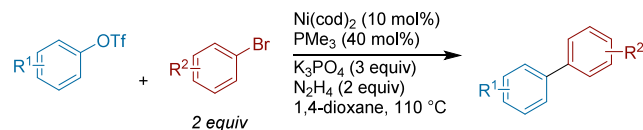
**Scheme 25. Ni-Catalyzed XEC of Aryl Bromides with Pyrimidin-2-yl Tosylates (2017)**



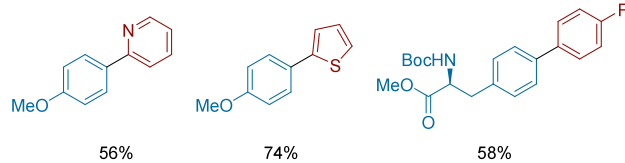
degree of electronic matching was required: lower yields were obtained with pyrimidin-2-yl tosylates bearing electron-donating groups. The authors proposed a sequential oxidative addition mechanism (**Figure 21A**) with initial oxidative addition of the pyrimidine tosylate.

In 2018, Chao-Jun Li and co-workers reported a Ni-catalyzed cross-electrophile coupling of aryl halides with aryl pseudohalides using N2H4 as a mediator.<sup>111</sup> The authors considered the reactivity of N2H4 when examining reaction conditions, concluding that a stronger ligand would be needed to outcompete the hydrazine for binding. Tested bidentate ligands were ineffective, but the small, electron-rich monodentate ligand PMe3 was effective. While coupling was hindered by substituents in the *ortho*-position, groups of varying electronics gave moderate to good yields (**Scheme 26**). Heteroaryl bromides were also well tolerated in this coupling.

**Scheme 26. Ni-Catalyzed XEC of Aryl Halides with Aryl Pseudohalides Using Hydrazine as the Reductant (2018)**



**Selected Examples**

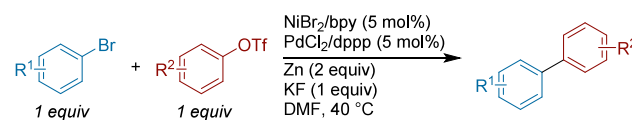


Mechanistic experiments suggested that aryl hydrazines are not intermediates. The authors proposed a sequential oxidative addition mechanism (Figure 21A).

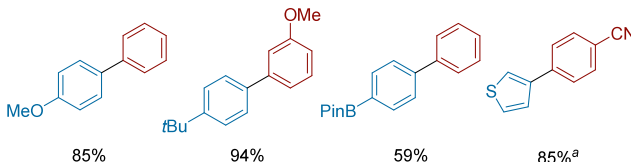
**3.2.2.2. Multimetallic Catalyzed Systems.** A general challenge for monometallic systems is differentiation of the two electrophiles by the same catalyst. In many cases, it is proposed that oxidative addition selectivity can change with oxidation state (Figure 21A), but transmetalation-based mechanisms suffer from lower selectivity (Figure 21B,C). Multimetallic approaches allow the use of two catalysts, one tuned to react with each electrophile, but this approach is less developed.<sup>58</sup>

In 2015, our group disclosed the nickel and palladium multimetallic catalyzed XEC of aryl bromides with aryl triflates.<sup>109</sup> Based upon literature precedents, the palladium catalyst is selective for oxidative addition of the aryl triflate and the nickel catalyst is selective for the aryl bromide. Potassium fluoride was found to further enhance both selectivity and rate. A range of substrates were able to be coupled, including electronically similar and dissimilar aryl bromides and aryl triflates (Scheme 27). The transmetalation mechanism (Figure

**Scheme 27. Nickel and Palladium Multimetallic XEC of Aryl Bromides with Aryl Triflates (2015)<sup>a</sup>**



**Selected Examples**

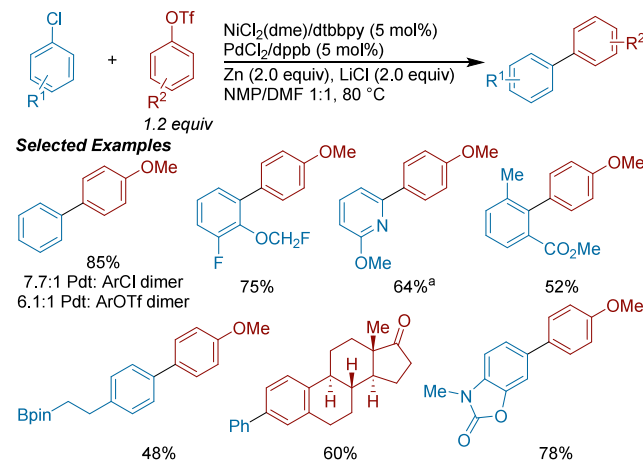


<sup>a</sup>With aryl triflate (3 equiv).

21B) is proposed to be selective because of the differential stability of the two intermediates. This “persistent metal effect” provides selective transmetalation because the (dppp)Pd(Ar)-(X) is stable and unreactive with itself (persistent), but reacts quickly with the (bpy)Ni(Ar) complex.<sup>58</sup> This situation, analogous to the persistent radical effect,<sup>112</sup> can engender high cross-selectivity as long as both oxidative addition steps and reduction steps are fast.

In 2019, our group extended Pd and Ni multimetallic XEC to the coupling of aryl chlorides with aryl triflates (Scheme 28).<sup>113</sup> High selectivity for the product over the homodi-

**Scheme 28. Nickel and Palladium Multimetallic-Catalyzed XEC of Aryl Chlorides with Aryl Triflates (2019)<sup>a</sup>**

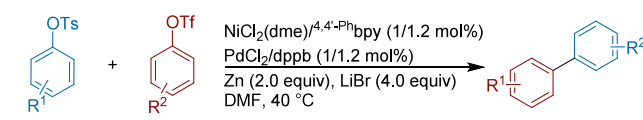


<sup>a</sup>With  $^{6,6'}\text{-Br}\text{bpy}$  (5 mol%).

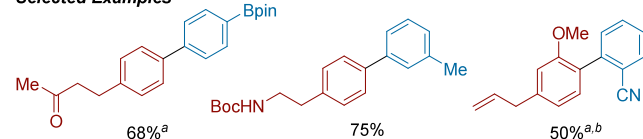
merized side products could be achieved with this method. LiCl proved to be a critical additive, enabling reduction of Ni on the Zn surface. It was observed that  $\text{ZnCl}_2$  and  $\text{Zn}(\text{OTf})_2$  salts inhibited the reduction of  $(\text{L})\text{Ni}^{\text{II}}(\text{X}_2)$  and LiCl could overcome this poisoning effect. Broad chemical diversity was demonstrated, including electron-rich and neutral aryl chlorides as well as sterically hindered di-*ortho*-substituted substrates.

This nickel and palladium system could be further extended to the coupling of two different phenol derivatives: aryl tosylates with aryl triflates (Scheme 29).<sup>20</sup> A series of

**Scheme 29. Nickel and Palladium Multimetallic XEC of Aryl Tosylates with Aryl Triflates (2020)<sup>a</sup>**



**Selected Examples**

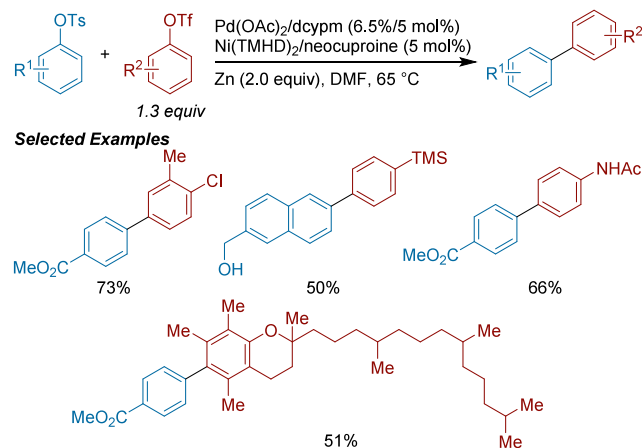


<sup>a</sup>(a) With aryl tosylate (1.5 equiv). (b) At 60 °C.

mechanistic studies established a  $\text{ZnX}_2$ -mediated transmetalation mechanism (Figure 21C) and selective oxidative of tosylate at nickel and triflate at palladium. A wide range of substrates could be coupled, in particular where phenol derivatives are the most convenient arene source (compared to arylmetal reagents).

Concurrently, Kramer and Zhong Lian published a closely related approach to the coupling of aryl tosylates with aryl triflates (Scheme 30).<sup>114</sup> It is exciting to note that the conditions were quite different from those in Scheme 29: the bisphosphine used has a different bite angle and is more

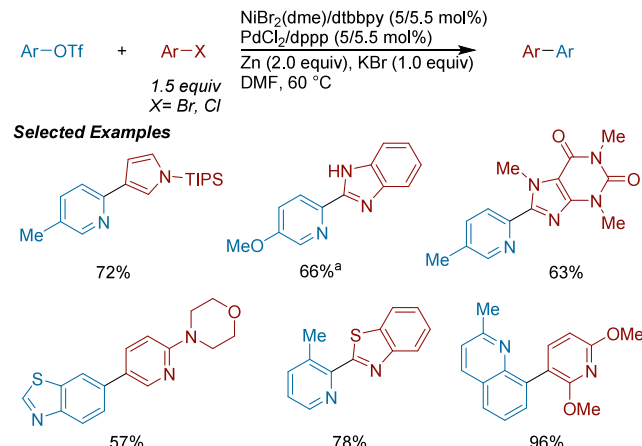
**Scheme 30. Nickel and Palladium Multimetallic XEC of Aryl Tosylates with Aryl Triflates (2020)**



electron-rich, the nitrogen ligand is more sterically hindered, and no additive halide salts were required. The substrate scope is also excellent and includes an extensive number of sterically hindered substrates. Notably, protic substrates were tolerated such as benzyl and aliphatic alcohols, that can be problematic in other nickel and palladium multimetallic systems.

Our group later reported on refined conditions for a general coupling of heteroaryl triflates with heteroaryl bromides and chlorides to form biheteroaryl products (**Scheme 31**).<sup>115</sup>

**Scheme 31. Nickel and Palladium Multimetallic XEC of Heteroaryl Triflates with Heteroaryl Bromides and Chlorides (2021)<sup>a</sup>**

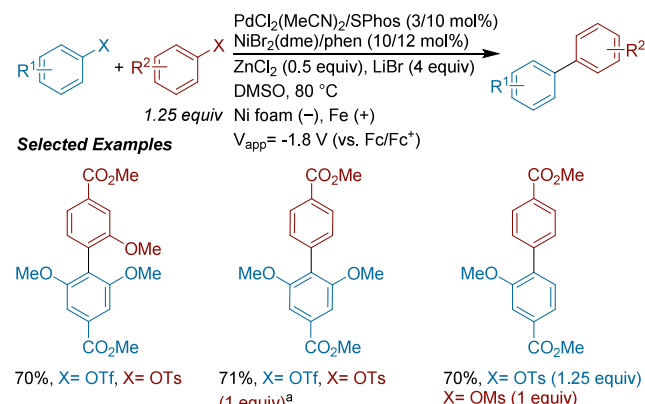


<sup>a</sup>X = Br unless otherwise noted. (a) With X = Cl.

Substrates with varying electronics, sterics, 5-membered, 6-membered, and fused heteroaryl rings were all tolerated in this method. This included the synthesis of biheteroaryl substrates which could strongly coordinate to the catalysts. Furthermore, the chemistry was demonstrated in 96-well plate format and a “toolbox plate” (consisting of various ligands, additives, and reductants) was developed to allow for rapid optimization of difficult substrate combinations.

In 2023, Beckham, Stahl, Weix, and co-workers developed an electrochemical adaptation of the reported multimetallic XEC methods from our group and applied them to the synthesis of lignin-derived plasticizers (**Scheme 32**).<sup>116</sup> Of

**Scheme 32. Synthesis of Lignin-Derived Biaryls by Palladium and Nickel Multimetallic Electrochemical XEC of Two Sulfonate Esters (2023)<sup>a</sup>**

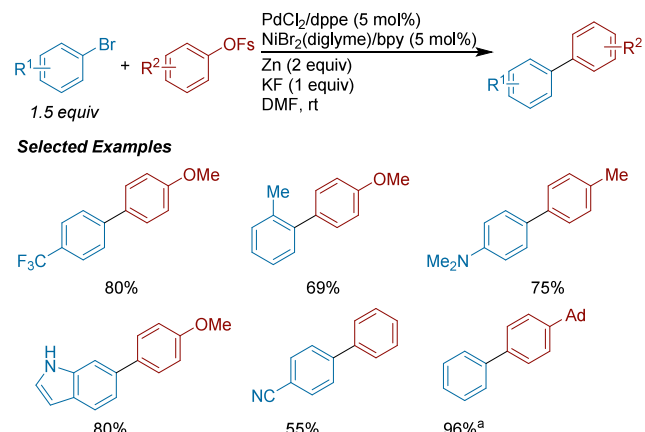


<sup>a</sup>With PdCl<sub>2</sub>(MeCN)<sub>2</sub> (2 mol%).

particular note was the use of chemical reductants in HTE to efficiently find optimal catalyst conditions followed by a relatively easy translation to electrochemical conditions. Also of note is the coupling of an aryl tosylate with an aryl mesylate. These coupling partners are more attractive on scale than triflates but are relatively unreactive. In some examples, synthesized plasticizers exhibited superior properties compared to traditional plasticizers.

Chengrong Ding reported the palladium and nickel multimetallic XEC of aryl bromides with aryl fluorosulfonates (**Scheme 33**).<sup>117</sup> Key to this protocol was the use of both Pd

**Scheme 33. Palladium and Nickel Multimetallic XEC of Aryl Bromides with Aryl Fluorosulfonates (2023)<sup>a</sup>**



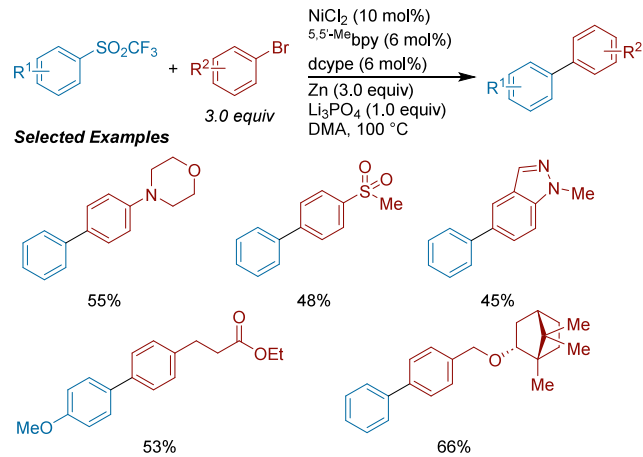
<sup>a</sup>At 40 °C.

and Ni, as yields dramatically decreased under a monometallic system. A transmetalation mechanism similar to other Pd and Ni XEC reactions was proposed. Fluorosulfonates are attractive alternatives to triflates and tosylates because they are easily synthesized on scale with sulfonyl fluoride and are more stable than triflates.

**3.2.3. XEC of Aryl Halides with Other Coupling Partners.** **3.2.3.1. Ni-Catalyzed Systems.** In 2023, Yuanhong Ma and co-workers described a method for the synthesis of biaryls by Ni-catalyzed XEC of aryl trifluoromethyl sulfones with aryl bromides (**Scheme 34**).<sup>118</sup> The combination of

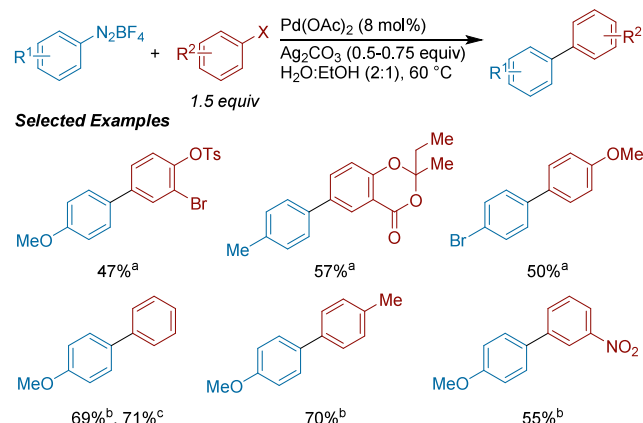
bipyridine and phosphine ligands was necessary for achieving good yields. The authors propose a sequential oxidative addition mechanism (Figure 21A).

**Scheme 34. Synthesis of Biaryls via Ni-Catalyzed XEC Between Aryl Sulfones and Aryl Bromides (2023)**



**3.2.3.2. Pd-Catalyzed Systems.** In 2023, Ranjan Jana demonstrated a Pd-catalyzed XEC of aryl diazonium salts, which are readily made from anilines, with aryl iodide or diaryliodonium salts (Scheme 35).<sup>119</sup> Several notable features

**Scheme 35. Pd-Catalyzed XEC of Aryl Diazonium Salts with Aryl Iodides or Diaryliodonium Salts (2023)<sup>a</sup>**

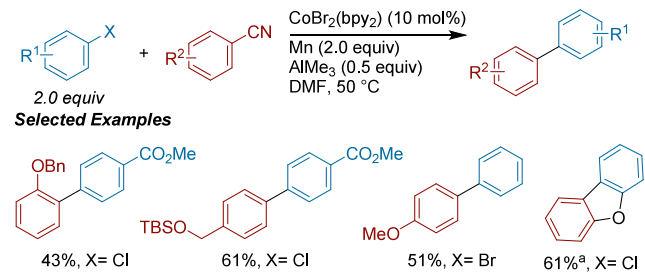


<sup>a</sup>(a) With X= I. (b) With X= I<sup>+</sup>-Mes<sup>-</sup>OTf. (c) With X= I<sup>+</sup>-Ph<sup>-</sup>BF<sub>4</sub>.

of these conditions include the addition of ethanol for activation of Pd(0), and utilizing Ag<sub>2</sub>CO<sub>3</sub> to preserve the catalytic activity of Pd and abstract iodide ions. Chemo-selectivity was high throughout their substrate scope and various diaryliodonium salts could be used.

**3.2.3.3. Cobalt-Catalyzed Systems.** In 2020, Gandon and Gosmini reported a cobalt-catalyzed XEC between benzonitriles and aryl bromides/chlorides to form biaryls (Scheme 36).<sup>120</sup> AlMe<sub>3</sub> was an effective additive for increasing cross-selectivity, presumably by increasing the reactivity of Aryl-CN bonds. Two viable transmetalation mechanisms (Figure 21B) were proposed that started from [Co<sup>0</sup>] or [Co<sup>-1</sup>]. Remarkably, reductive elimination from [(bpy)<sub>2</sub>Co<sup>II</sup>(Ar<sup>1</sup>)(Ar<sup>2</sup>)] ( $\Delta G^\ddagger = 16.4$  kcal/mol) was easier than from [(bpy)<sub>2</sub>Co<sup>III</sup>(Ar<sup>1</sup>)(Ar<sup>2</sup>)]<sup>+</sup> ( $\Delta G^\ddagger = 23.7$  kcal/mol). This unexpected result could perhaps

**Scheme 36. Cobalt-Catalyzed XEC of Benzonitriles with Aryl Halides (2020)<sup>a</sup>**

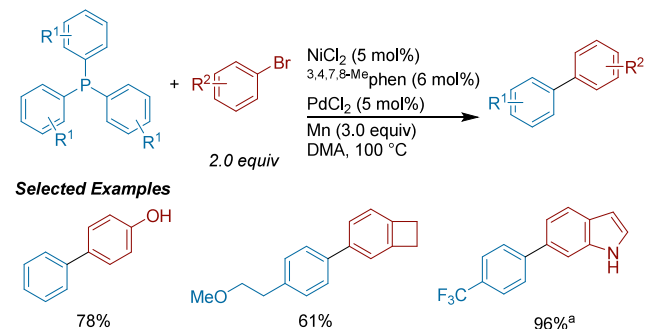


<sup>a</sup>Intramolecular reaction.

be understood by the Co<sup>II</sup> complex being formally 19-electron vs 18-electron for the Co<sup>III</sup> complex.

**3.2.3.4. Multimetallic Catalyzed Systems.** Yuanhong Ma and co-workers reported the Ni and Pd multimetallic XEC of triarylphosphines (symmetric and nonsymmetric) with aryl bromides to form biaryls (Scheme 37).<sup>121</sup> The conditions

**Scheme 37. Pd and Ni Multimetallic Catalyzed XEC of Triarylphosphines with Aryl Bromides (2022)<sup>a</sup>**



<sup>a</sup>With diphenyl(4-(trifluoromethyl)phenyl)phosphane.

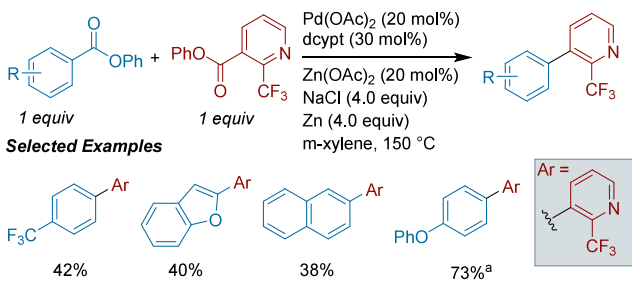
tolerated free -NH<sub>2</sub> and -OH groups, which is not always the case for other examples of this system. The authors optimized against a variety of challenges relevant to this uncommon class of electrophiles, including strong coordination of the triarylphosphines to metals and steric hindrance. The authors propose a sequential oxidative addition mechanism (Figure 21A) via a key tetraarylphosphonium intermediate, rather than the usual transmetalation mechanism invoked for reactions catalyzed by this system.

**3.2.4. XEC of Aryl Carboxylic Acid Esters, Aryl Ethers, and Anilines.** Aryl carboxylic acids and anilines are both attractive substrate pools that complement phenols and aryl halides but are rarely utilized in XEC reactions. While phenols are often coupled via sulfonate esters (vide supra), aryl ethers are attractive because they are very stable and atom economic (for methyl ethers). The following section addresses reactions of these useful, but unreactive, substrates.

**3.2.4.1. Pd-Catalyzed Systems.** In 2022, Junichiro Yamaguchi published a Pd-catalyzed doubly decarbonylative XEC of aryl esters to form unsymmetrical biaryls (Scheme 38).<sup>122</sup> Interestingly, this method resulted in higher yields when utilizing *m*-xylene as solvent, compared to amide-based solvents more commonly used in XEC reactions, such as DMF.

**3.2.4.2. Cr-Catalyzed Systems.** Several methods using chromium catalysis for XEC have been reported by Xiaoming

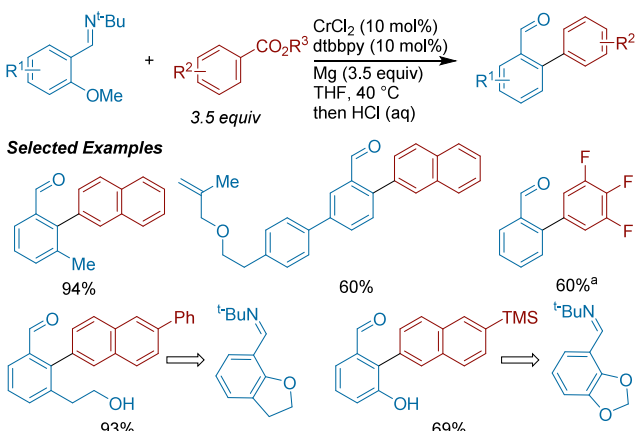
**Scheme 38. Pd-Catalyzed XEC of Aryl Esters (2022)<sup>a</sup>**



<sup>a</sup>With 1.5 eq of Ar.

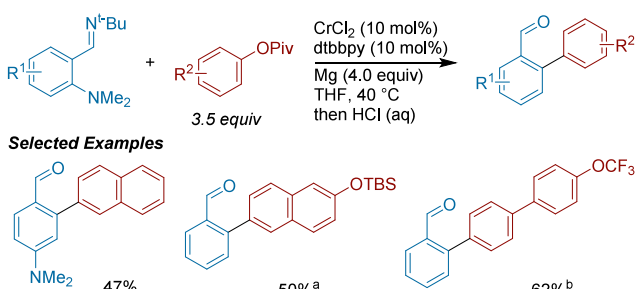
Zeng<sup>123,124</sup> and co-workers (Schemes 39 and 40) and most recently by Xiaoming Zeng and Meiming Luo<sup>125</sup> (Scheme 41)

**Scheme 39.** Cr-Catalyzed XEC of Aryl Ethers with Aryl Esters (2020)<sup>a</sup>



<sup>a</sup>R<sup>3</sup> = t-Bu unless otherwise noted. (a) With R<sup>3</sup> = 1-Ad, CrCl<sub>2</sub>/dtbbpy (5 mol%) at 60 °C.

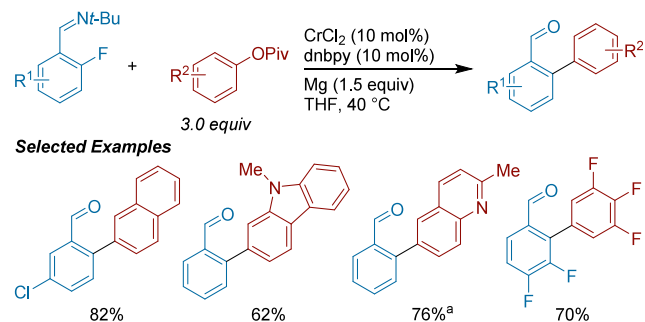
**Scheme 40. Cr-Catalyzed XEC of Aryl Amines with Aryl Esters (2020)<sup>a</sup>**



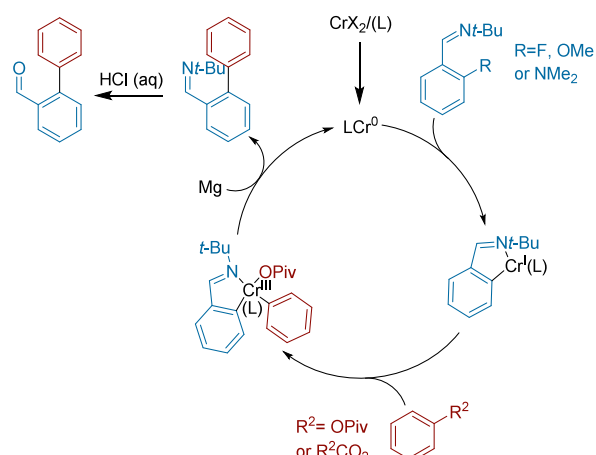
<sup>a</sup>(a) With CO<sub>2</sub>t-Bu coupling partner. (b) With CO<sub>2</sub>Ad coupling partner.

for unactivated aryl C–N, C–O, and C–F bonds coupled with aryl esters via decarbonylation ([Scheme 40](#)) or Aryl–OPiv oxidative addition ([Scheme 40](#) and [41](#)). Several mechanistic studies were conducted to tentatively rule out arylmagnesium species, and the authors prefer a sequential oxidative addition mechanism ([Figure 21A](#) and [Scheme 41](#)). Selective coupling of these typically inert aryl–X bonds is enabled by the imine directing group (as in directed C–H activation).

**Scheme 41.** Cr-Catalyzed XEC of Aryl Fluorides with Aryl Esters (2022)<sup>a</sup>



### ***Proposed Mechanism***



<sup>a</sup>With adamantyl ester coupling partner, CrCl<sub>2</sub>/dnbpy (20 mol%), at 60 °C.

### 3.3. Vinyl Arenes

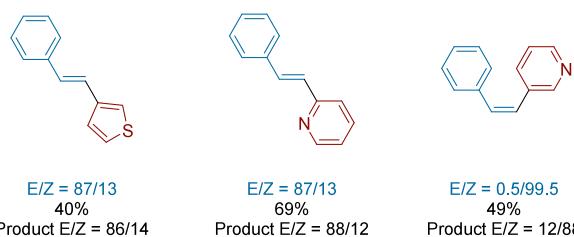
### 3.3.1 XEC of Vinyl Halides with Aryl Halides

**3.3.1.1. *Ni-Catalyzed Systems.*** In 2000, Condon and Durandetti reported the electrochemical Ni-catalyzed cross-electrophile coupling of vinyl bromides with heteroaryl bromides.<sup>126</sup> The coupling was investigated using bromostyrene and 2- and 3-halopyridines and thiophenes (**Scheme 42**). The authors found that 2-bromoheteroarenes resulted in higher yields than 3-bromoheteroarenes, and that (*E*)- $\beta$ -bromostyrene dimerizes more quickly than (*Z*)- $\beta$ -bromostyrene.

**Scheme 42.** Ni-Catalyzed Electrochemical XEC of Vinyl Bromides with Heteroaryl Bromides (2000)



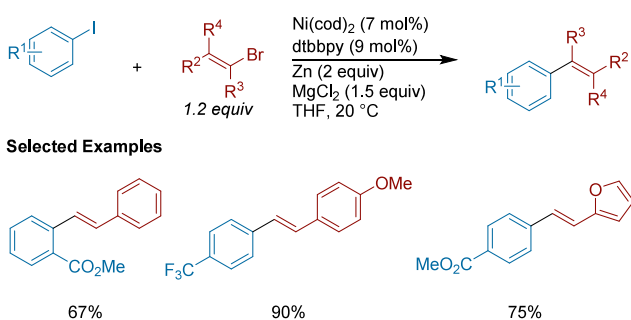
### ***Selected Examples***



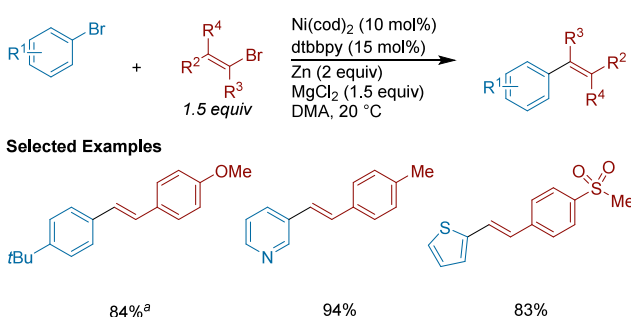
ene. The coupling of bromothiophenes with bromostyrene was found to be more stereoselective than the same coupling with bromopyridines.

Qinghua Ren, Xinghua Zhang, and Hegui Gong reported a Ni-catalyzed cross-electrophile coupling of aryl iodides with vinyl bromides.<sup>127</sup> In control experiments, the (*E*)-vinyl bromide coupled successfully, but the (*Z*)-vinyl bromide failed to couple with aryl halides. The authors developed three sets of conditions depending on substituent identity. Aryl iodides containing neutral or electron-withdrawing groups required the conditions shown in Scheme 43. A second set of conditions (Scheme 44) was tailored for coupling aryl bromides with styryl bromides.

**Scheme 43. Ni-Catalyzed Cross-Electrophile Coupling of Electron-Poor Aryl Iodides with Vinyl Bromides (2016)**



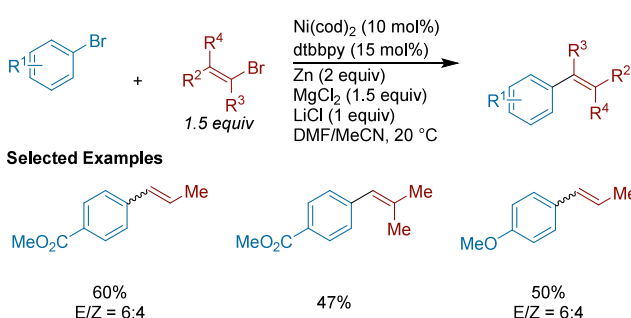
**Scheme 44. Ni-Catalyzed XEC of Electron-Rich Aryl Bromides with Vinyl Bromides (2016<sup>a</sup>)**



<sup>a</sup>With KF (1 equiv).

Finally, conditions to couple aryl bromides with alkyl-substituted vinyl bromides were developed (Scheme 45). Aryl bromides with both electron-poor and electron-rich groups

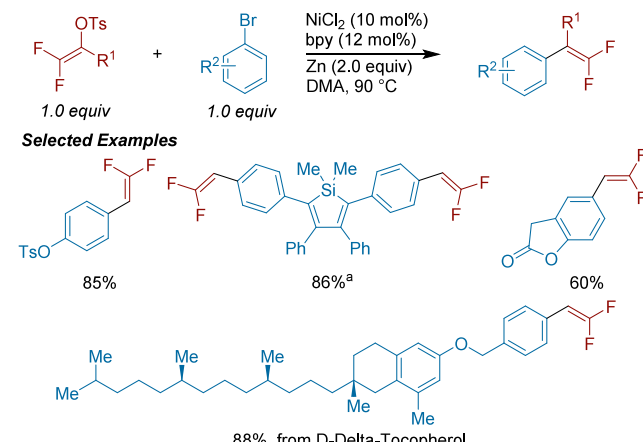
**Scheme 45. Ni-Catalyzed Cross-Electrophile Coupling of Aryl Bromides with Alkyl Functionalized Vinyl Bromides (2016)**



were tolerated. Some products maintained their double bond configuration, but others yielded a mixture of the *E*- and *Z*-isomers. The authors propose a sequential oxidative addition mechanism (Figure 21A).

Kramer, Gui-Juan Cheng, and Zhong Lian developed a Ni-catalyzed XEC of aryl bromides with *gem*-difluorovinyl tosylates (Scheme 46).<sup>128</sup> A variety of aryl bromides were

**Scheme 46. Ni-Catalyzed XEC of Aryl Bromides with Vinyl Tosylates (2020)<sup>a</sup>**



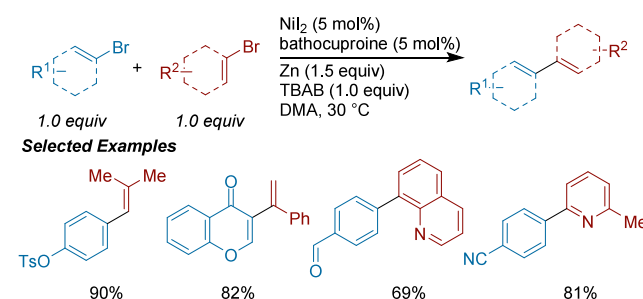
<sup>a</sup>with vinyl tosylate (4 equiv), NiCl<sub>2</sub> (20 mol%), bipy (24 mol%), and Zn (4 equiv).

utilized. These include interesting applications in ligand synthesis, late-stage modification of drug-like small molecules, and material science (i.e., derivatization of tetraphenylsiloles). While coupling of 2-substituted-1,1-difluorovinyl tosylates with aryl bromides was unsuccessful, the authors demonstrated a proof-of-concept for XEC of an aryl iodide with *gem*-difluorovinyl tosylate. Based on mechanistic studies, kinetic experiments, and DFT calculations the authors proposed two possible mechanisms involving Ni(0)/Ni(II) species (Figure 21B,C).

Yuqiang Li and Guoyin Yin examined the synthesis of alkenylarenes and biaryls from aryl bromides and vinyl bromides/iodides (Scheme 47).<sup>129</sup> Bathocuproine was superior to other ligands tested. Despite the equimolar substrate ratios, in some cases high yields could be obtained.

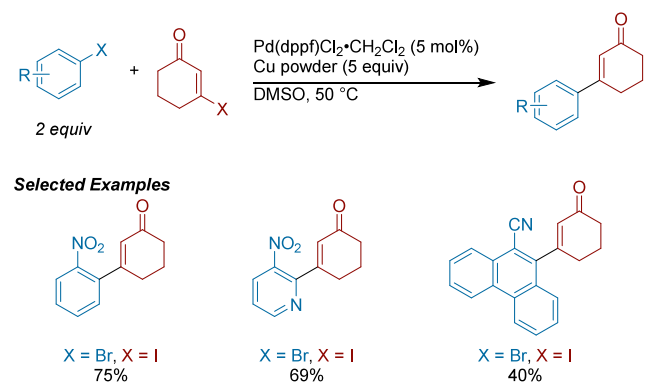
**3.3.1.2. Pd-Catalyzed Systems.** As an expansion upon their previous work,<sup>130</sup> Banwell and co-workers reported the Pd-catalyzed XEC of  $\beta$ -iodoenones with aryl halides (Scheme 48).<sup>131</sup> The aryl scope was focused on activated substrates.

**Scheme 47. Ni-Catalyzed XEC of Aryl Bromides with Vinyl Bromides and Other Aryl Bromides (2021)**



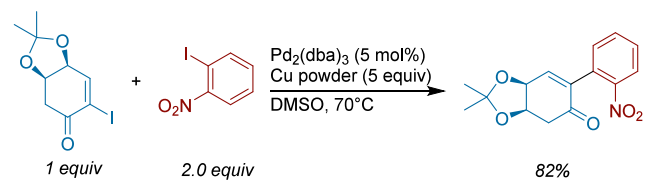
The copper reductant does not reduce the sensitive nitro group, which is not tolerated with stronger reductants.

**Scheme 48. Pd-Catalyzed XEC of  $\beta$ -Iodoenones with Aryl Halides (2018)**



In 2022 Banwell and White described a practical and operationally straightforward synthesis of enantiopure building blocks derived from quinic acid (Scheme 49).<sup>132</sup> An important

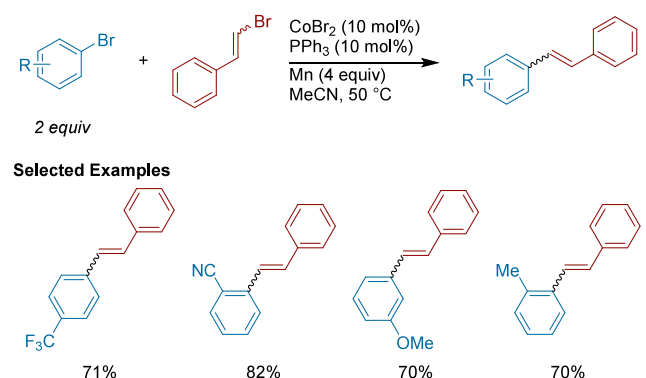
**Scheme 49. Multigram-Scale XEC of  $\alpha$ -Iodoenone With  $\alpha$ -Iodonitrobenzene (2022)**



step was the XEC of  $\alpha$ -iodoenone with  $\alpha$ -iodonitrobenzene, which was conducted on a multigram-scale to deliver the product in high yield. This intermediate was then cyclized upon treatment with  $\text{PtO}_2$  and  $\text{H}_2$  to afford the enantiopure tetrahydrocarbazole.

**3.3.1.3. Cobalt-Catalyzed Systems.** Gosmini and co-workers reported a cobalt-catalyzed XEC of aryl halides with  $\beta$ -bromostyrenes (Scheme 50).<sup>133</sup> Control experiments showed that slow addition of the bromostyrene allowed for fewer equivalents to be used by slowing down dimerization of the more reactive coupling partner. Aryl bromides bearing electron-withdrawing and electron-donating groups were well

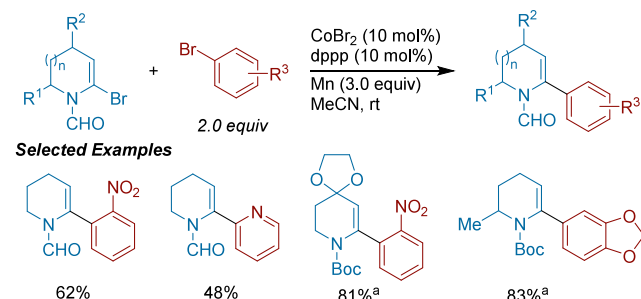
**Scheme 50. Cobalt-Catalyzed XEC of Aryl Halides with  $\beta$ -Bromostyrenes (2012)**



tolerated, and *ortho*-substituted aryl halides gave good yields. Supported by DFT calculations, the authors proposed a sequential oxidative addition mechanism (Figure 21A).

Beng and co-workers detailed a cobalt-catalyzed XEC of  $\alpha$ -bromo eneformamides and enecarbamates with aryl bromides (Scheme 51).<sup>134</sup> Several alkenyl bromides, in place of aryl

**Scheme 51. Cobalt-Catalyzed XEC of  $\alpha$ -Bromo Eneformamides and Enecarbamates with Aryl Bromides (2015)<sup>a</sup>**

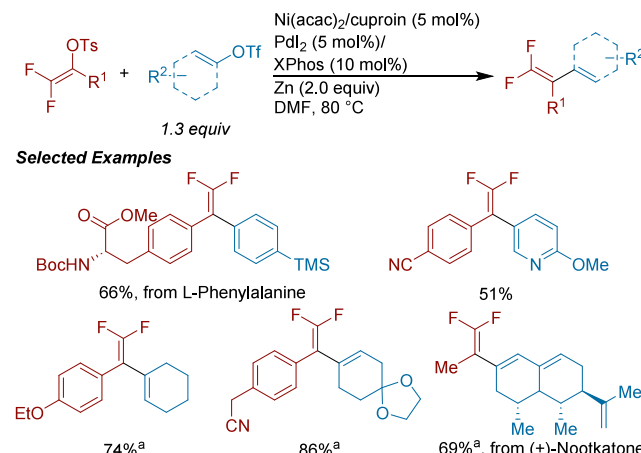


<sup>a</sup>At 40 °C.

bromides, were also successfully utilized in the coupling. The authors further derivatized the coupled products to access functionalized piperidines and azepanes.

**3.3.1.4. Multimetallic Catalyzed Systems.** Xuemei Zhang, Zhong Lian, and co-workers reported a multimetallic XEC with Pd and Ni for the synthesis of *gem*-difluoroalkenes (Scheme 52).<sup>135</sup> Both aryl and vinyl triflates could be coupled

**Scheme 52. Palladium- and Ni-Catalyzed XEC of Vinyl Tosylates with Aryl and Vinyl Triflates (2022)<sup>a</sup>**



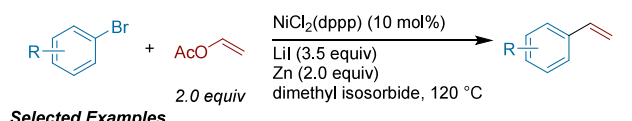
<sup>a</sup>with dcypm (5 mol%) at 65 °C.

with vinyl tosylates. Unlike in their previous work,<sup>128</sup> a wide variety of 2-substituted 1,1-difluorovinyl tosylates could be used. Supported by mechanistic experiments, the authors proposed a  $\text{ZnX}_2$ -mediated transmetalation mechanism (Figure 21C).

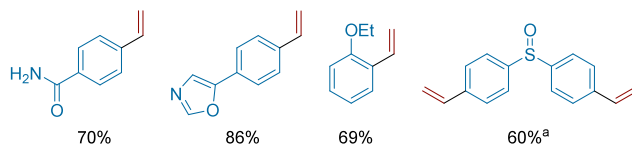
### 3.3.2. XEC of Aryl Halides with Vinyl Acetates.

**3.3.2.1. Ni-Catalyzed Systems.** Chuanhu Lei and Jian Jin reported the XEC of aryl bromides with vinyl acetate (Scheme 53).<sup>136</sup> Dimethyl isosorbide, a more sustainable solvent derived from glucose biomass, could be used instead of less-favorable amide solvents. Although substituted alkenyl acetates

**Scheme 53. Ni-Catalyzed XEC Between Aryl Bromides with Vinyl Acetate (2022)<sup>a</sup>**



**Selected Examples**

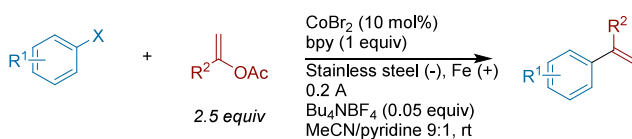


<sup>a</sup>With vinyl acetate (10 equiv) and zinc (4 equiv).

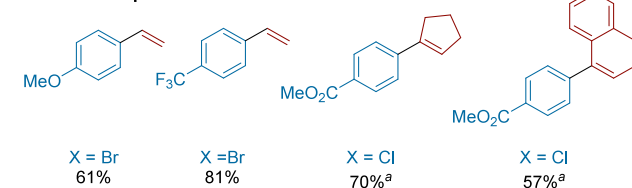
could not be used, the scope of heteroaryl and aryl bromides was broad.

**3.3.2.2. Cobalt-Catalyzed Systems.** Gosmini and co-workers reported a cobalt-catalyzed electrochemical XEC of aryl halides with vinylic acetates to form styrene derivatives (Scheme 54).<sup>137</sup> Notably, one equivalent of 2,2'-bipyridine

**Scheme 54. Cobalt-Catalyzed Electrochemical XEC of Aryl Halides with Alkenyl Acetates (2003)<sup>a</sup>**



**Selected Examples**



<sup>a</sup>With CoBr<sub>2</sub> (20 mol%).

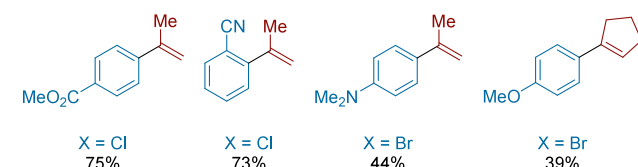
(bpy) was required for yields greater than 15%. Without the ligand, the reduced product dominated because the generated Fe(II) ions competitively complexed with the cobalt. Good yields were achieved using aryl chlorides and aryl bromides with substituents with varied electronics, but *ortho*-substituted aryl halides resulted in poor yields.

Gosmini and co-workers were also able to achieve the XEC of aryl halides with vinylic acetates using a metal reductant instead of electrochemistry with a sacrificial anode (Scheme 55).<sup>138</sup> Manganese was shown to be the only metal to give good yields. However, trifluoroacetic acid (TFA) was needed to activate its surface. Zinc could reduce the cobalt complex to yield the organozinc chloride byproduct but did not result in the coupled product. The use of aryl chlorides was reported, but an electron-withdrawing group is necessary for reaction with the reduced cobalt species. Substitutions in the *para*-, *meta*-, and *ortho*- positions are tolerated, but large substituents in the *ortho*- positions shut down reactivity regardless of the halide identity.

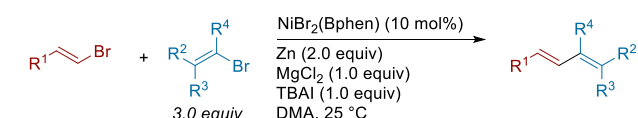
### 3.4. Synthesis of 1,3-Dienes

**3.4.1. Coupling of Vinyl Halides with Vinyl Halides and Pseudo Halides.** **3.4.1.1. Ni-Catalyzed Systems.** Da Wu and Hegui Gong reported a Ni-catalyzed XEC of vinyl bromides for the synthesis of 1,3-dienes (Scheme 56).<sup>139</sup> The

**Scheme 55. Cobalt-Catalyzed XEC of Aryl Halides with Alkenyl Acetates (2005)**



**Scheme 56. Ni-Catalyzed XEC of Vinyl Bromides to Form 1,3-Dienes (2021)<sup>a</sup>**



**Selected Examples**



<sup>a</sup>with 1 equiv LiCl, no TBAI. PMP = *p*-methoxyphenyl.

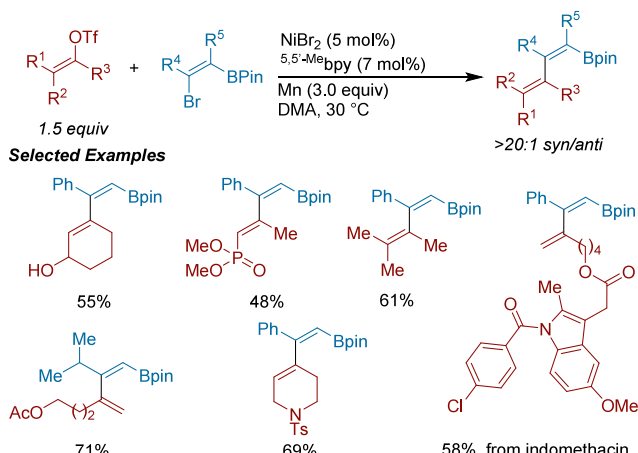
authors propose the beneficial effects of the MgCl<sub>2</sub> and TBAI may be due to activating the Zn surface. MgCl<sub>2</sub> may also promote halide exchange to form vinylnickel(II) intermediates and TBAI may act to solubilize salts in the mixture. A breadth of compounds could be made, including 2,4-disubstituted dienes. The method was also applied to the total synthesis of solanone. However, more sterically hindered vinyl bromides such as 2-bromo-3-methylbut-2-ene and 1-bromo-2-methylprop-1-ene could not be coupled.

Xing-Zhong Shu reported a Ni-catalyzed XEC of  $\beta$ -bromovinylboronates with vinyl triflates to form 1,3-dienylboronate esters with good stereocontrol (Scheme 57).<sup>140</sup> Varying levels of substitution on the diene, as well as acyclic and cyclic dienes, could be synthesized. However, fully substituted  $\beta$ -bromovinylboronates lead to lower or no product formation.

Dayong Shi and co-workers reported the synthesis of monofluoro 1,3-dienes by XEC between *gem*-difluoroalkenes and alkenyl electrophiles (Scheme 58).<sup>141</sup> The use of MgCl<sub>2</sub>, YbCl<sub>3</sub>, and TMSCl were suggested to activate the surface of Mn and/or undergo halide or anionic ligand exchange on Ni. The proposed mechanism involves oxidative addition of the vinyl triflate, migratory insertion of the *gem*-difluoroalkene, and  $\beta$ -F elimination to form product. Beyond a host of vinyl triflates used, the authors also demonstrated that aryl triflates, bromides, and iodides as well as vinyl tosylates, chlorides, bromides, and iodides could be utilized.

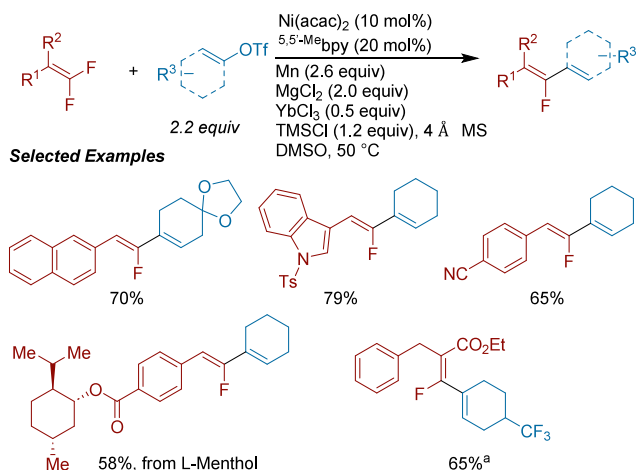
**3.4.1.2. Cobalt-Catalyzed Systems.** Beng and co-workers reported a method for the synthesis of azepines and benzotropones by a cobalt-catalyzed XEC of  $\alpha$ -bromo enones with  $\alpha$ -bromo enamides (Scheme 59).<sup>142</sup> In addition to tropone-type coupling partners, dibromonaphthoquinone, bromostyrenes, and bromoarenes were also good substrates for

**Scheme 57. Ni-Catalyzed Synthesis of Dienylboronates from the XEC of Vinyl Electrophiles (2022)<sup>a</sup>**



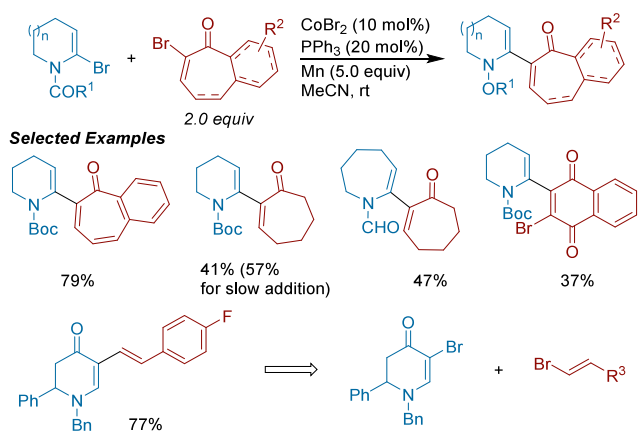
<sup>a</sup>The syn/anti configuration is defined as the Bpin group syn/anti to the alkene from the alkenyl triflate coupling partner.

**Scheme 58. Synthesis of Monofluoro 1,3-dienes via XEC of gem-Difluoroalkenes with Alkenyl Triflates (2023)<sup>a</sup>**



<sup>a</sup>With vinyl triflate (1.5 equiv), Mn (2.0 equiv), 4,4'-Me2bpy, at 30 °C.

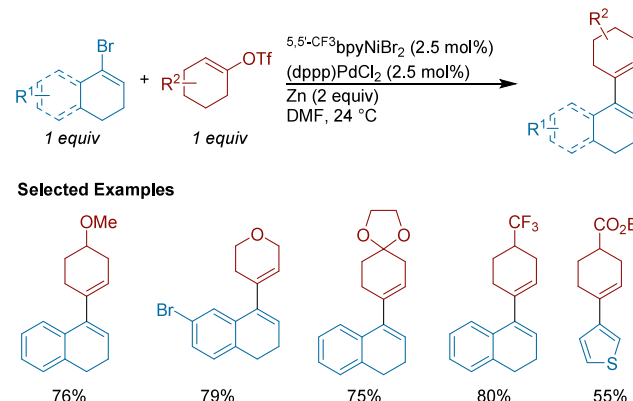
**Scheme 59. Cobalt-Catalyzed XEC of  $\alpha$ -Bromo Enones with  $\alpha$ -Bromo Enamides (2015)**



this method. The authors demonstrated further elaboration of the coupled products to access densely functionalized azaheterocycles.

**3.4.1.3. Multimetallic Catalyzed Systems.** In 2018, our group reported the Ni and Pd multimetallic catalyzed XEC of vinyl bromides with vinyl triflates to form substituted 1,3-dienes (Scheme 60).<sup>143</sup> Our studies showed that the bipyridine

**Scheme 60. Nickel and Palladium Multimetallic Catalyzed XEC of Vinyl Bromides with Vinyl Triflates (2018)**

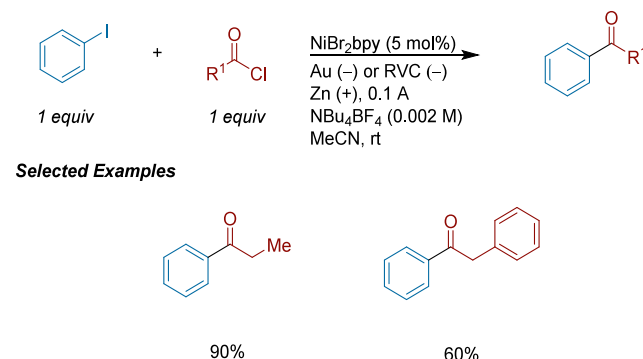


ligand influenced selectivity but the phosphine ligand did not, and higher temperatures resulted in lower selectivity. Control experiments revealed that a zinc-mediated transfer of the vinyl bromide from nickel to palladium is a key step in the reaction, and a transient vinylzinc intermediate is formed, but does not accumulate under standard conditions. Sterically hindered vinyl halides resulted in lower yields.

### 3.5. Ketones

**3.5.1. XEC with Acid Halides.** **3.5.1.1. Ni-Catalyzed Systems.** Nédélec, Périchon, and co-workers reported an electrochemical synthesis of ketones through Ni-catalyzed XEC of aryl iodides with acid chlorides (Scheme 61).<sup>144</sup> The

**Scheme 61. Ni-Catalyzed Electrochemical XEC of Acid Chlorides with Aryl Iodides (1989)**

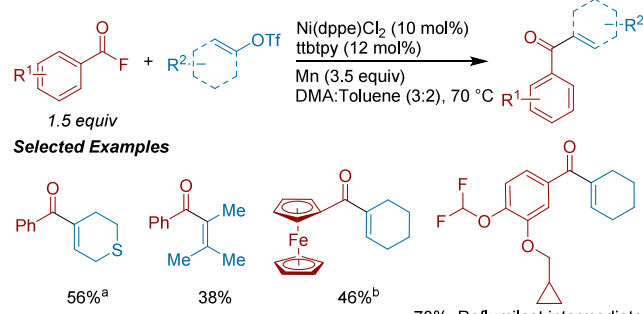


anodic material was found to be important, with a magnesium anode only yielding ketone when a five-time excess of acid chloride was used. Furthermore, reduction of the product is seen with the magnesium anode. However, the optimal zinc anode results in high Faradaic and chemical yields when a one-to-one ratio of starting materials is employed.

Xing-Zhong Shu and co-workers reported the synthesis of enones from Ni-catalyzed XEC of vinyl triflates with acid

fluorides (Scheme 62).<sup>145</sup> Acid fluorides were advantageous in this system, and other acyl electrophiles such as acyl chlorides

**Scheme 62. Synthesis of Enones by Ni-Catalyzed XEC of Vinyl Triflates with Acid Fluorides (2019)<sup>a</sup>**

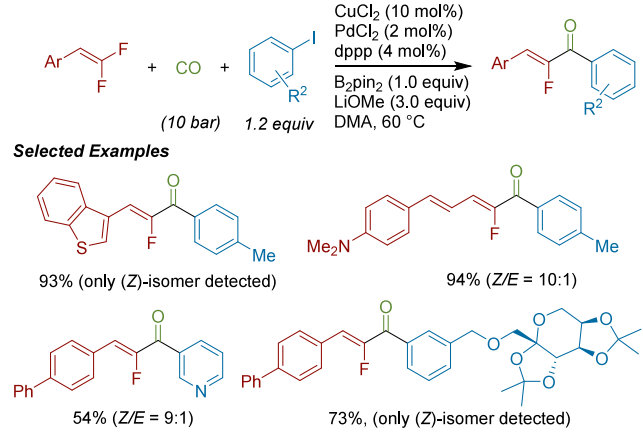


<sup>a</sup>(a) At 50 °C. (b) With tpy (15 mol%).

gave little to no yield of desired product. A variety of substrates were compatible, but only trace product was observed for 1,2-disubstituted, 1-substituted, or 2-substituted vinyl triflates. The authors propose a double oxidative addition mechanism (Figure 21A), but did not rule out a radical chain mechanism.

**3.5.2. Carbonylative XEC to Form Ketones.** **3.5.2.1. Multimetallic Catalyzed Systems.** Xiao-Feng Wu and co-workers reported a Pd and Cu multimetallic carbonylative XEC of *gem*-difluoroalkenes with aryl iodides that exhibits excellent Z-selectivity (Scheme 63).<sup>146</sup> Instead of a

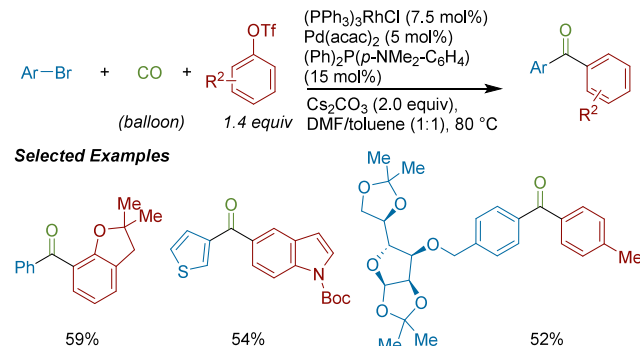
**Scheme 63. Palladium and Copper Catalyzed Carbonylative XEC of *gem*-Difluoroalkenes with Aryl Iodides (2021)**



metallic reductant, this approach uses bis(pinacolato) diborane ( $B_2Pin_2$ ) with LiOMe, a system introduced by Hegui Gong for XEC.<sup>52</sup> Alternative aryl electrophiles such as aryl bromides, aryl triflates, and aliphatic *gem*-difluoroalkenes were not good coupling partners. However, a broad range of  $\alpha$ -fluorochalcones could be synthesized (and further derivatized). While the (Z)-fluorinated vinylboronate ester, derived from the  $B_2Pin_2$  reductant, was a side product of the reaction, several control studies lead the authors to believe they are not intermediates in the cross-coupling reaction. The authors propose a dual catalytic cycle in which the Pd performs all of the bond-breaking and forming steps while copper activates the  $B_2Pin_2$  to enable turnover of the Pd.

Kramer, Gui-Juan Cheng, and Zhong Lian disclosed a multimetallic Pd and Rh catalyzed carbonylative XEC of aryl bromides with aryl triflates to form a wide range of diaryl ketones (Scheme 64).<sup>147</sup> Intriguingly, carbon monoxide serves

**Scheme 64. Palladium and Rhodium Multimetallic Catalyzed Carbonylative XEC of Aryl Bromides with Aryl Triflates (2022)**



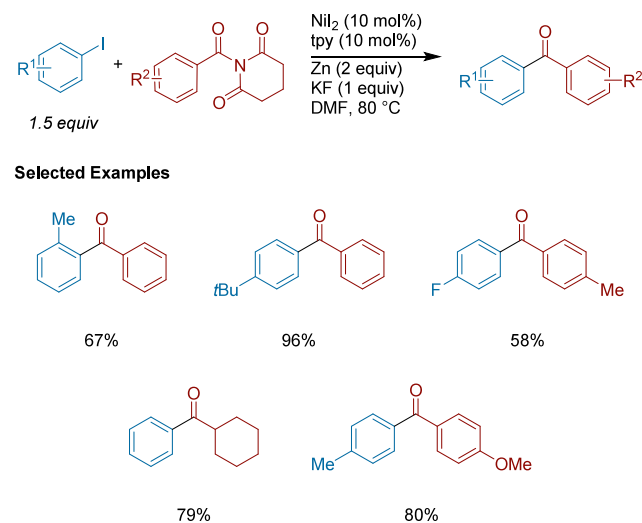
as both the reductant and carbonyl source, removing the need for a stoichiometric metal reductant. Evidence for CO as the reductant was shown by conducting isotope-labeling experiments and DFT calculations. The authors propose a mechanism in which Pd activates both aryl electrophiles and Rh mediates transmetalation and carbonylation steps. Mechanistic data showed that the reaction is first order in [ArBr] and [Pd(acac)<sub>2</sub>], zero-order in [ArOTf] and [(PPh<sub>3</sub>)<sub>3</sub>RhCl], and that oxidative addition is the rate-limiting step.

### 3.5.3. XEC of Aryl Halides with Other Activated Acids.

**3.5.3.1. Ni-Catalyzed Systems.** Jianlin Han and co-workers developed a Ni-catalyzed cross-electrophile coupling of aryl iodides with *N*-benzoyl glutarimides to form unsymmetrical diaryl ketones (Scheme 65).<sup>148</sup> Substitution on the aryl iodide included both electron-donating and -withdrawing groups, but the activated benzoic acids only contained electron donating or neutral groups.

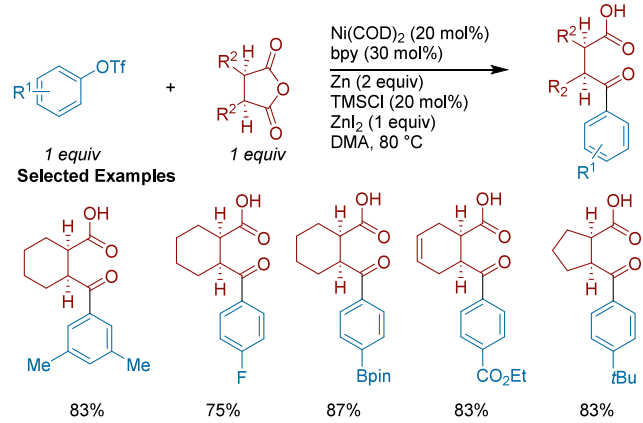
Jianyou Mao and Patrick Walsh reported the XEC of cyclic meso-anhydrides with aryl triflates to form  $\gamma$ -keto acids

**Scheme 65. Ni-Catalyzed XEC of Aryl Iodides With *N*-Benzoyl Glutarimides (2017)**



(Scheme 66).<sup>149</sup> Optimization experiments revealed that a higher catalyst loading (20 mol%) resulted in a large increase

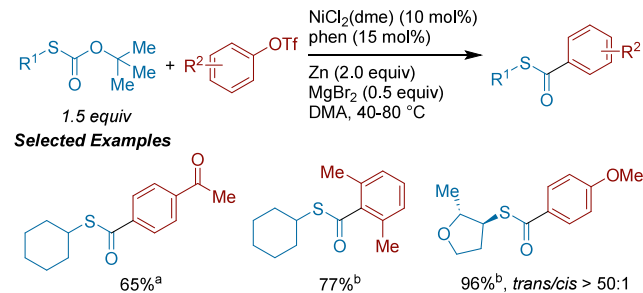
**Scheme 66. Ni-Catalyzed XEC of Aryl Triflates with Cyclic Meso-Anhydrides (2018)**



in yield. The scope of aryl triflates tolerated in this coupling included those with electron-donating and electron-withdrawing groups. Sterically hindered aryl triflates also gave good yields.

Weichao Xue and Hegui Gong published a method for the synthesis of thioesters via XEC of aryl triflates with *S*-alkyl thiocarbonates (Scheme 67).<sup>150</sup> Electron-poor aryl triflates

**Scheme 67. Synthesis of *S*-alkyl Aroyl Thioesters by XEC of Aryl Triflates with *S*-Alkyl O-*tert*-butyl Thiocarbonates (2021)<sup>a</sup>**

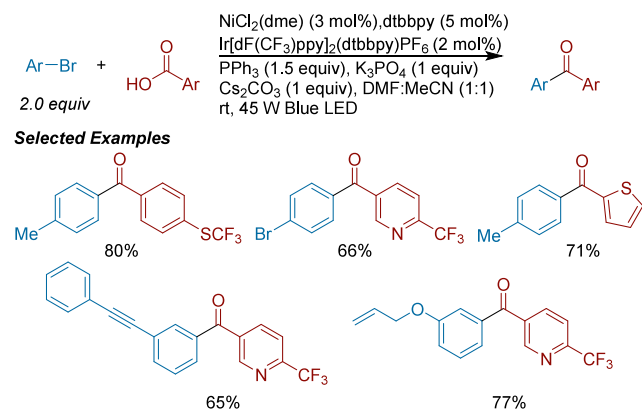


<sup>a</sup>(a) At 40 °C. (b) At 80 °C and *n*-Bu4NCl (2.0 equiv).

worked well, and slight modification of the conditions such as increased temperature and addition of tetrabutylammonium chloride, provided access to electron-rich and -neutral aryl triflates. The authors suggest sequential oxidative addition (Figure 21A) for the mechanism and ruled out a radical pathway.

Jin Xie and co-workers reported the XEC of aryl bromides with aryl carboxylic acids by dual Ni and Ir catalysis (Scheme 68).<sup>151</sup> Alkyl bromides could also be used as substrates (not shown here). In this system, triphenylphosphine is the terminal reductant/activating agent for the carboxylic acid. It is proposed to be oxidized and react with the carboxylic acid to generate a phosphoranyl radical intermediate. This species can undergo homolysis to form an acyl radical and triphenylphosphine oxide. The acyl radical is proposed to react with an arynickel(II) intermediate to generate the product. The authors demonstrate a broad scope, particularly for substrates which have functional groups incompatible with

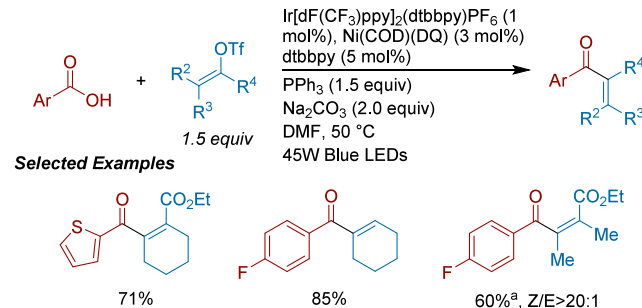
**Scheme 68. Nickel and Iridium Photochemical XEC of Benzoic Acids with Aryl Bromides to Form Diaryl Ketones (2020)**



the traditional Weinreb ketone synthesis such as aldehydes, esters, and ketones.

Jin Xie and co-workers, in collaboration with Chengjian Zhu and Xiao-Song Xue, later disclosed a method under modified conditions from their previous report for the synthesis of tetrasubstituted alkenes (Scheme 69).<sup>152</sup> Interestingly, the

**Scheme 69. Synthesis of  $\alpha,\beta$ -Unsaturated Ketones by Nickel and Iridium Photochemical XEC of Carboxylic Acids with Vinyl Triflates (2022)<sup>a</sup>**



<sup>a</sup>With [Ir] (2 mol%), [Ni] (6 mol%), and Cs2CO3 (1.5 equiv) at rt.

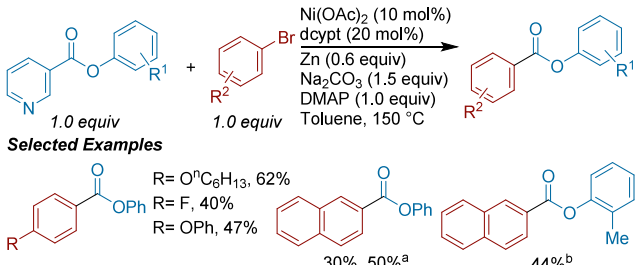
reaction could be run under air using Ni(COD)(duroquinone (DQ)) as the nickel precatalyst. The authors propose that this method is mechanistically similar to their previous report. Furthermore, DFT calculations support the authors claims of a Ni(0)/Ni(II)/Ni(III) mechanistic cycle.

### 3.6. C–C Bond Activation XEC

Junichiro Yamaguchi described the synthesis of aryl esters by Ni-catalyzed XEC between *O*-aryl nicotinic acid (as a *O*-aryl formyl source) and aryl bromides (Scheme 70).<sup>153</sup> The authors propose a transmetalation mechanism (Figure 21B) with C–CO<sub>2</sub>Ar bond activation. A variety of electrophiles could be utilized in the reaction, including aryl bromides, aryl chlorides, aryl pivalates, aryl carbamates, and arenols. Aryl iodides were less suitable for the reaction.

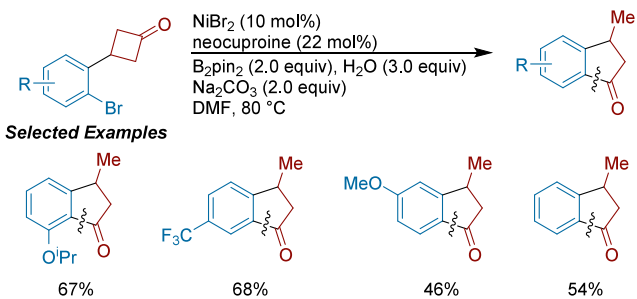
Peilin Han, Jinbo Zhao, and Yu Liu report a ring-expansion cross-electrophile coupling of cyclobutanones to form indanones (Scheme 71).<sup>154</sup> Interestingly, B<sub>2</sub>pin<sub>2</sub> and base (presumably NaOH) could effectively be used as the reductant in place of metallic reductants. The mechanism is proposed to proceed by C–Br oxidative addition, nucleophilic addition of

**Scheme 70. Synthesis of Aromatic Esters by Ni-Catalyzed XEC (2020)<sup>a</sup>**

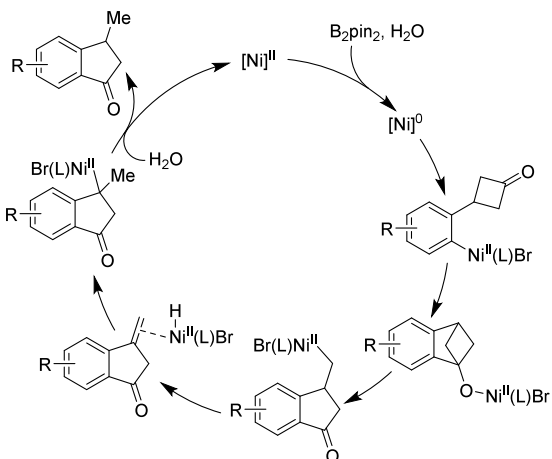


<sup>a</sup>(a) With aryl chloride, aryl ester (1.5 equiv), without DMAP. (b) With phenol, aryl ester (3 equiv), dcypt, (15 mol%), KF (2.0 equiv), and without DMAP.

**Scheme 71. Synthesis of Indanones by an Intramolecular XEC Involving C–C Bond Cleavage (2022)**



#### Proposed Mechanism

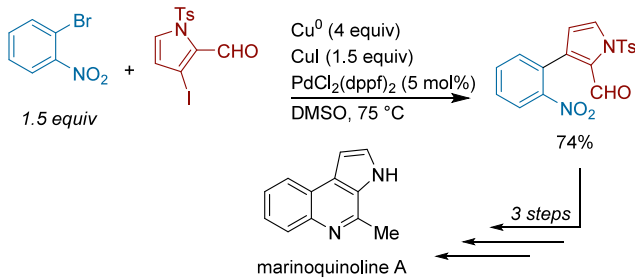


arylnickel(II) to the cyclobutanone carbonyl,  $\beta$ -carbon elimination,  $\beta$ -hydride elimination, migratory insertion, and protonation to generate the indanone.

#### 3.7. Synthetic Applications of C(sp<sup>2</sup>)–C(sp<sup>2</sup>) XEC

**3.7.1.1. Multimetallic Catalyzed Systems.** In 2012 Banwell and co-workers reported a convergent synthesis of marinoquinoline A that used a Pd-catalyzed cross-Ullman coupling (or XEC) as one of its key steps (Scheme 72).<sup>130</sup> It is proposed that the addition of stoichiometric Cu and CuI facilitates the formation of an arylcopper species that undergoes nucleophilic substitution with a C(sp<sup>2</sup>) palladium intermediate which, following reductive elimination, forms the cross-coupled product.<sup>67</sup> Initial attempts utilized 1-iodo-2-nitrobenzene as the coupling partner, but the major product was the homocoupled dimer. When switching to 1-bromo-2-nitro-

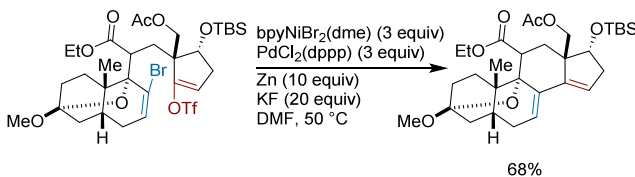
**Scheme 72. XEC of 1-Bromo-2-nitrobenzene with 3-Iodopyrrole-2-carboxaldehyde Towards Marinoquinoline A (2012)**



benzene the authors saw the cross-coupled product in 74% yield. This product was carried forward in the synthesis of marinoquinoline A.

Masayuki Inoue and co-workers reported a new synthesis of neurotoxin batrachotoxin in 2017.<sup>135</sup> Their method utilizes a palladium and nickel-mediated cross-electrophile coupling of vinyl bromides and vinyl triflates to perform a ring closure (Scheme 73). Initial attempts using only nickel resulted in a

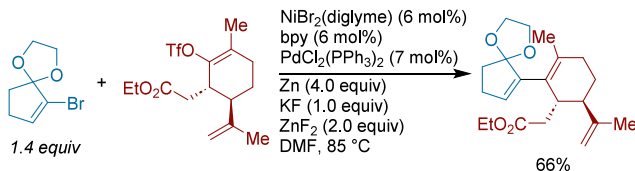
**Scheme 73. Synthesis of Batrachotoxin Using a Palladium and Nickel-Mediated Cross-Electrophile Coupling (2018)**



yield of 23%, but addition of palladium increased the yield to 68%. The authors note that heating of the reaction to 50 °C was necessary for appreciable yields.

Stoltz reported the use of XEC in progress toward the total synthesis of natural products curcusones A–D (Scheme 74).<sup>136</sup> The authors attempted more common cross-coupling

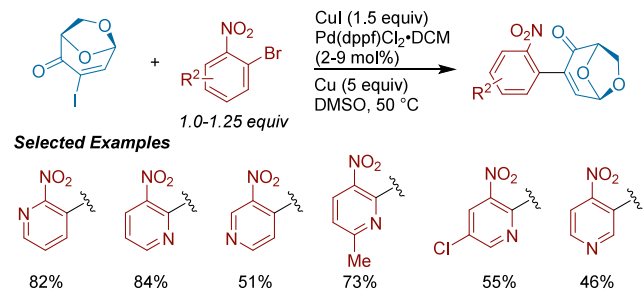
**Scheme 74. Key Nickel and Palladium XEC Step Used in Studies Towards the Synthesis of Curcusones A–D (2019)**



approaches, but these failed to give product. A Pd and Ni multimetallic system proved optimal and the use of a syringe pump for slow addition of vinyl bromide significantly increased the yield, presumably by suppressing hydrodehalogenation and homodimerization side products. The reaction was scaled up to gram-scale, with the addition of ZnF<sub>2</sub> crucial to maintaining high and consistent yields. The authors note this may be due to the Zn(II) salts competitively coordinating to KF and hindering transmetalation step(s). The authors then carried the product forward to construct the tricyclic cores of the diterpenoid natural products.

The Banwell group reported a Pd-catalyzed XEC of various bromonitropyridines with iodinated *iso*-levoglucosanone (*iso*-LGO) to form biologically active molecules (Scheme 75).<sup>137</sup>

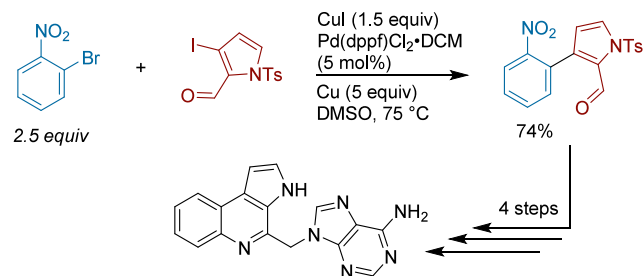
**Scheme 75.** Pd-Catalyzed XEC of Vinyl Iodides with Aryl Bromides Used to Form Biologically Active Compounds (2020)



They also made the analogous levoglucosenone-derived compounds. This is a synthetically convenient approach as the densely functionalized iodinated levoglucosenone electrophile can be accessed in just two steps from cellulose. Several of the analogues made in this study displayed potent antimicrobial properties and/or cytotoxicity.

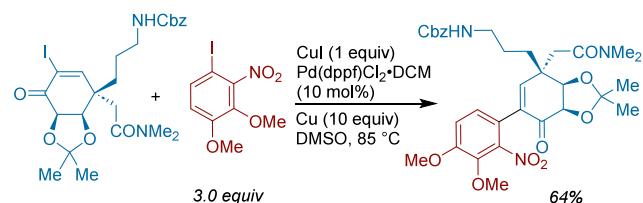
In 2020 Banwell and co-workers synthesized a variety of marinoquinoline natural products, in which a Pd-catalyzed XEC was a key C–C bond forming step en route to Aplidiopsamine A (Scheme 76).<sup>158</sup> Aplidiopsamine A's structure was confirmed by single-crystal X-ray analysis and tested for its biological activity as a potential inhibitor of acetylcholinesterase.

**Scheme 76.** Pd-Catalyzed XEC Towards Aplidiopsamine A (2020)



In 2022, Banwell and Ye disclosed the formal total syntheses of (+)- and (−)-Aspidophytine, of which (−)-Aspidophytine is a biosynthetic precursor to halophytine.<sup>159</sup> The authors began the synthetic efforts with cis-1,2-dihydrocatechol, eventually leading to the XEC of an aryl iodide with an  $\alpha$ -idoenone to afford the desired intermediate in 64% yield (Scheme 77).

**Scheme 77.** XEC Used in an Initial Synthetic Route Towards the Total Synthesis of (+)-Aspidophytine (2022)

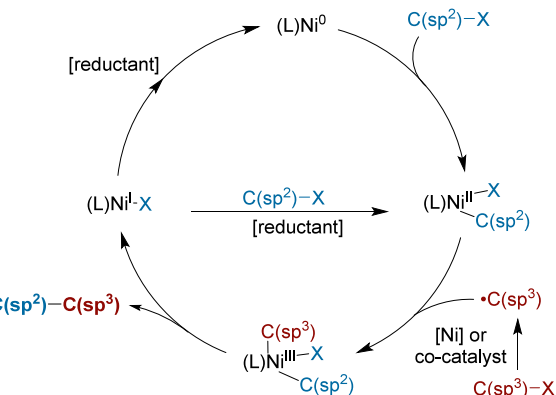


## 4. C(sp<sup>2</sup>)–C(sp<sup>3</sup>) Bond Formation

### 4.1. Overview

The cross-electrophile coupling of C(sp<sup>2</sup>) electrophiles, especially aryl, vinyl, and acyl electrophiles, with C(sp<sup>3</sup>) electrophiles has developed rapidly in the past decade and is the largest section in this review. The pace of development continues to increase and, in early 2024, one new report appears, on average, every 2 days. Increasingly, these approaches are used by chemists for the synthesis of natural products and drug candidates.

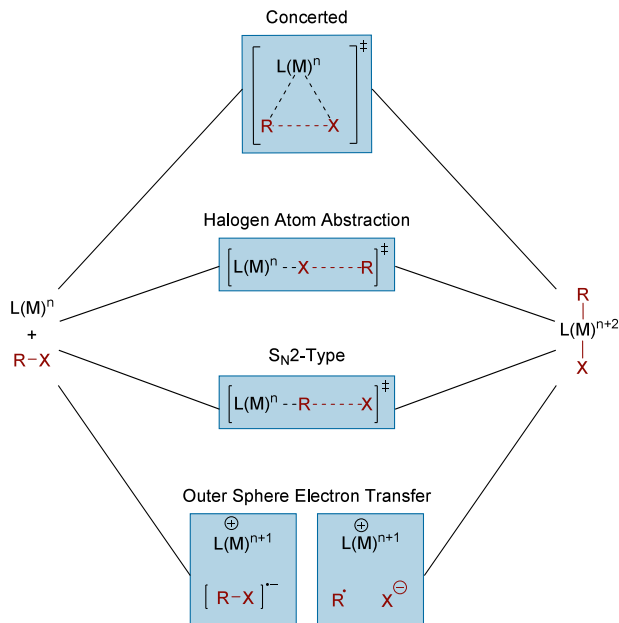
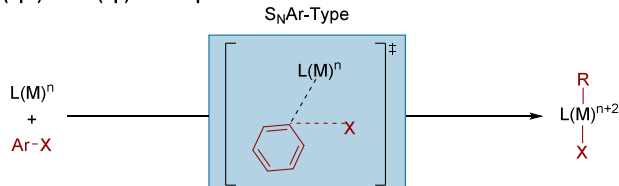
One reason for the current flowering of the field is that the essential design principles for the reactions have been established (Figure 22).<sup>160</sup> In the vast majority of reactions



**Figure 22.** Simplified mechanism for C(sp<sup>2</sup>)–C(sp<sup>3</sup>) bond forming cross-electrophile coupling with nickel.

catalyzed by nickel, the “recipe” for a productive reaction is relatively simple: a C(sp<sup>2</sup>) electrophile that can be activated by nickel through a nonradical mechanism can be coupled with a radical-forming C(sp<sup>3</sup>) electrophile in high yield, as long as their reactivities are well-matched. The primary challenges involve balancing reactivity and finding the right catalyst capable of the activation steps and the bond-forming steps. It is important to note that, despite the presence of alkyl radicals and the complexities of activating two different electrophiles, very high selectivities can be obtained (>99% cross-selectivity).<sup>161</sup>

This simplification, while enabling reaction development, obscures the fact that many of the key details of these reactions remain under study and debate. While some reactions occur with high selectivity, some reactions are unexpectedly challenging (e.g., the coupling of aryl triflates or alkyl chlorides). A better understanding of the mechanism could be key to overcoming these challenges. For example, the oxidative addition step for first-row metals could occur from several oxidation states (e.g., Ni<sup>0</sup> or Ni<sup>1</sup>, Co<sup>0</sup> or Co<sup>1</sup>) and proceed through a variety of mechanisms (Figure 23).<sup>79,162–169</sup> In these cases, the essential questions are the ordering of reduction and oxidative addition steps. The intermediate (LNi<sup>II</sup>(Csp<sup>2</sup>)X species does seem likely to be a resting state of the catalyst and accept the radical (often referred to as “radical capture”, but most correctly an oxidative ligation). However, it has been noted that if this species is reduced to (LNi<sup>I</sup>(Csp<sup>2</sup>), it is capable of generating an alkyl radical and regenerating (LNi<sup>II</sup>(Csp<sup>2</sup>)X).<sup>170</sup> The radical recombination in this case could be faster than diffusion. Regardless, the resulting (LNi<sup>III</sup>(Csp<sup>2</sup>)(Csp<sup>3</sup>)X species seems likely to perform the

**C(sp<sup>2</sup>) and C(sp<sup>3</sup>) Electrophiles****C(sp<sup>2</sup>) and C(sp<sup>3</sup>) Electrophiles**

**Figure 23.** Mechanisms of oxidative addition of C(sp<sup>2</sup>) and C(sp<sup>3</sup>) electrophiles. A number of oxidative addition mechanisms are known for both classes of electrophile.

reductive elimination step.<sup>171,172</sup> The (L)Ni<sup>I</sup>(X) species formed by reductive elimination could be reduced, or it could react with one of the electrophiles before being reduced.<sup>163,173</sup> The relative reactivity of nickel(0) and nickel(I) with C(sp<sup>2</sup>) and C(sp<sup>3</sup>) electrophiles has shown that selectivity is variable and ligand-dependent. The mechanism of radical generation appears to be especially variable and sometimes requires a cocatalyst.<sup>50,174–176</sup> Indeed, it is possible that different catalysts and conditions proceed by different mechanisms.<sup>177</sup> Even “radical first” mechanisms have been proposed to proceed by (L)Ni<sup>I</sup>(Csp<sup>3</sup>) intermediates under certain conditions.<sup>170,176,178–181</sup> While less commonly invoked, alkynickel(II) intermediates have been shown to react with aryl iodides to form C(sp<sup>2</sup>)–C(sp<sup>3</sup>) bonds.<sup>182–187</sup> Further comparative studies on different catalysts and metals are needed to enable further improvement.

The reliance of most systems on heterogeneous reduction steps (e.g., metal powders, electrode surfaces) or photoredox cocatalysis further complicates the study of these systems. The unknown extent to which side products of the reduction step (especially metal salts) alter catalyst reactivity and the mechanism of this step (electron-transfer or inner-sphere atom transfer) may contribute to discrepancies observed when these reactions are studied under different conditions. For instance, generation of M<sup>0</sup> might not be possible for some

reductant systems but possible for others or disproportionation/comproportionation mechanisms may be more favorable under certain conditions. A better understanding of these mechanistic features should be widely enabling, and further studies are needed.

Our own current understanding of this system is that these reactions are yet another example of the persistent radical (or metal) effect (Figure 24). Initially proposed by Griller and

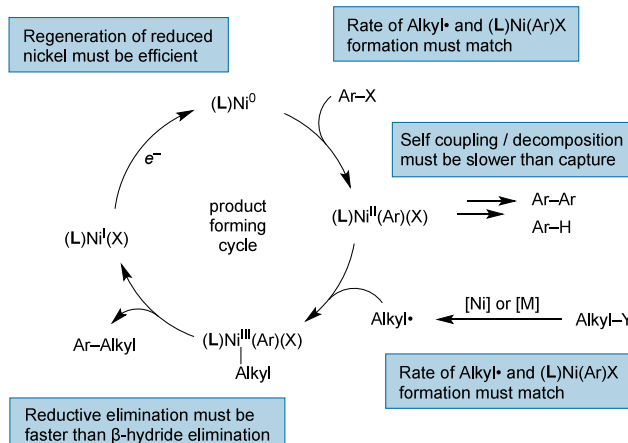


**Figure 24.** Persistent radical/metal effect for XEC. If the rate of formation of the radical and accepting metal are about equal, then the reaction can be cross-selective as long as the rate of cross-reaction of metal and radical is about 10× the decomposition of the metal species.

Ingold,<sup>188</sup> Liefert and Studer have recently collected the available data and provided modeling studies to demonstrate how this effect works to engender selectivity.<sup>112</sup> In summation: what is needed for selective coupling is for the rates of formation of •C(sp<sup>3</sup>) and (L)Ni<sup>II</sup>(Csp<sup>3</sup>)X to be about equal and for the homocoupling/decomposition of (L)Ni<sup>II</sup>(Csp<sup>3</sup>)X to be about 10× slower than the oxidative ligation/reductive elimination step. These parameters can exist for systems with selective electrophile activation steps, *but they can also exist for unselective activation*. That these conditions can be satisfied under a number of scenarios explains the broad success in the application of this system to a wide array of coupling reactions and the conflicting mechanistic reports.

The rapid development of the area has led to broad improvements in the scope of these reactions, but there are several areas that future studies must address. First, certain alkyl radicals still provide challenges: tertiary radicals are difficult to couple and tend to occur with unacceptable levels of isomerization (10% or more); certain classes of important radicals provide low yields (•CF<sub>3</sub>), yields with many classes of heterocycles remain low (pyrazoles, imidazoles, isoxazoles); sterically hindered bonds are a challenge generally, and some functional groups are not tolerated (–NO<sub>2</sub>, –N<sub>3</sub>, unprotected alkyne, some N–O bonds). Second, high enantioselectivity and diastereoselectivity are possible, but only for select coupling partners (2° benzylic, α-sulfone, α-phosphonate, α-nitrile) and there is significant room to explore this area. Third, cross-coupling with less reactive electrophiles is challenging to achieve with high selectivity and yield (e.g., aryl tosylates, aryl pivalates, aryl chlorides, alkyl chlorides).<sup>189</sup>

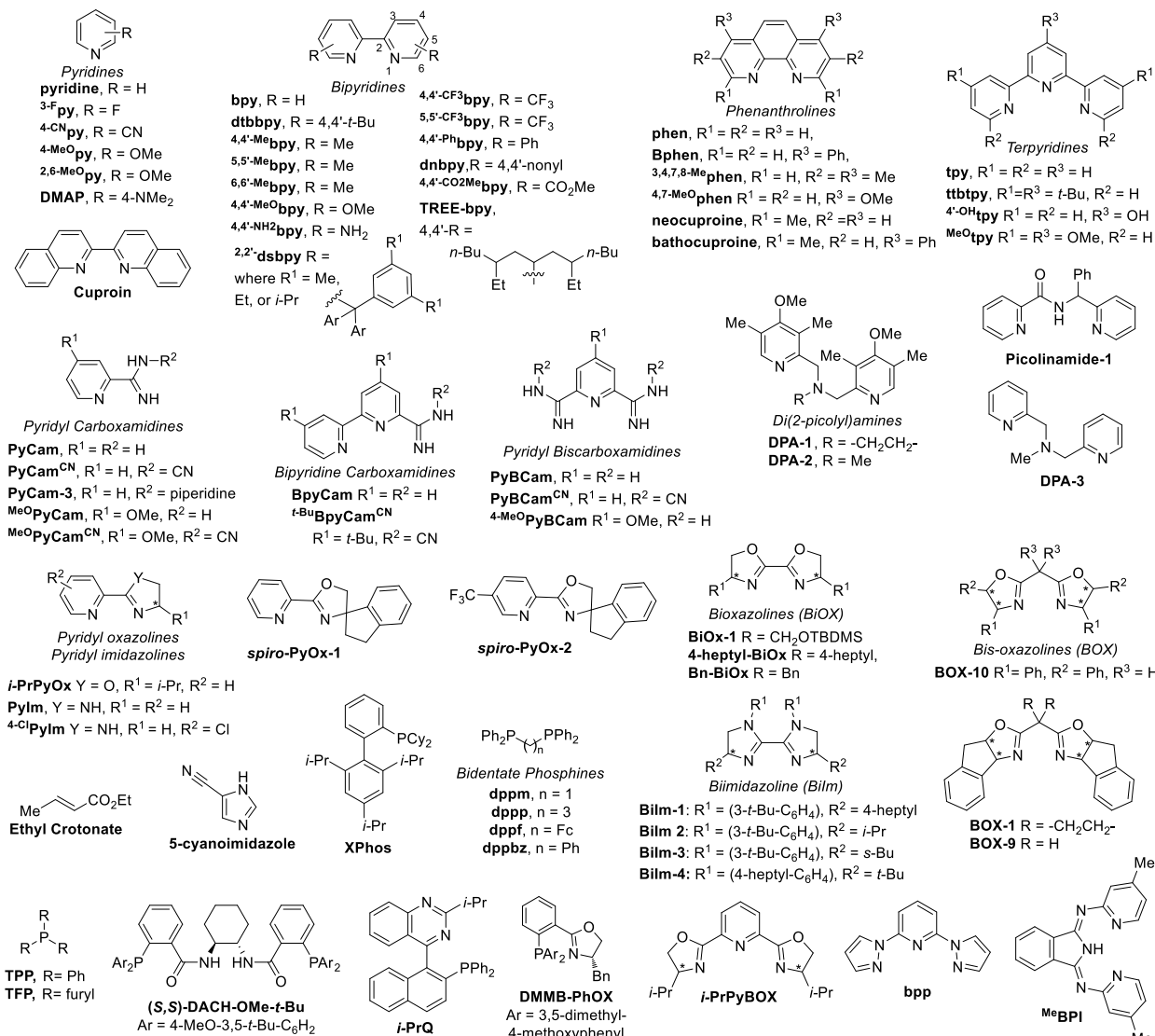


Figure 25. Ligands used in Aryl–Alkyl C(sp<sup>2</sup>)–C(sp<sup>3</sup>) XEC. \*Denotes chiral center.

#### 4.2. Alkylated Arenes

Recently, the medicinal chemistry community has become interested in increasing three-dimensionality from cross-coupling, leading to an explosion in the area of C(sp<sup>2</sup>)–C(sp<sup>3</sup>) bond-formation. In particular, Ni-catalyzed cross-electrophile coupling reactions have proven to be particularly well-suited for the construction of these challenging bonds. To this end, the use of cross-electrophile coupling to form C(sp<sup>2</sup>)–C(sp<sup>3</sup>) bonds has quickly transformed into an indispensable tool for any practicing organic chemist, resulting in a surge in development of increasingly efficient systems with broader scope. Note that this report is limited to reactions that fit our definition of XEC (Figure 2). A number of equally useful formal XEC reactions were not included, but are cited here for the interested reader.<sup>16,55,190–201</sup>

The large number of reports has led to a wide variety of reported precatalysts and ligands. In contrast to Ni and Pd-catalyzed cross-coupling reactions, which are dominated by strong σ-donor ligands like phosphines and N-heterocyclic carbenes, cross-electrophile coupling reactions appear to work best with nitrogen ligands (Figure 25). Indeed, 93% of reactions use nitrogen ligands (Figure 26). Although many

nitrogen ligands have been reported, the vast majority of reactions utilize bipyridine, phenanthroline, or (for enantioselective reactions) BOX and BiOX ligands. Because the nickel precatalyst is necessarily reduced during the catalytic cycle, a wide array of nickel salts are effective, but nickel(II) precatalysts dominate over nickel(0) precatalysts in number of reports by a wide margin (Figure 27). Differences observed between different precatalysts are likely related to adventitious salts formed during the reduction step (e.g., I<sup>–</sup> introduced through NiI<sub>2</sub> can be helpful for reactions), solubility (anhydrous NiX<sub>2</sub> salts have poor solubility), as well as commercial availability and practicality.

**4.2.1. Alkyl Bromides as Electrophiles.** As noted, the greater commercial abundance of alkyl halide electrophiles in comparison to their nucleophilic counterparts has driven the rise of reports in the cross-electrophile coupling literature that employ them. As a result, alkyl bromides have become the leading choice of alkyl electrophile within the past decade, with 12% of all reactions in this Review utilizing an alkyl bromide as a coupling partner. Among aryl–alkyl bond forming reactions, 36% of all reports involve an alkyl bromide.

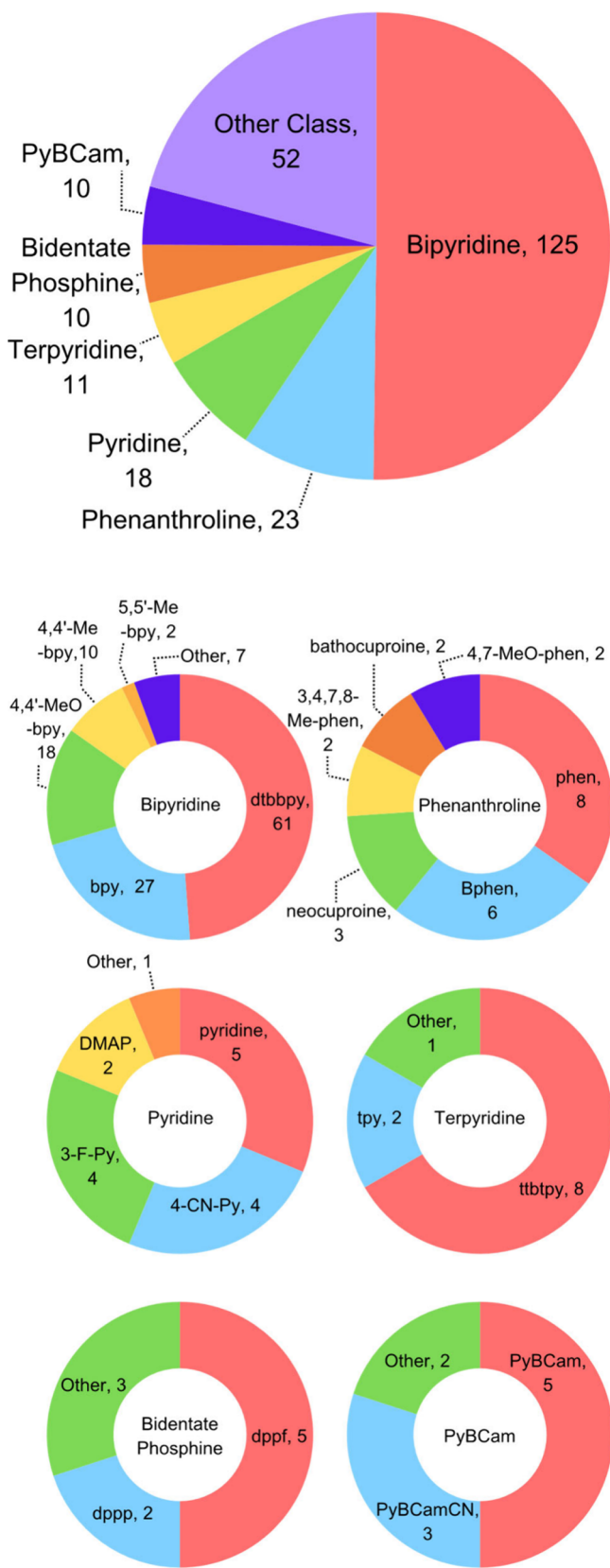


**Figure 26.** Distribution of ligands used in Aryl–Alkyl XEC. “Other” = ligands with 1 report. “Other Class” = ligand classes with <10 reports.

**4.2.1.1. XEC with Aryl Halides.** In 2009, Jacobi von Wangenheim and co-workers demonstrated an early example of the XEC of aryl halides with alkyl halides (Scheme 78).<sup>202</sup>

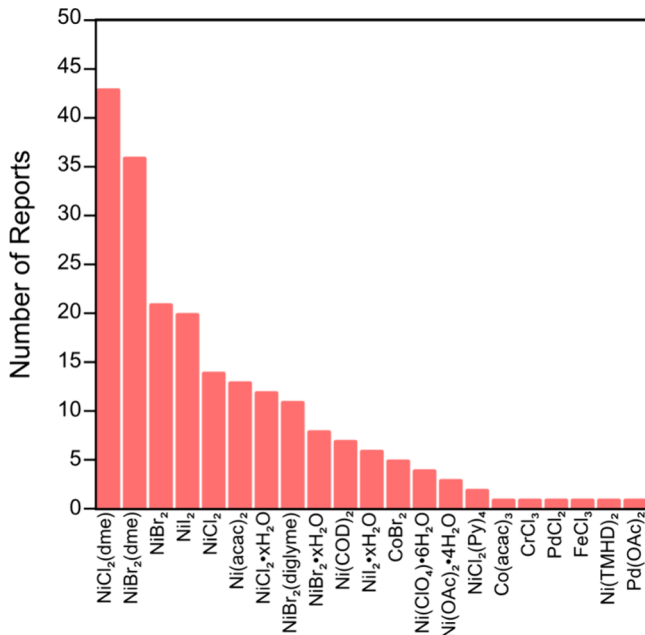
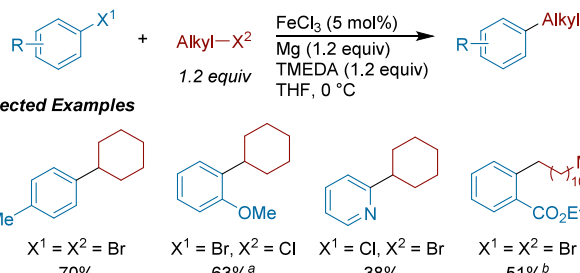


**Figure 27.** Metal sources used in Aryl–Alkyl XEC. NiCl<sub>2</sub>(dme) = 45 reports.

**Scheme 78. Fe-Catalyzed XEC of Aryl Halides with Alkyl Halides (2009)<sup>a</sup>**

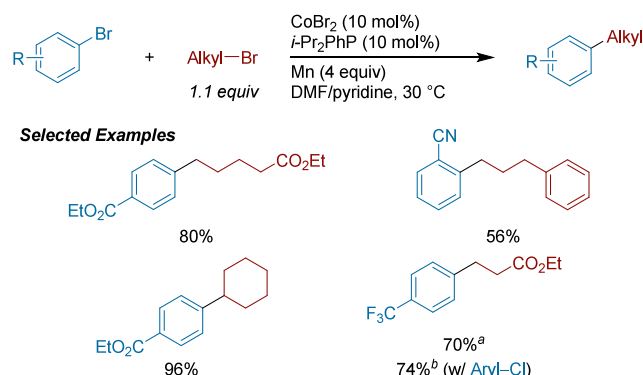


<sup>a</sup>(a) Reaction run for 2 h at 0 °C then at 20 °C for another 2 h. (b) With Mg (1.6 equiv) Mg and TMEDA (20 mol%).

They observed high selectivities for the cross-coupled product in the presence of FeCl<sub>3</sub> and noted that dilute reaction conditions minimized biaryl formation. Stoichiometric TMEDA improved cross-selectivity, likely due its role in metal complex stabilization. The conditions tolerate both primary and secondary alkyl bromides, and they also found success in couplings with alkyl chlorides under modified conditions. Time-course experiments revealed that iron catalyzed Grignard reagents formation, but that the Grignard intermediates did not accumulate. It appears that magnesium acts as a “shuttle” for the coupling partners between two different iron centers.

In 2010, the Gosmini group reported a cobalt-catalyzed XEC of aryl bromides and chlorides with 1° and 2° alkyl bromides (Scheme 79).<sup>203</sup> A survey of ligands found both bipyridine and monodentate phosphines to all be effective, although a 1:1 ratio of CoBr<sub>2</sub> and *i*-Pr<sub>2</sub>PPh could provide up to 99% yield! Pyridine cosolvent enabled even ligand-free conditions to provide considerable amounts of product. A variety of electron-poor aryl bromides and chlorides reacted well and cyclohexyl bromide coupled in remarkably high yield (96%). Finally, with bipyridine, the coupling of ethyl 4-bromobenzoate

**Scheme 79. Cobalt-Catalyzed XEC of Aryl Bromides With 1°, 2° Alkyl Bromides, and Benzyl Chloride (2010)<sup>a</sup>**

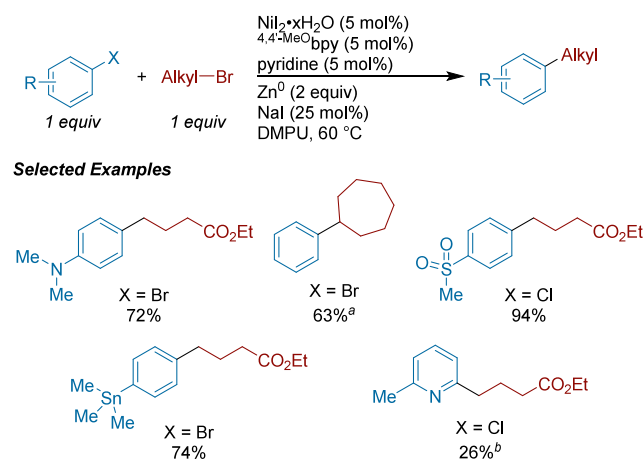


<sup>a</sup>(a) Modified conditions: CoBr<sub>2</sub> (20 mol%) and bpy (20 mol%) instead of *i*-Pr<sub>2</sub>PhP with alkyl bromide (2 equiv) at 50 °C. (b) Modified conditions: CoBr<sub>2</sub> (20 mol%) and bpy (20 mol%) instead of *i*-Pr<sub>2</sub>PhP, and alkyl bromide (3 equiv) of Alkyl-Br at 65 °C.

with benzyl chloride formed the diarylmethane in 85% yield. Evidence of an alkyl radical intermediate was provided by a cyclopropylmethyl bromide coupling.

Building on our initial report focused on organic iodides (see section 4.2.3.1, Scheme 153),<sup>44</sup> we reported general conditions for the coupling of aryl bromides with 1° and 2° alkyl bromides (Scheme 80).<sup>41</sup> Key findings in the

**Scheme 80. Ni-Catalyzed XEC of Aryl Bromides and Chlorides with 1° and 2° Alkyl Bromides (2012)<sup>a</sup>**



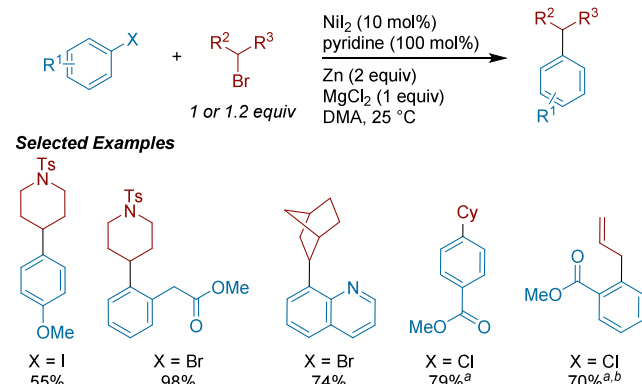
<sup>a</sup>(a) With alkyl bromide (1.25 equiv). (b) With Phen as ligand.

optimization that have proven broadly useful were the use of more-electron-rich bipyridine ligands (<sup>4,4'-MeO</sup>bpy vs dtbbpy<sup>161</sup>) and the addition of sodium iodide. For more electron-poor aryl bromides, phenanthroline outperformed bpy-type ligands. While a single *ortho*-substituent on the aryl coupling partner did not hinder reactivity, 2,6-disubstitution, such as in 2-bromomesitylene, turned off product formation entirely. Couplings with trisubstituted alkenyl halides proceeded well, but terminal monosubstituted alkenes suffered from isomerization. This report had an extensive survey of functional groups and noted several general trends: 1) acidic protons are well-tolerated (−OH, -NHR), π-electrophiles do not react (−CHO), common nucleophilic coupling partners in

cross-coupling are unreactive (C–SnR<sub>3</sub>, C–Bpin, C–SiMe<sub>2</sub>OH), β-leaving groups on the alkyl partner are tolerated, and arylsulfonate esters are unreactive (C–OTf, C–OTs). While an electron-rich protected indole coupled in good yield, 2-bromopyridine provided a low yield. Electron-poor chloroarenes coupled well to primary alkyl bromides, but simple bromobenzene provided only 22% yield. Mechanistically, this report detailed methods to activate the Zn reductant, showed organozinc intermediates were not likely on-cycle, and showed that the reaction rate had a positive dependence on alkyl halide and nickel catalyst concentration, but an inverse dependence on aryl halide concentration.

Also in 2012, Hegui Gong and co-workers reported a set of conditions for coupling aryl halides with 1° and 2° alkyl bromides (Scheme 81).<sup>204</sup> Early reactions were run at 80 °C

**Scheme 81. Ni-Catalyzed XEC of Aryl Iodides and Bromides with 1° and 2° Alkyl Bromides and Allylic Acetates (2012)<sup>a</sup>**

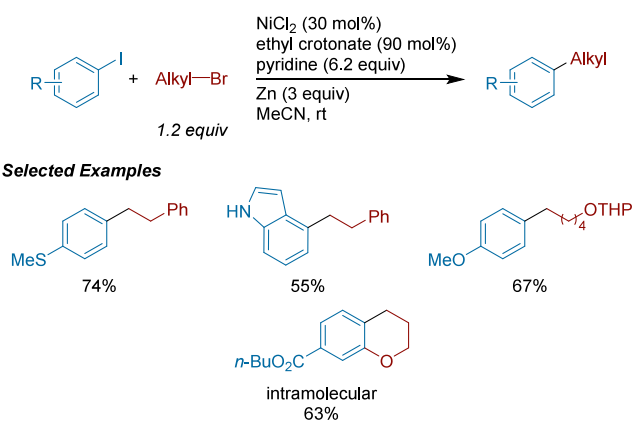


<sup>a</sup>(a) With *n*-BuNBr (1 equiv) added. (b) With allyl acetate (1 equiv).

but the authors found a significant improvement in yield when lowered to 25 °C in the presence of pyridine. MgCl<sub>2</sub> was a key additive, and has multiple roles in activating of the Zn surface and enhancing the rate of nickel(II) reduction. These conditions were general for a range of aryl iodides, bromides, and, in one instance, an activated chloride. The conditions are more suitable for electron-rich aryl coupling partners but still afford moderate yields for their electron-poor counterparts. Functional group compatibility was excellent. Heterocycles like pyridine and quinoline were shown to couple in promising yield. These conditions were also useful for coupling with allylic acetates.

In 2012, Yu Peng and co-workers identified a method for coupling aryl iodides with alkyl bromides both inter- and intramolecularly using nickel cross-electrophile coupling (Scheme 82).<sup>205</sup> The authors propose that ethyl crotonate and pyridine are ligated to the resulting nickel(0) complex. In DMF, they observed alkyl dimerization as the major product with near full recovery of the aryl iodide. After switching to MeCN as solvent and increasing catalyst loading, the reaction afforded 60% desired cross-product yield. A range of aryl electronics were tolerated in addition to free phenol. Its utility was demonstrated in the ability to use more complex, chiral structures, relevant to natural product synthesis. The reaction proceeded with moderate success intramolecularly, capable of forming heterocycles such as indolines and tetrahydroquinolines. Initial attempts were made in this report to expand these

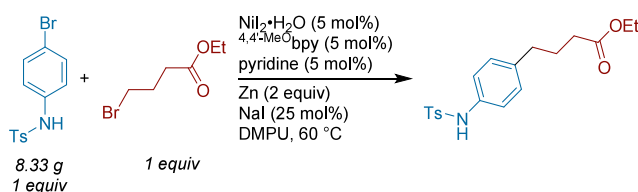
**Scheme 82. Inter- and Intramolecular Ni-Catalyzed XEC of Aryl Iodides with Alkyl Bromides (2012)**



conditions toward intramolecular alkene difunctionalization (see section 7.1.2.2, Schemes 421 and 422). Intramolecular XEC is still an outstanding challenge, and this remains one of the best reports in this area.

In 2013, we reported on the scalability of the conditions from our 2012 report<sup>41</sup> (Scheme 83).<sup>206</sup> The reaction was

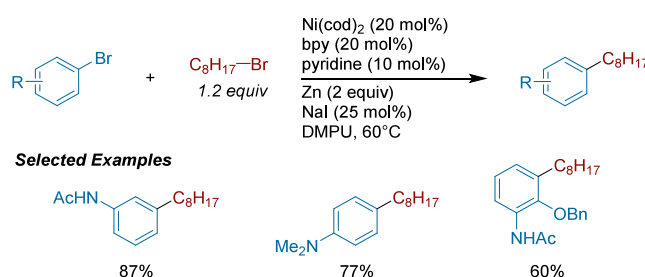
**Scheme 83. Example Large-Scale Ni-Catalyzed XEC of an Aryl Bromide with an Alkyl Bromide (2013)**



conducted on 8.33 g (25.5 mmol) of the aryl bromide. The key findings were 1) oxygen is tolerated in the headspace, but too much oxygen leads to incomplete conversion; 2) stirring the heterogeneous mixture works best with a mechanical stirrer in a Morton flask (to induce turbulent mixing). The challenges of mixing on scale are perhaps the largest barrier to scale-up.

A procedure for the cross-electrophile coupling of aryl bromides with alkyl bromides was detailed by Yuehai Shen and co-workers (Scheme 84).<sup>207</sup> This report focused on the reaction's applicability for the synthesis of functionalized natural product intermediates. Inspired by the retrosynthetic possibilities for benzenoid ansamycins, they modified a cross-electrophile coupling reaction to pair bromoanilines with alkyl bromides. They found that using a slight excess of alkyl bromide contributed to a noticeable increase in yield as

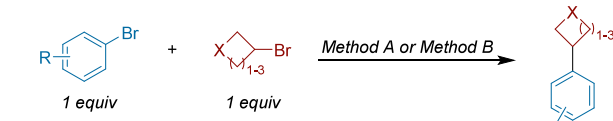
**Scheme 84. Ni-Catalyzed XEC of Alkyl Bromides with Amine-Functionalized Aryl Bromides (2014)**



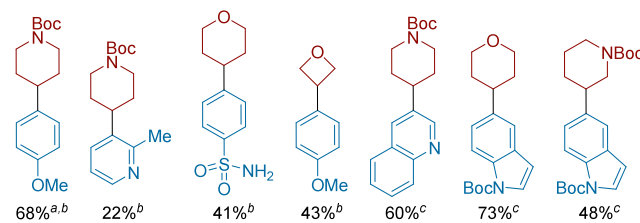
compared to an excess of aryl bromide. In contrast to previous studies, they found that introduction of MgCl<sub>2</sub> or Bu<sub>4</sub>NBr into the system hindered product formation. To test the reaction's feasibility in natural product synthesis, they applied their protocol to the preparation of an intermediate toward the synthesis of autolytimycin in up to 60% yield.

In collaboration with O'Neill at Pfizer, Molander and Traister were the first to apply a high-throughput experimentation (HTE) approach to optimize XEC reactions with heterocycles of interest to medicinal chemistry in 2014 (Scheme 85).<sup>208</sup> A detailed summary of pyridine derivatives,

**Scheme 85. Ni-Catalyzed XEC of Aryl Bromides with Unsaturated Heterocycle Alkyl Bromides (2014)<sup>a</sup>**



**Selected Examples**



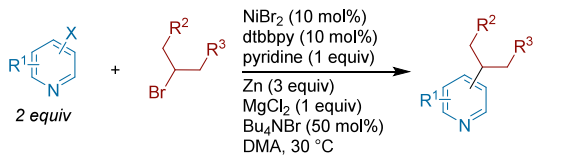
<sup>a</sup>(a) Conducted on a scale of 6 mmol with NiCl<sub>2</sub>(dme) (5 mol%) and phen (10 mol%). (b) Method A conditions: NiCl<sub>2</sub>(dme) (10 mol%), phen (20 mol%), 4-ethylpyridine (50 mol%), Mn (2 equiv), NaBF<sub>4</sub> (50 mol%), and MeOH (0.2 M) at 60 °C. (c) Method B conditions: NiI<sub>2</sub> (10 mol%), dtbbpy (10 mol%), 4-ethylpyridine (1 equiv), Mn (2 equiv), MgCl<sub>2</sub> (50 mol%), and DMA (0.2 M) at 60 °C.

additives, and physical conditions tested are outlined, including a breakdown of product to side products ratios. Key new findings were the use of a protic solvent (MeOH) and the superiority of 4-ethylpyridine to pyridine. This chemistry displayed compatibility with heterocycles, both aromatic and nonaromatic in nature, with modified reaction conditions.

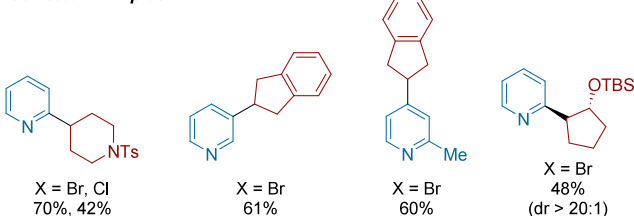
Interested in expanding these reaction types to heteroaryl bromides, Huiyan Liu, Qun Qian, and co-workers described conditions in which secondary alkyl bromides could successfully couple with multifunctionalized bromopyridines (Scheme 86).<sup>209</sup> They observed a significant dependence on solvent, requiring DMA for the best results. Both MgCl<sub>2</sub> and Bu<sub>4</sub>NBr were essential additives. They hypothesize that the two additives are crucial for zinc activation but also suggest a coordination effect between MgCl<sub>2</sub> and nickel. The reaction appears to tolerate electron-rich pyridines best, with lower yields obtained for -CF<sub>3</sub> substituted pyridines. This is an early example showing that Lewis basic nitrogen heterocycles could be a good match for XEC chemistry.

Also in 2014, our group reported conditions for the coupling of 2-chloropyridines with primary and secondary alkyl bromides (Scheme 87).<sup>210</sup> Ultimately, bathophenanthroline (Bphen), a ligand we had in quantity due to a gift from Kodak, proved to be best; reactions with tridentate ligands favored aryl dimer. In comparing Zn and Mn as the reductant, we discovered a bias toward the hydrodehalogenation pathway of the heteroaryl chloride when using Zn, supporting the idea that formation of an arylzinc species is an undesirable, off-cycle

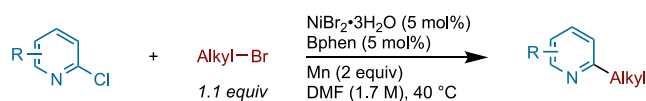
**Scheme 86. Ni-Catalyzed XEC of Halopyridines with Secondary Alkyl Bromides (2014)**



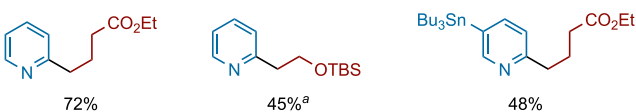
**Selected Examples**



**Scheme 87. Ni-Catalyzed XEC of 2-Chloropyridines with Alkyl Bromides (2014)<sup>a</sup>**



**Selected Examples**

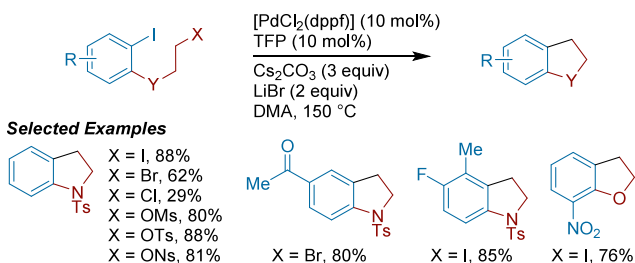


<sup>a</sup>With NiBr<sub>2</sub>•3H<sub>2</sub>O (10 mol%).

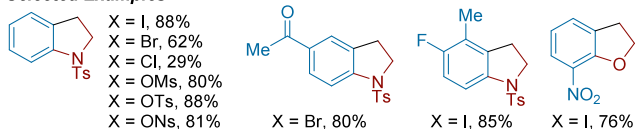
pathway. Sodium iodide was again found to be helpful for reactions with more reactive pyridyl substrates.

Xuefeng Jiang and co-workers reported a Pd-catalyzed intramolecular XEC of aryl iodides with alkyl electrophiles in 2014 (Scheme 88).<sup>211</sup> Optimal conditions utilized a dppf-

**Scheme 88. Pd-Catalyzed Intramolecular XEC of Aryl Iodides with Alkyl Halides (2014)<sup>a</sup>**



**Selected Examples**

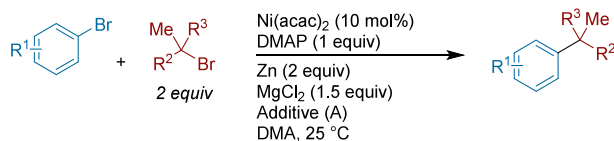


<sup>a</sup>TFP = tris(2-furyl)phosphine.

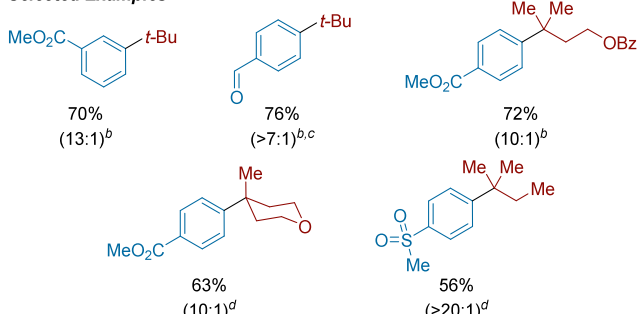
ligated palladium catalyst with added tri(2-furyl)phosphine, base, and LiBr in DMA. There is no explicit terminal reductant, but the authors provided evidence that, at 150 °C, DMA serves this role. The scope is impressive: in addition to indolines, these conditions allowed access to a tetrahydropyridine, a hexahydro-1*H*-indole, and a hexahydrocyclopenta[*b*]pyrrole. The isolated aryl oxidative addition Pd(II) complex, when heated in benzene at 100 °C, formed the indoline product in high yield, suggesting that a second oxidative addition is operative (via Pd(IV)). The complementary reactivity of Pd and Ni suggests that further exploration is warranted.

The formation of all-carbon quaternary centers by cross-coupling is generally challenging. In 2015, the group of Hegui Gong detailed the first XEC approach utilizing tertiary alkyl bromides and primarily electron-poor aryl bromides (Scheme 89).<sup>45</sup> MgCl<sub>2</sub> was a crucial additive in both sets of conditions

**Scheme 89. Ni-Catalyzed XEC of Aryl Bromides with Tertiary Alkyl Halides (2015)<sup>a</sup>**



**Selected Examples**



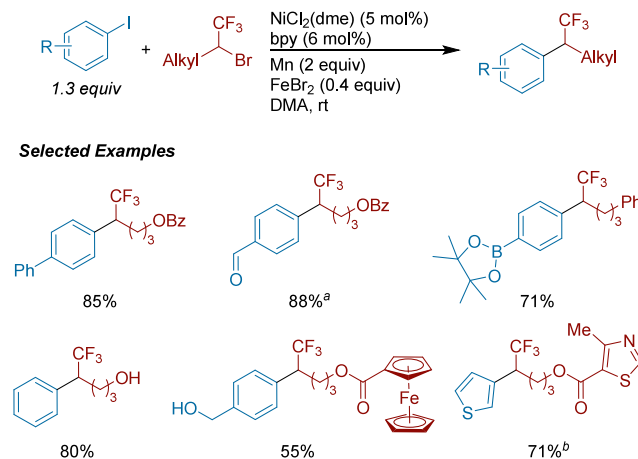
<sup>a</sup>(a) Ratio of product with quaternary center to isomerized product given below yields. (b) A = *i*-Pr-Im-HCl (30 mol%). (c) Pyridine (100 mol%) instead of DMAP. (d) A = *t*-Bu-Im-HCl (30 mol%).

they developed. MgCl<sub>2</sub> plays a variety of roles including solubilization of nickel intermediates and activation of the zinc surface, which enhances the rate of the reaction. As seen in previous examples, DMAP, or in some instances pyridine, appears to act as the ligand and altered the amount of isomerization (or chain-walking) observed. In their first method, *t*-BuBr was coupled favorably across a range of aryl bromides, including those that contained *ortho*-functionalization, aldehydes, and sulfones. While isomerization of tertiary alkyl groups can be an issue,<sup>212</sup> most of these reactions occurred with significant retention of the quaternary product. By altering the limiting reagent to be the alkyl coupling partner, more sterically hindered alkyl bromides could also be coupled. However, too much steric bulk, as seen when attempting to use 3-bromo-3-ethylpentane as a coupling partner, drastically reduced reactivity and increased the alkyl isomerization.

As a way to engage trifluoromethyl containing compounds, Xingang Zhang, Zhong-Xing Jiang, and co-workers described the XEC of  $\alpha$ -trifluoromethyl alkyl bromides with aryl iodides (Scheme 90).<sup>213</sup> Notably, FeBr<sub>2</sub> was a crucial additive for improved reaction outcome. While they were unable to elucidate the role of the iron salts, they attributed its benefits to low valent iron species, which had been shown to form under the presence of manganese.<sup>214</sup> A positive correlation was noted between catalyst loading and aryl dimerization: better results were obtained at lower catalyst loadings. Heteroaryl iodides with pyridine, quinoline, and thiophene backbones were shown to be competent coupling partners.

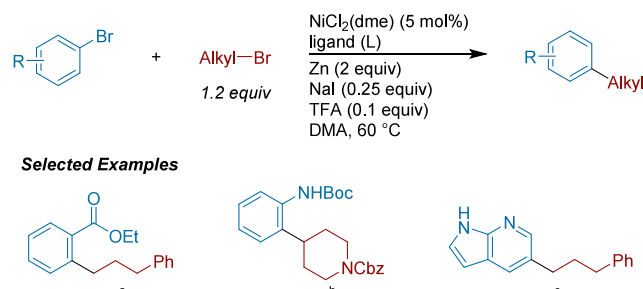
Inspired by the importance of nitrogen ligands and the relative lack of diversity in this class, we collaborated with Pfizer to explore pharmaceutical compound libraries to find new ligands that could solve challenging coupling reactions

**Scheme 90.** Ni-Catalyzed XEC of Aryl Iodides with  $\alpha$ -Trifluoromethyl Alkyl Bromides (2015)<sup>a</sup>



<sup>a</sup>(a) Ran reaction for 48 h at 50 °C. (b) With NiCl<sub>2</sub>(dme) (8 mol%) and bipy (9.6 mol%).

**Scheme 91.** New Ligands for Nickel and Application to the XEC of Challenging Aryl Bromides with Alkyl Bromides (2016)<sup>a</sup>

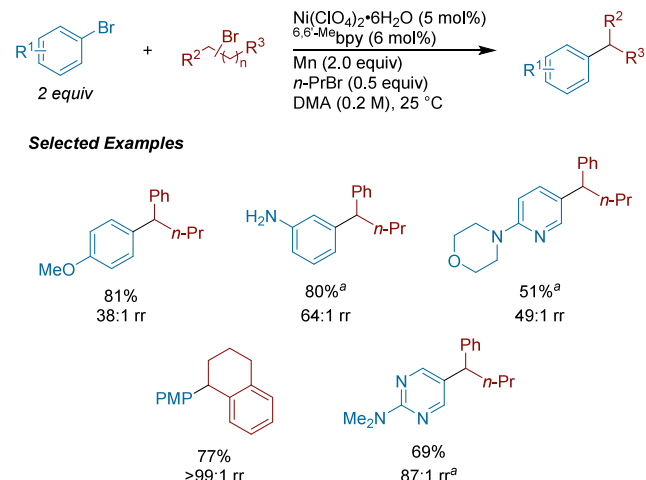


<sup>a</sup>(a) L = MeO<sup>4,4'</sup>-bipyCam<sup>CN</sup>, assay yield by GC or UPLC. (b) L = MeO<sup>4,4'</sup>-bipyCam. (c) L = PyBCam

(Scheme 91).<sup>32</sup> In total, 82 diverse ligands were screened in an XEC model reaction. Using  $4,4'$ -MeO<sup>4,4'</sup>bipy as the standard, nine hits were identified, two of which belonged to unexplored structural backbones. Additional pyridyl-2-carboxamidines and (2-pyridyl)-substituted aliphatic N-heterocycles were then mined from the database at Pfizer giving a total of 31 potential ligands to assess. After further testing, pyridyl-2-carboxamidines were identified as the most promising. Pyridine carboxamidine (PyCam) ligands were better than all known ligands for aryl bromides with a coordinating functional group in the *ortho*-position. A tridentate version, PyBCam, was found to be promising for Lewis basic nitrogen heterocycles.

Shaolin Zhu, Yi-Ming Wang, and co-workers reported on a chain-walking XEC reaction in 2017 between aryl and alkyl bromides (Scheme 92).<sup>215</sup> Using a modification of their previous conditions with alkenes instead of alkyl bromides, they observed isomerized coupling products indicative of chain-walking processes (i.e.,  $\beta$ -hydride elimination to form Ni–H, reinsertion to form different alkynickel).<sup>216</sup> The previous conditions already demonstrated high regioselectivity, up to 17:1 rr, favoring the migratory coupling product but this

**Scheme 92.** Ni-Catalyzed Chain-Walking XEC of Alkyl Bromides with Aryl Bromides (2017)<sup>a</sup>

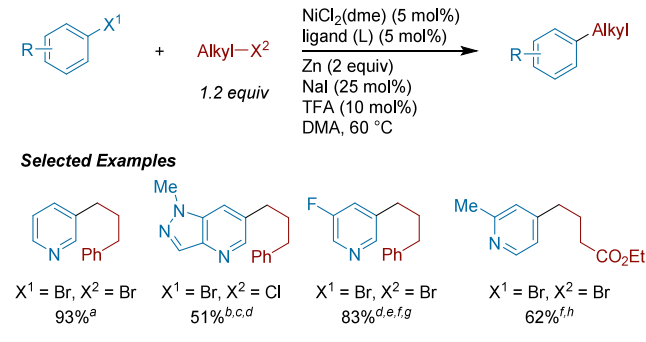


<sup>a</sup>With NiI<sub>2</sub>·xH<sub>2</sub>O as precatalyst.

did not translate to bromides. It was found that *n*-PrBr was a useful additive to generate the Ni–H species (via  $\beta$ -hydride elimination). In analogy to previous chain-walking reactions, more hindered ligands ( $6,6'$ -MeO<sup>4,4'</sup>bipy) promoted migration. The scope was just as broad as XEC reactions that proceed without isomerization. Based upon extensive mechanistic experiments, the authors propose an alkyl-first mechanism where the chain-walking happens via an alkynickel(I) intermediate. Product formation would then proceed by oxidative addition of the aryl bromide to the alkynickel(I) and reductive elimination to form product.

In collaboration with Pfizer and Asymchem Life Science, our group reported general conditions for the XEC of halogenated Lewis basic nitrogen heterocycles with alkyl bromides (Scheme 93).<sup>33</sup> This report was the first to systematically address

**Scheme 93.** Ni-Catalyzed XEC of Heteroaryl Halides with Alkyl Halides Enabled by Carboxamidine Ligands (2017)<sup>a</sup>



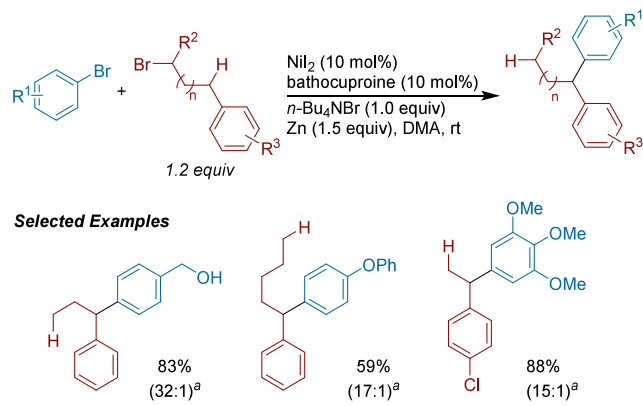
<sup>a</sup>(a) L = PyBCam. (b) L = PyBCam<sup>CN</sup>. (c) NiCl<sub>2</sub>(dme) and ligand used in 7 mol%. (d) Used 2.0 equiv of alkyl halide. (e) L = PyCam. (f) Precatalyst of NiI<sub>2</sub> used. (g) Run at 40 °C. (h) L = PyCam<sup>CN</sup>.

coupling on every position of the pyridine core with variation of the pyridine substitution and electronics. It was found that PyCam and PyBCam ligands were superior for these challenging substrates. Though multiple ligands were assessed, PyBCam, PyBCam<sup>CN</sup>, and PyCam were the most useful (and are now commercially available). Notably, it was found that homodimerization of the alkyl bromide coupling partner could

be overcome by switching to the analogous alkyl chloride, demonstrating a different approach to matching alkyl and aryl reactivity. While the scope was broad, these reactions are less effective for more electron-rich 5-membered azoles such as bromopyrazoles and bromoimidazoles.

In 2018, Guoyin Yin and co-workers reported a chain-walking cross-coupling of alkyl bromides and aryl bromides to generate diarylalkanes (**Scheme 94**).<sup>217</sup> The optimal catalyst,

**Scheme 94.** Ni-Catalyzed Chain Walking XEC of Alkyl Bromides with Aryl Bromides (2018)<sup>a</sup>

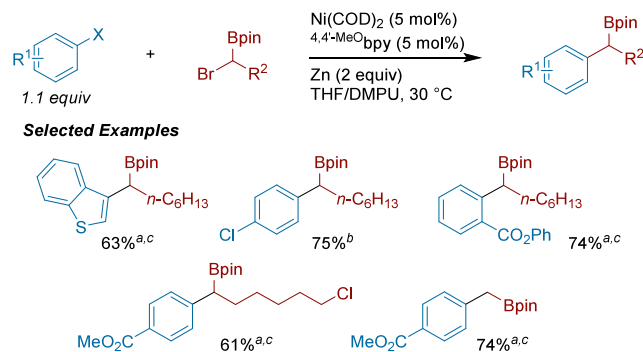


<sup>a</sup>Ratio of remote-/ipso-products.

like previous chain-walking XEC, featured methyl groups flanking the nitrogen atoms (<sup>6,6'-Me</sup>bpy and bathocuproine). The alkyl bromides examined were simple *n*-alkylarenes with halogenation distal to the aryl group. Efficient chain-walking enabled coupling at the benzylic position to form 1,1-diarylalkane products in good yield and high regioselectivity, including the synthesis of three anticancer isoerianin analogues. A gram-scale example (12-fold scale up) was demonstrated with 73% yield and excellent regioselectivity.

Martin and co-workers reported the Ni-catalyzed cross-electrophile coupling of aryl bromides and iodides with  $\alpha$ -boryl alkyl bromides (**Scheme 95**).<sup>218</sup> While functional group tolerance was excellent and both 1° and 2° alkyl bromides coupled,  $\alpha$ -quaternary substrates were unreactive. The authors highlighted the synthetic application of this method by further derivatizing products at the boronic ester using oxidation, Suzuki coupling, and lithiation. An isolated (L)Ni<sup>II</sup>(Ar)Br

**Scheme 95.** Ni-Catalyzed XEC of Aryl Bromides with  $\alpha$ -Boryl Alkyl Bromides (2018)<sup>a</sup>

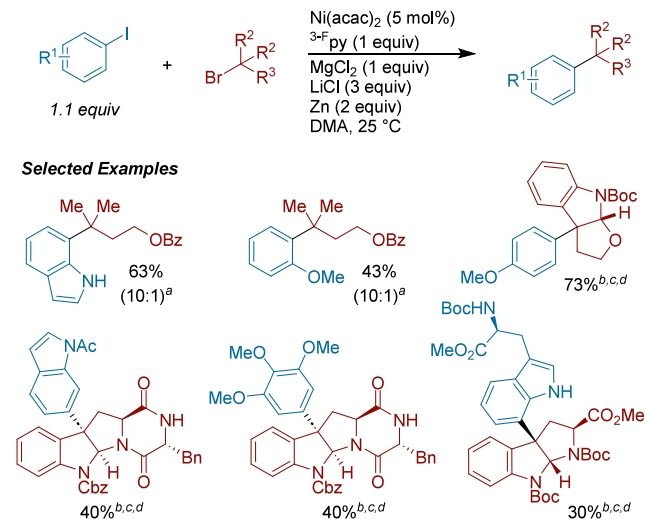


<sup>a</sup>(a) X = Br. (b) X = I. (c) Ni(COD)<sub>2</sub> (10 mol%).

complex was demonstrated to react with an  $\alpha$ -boryl alkyl bromide with or without added reductant, although the coupling yield was higher with Zn.

In 2018, Hegui Gong, Xiaotai Wang, and co-workers published a comprehensive follow-up study (see **Scheme 89**) on the XEC of tertiary alkyl bromides with aryl halides to form all-carbon quaternary centers (**Scheme 96**).<sup>219</sup> Their previous

**Scheme 96.** Ni-Catalyzed XEC of Electron-Rich Aryl Iodides with Tertiary Alkyl Bromides and Mechanistic Studies (2018)<sup>a</sup>

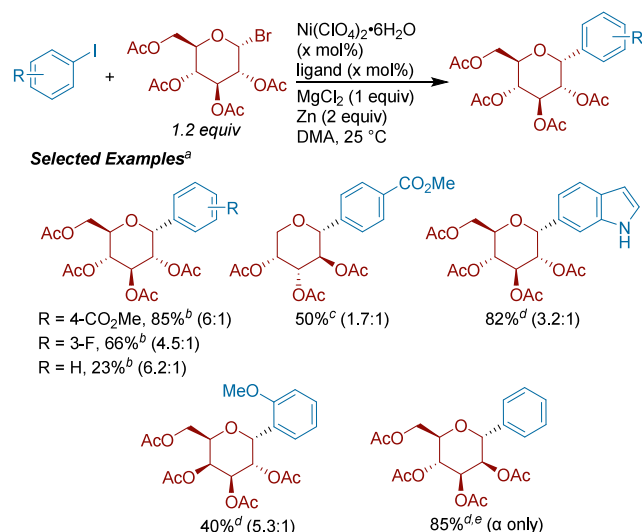


<sup>a</sup>(a) Ratio of retention product to rearranged product. (b) With Ni(acac)<sub>2</sub> (20 mol%) instead. (c) With DMF as solvent. (d) With alkyl chloride.

conditions worked poorly with electron-rich aryl bromides. Switching to aryl iodides and adjusting the ligand (3-fluoropyridine vs DMAP), salt additives (+LiCl), and nickel precursor (Ni(acac)<sub>2</sub>) resulted in satisfactory yields. DFT calculations and stoichiometric studies suggested the reason that monodentate pyridines work best for tertiary alkyl coupling reactions: pyridine ligands can dissociate to relieve steric congestion and reduce the barrier for reductive elimination. Of particular interest are studies that shed light on the role of MgCl<sub>2</sub> and LiCl in forming an active nickel intermediate, solubilization of nickel intermediates, and activation of the zinc surface.

Hegui Gong developed conditions for the XEC of glycosyl bromides with aryl iodides (**Scheme 97**).<sup>220</sup> For some substrate pairs, they found that addition of HBr was needed to initiate the reaction, which they attribute to Zn activation. Two sets of conditions were optimized based on the electronics of the aryl iodides used. In general, electron-deficient arenes proceeded with a monodentate amine ligand, while electron-rich arenes required a bidentate ligand to enhance reactivity (at the cost of  $\alpha/\beta$  selectivity). Stoichiometric reactions with arylnickel(II) complexes in the absence of Zn afforded product, supporting a radical chain mechanism. MgCl<sub>2</sub> provided improved yields, which may be due to a beneficial anion exchange with the Ni complexes, forming more stable bonds.<sup>219</sup> The authors attribute the high  $\alpha$ -selectivity to sterics and suggest that the anomeric oxygen's lone pair in  $\alpha$ -isomer is aligned to allow for stabilization of the Ni–C bond through donation into its antibonding orbital. They suggest that the lability of DMAP is

**Scheme 97.**  $\alpha$ -Selective Ni-Catalyzed XEC of Aryl Iodides with Glucosyl Bromides (2018)<sup>a</sup>

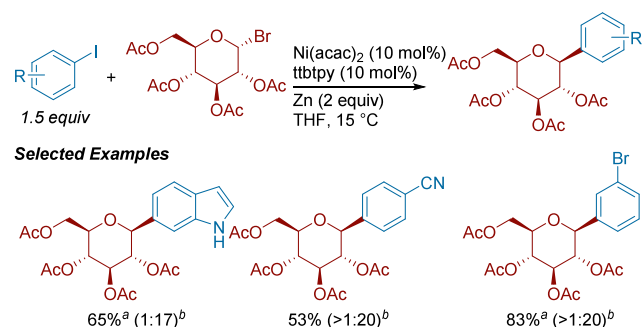


<sup>a</sup>(a) Numbers in parentheses represent  $\alpha/\beta$  ratios. (b) With 20 mol% [Ni], DMAP (80 mol%), trace HBr/AcOH, and DMA/THF (2:3) at 0 °C. (c) With 10 mol% [Ni] and DMAP (40 mol%). (d) With 10 mol% [Ni] and dtbbpy (15 mol%). (e) In DMA/THF (1:4).

key to high  $\alpha/\beta$  ratios as well. In this study, they also developed distinct conditions to couple vinyl bromides with glucosyl bromides (see section 4.3.2, Scheme 256).

Hegui Gong, Chuanhu Lei, Jiandong Liu, and co-workers then disclosed the  $\beta$ -selective cross-coupling of glucosyl bromides with aryl iodides to access a variety of C-aryl glucosides in moderate to high yields (Scheme 98).<sup>221</sup>

**Scheme 98.**  $\beta$ -Selective Ni-Catalyzed XEC of Aryl Iodides with Glucosyl Bromides (2019)<sup>a</sup>



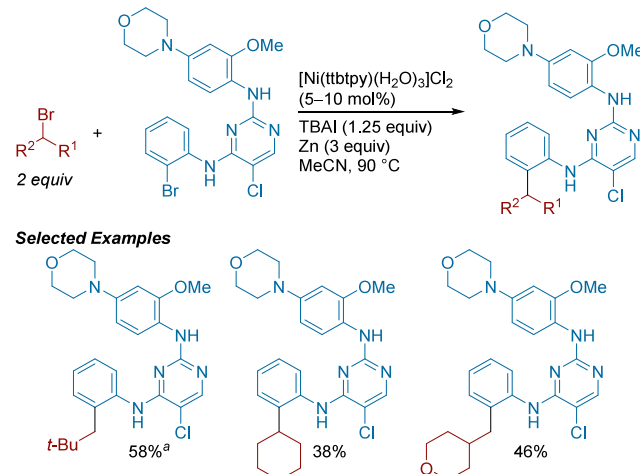
<sup>a</sup>(a) With 1.5 equiv glucosyl bromide and 15 mol% MgCl<sub>2</sub>. (b) Ratio in parentheses refers to  $\alpha/\beta$  ratio.

analogy to other Ni XEC reactions, the mechanism is proposed to involve a glucosyl radical intermediate that reacts with an arylnickel(II) intermediate. High  $\beta$ -selectivity is proposed to arise from the steric bulk of the terpyridine ligand, favoring  $\beta$ -attack of the glucosyl radical by nickel. This complements their previous report<sup>220</sup> with monodentate pyridine as ligand, which allows for  $\alpha$ -selective XEC due to the lability and decreased steric profile of pyridine compared to ttbtpy (see section 4.3, Scheme 257). For electron-rich aryl iodides, MgCl<sub>2</sub> was necessary to maintain high selectivity, presumably through activation of Zn for nickel(II) reduction to nickel(0). In addition to a broad scope, this method enabled access to

intermediates of pharmaceutically relevant compounds Salmo-chelin and Canagliflozin.

Merck & Co department of Discovery Chemistry, led by Mennie and Levi, described the alkylation of a complex aryl bromide scaffold to produce a variety of ATP-competitive kinase inhibitor derivatives through XEC (Scheme 99).<sup>222</sup>

**Scheme 99.** Late-Stage Ni-Catalyzed XEC of a Complex Aryl Bromide with Alkyl Bromides (2020)<sup>a</sup>

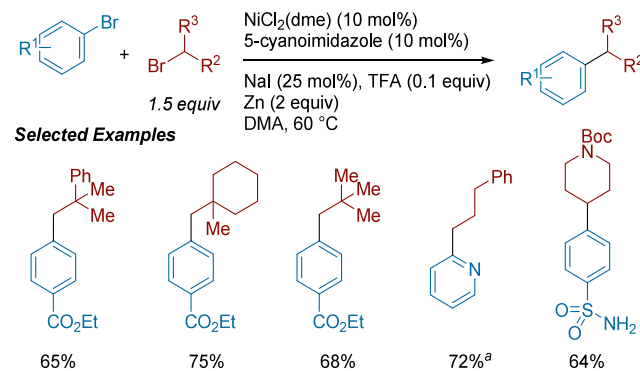


<sup>a</sup>With alkyl iodide instead.

Using a high-throughput screening approach, the authors identified an optimal set of conditions that gave high chemoselectivity and product formation, enabling derivatization of the model aryl bromide with a number of primary and secondary alkyl bromides. Notably, sterically challenging neopentyl coupling was improved significantly using the more reactive iodide.

Neopentyl alkyl bromides can be especially challenging substrates for most XEC conditions, usually requiring large amounts of NaI or switching to the neopentyl iodide. Bo Qu and Desrosiers reported that a nickel catalyst with a 5-cyanoimidazole ligand (along with other 2-cyanopyridine ligands) was especially effective for the XEC of aryl bromides with neopentyl bromides (Scheme 100).<sup>223</sup> This new catalyst was discovered by mining the large Boehringer Ingelheim

**Scheme 100.** Ni-Catalyzed XEC of Aryl Bromides with Neopentyl Bromides Enabled by 5-Cyanoimidazole Ligand (2020)<sup>a</sup>

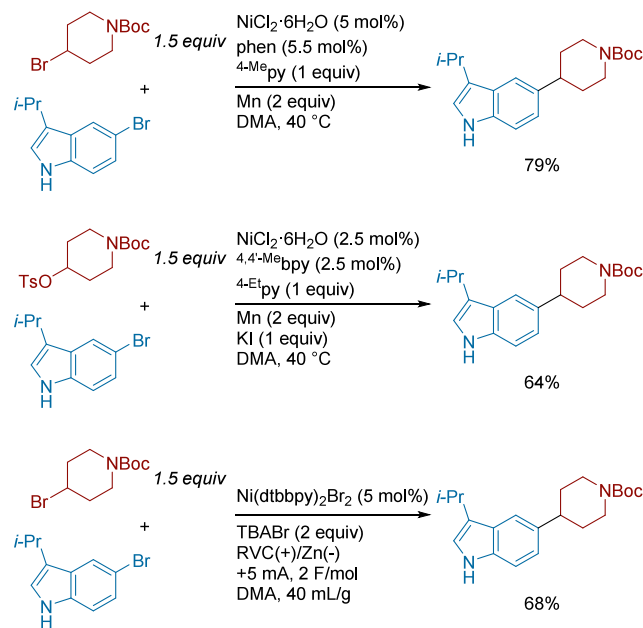


<sup>a</sup>With 2 mmol of aryl bromide.

compound library for new ligands, using a strategy we had previously developed with Pfizer ([Scheme 91](#)).<sup>32</sup> Results from structure activity relationship studies showed that the presence and positioning of the nitrile moiety on the imidazole core was crucial for reactivity.

The Chemical Process Development team at Bristol Myers Squibb, led by Beutner and Simmons, evaluated several  $C(sp^2)-C(sp^3)$  cross-coupling methodologies, to form a representative pharmaceutical intermediate (**Scheme 101**).<sup>46</sup>

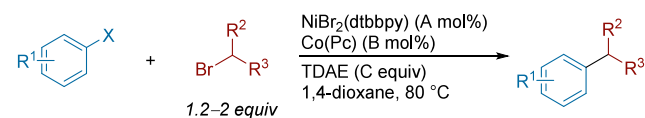
**Scheme 101. Process Chemistry Evaluation of XEC Against Various Other C(sp<sup>2</sup>)–C(sp<sup>3</sup>) Cross-Coupling Approaches (2021)**



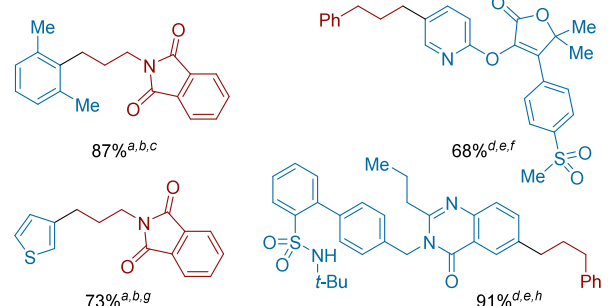
The authors report a variety of conditions, including both cross-coupling and XEC, as well as couplings using alkyl bromides and tosylates. While the authors also attempted photochemical-mediated XEC and XEC with organic reductants, these methods were less appealing, due to lower assay yields or poor commercial availability of the reductant, respectively. While the XEC methods offered advantages over Suzuki coupling methods also explored in this work, the authors attributed major outstanding challenges to the heterogeneous reaction conditions and cost of alkyl halides (relative to the analogous alcohol). Deuterium studies of the electrochemically driven XEC reaction unequivocally demonstrated that the Ar–H side product was derived from  $\beta$ -hydride elimination of the alkyl coupling partner. This is a key finding for the field. The authors conclude the work with a quantitative comparison of all available C(sp<sup>2</sup>)–C(sp<sup>3</sup>) catalytic coupling methods and a process chemistry viewpoint on their relative merits and challenges.

A breakthrough in the use of tetrakis(dimethylamino)-ethylene (TDAE), a homogeneous reductant, for XEC was reported by Hazari and co-workers in collaboration with a Merck team led by Zultanski. Utilizing a cobalt phthalocyanin cocatalyst for radical generation in dioxane greatly broadened the scope of XEC couplings using (dtbbpy)NiBr<sub>2</sub> and TDAE (**Scheme 102**).<sup>50</sup> In accordance with literature precedent and their own mechanistic studies,<sup>174,224</sup> Co(Pc) was proposed to form the alkyl radical from the alkyl bromide by S<sub>N</sub>2 followed

**Scheme 102. Homogeneous Nickel and Cobalt Co-Catalyzed XEC of Aryl Halides with Alkyl Bromides (2020)<sup>a</sup>**



## ***Selected Examples***



<sup>a</sup>Co(Pc) = cobalt phthalocyanin. (a) With 2 equiv alkyl bromide. (b) With aryl bromide, (c) A = 10, B = 0.5, C = 1.6, (d) With aryl iodide. (e) With 1.6 equiv alkyl bromide. (f) A = 5, B = 0.5, C = 1.4, (g) A = 0.5, B = 5, C = 1.6. (h) A = 5, B = 5, C = 1.4.

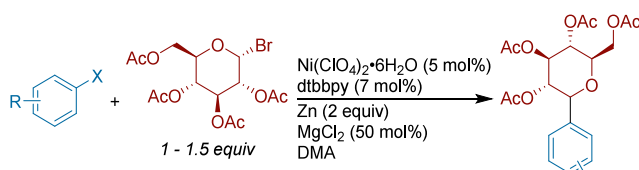
by homolysis. Branched secondary alkyl iodides and branched benzyl chlorides were successfully coupled in moderate yields, but secondary alkyl bromides were unsuccessful (perhaps due to the S<sub>N</sub>2 mechanism). As in other cocatalyst systems, the ratio of the two catalysts could be tailored to the substrate pair to optimize the yield. As homogeneous conditions greatly simplify both large- and small-scale chemistry, further advances in this area would be impactful.

While the cross-electrophile coupling of glycosides with electron-rich aryl bromides and iodides had been investigated in previous studies, Qun Qian and co-workers noted that further development in this area to include electron-poor aryl halides was needed (**Scheme 103**).<sup>225</sup> As an additional study, they also evaluated a modified version of their conditions to couple glycosyl bromides with electron-rich aryl iodides that had not been previously utilized. These reactions show slight favorability toward the  $\alpha$ -product in both methods. Their methods tolerated multiple electron-withdrawing functionalities such as ester and cyano groups. In their scope of electron-rich arenes, *ortho*-substitution and heterocycles were compatible.

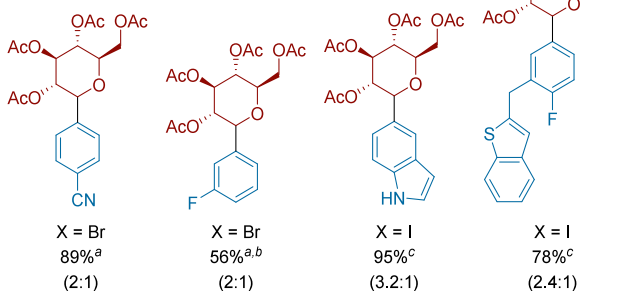
In 2021, our group, in collaboration with Ying Wang and the Advanced Chemistry Technologies Group at AbbVie, described the application of XEC in 96-well plate format for small molecule library synthesis (**Scheme 104**).<sup>226</sup> Using the ChemBead technology previously developed at AbbVie<sup>227,228</sup> problems with weighing and stirring small quantities of metal powders could be solved by using calibrated scoops and a simple plate shaker. Application of XEC to a wide array of challenging heteroaryl halides and alkyl bromides led to the discovery of a new ligand, BpyCam. Out of 222 reactions tested, a 55% hit rate was observed with three different sets of conditions. This compared favorably to other common cross-coupling reactions used at AbbVie.

Dawei Teng and co-workers reported a new spirocyclic PyOx ligand for the XEC of aryl bromides with secondary alkyl bromides (**Scheme 105**).<sup>229</sup> The authors highlight the design of the ligand: the pyridyl moiety promoting reductive

**Scheme 103. Ni-Catalyzed XEC of Aryl Halides with Glycosyl Halides (2021)<sup>a</sup>**



**Selected Examples**

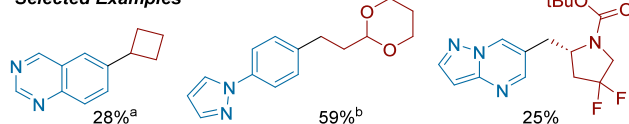


<sup>a</sup>(a) With DMA/THF (1:4) at 25 °C. (b) Aryl iodide was used. (c) Modified conditions: 10 mol% of Ni catalyst, 15 mol% of ligand, and 100 mol% of MgCl<sub>2</sub> in an ice-bath. Parentheses refer to  $\alpha/\beta$  ratio.

**Scheme 104. Ni-Catalyzed XEC of Aryl Bromides with Alkyl Bromides in 96-Well Plates Enabled by ChemBeads (2021)<sup>a</sup>**

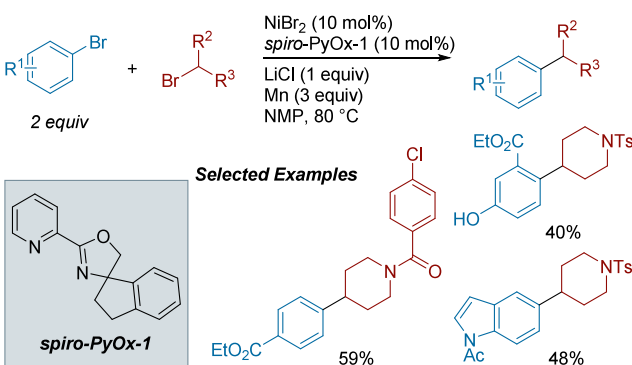


**Selected Examples**



<sup>a</sup>(a) Isolated yield on 0.1 mmol scale using ChemBeads. (b) Isolated on 0.5 mmol scale using Zn powder and stir bars.

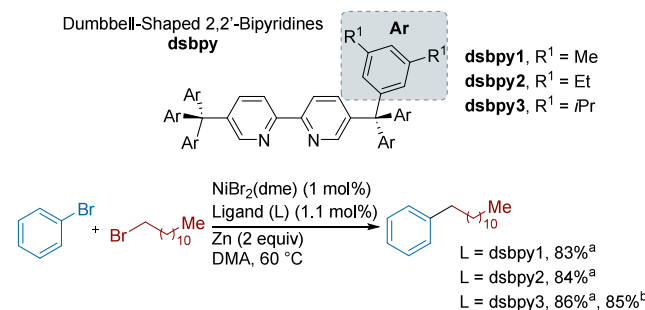
**Scheme 105. New Spirocyclic PyOx Ligand for Ni-Catalyzed XEC of Aryl Bromides with 2° Alkyl Bromides (2021)**



elimination, the oxazole promoting oxidative addition, and the spiro moiety modulating the ability for the ligand to bind to the metal center. A wide array of secondary heterocyclic alkyl bromides was tested.

Sawamura, Iwai, and co-workers reported on the design of a “dumbbell-shaped” bipyridines for XEC of aryl bromides with alkyl bromides at low catalyst loadings (Scheme 106).<sup>230</sup> The

**Scheme 106. Dumbbell-Shaped Ligands Enable Ni-Catalyzed XEC of Aryl Bromides with Alkyl Bromides at Low Catalyst Loading (2021)<sup>a</sup>**



<sup>a</sup>(a) NMR yield. (b) Isolated yield.

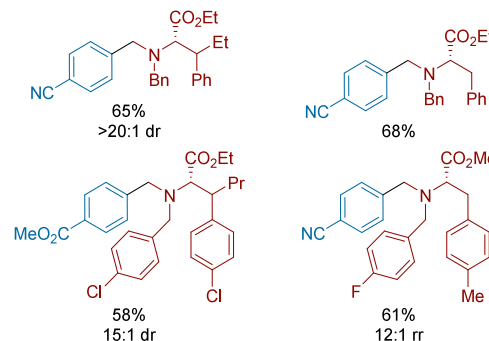
2,2'-bipyridine ligands featured large triarylmethyl groups at the 5 and 5' positions and the authors show evidence that these prevent the formation of (L)<sub>2</sub>Ni and (L)<sub>3</sub>Ni complexes that might hinder catalytic efficiency. The optimal ligands (depicted in Scheme 106) afforded excellent yields at low catalyst loading (1 mol% [Ni]). These same ligands were also helpful for dual catalytic photoredox Ni and Ir decarboxylative coupling reactions.

Shi Tang, Jin-Heng Li, and co-workers reported an unusual 1,4-aryl migration/arylation cascade XEC of  $\alpha$ -amino- $\beta$ -bromo acid esters with aryl bromides (Scheme 107).<sup>231</sup> Using DFT

**Scheme 107. Ni-Catalyzed 1,4-Aryl Migration XEC of  $\alpha$ -Amino- $\beta$ -bromo Acid Esters with Aryl Bromides (2021)**



**Selected Examples**

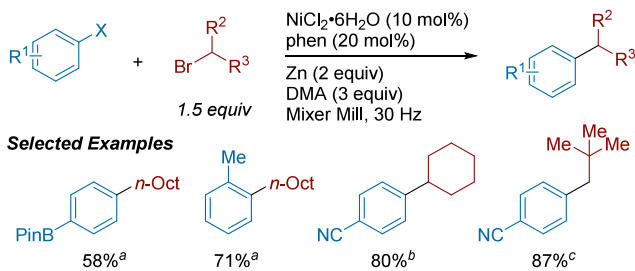


calculations, the authors propose that the 1,4-aryl migration occurs via an intramolecular *ipso*-attack from the  $\beta$ -alkyl radical, forming a spiro 5-membered *N*-heterocycle bound to a benzene radical. This intermediate then undergoes C–C homolytic cleavage, followed by rearomatization of the aryl group to furnish an  $\alpha$ -aminoalkyl radical that is coupled in the usual fashion. The authors employ melamine (2,4,6-triamino-*s*-triazine) as a reaction additive, and propose it may act as a labile ligand, as the amount of migratory coupling was greatly

diminished when melamine was excluded from the reaction. A majority of their scope involves symmetric dibenzyl substituted amines (e.g.,  $R^4 = \text{CH}_2\text{Ar}$ ), but the authors see selective aryl migration of the more electron-rich aromatic ring in unsymmetrical dibenzyl substituted amines. Amino acid esters with  $R^4 = \text{Me}$  or  $\text{H}$  are inefficient substrates in this reaction.

Browne and co-workers employed ball-milling technique in the XEC of aryl and alkyl bromides and iodides (**Scheme 108**).<sup>232</sup> Using only 3 equiv of DMA as a liquid-assisted

**Scheme 108. Mechanochemical Ni-Catalyzed XEC of Aryl Halides with Alkyl Halides in a Ball Mill (2021)<sup>a</sup>**

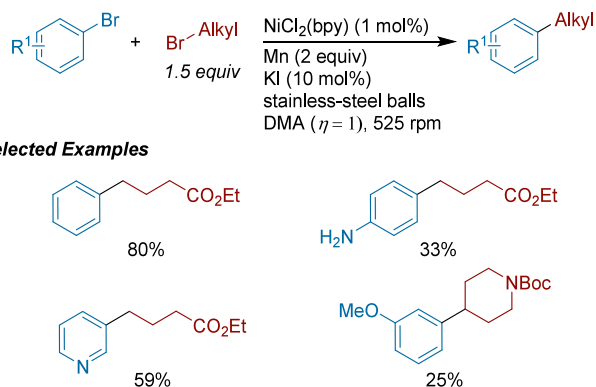


<sup>a</sup>(a) With aryl bromide and alkyl iodide. (b) With aryl iodide and alkyl bromide. (c) With aryl iodide and alkyl iodide.

grinding (LAG) agent, the method is virtually solvent-free and was successful in the cross-coupling of a variety of aryl halides with primary and secondary alkyl halides in good yields. Although ball-milling is relatively unexplored, this approach is exciting because it can address the problems of using amide solvents and mixing.

Gang Zou, Weijia Shi, and Sisi Wu concurrently reported the coupling of aryl and alkyl bromides using liquid-assisted grinding via ball milling (**Scheme 109**).<sup>233</sup> In addition to

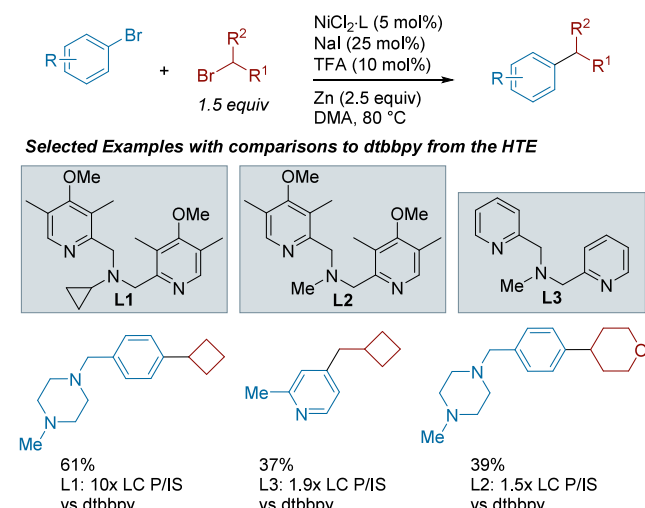
**Scheme 109. Mechanochemical Ni-Catalyzed XEC of Aryl Halides with Alkyl Halides in a Ball Mill (2021)**



evaluating standard reaction parameters, the authors found that optimizing the mechanical conditions, such as rotational speed of the mill, stainless steel ball size and count, and the percentage of the jar that is filled, was crucial for reaction efficiency. Control experiments showed a better water-tolerance under mechanochemical conditions than in previous chemical reports, with the reaction still proceeding under air, albeit with an increased reaction time. The functional group tolerance is wide, particularly with respect to diversity of the aryl coupling partner, and catalyst loading is low compared to other XEC reports.

Using microscale HTE techniques, the Advanced Chemical Technologies Group at AbbVie reported the discovery of di(2-picoly)amines (DPA) as a new class of ligands for cross-electrophile coupling reactions of aryl bromides and alkyl bromides (**Scheme 110**).<sup>234</sup> The new set of ligands are readily

**Scheme 110. Development of DPA Ligands and Application to Ni-Catalyzed XEC of Diverse Aryl Bromides with Alkyl Bromides (2022)**

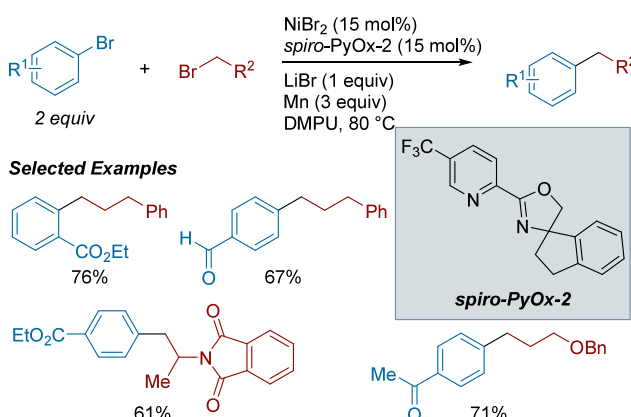


accessible through a single step reaction of commercially inexpensive starting materials. The generality of the new DPA ligands was tested through an HTE approach using 5 different aryl bromides with various electronic properties and 15 different primary and secondary alkyl halides, while using Zn as a terminal reductant (on ChemBeads). The results from HTE suggested that the DPA ligands are effective in most cases and desired cross-coupled products could be obtained. Furthermore, head-to-head comparisons of the DPA ligands with dtbbpy were also carried out for selected substrate pairs under identical reaction conditions. For these substrate pairs, DPA ligands gave higher yields compared to dtbbpy in most cases, highlighting the utility of this new type of ligand. These ligands are a rare example of a bidentate, but redox-innocent ligand in XEC.

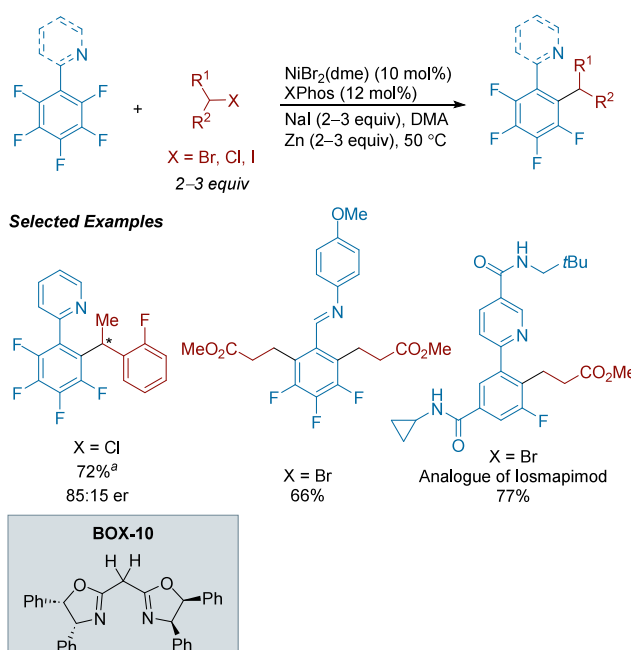
Dawei Teng and co-workers reported the use of one of their spiro-ligands for the cross-electrophile coupling of aryl bromides with primary alkyl bromides (**Scheme 111**).<sup>235</sup> Modification of the previously reported spiro ligand with a  $\text{CF}_3$  group on the 5-position of the pyridine ring resulted in improved yields. Using this ligand, a select number of alkyl bromides were successfully coupled with electron-deficient aryl bromides to give the desired alkylated arenes, including the formation of an intermediate toward the synthesis of 5-HT<sub>2A</sub> agonists.

An attractive approach to alkylated fluoroarenes is the selective alkylation of C–F bonds. Zhuanzhi Shi and co-workers reported the first site-selective defluorinative alkylation of polyfluoroarenes using an XEC strategy (**Scheme 112**).<sup>236</sup> The method achieves selective alkylation at the C–F bond(s) *ortho*- to directing groups such as 2-pyridyl substituents and imines. A variety of primary and secondary alkyl halides could be successfully engaged in cross-coupling, including examples with methyl and benzylic substrates. Furthermore, the method could be rendered asymmetric by employing a chiral

**Scheme 111. Development of Spiro-PyOx Ligand and Application to XEC of Aryl Bromides with 1° Alkyl Bromides (2022)**



**Scheme 112. Ni-Catalyzed XEC of Aryl Fluorides with Alkyl Halides by a Directing-Group Approach (2022)<sup>a</sup>**

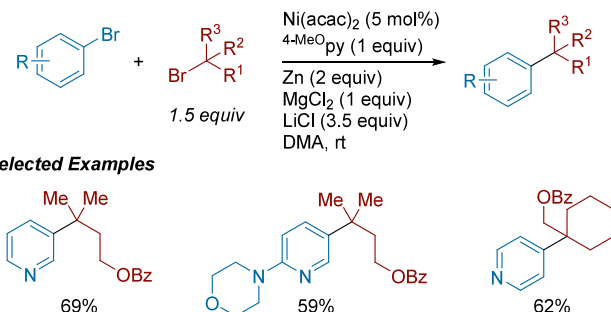


<sup>a</sup>With bis((4*R*,5*S*)-4,5-diphenyl-4,5-dihydrooxazol-2-yl)methane (BOX-10) (12 mol%) as ligand.

bisoxazoline ligand, and a set of secondary benzylic chlorides were arylated in high yields with good enantioselectivity. An examination of polyfluoroarenes showed that substrates with higher fluorine substitution were most effective for cross-coupling, but substrates with fluoride substitution as low as two could give the desired monofluorinated product, albeit in diminished yields. Mechanistically, the presence of an alkyl radical intermediate was established by the observation of alkylated adducts with 1,1-diphenylethylene. To demonstrate the feasibility of oxidative addition to C–F bonds by Ni(0), the authors isolated and characterized an (aryl)nickel(II) complex from treatment of Ni(COD)<sub>2</sub> with a perfluoroarene bearing two pyridyl directing groups. The resulting complex was found to be competent in producing the cross-coupled product in the presence of alkyl bromide under standard reaction conditions.

Fan Wu, Hegui Gong, and Quan Lin reported a cross-electrophile coupling of heteroaryl bromides with tertiary alkyl halides (Scheme 113).<sup>237</sup> Heteroaromatics including substituted

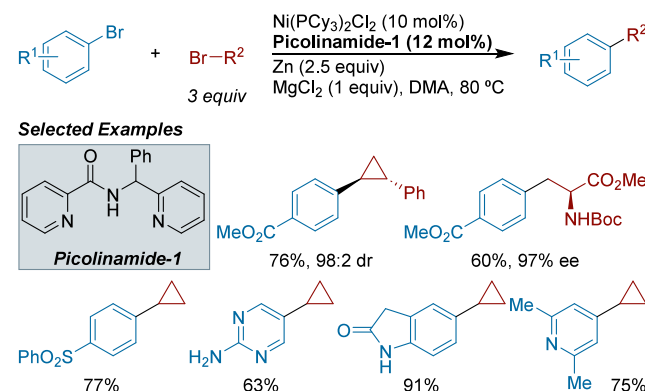
**Scheme 113. Ni-Catalyzed XEC of Heteroaryl Iodides with Tertiary Alkyl Bromides (2022)**



pyridine, thiophene, quinoline, carbazole, dibenzofuran, and dibenzothiophene were all shown to couple with tertiary alkyl bromides in good yields. It is worth noting that 2-bromopyridines were not tolerated in this reaction. This was explained by the homocoupling byproducts, 2,2'-bipyridines, likely inhibiting the productive catalytic cycle. MgCl<sub>2</sub> and LiCl were observed to be crucial for the reaction to occur, and the authors indicated that it was likely that these chloride salts were accelerating the stoichiometric reaction between arylnickel(II) and *tert*-butyl bromide. As with previous reports with tertiary alkyl coupling, an electronically tuned pyridine ligand played a central role (4-MeOpy).

Jian Jin and co-workers developed a novel picolinamide derived NNN pincer ligand to successfully couple a variety of aryl bromides with alkyl bromides, with a focus on cyclopropyl bromides (Scheme 114).<sup>238</sup> The authors hypothesized that

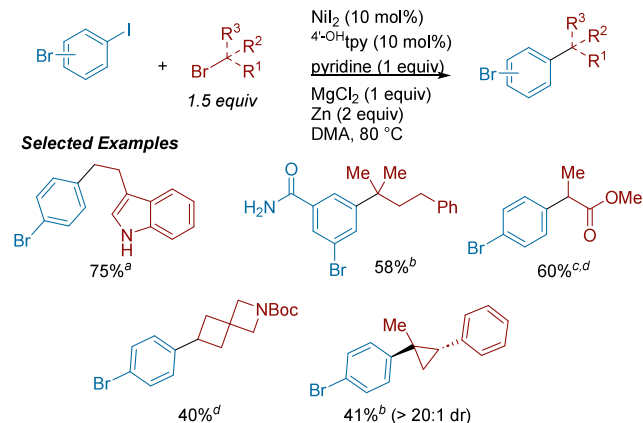
**Scheme 114. Design of Picolinamide Ligands for Ni-Catalyzed XEC of (Hetero)Aryl Bromides with Alkyl Bromides (2022)**



most ligands used in XEC are not bulky enough and are too rigid for these types of alkyl electrophiles. They turned toward picolinamide ligands for their sterically congested but flexible nature and adding substituents to the 2-pyridinylmethyl position of the ligand backbone increased the yield of the desired product. The authors explored a large variety of (hetero)aryl bromide coupling partners with a variety of functional groups. Broadly, electron-rich (hetero)aryl coupling partners proceeded with higher yields than their electron-deficient counterparts.

Chao Li and co-workers developed a C(sp<sup>2</sup>)–I selective coupling of bromo(iodo)arenes with a variety of alkyl bromides (**Scheme 115**).<sup>178</sup> This reaction proves synthetically

**Scheme 115.** Ni-Catalyzed, C(sp<sup>2</sup>)–I Selective XEC of Bromo(iodo)arenes Iodides with Alkyl Bromides (2023)<sup>a</sup>

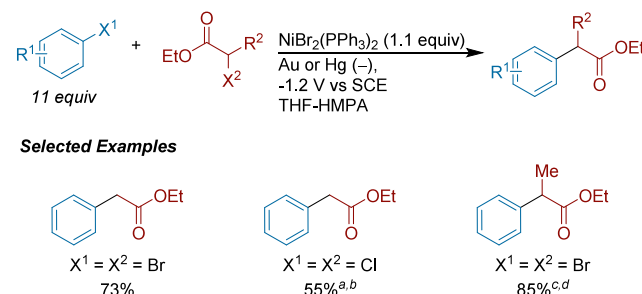


useful in combination with other common XEC methods, allowing for iterative routes to more complex structures. Ligand optimization found several trends: (1) tridentate ligands prevented isomerized product formed from tertiary radical rearrangement and (2) more electron rich terpyridine ligands delivered higher yields of the desired cross product. The scope exhibits excellent functional group compatibility with high retention/isomerization ratios, as well as excellent C(sp<sup>2</sup>)–I selectivity. Based on mechanistic studies, the authors propose that a nickel(I) complex activates the alkyl bromide via an SET process, followed by reduction to generate an alkynickel(I) complex. This complex then undergoes oxidative addition with bromo(iodo)arene to generate a nickel(III) adduct, which then forms the desired product by reductive elimination. This is a rare example of *tert*-alkyl bromide coupling with a tridentate ligand (vs monodentate pyridine ligands).

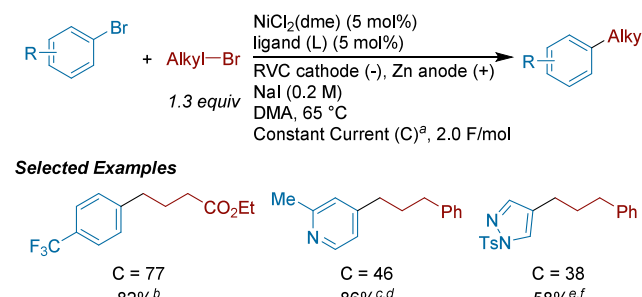
**4.2.1.2. Photochemical and Electrochemical Approaches.** In 1988, Jutand and co-workers published an electrochemical method to couple aryl halides with  $\alpha$ -haloesters in the presence of a nickel catalyst using gold or mercury cathodes (**Scheme 116**).<sup>239</sup> Under these conditions, the typical reductive side-products associated with cross-electrophile coupling were observed including protodehalogenated aryl halide as well as aryl dimer. They had investigated the use of NiBr<sub>2</sub>(diphos) as the active catalyst, but focused on NiBr<sub>2</sub>(PPh<sub>3</sub>)<sub>2</sub>. Using a solvent mixture consisting either of THF and HMPA or THF and NMP, the group was successfully able to couple both aryl bromides and chlorides with  $\alpha$ -bromo- and  $\alpha$ -chloroesters. In some examples, yields were further improved with the addition of triethylamine but in other cases this could inhibit catalysis.

Perkins, Pedro, and Hansen at Pfizer Process noticed the existing limitations of electrochemical applications in cross-electrophile coupling and, in consultation with our group, developed an approach for the coupling of unactivated aryl and alkyl bromides (**Scheme 117**).<sup>240</sup> Their setup consisted of an undivided cell with an RVC cathode and a Zn anode, and NaI

**Scheme 116.** Electrochemical Ni-Catalyzed XEC of Aryl Halides with Alkyl Halides (1988)<sup>a</sup>



**Scheme 117.** Electrochemical Ni-Catalyzed XEC of Aryl Bromides and Alkyl Bromides (2017)<sup>a</sup>

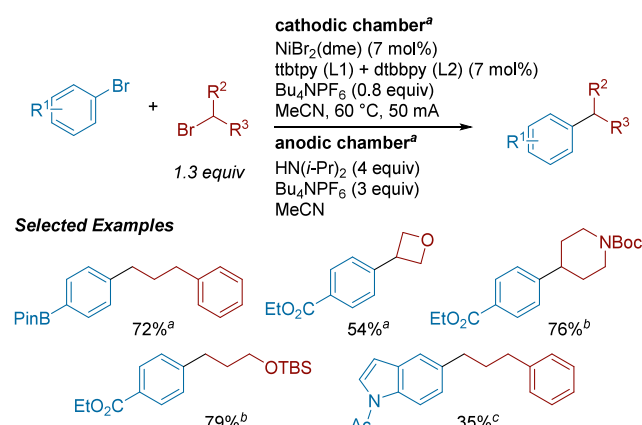


served as both additive and electrolyte. It should be noted that using Fe as an anode also worked well (as preceded in other classes of XEC). In addition to other more usual variables, selectivity could be improved by tuning the current. A variety of standard ligands were compatible: <sup>4,4'-MeO</sup>bpy as well as <sup>MeO</sup>PyBCam, PyBCam, and <sup>MeO</sup>PyCam. In cases where metallic powder reductants afforded low yields, such as in coupling some electron-poor heterocycles, these electrochemical conditions prove beneficial with yields above 50%.

Electrochemical reactions most often use a sacrificial anode in an undivided cell for simplicity, but a divided cell offers opportunities for driving XEC with a wide array of anodic processes. In collaboration with our group, Pfizer, led by Hansen, demonstrated an electrochemical XEC of aryl bromides with alkyl bromides in a divided cell utilizing amine oxidation at the anode (**Scheme 118**).<sup>49</sup> Notably, acetonitrile, a more process- and environmentally friendly solvent, could be utilized instead of amide solvents. Finally, echoing early reports on cross-electrophile coupling, the optimal conditions utilized a synergistic mixture of two catalysts (with ttbipy and dtbbpy as ligands), both of which were not efficient when used alone. The terpyridine favors activation of the alkyl bromide while the bipyridine favors activation of the aryl bromide, and reactivity could be tuned by adjusting the ratio of catalysts (see also **Scheme 122**).<sup>241</sup>

Tian-Sheng Mei and co-workers reported the electrochemical chain-walking cross-electrophile coupling of aryl halides with  $\omega$ -bromoalkyl arenes to give 1,1-diaryllalkanes

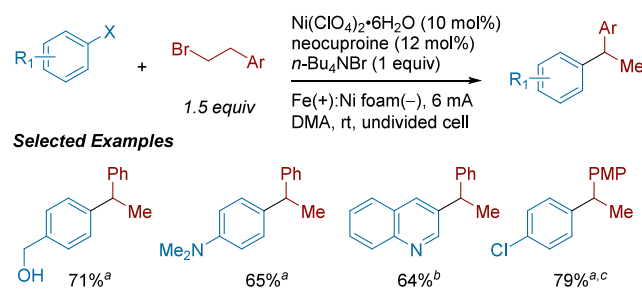
**Scheme 118. Electrochemical Ni-Catalyzed XEC of Aryl Bromides with Alkyl Bromides Using Amine Terminal Reductant in Acetonitrile (2019)<sup>a</sup>**



<sup>a</sup>(a) Chamber equipped with RVC electrode. (b) L1:L2 = 1:2. (c) L1:L2 = 1:1. (d) L1:L2 = 1:4.

(Scheme 119).<sup>242</sup> The catalyst is similar to that used with chemical reductants, possessing steric hindrance around the

**Scheme 119. Electrochemical Ni-Catalyzed Chain-Walking XEC of Aryl Halides with Alkyl Bromides (2019)<sup>a</sup>**

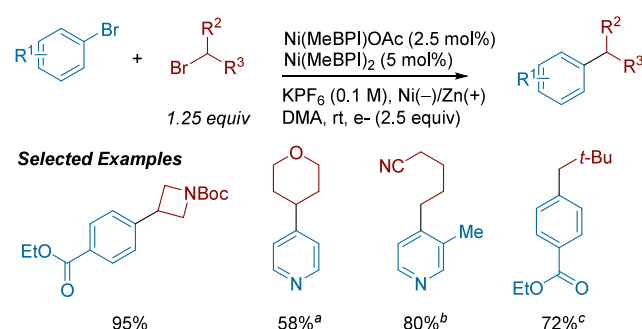


<sup>a</sup>(a) X = Br, (b) X = Cl. (c) PMP = 4-methoxyphenyl.

binding nitrogen atoms. A broad scope of electron-rich aryl bromides and electron-deficient aryl chlorides could be coupled with 1-bromo-3-aryl alkanes with good functional group tolerance. Experimental studies at different constant potentials combined with cyclic voltammetry (CV) studies on individual reaction components led the authors to propose preferential oxidative addition of the aryl bromide followed by radical capture at arylnickel, consistent with previous reports.<sup>160</sup> The authors propose a more thermodynamically stable benzynickel intermediate is formed via  $\beta$ -hydride elimination/reinsertion, followed by reductive elimination to furnish the desired product.

Utilizing strategies adapted from the flow battery literature, Sevov and co-workers took advantage of a variety of homogeneous redox shuttles for use as overcharge protection in an electroreductive XEC reaction of aryl iodides with alkyl bromides (Scheme 120).<sup>243</sup> As a showcase of the utility of redox shuttles, secondary alkyl bromides gave significantly higher yields with the shuttle than without. The authors propose the shuttle serves as an internal limiter that is enabled when the current exceeds the rate of catalysis. This allows for productive coupling at larger scales (75 mmol) with higher current density (15 mA/cm<sup>2</sup>) and a minimal decrease in yield,

**Scheme 120. Electrochemical Ni-Catalyzed XEC of Aryl Bromides with Alkyl Bromides Enabled by Overcharge Protection (2020)<sup>a</sup>**

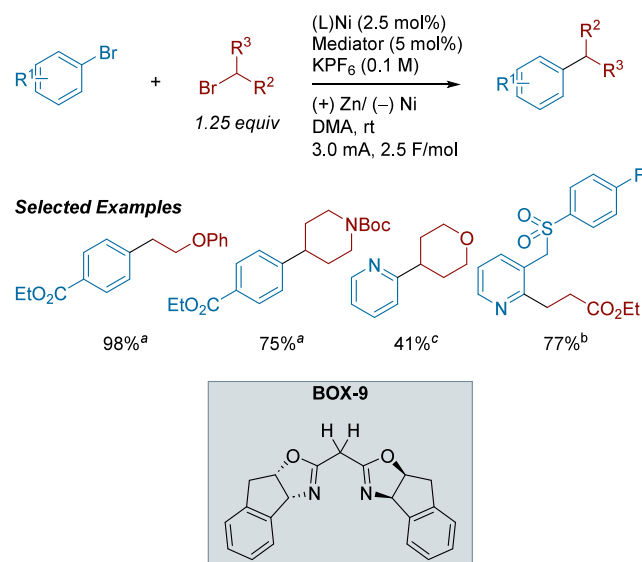


<sup>a</sup>(a) With 2 equiv alkyl bromide and NaI in place of KPF<sub>6</sub>. (b) With 1.5 equiv alkyl bromide and NaI in place of KPF<sub>6</sub>. (c) With 2 equiv alkyl bromide and added  $\text{PPh}_3$  (2.5 mol%).

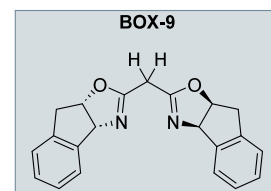
which the authors attribute to increased reaction temperature from increased resistance.

Utilizing mediator-assisted electrocatalytic conditions, the Sevov lab reported the XEC of aryl and alkyl bromides (Scheme 121).<sup>39</sup> The authors report a set of catalyst-mediator

**Scheme 121. Electrochemical Ni-Catalyzed XEC of Aryl Bromides with Alkyl Bromides Enabled by Combinations of Catalysts and Overcharge Protectors (2022)<sup>a</sup>**



<sup>a</sup>(a) With  $\text{Ni}(\text{MeBPI})\text{OAc}$  as (L)Ni and  $\text{Ni}(\text{MeBPI})_2$  as mediator. (b) With (BOX-9)NiBr<sub>2</sub> as (L)Ni and  $\text{Ni}(\text{MeBPI})_2$  as mediator. (c) With (dtbbpy)NiBr<sub>2</sub> as (L)Ni and [(tpy)<sub>2</sub>Ni](PF<sub>6</sub>)<sub>2</sub> as mediator.

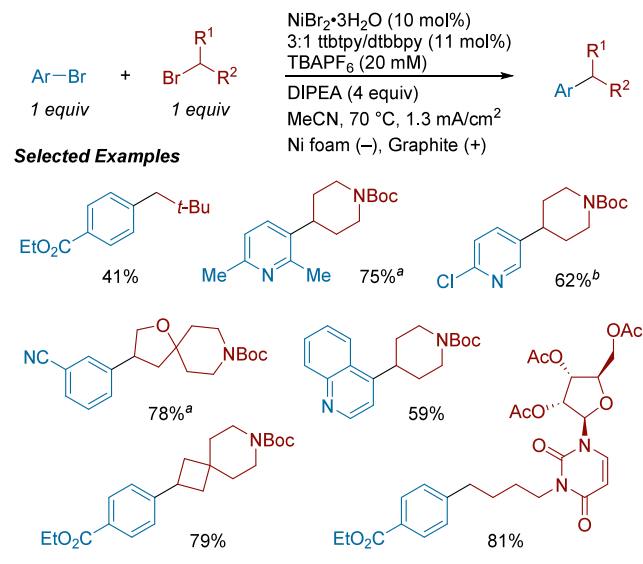


combinations, comprised of ligands from four separate classes (BPI, BOX, bpy, and PyOX), which the authors propose offers complementary reactivity and stability, and could be used both in electrochemical XEC, as well as in reactions with stoichiometric metal reductants. Combinations where the reduction potential of the catalyst and mediator are well matched resulted in overcharge protection of the catalyst, and, based on mechanistic studies, the authors propose that the mediator is acting as a redox shuttle, rather than a masked form of the operative catalyst. Of these catalyst-mediator systems, the authors found that  $\text{Ni}(\text{MeBPI})\text{OAc}/\text{Ni}(\text{MeBPI})_2$  and (BOX-

9)NiBr<sub>2</sub>/Ni(<sup>Me</sup>BPI)<sub>2</sub>, which are reduced at the most negative potentials, were the most effective catalyst-mediator systems in the coupling of primary alkyl electrophiles; all four catalyst-mediator systems proved effective in the coupling of secondary alkyl bromides where more common conditions for electrochemical XEC proved ineffective.

Our group reported scalable, greener conditions for the electrochemical XEC of aryl bromides with alkyl bromides (**Scheme 122**).<sup>241</sup> The conditions employ a mixed ligand

**Scheme 122. Electrochemical Ni-Catalyzed XEC of Aryl Bromides with Alkyl Bromides Under Process-Friendly Conditions (2022)<sup>a</sup>**

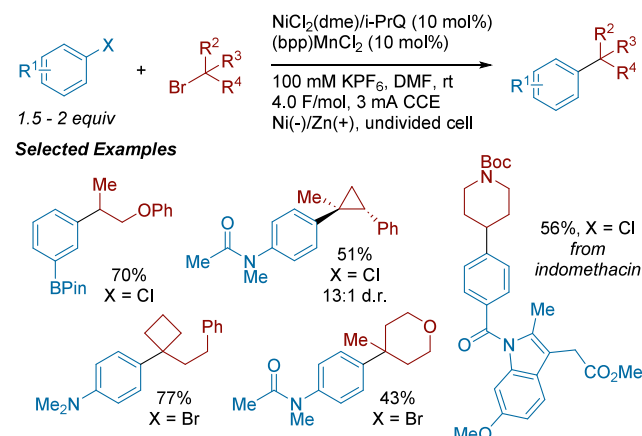


<sup>a</sup>(a) 1:1 ratio of ttbipy/dtbppy. (b) 5:1 ratio of ttbipy/dtbppy.

system to achieve high cross-selectivity, which was found to result from the selective activation of alkyl bromides by ttbipy and aryl bromides by dtbppy. An advantage of mixed ligand systems is that the ratio of each ligand can be tuned based on the rate of activation of each coupling partner, enabling higher cross-selectivities. The reaction can be performed in an undivided cell with a nonamide solvent, acetonitrile, and Hünig's base as the terminal reductant. A broad set of aryl and heteroaryl bromides could be cross-coupled with primary and secondary alkyl bromides in good yields and with good functional group tolerance.

Sevov and co-workers reported the XEC of secondary and tertiary alkyl bromides with aryl halides and triflates using a dual ligand system under electrochemical conditions (**Scheme 123**).<sup>244</sup> The authors capitalized on the differences in reactivity resulting from pyridyl type ligands and phosphines, in which an electrochemically inactive phosphine-ligated nickel(0) complex can selectively activate aryl (pseudo)halides via a 2 e<sup>-</sup> pathway, in conjunction with an electrochemically active complex that selectively activates alkyl halides via a 1 e<sup>-</sup> pathway. The formation of these complexes could occur at mild potentials through a dynamic ligand exchange, allowing for easy control of the redox states of nickel. By employing (bpp)MnCl<sub>2</sub>, the authors avoided the formation of isomerized byproduct, which was observed when using (bpp)NiCl<sub>2</sub> and other first row transition metal bpp complexes. Stoichiometric studies make a convincing case for the ligand exchange process not seen in previous dual-catalyst systems. The substrate scope

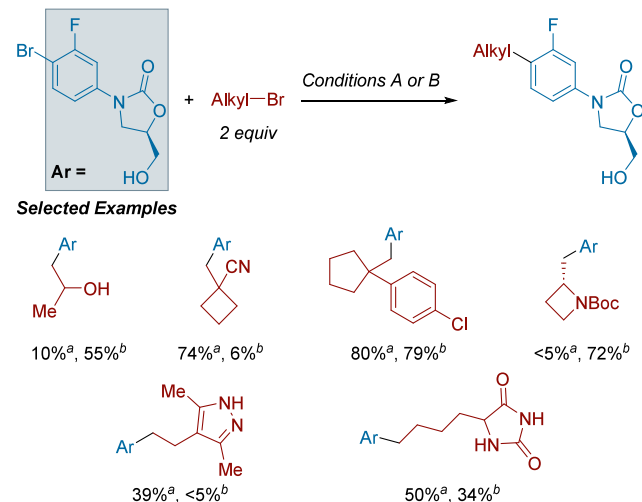
**Scheme 123. Electrochemical Ni-Catalyzed XEC of ArBr/ArCl with 2° and 3° Alkyl Bromides Enabled by Dynamic Ligand Exchange (2022)**



is particularly broad and among the best reported for these challenging classes of couplings. Again, it is notable that monodentate (pyridine) and tridentate (bpp or tpy) ligands appear to work better for tertiary alkyl radicals than bidentate ligands.

Merck, led by Bastidas and El Marrouni, utilized either photo- or electrocatalyzed XEC with a variety of alkyl bromides relevant for medicinal chemistry to access novel tedizolid analogues (**Scheme 124**).<sup>245</sup> In studying the photo-

**Scheme 124. Comparison of Electrochemical and Photochemical XEC Conditions for Coupling Aryl Bromides with Alkyl Bromides (2023)<sup>a</sup>**



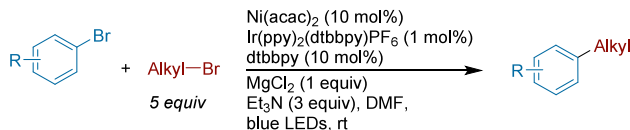
<sup>a</sup>(a) Ir[ dF(CF<sub>3</sub>)ppy]<sub>2</sub>(dtbppy)PF<sub>6</sub> (1 mol%), Ni(dtbppy)Cl<sub>2</sub>·H<sub>2</sub>O (20 mol%), (TMS)<sub>3</sub>SiH (1 equiv), 2,6-lutidine (2 equiv), DME, 450 nm, rt. (b) NiCl<sub>2</sub>(dme) (20 mol%), <sup>4</sup>-MeO-PyCam (20 mol%), C(-)/Zn(+), 0.5 V, NaI (0.8 equiv), DMA.

catalyzed reaction, the authors observed that high light intensity was necessary to achieve high conversion; similarly, for electrocatalyzed XECs, constant voltage showed higher conversion than constant current. In this work, the authors categorized alkyl bromides by coupling efficiency under photo- or electrocatalyzed systems, allowing for some preliminary

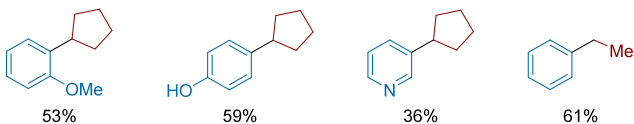
trends to be observed, such as bromoketones and alkyl fluorides only being tolerated under photochemical conditions.

Wu Li, Aiwen Lei, and co-workers developed conditions for a photochemical XEC of aryl bromides with alkyl bromides, utilizing triethylamine as a terminal reductant and  $MgCl_2$  as an additive (**Scheme 125**).<sup>246</sup> While the authors do not propose a

**Scheme 125. Photochemical Nickel and Iridium Co-Catalyzed XEC of Aryl Bromides with Alkyl Bromides (2016)**



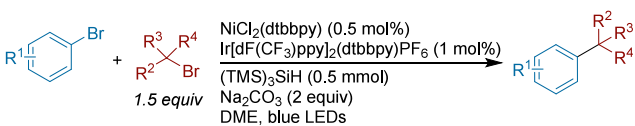
**Selected Examples**



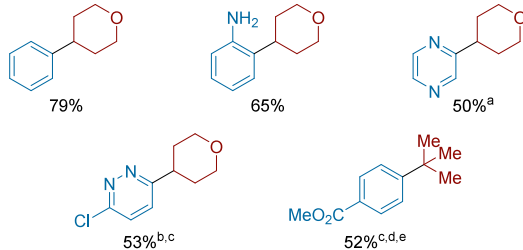
potential role for  $MgCl_2$ , they report a significant decrease in yield in its absence. With  $Ni(acac)_2$  and  $Ir(ppy)_2(dtbbpy)PF_6$ , they found reasonable chemoselectivity and no major bias toward electron-rich or electron-poor aryl bromides. Branching secondary alkyl bromides and primary alkyl bromides were both tolerated, giving moderate to high yields.

In 2016, MacMillan and co-workers designed a photochemical approach to XEC of aryl bromides with alkyl bromides that relies upon a silane reductant to handle alkyl radical generation by halogen atom transfer (**Scheme 126**).<sup>43</sup>

**Scheme 126. Photochemical Nickel and Iridium Co-Catalyzed XEC of Alkyl Bromides and Aryl Bromides with Silyl-Mediated Radical Formation (2016)<sup>a</sup>**



**Selected Examples**



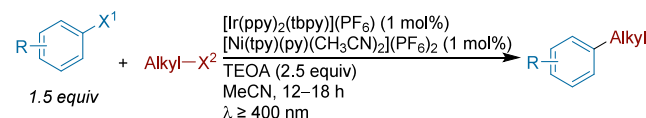
<sup>a</sup>(a) Used LiOH in place of  $Na_2CO_3$ . (b) Aryl chloride was used. (c) 10 mol% of Ni catalyst added. (d) Dioxane used as solvent. (e) Reaction ran for 48 h.

This photochemical setup operates on the hypothesis that when excited, this catalyst can oxidize bromide to  $Br\bullet$ . The  $Br\bullet$  can abstract the H atom from  $(TMS)_3Si-H$  to form the  $(TMS)_3Si\bullet$ , and  $(TMS)_3Si\bullet$  abstracts a bromine atom from the alkyl halide to generate  $Alkyl\bullet$ . This radical then participates in oxidative ligation with  $(L)Ni^{II}(Ar)Br$  in the usual fashion. In this mechanism, the iridium catalyst acts both as an oxidant, cultivating the radical generation pathway, and

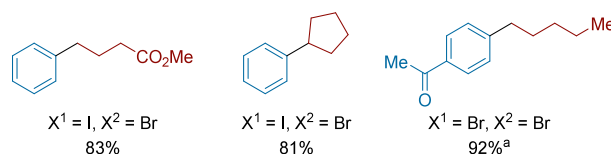
as a reductant to turn over the nickel. Couplings with sterically hindered alkyl partners were generally well-tolerated in addition to a variety of heterocycles. Primary, secondary, and tertiary alkyl coupling partners proceeded successfully in addition to saturated ring systems. Separating the radical generation step from the nickel catalyst has several particularly beneficial effects and this system has seen widespread use.

Concurrently with these other seminal reports, the Vannucci group described a method for the coupling of alkyl bromides with aryl iodides and bromides using photochemical XEC and triethanolamine (TEOA) as the terminal reductant (**Scheme 127**).<sup>247</sup> In XEC conditions under white light, filtering UV and

**Scheme 127. Photochemical Nickel and Iridium Co-Catalyzed XEC of Aryl Bromides with Alkyl Bromides (2017)<sup>a</sup>**



**Selected Examples**



<sup>a</sup>Used 3 equiv of aryl bromide.

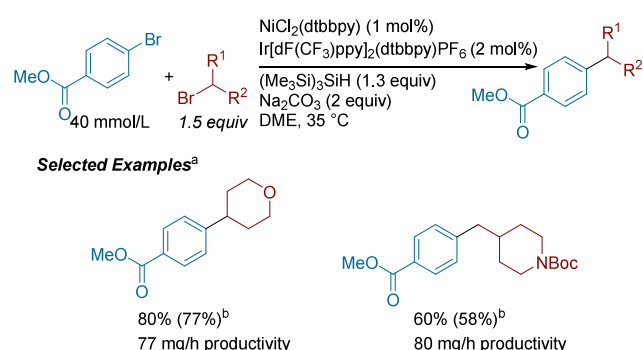
near-UV light with a 400 nm long-pass filter, the authors observed minimal dimerization and good yields of product with a broad range of substrates. While the reaction proceeded well with 1° and 2° alkyl halides, 3° partners were not effective. Throughout this reaction, they observed formation of an insoluble white precipitate, which was characterized as a TEOA halide salt; from this, the authors propose that TEOA, while acting as the reductant, also serves as a halide scavenger.

Scale-up of heterogeneous and photochemical conditions can be challenging, thus Jensen and co-workers, in collaboration with scientists at Novartis, developed a continuous stirred-tank reactor (CSTR) cascade, demonstrating the technology on a silyl radical-mediated metallaphotoredox cross-coupling of ethyl 4-bromobenzoate and alkyl bromides using an insoluble, inorganic base (**Scheme 128**).<sup>248</sup> Using this technology, the authors showed efficient gram-scale coupling of methyl 4-bromobenzoate in continuous flow (40 mmol/L) with a primary and secondary alkyl bromide in 60% and 80% yields, respectively.

AbbVie Medicinal Chemistry, led by Dombrowski and Gesmundo, compared XEC reactions under heterogeneous metal reductant and photoredox-mediated conditions, as well as redox-neutral cross-coupling analogues (**Scheme 129**).<sup>249</sup> Both reaction methods were tolerant of primary and secondary alkyl bromides, and, when directly comparing the two cross-electrophile coupling methods, the methods afforded complementary reactivity. Overall, this work provides a rare comparative study of XEC reactions against other cross-coupling methods, highlighting the benefits of each method toward synthetic use in medicinal chemistry applications.

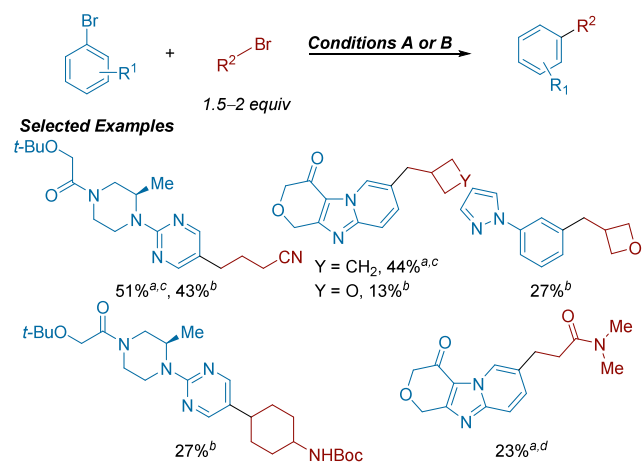
Another approach to handle the challenges of heterogeneous photochemical conditions was reported by Debrouwer and co-

**Scheme 128. Photochemical Nickel and Iridium Co-Catalyzed XEC in Continuous Flow Using a Series of CSTR (2019)<sup>a</sup>**



<sup>a</sup>(a) Yields determined by HPLC analysis. (b) Yields in parentheses obtained from flow setup.

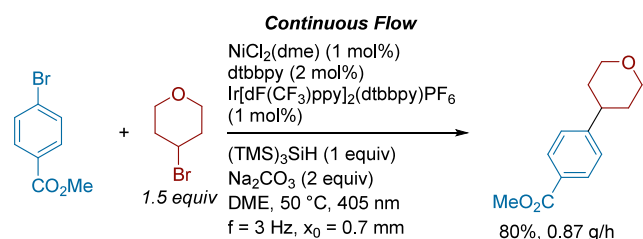
**Scheme 129. Comparison of Chemical and Photochemical XEC of “Drug-Like” Aryl Bromides and Alkyl Bromides (2020)<sup>a</sup>**



<sup>a</sup>(a) Conditions A: Alkyl-Br (2 equiv), NiCl<sub>2</sub>(dme) (7 mol%), ligand (7 mol%), NaI (25 mol%), Zn flake (2 equiv), TFA (10 mol%), DMA, 60 °C. (b) Condition B: Alkyl-Br (1.5 equiv), NiCl<sub>2</sub>(dtbbpy) (0.5 mol%), Ir(dF(CF<sub>3</sub>)ppy)<sub>2</sub>(dtbbpy)PF<sub>6</sub> (1.0 mol%), 2,6-lutidine (2 equiv), (TMS)<sub>3</sub>SiH (1.2 equiv), DME, 450 nm LEDs. (c) Ligand = BpyCam. (d) Ligand = PyBCam<sup>CN</sup>.

workers. The authors employed a HANU plate reactor as a continuous plug flow system, which employs Continuous processing utilizing an Oscillatory flow with STAtic mixing (COSTA) (Scheme 130).<sup>250</sup> This technology was applied to handle a photochemical XEC of methyl 4-bromobenzoate and 4-bromotetrahydropyran at 0.87 g/h. The authors found that

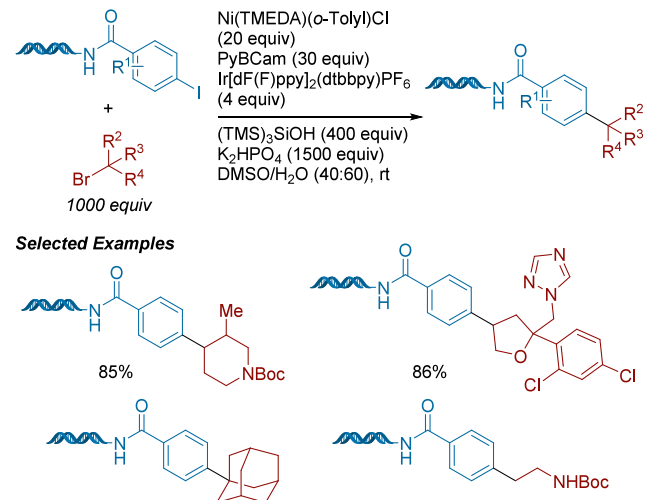
**Scheme 130. Photochemical Nickel and Iridium Co-Catalyzed XEC in Continuous Flow Using COSTA (2020)**



the oscillatory flow regime was necessary to successfully maintain stable reactant suspensions. The authors were also able to decrease the reaction time from 6 h in batch to 20 min in continuous flow.

Pfizer, led by Kölmel and Flanagan, expanded the scope of their previous report to include alkyl bromides in on-DNA cross-electrophile coupling, enabling access to unstabilized alkyl radical precursors (Scheme 131).<sup>251</sup> Starting from their

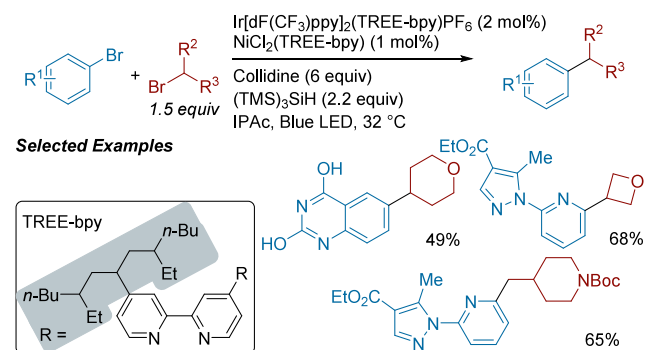
**Scheme 131. Photochemical Nickel and Iridium Co-Catalyzed XEC for DNA-Encoded Libraries (2020)**



previously published conditions, the authors found several key changes to achieve success under the current coupling manifold: (1) PyBCam was crucial for high reaction efficiency and minimization of protodehalogenation of aryl iodide, and (2) inclusion of silanol reductant (TMS)<sub>3</sub>SiOH, which led to a substantial boost in yield. These mild conditions resulted in the successful XEC of a broad range of aryl iodides with primary and secondary alkyl bromides in good yields and good DNA-compatibility, including the use of a parallel-synthesis format to demonstrate DEL preparation.

Novartis Discovery Chemistry SynTech group, led by Delgado and Tan, developed a lipophilic Ni/Ir dual catalytic system for use in the XEC of aryl halides with alkyl bromides in greener, nonamide solvents (Scheme 132).<sup>36</sup> The authors propose that the low efficiency reported for XEC reactions in green solvents can be improved by the incorporation of

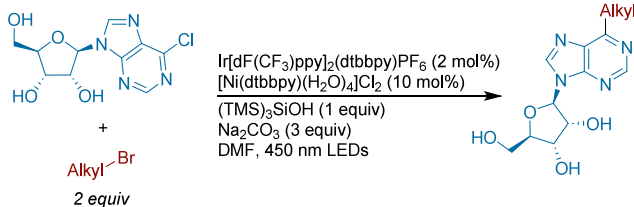
**Scheme 132. Photochemical Nickel and Iridium Co-Catalyzed XEC in Green Solvents Enabled by Lipophilic TREE ligands (2021)**



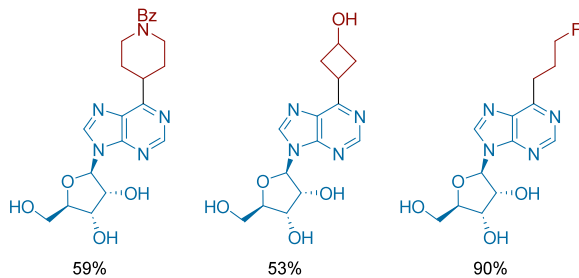
lipophilic groups to increase the solubility of nickel and iridium catalysts in such solvents as IPAc and EtOAc, leading to the development of the TREE-bpy ligand.

Researchers at Merck sought to develop an XEC method that allowed for nucleoside functionalization using a dual catalyst photoredox approach with nickel and iridium (Scheme 133).<sup>252</sup> They used halogenated nucleosides with alkyl

**Scheme 133. Photochemical Nickel and Iridium Co-Catalyzed XEC of Halogenated Nucleosides with Alkyl Bromides (2021)**



*Selected Examples*

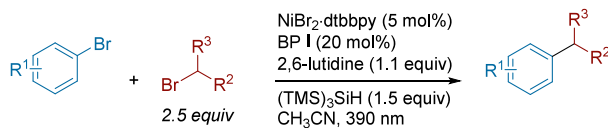


bromides to achieve C(sp<sup>2</sup>)–C(sp<sup>3</sup>) bond formation. Although the optimized conditions employ an iridium photocatalyst, they also noted success with the organic dye 4CzIPN, but longer reaction times. To rule out the possibility of direct radical addition through homolytic aromatic substitution, they performed the reaction without nickel and observed trace product. Four-, five-, and six-membered cyclic alkyl bromides were found to be compatible with these conditions as well as primary alkyl chains. Tertiary alkyl bromides were not applicable in this protocol. Free alcohols were well-tolerated and fluorinated alkyl substrates could be coupled with good yield.

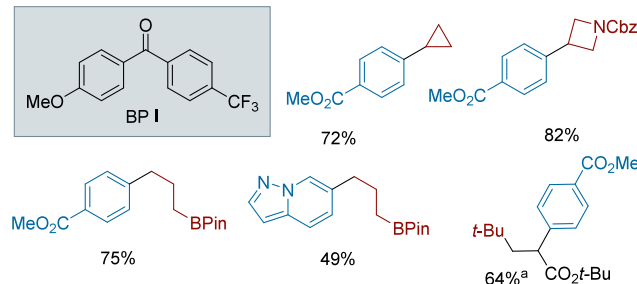
The Noël lab reported a photoredox/nickel dual catalysis system to couple aryl bromides with alkyl bromides (Scheme 134).<sup>253</sup> The authors were able to use benzophenone in place of Ir dyes as a photocatalyst along with tris(trimethylsilyl)silane as the terminal reductant and XAT mediator. The tuned benzophenone catalyst is capable of HAT (from the silane to the ketyl radical), avoiding the need to generate Br• by oxidation. The resulting reaction scope is broad with primary and secondary alkyl bromides reacting well with various aryl/heteroaryl bromides to yield modest to good reaction yield. The authors further applied the reaction system to the arylalkylation of *tert*-butyl acrylate. Given the wide use of the Ir and Ni system and the high cost of Ir, this Ir-free system is an exciting advance.

In collaboration with Global Medicinal Chemistry groups of Merck KGaA and EMD Serono, the Kappe, Williams, Eggenweiler and co-workers disclosed a photoredox/nickel XEC reaction of alkyl bromides with thalidomide bromides to provide a streamlined approach to proteolysis targeting

**Scheme 134. Photochemical Nickel and Benzophenone Co-Catalyzed XEC with Silane Mediated Radical Generation (2022)<sup>a</sup>**



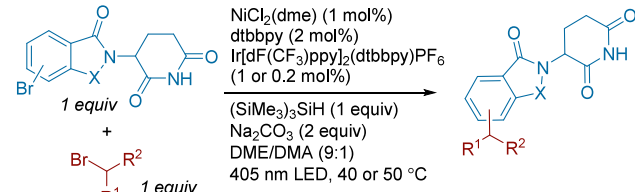
*Selected Examples*



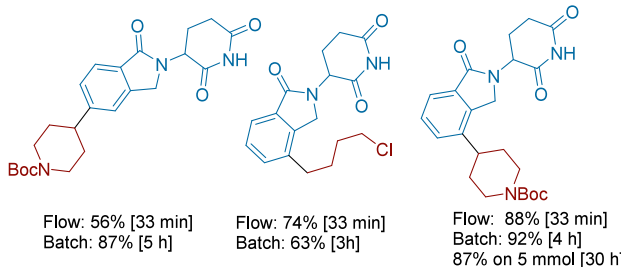
<sup>a</sup>With *tert*-butyl acrylate (3 equiv) added as reactant for dicarbofunctionalization reaction.

chimeras (PROTACs) (Scheme 135).<sup>254</sup> While the standard conditions provided good yields for the coupling of

**Scheme 135. Photochemical Nickel and Iridium Co-Catalyzed XEC of Thalidomide Bromides with Alkyl Bromides in an Oscillatory Flow Reactor (2022)**



*Selected Examples*

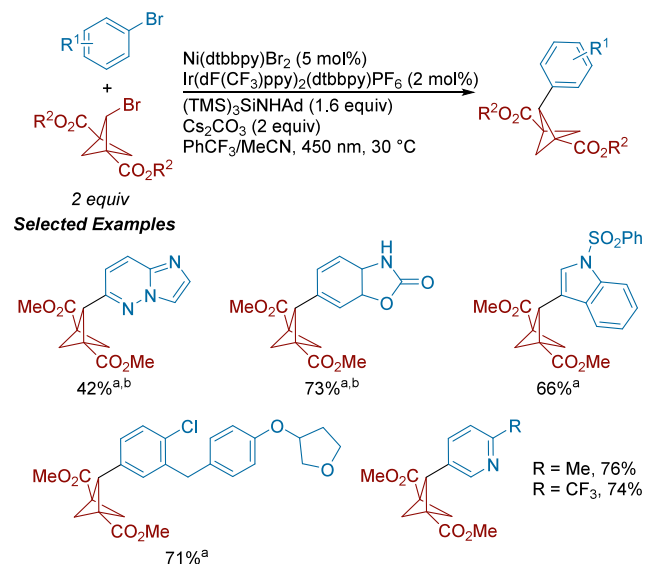


lenalidomide bromide and thalidomide bromide with *N*-Boc-4-bromopiperidine in batch reactions, the heterogeneity resulting from the use of Na<sub>2</sub>CO<sub>3</sub> was a barrier to developing a flow process. Replacing Na<sub>2</sub>CO<sub>3</sub> with a homogeneous organic base, such as 2,6-lutidine, resulted in a slow reaction rate. Finally, by engaging a smaller particle size of Na<sub>2</sub>CO<sub>3</sub> ( $X_{50}$  = 13  $\mu$ m compared to 116  $\mu$ m for commercial samples), the batch reaction was successfully transferred to a flow process in an oscillatory flow reactor with increased reaction rate and selectivity. To highlight the utility of the methodology, the authors conducted a 5 mmol scale reaction with an 87% HPLC yield, albeit longer reaction time was needed to reach completion (30 h vs 4 h).

The MacMillan lab, in collaboration with the Merck Department of Discovery Chemistry, developed reaction

conditions for the synthesis of 1,2,3-trifunctionalized bicyclo[1.1.1]pentanes (BCPs) by selective 2-bromination followed by photochemical XEC with aryl bromides (**Scheme 136**).<sup>255</sup> One initial concern of their work was the high s

**Scheme 136. Photochemical Nickel and Iridium Co-Catalyzed XEC of BCP Bromides with Aryl Bromides (2023)<sup>a</sup>**

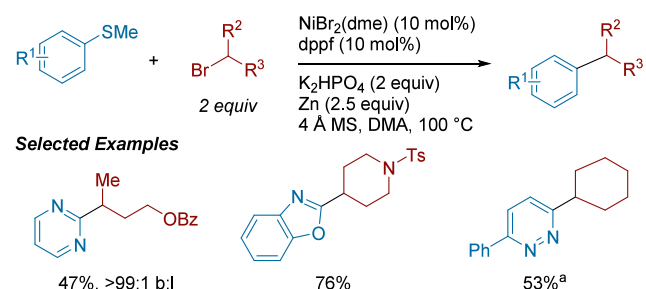


<sup>a</sup>(a) With 10 mol % Ni(dtbbpy)Br<sub>2</sub>. (b) In PhCF<sub>3</sub>/t-BuOH.

character of the BCP radical intermediate, which may instead favor protodebromination side product over desired cross-coupling. To circumvent this issue, the authors found that use of solvents lacking weaker, hydridic C–H bonds (e.g., PhCF<sub>3</sub>), in conjunction with careful control of the reaction temperature, slow addition of the aryl bromide, and a modified silane afforded the desired product in good to high yields. The reaction is tolerant of a wide variety of functional groups, including electron-deficient and electron-rich substituents, as well as acidic functionalities.

**4.2.1.3. XEC with Aryl Pseudohalides.** Cornella and co-workers reported the use of heteroaryl thioethers in XEC with alkyl bromides (**Scheme 137**).<sup>256</sup> Heteroaryl thioether substrates can be convenient in multistep synthesis because they act as “protecting groups” for reactive sites on multihalogenated heteroarenes for sequential S<sub>N</sub>Ar reactions. However, thioethers are usually unreactive and must be

**Scheme 137. Ni-Catalyzed XEC of Aryl Thioethers with Alkyl Bromides (2019)<sup>a</sup>**

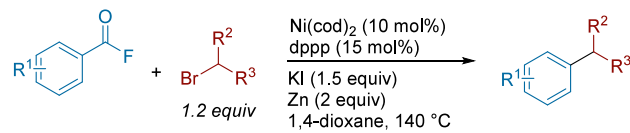


<sup>a</sup>With 3 equiv alkyl bromide at 50 °C.

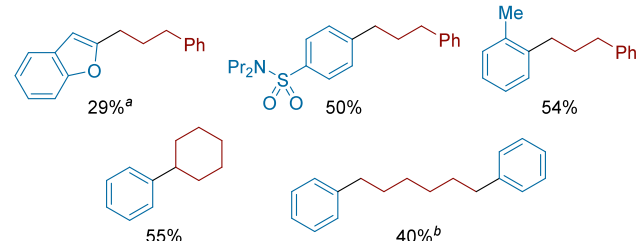
activated by oxidation to the sulfone. Key to overcoming this low reactivity was identification of dppf as a bidentate, electron-rich ligand that enabled oxidative addition. A variety of heteroaryl thioethers were competent coupling partners with secondary alkyl bromides to give the desired products with good functional group tolerance. In contrast to problematic isomerization observed in previous reports employing dppf as ligand, open-chain secondary alkyl bromides led to exclusively the branched products. Alkylation of the zinc thiolate is not observed, even at 100 °C, perhaps due to strong Zn–S bonding or phase-separation. The ratio of cyclized to uncyclized cross-coupled product in a 5-exo-trig cyclization mechanistic study did not vary with the concentration of catalyst, providing evidence that the alkyl radical is formed and reacts at the same nickel center.

Nishihara and co-workers reported on the decarbonylative reductive alkylation of aryl fluorides with alkyl bromides (**Scheme 138**).<sup>257</sup> The authors propose that the reaction

**Scheme 138. Ni-Catalyzed Decarbonylative XEC of Aryl Fluorides with Alkyl Bromides (2022)<sup>a</sup>**



**Selected Examples**

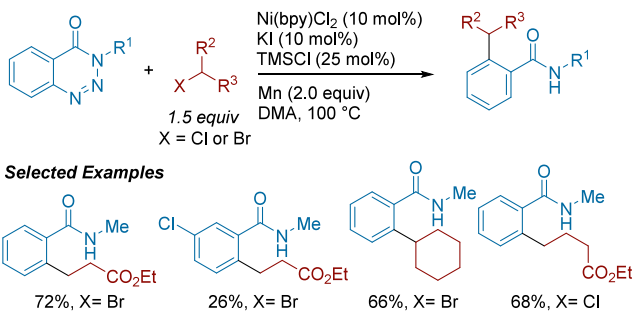


<sup>a</sup>(a) With alkyl bromide (1.5 equiv). (b) With aryl fluoride (3 equiv).

proceeds through oxidative addition of the aryl fluoride to nickel(0), followed by alkyl radical capture, decarbonylation, and reductive elimination to generate the product. A number of aryl fluorides bearing electron-donating and electron-withdrawing functional groups as well as *ortho*-substituents could undergo decarbonylative coupling with primary alkyl bromides to give the desired products, including one example with a secondary alkyl bromide. Under these conditions, the authors found that neither aryl chlorides nor alkyl acid fluorides were competent coupling partners.

The Gang Zou group developed an XEC reaction to access *ortho*-alkylated benzamides by coupling benzotriazinones and alkyl halides via a denitrogenation pathway (**Scheme 139**).<sup>258</sup> The authors report addition of KI is essential to ensure good yields, as it is proposed to (1) convert alkyl bromides and chlorides into more reactive alkyl iodides and (2) facilitate reduction of the nickel(II) species to nickel(0). While the optimal condition was at 100 °C, control reactions revealed that the reaction could be conducted at room temperature for a longer reaction time, albeit with a slightly diminished yield. The denitrogenation step was proposed to occur via oxidative addition of 1,2,3-benzotriazinones to nickel(0), followed by the extrusion of nitrogen, resulting in a five membered azanickelacycle intermediate. The report shows high yields

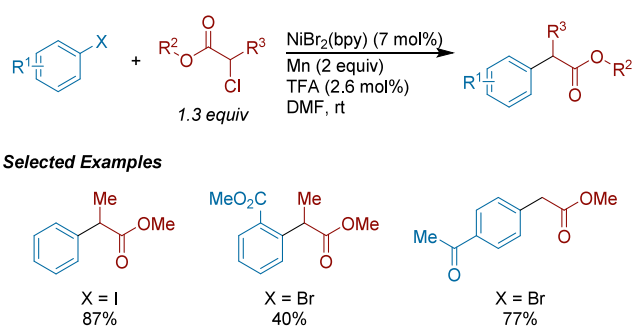
**Scheme 139.** Ni-Catalyzed Denitrogenative XEC of 1,2,3-Benzotriazinones with Alkyl Halides (2022)



with primary alkyl bromides, and a few primary alkyl chlorides also afforded decent yields of the cross-coupled products.

**4.2.2. Alkyl Chlorides as Electrophiles.** **4.2.2.1. XEC with Aryl Halides.** In 2006, Durandetti, Gosmini, and Périchon reported the cross-electrophile coupling of aryl halides with  $\alpha$ -chloroesters (Scheme 140).<sup>259</sup> These reactions generally

**Scheme 140.** Ni-Catalyzed XEC of Aryl Halides with  $\alpha$ -Chloroacetates (2007)

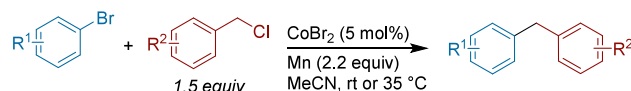


required lower equivalencies of  $\alpha$ -chloroester compared to previous methods. Careful selection of temperature (ranging from rt to 70 °C) based on the coupling partners was important for productive reactivity. Adding TFA to activate the Mn reductant resulted in a more efficient reaction. These modified conditions allowed for increased yields among a range of electronically different arenes. When electron-rich substituents are present, aryl iodides provided improved results, whereas electron-deficient aryl bromides and iodides are both compatible. The reaction is compatible with primary  $\alpha$ -chloroesters as well, providing access to arylacetates without over arylation.

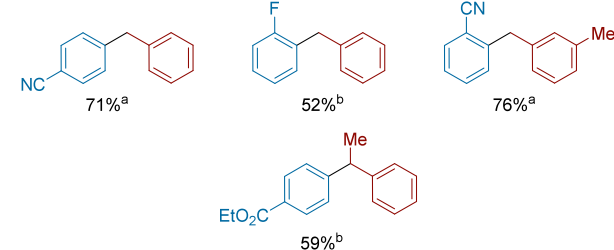
Gosmini and Auffrant developed an XEC procedure that relies on a cobalt catalyst, rather than nickel, to catalyze the coupling of benzylic chlorides with aryl bromides (Scheme 141).<sup>260</sup> Compared to previous cobalt-catalyzed XEC reactions, the authors were able to use MeCN in place of DMF/pyridine mixtures. Although a dipicolylamine ligand was identified during optimization (and related ligands have since found use in nickel catalysis), ligand-free conditions were equally effective. Slightly diminished yields were observed with electron rich aryl halides. Benzylic chlorides with electron-donating groups were prone to forming bibenzyl homodimers.

Our group reported on the use of organic reductants in place of metallic powders (Zn, Mn, etc.) in Ni-catalyzed XEC reactions (Scheme 142).<sup>34</sup> Metal powders can cause issues on scale-up and generate stoichiometric metal waste. Noting

**Scheme 141.** Cobalt-Catalyzed XEC of Aryl Bromides with Benzyl Chlorides (2016)<sup>a</sup>

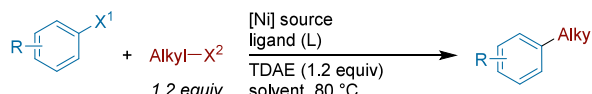


#### Selected Examples

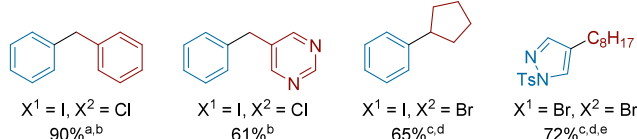


<sup>a</sup>(a) At 35 °C. (b) At rt.

**Scheme 142.** Ni-Catalyzed XEC of Aryl Halides with Benzyl Chlorides and Alkyl Bromides with a Homogeneous Reductant (2016)<sup>a</sup>



#### Selected Examples



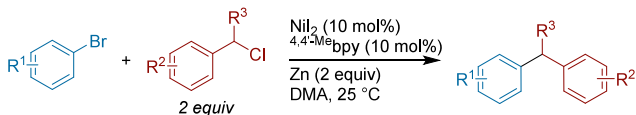
<sup>a</sup>(a) With 2 equiv of TDAE. (b) [Ni]/L = NiBr<sub>2</sub>(dtbbpy) (7 mol%), Solvent = propylene carbonate. (c) [Ni] = NiI<sub>2</sub>•xH<sub>2</sub>O (10 mol%), L = dtbbpy (10 mol%), Solvent = MeCN. (d) With 25 mol% NaI. (e) Reaction run at 60 °C.

earlier work by Tanaka, on the use of tetrakis(dimethylamino)-ethylene (TDAE) in reductive Ni/Cr chemistry,<sup>261</sup> we explored the use of TDAE in XEC reactions. TDAE was compared to Zn in various solvents in the XEC of benzyl chloride with aryl iodides. Notably TDAE lead to comparable yields as Zn in DMA, and outperformed Zn when using a variety of nonamide solvents (a common challenge for metal powder reductants). TDAE also outperformed Zn with coupling partners prone to direct metalation (electron-poor pyrimidine and pyrazole). For large scale XEC reactions, liquid reductants enable the reaction to be paused and restarted without any loss in activity by controlling the addition of the reductant.<sup>34</sup>

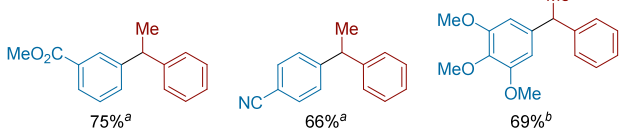
Hegui Gong, Qun Qian, and co-workers reported a strategy to couple benzylic chlorides with aryl bromides (Scheme 143).<sup>262</sup> Two methods were developed: MgCl<sub>2</sub> and pyridine were key additives for successful XEC with electron-poor aryl bromides, while KF was identified as the critical additive when electron-rich aryl bromides were employed. The scope encompassed *ortho*-substituted aryl coupling partners as well as those containing aldehydes and ketones. Unfortunately, no reactivity was seen with heterocycles.

Hazari and co-workers synthesized, characterized, and examined the reactivity of polypyridyl Ni<sup>I</sup> halide complexes in the cross-electrophile coupling of iodobenzene with benzyl

**Scheme 143. Ni-Catalyzed XEC of Aryl Bromides with Benzyl Chlorides (2016)<sup>a</sup>**



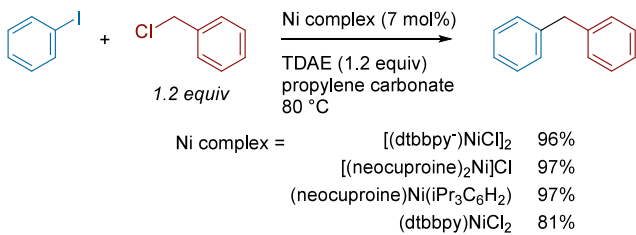
**Selected Examples**



<sup>a</sup>(a) With MgCl<sub>2</sub> (1 equiv) and pyridine (1 equiv). (b) With KF (1 equiv).

chloride using TDAE as reductant (Scheme 144).<sup>173</sup> The authors showed that  $[(\text{dtbbpy})\text{Ni}^{\text{I}}\text{Cl}]_2$  complex could be

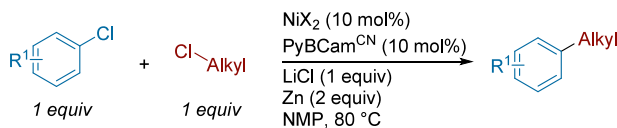
**Scheme 144. Stoichiometric Studies on Nickel Polypyridyl Complexes as Catalysts for XEC (2019)**



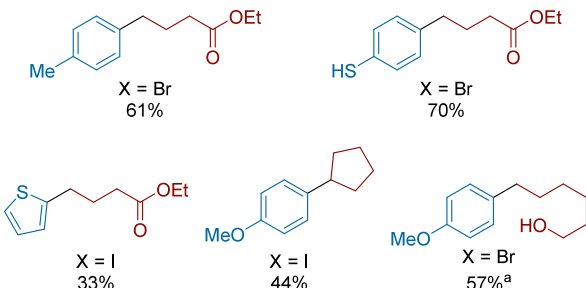
synthesized through oxidative addition of an aryl chloride to  $\text{Ni}(\text{COD})_2$  and ligand. It is proposed to proceed by reductive elimination of biaryl and comproportionation. The resulting complex was competent in alkyl radical generation as demonstrated with triptyl chloride, providing support for the proposed role of Ni(I) in the typical radical chain mechanism. However, the dimeric Ni(I) halide complex showed no reactivity toward either iodobenzene or TDAE.

Our group reported the first general XEC of aryl chlorides with alkyl chlorides (Scheme 145).<sup>263</sup> The pyridine bis(carboxamidine) ligand class was necessary for productive

**Scheme 145. Ni-Catalyzed XEC of Aryl Chlorides with Alkyl Chlorides Enabled by Carboxamidine Ligands (2020)<sup>a</sup>**



**Selected Examples**

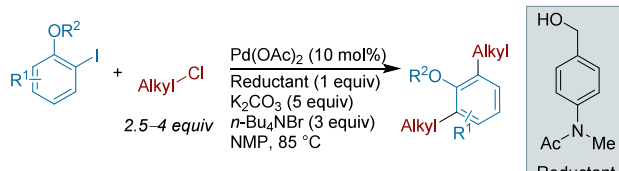


<sup>a</sup>With alkyl chloride (1.25 equiv)

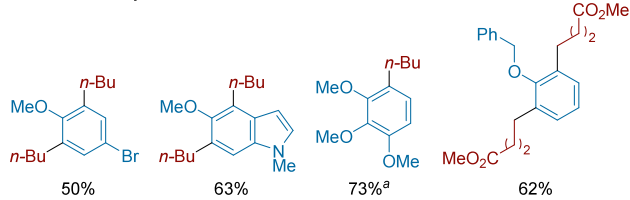
coupling, with PyBCam<sup>CN</sup> resulting in the highest yield of cross product and minimal formation of homodimers. A catalytic amount of either bromide or iodide was necessary for successful coupling, which was attributed to a fast, unfavorable halide exchange that increased the reactivity of the alkyl chloride. The addition of zinc and lithium halide salts favored this halide exchange equilibrium, which we proposed to occur via the favorable formation of  $\text{LiZnCl}_3$ , resulting in chloride sequestration. Primary alkyl chlorides were better substrates than secondary alkyl chlorides.

Yanghai Zhang and co-workers reported a Pd-catalyzed cross-electrophile coupling of aryl iodides with alkyl chlorides in the presence of *N*-(4-(hydroxymethyl)phenyl)-*N*-methylacetamide (Scheme 146).<sup>264</sup> The reaction works best with a

**Scheme 146. Pd-Catalyzed XEC of Aryl Iodides and Alkyl Chlorides by a Cyclometalation Mechanism (2021)<sup>a</sup>**



**Selected Examples**



<sup>a</sup>With  $\text{K}_2\text{CO}_3$  (4 equiv) and  $n\text{-Bu}_4\text{NBr}$  (2 equiv).

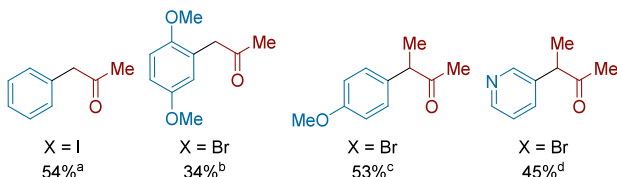
substituted-benzyl alcohol as a terminal reductant in NMP. With these conditions at 85 °C and TBAB as an additive, the group was successful at obtaining dialkylation of *ortho*-iodoanisole. The reaction mechanism is complex, but good evidence is provided to support oxidative addition to form arylpalladium(II) and cyclometalation onto the  $\text{OCH}_2\text{R}$  group. This species might participate in oxidative addition of alkyl halide followed by reductive elimination to form the first coupling product. Dialkylation would involve a second cyclometalation, oxidative addition, and reductive elimination. Electronically diverse aryl iodides were well tolerated and a few heterocycles, namely indole, benzofuran, and indoline, gave moderate yields. In substrates where the *meta*-position was significantly sterically hindered, only monosubstitution products were formed. Monosubstitution also proceeds in high yield when the nonhalogenated *ortho* site is functionalized.

**4.2.2.2. Photochemical and Electrochemical Approaches.** In 1994, a report on the XEC of aryl halides and  $\alpha$ -chloroketones was published by Durandetti and co-workers (Scheme 147).<sup>265</sup> The group used a variety of equivalencies of  $\alpha$ -chloroketone, ranging from 1.2 to 3.9 equiv. They hypothesized that the oxidative addition of the aryl halide to the nickel would be slow, requiring only small amounts of alkyl coupling partner to be present at a time to mitigate competing reactivity. Thus, for these reactions, the  $\alpha$ -chloroketone was introduced via slow addition into the electrochemical cells. Running the reactions at 80 °C, the authors were able to see moderate yields for both electron-rich and electron-poor aryl iodides and bromides. The reaction was tolerant of sterically

**Scheme 147.** Electrochemical Ni-Catalyzed XEC of Aryl Halides with  $\alpha$ -Chloroketones (1994)<sup>a</sup>



**Selected Examples**

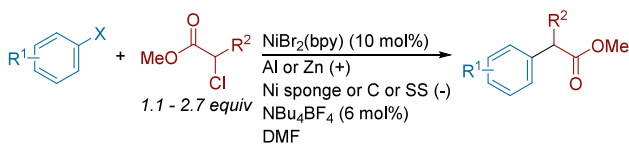


<sup>a</sup>(a) With 2.9 equiv of  $\alpha$ -chloroketone at rt. (b) With 3.5 equiv of  $\alpha$ -chloroketone. (c) With 2.6 equiv of  $\alpha$ -chloroketone. (d) With 2.2 equiv of secondary  $\alpha$ -chloroketone.

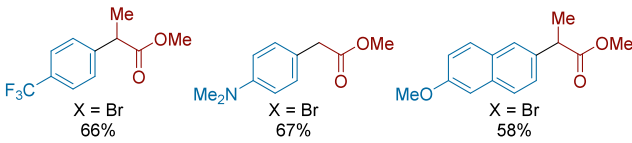
hindered substrates and both primary and secondary alkyl chlorides were compatible. One entry with the coupling of pyridine demonstrated this method's promise toward forming C–C bonds with heterocycles.

In a seminal publication for the field of XEC, Durandetti, Nédélec, and Périchon reported on the electrochemically driven XEC of  $\alpha$ -chlorocarbonyls with aryl halides (Scheme 148).<sup>266</sup> In their studies, they found low-yielding reactions

**Scheme 148.** Electrochemical Ni-Catalyzed XEC of Aryl Halides with  $\alpha$ -Chloroketones and  $\alpha$ -Chloroesters (1996)



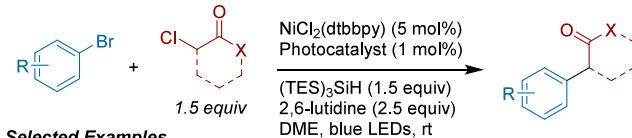
**Selected Examples**



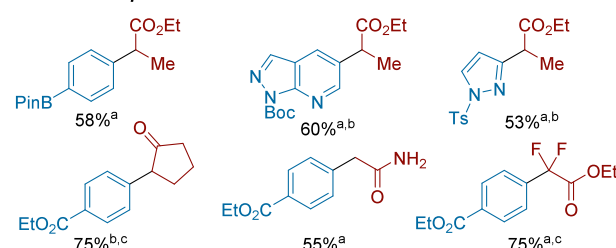
suffered from fast production of alkyl dimer followed by slow formation of biphenyl once the alkyl partner had been depleted. A correlation between aryl halide reactivity and the optimal temperature for XEC was observed (more reactive aryl halides work best at lower temperature) and slow addition of the more reactive substrate of the pair improved yields. Primary and secondary alkyl partners, both ketones and esters, reacted effectively to form product. Allylic electrophiles were compatible as well, giving moderate yields. They were also able to collect results for other activated alkyl electrophiles such as benzyl halides. These early trials demonstrated both primary and secondary alkyl halide compatibility as well as tolerance of heterocycles. In addition, in the  $C(sp^2)$ – $C(sp^2)$  coupling 1-bromo-1-propene (initially as a 50:50 mixture of *E/Z* isomers) with several aryl bromides, the authors report convergence to the (*E*)-isomer of the cross-coupled product (ratios range from 3:1 to 4:1 *E/Z*) but did not explore the stereochemical outcome further. This convergence is likely due to increased sterics present in the (*Z*)-isomer, which are minimized in the (*E*)-isomer.

MacMillan and co-workers employed a metallaphotoredox strategy in the arylation of  $\alpha$ -chlorocarbonyls (Scheme 149).<sup>267</sup> The reaction proceeds through the generation of

**Scheme 149.** Photochemical Nickel and Iridium Co-Catalyzed XEC of Aryl Bromides with  $\alpha$ -Chloroketones and  $\alpha$ -Chloroesters by Silane-Mediated XAT (2019)<sup>a</sup>



**Selected Examples**

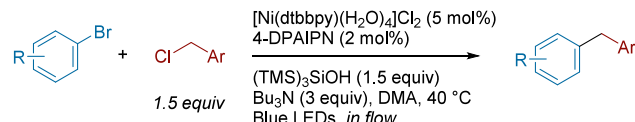


<sup>a</sup>(a)  $[Ir(d(F)(CF_3)pp)]PF_6$  as photocatalyst. (b)  $Na_2CO_3$  as base. (c)  $[Ir(d(CF_3)(Me)pp)]PF_6$  as photocatalyst.

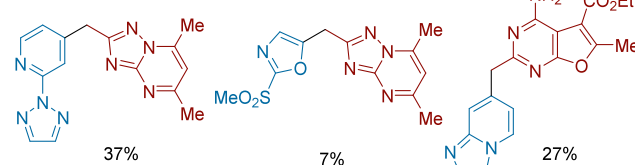
alkyl radical from chlorine atom abstraction by a tris-(triethylsilyl)silyl radical, which itself is generated through hydrogen-atom abstraction by bromine radical resulting from oxidation of bromine anion by excited state Ir photocatalyst. The reaction can be applied to a number of electronically activated aryl and heteroaryl bromides to form the corresponding  $\alpha$ -arylation products in good yields. A variety of activated alkyl chlorides were effective, including  $\alpha$ -chloroesters, amides, and ketones as well as benzyl chlorides. Notably,  $\alpha$ -chloro carboxylic acids can also be utilized through *in situ* masking as the TMS esters.

Merck Discovery Chemistry, led by Brill, described the use of a continuous flow approach for a photochemical XEC of (hetero)aryl bromides with (hetero)aryl benzylic chlorides to give a number of complex medicinally relevant di(hetero)-arylmethanes in synthetically useful yields (Scheme 150).<sup>268</sup> The authors identified key design features for compatibility in a flow reactor setting and optimized reaction yield, which involved the development of a fully homogeneous system using  $Bu_3N$  as base in DMA,  $(TMS)_3SiOH$  as reductant to decrease protodehalogenation of the alkyl substrate, and a residence time of 30 min to maximize workflow efficiency. Using a

**Scheme 150.** Photochemical Nickel- and Iridium-Catalyzed XEC of Aryl Bromides with Benzyl Chlorides in Flow (2019)



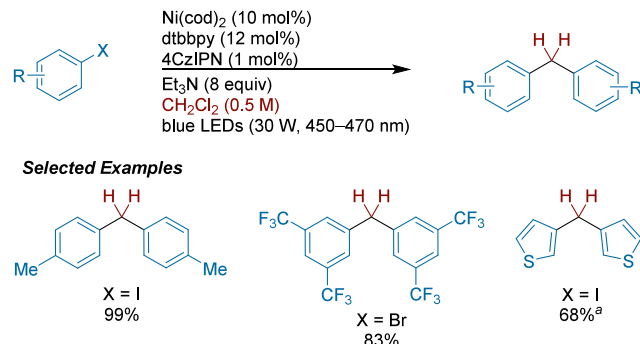
**Selected Examples**



Vaportec flow chemistry system equipped with an autosampler, the authors successfully prepared two compound libraries to give a total of 23 isolated products.

In 2020, Tao Xu and co-workers described an XEC approach that utilized dichloromethane as both solvent and methylene source in the formation of diarylmethanes (**Scheme 151**).<sup>269</sup> The authors were able to access the chloromethane

**Scheme 151.** Nickel/Photoredox XEC of Aryl Halides with Dichloromethane (2019)<sup>a</sup>

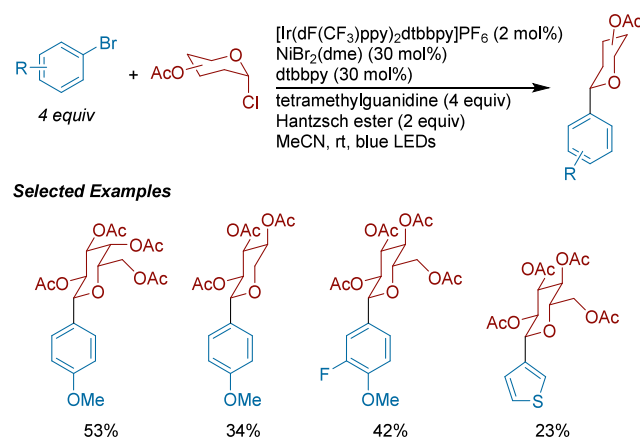


<sup>a</sup>With CH<sub>2</sub>Cl<sub>2</sub> (0.25 M).

radical via single-electron reduction, overcoming the typically inert nature of C–Cl bonds. Attempting the reaction with traditional Zn or Mn reductants led to trace product. The reaction can also be run with CD<sub>2</sub>Cl<sub>2</sub> to afford deuterated diarylmethanes. The authors showed that benzyl chloride is a competent intermediate in this reaction, which presumably forms after the first XEC of the aryl halide and CH<sub>2</sub>Cl<sub>2</sub>.

Building upon the works of Hegui Gong<sup>220</sup> and Tianning Diao<sup>270</sup> in the area of reductive glycoside arylation via nickel XEC, Xia Zhang, Dawen Niu, and co-workers reported a photochemical nickel/iridium XEC of glycosyl chlorides with aryl bromides (**Scheme 152**).<sup>271</sup> Other reductants outside of the optimal Hantzsch ester, such as tris(trimethylsilyl)silane and Zn, as well as inorganics bases, like K<sub>2</sub>CO<sub>3</sub>, resulted in diminished yields. Using the most productive conditions, a variety of glycosyl chlorides, derived from galactose, rhamnose, and arabinose (among others), fared well in the coupling and favored the  $\beta$ -products. Both electron-rich and -neutral aryl

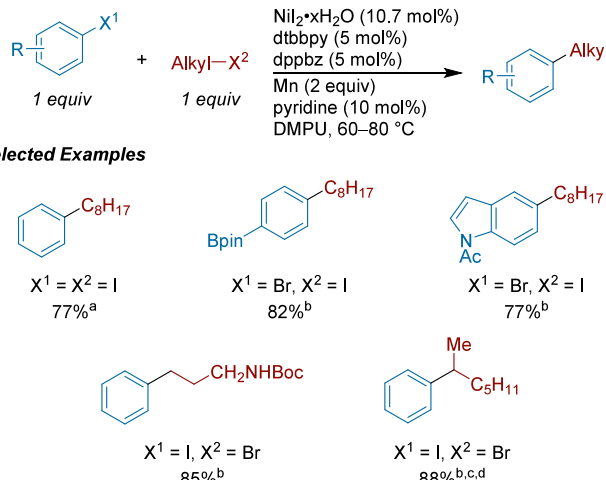
**Scheme 152.** Photochemical Nickel and Iridium Co-Catalyzed XEC of Aryl Bromides with Glycosyl Chlorides (2021)



bromides were tolerated as well as some heterocycles (thiophenes and indoles). It is notable that Hantzsch ester could be used in place of silanes in this system.

**4.2.3. Alkyl Iodides as Electrophiles.** **4.2.3.1. XEC with Aryl Halides.** In 2010, our group reported a cross-electrophile coupling protocol that forgoes the formation of organometallic reagents (**Scheme 153**).<sup>44</sup> Synergy between two different

**Scheme 153.** Ni-Catalyzed XEC of Aryl Iodides with Alkyl Iodides (2010)<sup>a</sup>



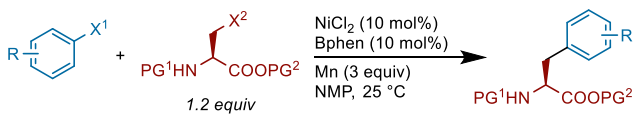
<sup>a</sup>(a) Run at 80 °C. (b) Run at 60 °C. (c) Required 26–37 h. (d) Used technical grade 2-bromoheptane (1.2 equiv).

nickel catalysts (derived from dtbbpy and dppbz) was observed: although dppbz was a poor catalyst alone, it improved yields when combined with dtbbpy. The conditions were general for the coupling of a variety of aryl iodides with alkyl iodides and provided promising yields with combinations of iodides and bromides. Esters, nitriles, and ketones were all tolerated, demonstrating the now common orthogonality of XEC to more traditional cross-coupling reagents. Substrates containing free alcohols and other acidic protons also coupled in good yield and *ortho*-substitution on the aryl substrate did not significantly impede reactivity. Control experiments ruled out the formation of arylmanganese intermediates, and the reaction could proceed with an organic reductant (TDAE).

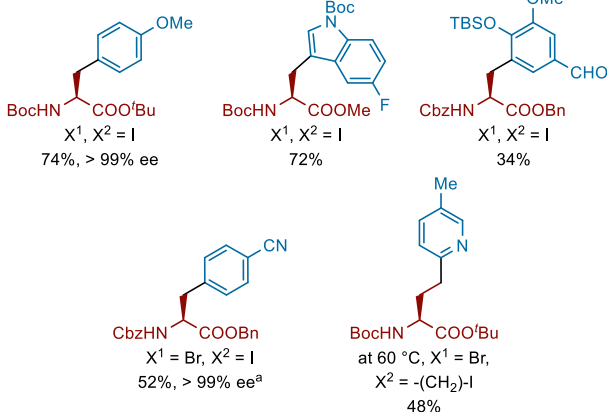
Lei Liu, Bin Xiao, and co-workers described a general approach to enantioenriched  $\alpha$ -amino acid derivatives by the XEC of alkyl iodides derived from serine and homoserine with aryl iodides and bromides (**Scheme 154**).<sup>272</sup> Using Bphen as the ligand and NMP as the solvent, this room temperature reaction tolerated a variety of common protecting groups on nitrogen and the acid. Besides simple aryl halides, a few heterocycles were tolerated (pyridine and pyrimidine). The reactions largely proceeded without racemization of the starting material. In addition to aryl halides, acid chlorides could be coupled with similar success. However, swapping the aryl halide for a 1° alkyl iodide resulted in a good yield of C(sp<sup>3</sup>)–C(sp<sup>3</sup>) coupled product, but with substantial racemization. The chemistry was also demonstrated on a dipeptide.

Inspired by the pharmaceutical relevance of borazonaphthalenes, Molander and co-workers targeted C–C bond formation at the 3-position (**Scheme 155**).<sup>273</sup> Previously, they had failed to efficiently form the B–N bond via a cyclization with starting materials prefunctionalized at this

**Scheme 154.** Ni-Catalyzed XEC of Amino Acid Derived Alkyl Iodides with Aryl Halides (2014)<sup>a</sup>

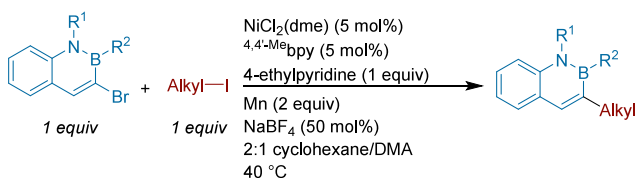


**Selected Examples**

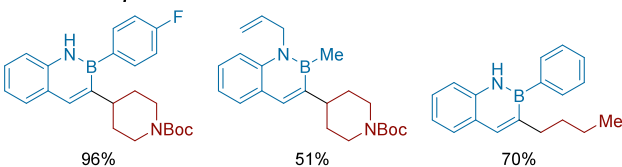


<sup>a</sup>With 2 equiv NaI.

**Scheme 155.** Alkylation of Bromoborazaronaphthalenes Through Ni-Catalyzed XEC with Alkyl Iodides (2014)



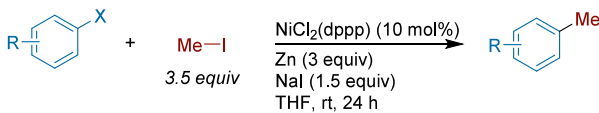
**Selected Examples**



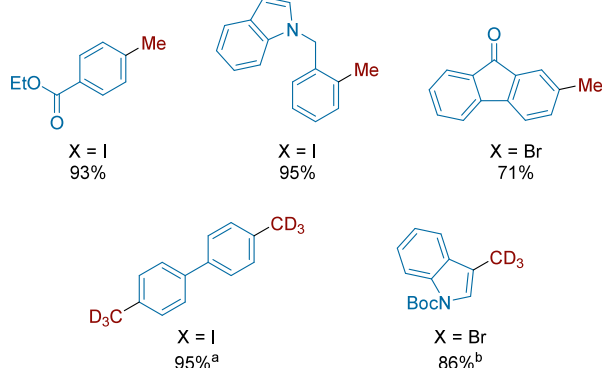
position. After encountering challenges using cross-coupling approaches, an XEC approach was explored. Using brominated 2,1-borazaronaphthalenes and alkyl iodides, they developed conditions analogous to their previously described work. The use of degassed solvents was not required. A variety of nonaromatic heterocycles were tolerated as the alkyl coupling partner. Though not compatible with tertiary alkyl partners or other hindered alkyl iodides, significant steric bulk at the boron were handled under these conditions.

Understanding the significance of methylation in medicinal chemistry, Xuebin Liao and colleagues studied the XEC of methyl iodide with aryl iodides/bromides (Scheme 156).<sup>274</sup> Typical bidentate amine ligands did not form the desired cross-product and it was hypothesized that these ligands may be undergoing *N*-methylation instead. Switching to phosphine ligands, they observed improved reactivity with 1,3-bis(diphenylphosphino)propane (dppp) and NaI additive. In addition to tolerating various electronics and *ortho*-sterics, these conditions are also compatible with aryls containing amides, sulfonamides, aldehydes, and a heterocyclic core. They

**Scheme 156.** Ni-Catalyzed XEC Methylation of Aryl Halides (2016)<sup>a</sup>



**Selected Examples**

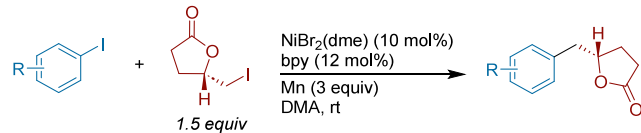


<sup>a</sup>(a) Used CD<sub>3</sub>I (7 equiv) as coupling partner with Zn (6 equiv) and NaI (3 equiv). (b) Used CD<sub>3</sub>I (3.5 equiv) as coupling partner.

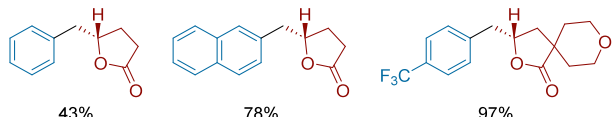
were also successful in demonstrating their chemistry's capabilities in CD<sub>3</sub>-functionalization.

In a report showcasing photoredox and copper-catalyzed iodolactonization techniques, Wei Li and co-workers demonstrated the XEC of aryl iodides with their iodolactone products (Scheme 157).<sup>275</sup> This a potentially challenging reaction

**Scheme 157.** Applications of XEC in the Formation of C(sp<sup>2</sup>)–C(sp<sup>3</sup>) Bonds Between Aryl Iodides and Iodolactones (2018)



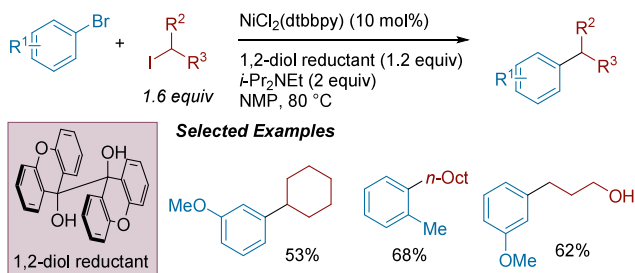
**Selected Examples**



because  $\beta$ -carboxylate elimination would open the lactone and is a fast process for many carbanion equivalents. These conditions were tolerant of both electron-rich and electron-poor aryl coupling partners. They also focused on showcasing XEC on the wide range of functionalized iodolactones that could be formed with the methods presented in their paper, such as benzolactones and spirolactones.

Murakami, Ishida, and co-workers employed a strained vicinal diol as an organic reductant in the cross-coupling of aryl bromides with alkyl iodides (Scheme 158).<sup>276</sup> With these conditions, several aryl bromides bearing sensitive functional groups were successfully coupled with primary and secondary alkyl iodides in good yields. The reductant can be easily synthesized and regenerated after use through photoinduced dimerization of xanthone under natural sunlight, and the energy stored in the form of steric strain is released in the

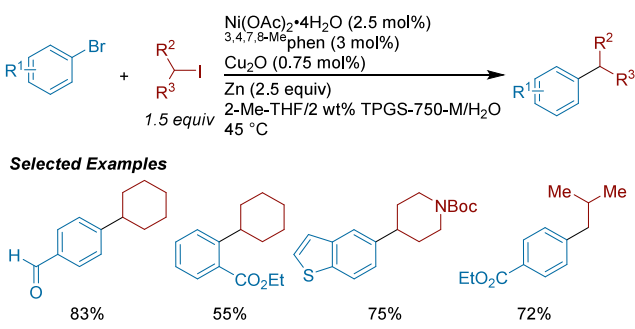
**Scheme 158. Ni-Catalyzed XEC of Aryl Bromides with Alkyl Iodides Using a Homogeneous Organic Reductant (2019)**



presence of Hünig's base to enable reduction of Ni(II) to Ni(0). The authors propose that the reaction follows a typical radical chain mechanism with direct replacement of the reductant.

In 2021, scientists at Novartis, led by Fabrice Gallou, Bin Wu, and Ning Ye, published a Ni and Cu cocatalyzed cross-electrophile coupling reaction of aryl bromides with alkyl iodides in water/surfactant mixtures (Scheme 159).<sup>277</sup>

**Scheme 159. Nickel- and Copper-Catalyzed XEC of Aryl Bromides with Alkyl Iodides in Water, Solvent, and Surfactant Mixtures (2021)**

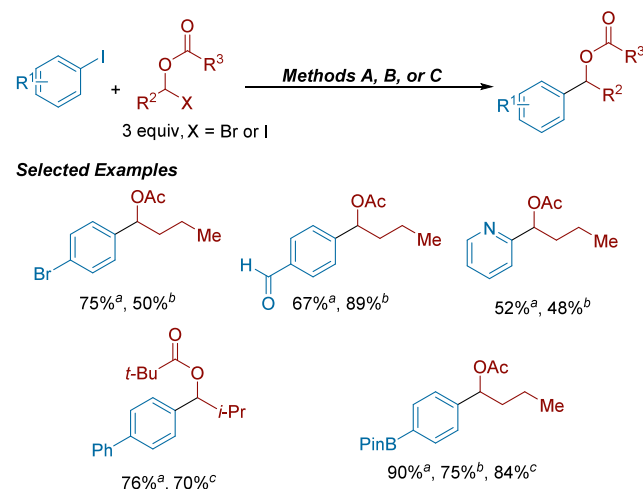


Stemming from a finding with copper-contaminated aryl bromide, this project found catalytic amounts of copper promoted alkyl transmetalation onto nickel, though its exact role is not defined in this study. These process-friendly, green conditions give rise to successful couplings between primary and secondary, cyclic or noncyclic, alkyl iodides and bromides with aryl bromides of different electronics. Heterocycles, both aromatic and saturated, were compatible, encompassing indoles, benzofurans, and benzothiophenes, among others. The reaction shows chemoselectivity over alkyl and aryl chlorides and tolerates more strained alkyl systems, such as the coupling of azetidines or cyclopropyl rings. This chemistry showcases the compatibility of XEC chemistry with protic solvents, even water!

Rueping and Huijing Yue reported the coupling of a variety of C(sp<sup>2</sup>) and C(sp) electrophiles with  $\alpha$ -oxy halides (derived from aldehydes) under three different reduction approaches (Scheme 160).<sup>278</sup> The diverse reaction conditions all converge on the use of NiCl<sub>2</sub>(dme) and 4,7-MeO-phen as the precatalyst and ligand. On the basis of DFT and experimental studies, the authors propose that the  $\alpha$ -oxy halide is a source of ketyl radical under these coupling conditions.

**4.2.3.2. XEC with Aryl Pseudohalides.** To couple alkyl iodides with aryl triflates and nonaflates, Hosoya and Sumida reported a method using Bphen, LiBr as an additive, and a Mn

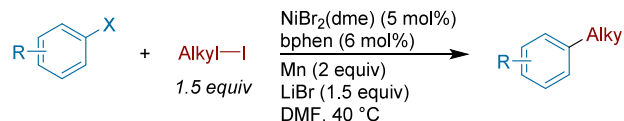
**Scheme 160. Photochemical, Electrochemical, and Mechanochemical Ni-Catalyzed XEC of  $\alpha$ -Oxy Alkyl Halides with Aryl Iodides (2022)<sup>a</sup>**



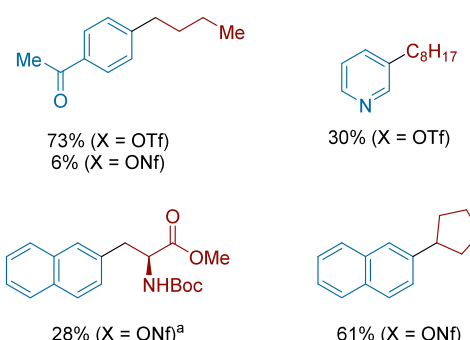
<sup>a</sup>(a) Method A: NiCl<sub>2</sub>(dme) (10 mol%), 4,7-MeO-phen (10 mol%), Mn (2 equiv), DMA, rt. (b) Method B: 3CzClIPN (5 mol%), NiCl<sub>2</sub>(dme) (10 mol%), 4,7-MeO-phen (10 mol%), Hantzsch Ester (2 equiv), (n-Bu)<sub>4</sub>N (5 equiv), DMA, 440 nm LED. (c) NiCl<sub>2</sub>(dme) (10 mol%), 4,7-MeO-phen (10 mol%), TBAPF<sub>6</sub> (0.2 M), DMA, Fe rod(+) / Ni foam(-), 8 mA, rt.

reductant to achieve selectivity (Scheme 161).<sup>279</sup> While couplings with electron-withdrawing triflates proceed effec-

**Scheme 161. Ni-Catalyzed XEC of Aryl Triflates and Nonaflates with Alkyl Iodides (2017)<sup>a</sup>**



**Selected Examples**

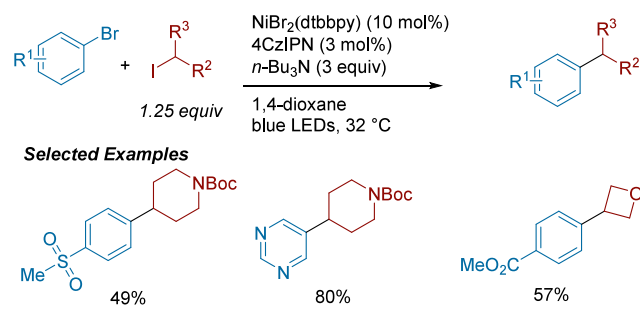


<sup>a</sup>At 80 °C.

tively, their nonaflate counterparts resulted in no detected yield and it was found that, across the board, electron-rich arenes are not compatible with these conditions. A series of aryl nonaflates were tested with alkyl iodides and moderate yields were obtained for both primary and secondary alkyl iodides. This work also briefly covers applicability to alkynyl triflates.

**4.2.3.3. Photochemical Methods.** Yatham and co-workers reported the visible-light mediated cross-electrophile coupling of alkyl iodides with aryl bromides (Scheme 162). Inspired

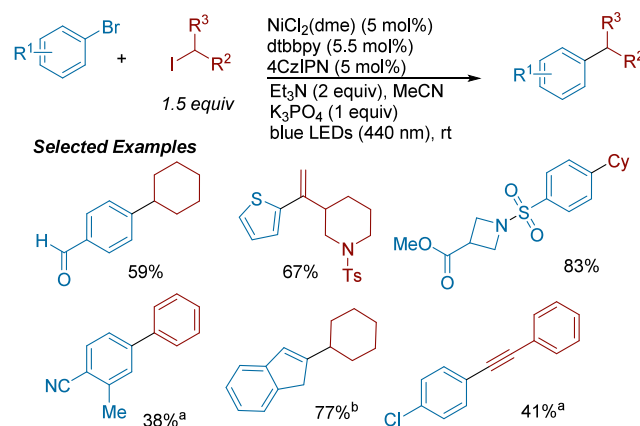
**Scheme 162.** XAT-Mediated XEC of Aryl and Heteroaryl Bromides with Alkyl Iodides Catalyzed by Nickel and 4CzIPN (2022)



by reports from the Leonori group that described alkyl radical formation through halogen-atom transfer (XAT) on alkyl iodides by photoredox-generated  $\alpha$ -amino radicals for use in metal-catalyzed cross-coupling reactions,<sup>281</sup> the authors extended this XAT approach to XEC. Mechanistic experiments support a radical pathway mediated by  $\alpha$ -amino radicals as Stern–Volmer experiments that show only *n*-Bu<sub>3</sub>N among the reaction components is able to quench excited state 4-CzIPN. A number of aryl and heteroaryl bromides were competent coupling partners with primary and secondary alkyl iodides to give the desired products with good functional group tolerance.

The Barham lab disclosed the XEC of aryl bromides with various electrophiles, including alkyl iodides, aryl iodides and alkenyl iodides, using  $\alpha$ -amino radical XAT agents under metallaphotoredox catalysis (Scheme 163).<sup>71</sup> Also inspired by

**Scheme 163.** XAT-Mediated XEC of Aryl Bromides with Organic Iodides Catalyzed by Nickel and 4CzIPN (2022)<sup>a</sup>

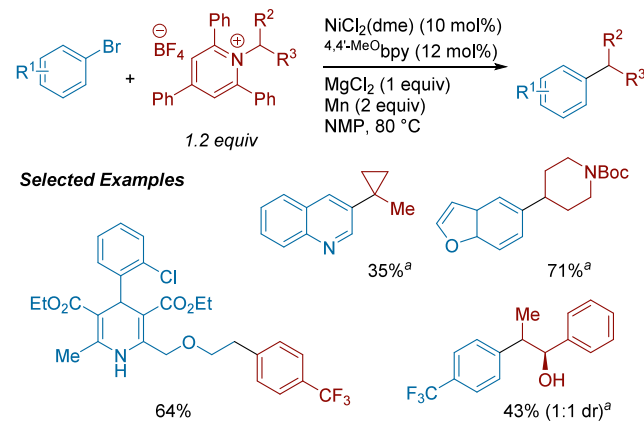


<sup>a</sup>(a) 3 Equiv organic iodide was used. (b) Ratio of aryl bromide to organic iodide is 1.5:1.

Leonori, the authors married XAT radical generation by photoredox-generated  $\alpha$ -aminoalkyl radicals with nickel catalysis to develop a variety of XEC reactions with aryl bromides. This strategy was general for a range of different types of iodinated carbon electrophiles and the formation of C(sp<sup>2</sup>)–C(sp<sup>3</sup>), C(sp<sup>2</sup>)–C(sp<sup>2</sup>) and C(sp<sup>2</sup>)–C(sp) bonds were all possible. While secondary alkyl iodides and alkenyl iodides coupled well with aryl bromides to form products with good yields, primary alkyl iodides, aryl iodides and alkynyl iodides often suffered from low reactivity with low product yields observed across the substrate scope.

**4.2.4. Alkyl Amines as Electrophiles.** 4.2.4.1. XEC of N-Alkylpyridinium Salts with Aryl Halides and Pseudohalides. Watson, Garnsey, and co-workers reported the deaminative cross-electrophile coupling of N-alkylpyridinium salts with aryl bromides (Scheme 164).<sup>282</sup> A broad range of aryl and

**Scheme 164.** Coupling of Aryl and Heteroaryl Bromides with N-Alkyl Pyridinium Salts via Ni-Catalyzed XEC (2019)<sup>a</sup>

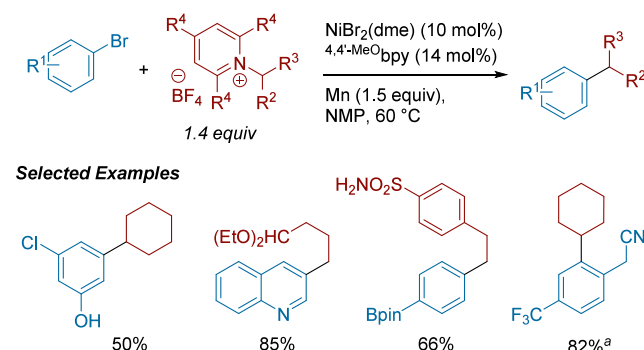


<sup>a</sup>With slow addition of pyridinium salt (1 equiv) and aryl bromide (1.1 equiv).

heteroaryl bromides were competent coupling partners with primary and secondary alkylpyridinium salts. In addition, the authors demonstrate a sterically challenging coupling with a tertiary alkylpyridinium salt. To simplify reaction setup, the authors demonstrated a one-pot protocol for direct use of an alkylamine through in situ pyridinium formation without intermediate purification to give the desired product with slightly reduced efficiency.

Martin and co-workers reported the cross-electrophile coupling of N-alkylpyridinium salts with aryl bromides to give the desired products with good functional group tolerance (Scheme 165).<sup>283</sup> The utility of this method was demonstrated through derivatization of amine-containing bioactive compounds such as Mexiletine and Mosapride. Control and radical trapping experiments suggest that alkylpyridinium fragmentation to alkyl radical is likely a Zn-mediated SET process rather than Ni-mediated.

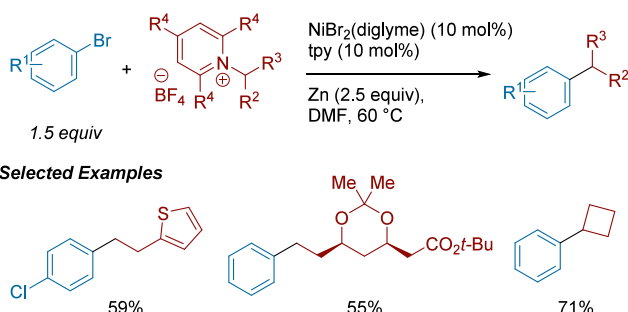
**Scheme 165.** Ni-Catalyzed XEC of Aryl and Heteroaryl Bromides with Primary and Secondary Pyridinium Salts (2019)<sup>a</sup>



<sup>a</sup>At 45 °C.

Hong Yan, Yi Wang, Jianlin Han, and co-workers reported the deaminative cross-coupling of *N*-alkylpyridinium salts with aryl iodides (**Scheme 166**).<sup>284</sup> Primary, as well as some

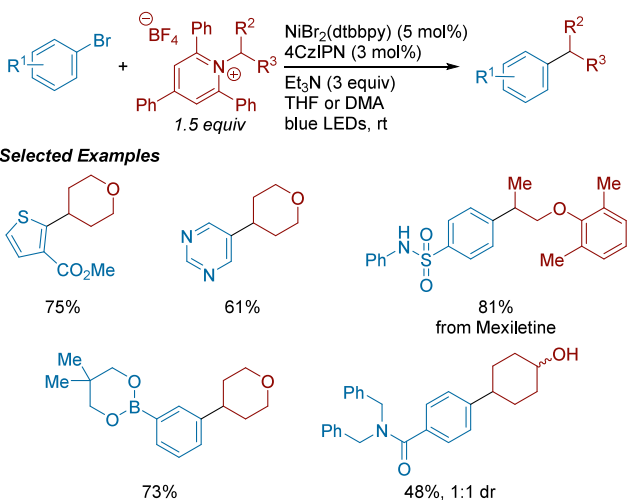
**Scheme 166.** In Situ Generation of *N*-Alkyl Pyridinium Salts for Ni-Catalyzed XEC with Alkyl Halides (2019)



secondary, alkylpyridinium salts were competent coupling partners. A one-pot protocol was demonstrated with one example to provide the desired product with essentially no loss of efficiency. The authors applied this method to the synthesis of an advanced common intermediate toward the natural products (+)-compactin and (+)-mevinolin in two steps in 55% yield, which was previously synthesized in ten steps in lower yield.

Molander and co-workers demonstrated the deaminative cross-electrophile coupling of *N*-alkyl pyridinium salts with aryl bromides using a metallaphotoredox strategy (**Scheme 167**).<sup>285</sup>

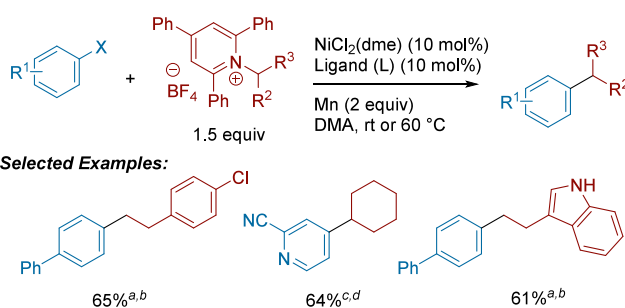
**Scheme 167.** Nickel/Photoredox XEC of Aryl Bromides with *N*-Alkyl Pyridinium Salts Using 4-CzIPN (2019)



While iridium photocatalysts were equally effective in promoting cross-coupling, 4-CzIPN was chosen as the optimal, more affordable option. Aryl and heteroaryl bromides of varying electronics bearing sensitive functional groups were effective coupling partners with several cyclic and acyclic alkyl pyridinium salts. Stern–Volmer quenching studies indicate that direct SET reduction of the pyridinium salt by excited state 4-CzIPN is possible, but further studies would be needed to rule out reduction by nickel.

Cavallo, Rueping, and co-workers reported on the deaminative cross-coupling of *N*-alkylpyridinium salts with aryl halides (**Scheme 168**).<sup>286</sup> A number of aryl and heteroaryl

**Scheme 168.** Coupling of Aryl and Heteroaryl Halides with *N*-Alkyl Pyridinium Salts via Nickel XEC (2019)<sup>a</sup>

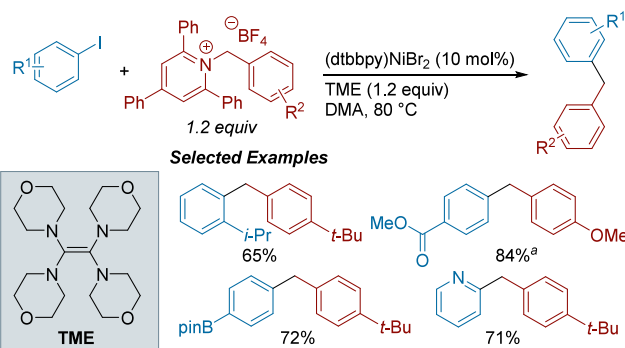


<sup>a</sup>(a) X = I, (b) L = ttbipy. (c) X = Br. (d) L = bpy.

bromides and iodides bearing groups of varying electronic effects provided the cross-coupled products in good yields. Both cyclic and acyclic alkylpyridinium salts were viable coupling partners. Notably, primary alkylpyridinium salts were also suitable for deaminative cross-coupling, and even methylation was viable under these conditions.

Hazari, Uehling, Zultanski, and co-workers developed a family of tetraaminoethylene-based reductants with improved stability and a range of reduction potentials compared to TDAE (**Scheme 169**).<sup>51</sup> The authors designed a three step

**Scheme 169.** Ni-Catalyzed XEC of Aryl Iodides with Benzylic *N*-Alkyl Pyridinium Salts Using a Homogeneous Organic Reductant (2021)<sup>a</sup>

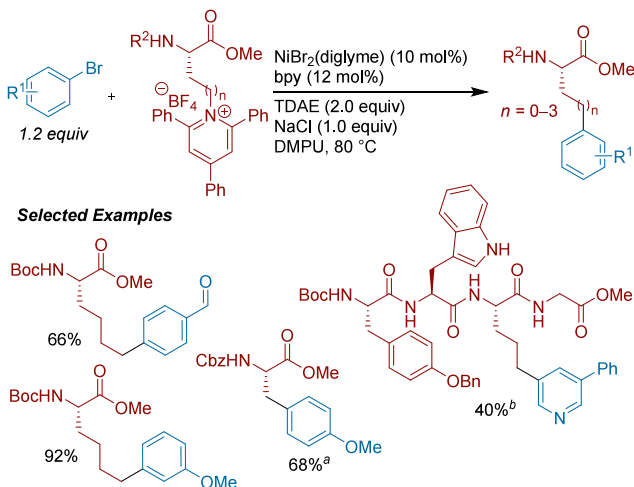


<sup>a</sup>With 20 mol% (dtbbpy)NiBr<sub>2</sub>.

synthesis of the air-stable solid reductants that are conveniently purified through filtration and washing under air, a stark contrast to the rigorously air-free conditions required for purification of TDAE. Using the range of reduction potentials to their advantage, the authors demonstrate fine-tuning of electron-transfer in several cross-electrophile coupling reactions between aryl halides and alkyl bromides or pyridinium salts. In fact, the reductant with the lowest potential enabled the first general cross-coupling of highly reactive benzylpyridinium salts and aryl iodides to give a variety of diarylmethanes in good yields and with good functional group tolerance.

In collaboration with Dion and Kalyani at Merck, Watson and co-workers reported a method to synthesize noncanonical amino acids through the XEC of *N*-alkylpyridinium salts with aryl bromides (**Scheme 170**).<sup>287</sup> These conditions employ amino acids with terminal amine side chains, enabling the

**Scheme 170.** Ni-Catalyzed XEC of Amino Acid-Derived N-Alkyl Pyridinium Salts with Aryl Bromides (2023)<sup>a</sup>



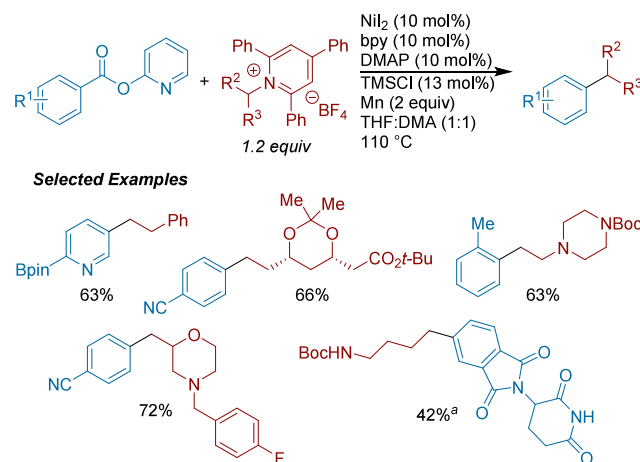
<sup>a</sup>(a) Modified conditions: NiBr<sub>2</sub>(diglyme) (10 mol%), PyBCam•2HCl (12 mol%), Mn (2.0 equiv), and DMPU (0.1 M) at 80 °C. (b) Modified conditions: aryl bromide (2.5 equiv), NiBr<sub>2</sub>(dme) (60 mol%), PyBCam•2HCl (72 mol%), Zn (3.0 equiv), TBAI (1 equiv), Boc-Trp-OMe (1 equiv), DMA at 80 °C.

synthesis of enantioenriched products from chiral pool materials. While substrates containing amides were tolerated, others containing acidic hydrogens (phenols, carboxylic acids, etc.) reacted poorly. The authors were motivated to undertake a high-throughput experimentation (HTE) approach to address these limitations. Using 96-well ( $\mu$ mol scale) and 1536-well (100 nMol scale) set-ups, they studied a range of parameters and found additional complementary reaction conditions that gave promising yields. Modified conditions with Zn or Mn better tolerated acidic functionality than the first set of conditions, possibly due to the inherent basicity of TDAE. However, the original TDAE conditions gave the highest yields across the broadest range of coupling partners. The stability of the N-alkylpyridinium amino acids allowed for solid-phase peptide synthesis where this functionality was carried through. XEC could be successfully performed on the peptide products, even before cleavage of the resin.

Our group reported the decarbonylative XEC of carboxylic acid substrate pools (as the aryl 2-pyridyl ester) with alkylamine substrate pools (as the N-alkylpyridinium, Scheme 171).<sup>288</sup> Through stoichiometric reactions and <sup>13</sup>CO labeling studies, we found that oxidative addition and decarbonylation of the aryl pyridyl esters is fast and reversible. 2-pyridone acts as a ligand to promote decarbonylation and stabilize the resulting arylnickel(II) complex. As with other reports in this area, elevated temperature was necessary to effectively remove CO from the reaction system and disfavor ketone formation. The conditions were also compatible with alkyl halide coupling partners. We successfully applied this strategy to efficiently form C(sp<sup>2</sup>)–C(sp<sup>3</sup>) linkages on proteolysis targeting chimera (PROTAC) anchors.

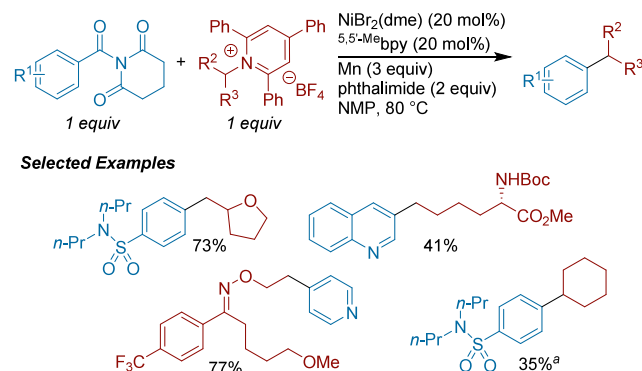
Concurrently, the Cernak lab developed the decarbonylative XEC of the same substrate pools, coupling N-acyl glutarimides with N-alkylpyridinium salts at relatively low temperatures (Scheme 172).<sup>289</sup> Using the latest in HTE optimization, the authors found that a stoichiometric phthalimide additive enabled high yields. DFT calculations and mechanistic studies

**Scheme 171.** Ni-Catalyzed Decarbonylative XEC of Carboxylic Acid Esters with N-Alkyl Pyridinium Salts (2023)<sup>a</sup>



<sup>a</sup>Modified conditions: alkylpyridinium (1.5 equiv), NiI<sub>2</sub> (20 mol%), 4,4'-MeO<sub>2</sub>bipy (20 mol%), Mn (2 equiv), THF/DMA (1:1) at 110 °C.

**Scheme 172.** Ni-Catalyzed Decarbonylative XEC of Aryl N-Acyl-Glutarimides with N-Alkyl Pyridinium Salts (2023)<sup>a</sup>

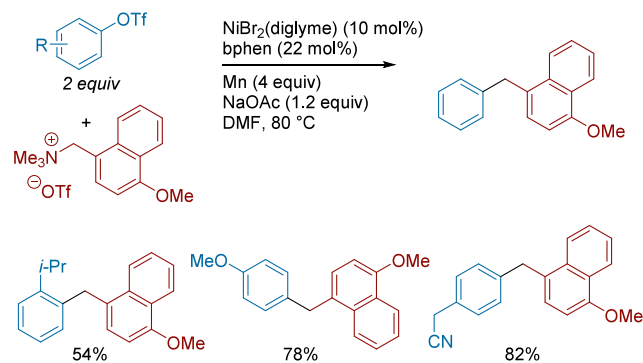


<sup>a</sup>Modified conditions: NiBr<sub>2</sub>(dme) (20 mol%), 5,5'-CF<sub>3</sub>bipy (20 mol%), Mn (2 equiv), phthalimide (2 equiv), RuCl<sub>3</sub> (50 mol%), GaCl<sub>3</sub> (50 mol%), NMP at 40 °C.

ruled out the phthalimide undergoing a transamidation reaction prior to XEC. The authors suggest that phthalimide may be assisting in prevention of nickel oligomerization or the formation of an off-cycle N-acyl-imide nickel complex. Electron-rich aryl acids were generally lower yielding under these conditions, favoring the ketone product instead. In the coupling with benzyl and secondary N-alkylpyridiniums, the authors found that addition of RuCl<sub>3</sub> and GaCl<sub>3</sub> reduced the amount of ketone byproduct and improved the yields for the decarbonylated product in the process.

**4.2.4.2. XEC of Ammonium Triflates with Aryl Pseudohalides.** Xing-Zhong Shu and co-workers described the use of benzyl ammonium triflates in deaminative cross-coupling with aryl triflates (Scheme 173).<sup>290</sup> This report marks one of the first combinations of C–O and C–N electrophiles for C–C bond formation in cross-electrophile coupling. The method was successful in providing a variety of diarylmethane products in good yields. Radical trapping and radical clock experiments indicate the involvement of benzyl radical from C–N bond

**Scheme 173. Ni-Catalyzed XEC of Aryl Triflates and Benzylic Ammonium-Functionalized Substrates (2019)**

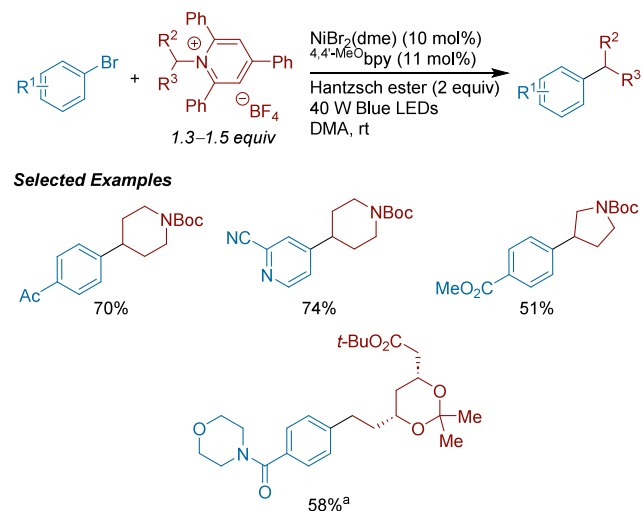


fragmentation, rather than through an oxidative addition mechanism with Ni.

**4.2.4.3. Electrochemical and Photochemical Approaches.**

Ming Joo Koh and co-workers reported a photochemical approach to cross-couple primary and secondary *N*-alkylpyridinium salts with aryl bromides (Scheme 174).<sup>291</sup> Aryl

**Scheme 174. Coupling Aryl Bromides with *N*-Alkylpyridinium Salts Through Nickel XEC (2021)<sup>a</sup>**

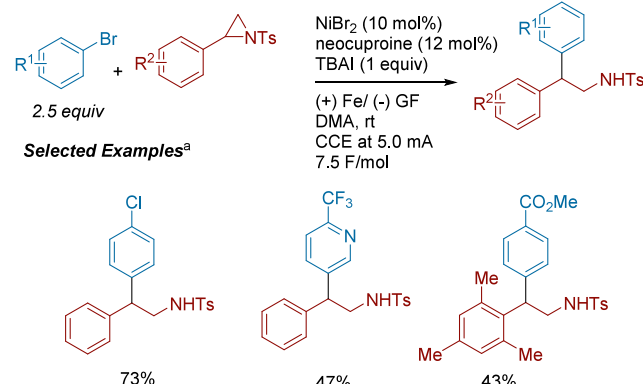


<sup>a</sup>With  $\text{NiBr}_2(\text{dme})$  (10 mol%), dtbbpy (12 mol%),  $\text{Et}_3\text{N}$  (3 equiv), and 1.5 equiv of the pyridinium salt.

bromides of various electronic profiles were tolerated in addition to substrates with sensitive functionalities like aldehydes and free alcohols. Both cyclic and acyclic secondary alkyl coupling partners coupled in moderate to high yield. Saturated heterocycles fared well and a few compounds, derived from bioactive precursors, were formed efficiently. They also described a few examples of alkyl–alkyl coupling using the same class of substrates. A few mechanistic experiments were conducted to test for the presence of a radical and for the intermediacy of an organonickel species; all results obtained do support these claims. Their proposed mechanism first involves the photoexcitation of Hantzsch ester which forms an EDA complex with the *N*-alkylpyridinium salt. After an SET step, the alkyl substrate undergoes fragmentation of the pyridinium group to form an alkyl radical which can then enter the nickel catalytic cycle.

Youai Qiu and co-workers report the synthesis of  $\beta$ -arylethylamines by electrochemically driven XEC of aryl aziridines and aryl bromides (Scheme 175).<sup>292</sup> The resultant

**Scheme 175. Coupling of Aryl Bromides with Tosyl-Protected Aziridines Using Electrochemically-Driven Nickel XEC (2023)<sup>a</sup>**

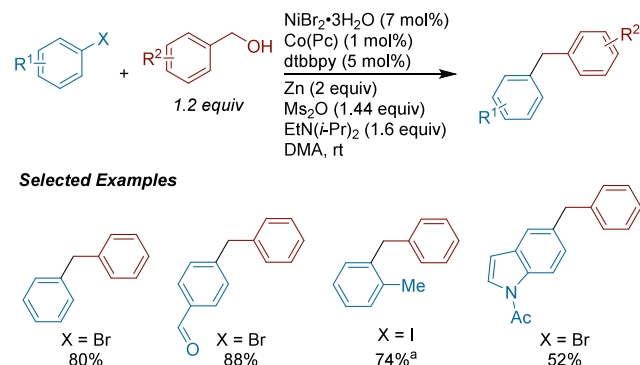


<sup>a</sup>GF = graphite felt.

coupling has high chemo- and regioselectivity. A broad range of electronic differences about the aryl bromide are tolerated, but electron-deficient aryl bromides typically outperformed electron-rich aryl bromides. With respect to the aryl aziridine, a broad range of functional groups were tolerated, including sterically hindered mesityl aziridine. From CV studies, the authors propose that neocuproine may be acting as a single-electron transfer mediator for the reduction of aryl aziridines, which generates a benzyl radical intermediate as the active species.

**4.2.5. Alkyl Alcohols as Electrophiles.** **4.2.5.1. XEC of *In Situ* Activated Alcohols with Aryl Halides and Pseudohalides.** Using a cobalt-based cocatalyst, we reported a pathway for the generation of benzylic C–C bonds through XEC (Scheme 176).<sup>174</sup> This method relies on the ability of  $\text{Co}(\text{Pc})$ , cobalt phthalocyanine, to generate benzyl radicals from benzylic mesylates; under optimized conditions, the mesylate is formed *in situ* from benzylic alcohols using methanesulfonic anhydride. Functional groups sensitive to organometallic reagents such as aldehydes and ketones are tolerated under

**Scheme 176. Cobalt- and Ni-Catalyzed XEC of Aryl Halides and Benzyl Alcohols Through *In Situ* Mesylate Formation (2015)<sup>a</sup>**

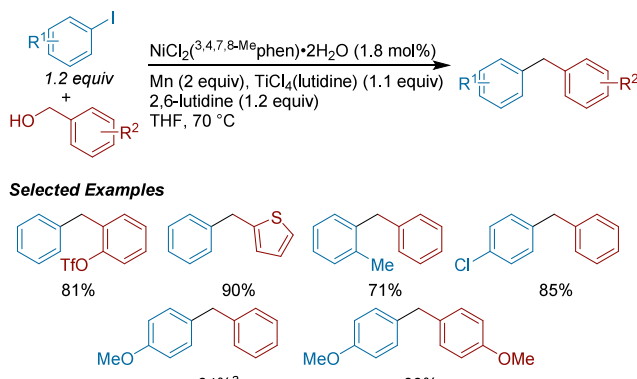


<sup>a</sup>With 3 mol%  $\text{Co}(\text{Pc})$  and at 60 °C.

this method. Added steric effects on the alcohol did not hinder reactivity and the conditions could be transferred to a vinyl bromide with similar success. With increased catalyst loading and temperature, benzyl diethyl phosphates could be employed in this reaction. A preliminary enantioconvergent coupling to  $\alpha$ -chloroethylbenzene using a chiral bis(oxazoline) ligand was also reported in 41% yield and 43% ee.

Ukaji and Suga reported the Ni-catalyzed cross-electrophile coupling of aryl iodides and benzyl alcohols with a Ti cocatalyst (Scheme 177).<sup>175</sup> The conditions tolerated benzyl

**Scheme 177. Titanium-Assisted Ni-Catalyzed XEC of Aryl Halides with Benzyl Alcohols (2018)<sup>a</sup>**

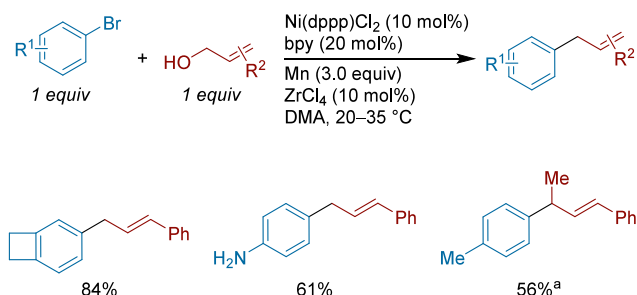


<sup>a</sup>With aryl bromide (3 equiv) instead of aryl iodide.

alcohols bearing electron-withdrawing and donating groups as well as reactive functional groups such as triflate and chloride but was limited to primary benzyl alcohols. Mechanistic experiments showed that a benzyl titanate is formed during the reaction, which is solely responsible for benzyl radical generation without involvement of Ni.

Xing-Zhong Shu and co-workers demonstrated the ability to employ both nickel and Lewis acids for the coupling of aryl bromides with allylic alcohols (Scheme 178).<sup>293</sup> The chosen

**Scheme 178. Employing Lewis Acids Alongside Nickel in the XEC of Aryl Halides with Allylic Alcohols (2018)<sup>a</sup>**



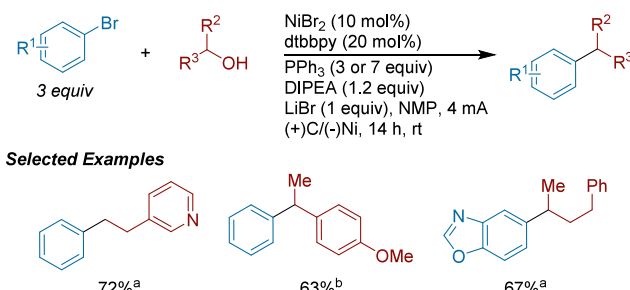
<sup>a</sup>With 15 mol% Ni(dppp)Cl<sub>2</sub>.

Lewis acid, ZrCl<sub>4</sub>, allows for effective activation of the alcohol via chelation. With no Lewis acid, they observed significant aryl dimer and no cross-product. Interestingly, these conditions use Ni(dppp)Cl<sub>2</sub> as their nickel precursor but have 2,2'-bipyridine as their active ligand. Additionally, NiBr<sub>2</sub>(dme) was used for sterically hindered aryls. The reaction proved chemoselective toward bromides over chlorides and couplings with heterocycles were also possible. Aryl coupling partners with free

alcohols and amines performed well in this protocol, as did both primary and secondary allylic alcohols. Mechanistic studies were conducted to elucidate the role of the Lewis acid, the kinetics and order of oxidative addition, and the possibility of a radical-containing process.

Chao Li and co-workers published an electrochemically driven cross-coupling method to form C(sp<sup>2</sup>)—C(sp<sup>3</sup>) bonds from alkyl alcohols and aryl bromides (Scheme 179).<sup>294</sup> The

**Scheme 179. Electrochemical Ni-Catalyzed XEC of Aryl Bromides with Primary and Secondary Alcohols (2021)<sup>a</sup>**

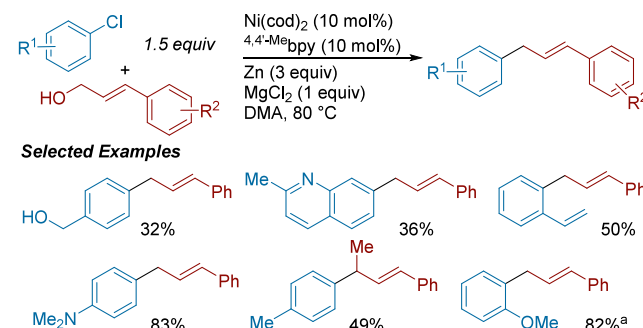


<sup>a</sup>(a) With 7 equiv of PPh<sub>3</sub>. (b) With 3 equiv of PPh<sub>3</sub>.

reaction takes place in an undivided cell at a constant current of 4 mA with a graphite anode and nickel foam cathode. Under these conditions, alkyl bromide is generated in situ via an Appel reaction between Br<sub>2</sub> and the triphenylphosphine-activated alcohol. They suggest that molecular bromine can be generated on the anode from bromide ions in solution. This reaction tolerates a variety of functional groups including protected amines, benzylic heterocycles, and ethers and can be used for primary or secondary alcohols. Additionally, heterocycles, such as indoles, carbazoles, and indazoles, can be functionalized. As an initial test, they also showed the coupling of a secondary alcohol with a vinyl bromide.

Zhong-Xia Wang and co-workers reported the coupling of aryl chlorides with allylic alcohols (Scheme 180).<sup>295</sup> The

**Scheme 180. Nickel-Catalyzed XEC of Aryl Chlorides with Alkyl Alcohols (2021)<sup>a</sup>**

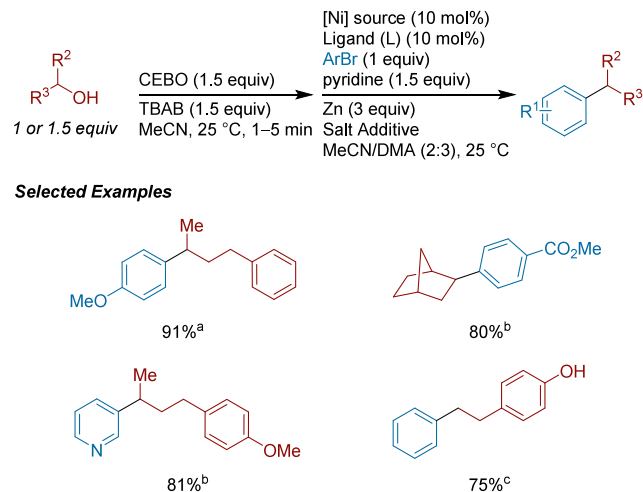


<sup>a</sup>With 4,4'-NH<sub>2</sub>bpy as ligand.

authors employ MgCl<sub>2</sub> to activate the allylic alcohol toward oxidative addition to the arylnickel(II) complex, resulting in the formation of an  $\eta^3$ -allylnickel(III) complex. 1,3- and 3-substituted allylic alcohols coupled effectively to furnish the (*E*)-configured products, and a variety of functional groups were tolerated on both coupling partners.

Hegui Gong, Guobin Ma, and Quan Lin reported a method, which employed a halogenation strategy developed by Mukaiyama, to couple primary and secondary alcohols with aryl bromides (**Scheme 181**).<sup>296</sup> This method involves a

**Scheme 181.** In Situ Generation of Alkyl Bromides from Alcohols for XEC with Aryl Bromides (2021)<sup>a</sup>

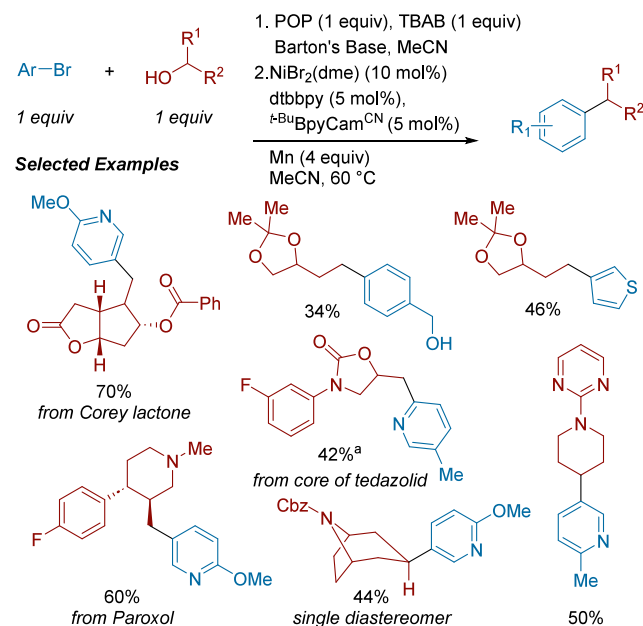


<sup>a</sup>(a) Conditions: [Ni] = NiCl<sub>2</sub>(Py)<sub>4</sub> (10 mol%), L = dtbbpy (10 mol %), and MgCl<sub>2</sub> (2 equiv). (b) Conditions: [Ni] = NiCl<sub>2</sub>(Py)<sub>4</sub> (5 mol %), L = dtbbpy (30 mol%), and MgCl<sub>2</sub> (2 equiv). (c) Conditions: [Ni] = Ni(acac)<sub>2</sub> (10 mol%), L = <sup>3,4,7,8-Me</sup>Phen (10 mol%), LiI (75 mol%), DMPU, 60 °C.

preactivation step, using 2-chloro-3-ethylbenzo[d]oxazol-3-ium (CEBO) and TBAB to generate alkyl bromides after which an aryl bromide is added with NiCl<sub>2</sub>(Py)<sub>4</sub>, dtbbpy, zinc, and MgCl<sub>2</sub> to initiate the XEC. CEBO is preceded in chlorination and this activation was near quantitative and fast in MeCN. The scope includes substrates with amides, saturated heterocycles, and macrocycles. They also show diastereoselective examples with >20:1 dr as well as examples where heterocycles were compatible. In their trials with diols, they show effective coupling even under the presence of free alcohols in addition to examples of diarylation when an excess of brominating agent is utilized.

Our group reported the in situ bromination/cross-coupling of unactivated aliphatic alcohols with aryl bromides (**Scheme 182**).<sup>297</sup> Employing Hendrickson's POP reagent in the presence of a bromide source and base, we quantitatively generated alkyl bromides from alcohols within a minute. The resulting mixture could be directly used in subsequent cross-coupling with aryl bromides without purification steps. The identification of an appropriate in situ bromination reagent was crucial to ensure compatibility of byproducts with the Ni-catalyzed cross-coupling step. A combination of dtbbpy and <sup>t-Bu</sup>BpyCam<sup>CN</sup> as ligands were found to be necessary for productive catalysis, in which dtbbpy was important aryl bromide activation whereas <sup>t-Bu</sup>BpyCam<sup>CN</sup> was key to alkyl bromide consumption. A variety of aryl and heteroaryl bromides were competent coupling partners with a diverse set of primary and secondary alcohols, including the deoxygenative arylation of the prostaglandin precursor Corey lactone and medicinally relevant compounds such as Paroxol, the core of tedizolid, and a tropine derivative.

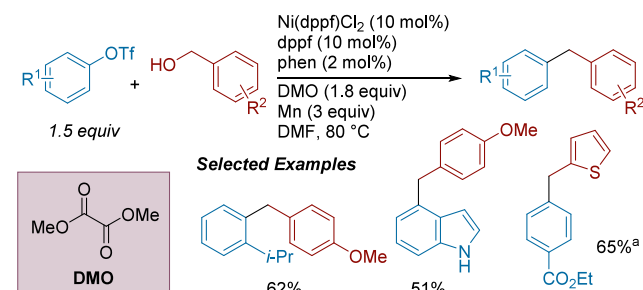
**Scheme 182.** Ni-Catalyzed XEC of Aryl Halides with Primary and Secondary Alcohols Through an In Situ Bromination Strategy (2022)<sup>a</sup>



<sup>a</sup>With <sup>t-Bu</sup>BpyCam<sup>CN</sup> (10 mol%) and no dtbbpy.

Xing-Zhong Shu and co-workers reported the deoxygenative cross-coupling of benzyl alcohols with aryl triflates (**Scheme 183**).<sup>298</sup> Free benzylic alcohols are activated in situ as redox-

**Scheme 183.** Ni-Catalyzed XEC of Aryl Triflates with Benzyl Alcohols (2021)<sup>a</sup>



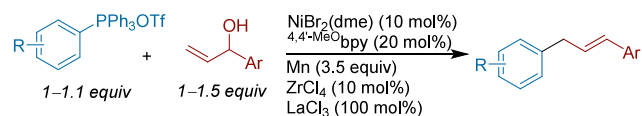
<sup>a</sup>With NiBr<sub>2</sub>(diglyme) (10 mol%) as catalyst, pyridine (10 mol%), and AlCl<sub>3</sub> (10 mol%).

active oxalates, via transesterification with dimethyl oxalate (DMO), which undergo fragmentation to benzylic radicals upon SET. When employing heterobenzyl alcohols, the authors found that the addition of AlCl<sub>3</sub> was necessary for successful coupling; mechanistic studies show that AlCl<sub>3</sub> may enhance reactivity of aryl triflates and/or slow down the transesterification of alcohols to form oxalates, resulting in better matched rates of reactivity. In subjecting both coupling partners to a preformed nickel(0) complex, the authors observed a higher percentage of benzyl homodimer and protodefunctionalization side products over the analogous aryl triflate side products, implying that the benzyl oxalate is first to react with the nickel complex in a catalytic system via a radical type pathway.

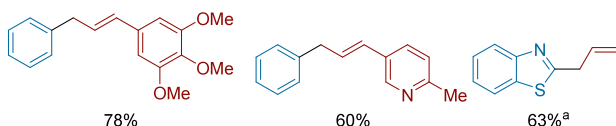
Huifei Wang, Hongze Liang, and co-workers detailed the cross-electrophile coupling of aryl phosphonium salts and

allylic alcohols using a nickel catalyst and a Lewis acid for alcohol activation (Scheme 184).<sup>299</sup> When investigating Lewis

**Scheme 184.** Ni-Catalyzed XEC of Allylic Alcohols and Aryl Phosphonium Salts (2021)<sup>a</sup>



**Selected Examples**

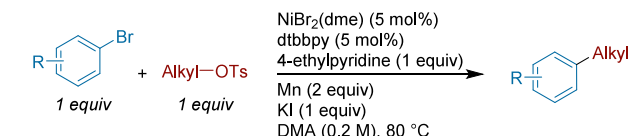


<sup>a</sup>Modified conditions for allylic carbonates: Josiphos (20 mol%) used as ligand, Mn (3 equiv), no ZrCl<sub>4</sub> or LaCl<sub>3</sub> added, and rt. From methyl 3-butenoate.

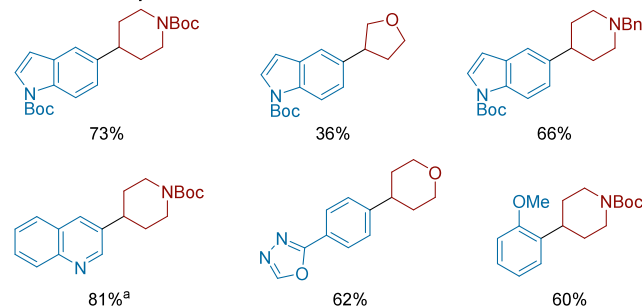
acids, LaCl<sub>3</sub> was shown to give poor yields but excellent cross-selectivity. Ultimately, they found that a mixture of ZrCl<sub>4</sub> and LaCl<sub>3</sub> balanced both aspects well. Both electron-rich and electron-poor arenes displayed compatibility with these conditions, in addition to *ortho*-substituted aryl substrates. Heterocycles, such as dibenzofuran, pyridine, and indole, were effectively coupled, generally in yields above 60%. They attempted to apply these findings to couple benzothiazole derivatives with allylic carbonates under slightly modified conditions using a Josiphos ligand. These initial results demonstrated successful coupling with both electron-rich and electron-poor benzothiazoles.

**4.2.5.2. XEC with Alkyl Sulfonates.** The Molander group adapted their previous findings to encompass more readily available alkyl coupling partners, (Scheme 185).<sup>300</sup> Envisioning an alcohol preactivation step, they described a pathway in which alkyl tosylates could be coupled with aryl bromides. They found that pyrrolidines, piperidines, and tetrahydropyrans among other nonaromatic heterocycles were compatible. When attempting a coupling with the respective mesylates, reactivity was still observed although at lower yields. Similarly

**Scheme 185.** Ni-Catalyzed XEC of Heteroaryl Bromides and Heterocyclic Alkyl Tosylates (2015)<sup>a</sup>



**Selected Examples**

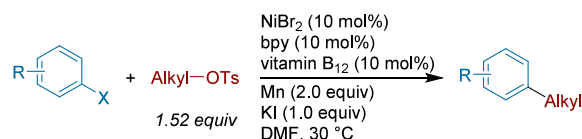


<sup>a</sup>Run on a 3.0 mmol scale.

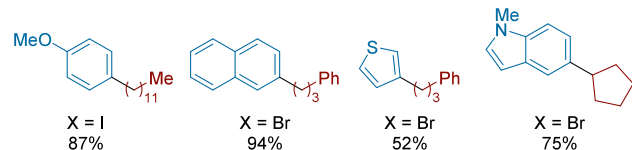
to other proposals, they suggest one role of KI is halogen exchange with the alkyl tosylate, forming an alkyl iodide. They also propose that this additive may serve as an intermediate stabilizer or bridging ligand within the nickel cycle.

Inspired by developments in cocatalyzed nickel and cobalt cross-electrophile coupling, Komeyama and co-workers described a method in which vitamin B<sub>12</sub> (VB<sub>12</sub>) could act as a suitable replacement for other previously used cobalt cocatalysts (Scheme 186).<sup>301</sup> They were interested in the

**Scheme 186.** XEC of Aryl Halides with Alkyl Tosylates Using Nickel and Vitamin B<sub>12</sub> Co-Catalysis (2017)



**Selected Examples**

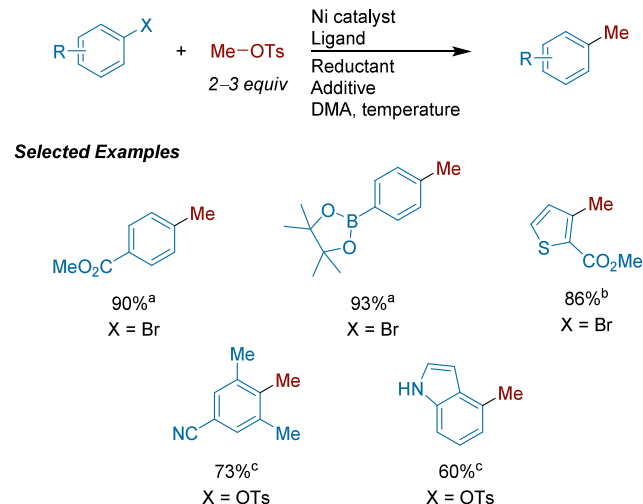


couplings of aryl halides with alkyl tosylates and found a dependence of alkyl tosylate consumption on the presence of VB<sub>12</sub> while aryl halide consumption was controlled by the nickel catalyst. Furthermore, VB<sub>12</sub> outperformed a variety of other cobalt cocatalysts. The KI additive enhanced yields, although the reaction still proceeded without added iodide. The reaction was compatible with aryl iodides and bromides, and an example of an electron-deficient aryl chloride was also included.

Hegui Gong, Jianhong Zhao, and Jiawang Wang disclosed a methylation technique in which aryl bromides and tosylates could undergo Ni-catalyzed XEC with methyl tosylate (Scheme 187).<sup>302</sup> The methods vary widely from bromides to tosylates, requiring careful selection of reagents and catalyst loadings in almost all aspects. When using aryl bromides, they observed a strong dependence on TBAI and MgCl<sub>2</sub> for reactivity. The reaction covers a wide range of electronically diverse substrates and is successful with hindered arene coupling partners. More sensitive functional groups are tolerated, such as alkenes and boronate esters, and heterocycles could also be coupled. To increase the generality of their system and include substrates derived from phenols, they describe a second set of conditions that can be used with aryl tosylates. The scope here is relatively similar but also allows for the methylation of sterically congested substrates with 2,6-di-*ortho*-substitution.

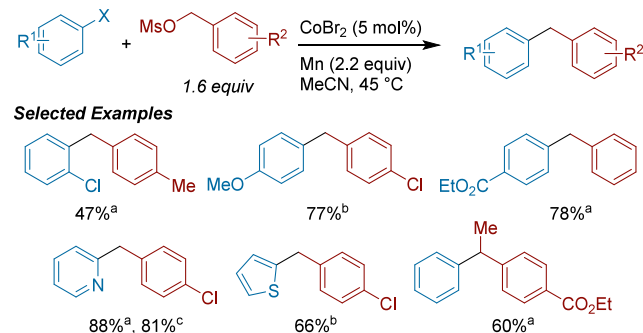
Gosmini, Auffrant, and co-workers reported a cobalt-catalyzed XEC of aryl bromides and iodides with benzyl mesylates (Scheme 188).<sup>303</sup> The protocol can also be streamlined to start from the benzyl alcohol without isolation of the mesylate, although a centrifugation step prior to XEC was needed to remove ammonium salt byproducts. Aryl halides with various electronics could be coupled. The mechanism is proposed to undergo initial reduction of Co<sup>II</sup> salt to catalytically active Co<sup>I</sup> species, which reacts with the aryl bromide to form a Co<sup>III</sup> complex. This complex undergoes reduction by Mn and subsequent capture of a benzyl radical

**Scheme 187.** Ni-Catalyzed Methylation of Aryl Halides and Tosylates with Methyl Tosylate (2017)<sup>a</sup>



<sup>a</sup>(a) Conditions A:  $\text{NiI}_2$  (5 mol%),  $4,4'\text{-Me}\text{bpy}$  (7 mol%), Zn (2 equiv),  $\text{MgCl}_2$  (1.5 equiv), and TBAI (1 equiv) at rt. (b) Conditions B:  $\text{NiI}_2$  (10 mol%),  $4,4'\text{-Me}\text{bpy}$  (15 mol%), and MeOTs (2 equiv). (c) Conditions C:  $\text{NiCl}_2(\text{dme})$  (10 mol%), dppf (20 mol%), Zn (6 equiv), LiCl (6 equiv), and TBAI (1.5 equiv) at 40 °C.

**Scheme 188.** Cobalt-Catalyzed XEC of Aryl Halides with Benzylmesylates (2018)<sup>a</sup>



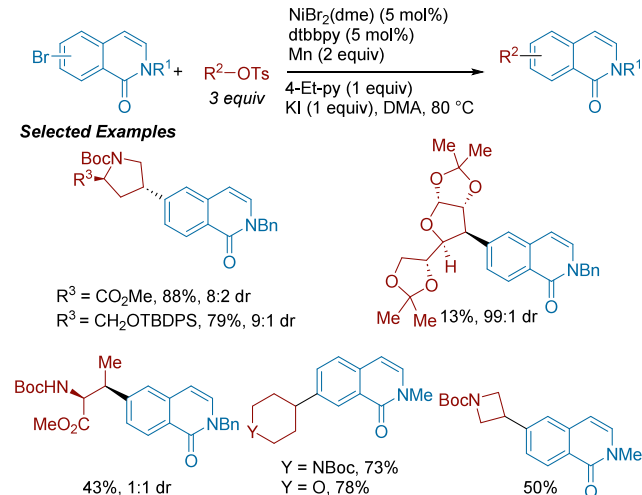
<sup>a</sup>(a) With aryl bromide. (b) With aryl iodide. (c) Telescoped from benzyl alcohol without isolation of the mesylate.

from benzyl bromide, which was detected in the reaction (*in situ* generated from the mesylate).

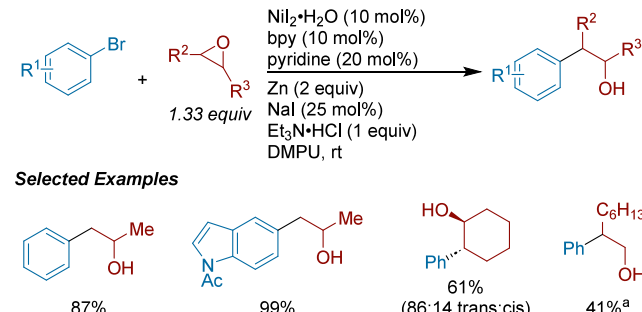
Hanessian and co-workers reported the XEC of bromoisouquinolones with alkyl tosylates to introduce saturated heterocycles, as well as acyclic aminoalkyl moieties, at the C-6 and C-7 positions of the isoquinolone core (Scheme 189).<sup>304</sup> The authors report good yields and high diastereoselectivity in coupling chiral azacyclic tosylates, and were able to translate this to the coupling of a sugar derivative, albeit in low yield. Acyclic amino acid derived tosylate coupling partners were also successful but saw decreased yield and diastereoselectivity. While the authors do show that KI and 4-ethyl-pyridine are necessary additives for improving reaction selectivity, the exact role is not concretely understood.

**4.2.5.3. XEC with Epoxides.** In 2014, our group reported a cross-electrophile coupling strategy with epoxides as coupling partners (Scheme 190).<sup>305</sup> While initial conditions favored terminal insertion to afford the secondary alcohol, the addition of a titanium cocatalyst under modified conditions flips

**Scheme 189.** Ni-Catalyzed XEC of Bromoisouquinolones with Alkyl Tosylates (2020)



**Scheme 190.** Nickel/Titanium Co-Catalyzed Regiodivergent Cross-Electrophile Coupling of Aryl Halides with Epoxides (2014)<sup>a</sup>

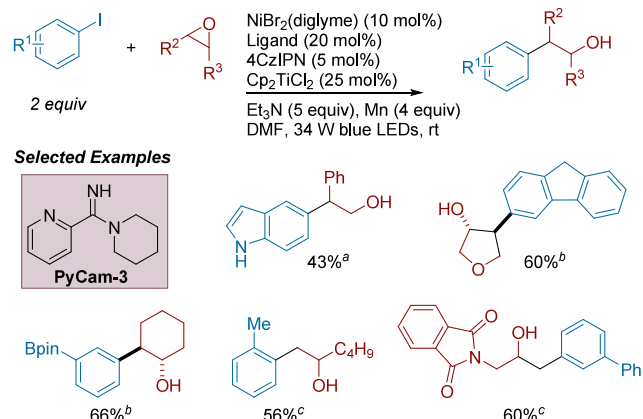


<sup>a</sup>Conditions for branched product:  $\text{NiCl}_2(\text{dme})$  (10 mol%), bipy (10 mol%),  $\text{Cp}_2\text{TiCl}_2$  (10 mol% + 4 mol% after 2 h),  $\text{Et}_3\text{N}\text{-HCl}$  (1 equiv), Mn (2 equiv), and DMPU.

regioselectivity and favors ring-opening at the more hindered site. Adding NaI improved the rate of formation of cross-product, but the reaction reaches comparable yields with longer reaction times, as the precatalyst introduces catalytic amounts of iodide. The possibility of an organozinc reagent was ruled out by the fact that TDAE was a competent reductant. When forming the secondary alcohol, the reaction proceeded with high enantiospecificity and regioselectivity. In the case when forming a primary alcohol, regioselectivity was substrate dependent with regards to the alkyl bromide. Alterations to the aryl bromide were well-tolerated.

Doyle and co-workers reported the regioselective cross-coupling of aryl iodides with epoxides using a Ni/Ti/photocatalytic system (Scheme 191).<sup>306</sup> The optimal ligand for cross-coupling was dependent on the epoxide structure, with styrene oxides most generally effective with piperidinyl-PyCam (PyCam-3), cyclic epoxides with Bphen, and terminal aliphatic epoxides with ttbtpy. The authors noted that enantioenriched styrene oxides racemize under reaction conditions and favor the branched product, while enriched aliphatic epoxides retain their stereocenter and favor the linear product. Accordingly two mechanisms are proposed: styrene oxides engage with Ti(III) species to generate alkyl radical,

**Scheme 191.** Nickel and Titanium Catalyzed Photoredox-Enabled XEC of Aryl Iodides with Epoxides (2020)<sup>a</sup>

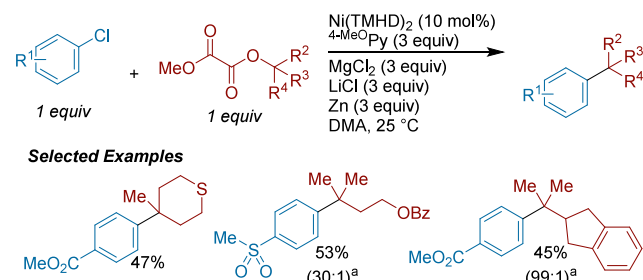


<sup>a</sup>(a) Ligand = PyCam-3, (b) Ligand = Bphen, MeCN instead of DMF, (c) Ligand = dtbbpy.

while aliphatic epoxides undergo *in situ* ring-opening to form iodohydriins as intermediates.

**4.2.5.4. XEC with Oxalates.** Hegui Gong and co-workers reported conditions for the deoxygenative coupling of tertiary alkyl oxalates with electronically activated aryl chlorides to give all-carbon quaternary centers with high selectivity for the retention product over isomerization (Scheme 192).<sup>307</sup> MgCl<sub>2</sub>

**Scheme 192.** Formation of Quaternary Centers via Ni-Catalyzed XEC of Aryl Chlorides with Tertiary Alkyl Oxalates (2019)<sup>a</sup>

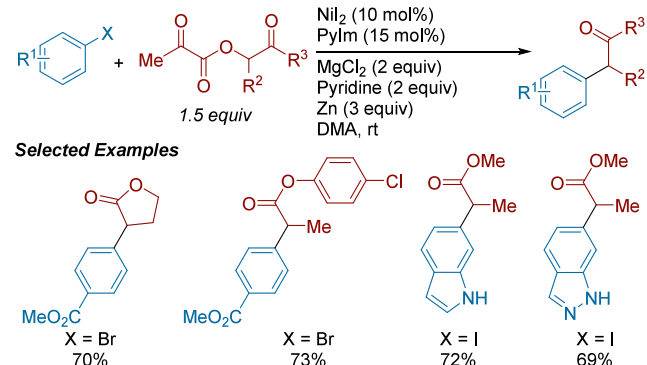


<sup>a</sup>Ratio of quaternary product to isomerization product.

is proposed to activate the oxalate for reduction by Zn to generate the putative tertiary alkyl radical. The authors demonstrate the synthetic utility of this method through the derivatization of the aryl chloride-containing drug fenofibrate in 65% yield under slightly modified reaction conditions. Modified conditions for trapping the tertiary alkyl radical with electron-deficient alkenes were also demonstrated.

Hegui Gong and co-workers then disclosed the activation of  $\alpha$ -hydroxy carbonyls as redox-active oxalates, which can undergo C–O bond fragmentation and subsequent Ni-catalyzed cross-coupling with aryl halides (Scheme 193).<sup>308</sup> The method was successful in providing the deoxygenated cross-coupled products for a variety of aryl bromides and iodides in good yields. Cyclic voltammetry measurements indicated that Zn alone is not sufficiently reducing for C–O bond fragmentation, suggesting that coordination to MgCl<sub>2</sub> may be necessary to promote reduction of the oxalate. Mechanistic experiments with a 5-hexenyl radical clock probe

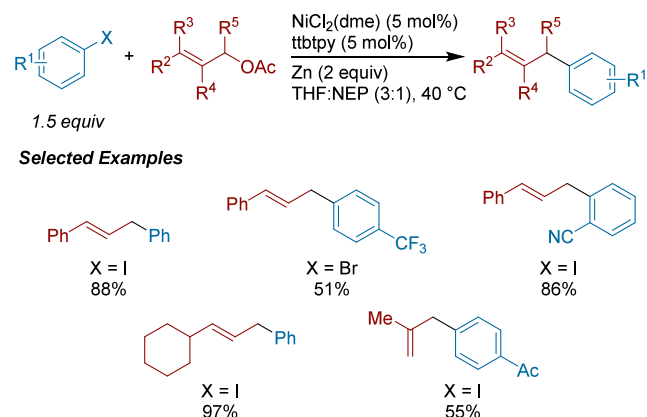
**Scheme 193.** Ni-Catalyzed XEC of Aryl Halides with Oxalates Derived from  $\alpha$ -Hydroxy Esters (2019)



at varying catalyst concentrations supported a radical chain mechanism.

**4.2.5.5. XEC with Allylic Acetates.** Following our first report on XEC, we reported conditions to couple aryl bromides and iodides with allylic acetates (Scheme 194).<sup>309</sup> Using

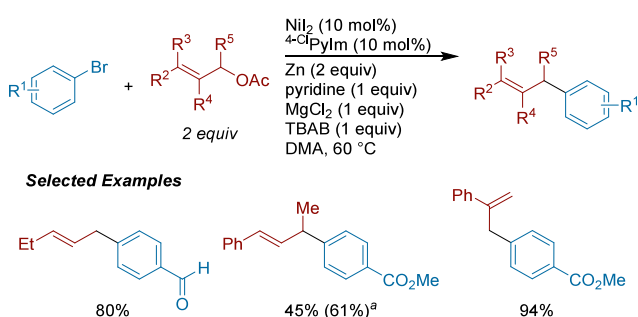
**Scheme 194.** Ni-Catalyzed XEC of Aryl Halides with Allylic Acetates (2012)



NiCl<sub>2</sub>(dme) and ttbipy as our catalytic system, effective coupling of cinnamyl acetate with iodobenzene could be achieved in 90% yield. Tracking the mass balance, we observed minimal formation of biphenyl and alkyl dimer. The most significant competing reaction was hydrodehalogenation of the aryl coupling partner. A solvent mixture consisting of *N*-ethylpyrrolidinone (NEP)/THF was used but a DMA/THF mixture can be substituted if needed without a significant decrease in yield. A variety of electron-rich/neutral aryl iodides and electron-poor aryl bromides were compatible. Primary and secondary allylic acetates are tolerated with a preference for linear over branched products. This report also demonstrates couplings of allylic acetates with alkyl bromides and enones, which is highlighted in section 6.3.1, Scheme 355.

Hegui Gong, Qun Qian, and co-workers developed the Ni-catalyzed cross-electrophile coupling of aryl bromides with allylic acetates (Scheme 195).<sup>310</sup> During optimization, they discovered that 4-chloro-pyridinylimidazole (<sup>4-Cl</sup>PyIm) was the best-performing ligand and that the reaction benefitted greatly from the presence of MgCl<sub>2</sub> and Bu<sub>4</sub>NBr; it was suggested that these additives aid in zinc activation to participate in the reduction of nickel. In cases where it is more sterically favorable, regiosomers may form via transfer of nickel within

**Scheme 195.** Cross-Electrophile Coupling of Aryl Bromides with Allylic Acetates (2013)<sup>a</sup>

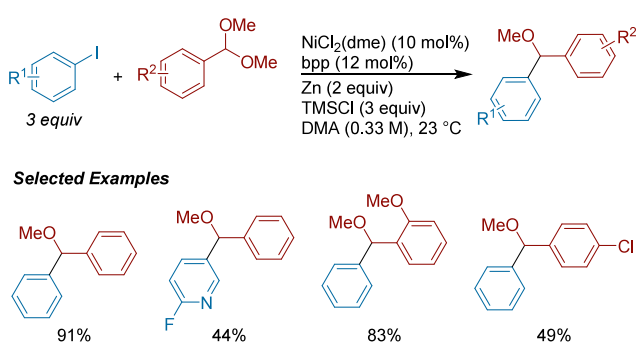


<sup>a</sup>With aryl chloride.

the  $\pi$ -allyl-nickel(II) complex. An initial test toward enantioselective XEC was made in this study using a PyBOX ligand resulting in 45% yield and 10% ee. The authors reasoned that the mechanism did not proceed through organozinc species since primarily unreacted starting material was observed when the reaction was run without ligand.

**4.2.5.6. XEC with Alkyl Ethers.** Doyle and co-workers applied their understanding of  $\alpha$ -oxy radical generation in cross-electrophile coupling to form dialkyl ethers (Scheme 196) from aryl iodides and acetals.<sup>311</sup> It is notable that the

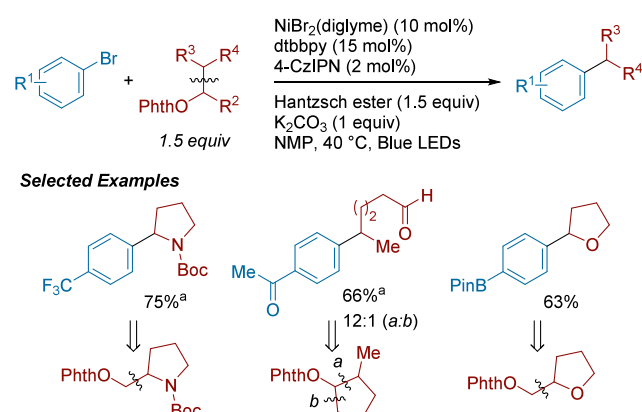
**Scheme 196.** Ni-Catalyzed Cross-Electrophile Coupling of Aryl Iodides with Acetals (2015)



synthesis of dialkyl ethers generally relies on C–O bond formation (e.g., Williamson ether synthesis) or C(sp<sup>3</sup>)–C bond formation with organic nucleophiles, both of which exhibit limitations in functional group tolerance. Their conditions tolerate electronically diverse arenes including carbonyl functional groups, with no sign of ketyl formation. Using TMSCl as a Lewis acid and Zn as the reductant, they could generate the  $\alpha$ -oxy radical as indicated by trapping experiments. Although less commonly applied in nickel XEC up to that point, 2,6-bis(*N*-pyrazolyl)pyridine (bpp), a tridentate amine ligand, proved to be the optimal choice. X-ray diffraction of the Ni(bpp) complex indicated a distorted octahedral geometry as opposed to square planar, the geometry seen in Ni(tpy) complexes. They suggest, however, that the redox potentials of the ligands contribute to the unique selectivity differences between the two conditions given their otherwise similar features.

Martin and co-workers reported the alkylation of aryl bromides via  $\beta$ -scission of alkoxy radicals derived from *N*-alkoxyphthalimide ethers (Scheme 197).<sup>312</sup> The authors propose that alkoxy radical generation proceeds through an

**Scheme 197.** Ni-Catalyzed Photoredox Approach to the XEC of Aryl Bromides with *N*-Alkoxyphthalimide Ethers (2020)<sup>a</sup>

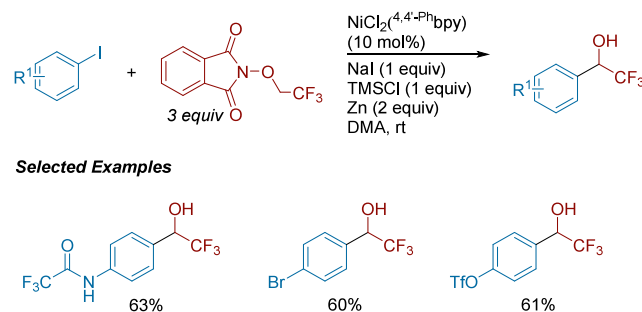


<sup>a</sup>With 2 equiv *N*-alkoxyphthalimide ether and 2 equiv Hantzsch ester.

initial electron-donor–acceptor (EDA) complex between Hantzsch ester reductant and the *N*-alkoxyphthalimide ethers. Subsequent C–C  $\beta$ -scission results in the more substituted alkyl radical, which engages in cross-coupling to give the desired product. Notably, the method could be used to functionalize a variety of saccharide-derived coupling partners in good yields. The authors also demonstrated C(sp<sup>3</sup>)–C(sp<sup>3</sup>) coupling of alkyl bromides with *N*-alkoxyphthalimide ethers under modified conditions.

Bandini, Bertuzzi, Silva López, and co-workers disclosed a Ni-catalyzed cross-electrophile coupling approach for the synthesis of  $\alpha$ -aryl- $\alpha$ -trifluoromethyl alcohols (Scheme 198).<sup>313</sup> The authors found that the redox-active ether *N*-

**Scheme 198.** Ni-Catalyzed XEC of Aryl Iodides with *N*-trifluoroethoxyphthalimide (2022)

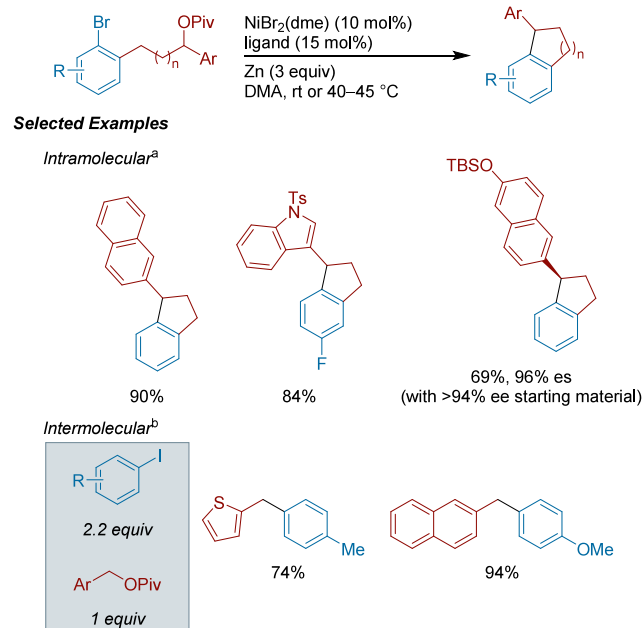


trifluoroethoxyphthalimide could be reduced through N–O bond cleavage. This affords a highly electrophilic oxygen radical, which undergoes a rapid intramolecular 1,2-HAT process, resulting in a more stable alkyl radical. The substrate scope shows broad functional group compatibility for the aryl iodide coupling partner, as bromide, boronate ester, triflate, and a TMS-protected alkyne were all well-tolerated in this reaction. An example of a pentafluoropropanol-derived *N*-alkoxyphthalimide coupling partner was low yielding (22%). DFT computations supported that Zn helps promote the N–O bond cleavage and that the key 1,2-HAT process is mediated by DMA.

**4.2.5.7. XEC with Alkyl Acetates and Pivalates.** In 2016, the Jarvo group outlined both an intra- and intermolecular pathway for the coupling of alkyl pivalates with aryl bromides

and iodides (Scheme 199).<sup>314</sup> They observed high selectivity for the intramolecularly cyclized product, with lower yielding

**Scheme 199. Inter- and Intramolecular Ni-Catalyzed XEC of Aryl Halides with Benzylidic Pivalates (2016)<sup>a</sup>**



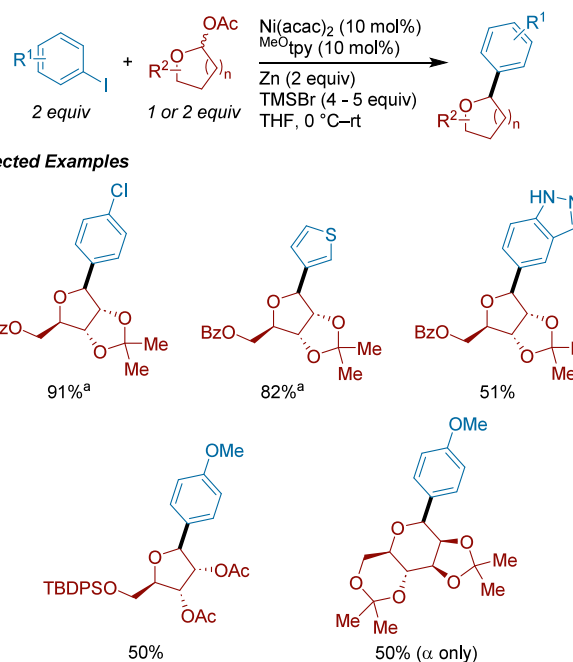
<sup>a</sup>(a) With Bphen as ligand. (b) With dppf as ligand.

reactions being attributed to accelerated hydrodehalogenation. Adding pyridine or NaI disfavored product formation and led to increased hydrodehalogenation. The reaction could form 5- and 6-membered rings with various functionality at the alkyl site of reactivity, including heterocycles. A stereospecific version of this cyclization was described, which proceeded in good to high enantiospecificity (83–96% es). In addition, they adapted their conditions to apply to intermolecular examples, requiring a swap of the ligand to dppf. These examples were limited to benzylic coupling partners, but good yields were achieved.

In 2022, Chao Li and co-workers reported a diastereoselective procedure for the cross-electrophile coupling of furanosyl acetates with aryl iodides (Scheme 200).<sup>315</sup> During optimization, the  $\beta$ -anomer was selectively formed though a few scope entries favor the  $\alpha$ -anomer. Generally, sterically hindered *ortho*-substituted arenes are tolerated, although they give lower yields. The conditions also tolerate a range of electronic aryl iodide profiles, and these conditions are chemoselective for aryl iodides over bromides and chlorides. A variety of sugars, such as ribofuranoses and mannofuranoses, as well as different classes of heterocycles, were compatible. The researchers were successful in scale up attempts, running this reaction at the gram scale.

**4.2.6. Carboxylic Acids as Electrophiles. 4.2.6.1. XEC with N-Hydroxyphthalimide Esters.** Prior to their use in XEC reactions, *N*-hydroxyphthalimide (NHP) esters had been previously shown to generate alkyl radicals following single electron transfer,<sup>316,317</sup> providing motivation that NHP esters could be competent coupling partners in XEC methods. Concurrent with our work in XEC, Baran and co-workers reported impressive results coupling NHP esters with arylzinc reagents.<sup>318</sup>

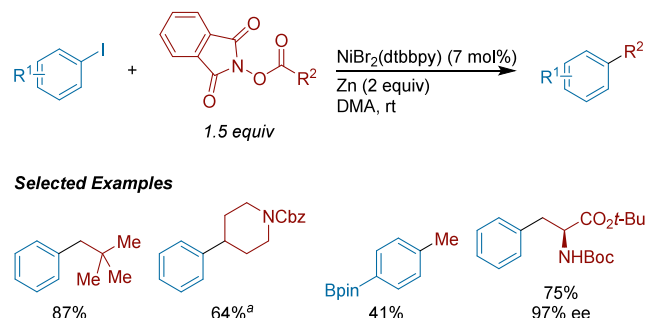
**Scheme 200. Ni-Catalyzed XEC of Aryl Iodides and Furanosyl Acetates (2022)<sup>a</sup>**



<sup>a</sup>With 5 equiv of TMSBr.

Our group developed the Ni-catalyzed decarboxylative cross-electrophile coupling of NHP esters with aryl iodides (Scheme 201).<sup>319</sup> Notably for the time, this report represented a

**Scheme 201. Ni-Catalyzed XEC of Aryl Iodides and *N*-Hydroxyphthalimide Esters (2016)<sup>a</sup>**

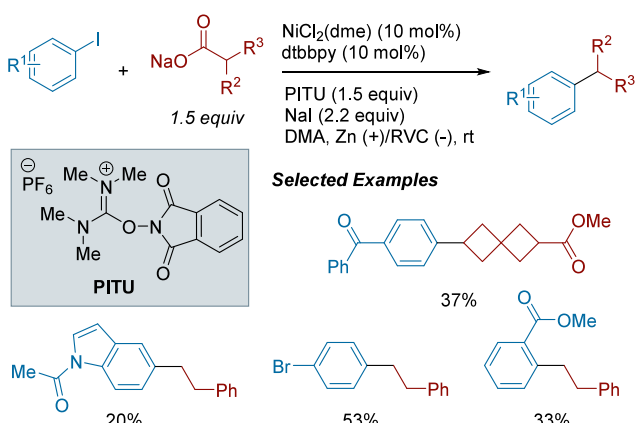


<sup>a</sup>With 1 equiv of NHP ester and 12 mol% NiBr<sub>2</sub>(dtbbpy).

complementary approach to alkyl radical generation from carboxylic acids instead of photochemistry. This method proved especially useful in cases where the corresponding alkyl halide is not commercially available, unstable, or simply fails to couple. We utilized a preformed nickel(II)aryl complex and subjected it to reaction conditions with and without zinc powder and saw comparable yields of product formation. These results suggest that the formation of an arylzinc intermediate is unlikely.

Loren and co-workers reported the use of NHP esters, generated *in situ* from alkyl carboxylates, in an electrochemical decarboxylative cross-coupling with aryl iodides (Scheme 202).<sup>320</sup> The one-pot protocol involves initial conversion of sodium alkyl carboxylates to redox-active NHP esters using *N*-hydroxyphthalimide tetramethyluronium hexafluorophosphate

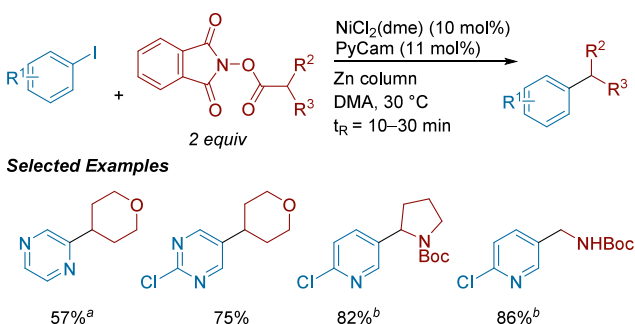
**Scheme 202. Electrochemical Coupling of Aryl Iodides with in Situ Generated Redox Active Esters in a One-Pot Nickel XEC Protocol (2019)**



(PITU) as the activating reagent, followed by addition of the remaining reagents and catalyst for subsequent cross-coupling. Notably, the use of an undivided cell further simplifies reaction setup. Electron-poor aryl iodides were generally better performing than electron-rich iodides, and a variety of primary and secondary alkyl carboxylates were compatible.

Ley and co-workers described the use of a packed zinc bed column in a continuous flow system for the cross-electrophile coupling of *N*-hydroxypythalimide esters with aryl iodides (Scheme 203).<sup>321</sup> Through the use of a packed zinc bed

**Scheme 203. Continuous Flow Ni-Catalyzed XEC of Aryl and Heteroaryl Halides with Redox-Active Esters (2020)<sup>a</sup>**

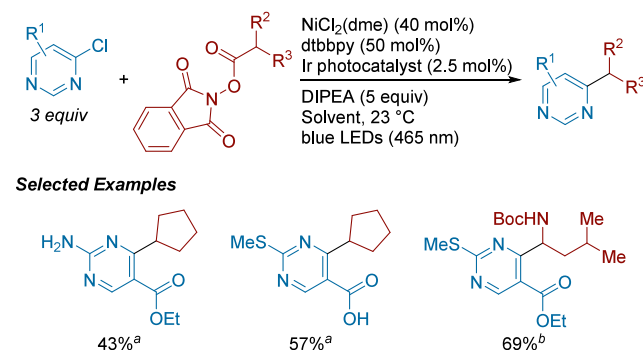


<sup>a</sup>(a) With aryl bromide, NiCl<sub>2</sub>(dme) (20 mol%), PyCam (22 mol%) under 20 min t<sub>R</sub>. (b) Using crude redox-active ester.

column, the authors were able to run this previously heterogeneous reactions homogeneously in flow, and avoid downstream removal of zinc and its byproducts from the reaction solution. The authors report that the zinc column can be reused ten times on 0.4 mmol scale with no loss in efficiency. In addition, their preparation of the reaction mixture did not require rigorous exclusion of air or water. Under this flow setup, the reaction time was significantly decreased (from 12 h in batch to 10 min in flow). As a showcase of the utility of this setup, the authors ran the flow setup for 31 h, delivering >11.7 g of cross-coupled product without significant diminished efficiency of the remaining zinc bed.

Janssen Discovery Process Research, led by Herrmann, reported the decarboxylative cross-electrophile coupling of pyrimidinyl and pyridyl halides with *N*-hydroxypythalimide esters using a metallaphotoredox strategy (Scheme 204).

**Scheme 204. Coupling of Heteroaryl Halides with NHP Esters Through Nickel/Photoredox XEC (2021)<sup>a</sup>**

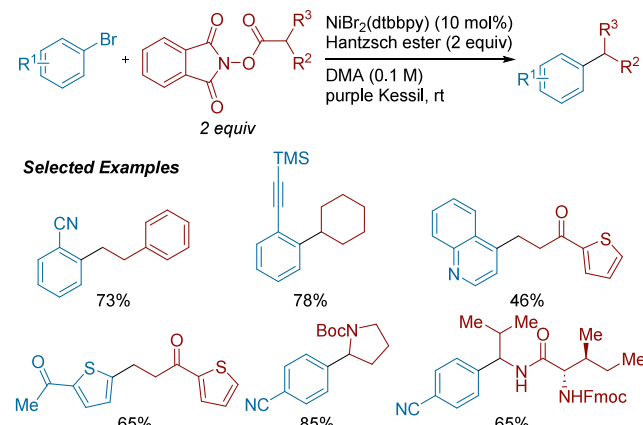


<sup>a</sup>(a) With Ir(p-CF<sub>3</sub>-ppy)<sub>3</sub> and DMSO. (b) With [(Ir[dF(CF<sub>3</sub>)-ppy]<sub>2</sub>(dtbbpy)]PF<sub>6</sub>, 1 equiv aryl chloride, 2 equiv NHP ester, and 1,4-dioxane.

Using Hünig's Base as terminal reductant, the authors focused on medicinally relevant heterocycles bearing sensitive functional groups that are challenging substrates in the cross-electrophile coupling literature. The authors found that, under these conditions, an electron-donating group at the 2-position and an electron-withdrawing group at the 5-position was necessary for optimal success. However, they saw some success with electron neutral groups at the 2- and 6- positions when changing from heteroaryl chlorides to the more reactive heteroaryl bromides.

The Molander lab reported the nickel/photochemical XEC of aryl bromides with NHP esters (Scheme 205).<sup>56</sup> The

**Scheme 205. Photochemical/Nickel Dual Catalyzed XEC of Aryl Bromides and NHP Esters via an EDA Complex (2021)**

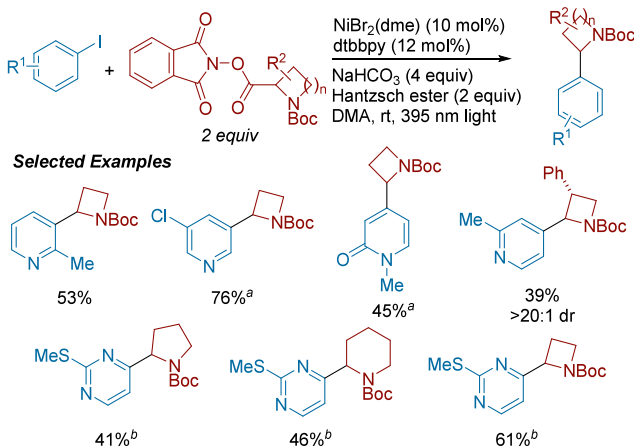


authors propose that decarboxylative activation of the NHP ester occurs via formation of an electron donor–acceptor (EDA) complex. By utilizing Hantzsch ester as both a photocatalyst and an organic reductant, the authors preclude the need for an exogenous photocatalyst and a metal reductant. The scope is broad, with better reactivity observed with electron deficient (hetero)aryl bromides, and *ortho*-substituted aryl substrates did not hinder reactivity.

Azetidines are of interest for medicinal chemistry development as they present a low-molecular weight scaffold to introduce three-dimensionality. While significant advancements have been made toward their syntheses, these have mainly focused on derivatizing the 3-position. Pfizer Medicinal

Chemistry, led by Brewster and Hinklin, described the synthesis of 2-heteroaryl azetidines through decarboxylative cross-electrophile coupling of *N*-Boc azetidine NHP esters with heteroaryl iodides (**Scheme 206**).<sup>323</sup> The NHP ester is

**Scheme 206.** Nickel/Photochemical XEC of Heteroaryl Iodides with NHP-Functionalized Azetidines (2022)<sup>a</sup>



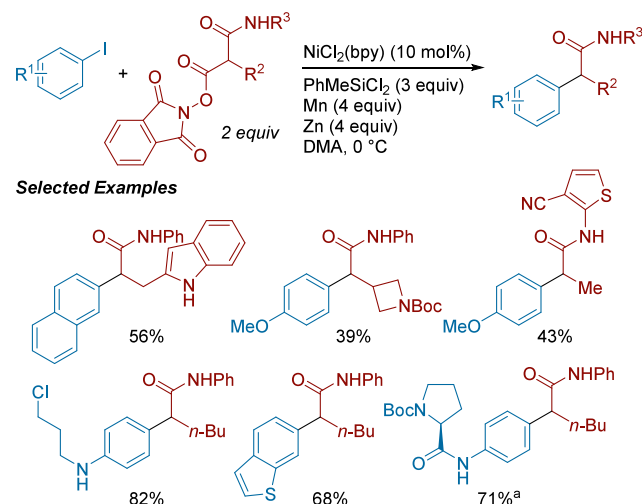
<sup>a</sup>(a) With 3 equiv aryl iodide, 5 equiv NaHCO<sub>3</sub>, and 1.25 equiv Hantzsch ester. (b) With 2 equiv aryl iodide, 1 equiv NHP ester, 1.2 equiv Hantzsch ester.

proposed to form an electron donor–acceptor (EDA) complex with an excited state Hantzsch ester before SET reduction to generate the azetidinyl radical and phthalimide anion. Under these conditions, a diverse set of heteroaryl iodides with electron-donating and -withdrawing groups, sensitive functional groups, and *ortho*-substitution were competent coupling partners. Using a substituted azetidine NHP ester, the authors observed high diastereoselectivity. The high chemoselectivity of this XEC with a chloro-substituted heteroaryl iodide allowed further functionalization of the chloride via a Pd-catalyzed Suzuki cross-coupling.

Rousseaux and co-workers, in collaboration with Merck Process Chemistry, reported the  $\alpha$ -arylation of secondary amides using aryl iodides and NHP esters (**Scheme 207**).<sup>324</sup> The authors found that an equimolar ratio of Zn and Mn as terminal reductants provided the highest yields of cross-coupled product and minimized aryl dimerization. The chlorosilane additive was critical for reactivity, and TMSCl can be swapped for the less common PhMeSiCl<sub>2</sub> with only a small decrease in yield. These conditions tolerate other cross-coupling functionality on the aryl iodide (e.g., bromide, tosylate). These methods were also extended to the functionalization of *N*- and *C*-terminus functionalized amino acids, which can be applied to the synthesis of peptide analogues.

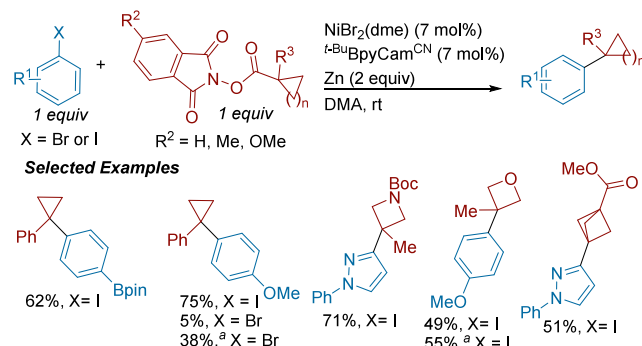
Our group, in collaboration with Janssen Research and Development, disclosed a general approach to couple aryl halides with strained ring derived NHP esters through XEC (**Scheme 208**).<sup>325</sup> Conventional NHP esters of cyclopropanes, bicyclopentanes, azetidines, and other strained rings were compatible. We also demonstrated that tuning the electronics of the NHP esters can control the rate of radical generation (by tuning the reduction potential), enabling improved rate-matching of coupling partners. More electron-rich <sup>Me</sup>NHP and <sup>MeO</sup>NHP esters could slow down radical generation and provide increases in yields of couplings with electron-rich aryl

**Scheme 207.** Ni-Catalyzed XEC of Aryl Iodides with NHP Esters for the  $\alpha$ -Arylation of Amides (2022)<sup>a</sup>



<sup>a</sup>With TMSCl (3 equiv) instead of PhMeSiCl<sub>2</sub>.

**Scheme 208.** Arylation of Strained Rings Through the Ni-Catalyzed XEC of Aryl Halides with NHP Esters (2022)<sup>a</sup>



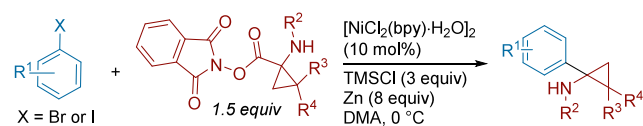
<sup>a</sup>Reactions run with NHP ester ( $R^2 = H$ ) unless noted. (a)  $R^2 = OMe$ .

halides. We also showed that these conditions could be scaled up using a continuous flow setup and scaled down to a 96-well plate format on 10  $\mu$ mol scale. An X-ray structure of an arylnickel(II) oxidative addition complex with <sup>t-Bu</sup>BpyCam<sup>CN</sup> was also reported, providing structural insights to the binding mode of this new ligand.

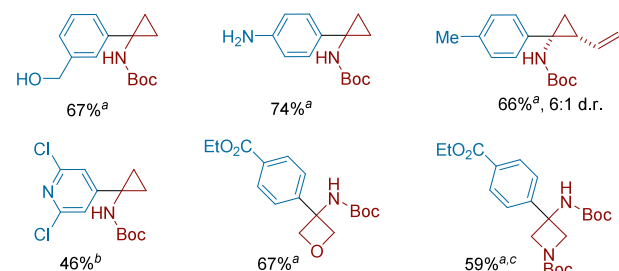
Rousseaux, Huestis, and co-workers reported a decarboxylative cross-electrophile coupling of strained ring NHP esters derived from amino acids with a range of aryl halides (**Scheme 209**).<sup>326</sup> While the focus was on cyclopropylamines, the authors also showed that their conditions were compatible with NHP esters of cyclobutylamine, *N*-Boc-aminoctetane, and *N,N*-Boc-protected aminoazetidine. It is worth noting that the use of TMSCl additive was essential for the product formation.

The Baran lab in collaboration with scientists at Biogen, Pfizer, Bristol Myers Squibb, Minakem Recherche, LEO Pharma and Enamine reported conditions for electrochemically driven XEC of NHP esters with aryl halides (**Scheme 210**).<sup>327</sup> They found that their Ag–Ni electrocatalysis setup could address challenging couplings with electron-rich aryls and heterocycles. In situ activation of the NHP ester was also demonstrated for substrates challenging to isolate. To support

**Scheme 209.** Ni-Catalyzed XEC of Aryl Halides with Strained Ring NHP Esters Derived from Amino Acids (2022)<sup>a</sup>

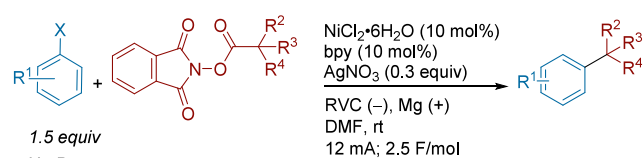


**Selected Examples**

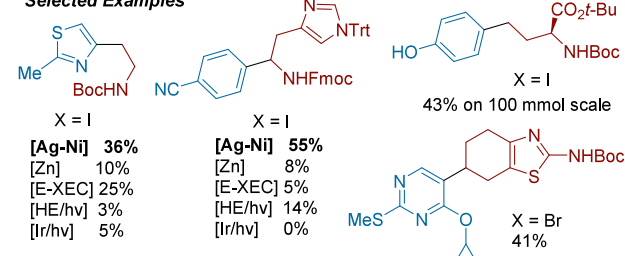


<sup>a</sup>(a) X = I. (b) X = Br. (c) With  $\text{NiCl}_2(\text{dtbbpy})$  (20 mol%).

**Scheme 210.** Ni-Catalyzed Electrochemical Approach to the Decarboxylative XEC of Aryl Halides with Redox-Active Esters (2022)



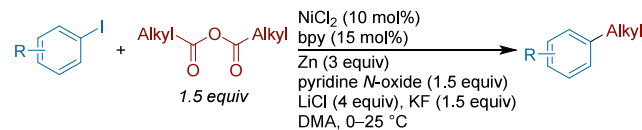
**Selected Examples**



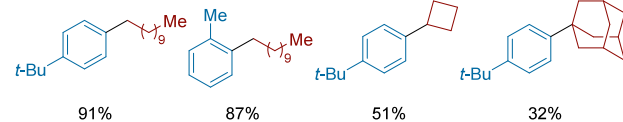
the beneficial effects of the newly discovered system, the authors conducted a head-to-head comparison with four reported methods for such types of reaction for selected substrates that pose challenges in those previous reports. They also showcased a 100 mmol scale synthesis with a recirculating flow setup for two of the selected examples. The role of in situ-formed electrode-bound Ag-nanoparticles was observed to be beneficial in (1) extending catalyst lifetime, (2) preventing background NHP-ester decomposition, and (3) lowering the required overpotential, which results in better functional group tolerance.

**4.6.2.2. XEC with Anhydrides.** Xuebin Liao and co-workers published the cross-electrophile coupling of aryl halides with organic anhydrides through a decarboxylative process (Scheme 211).<sup>328</sup> Inspired by previous work in the decarboxylative coupling of NHP esters, they show that pyridine N-oxide reacts with the anhydride to form an O-acylated species that can be reduced to form pyridine,  $\text{CO}_2$ , and the alkyl radical. Both primary and secondary carboxylic acid anhydrides were coupled successfully, with secondary anhydrides providing slightly lower yields. Due to the reaction's high chemoselectivity, it can be applied to a variety of substrates.

**Scheme 211.** Decarboxylative Ni-Catalyzed XEC of Aryl Iodides with Anhydrides (2018)



**Selected Examples**

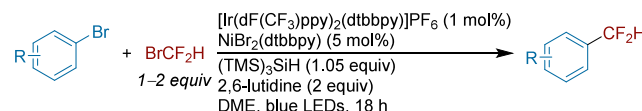


selectivity for alkyl carboxylic acids, mixed anhydrides with *p*-toluic acid could also be used to avoid wasting valuable carboxylic acid coupling partners.

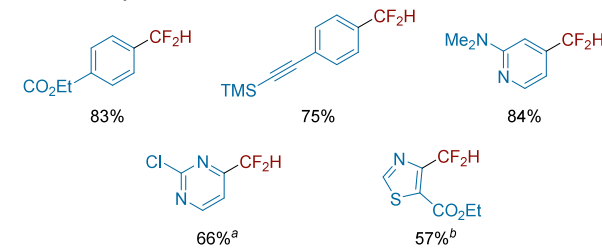
**4.2.7. Fluoroalkylation.** The incorporation of fluorinated alkyl fragments in bioactive molecules has become increasingly important in drug discovery. Cross-electrophile coupling strategies to directly install fluorinated fragments are an attractive alternative to many current methods that employ nucleophilic fluorinating reagents. Methods which utilize environmentally friendly and easy-to-handle solid reagents (over gaseous fluorinating reagents) are becoming increasingly reported in the literature.<sup>329,330</sup>

**4.2.7.1. Alkyl Bromides as Fluoroalkylating Reagents.** The MacMillan group applied their metallaphotoredox silyl-radical strategy to difluoromethylarene synthesis from the cross-coupling of aryl bromides with  $\text{BrCF}_2\text{H}$  (Scheme 212).<sup>43,331</sup>

**Scheme 212.** Nickel/Photoredox XEC of Aryl Bromides with Bromodifluoromethane (2018)<sup>a</sup>



**Selected Examples**



<sup>a</sup>(a)  $^{19}\text{F}$  NMR yield. (b) With DABCO (3 equiv) instead of 2,6-lutidine.

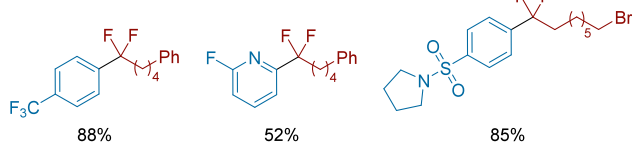
The conditions tolerate a variety of sensitive functionality as well as *ortho*-substituted arenes, and heterocycles. Electron-deficient aryl bromides required a significant excess of bromodifluoromethane, as the faster oxidative addition of the aryl species requires an excess of the alkyl partner to match reactivities. Conversely, electron-rich arenes required fewer equivalents of bromodifluoromethane. To demonstrate the pharmaceutical relevance of this reaction, they performed late-stage difluoromethylation on four medicinally relevant compounds, in 64–82% yield.

Xingang Zhang and co-workers disclosed a Ni-catalyzed XEC strategy for the difluoroalkylation of aryl bromides (Scheme 213).<sup>332</sup> Initially they observed low conversion of the

**Scheme 213.** Ni-Catalyzed XEC of Aryl Bromides with 1-Bromo-1,1-difluoroalkanes (2018)



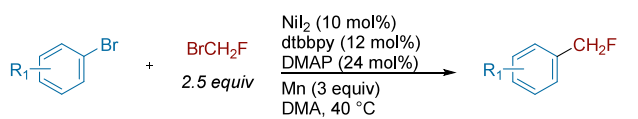
**Selected Examples**



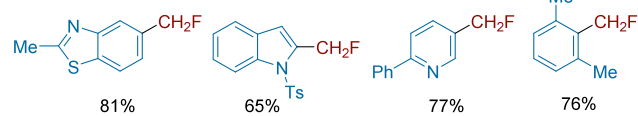
aryl bromide, but adding NaI improved yields and inhibited the formation of protodebrominated side-products. Incorporating 3 Å MS further improved yields, although the exact reason is unknown. The reaction is tolerant of functional groups such as aldehydes, nitriles, silyl groups, and free alcohols. The reaction was highly chemoselective for alkyl  $\text{CF}_2\text{-Br}$  activation over alkyl  $\text{CH}_2\text{-Br}$ . Control experiments and  $^{19}\text{F}$  NMR monitoring ruled out the formation of difluoroalkylzinc species.

Xi-Sheng Wang and co-workers reported the monofluoromethylation of aryl bromides, with  $\text{BrCH}_2\text{F}$  as the radical precursor (Scheme 214).<sup>333</sup> Control experiments rule out the

**Scheme 214.** Ni-Catalyzed XEC of Aryl Bromides with Bromofluoromethane (2019)



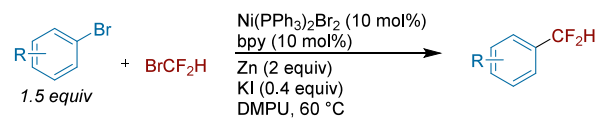
**Selected Examples**



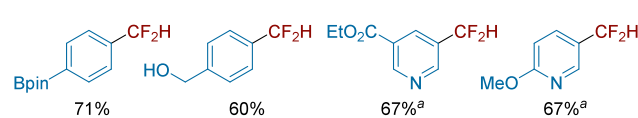
possibility of monofluoromethyl manganese species participating in the reaction and is instead proposed to proceed via a monofluoromethyl radical.

Xingang Zhang and co-workers reported the XEC of aryl bromides with  $\text{BrCF}_2\text{H}$  (Scheme 215).<sup>334</sup> The authors ruled out formation of difluoromethylzinc intermediates by monitor-

**Scheme 215.** Difluoromethylation of Aryl Bromides with Bromodifluoromethane through Ni-Catalyzed XEC (2019)<sup>a</sup>



**Selected Examples**

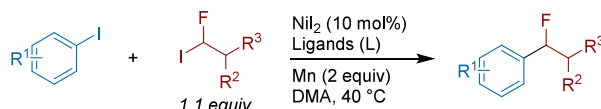


<sup>a</sup>With aryl bromide (2 equiv),  $\text{Ni}(\text{PPh}_3)_2\text{Br}_2$  (5 mol%), dtbbpy (5 mol%), and 3 Å MS.

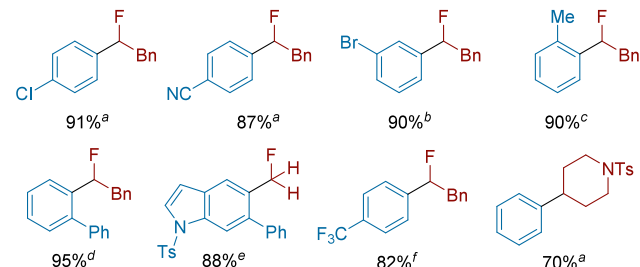
ing the reaction with  $^{19}\text{F}$  NMR. In addition, radical clock experiments indicated the intermediacy of a difluoromethyl radical. A variety of arene electronics and heterocycles were coupled successfully in this protocol.

**4.2.7.2. Alkyl Iodides as Fluoroalkylating Reagents.** Xi-Sheng Wang and co-workers reported the Ni-catalyzed monofluoroalkylation of aryl bromides and iodides (Scheme 216).<sup>335</sup> The authors found that a combination of bipyridine

**Scheme 216.** Ni-Catalyzed XEC of Aryl Iodides with Monofluoroalkyl Iodides (2018)<sup>a</sup>



**Selected Examples**

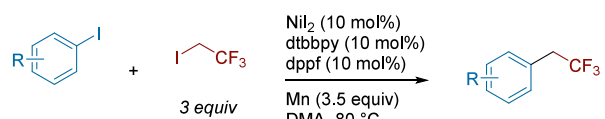


<sup>a</sup>(a)  $L = 4,4'\text{-MeO bpy}$  (10 mol%)/ $4\text{-CN bpy}$  (20 mol%), (b)  $L = 4,4'\text{-MeO bpy}$  (10 mol%)/ $py$  (20 mol%), (c)  $L = 4,4'\text{-MeO bpy}$  (10 mol%)/ $2,6\text{-MeO Py}$  (20 mol%), (d)  $L = dtbbpy$  (10 mol%)/ $4\text{-CN bpy}$ , (e) With  $\text{BrCFH}_2$  (1.5 equiv) instead of alkyl iodide, (f) With aryl bromide instead of aryl iodide and NaI (1 equiv) at 80 °C.

and pyridine ligands was optimal for cross-coupling, with the mixed ligand system dependent upon the substrate pair. Through combinatorial screening of ten monodentate ligands with five bidentate ligands, five ligand combinations afforded ~90% yield in their model cross-coupling. The conditions could also be extended to the coupling of aryl iodides with nonfluorinated alkyl fragments. Mechanistic experiments support the involvement of a monofluoroalkyl radical instead of an alkylmanganese species.

Xi-Sheng Wang and co-workers reported the trifluoroethylation of aryl halides using a cross-electrophile coupling strategy (Scheme 217).<sup>336</sup> The authors attribute the high reaction efficiency to the combination of dtbbpy and dppf ligands. Under these conditions, an electronically diverse set of aryl iodides bearing a variety of sensitive functional groups and *ortho*-sterics were trifluoroethylated in high yields. Notably, the authors successfully applied this method to the trifluoroethyl-

**Scheme 217.** Ni-Catalyzed XEC of Aryl Iodides with 1,1-Trifluoro-2-Iodoethane (2020)



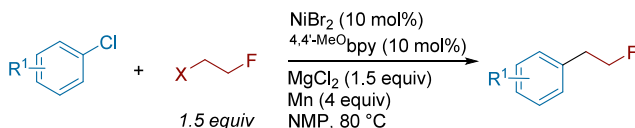
**Selected Examples**



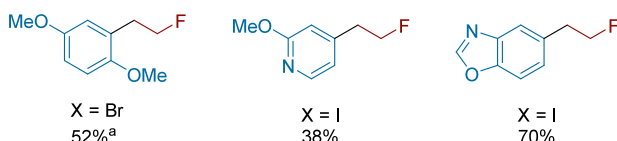
lation of several bioactive compounds, including the aryl iodide derivatives of fenofibrate, ezetimibe, and loratadine. The presence of a trifluoroethyl radical was supported through radical trapping with TEMPO, and control experiments with Mn indicated no formation of trifluoroethylmanganese species.

Yi Yang, Yingle Liu, and co-workers reported the  $\beta$ -fluoroethylation of aryl chlorides using nickel XEC (Scheme 218).<sup>337</sup> The method was utilized in the derivatization of

**Scheme 218. Ni-Catalyzed XEC of Aryl Halides with  $\beta$ -Fluoroethyl Alkyl Halides (2020)<sup>a</sup>**



**Selected Examples**

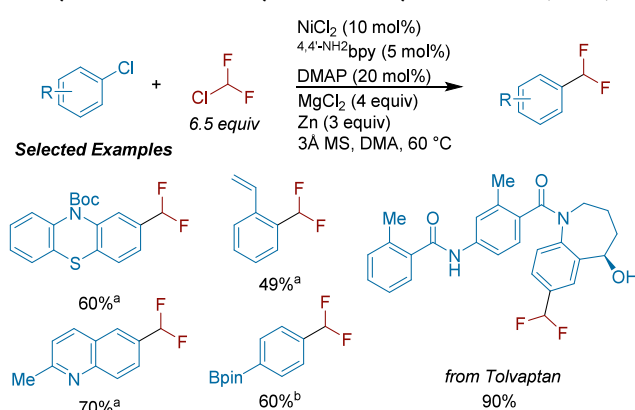


<sup>a</sup>With aryl bromide, 4,4'-MeO-bpy (10 mol%) as ligand, and TBAI (20 mol%) instead of MgCl<sub>2</sub>.

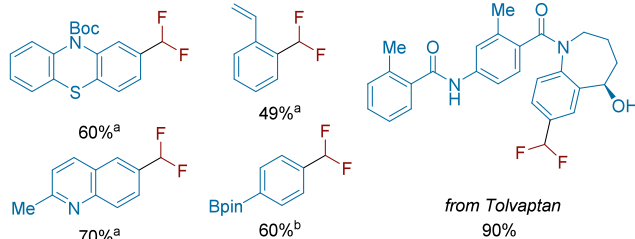
several aryl chloride containing pharmaceuticals, such as clofibrate, fenofibrate, and loratadine. An extension of the scope to aryl triflates and  $\beta$ -fluoroalkyl halides as coupling partners was demonstrated in lower yields. Control experiments rule out the formation of organomanganese species.

**4.2.7.3. Alkyl Chlorides as Fluoroalkylating Reagents.** Xingang Zhang and co-workers in 2018 reported the difluoromethylation of aryl chlorides through XEC (Scheme 219).<sup>338</sup> The authors found that a combination of electron-rich

**Scheme 219. Use of Chlorodifluoromethane for the Ni-Catalyzed Difluoromethylation of Aryl Chlorides (2018)<sup>a</sup>**



**Selected Examples**



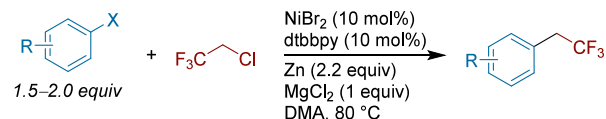
<sup>a</sup>(a) With 15 mol% NiCl<sub>2</sub> and 10 mol% 4,4'-NH<sub>2</sub>bpy. (b) With 20 mol% NiCl<sub>2</sub> and 10 mol% 4,4'-NH<sub>2</sub>bpy.

ligands 4,4'-NH<sub>2</sub>bpy and DMAP was optimal for aryl chloride activation. Radical clock experiments support the formation of difluoromethyl radical. Furthermore, control experiments showed that difluoromethylzinc was not a competent intermediate in this reaction. The authors showed the arynickel(II) complex [(dtbbpy)Ni(4-t-Bu-C<sub>6</sub>H<sub>4</sub>)Cl] to be a

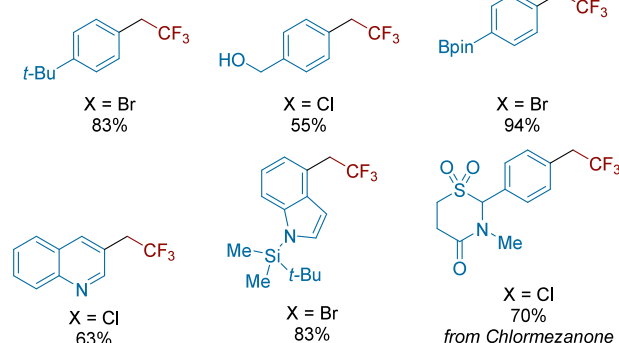
competent precatalyst, suggesting that the reaction begins through oxidative addition to the aryl chloride. The method can be applied to a diverse set of aryl chlorides with good functional group tolerance, including the difluoromethylation of several aryl chloride containing pharmaceuticals.

Xingang Zhang and co-workers demonstrated a Ni-catalyzed cross-electrophile coupling of aryl halides with chlorotrifluoroethane (Scheme 220).<sup>339</sup> They also successfully encompassed

**Scheme 220. Ni-Catalyzed Trifluoroethylation of Aryl Bromides via XEC (2021)**



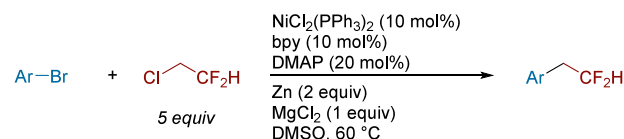
**Selected Examples**



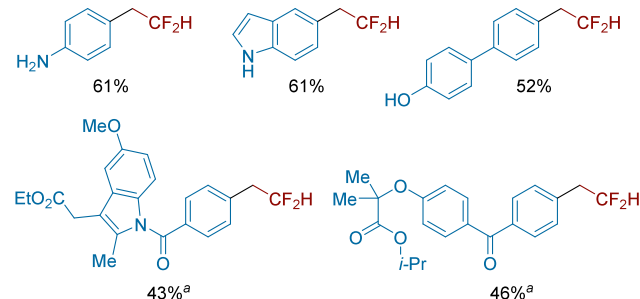
heteroaryl halides within their scope, coupling quinolines, indoles, and benzoxazoles. It was noted, however, that simple pyridines were an exception and did not couple well. Several aryl chloride containing pharmaceuticals were successfully trifluoroethylated, such as chlormezanone and loratadine.

Xinjin Li and co-workers reported the 2,2-difluoroethylation of aryl bromides with 2-chloro-1,1-difluoroethane (HCFC-142) using a cross-electrophile coupling strategy (Scheme 221).<sup>340</sup> Similar to other reports in this area, the authors propose that DMAP may function as a coligand in the reaction. From comparative studies, there appears to be a fluorine effect,

**Scheme 221. Ni-Catalyzed XEC of Aryl Bromides with 2-Chloro-1,1-Difluoroethane (2022)<sup>a</sup>**



**Selected Examples**

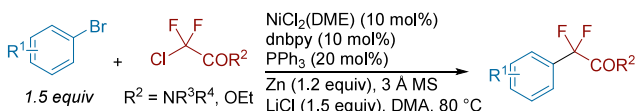


<sup>a</sup>With dtbbpy (10 mol%) and DMAP (20 mol%) at 110 °C.

with di- and trifluoroethylated products resulting in a higher yield than the monofluoroethylated product. All fluorinated reagents resulted in higher reactivity than 1,2-dichloroethane or 1-chloropropane.

Xingang Zhang and co-workers developed a Ni-catalyzed XEC of heteroaryl halides with chlorodifluoroacetamides and chlorodifluoroacetate (Scheme 222).<sup>341</sup> The authors proposed

**Scheme 222. Ni-Catalyzed Fluoroalkylation of Heteroaryl Halides with Chlorodifluoroacetamides (2022)**



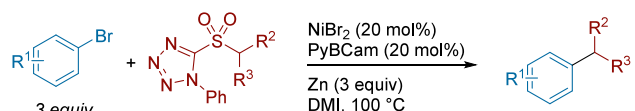
**Selected Examples**



that the use of a soft phosphine coligand, which are more labile on the nickel center than hard bipyridine ligands, may protect the active nickel species from decomposing. The authors utilized these conditions to prepare several biologically active molecules, including an AMPAR allosteric modulator and FKBP12 inhibitor. Mechanistic experiments ruled out the formation of difluoroacetylzinc intermediates.

**4.2.8. Other Alkyl Precursors.** Hughes and Fier reported a desulfonylative cross-electrophile coupling of aryl bromides with alkyl phenyltetrazole sulfones (Scheme 223).<sup>342</sup> The

**Scheme 223. XEC of Aryl Bromides with Redox-Active Alkyl Sulfones via Nickel Catalysis (2019)**



**Selected Examples**

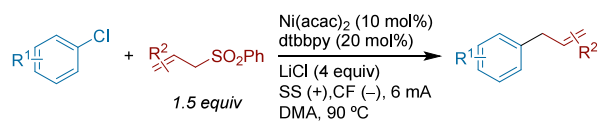


optimized reaction conditions were developed from an initial hit found by microscale-high throughput experimentation. As applications, the authors demonstrated the synthesis of complex diarylmethanes and the straightforward derivatization of a methyl sulfone to enable the preparation of an aryl indane core. A cyclopropylmethyl radical clock experiment supported the formation of alkyl radical intermediates.

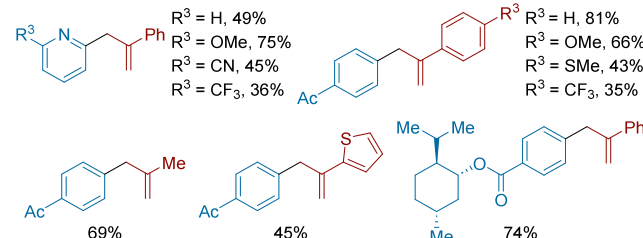
Jie Liu and co-workers reported the electroreductive allylation of aryl chlorides with allylic sulfones (Scheme 224).<sup>343</sup> The reaction conditions are tolerant of a variety of electronics on both the aryl chloride and allyl sulfone. The authors also report initial results coupling aryl triflates with allyl sulfones, as well as aryl chlorides with aliphatic sulfones. Addition of  $\text{LiCl}$  was necessary for efficient reduction of the nickel catalyst.

Xiaomeng Zeng and co-workers reported the Cr-catalyzed deoxygenative coupling of aryl pivalates with C = O bonds of

**Scheme 224. Electrochemically-Driven Ni-Catalyzed XEC of Aryl Chlorides with Allylic Sulfones (2023)**

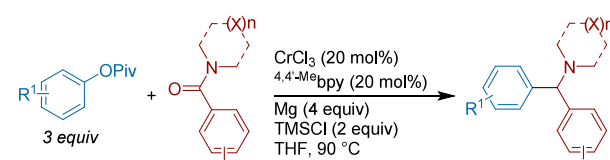


**Selected Examples**

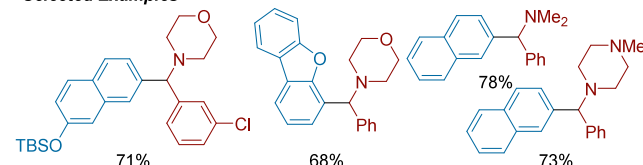


aryl amides to form diarylmethylated tertiary amines (Scheme 225).<sup>344</sup> Through stoichiometric and deuterium-labeling

**Scheme 225. Deoxygenative Chromium-Catalyzed XEC of Aryl Pivalates with and Aryl Amides (2023)**



**Selected Examples**

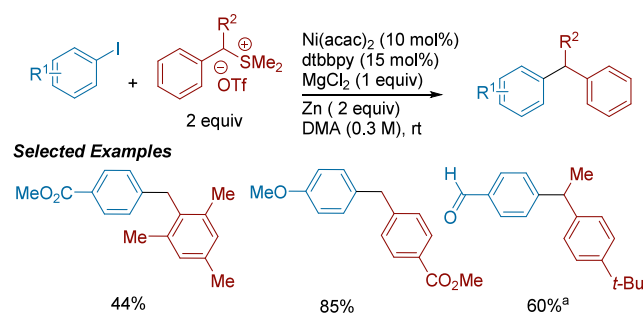


experiments, the authors propose that upon oxidative addition of the aryl ester to the chromium catalyst, the resulting complex reacts with Mg and TMSCl to form the arylated silachromate(II) complex. Addition of this complex to the amide carbonyl bond is expected to occur in a regioselective manner to form the aryl-alkylchromium complex. Upon reductive elimination, the silyloxy group undergoes deoxygenative HAT to give the arylated tertiary diarylmethylamine. This method was applied to the derivatization of tertiary amide-containing drugs such as trimetozine and trocimine.

Fan Wu and co-workers disclosed the Ni-catalyzed XEC of benzyl sulfonium salts with aryl iodides (Scheme 226).<sup>345</sup> The reaction conditions appear best with electron-neutral and electron-rich sulfonium salts. The authors describe two sets of conditions for primary and secondary benzyl sulfonium salts. Preliminary mechanistic experiments appear to rule out the formation of benzylzinc intermediates.

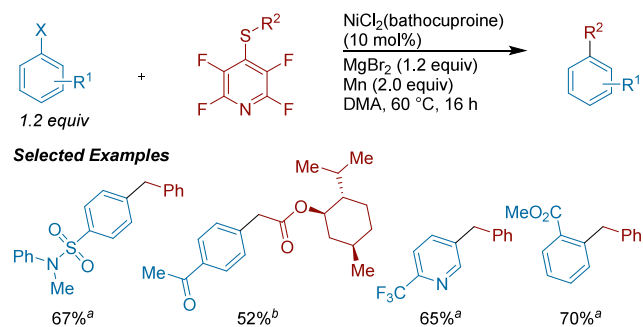
Husan-Hung Liao and co-workers reported the XEC of benzyl mercaptans or mercaptoacetates with aryl halides via desulfurative benzyl radical generation from a tetrafluoropyridine thioether source (Scheme 227).<sup>346</sup> Primary alkyl sources resulted in higher yields than secondary, which the authors attribute to stabilized secondary radicals favoring homodimerization. To achieve good yields with electron-rich aryls, the authors swapped from the aryl bromide to the iodide. The authors showed that the tetrafluoropyridine thioether can be

**Scheme 226.** Ni-Catalyzed XEC of Aryl Iodides with Benzylic Sulfonium Salts (2021)<sup>a</sup>



<sup>a</sup>Conditions for R<sup>2</sup> = Me or Et: NiI<sub>2</sub> (10 mol%), dtbbpy (15 mol%), Zn (2.0 equiv), MgBr<sub>2</sub> (30 mol%), DMA (0.6 M) at 40 °C.

**Scheme 227. Desulfurative Arylation of Benzyl Mercaptans and Mercaptoacetates with Aryl Halides (2022)**<sup>a</sup>

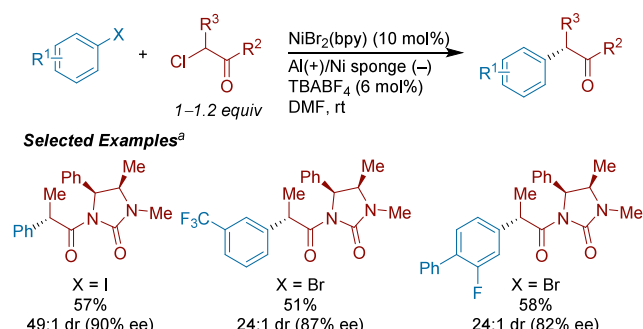


<sup>a</sup>(a) X = Br. (b) X = I.

formed from the thiol precursor and directly used crude in coupling with no decrease in yield.

**4.2.9. Stereocontrolled XEC of Aryl-X with Alkyl-X.** **4.2.9.1. Alkyl Chlorides as Electrophiles.** Durandetti and co-workers extended their electrochemical strategy to an asymmetric method, using chiral auxiliaries to control stereochemistry in the XEC of aryl halides with α-chloropropionates (Scheme 228).<sup>347</sup> In an evaluation of common chiral auxiliaries, the highest levels of diastereoselectivity were obtained with imidazolidinone derivatives. No racemization of the stereocenter was observed when removing the chiral auxiliary.

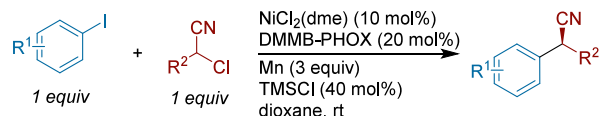
**Scheme 228. Electrochemically Driven Asymmetric Ni-Catalyzed XEC of Aryl Halides with α-Chloropropionic Acid Derivatives (1997)**<sup>a</sup>



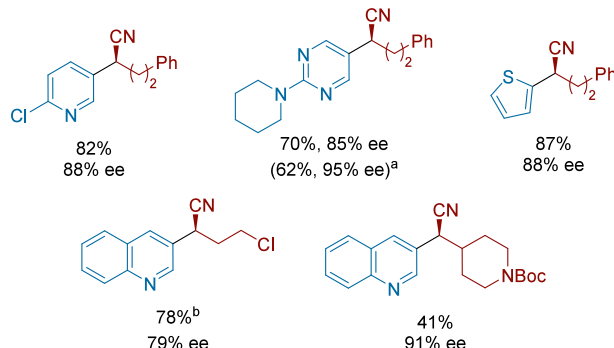
<sup>a</sup>ee calculated after removal of auxiliary group.

In 2015, the Reisman group detailed a Ni-catalyzed asymmetric cross-coupling reaction of heteroaryl iodides with α-chloronitriles (Scheme 229).<sup>348</sup> Initially starting with BOX

**Scheme 229. Asymmetric Ni-Catalyzed XEC of Heteroaryl Iodides with α-Chloronitriles (2015)**<sup>a</sup>



**Selected Examples**



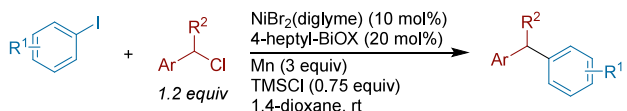
<sup>a</sup>(a) Yield and %ee after one recrystallization. (b) With 2.0 equiv of heteroaryl iodide.

ligands, they found rapid consumption of the α-chloronitrite to the hydrodehalogenation product. Swapping to electron-rich DMMB-PHOX as ligand led to improved yields and enantioselectivity which they hypothesized was due to the increased rate of oxidative addition step. The conditions are chemoselective for aryl iodides over other halogens. In general, a variety of aromatic and saturated heterocycles were tolerated. Pyridines and pyrimidines that had open C2 positions were low yielding substrates, which was attributed to the nitrogen's Lewis basicity. Good to excellent enantioselectivity was generally observed (>80% ee). Increased steric hindrance at the alkyl coupling was shown to benefit enantioselectivity but at the cost of yield.

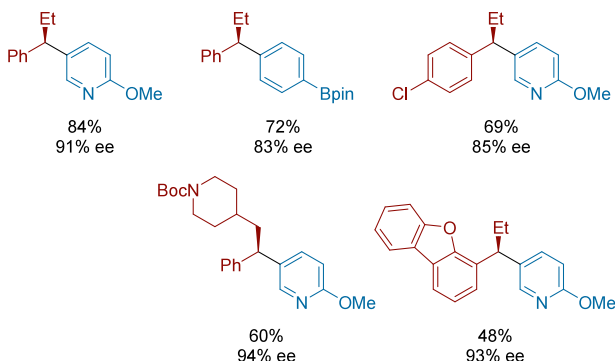
In 2017, the Reisman group reported a method for the Ni-catalyzed asymmetric cross-electrophile coupling of secondary benzyl chlorides with aryl iodides enabled by the use of a chiral BiOX ligand (Scheme 230).<sup>349</sup> While investigating ligand effects on the reaction, they observed that the length of the alkyl chain on the BiOX ligand had a positive correlation to yield and enantioselectivity. Replacing the benzyl chloride with the corresponding bromide resulted in significant homocoupling of the alkyl coupling partner. Coupling pyridines, pyrimidines, and indoles resulted in high yields and good levels of stereocontrol (>80% ee). The reaction is chemoselective for benzylic over primary alkyl chlorides. To showcase their method further, the authors prepared a key chiral intermediate relevant for production of sertraline, an antidepressant.

Jianyou Mao and Walsh reported an enantioselective arylation of α-chloroesters with aryl iodides using a metal-lphotoredox strategy (Scheme 231).<sup>350</sup> A combination of 4-heptyl-substituted BiOX and a sterically bulky substituent on the ester were responsible for the high enantioselectivity. Both α-alkyl and α-aryl chloroesters were compatible in this protocol. The addition of Cy<sub>2</sub>NMe sequesters any HX

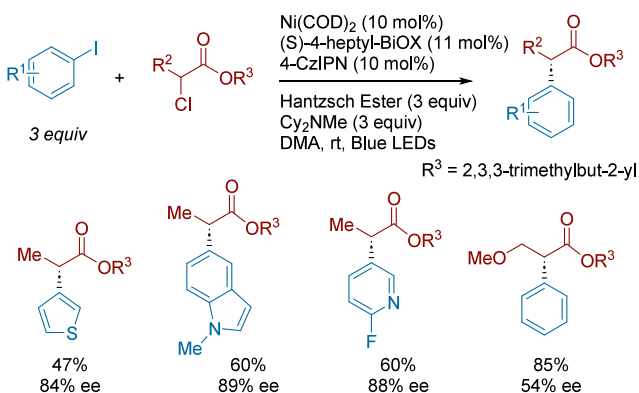
**Scheme 230. Asymmetric XEC of Secondary Benzyl Chlorides with Aryl Iodides (2017)**



### **Selected Examples**



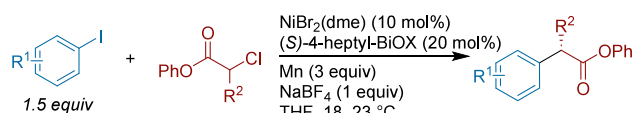
**Scheme 231. Asymmetric Cross-Coupling of Aryl Iodides with  $\alpha$ -Chloroesters via Nickel/4-CzIPN Photoredox Catalysis (2020)**



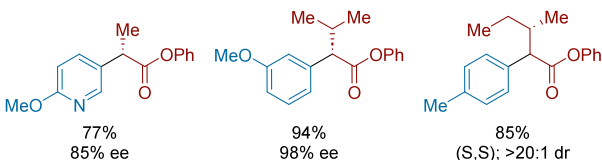
generated from the reaction. A reaction with stoichiometric Ni(COD)<sub>2</sub> and chiral ligand afforded identical enantioselectivity to the catalytic conditions, suggesting that the enantiodetermining step does not involve Hantzsch ester or Cy<sub>2</sub>NMe.

Reisman and co-workers developed conditions for the enantioselective cross-electrophile coupling of secondary  $\alpha$ -chloroesters with aryl iodides (Scheme 232).<sup>351</sup> They found bioxazoline (BiOX) ligands performed well in this reaction,

**Scheme 232. Asymmetric Ni-Catalyzed XEC of  $\alpha$ -Chloroesters with Aryl Iodides (2021)**



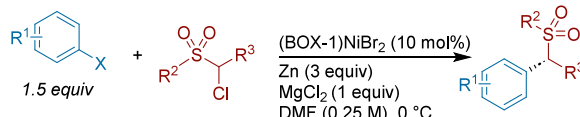
### **Selected Examples**



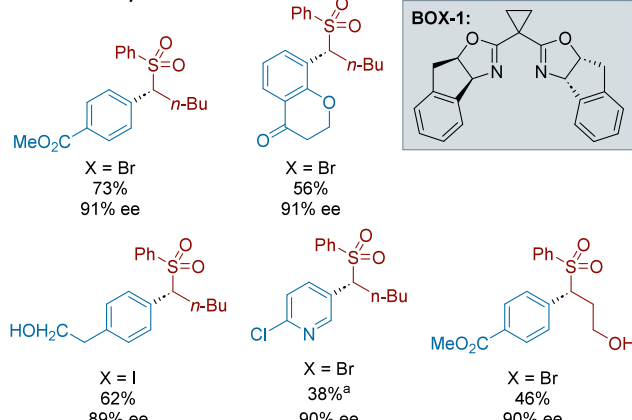
especially when equipped with alkyl substituents, and the highest enantioselectivity and yield was achieved with 4-heptyl-BiOX. They found that enantioselectivity increased with the size of the  $\alpha$ -chloroester substituent. To investigate this further, they, in collaboration with the Sigman group, investigated the reaction computationally. Using multivariate linear regression analysis, they concluded that this trend was indeed due to the steric matching of substrate with catalyst. They include the synthesis of (*S*)-naproxen from their method and show that manganese-enolates are not viable intermediates in the reaction.

Investigating the potential to modify sulfone-containing alkyl substrates, Hegui Gong, Chuanhu Lei, and co-workers developed an asymmetric cross-electrophile coupling of aryl halides with  $\alpha$ -chlorosulfones (Scheme 233).<sup>352</sup> For this

**Scheme 233. Cross-Electrophile Coupling of  $\alpha$ -Chlorosulfones with Aryl Halides via Enantioselective Nickel XEC (2021)<sup>a</sup>**



### ***Selected Examples***

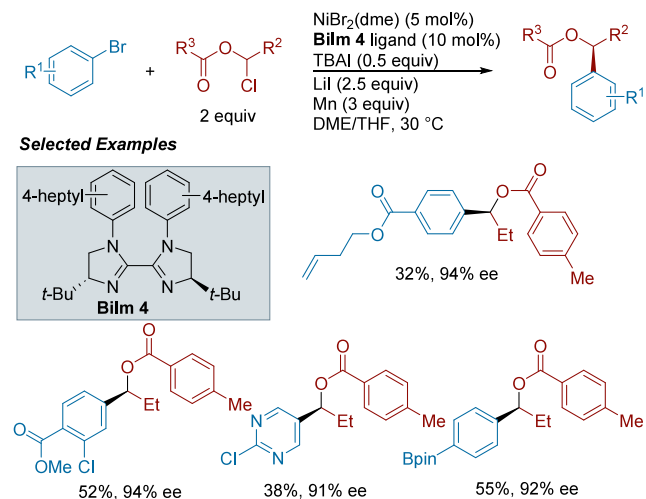


<sup>a</sup>Conditions: NiBr<sub>2</sub>(BOX-1) (10 mol%), Mn (3 equiv), aryl bromides (2 equiv), 1,4-dioxane at rt.

reaction, they determined a chiral BOX ligand to be optimal for both product yield and enantioselectivity. Substrates containing acidic protons were competent under these conditions. A variety of heteroaryl halides were compatible in this reaction as were a series of drug molecule cores (e.g., celecoxib). Stoichiometric experiments with (dtbbpy)-arylnickel(II) supported that radical capture and reductive elimination from nickel(III) is a viable pathway.

Yunrong Chen, Jifen Wang, Guobin Ma, and co-workers reported the enantioconvergent XEC of racemic 1-chloro-1-alkanol esters with aryl bromides (**Scheme 234**).<sup>353</sup> With the conditions employed, a variety of 1-chloro-1-alkanol esters with varying alkyl chain lengths and steric profiles could be efficiently coupled with aryl bromides in high yields and good enantioselectivity, in which lower steric bulk near the reactive center gave the highest yields. The demonstrated derivatization of several pharmaceutically relevant compounds such as Fenofibrate and Indomethacin as well as the synthesis of the key scaffolds of Pradefovir and Ezetimibe. Notably, the 1-chloro-1-alkanol starting material can be generated *in situ* from

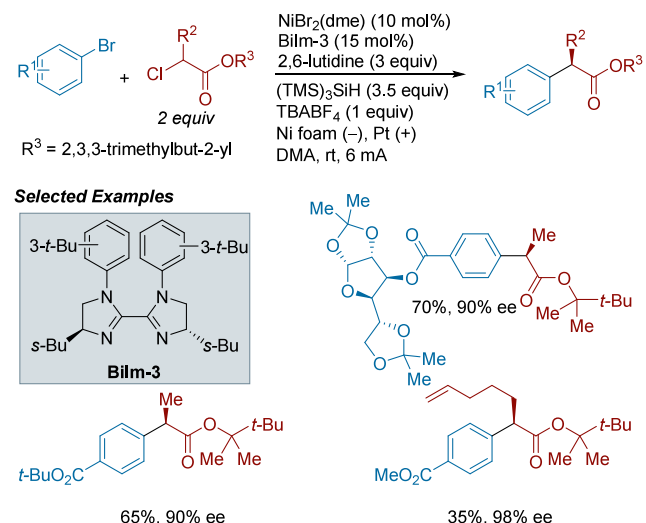
**Scheme 234.** Ni-Catalyzed Asymmetric Reductive Arylation of 1-Chloro-1-Alkanol Esters with Aryl Bromides (2022)



the corresponding aldehyde and acid chloride with only a minimal decrease in yield and enantioselectivity after cross-coupling.

Tian-Sheng Mei and co-workers disclosed an enantioselective cross-electrophile coupling between  $\alpha$ -chloroesters with aryl bromides through a paired electrolysis approach (Scheme 235).<sup>354</sup> Good enantioselectivities (>90% ee) and reactivities

**Scheme 235.** Enantioselective XEC of  $\alpha$ -Chloroesters with Aryl Bromides via Paired-Electrolysis (2022)

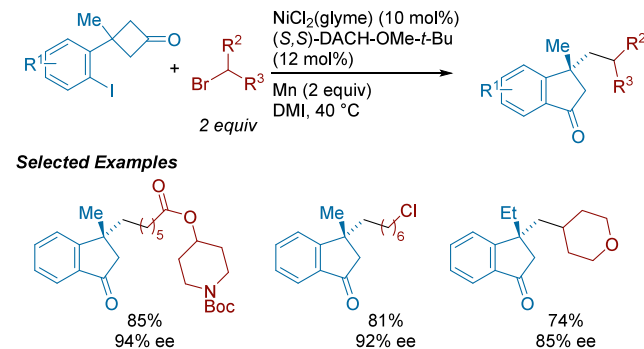


(>70% yield) were achieved in most cases by using a biimidazoline type ligand in combination of a nickel(II) precatalyst under a cell potential of 2.9 V. The reaction was proposed to go through an anode oxidation of the bromide anion to form bromine radical which rapidly abstracts a hydrogen atom from the silane. The resulting silyl radical was proposed to react with  $\alpha$ -chloroesters through chlorine atom abstraction to generate the desired alkyl radical which then engaged in the cross-coupling event.

**4.2.9.2. Alkyl Bromides and Iodides as Electrophiles.** The usual steps of an XEC reaction can be interwoven with other intramolecular steps to form complex cascades. Chuan Wang and co-workers reported an enantioselective domino arylation/

ring-opening/alkylation reaction between cyclobutanone tethered aryl iodides and alkyl bromides (Scheme 236).<sup>355</sup> This

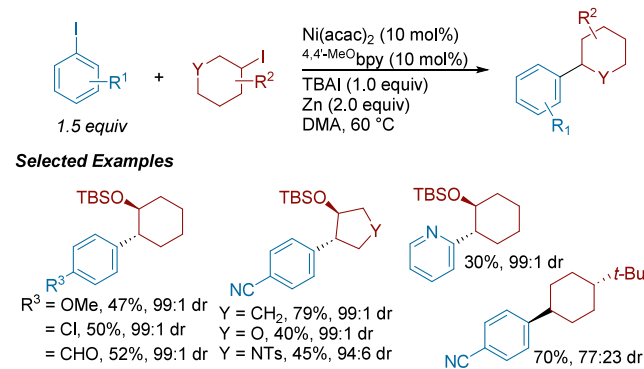
**Scheme 236.** Ni-Catalyzed XEC of Aryl Iodides with Alkyl Bromides Featuring Carbon Skeleton Rearrangement (2020)



reaction employs a chiral diphenylphosphinobenzoic acid (DPPBA)-based ligand, developed by Trost,<sup>356</sup> which is a rare ligand class in XEC. The authors propose that selective insertion of arylnickel(I) into the C–C  $\sigma$ -bond of the cyclobutanone as the enantiodetermining step. It is also notable because the aryl iodides are among the most hindered in this review (*ortho*-tertiary alkyl substitution).

Zhi-Liang Shen, Xiaocong Zhou, and co-workers reported the diastereoselective cross-electrophile coupling of cycloalkyl iodides with aryl iodides to afford the *anti*-diastereomer (Scheme 237).<sup>357</sup> While this study focused on 1,2-

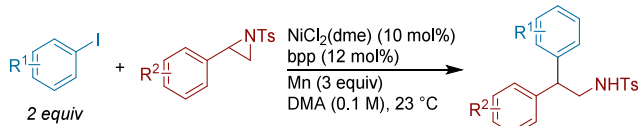
**Scheme 237.** Diastereoselective XEC of Cycloalkyl Iodides with Aryl Iodides (2021)



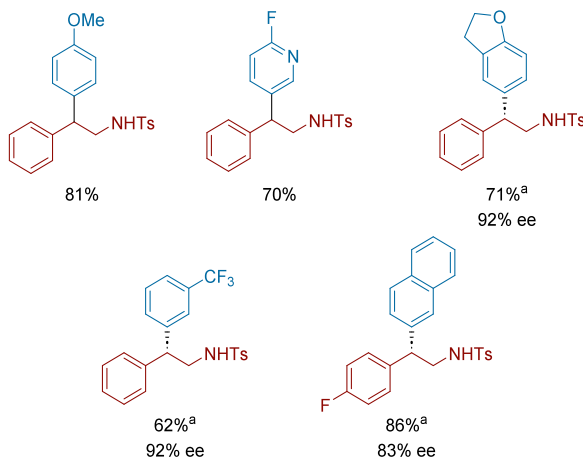
disubstituted cycloalkanes (generally in 99:1 dr), the authors report one example each of 1,3- and 1,4-disubstituted products, with good yields and lower diastereoselectivity (84:16 dr and 77:23 dr, respectively). A linear aliphatic iodide coupling partner was compatible, but it afforded lower diastereoselectivity (68:32 dr).

**4.2.9.3. Alkyl Amines as Electrophiles.** The Doyle and Sigman groups investigated the enantioselective coupling of styryl aziridines with aryl iodides (Scheme 238).<sup>358</sup> In line with previous findings from the Doyle group,<sup>311</sup> a racemic XEC approach with bpp ligand was developed. The electronics on both the aryl iodide and aziridine can be varied without substantial decreases in yield. To make this reaction enantioselective, the group employed (R)-4-heptyl-BiOX as ligand under slightly modified conditions. Parameterization

**Scheme 238. Ni-Catalyzed Racemic and Enantioselective XEC of Aryl Iodides with Styryl Aziridines (2017)<sup>a</sup>**



**Selected Examples**



<sup>a</sup>Modified conditions:  $\text{NiCl}_2(\text{dme})$  (15 mol%), (R)-4-heptyl-BiOX (18 mol%), NaI (2 equiv), TMSCl (20 mol%), Mn (3 equiv), THF (0.1 M) at  $-10^\circ\text{C}$ .

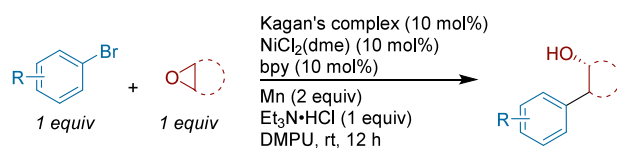
studies were undertaken to elucidate factors directly contributing to enantioselectivity. The three contributors were identified to be B1, NBO<sub>O</sub>, and Pol representing the minimum width of the R substituent of the ligand, the NBO charge of the oxygen atoms on the ligand, and the polarizability of the ligand, respectively.

**4.2.9.4. Epoxides as Electrophiles.** Following our report on the cross-coupling of epoxides with aryl halides (see section 4.2.5.3, Scheme 190),<sup>305</sup> we expanded this finding to an enantioselective approach (Scheme 239).<sup>309</sup> Using a traditional nickel catalyst, we employed a chiral titanium cocatalyst (Kagan's complex) to influence facial selectivity. Using *meso*-epoxides, a range of electronically diverse aryl bromides were coupled. C–Cl bonds were tolerated on aryls that contained multiple halides. This study also investigated the enantioselective coupling of vinyl halides/triflates with epoxides. In many of the scope examples, enantioselectivity was above 85% ee.

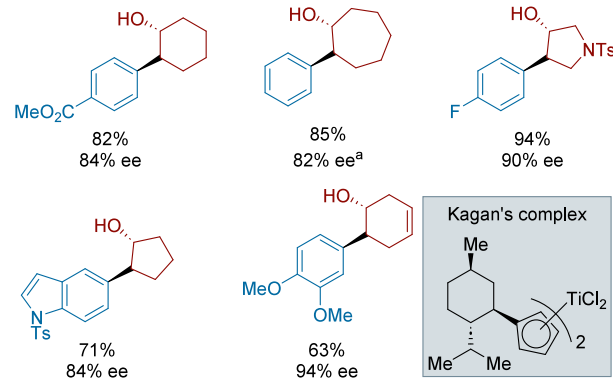
To address the regioselectivity issues arising from previously reported Ni-catalyzed XEC reactions between aryl halides and epoxides, Yamamoto and Banerjee hypothesized that hydroxy groups added  $\beta$ - to the epoxide could act as directing groups (Scheme 240).<sup>360</sup> Their approach was preceded by a previous finding they had published on regio- and enantioselective aminolysis.<sup>361</sup> Reaction development led them to design a chiral silyl-ether-based BiOX ligand which gave 90:10 dr and >99:1 regioselectivity in their model reaction. In all substrates investigated enantioselectivities were excellent (>90% ee). Removal of the hydroxy directing group diminished diastereoselectivity.

Doyle and co-workers expanded on their previous work and developed an enantioconvergent synthesis of chiral diarylmethanes using racemic styryl oxides with aryl iodides (Scheme 241).<sup>306,362</sup> While BiOX ligands, used in their

**Scheme 239. Enantioselective Ni-Catalyzed Cross-Electrophile Coupling of Aryl Halides with *meso*-Epoxides (2015)<sup>a</sup>**

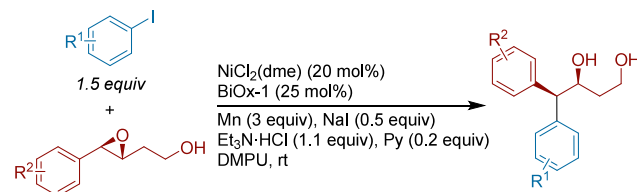


**Selected Examples**

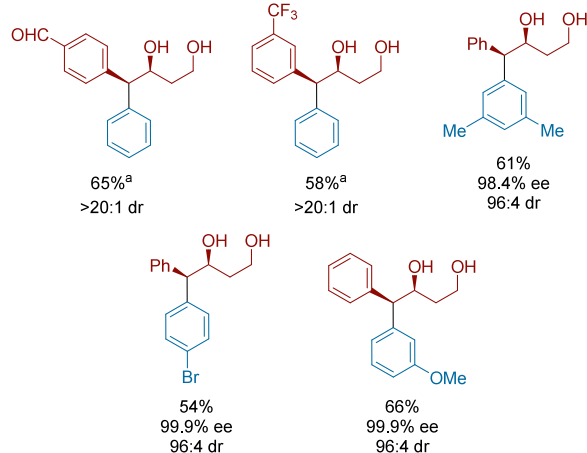


<sup>a</sup>Conducted on a 5 mmol scale.

**Scheme 240. Regio-, Diastereo-, and Enantioselective XEC of Aryl Iodides with Epoxides (2017)<sup>a</sup>**



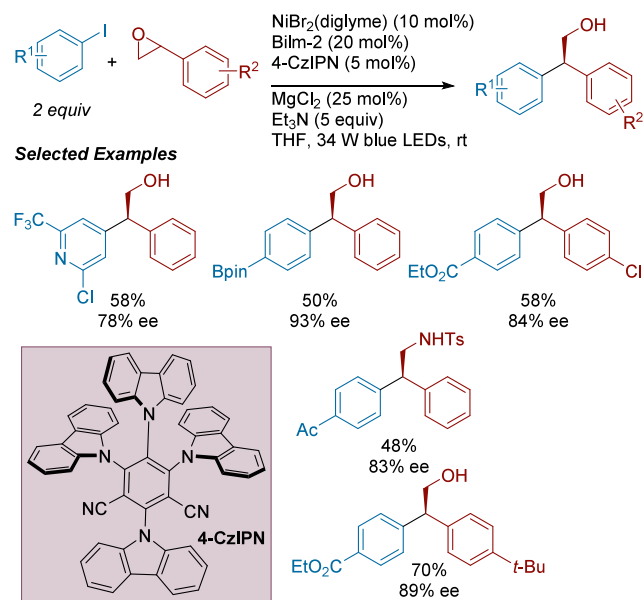
**Selected Examples**



<sup>a</sup>Racemic epoxyalcohol was used.

aziridine couplings, resulted in notable enantiocontrol with epoxides (50–75% ee), yields were moderate. Swapping to a more electron-rich biimidazoline (Bilm) improved yields with excellent enantioinduction. With comparable redox properties,  $[\text{Ir}(\text{dF}(\text{CF}_3)\text{ppy})_2(\text{dtbbpy})]\text{PF}_6$  could be substituted out with 4-CzIPN. Competition reactions ruled out epoxide oxidative addition to Ni(0) before aryl iodide and control experiments showed that halohydrin (from epoxide ring-opening with  $\text{Br}^-$ )

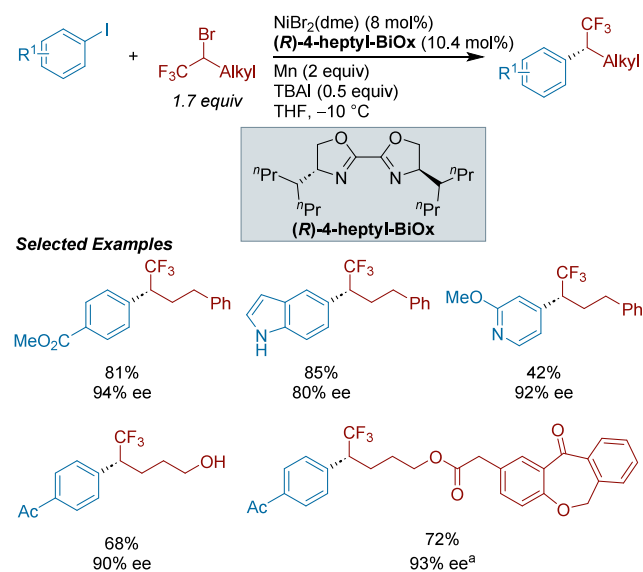
**Scheme 241.** XEC of Aryl Iodides with Styrene Oxides Enabled by a Nickel/Iridium Photoredox System (2021)



was a competent reaction intermediate. Swapping the aryl iodide with an aryl bromide or the epoxide with an *N*-aziridine was also viable under reaction conditions. Multi-variant linear regression analysis was conducted to further understand the effects of various ligand parameters on the reaction.

**4.2.9.5. Alkyl Halides as Fluoroalkylating Reagents.** Xi-Sheng Wang and co-workers developed an asymmetric approach to the trifluoroalkylation of aryl iodides (Scheme 242).<sup>363</sup> In their ligand evaluation, they found that secondary alkyl chains on the bioxazoline core increased enantioselectivity. With their optimized conditions, the authors showed generality toward coupling aryl substrates with aldehydes and free alcohols, in addition to a variety of heterocycles and

**Scheme 242.** Asymmetric Ni-Catalyzed XEC of  $\alpha$ -Trifluoromethyl Alkyl Bromides with Aryl Iodides (2021)<sup>a</sup>

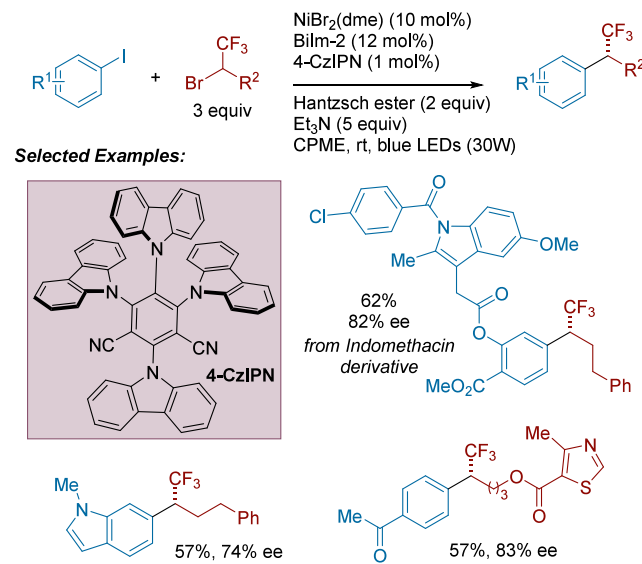


<sup>a</sup>With  $\text{NiBr}_2(\text{dme})$  (15 mol%), (*S*)-*n*-Pr-BiOx (20 mol%) at 0 °C.

bioactive molecules. Their alkyl scope included examples where functional groups such as unactivated chlorides, ferrocene, and cyclic protected amines are tolerated. High enantioselectivity was demonstrated, with most products generated above 90% ee. They also showed that these conditions can work with other alkyl- $\text{CF}_2\text{Br}$  coupling partners.

Tao Xu and co-workers reported the asymmetric trifluoroalkylation of aryl iodides through a nickel/photochemical XEC (Scheme 243).<sup>364</sup> The authors propose that the reaction

**Scheme 243.** Nickel/Iridium Photoredox Approach for the XEC of Aryl Iodides with  $\alpha$ -Trifluoromethyl Alkyl Bromides (2021)

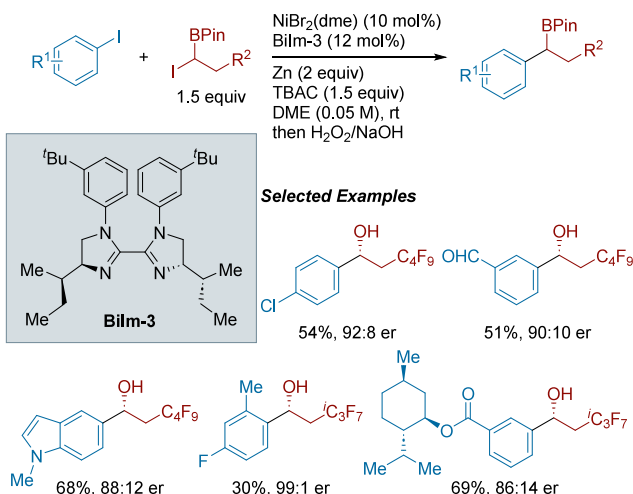


proceeds through alkyl radical formation, which does not occur through reduction of alkyl bromide by excited state 4-CzIPN\* as indicated by photoluminescence quenching experiments. Competition experiments between aryl iodides with different electronics showed a strong preference for consumption of the more activated substrate. A broad set of aryl iodides possessing electron-withdrawing and electron-donating groups were successfully trifluoroalkylated in high enantioselectivity, including the late-stage diversification of several drug-derived molecules.

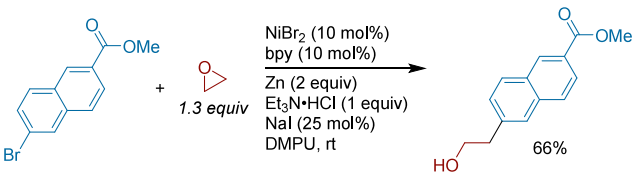
Tao Xu and co-workers also reported the coupling of aryl iodides with perfluoroalkylated  $\alpha$ -iodoboronates to form enantioenriched perfluoroalkylated boronate esters (Scheme 244).<sup>365</sup> The authors propose that addition of  $n\text{-Bu}_4\text{NCl}$  is necessary to accelerate the reduction of  $\text{Ni}^{II}\text{X}_2$  species, but all other chloride additives explored resulted in significantly diminished yields. The biimidazole (BiIm) ligand structure appears crucial, with a diamine or bis(oxazoline) ligand core resulting in no desired product, or diminished yield, respectively. Changing the steric bulk on the 2,8 positions from *i*-Pr to *s*-Bu resulted in a minimal increase in yield and enantiomeric ratio. The functional group tolerance of aryl iodides is broad, including electron rich and *ortho*-substituted aryls.

**4.2.10. Synthetic Applications of  $\text{C}(\text{sp}^2)-\text{C}(\text{sp}^3)$  Aryl-Alkyl XEC.** In a 2017 report describing the synthesis of GPR55 agonists, Croatt and co-workers applied cross-electrophile coupling into their synthetic plan (Scheme 245).<sup>366</sup> Their goal was to couple an intermediate aryl bromide with ethylene

**Scheme 244. Enantioconvergent Ni-Catalyzed XEC of Aryl Iodides with  $\beta$ -Perfluoroalkylated  $\alpha$ -Iodo Boronate Esters (2021)**



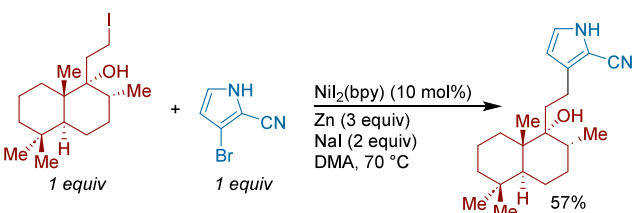
**Scheme 245. Application of Ni-Catalyzed XEC in the Synthesis of GPR55 Agonists (2017)**



oxide, later protecting the resulting alcohol with a silyl group. Initially, they thought to form an organometallic species through insertion of the C–Br bond. However, they found cross-electrophile coupling to be milder and more effective, giving product in 66% yield. This saved four steps and increased the overall yield by more than 30%.

In a report detailing the synthesis of (+)-vitепролоид A and (+)-vitепролоид B, Christmann and co-workers employed a late stage Ni-catalyzed cross-electrophile coupling with complex coupling partners (Scheme 246).<sup>367</sup> With an alkyl

**Scheme 246. Late-Stage Application of Ni-Catalyzed XEC for the Synthesis of (+)-Vitепролоид A and (+)-Vitепролоид B (2018)**

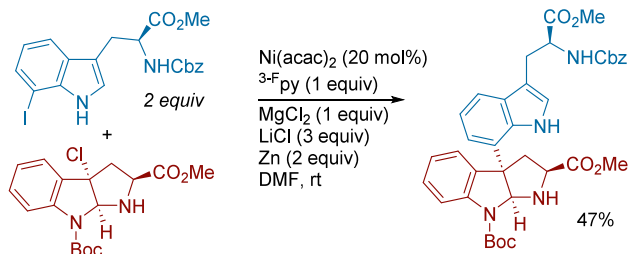


iodide and a heteroaryl bromide in hand, they sought to find a method that would eliminate the need for protecting groups and tolerate protic functionality. After testing multiple nickel- or palladium-based systems they found a hit with cross-electrophile coupling in 12% yield. This reaction was later optimized with the addition of  $\text{NaI}$  (2 equiv) and an increase in temperature affording 57% yield of product.

Hegui Gong, Yu Peng, and co-workers presented the divergent total syntheses of the diketopiperazine alkaloids

(+)-asperazine and (+)-pestalazine A. These syntheses proceed through a common intermediate constructed through cross-electrophile coupling of a tertiary alkyl chloride and iodotryptophan fragment (Scheme 247).<sup>368</sup> As a result of

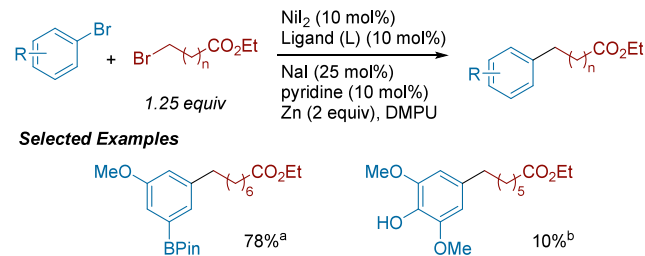
**Scheme 247. XEC of Aryl Iodide with Alkyl Chloride Intermediates in the Total Synthesis of (+)-Asperazine and (+)-Pestalazine (2018)**



this strategy, the syntheses of (+)-asperazine and (+)-pestalazine A was completed in an average overall yield of 14% and longest linear sequences of ten steps each. Furthermore, the preparation of two additional diketopiperazine alkaloids were achieved in similar yields with straightforward modification of the synthetic sequence.

Gellman and co-workers applied the cross-electrophile coupling of aryl bromides with alkyl bromides as a key step in the total synthesis of robustol (Scheme 248).<sup>369</sup> The

**Scheme 248. Synthesis of Robustol with Two Intermediate XEC Procedures Followed by Foldamer Catalysis (2019)<sup>a</sup>**



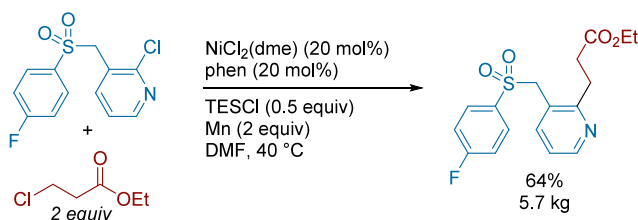
<sup>a</sup>(a) L = phen, 65 °C, (b) L = <sup>4,4'</sup>-MeO **bpy**, 75 °C.

coupling tolerated both boronate ester and phenol functionalities (the latter in a lower yield), which enabled further derivatization. Subsequent Chan-Lam coupling of the two fragments and aldol macrocyclization using foldamer catalysis afforded the natural product.

In 2020, Bristol Myers Squibb, led by Vaidyanathan, disclosed a cross-electrophile coupling reaction between 2-chloropyridine and ethyl 3-chloropropionate completed at a multikilogram scale (Scheme 249).<sup>47</sup> This report contains systematic studies on Mn powder activation (including using focused beam reflectance measurements), a new activating agent for Mn (TESCl), and systematic studies on stirring/reactor design for XEC reactions. Considerable detail is provided in the use of modeling and small-scale test reactions to determine the appropriate mixing speed to suspend the Mn in a given reactor geometry/stirrer combination. The title cross-coupling reaction was executed with 7 kg of aryl bromide to give the desired product in 64% yield (5.7 kg).

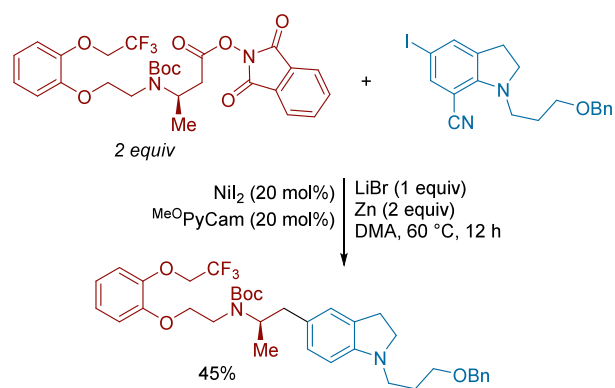
Baran and co-workers, in collaboration with Minakem, described the formal synthesis of silodosin using the

**Scheme 249. Cross-Coupling of Derivatized 2-Chloropyridine and Ethyl 3-Chloropropionate Through a Ni-Catalyzed Protocol (2020)**



decarboxylative cross-electrophile coupling of an NHP ester and iodoindoline intermediate as a key combinatorial step (Scheme 250).<sup>370</sup> Previous approaches to this molecule have

**Scheme 250. Synthesis of (R)-Silodosin Involving a Key XEC Step Between an Aryl Iodide and NHP ester (2021)**



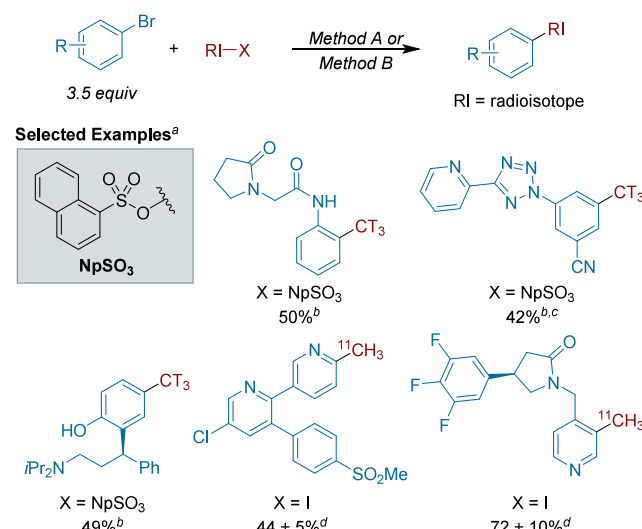
utilized either a hydrogenation/Curtius pathway<sup>371</sup> or a reductive amination based strategy.<sup>372–374</sup> By employing cross-electrophile coupling, the authors were able to take a more convergent approach to the synthesis and to lower the longest linear sequence to seven steps.

In collaboration with Merck, the University of Pennsylvania, and RTI International, MacMillan and co-workers applied cross-electrophile coupling for the synthesis of positron emission tomography (PET) radioligands (Scheme 251).<sup>375</sup> These compounds, containing tritium or carbon-11 labels could serve as competent characterization tools for diseases and drug candidates. The methylation reactions they proposed install either a tritriomethyl or <sup>11</sup>C-methyl group from [<sup>3</sup>CT<sub>3</sub>] methyl 1-naphthalenesulfonate (CT<sub>3</sub>ONp) and [<sup>11</sup>C]-iodomethane, respectively. Success of coupling was monitored by radiochemical yield (RCY), with the aim of obtaining higher than 10%. They achieved this goal with most targets and were able to apply their conditions to substrates with protic functional groups. Due to the stability of the –CT<sub>3</sub> source they chose, this method could be viable for applications where volatile precursors are traditionally avoided. To test the possibility of use in the medical field, they conducted PET imaging on a nonhuman primate using one of the <sup>11</sup>C-labeled molecules isolated.

#### 4.3. Alkylated Alkenes

**4.3.1. Overview.** Alkenyl electrophiles (such as vinyl halides, vinyl triflates, or vinyl acetates) react in cross-electrophile couplings analogously to aryl electrophiles, but it is common that distinct conditions from aryl–alkyl coupling

**Scheme 251. Nickel/Photoredox-Enabled Methylation Conditions for Radiolabeling (2021)<sup>a</sup>**



<sup>a</sup>(a) All yields given as radiochemical yields (RCY). (b) Conditions: NiBr<sub>2</sub> (10 mol%), dtbbpy (12 mol%), [Ir(dF(CF<sub>3</sub>)ppy)<sub>2</sub>](dtbbpy)]-PF<sub>6</sub> (1 mol%), (TMS)<sub>3</sub>SiH (3 equiv), LiBr (2 equiv), and 2,6-lutidine (5 equiv) in 1:1 DMA/toluene at rt, 450 nm LEDs. (c) Modified conditions: NiBr<sub>2</sub>(dtbbpy) (80 mol%), [Ir(dF(CF<sub>3</sub>)ppy)<sub>2</sub>](dtbbpy)]-PF<sub>6</sub> (4 mol%), and LiI (5 equiv) in acetone (0.01 M). (d) Conditions: NiBr<sub>2</sub> (0.75 μmol), dtbbpy (0.9 μmol), [Ir(dF(CF<sub>3</sub>)ppy)<sub>2</sub>](dtbbpy)]PF<sub>6</sub> (75 nmol), (TMS)<sub>3</sub>SiH (9 μmol), TBAI (2.4 μmol), and 2,6-lutidine (15 μmol) in acetone at rt, 450 nm LEDs.

are required for efficient vinyl–alkyl coupling.<sup>376</sup> This can be attributed to faster rates of oxidative addition and faster rates of homocoupling. This commonly results in rapid homocoupling of the vinyl–X partner before consuming the alkyl–X species. Nonetheless, strategies have emerged to promote cross-selectivity, such as lowering catalyst loading or using more activated alkyl–X electrophiles (such as benzyl–X or alkyl iodides) to better match reactivity.

The challenge of *E/Z* stereochemistry is an extra consideration for vinyl electrophiles. First, synthesis of the electrophiles with the desired stereochemistry can present a challenge. Second, the coupling reaction can result in erosion of stereochemistry. Despite this extra challenge, the diversification of a single vinyl electrophile to a wide array of substituted alkenes with stereocontrol is a major advantage of this approach. Conventional stereoselective olefination methods (e.g., Wittig, Horner-Wadsworth-Emmons modifications, Julia, etc.) often do not tolerate protic and electrophilic functional groups as well as cross-electrophile coupling.

In this section we describe cross-electrophile coupling reactions that have been directly optimized on a vinyl–X coupling partner. Despite this, the optimal ligands are similar to the Aryl–Alkyl section (Figure 28, Figure 29). Enantioselective couplings and total syntheses employing vinyl–X electrophiles are highlighted. We note that conditions optimized for aryl–alkyl coupling often work to some extent for vinyl–alkyl couplings (see section 4.2) (refs 41, 50, 71, 174, 206, 219, 232, 243, 244, 268, 269, 278, 279, 283, 289, 294, 297, 305, 308, 309, 311, 353, 354, and 359). Vinyl–alkyl couplings that are known to proceed via *in situ* Zn or Mg insertion into alkyl halides and concurrent Negishi/Kumada cross-coupling will not be covered in this review.<sup>377,378</sup> Another class of reactions

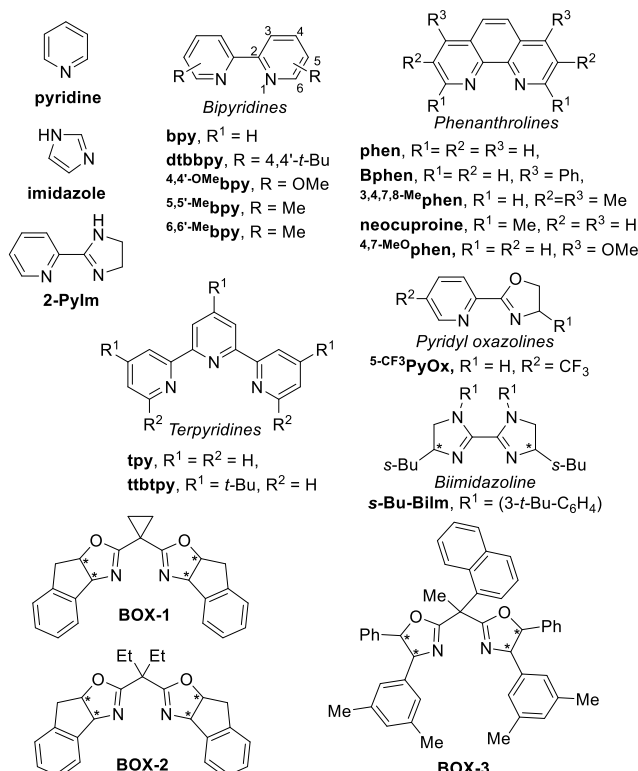


**Figure 28.** Ligands used in vinyl–alkyl XEC reactions.\* Denotes chiral center.

that is easily confused with XEC chemistry involve reductive, metal-mediated radical formation followed by substrate radical capture and bond formation that does not involve a metal catalyst.<sup>379–381</sup> This is prominent with styryl electrophiles and tertiary radicals, for example.<sup>379–381</sup> We note again that this is merely categorization—these are often excellent reactions that have all of the advantages of XEC reactions.

**4.3.2. XEC of Vinyl Halides with Alkyl Electrophiles.** An early example of vinyl cross-electrophile coupling was reported by Condon and Durandetti in 2000. They developed an electrochemical cross-electrophile coupling that could form C–C bonds from vinyl iodides, bromides, and chlorides with  $\alpha$ -chloroketones, esters, and nitriles in an undivided cell (**Scheme 252**).<sup>126,382</sup> They also demonstrated XEC of vinyl halides with aryl and vinyl electrophiles (see section 3.3.1.1, **Scheme 42**). They noted that vinyl iodides were susceptible to dimerization due to their increased reactivity, but this could be overcome through slow addition of the vinyl coupling partner to the alkyl halide in solution. Cross-coupled products in some cases retained the olefin geometry of the starting vinyl halide, with the degree of isomerization being variable.

In 2016, our group reported improved conditions from our initial report<sup>44</sup> for the Ni-catalyzed cross-electrophile coupling of vinyl bromides with alkyl halides (**Scheme 253**).<sup>383</sup> Key to the success of this approach was low catalyst loadings (2.5 mol %) to minimize undesired vinyl homodimerization. The dimerization appears to involve transmetalation between two vinylnickel(II) species, but the cross-product formation is closer to first order in nickel concentration. A variety of unhindered styryl and  $\beta$ -alkyl-substituted (*Z*)-vinyl bromides could be cross-coupled with alkyl bromides in high yields and good retention of olefin geometry. An (*E*)-vinyl bromide could also be coupled by lowering catalyst loading further to 0.5 mol

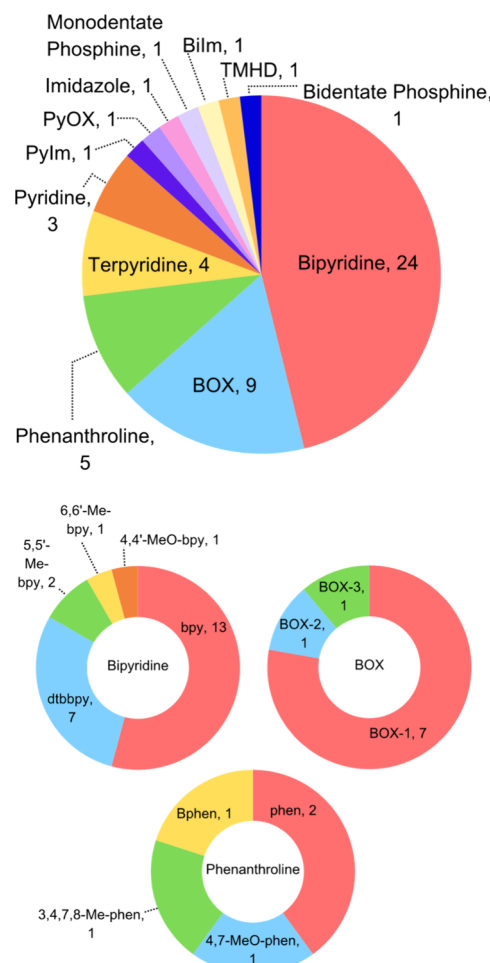
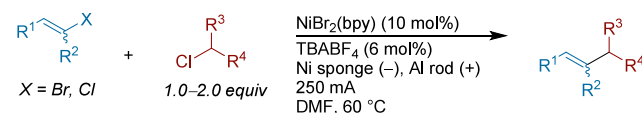
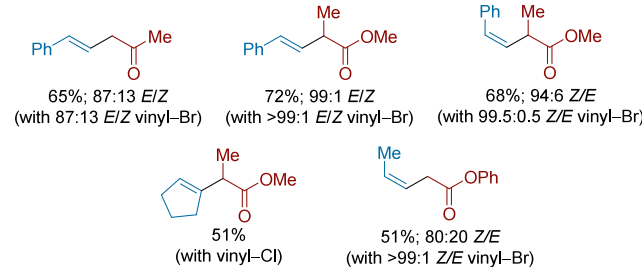


**Figure 29.** Distribution of ligands used in vinyl–alkyl XEC reactions.

### Scheme 252. Electrochemical XEC of Vinyl Halides with Alkyl Chlorides (2000)



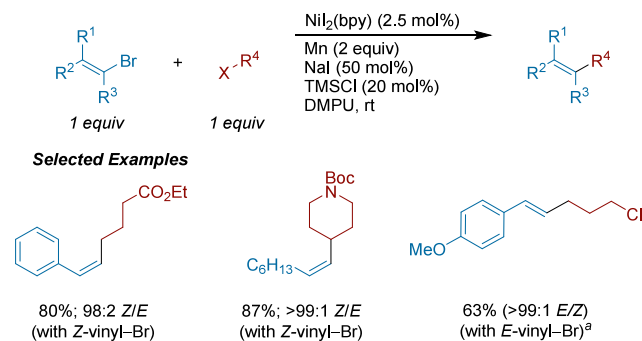
#### Selected Examples



% and employing a more electron-rich ligand, 4,4'-MeO<sup>o</sup>bpy. Control experiments suggested any olefin isomerization, when observed, occurred prior to C–C bond formation. These conditions were also directly applicable to the coupling of aryl bromides with alkyl bromides.

The Gong group reported on a series of XEC reactions of vinyl halides with both activated and unactivated alkyl halides. In 2016, Hegui Gong, Xinghua Zhang, and Ken Yao developed conditions for the Ni-catalyzed vinylylation of  $\alpha$ -halocarbonyls

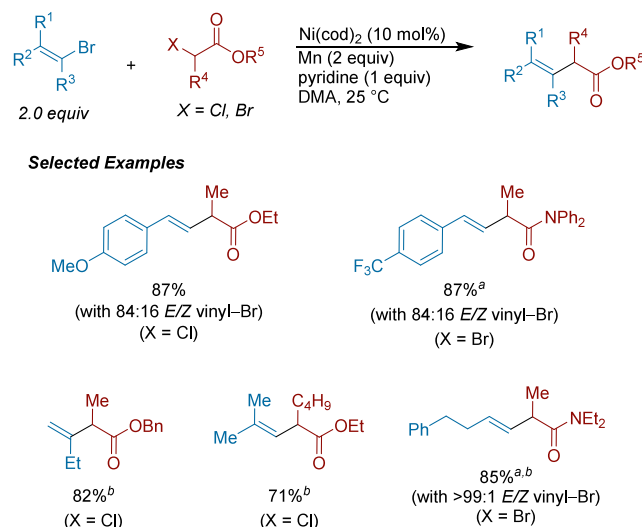
**Scheme 253. Ni-Catalyzed Cross-Electrophile Coupling of Vinyl Bromides with Alkyl Halides<sup>a</sup>**



<sup>a</sup>With  $\text{NiI}_2(4,4'\text{-MeO} \text{bpy})$  (0.5 mol%) as catalyst.

(Scheme 254).<sup>384</sup> When applying styryl bromides in this protocol, pyridine was sufficient as the sole ligand, while  $\beta$ -

**Scheme 254. Ni-Catalyzed Cross-Electrophile Coupling of  $\alpha$ -Halocarbonyl Derivatives with Vinyl Bromides (2016)<sup>a</sup>**

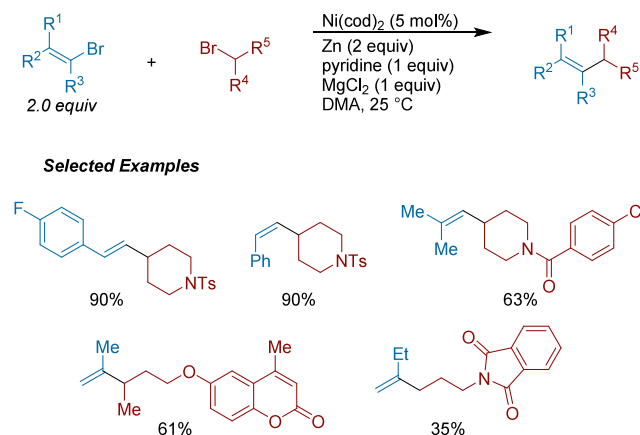


<sup>a</sup>(a)  $\text{MgCl}_2$  (1 equiv) was added. (b) bpy (30 mol%) was added.

alkyl-substituted vinyl halides required both bpy and pyridine for efficient reactivity. Both di- and trisubstituted olefin products could be accessed. Employing (*E*)-vinyl halides yielded the (*E*)-olefin product, while (*Z*)-vinyl halides isomerized, favoring the (*E*)-product. The authors propose a radical chain mechanism.

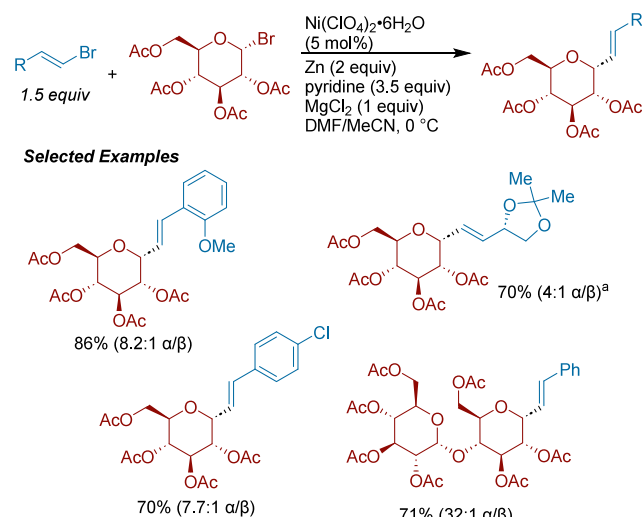
Later in 2017, Hegui Gong, Kunhua Lin, Qun Qian and co-workers reported the nickel cross-electrophile coupling of vinyl bromides with unactivated alkyl halides (Scheme 255).<sup>385</sup> As with their previous XEC reaction of vinyl bromides and  $\alpha$ -halocarbonyls, pyridine was the sole ligand for this transformation. Styryl and  $\beta$ -alkyl substituted vinyl bromides were both applicable under these conditions. Retention of olefin geometry of the substrate was observed in all examples, except for the coupling of (*Z*)-1-bromo-1-nonene, which isomerized from 99:1 *Z/E* vinyl bromide to 85:15 *Z/E* in the cross-product. Di- and trisubstituted vinyl bromides could be coupled, including nonstyryl- $\alpha$ -substituted vinyl bromides. One example of a tetrasubstituted olefin was also shown, albeit in a low yield.

**Scheme 255. Cross-Electrophile Coupling of Vinyl Bromides with Unactivated Alkyl Bromides (2017)**



Hegui Gong and co-workers then extended their Ni-catalyzed vinylation strategy to prepare  $\alpha$ -C-linked glycosides. The authors optimized two sets of conditions for the cross-coupling of glycosyl halides with aryl iodides (see section 4.2.1.1, Scheme 97) and with vinyl bromides (Scheme 256).<sup>220</sup>

**Scheme 256. Stereoselective Preparation of  $\alpha$ -C-Vinyl Glycosides via Ni-Catalyzed XEC of Glycosyl Bromides with Vinyl Bromides (2018)<sup>a</sup>**

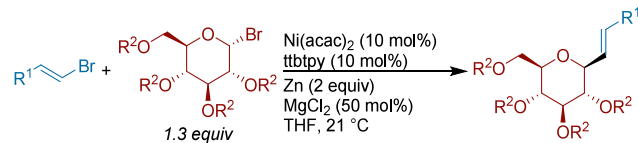


<sup>a</sup>With 10 mol%  $\text{Ni}(\text{ClO}_4)_2 \bullet 6\text{H}_2\text{O}$ .

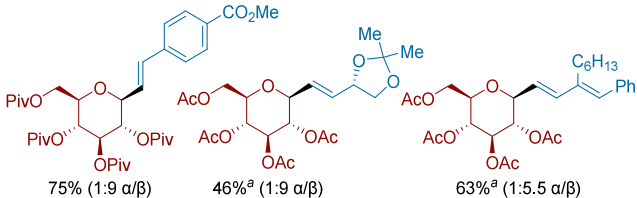
For glucosyl bromides, reported Ni, Fe, and Co cross-coupling reactions afforded either high  $\beta$ -selectivity or an unselective mixture of anomers. In contrast, their Ni-catalyzed XEC conditions provided good to excellent  $\alpha$ -diastereoselectivity in the vinylation of glucose (as well as galactose, mannose, and maltose derivatives). This unusual selectivity appeared to arise from the monodentate pyridine ligand: bidentate and tridentate ligands provided lower  $\alpha/\beta$  selectivity (2.8:1 to 1:1). The authors propose that the lability of pyridine and decreased steric profile are responsible.

Following their 2018 report, Hegui Gong, Chuanhu Lei, and Jiandong Li then reported modified conditions for  $\beta$ -selective cross-electrophile coupling of glucosyl bromides with aryl and vinyl halides (Scheme 257).<sup>221</sup> As previously, distinct conditions were required for coupling aryl iodides (see section

**Scheme 257.** Stereoselective Preparation of  $\beta$ -C–Vinyl Glycosides via Ni-Catalyzed XEC of Glycosyl Bromides with Vinyl Bromides (2019)<sup>a</sup>



**Selected Examples**

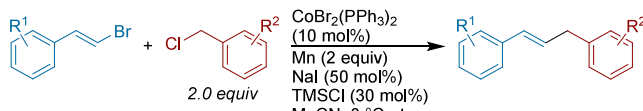


<sup>a</sup>With glycosyl bromide (2 equiv) and MgCl<sub>2</sub> (15 mol%) at 25 °C.

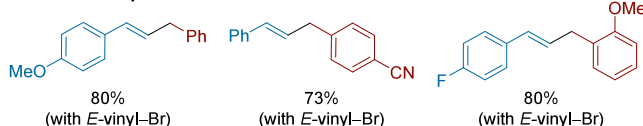
4.2.1.1, Scheme 98) and for coupling vinyl bromides. Glucose- and galactose-derived alkyl halides could be employed in this protocol, but mannosides only afforded the  $\alpha$ -anomer. The authors propose that diastereoselectivity arises from favorable  $\beta$ -attack of nickel to the boat conformation of the glucosyl radical, minimizing steric interactions between the glucoside substituents and the bulky tbtipy ligand on the nickel center.

The Gosmini group applied their cobalt cross-electrophile coupling catalyst system to the coupling of styryl bromides with primary benzyl chlorides (Scheme 258).<sup>386</sup> To achieve

**Scheme 258.** Cobalt-Catalyzed Cross-Electrophile Coupling of Styryl Bromides with Benzyl Chlorides (2017)



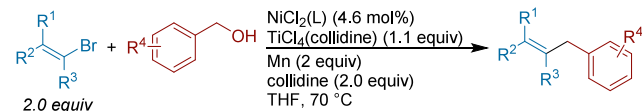
**Selected Examples**



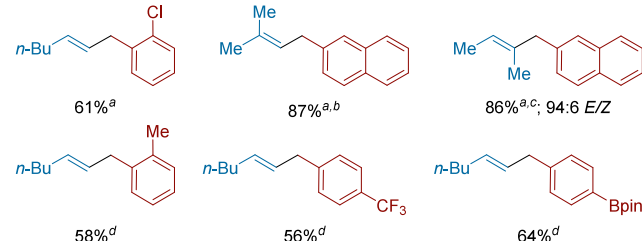
high yields, the authors noted the importance of performing the CoBr<sub>2</sub>(PPh<sub>3</sub>)<sub>2</sub> complex and employing TMSCl as an additive for manganese activation. A variety of electron-donating and electron-withdrawing substituents could be incorporated on either coupling partner, but  $\beta$ -alkyl substituted vinyl bromides provided no yield under reaction conditions. Importantly, they showed that this coupling proceeds with high retention of olefin *E/Z* stereochemistry, even for (*Z*)-olefins.

Ukaji, Suga, Takahashi and co-workers reported a nickel/titanium system to cross-couple vinyl bromides with benzyl alcohols (Scheme 259).<sup>387</sup> These are proposed to proceed without preactivation of the alcohol; instead, a low-valent titanium species initiates C–OH bond scission and generates the alkyl radical. Radical capture by a vinylnickel(II) species, followed by reductive elimination would then yield the product. The authors noted the judicious selection of ligand for nickel and titanium complex was important for each combination of coupling partner. In general, *E/Z* olefin geometry was retained, but when mixed vinyl bromides were

**Scheme 259.** Cross-Electrophile Coupling of Benzyl Alcohols with Alkenyl Halides Using a Ni/Ti/Mn System (2020)<sup>a</sup>



**Selected Examples**

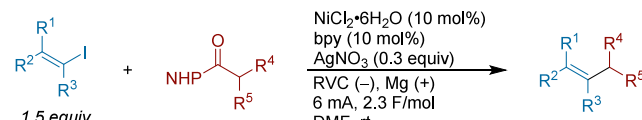


<sup>a</sup>(a) L = 3,4,7,8-Me<sub>4</sub>phen. (b) With vinyl bromide (1.2 equiv) and 2,6-lutidine instead of collidine. (c) With vinyl bromide (3.0 equiv) and 2,6-lutidine instead of collidine. (d) L = 4,7-Me<sub>2</sub>Ophen.

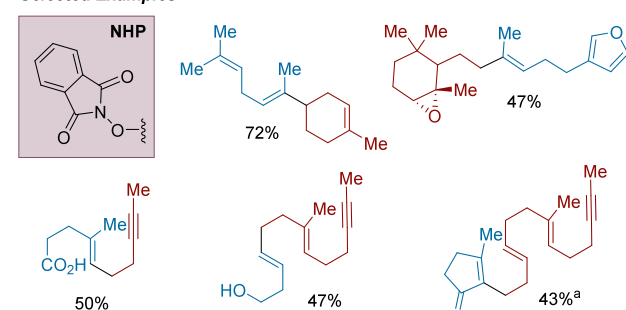
used, they saw faster consumption of the (*E*)-isomer. With additional optimization, a fully tetrasubstituted vinyl bromide was successfully coupled in good yield.

Baran, Anderson, Abruna, and co-workers reported an electrochemical approach to assemble terpene fragments through decarboxylative cross-electrophile coupling of vinyl iodides with NHP esters (Scheme 260).<sup>388</sup> Key to the success

**Scheme 260.** Electrochemical Cross-Electrophile Couplings of Vinyl Iodides with N-Hydroxyphthalimide Esters to Prepare Terpene Natural Products (2022)<sup>a</sup>



**Selected Examples**



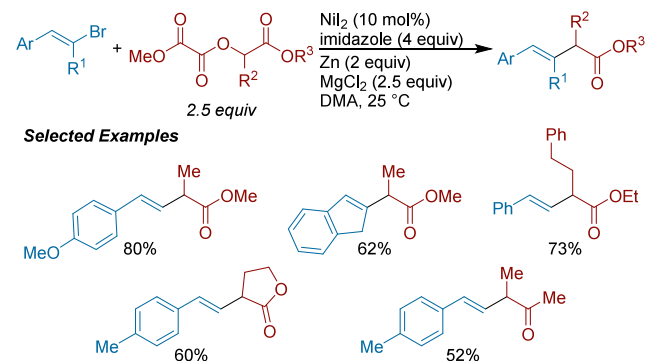
<sup>a</sup>With alkyl bromide instead of NHP ester.

of this strategy is the addition of silver salts that modify the surface of the RVC (carbon) cathode. The carboxylic acid could be activated as the NHP ester in situ, complete retention of olefin geometry was observed, and reactions tolerated the presence of sensitive functionality (e.g., free carboxylic acids, epoxides). This method was showcased in the preparation of 13 terpene-based natural products (see section 4.3.5 Scheme 297) and in a 100-g reaction conducted using a recirculating flow system. A series of spectroscopic experiments revealed that silver nanoparticles are deposited on the surface of the cathode, lowering the electrode's potential by +0.51 V. This

effectively lowers the overpotential of the system and inhibits over-reduction of the nickel catalyst. This prevents deposition of the catalyst on the cathode, which can occur when the reaction is run at higher potentials.

An approach for the preparation of  $\beta,\gamma$ -unsaturated carbonyls through the Ni-catalyzed cross-electrophile coupling of vinyl bromides with oxalate-activated  $\alpha$ -hydroxy carbonyls was developed by Fan Wu and co-workers (Scheme 261).<sup>389</sup>

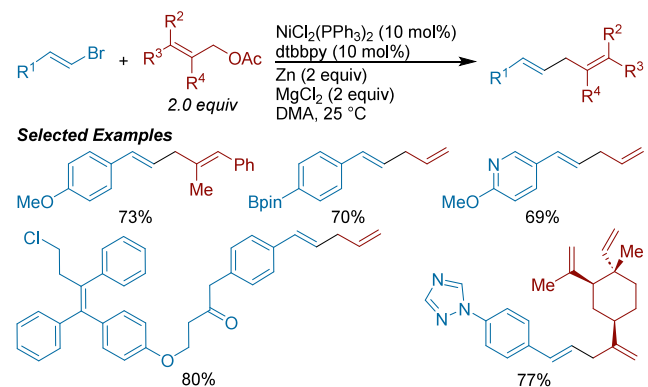
**Scheme 261.** Ni-Catalyzed Cross-Electrophile Coupling of Oxalates Derived from  $\alpha$ -Hydroxy Carbonyls with Vinyl Bromides (2022)



excess of imidazole was utilized instead of more common bi- or tridentate ligands. Electron-rich styryl bromides coupled well in this approach, as did oxalates derived from esters, ketones, and lactones.

Tian Xie, Xiang-Yang Ye, Yang Ye and co-workers described a strategy for the XEC of vinyl bromides with allylic acetates to prepare 1,4-dienes (Scheme 262).<sup>390</sup> They noted that

**Scheme 262.** Ni-Catalyzed Cross-Electrophile Coupling of Vinyl Bromides with Allylic Acetates (2022)

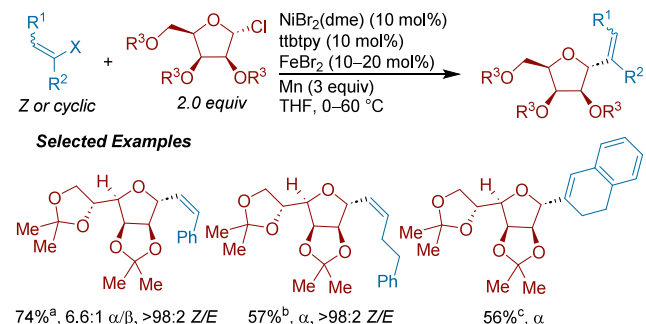


conditions previously reported for coupling aryl halides with allylic acetates (see section 4.2.5.5, Scheme 195)<sup>310</sup> gave low yields in the targeted vinyl allylation, and reoptimization of reaction conditions was necessary. Primary, secondary, and tertiary allylic acetates could be applied in good yields and excellent regioselectivity for the linear over branched products was observed. In addition to vinyl bromides, the corresponding chlorides, iodides, and triflates were compatible coupling partners. (*E*)- and (*Z*)-vinyl halides were both competent in this protocol with complete retention of olefin geometry. The authors highlighted their method in analogue syntheses of the  $\beta$ -elemene scaffold, a broad-spectrum antitumor natural

product. The triazole containing  $\beta$ -elemene analog (Scheme 261, bottom right) exhibited increased potency *in vivo* in cancer cell lines.

Ming Joo Koh, Gong Chen, and co-workers showcased an iron-catalyzed XEC approach to prepare C-linked glycosides by coupling chlorosugars with vinyl electrophiles (Scheme 263).<sup>391</sup> While reactions with (*E*)-vinyl bromides appear to

**Scheme 263.** Iron and Nickel Co-Catalyzed Cross-Electrophile Coupling of Vinyl Electrophiles with Glycosyl Chlorides (2022)<sup>a</sup>



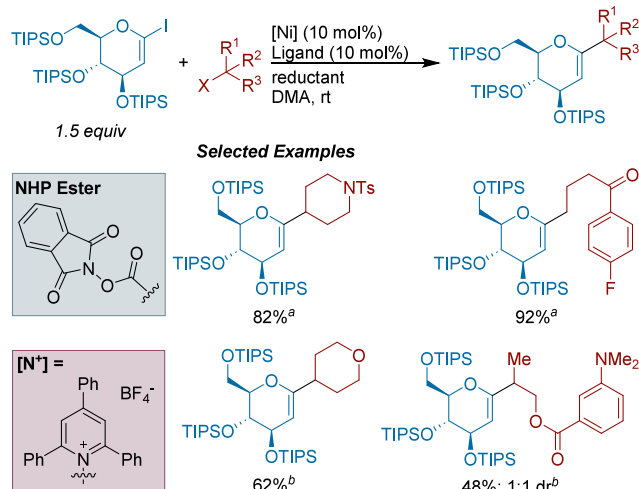
<sup>a</sup>(a) X = Br. (b) X = I. (c) X = OTf.

proceed by a pure radical addition/elimination process that is not a cross-electrophile coupling, (*Z*)-vinyl halides can be coupled stereospecifically with a nickel cocatalyst through an XEC mechanism. The authors also demonstrated that vinyl iodides and triflates, alkynyl iodides, and several classes of heteroaryl chlorides were all compatible with this protocol. Mechanistic studies were consistent with formation of a glycosyl radical by the iron salt followed by radical addition/elimination or a nickel mediated coupling process (depending upon the conditions). This reaction generally proceeds with high diastereoselectivity, dictated by radical addition/capture at the less-hindered face of the glycosyl radical. This method was demonstrated in two short syntheses of the anticancer agent (+)-varitriol and a fluorinated analogue.

Honggen Wang, Xu-Ge Liu, and co-workers reported an approach to prepare C-glycosides through the Ni-catalyzed cross-electrophile coupling of alkenyl glycoside iodides with NHP esters and *N*-alkylpyridinium salts (Scheme 264).<sup>392</sup> Primary, secondary, and tertiary NHP esters all coupled effectively in this protocol. With modified conditions, secondary *N*-alkylpyridiniums also coupled well in this approach.

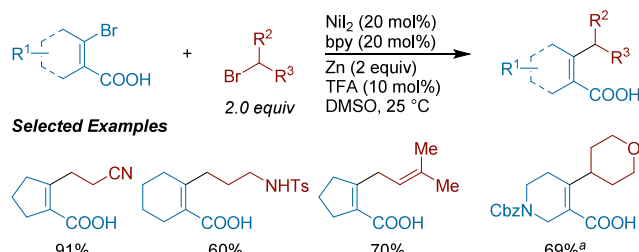
Yong Qin, Zhenlei Song, and co-workers described a strategy to couple sterically hindered 2-bromocycloalkenyl carboxylic acids with alkyl bromides (Scheme 265).<sup>393</sup> Notably, the free carboxylic acid did not cause significant side-reactivity. Primary alkyl bromides bearing varied functionality (such as nitrile, aldehyde, and acidic protons) coupled effectively. More sterically hindered secondary alkyl bromides could also be coupled by switching the additive to 3 equiv NaI instead of TFA. Cyclic vinyl bromides of various sizes (5–8 membered rings), including those derived from steroid frameworks, could be coupled in this protocol. Despite the similarity of the conditions to typical XEC conditions (DMSO vs amide solvent, room temperature conditions, etc.), control experiments showed that the carboxylic acid was essential for productive reactivity. This suggests the group directs oxidative addition or stabilizes the resulting intermediate. Further

**Scheme 264.** Ni-Catalyzed Cross-Electrophile Coupling of Vinyl Glycosyl Iodides with NHP Esters and *N*-Alkyl Pyridiniums (2023)<sup>a</sup>



<sup>a</sup>(a) With  $\text{NiBr}_2(\text{dme})$ , dtbbpy, Zn (3 equiv), X = NHP ester. (b) With  $\text{NiCl}_2(\text{dme})$ , bpy, Mn (2 equiv), X =  $[\text{N}^+]$ .

**Scheme 265.** Carboxylic Acid-Assisted, Ni-Catalyzed Cross-Electrophile Coupling of Cycloalkenyl Bromides with Alkyl Bromides (2023)<sup>a</sup>

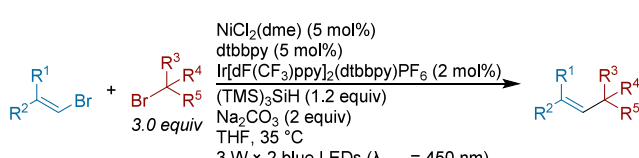


<sup>a</sup>With NaI (3 equiv) instead of TFA.

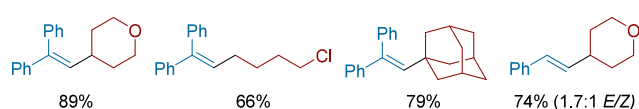
experiments with the radical clock 6-bromo-1-hexene showed the degree of rearrangement to be independent of catalyst concentration, consistent with a radical rebound process or an outer-sphere radical addition process.

Wen-Jing Xiao and König reported a dual catalytic protocol for the alkenylation of primary, secondary, and tertiary alkyl bromides based upon the previously reported silyl radical XAT strategy by the MacMillan group<sup>43</sup> (Scheme 266).<sup>394</sup> Two

**Scheme 266.** Alkenylation of Unactivated Alkyl Bromides through Visible Light Photocatalysis and Silyl Radical XAT (2019)



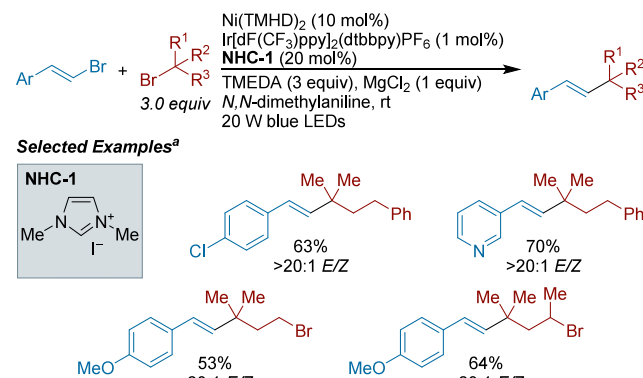
**Selected Examples**



classes of reactions were demonstrated in this work: radical additions into vinyl sulfones (not shown) and cross-electrophile coupling of vinyl bromides with alkyl bromides (Scheme 266). Consistent with MacMillan's studies,  $(\text{TMS})_3\text{Si}^\bullet$  radical is proposed to react with the alkyl halide to form the alkyl radical. Both di- and trisubstituted vinyl bromides could be applied in good yields, although *E/Z* ratios were modest in products with olefin stereochemistry (1.5:1 to 3:1 *E/Z* ratios).

Junkai Fu, Tao Wang, and co-workers reported the nickel photoredox cross-electrophile coupling of styryl bromides with tertiary alkyl bromides (Scheme 267).<sup>395</sup> TMEDA was used as

**Scheme 267.** Dual Nickel- and Photoredox-Catalyzed Cross-Electrophile Coupling of Styryl Halides and Unactivated Tertiary Alkyl Bromides (2019)<sup>a</sup>



<sup>a</sup>TMHD = 2,2,6,6-tetramethyl-3,5-heptanedione.

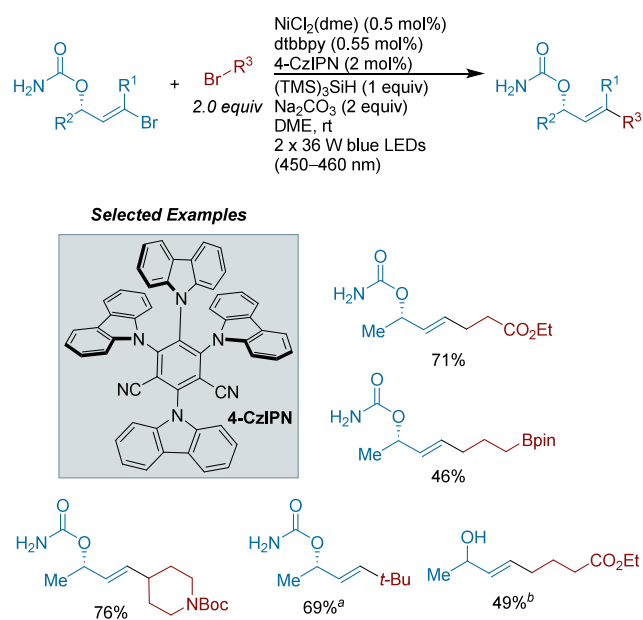
the terminal reductant and the combination of NHC-1 and  $\text{MgCl}_2$  provided the highest yields. The role of NHC-1 was somewhat unclear but had a notable effect. High (*E*)-selectivity was observed regardless of the starting configuration of the vinyl bromide. While radical addition followed by elimination does not require nickel catalysis,<sup>380</sup> the authors propose nickel mediates C–C bond formation as well as radical generation. Given some of the success with enantioselective versions of these reactions (see section 4.3.4), this is a reasonable proposal.

The Stecko group reported a nickel/iridium photocatalytic cross-electrophile coupling of nonstyryl vinyl bromides with alkyl bromides to form versatile chiral allyl carbamates (Scheme 268).<sup>396</sup> The authors applied chiral bromoallylic carbamates as substrates, and the stereocenter was preserved throughout the reaction. Importantly, complete retention of *E/Z* olefin geometry was also observed. Broad functional group tolerance was demonstrated, including epoxides, phosphonates, boronate esters, free alcohols, and acetals. The alkyl coupling partner scope was also broad, including 1°, 2°, and 3° alkyl bromides (3° required different conditions). In the case of activated alkyl coupling partners (e.g., benzyl), the authors found that utilizing a non-XEC nickel photoredox coupling of the carboxylic acid provided better results.

Stecko and co-workers applied their previous conditions<sup>396</sup> to the related amine-functionalized vinyl bromides to form useful chiral, branched allylamines from 3-bromoallylamines (Scheme 269).<sup>397</sup> A variety of *N*-protecting groups could be tolerated, and the substrate scope of alkyl substitution was broad, in analogy to their previous work.

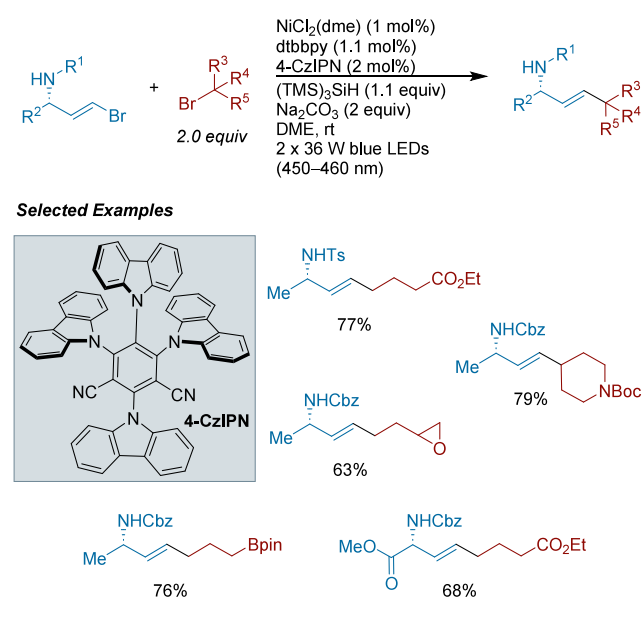
*gem*-Difluoroalkenes represent a distinct class of electrophile for cross-electrophile couplings. Yao Fu, Tian-Jun Gong, and

**Scheme 268.** Nickel/Photocatalytic Vinyl Cross-Electrophile Coupling to Prepare Chiral Allyl Carbamates (2020)<sup>a</sup>



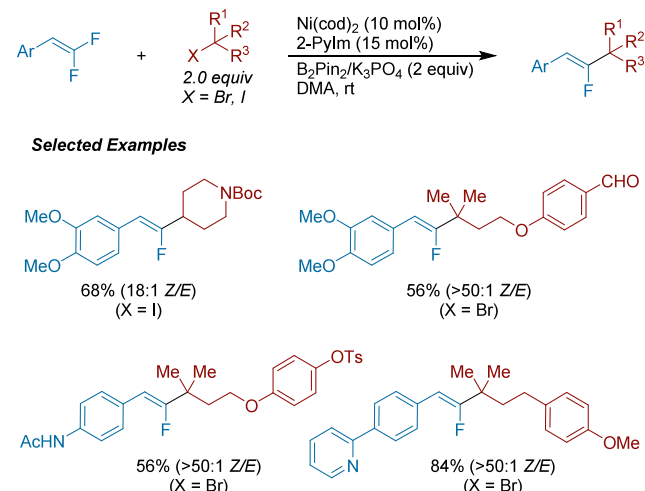
<sup>a</sup>(a) With Ni(TMHD)<sub>2</sub> (10 mol%) as catalyst. (b) Racemic vinyl bromide was used.

**Scheme 269.** Nickel/Photocatalytic Vinyl Cross-Electrophile Coupling to Prepare Chiral Allyl Amines (2021)



co-workers reported the cross-electrophile coupling of *gem*-difluoroalkenes with secondary and tertiary alkyl halides (Scheme 270).<sup>398</sup> This monofluorovinylation process proceeds with excellent (*Z*)-stereoselectivity. The authors demonstrated a broad substrate scope with sensitive functionality, such as heterocycles, aldehydes, and acidic protons. They also showed regioselectivity of tertiary alkyl bromides to be high in the presence of secondary and primary alkyl bromides. Mechanistic experiments ruled out the formation of borylated species and *in situ* and radical cyclization experiments showed alkyl

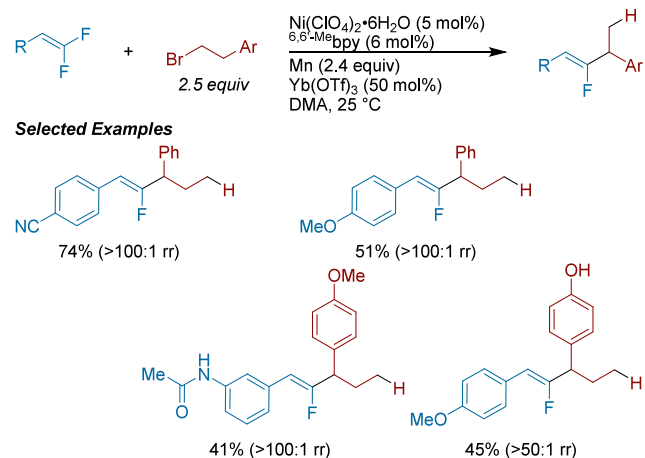
**Scheme 270.** Defluorinative Cross-Electrophile Coupling of *gem*-Difluoroalkenes with Unactivated Secondary and Tertiary Alkyl Halides (2017)



radicals are generated from the alkyl halide. While radical addition to difluoroalkenes does not always require nickel catalysis,<sup>399</sup> the authors propose nickel capture of the benzyl radical intermediate and  $\beta$ -fluoride elimination to afford the cross-coupled product. The authors showcased the utility of their method in the synthesis of substituted alkenylated prolines and the preparation of a LIM kinase inhibitor analogue.

Exploiting the propensity of unactivated alkyl bromides to undergo chain-walking type processes, Chao Feng and co-workers reported the migratory fluoroalkenylation of alkyl bromides containing a terminal aryl group (Scheme 271).<sup>400</sup>

**Scheme 271.** Ni-Catalyzed Migratory Fluoroalkenylation of Unactivated Alkyl Bromides with *gem*-Difluoroalkenes (2019)



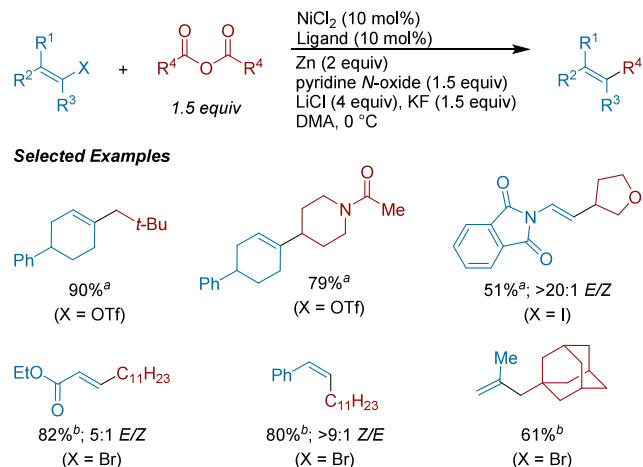
The authors propose oxidative addition of nickel to the alkyl bromide followed by chain-walking to form a benzylnickel species that then reacts with the difluoroalkene to form the coupled product. Alkyl chains of 2–5 carbons could be applied, albeit yields were lower for longer chains. Yb(OTf)<sub>3</sub> was found to be a necessary additive that offered improved yields to more conventional Lewis acidic additives. An experiment with stoichiometric nickel catalyst and ligand still

required the ytterbium salt for high yields, which may indicate the additive's role is activating the difluoroalkene for addition and C–C bond formation.

**4.3.3. XEC of Vinyl Triflates and Acetates with Alkyl Electrophiles.** While the majority of vinyl cross-electrophile couplings have used vinyl bromides (or other vinyl halides), these substrates can be relatively difficult to access in stereodefined way. This has driven interest in the use of vinyl triflates and acetates, which can be generated from ketones and leverage techniques for stereoselective enolate generation. Early studies focused on aryl halides had noted that vinyl triflates could react under related conditions,<sup>41</sup> but more recently more systematic reports have appeared.

Xuebin Liao and co-workers reported the decarboxylative XEC of alkyl carboxylic acid anhydrides with a variety of vinyl triflates and halides (Scheme 272).<sup>401</sup> In these reactions

**Scheme 272. Ni-Catalyzed Decarboxylative Alkenylation of Anhydrides with Vinyl Triflates and Halides (2019)<sup>a</sup>**



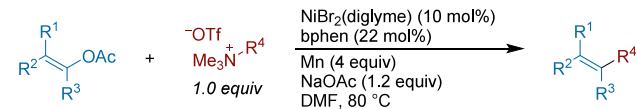
<sup>a</sup>(a) With phen as ligand. (b) With bpy as ligand.

pyridine *N*-oxide reacts with the anhydride to form an *O*-acylated species that can be reduced to form pyridine, CO<sub>2</sub>, and the alkyl radical. Notably, methylation and ethylation of vinyl triflates could be achieved. Olefin geometry was largely retained, especially in cases with vinyl iodides. Due to the reaction's high chemoselectivity for alkyl carboxylic acids, mixed anhydrides with *p*-anisic or *p*-toluic acid could also be used in this protocol. This enables the application of more valuable alkyl carboxylic acids as mixed anhydrides to avoid wasting 1.5 equiv of acid from the symmetrical anhydride.

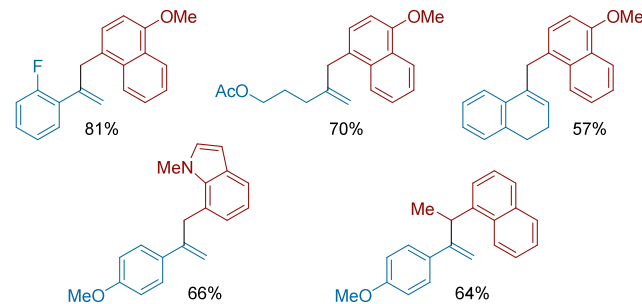
The group of Xing-Zhong Shu reported the XEC of vinyl acetates with benzyl trimethylammonium salts to form allylated arenes (Scheme 273).<sup>290,402</sup> Both styryl and  $\beta$ -alkyl-substituted vinyl acetates could be effectively coupled in this protocol, but fully substituted or unsubstituted vinyl acetates did not work as well. The authors also showed a few examples of aryl ammonium salts derived from anilines, as well as aryl triflates (see section 4.2.4.2, Scheme 173), in this cross-coupling. Studies showed that the benzyl ammonium coupling partners are a source of benzyl radical, rather than undergoing direct oxidative addition with nickel.

Continuing their work with C–O electrophiles, Xing-Zhong Shu and co-workers reported conditions for the XEC of vinyl triflates with alkyl mesylates (Scheme 274).<sup>403</sup> As has been observed before, iodide (from the precatalyst) turns on

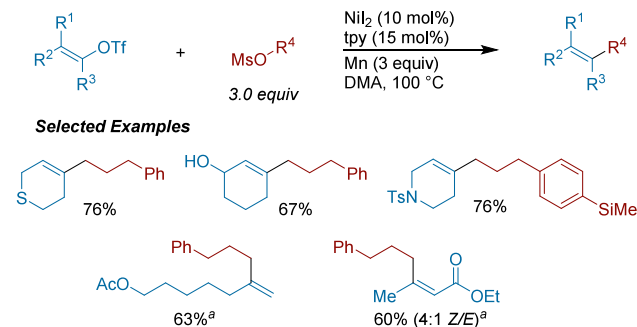
**Scheme 273. Ni-Catalyzed Cross-Electrophile Coupling between C–N and C–O Electrophiles (2019)**



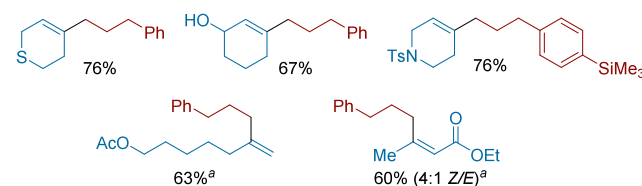
**Selected Examples**



**Scheme 274. Ni-Catalyzed Cross-Electrophile Coupling of Vinyl Triflates with Alkyl Sulfonates (2019)<sup>a</sup>**



**Selected Examples**



<sup>a</sup>With alkyl tosylate instead of alkyl mesylate.

reactivity by generating a constant, low concentration of alkyl iodide. Cyclic vinyl triflates reacted most effectively under these conditions, but acyclic vinyl triflates could also be employed by switching the alkyl coupling partner to the more reactive alkyl tosylate and adding 0.5 equiv of NaI. In these cases, isomerization of the olefin geometry occurred. In the same report they also demonstrated that peptide-based aryl triflates derived from tyrosine could be cross-coupled effectively with alkyl tosylates.

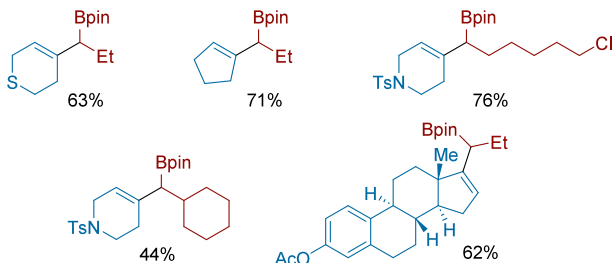
Xing-Zhong Shu and co-workers then reported an approach to prepare allylboronates through the XEC of vinyl triflates with  $\alpha$ -chloroboronates (Scheme 275).<sup>404</sup> This approach enabled straightforward access to cyclic allylboronates, which are versatile reagents. Acyclic vinyl triflates could also be applied by changing the ligand from bpy to Bphen.

More recently, Xing-Zhong Shu and co-workers reported conditions for the XEC of vinyl acetates with primary and secondary alkyl bromides (Scheme 276).<sup>405</sup> The vinyl acetate scope was notable: not only styryl acetates, but also those derived from cyclic ketones or 1,3-diones were effective (with small changes to the conditions). However, nonconjugated acyclic vinyl acetates reacted with lower yields and isomerization of olefin geometry. Functional-group compatibility included nitrile, ketone, aldehyde, and free phenol. Stoichiometric experiments with a nickel(0) complex afforded no consumption of the vinyl acetate, but the analogous nickel(I) complex was able to generate product without external

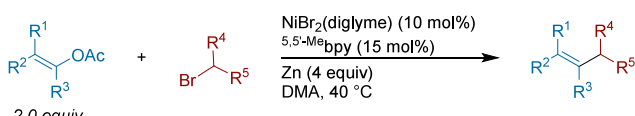
**Scheme 275.** Ni-Catalyzed Cross-Electrophile Coupling of Vinyl Triflates with  $\alpha$ -Chloroboronates (2020)



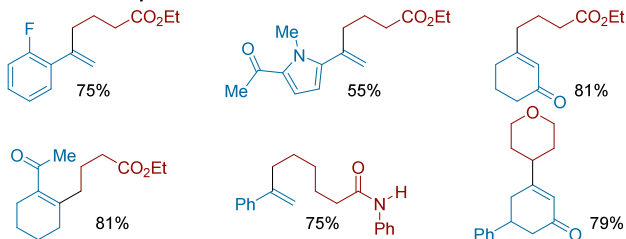
**Selected Examples**



**Scheme 276.** Ni-Catalyzed Cross-Electrophile Coupling of Alkenyl Acetates with Alkyl Bromides (2022)



**Selected Examples**

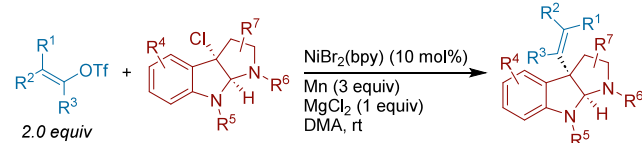


reductant. Additionally, radical cyclization experiments with 6-bromo-1-hexene indicated that radical formation and capture happen at two different nickel centers.

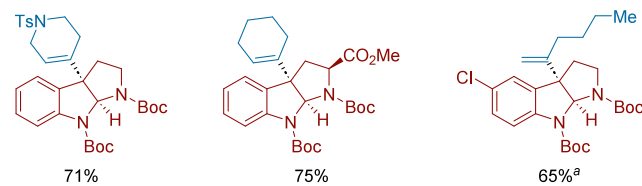
As an extension of their pioneering work (see section 4.2.1.1, Scheme 96)<sup>219</sup> on tertiary alkyl cross-coupling, Hegui Gong, Guobin Ma, and co-workers reported conditions to couple vinyl triflates with substituted chloro-hexahydropyrroloindolines (Scheme 277).<sup>406</sup> Complementary conditions for coupling cyclic and acyclic vinyl triflates were developed. In cases with olefin geometry, (*E*)-selectivity was observed in more hindered couplings, but mixtures of olefin isomers were observed with less hindered disubstituted vinyl triflates. Control experiments suggested that (*Z*)-vinyl triflates partially isomerize under reaction conditions to the less sterically hindered (*E*)-vinyl triflate, accounting for the overall (*E*)-selectivity for the cross-product.

Hegui Gong, Xiaotai Wang, and co-workers described a method to prepare  $\alpha$ -functionalized amino acids by XEC of  $\alpha$ -pivaloyloxyglycine with vinyl electrophiles (Scheme 278).<sup>407</sup> This process formed the (*E*)-olefin products, even when mixtures of vinyl bromide isomers were employed. Di-, tri-, and tetrasubstituted vinyl bromides could be applied in this reaction (Method A), and vinyl triflates could also be coupled with modified conditions (Method B). Furthermore, several examples with aryl halides were also demonstrated, affording the analogous  $\alpha$ -arylated amino acids. Based upon a series of mechanistic and computational experiments, the authors

**Scheme 277.** Ni-Catalyzed XEC of Chloro-Hexahydropyrroloindoline Derivatives with Vinyl Triflates (2021)<sup>a</sup>



**Selected Examples**

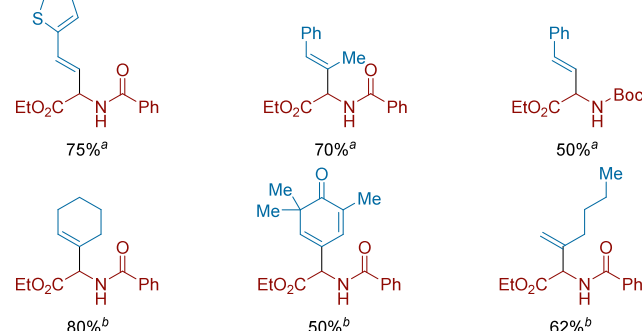


<sup>a</sup>Modified Conditions: With vinyl triflate (2.5 equiv), NiBr<sub>2</sub>(bpy) (12 mol%), Zn (3 equiv), MgCl<sub>2</sub> (60 mol%), and DMA at 30 °C.

**Scheme 278.** Ni-Catalyzed Cross-Electrophile Coupling of C(sp<sup>2</sup>) Triflates/Halides with  $\alpha$ -Pivaloyloxy Glycine (2021)<sup>a</sup>



**Selected Examples**



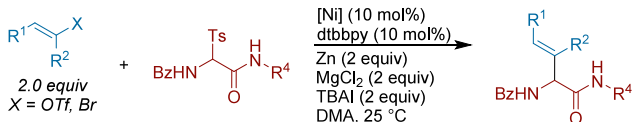
<sup>a</sup>(a) With X = Br, [Ni] = NiBr<sub>2</sub>, and MgCl<sub>2</sub> (1.5 equiv). (b) With X = OTf, [Ni] = NiCl<sub>2</sub>(Py)<sub>4</sub>, and MgCl<sub>2</sub> (2.0 equiv).

proposed glycine radical formation and that (L)Ni<sup>II</sup>(Ar)X was off-cycle. Computational studies suggested that a “radical first” pathway was viable with subsequent vinyl halide oxidative addition and reductive elimination.

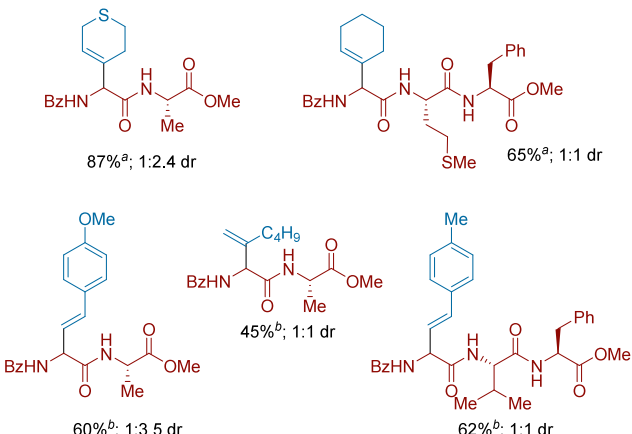
Deli Sun, Qun Qian, Yunrong Chen, and co-workers adapted the glycine radical strategy to the diversification of short peptides through the cross-electrophile coupling of vinyl halides/triflates with  $\alpha$ -tosylglycine-containing di- and tripeptides (Scheme 279).<sup>408</sup> The coupling proceeds with modest diastereoselectivity (ranging from 1:1 to 3.5:1 dr) but does not epimerize any of the stereocenters on the other amino acids within the peptide. A few examples with aryl iodides were also demonstrated.

Weichao Xue, Ken Yao, and Xianghua Tao reported an approach to synthesize  $\beta,\gamma$ -unsaturated ketones through XEC of vinyl triflates with oxalates derived from  $\alpha$ -hydroxy esters (Scheme 280).<sup>409</sup> Cyclic vinyl triflates coupled best but some acyclic vinyl triflates also could be utilized. In addition to  $\alpha$ -hydroxy esters,  $\alpha$ -hydroxy lactones and  $\alpha$ -hydroxy ketones

**Scheme 279.** Ni-Catalyzed Cross-Electrophile Coupling of  $\alpha$ -C-Tosyl Peptides with C( $sp^2$ ) Triflates/Halides (2021)<sup>a</sup>



*Selected Examples*

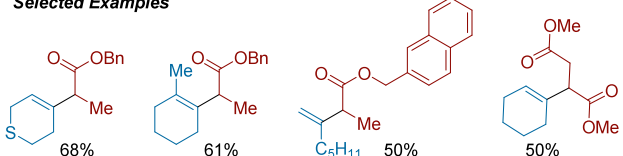


<sup>a</sup>(a) With X = OTf and [Ni] = NiCl<sub>2</sub>(Py)<sub>4</sub>. (b) With X = Br and [Ni] = NiBr<sub>2</sub>.

**Scheme 280.** Ni-Catalyzed Cross-Electrophile Coupling of  $\alpha$ -Hydroxy Carbonyl-Derived Oxalates with Vinyl Triflates (2021)



*Selected Examples*

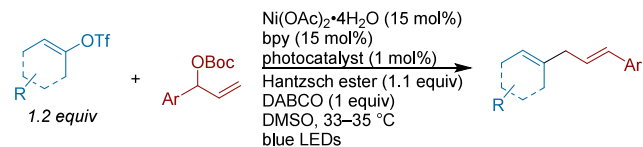


could be coupled in good yields, but low yields were observed with tertiary alkyl oxalates. The authors disclosed a preliminary result for an enantioconvergent coupling with low levels of enantiocontrol (15% ee) and showed that the reaction likely proceeds through a radical-based mechanism through radical trapping experiments.

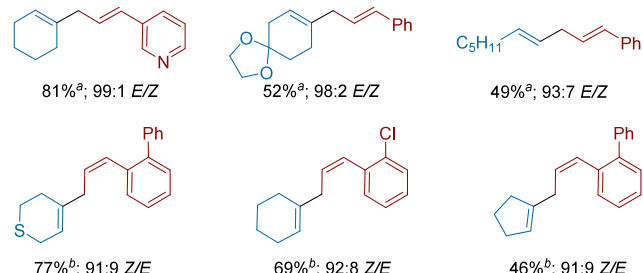
Lingling Chu and co-workers demonstrated a metal-lphotoredox approach to prepare stereodefined 1,4-dienes through XEC of vinyl triflates with allylic carbonates (Scheme 281).<sup>410</sup> The triplet energy of the photocatalyst alters the stereochemistry of the final product. The lower energy Ru(bpy)<sub>3</sub>(PF<sub>6</sub>)<sub>2</sub> catalyst affords the (*E*)-product because the product is not isomerized. The higher triplet energy of Ir(ppy)<sub>2</sub>(dtbbpy)PF<sub>6</sub> ( $E_T$  = 51.0 kcal/mol) affords the (*Z*)-product by preferential isomerization of the (*E*)-isomer.<sup>411</sup> This reaction yields the linear product regardless of whether the linear or branched allylic carbonate was employed.

**4.3.4. Stereocontrolled XEC of Vinyl-X with Alkyl-X.** The Reisman group has pioneered a series of enantioselective

**Scheme 281.** Nickel/Photoredox Stereodivergent Cross-Electrophile Coupling of Vinyl Triflates with Allylic Carbonates (2020)<sup>a</sup>



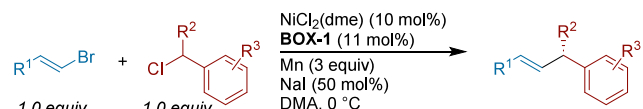
*Selected Examples*



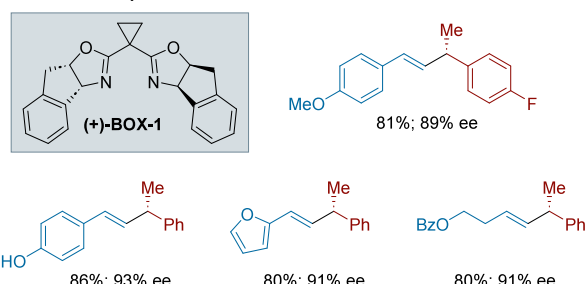
<sup>a</sup>(a) With Ru(bpy)<sub>3</sub>(PF<sub>6</sub>)<sub>2</sub> as photocatalyst. (b) With Ir(ppy)<sub>2</sub>(dtbbpy)PF<sub>6</sub> as photocatalyst.

cross-electrophile couplings of vinyl and alkyl electrophiles. In 2014, they reported an enantioconvergent cross-electrophile coupling of vinyl bromides with racemic secondary benzyl chlorides (Scheme 282).<sup>412</sup> The best results were obtained

**Scheme 282.** Ni-Catalyzed Enantioselective Cross-Electrophile Coupling of Vinyl Bromides with Benzyl Chlorides (2014)



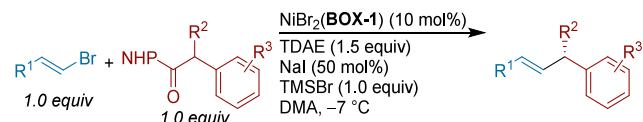
*Selected Examples*



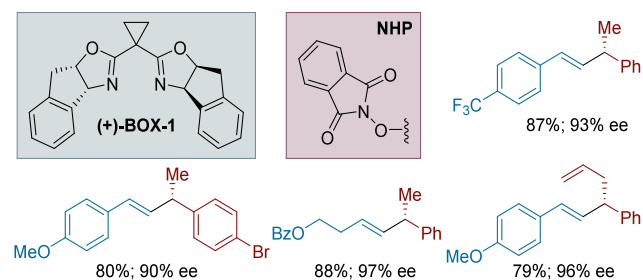
with an indanyl-substituted bisoxazoline ligand **BOX-1**, which improved both selectivity for cross-product and enantioselectivity in comparison to other substituted bisoxazoline ligands. A variety of disubstituted alkenes with  $\alpha$ -stereocenters could be accessed in 88–97% ee. (*E*)-vinyl bromides reacted without olefin isomerization, while (*Z*)-vinyl bromides reacted sluggishly and were susceptible to isomerization. Follow-up mechanistic work demonstrated that nickel(I)-**BOX-1** intermediate reacts with both vinyl bromide (oxidative addition) and the benzyl chloride (halogen atom transfer). Computational studies suggested that the enantiodetermining step is dictated by the facial selectivity of the radical addition, and subsequent reductive elimination is rapid.<sup>42</sup>

Continuing their work on enantioselective cross-electrophile vinylylation, Reisman and co-workers reported an alternative approach to the above products by the coupling of vinyl bromides with racemic  $\alpha$ -aryl NHP esters (**Scheme 283**).<sup>413</sup>

**Scheme 283.** Ni-Catalyzed Enantioselective Cross-Electrophile Coupling of Vinyl Bromides with *N*-Hydroxyphthalimide Esters (2017)



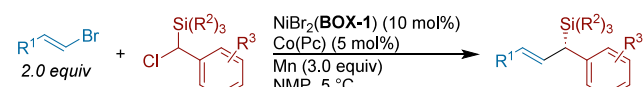
*Selected Examples*



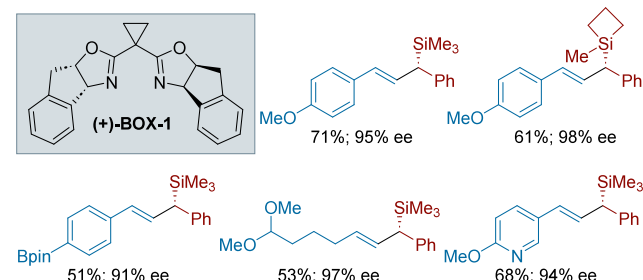
The combination of TDAE and TMS–Br was important for achieving high yields, and indanyl-substituted **BOX-1** was again the ligand of choice. The authors demonstrated a broad substrate scope and showcased how NHP esters can be applicable in this cross-coupling protocol in cases where the benzyl chloride is unstable (e.g., in alkyl coupling partners containing an  $\alpha$ -methoxy substituent). Subsequent detailed mechanistic studies from the Reisman group elucidated the role of TMS–Br as a Lewis acid and showed how radical formation is independent of nickel.<sup>42</sup> This second study has a wealth of useful mechanistic information.

In 2018, Reisman and co-workers applied their enantioselective cross-electrophile coupling strategy to couple vinyl bromides and chlorobenzyl silanes (**Scheme 284**).<sup>224</sup> The cobalt phthalocyanine [Co(Pc)] additive was important for high yields, possibly due to increasing the rate of radical generation at the benzyl chloride (as was observed for related racemic coupling reactions with aryl halides, see **section**

**Scheme 284.** Ni-Catalyzed Cross-Electrophile Coupling of Vinyl Bromides with Chlorobenzyl Silanes (2018)



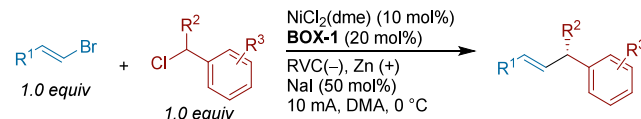
*Selected Examples*



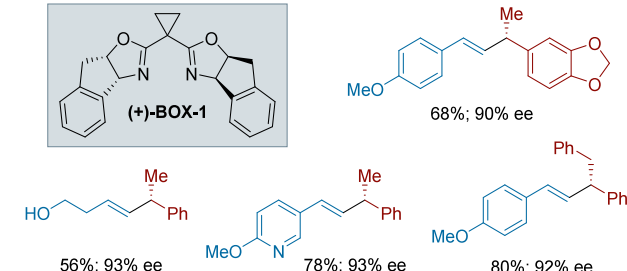
4.2.5.1, **Scheme 176**).<sup>174</sup> As with their previous work, indanyl-substituted **BOX-1** was the best-performing ligand for controlling enantioselectivity. A broad array of disubstituted (*E*)-alkenes reacted in good yields with retention of olefin geometry, but the authors noted (*Z*)-alkenes, as well as tri- and tetrasubstituted alkenes were unreactive in this protocol. The chiral allylic silanes formed were applied to Hosomi-Sakurai reactions, heterocycle synthesis, and the preparation of the natural product (+)-tashiromine with excellent retention of stereochemistry from the silane.

The Reisman Group then reported the first example of an electrochemically driven enantioselective cross-electrophile coupling reaction. This protocol enabled the coupling of vinyl bromides with secondary benzyl chlorides in an undivided cell with a zinc sacrificial anode (**Scheme 285**).<sup>414</sup>

**Scheme 285.** Enantioselective Electrochemical Cross-Electrophile Coupling of Vinyl Bromides with Benzyl Chlorides via Nickel Catalysis (2019)



*Selected Examples*

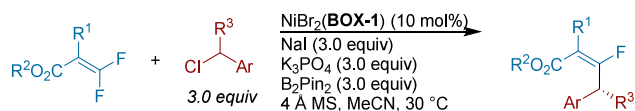


Careful selection of cathode, anode, current density, and electrolyte were critical for high yields and enantioselectivity. A broad range of electronics on both coupling partners were tolerated, and ligand control of diastereoselectivity was observed when a (−)-citronellal-derived vinyl bromide was employed.

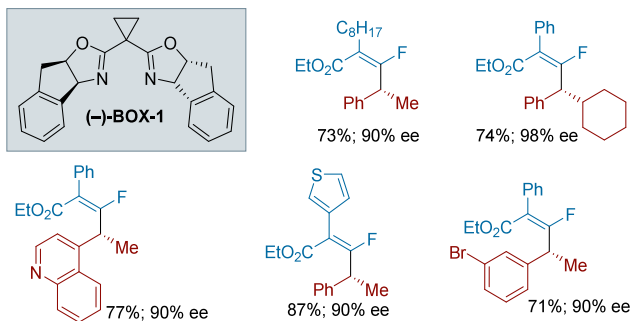
Zhuanzhi Shi and co-workers reported an enantioselective cross-electrophile coupling of *gem*-difluoroalkenes with secondary benzyl chlorides (**Scheme 286**).<sup>415</sup> The ester group on the difluoroalkene is proposed to act as a directing group to facilitate oxidative addition into the adjacent C–F bond, rendering the process highly stereoselective in terms of olefin geometry. The authors noted removal of sodium iodide, potassium phosphate, or molecular sieves led to no reactivity. Control experiments supported intermediacy of a benzyl radical and ruled out *in situ* formation of borylated intermediates. While radical additions to difluoroalkenes are known,<sup>399</sup> the high enantioselectivities provide strong evidence for a nickel-mediated mechanism.

All of the previous examples proceeded by secondary benzylic radical intermediates. Fan Wu, Deli Sun, and co-workers expanded enantioconvergent XEC to the coupling of racemic  $\alpha$ -chlorosulfones with styryl bromides (**Scheme 287**).<sup>416</sup> Indanyl-substituted **BOX-2** was employed as the chiral ligand in this transformation. Control experiments supported that cross-coupling proceeds through radical formation at the  $\alpha$ -chlorosulfone.

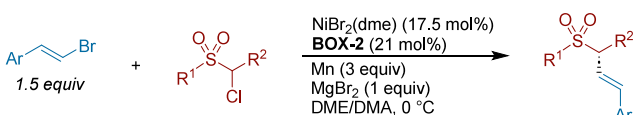
**Scheme 286.** Ni-Catalyzed Stereo- and Enantioselective Cross-Electrophile Coupling of *gem*-Difluoroalkenes with Benzyl Chlorides (2022)



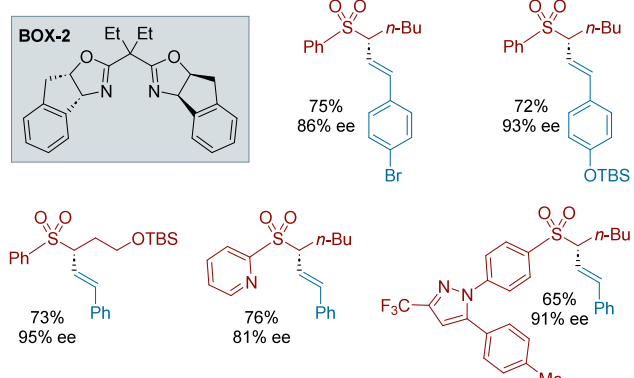
**Selected Examples**



**Scheme 287.** Ni-Catalyzed Enantioselective Cross-Electrophile Coupling of Vinyl Bromides with  $\alpha$ -Chlorosulfones (2022)



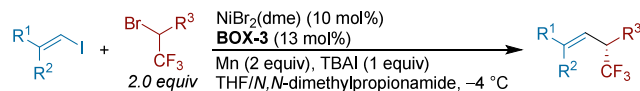
**Selected Examples**



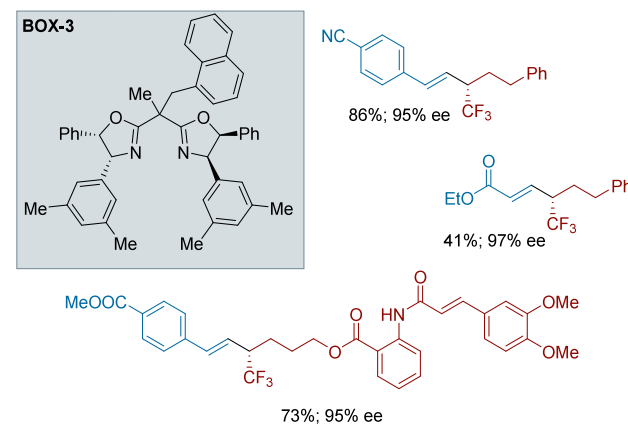
Xi-Sheng Wang and co-workers further expanded the substrate pool to racemic 2-bromo-1,1,1-trifluoroalkanes for enantioconvergent XEC with vinyl electrophiles (Scheme 288).<sup>417</sup> Systematic variation of the BOX ligand *gem*-substituents and increasing the steric profile of the oxazoline substituents led to the development of BOX-3. A variety of styryl,  $\beta$ -alkyl-substituted, and  $\alpha,\beta$ -unsaturated carbonyls work well in this protocol. As with similar reports, (*E*)-vinyl iodides reacted effectively and with retention of olefin geometry, while the more hindered (*Z*)-vinyl iodides afforded trace yields.

Zhan Lu, Qun Fang, and co-workers adapted the Reisman conditions for enantioconvergent cross-electrophile coupling of racemic benzylic chlorides with vinyl bromides to work with a photochemical system (an iridium catalyst and Hantzsch ester as terminal reductant) (Scheme 289).<sup>418</sup> The authors required a different ligand (*s*-BuBilm). This method worked well for both aryl bromides and for vinyl bromides. Highlighting a potential challenge with using photochemistry,

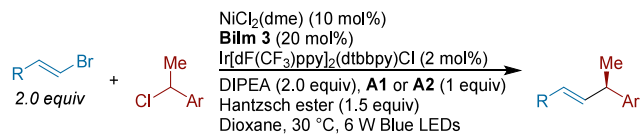
**Scheme 288.** Ni-Catalyzed Enantioselective Cross-Electrophile Coupling of Vinyl Iodides with  $\alpha$ -Trifluoromethyl Alkyl Bromides (2022)



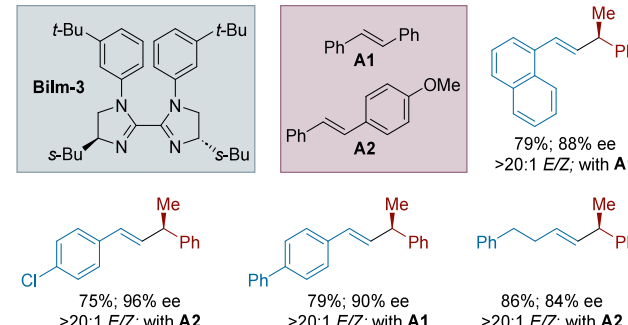
**Selected Examples**



**Scheme 289.** Nickel/Photoredox Enantioselective Cross-Electrophile Coupling of Vinyl/Aryl Bromides with Benzyl Chlorides (2022)



**Selected Examples**

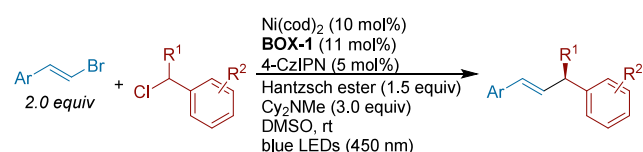


stilbene derivatives A1 or A2 were needed as triplet-energy-transfer inhibitors to preserve stereoselectivity in the vinyl halide coupling. The authors also demonstrated that the reaction could work with vinyl chlorides in more moderate yields but with high selectivity.

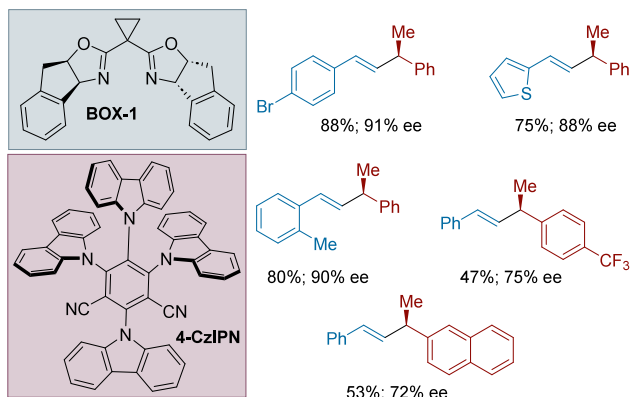
Concurrently, Jianyou Mao and co-workers found a way to drive enantioconvergent cross-electrophile coupling of benzylic chlorides with vinyl bromides by photoredox cocatalysis (Scheme 290).<sup>419</sup> This approach tolerated a variety of substitutions on both aryl rings and retention of (*E*)-selectivity for the cross-coupling was observed. As with analogous reports, (*Z*)-vinyl bromides did not react in this reaction. The reaction forms equivalent amounts of HX and a trialkylamine base ( $C_2NMe$ ) was added to sequester the acid.

The Nevado group reported an enantioselective Ni-catalyzed cross-electrophile coupling of vinyl bromides with

**Scheme 290.** Nickel/Photoredox-Catalyzed Enantioselective Cross-Electrophile Coupling of Vinyl Bromides with Benzyl Chlorides (2022)

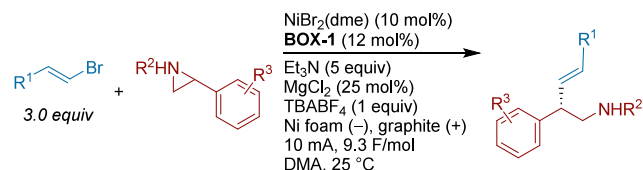


**Selected Examples**

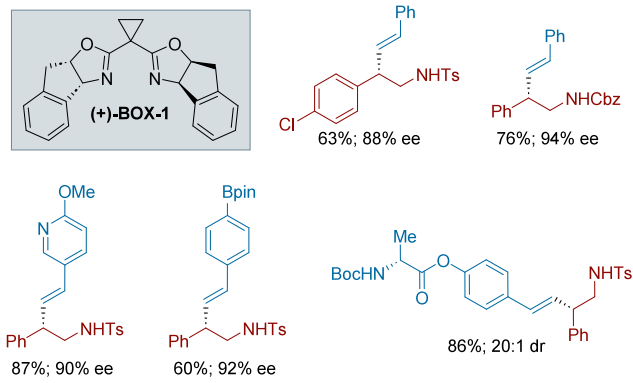


aryl aziridines (Scheme 291).<sup>420</sup> This process is driven electrochemically in an undivided cell with a graphite anode,

**Scheme 291.** Ni-Catalyzed Enantioselective Electrochemical Cross-Electrophile Coupling of Vinyl Bromides with Aryl Aziridines (2023)



**Selected Examples**

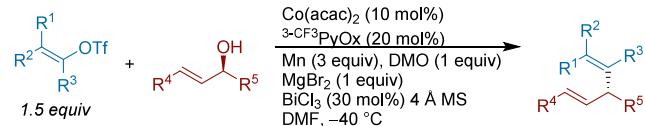


Ni foam cathode, and triethylamine as the terminal reductant. As with other enantioconvergent couplings of benzylic radicals with vinyl bromides, **BOX-1** afforded high enantioselectivities in this coupling. Furthermore, the reaction proceeded with high (*E*)-stereoselectivity, regardless of the *E/Z* ratio of the starting vinyl bromides. The substrate scope was broad with respect to aryl aziridine electronics and styryl bromide functionality. Alkyl-substituted vinyl bromides also coupled well with increased catalyst and ligand loading. Control experiments support activation of the aryl aziridine proceeding

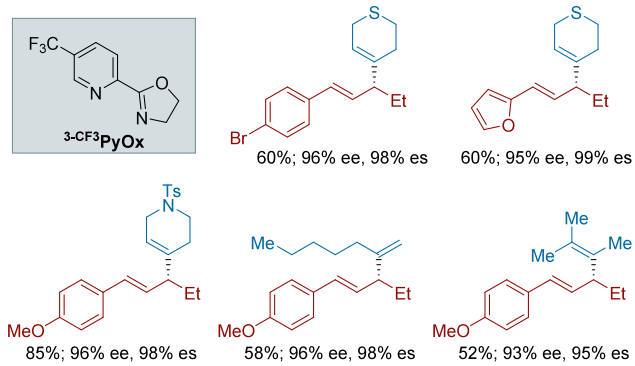
through a benzylic radical. CV and other mechanistic experiments further supported a mechanism where nucleophilic halide ring opening of the aziridine generates a  $\beta$ -halosulfonamide in situ, which is then reduced to the benzylic radical through a variety of pathways.

Xing-Zhong Shu and co-workers reported an enantiospecific cobalt-catalyzed cross-electrophile coupling of vinyl triflates with chiral allylic alcohols (Scheme 292).<sup>421</sup> The alcohols are

**Scheme 292.** Cobalt-Catalyzed Enantiospecific Dynamic Kinetic Cross-Electrophile Coupling of Vinyl Triflates with Allylic Alcohols (2021)<sup>a</sup>



**Selected Examples<sup>a,b</sup>**



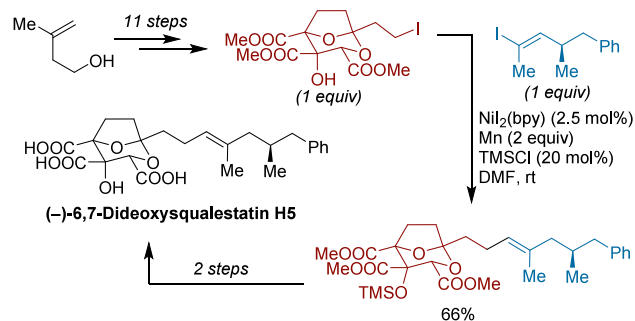
<sup>a</sup>(a) DMO = dimethyl oxalate. (b) %es = %ee(product)/%ee(starting material).

activated in situ by dimethyl oxalate (DMO), which is proposed to undergo a two-electron oxidative addition with cobalt. This enabled the reaction to proceed with high levels of enantiospecificity and obviated the need for a chiral ligand. The authors noted how the transformation failed to give product under Ni-catalyzed conditions. The  $MgBr_2$ ,  $BiCl_3$ , and molecular sieves were all critical for complete consumption of the starting materials. Di-, tri- and tetrasubstituted vinyl triflates were all productive coupling partners. Competition experiments revealed that cobalt reacts much more rapidly with the allylic oxalate than the vinyl triflate. Based on additional control experiments, the authors propose a mechanism in which cobalt(0) undergoes an anti- $S_N2'$  oxidative addition to the oxalate to generate a  $\pi$ -allylcobalt(II) complex and inverts the stereocenter. Manganese reduction to allylcobalt(I) followed by oxidative addition to the vinyl triflate affords a cobalt(III) complex. Reductive elimination then yields the cross-coupled chiral product. It is notable that this is the opposite sequence of events compared to the majority of reactions in this section.

**4.3.5. Synthetic Applications of C(sp<sup>2</sup>)–C(sp<sup>3</sup>) Vinyl–Alkyl XEC.** Hodgson and co-workers reported an asymmetric total synthesis of (−)-6,7-dideoxysqualenolide H5 that showcased a stereoretentive cross-electrophile coupling of a vinyl iodide with the tricarboxylate core of the natural product (Scheme 293).<sup>422</sup> The stereochemical configuration was achieved through a highly diastereoselective *N*-alkylation of (*R,R*)-tartrate acetonide. Presumably due to the thermal

**Scheme 293. Total Synthesis of (*-*)-6,7-Dideoxysqualenostatin H5 (2017)**

*Total Synthesis of (*-*)-6,7-Dideoxysqualenostatin H5*

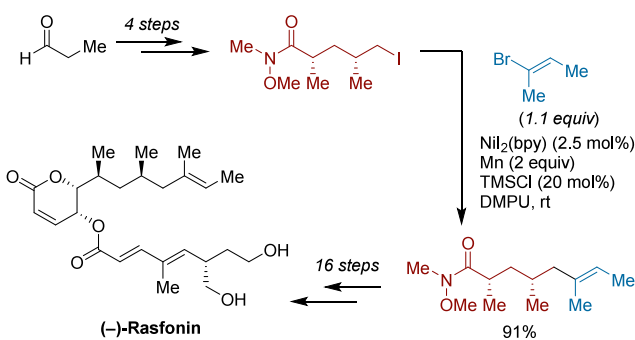


instability of the vinyl halide coupling partner, conventional cross-coupling processes failed to deliver the desired product. Cross-electrophile coupling was key for assembling the final natural product.

An improved strategy to (*-*)-rasfonin from their initial report<sup>423</sup> was described by Boeckman and co-workers in 2018 (Scheme 294).<sup>424</sup> The focus of this work was to improve

**Scheme 294. Total Synthesis of (*-*)-Rasfonin (2018)**

*Total Synthesis of (*-*)-Rasfonin*



scalability of several key steps and enable access to more material for biological testing. Notably, this synthesis features a high yielding cross-electrophile coupling early in the route between a vinyl bromide and an alkyl iodide. This offered a key fragment of the natural product in gram quantities following reduction and functionalization of the Weinreb amide.

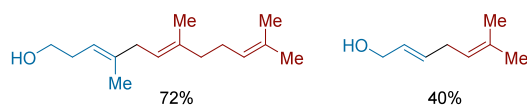
Jamison and co-workers reported a strategy for the cross-coupling of vinyl bromides with allyl trifluoroacetates toward the synthesis of skipped polyene fragments for natural product synthesis (Scheme 295).<sup>425</sup> This protocol is highly (*E*)-selective, but alkene isomerization could be limited by employing coupling partners that rapidly react. Importantly, this method tolerates free alcohols, which provides a functional handle for polyene cyclization to prepare natural product cores. The authors showcased a route to prepare a pentaene that utilized two vinyl cross-electrophile couplings in the sequence. Poly epoxidation of the pentaene followed by a ring-opening cascade cyclization afforded the “RST” fragment of maitotoxin.

In their total synthesis of the meroditerpenoid (*-*)-isoscopariisin, Pema-Tenzin Puno, Ang Li, and co-workers showcased a vinyl cross-electrophile coupling of an advanced alkyl bromide intermediate with a bromoallylic alcohol (Scheme 296).<sup>426</sup> The tricyclic core was prepared from

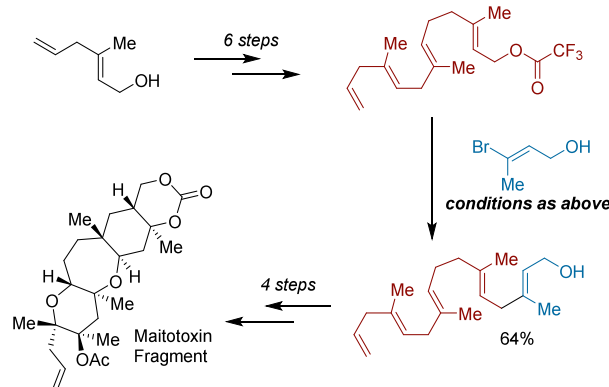
**Scheme 295. Ni-Catalyzed Cross-Electrophile Coupling for the Synthesis of Skipped Polyenes (2019)**



*Selected Examples*

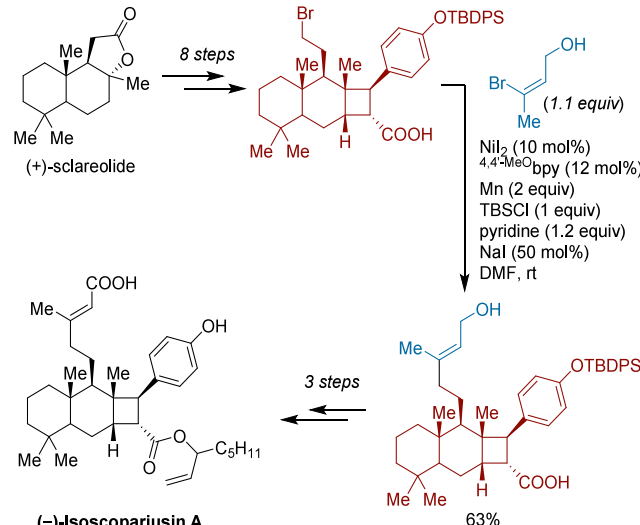


*Total Synthesis*



**Scheme 296. Total Synthesis of (*-*)-Isoscopariisin A (2021)**

*Total Synthesis of (*-*)-Isoscopariisin A*

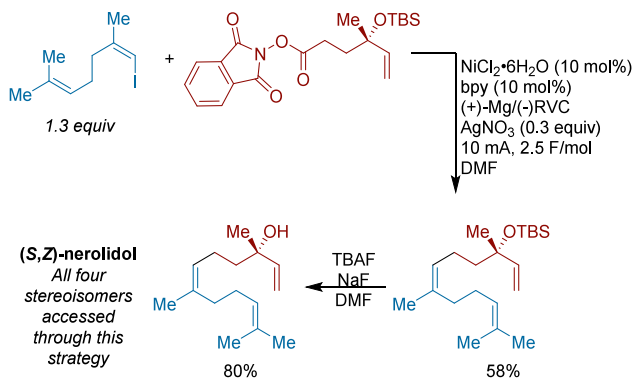


(+)-scclareolide, with a key intermolecular [2 + 2] cycloaddition. The cross-electrophile coupling was notable as it proceeded in good yield on gram scale in the presence of acidic functionality. The synthesis was completed by esterification of the acid, followed by oxidative and protecting group manipulations, which afforded (*-*)-isoscopariisin in gram quantities as the enantiopure natural product.

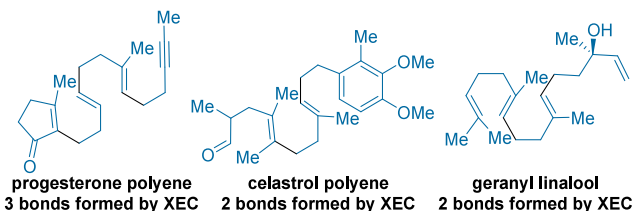
In their work on electrochemical cross-electrophile coupling, Baran and co-workers (see section 4.3.2, Scheme 260) showcased the utility and functional group tolerance of their method through the synthesis of 13 terpene-based natural products (Scheme 297).<sup>388</sup> Selected examples include efficient,

**Scheme 297. Applications of Electrochemical Cross-Electrophile Couplings of Vinyl Iodides with *N*-Hydroxyphthalimide Esters (2022)**

Divergent Synthesis of the Nerolidol Natural Products



Other Selected Natural Product Syntheses From This Work

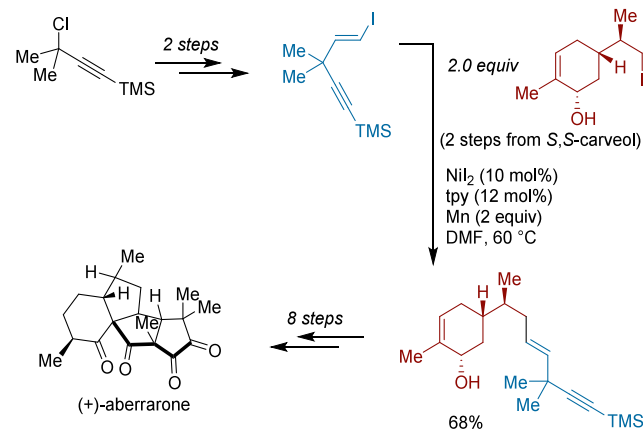


fragment-based couplings to prepare polyene precursors of progesterone and celastrol, as well as geranyl linalool. Many of these couplings were run on gram scale and even at 100-g scale in flow. Furthermore, they demonstrated the total synthesis of all four isomers of the olfactory terpene nerolidol in high stereochemical purity. (*S, Z*)-nerolidol, and the other three isomers were accessed by varying the olefin geometry of the vinyl iodide fragment and the stereochemistry of the alkyl NHP ester fragment.

In their synthesis of the diterpene (+)-aberrarone, Yanxing Jia and co-workers demonstrated a Ni-catalyzed cross-electrophile coupling between a vinyl iodide and an alkyl iodide to join two key fragments (Scheme 298).<sup>427</sup> After optimization of the process, they found tpy as ligand to give the best results.

**Scheme 298. Total Synthesis of (+)-Aberrarone (2023)**

Total Synthesis of (+)-Aberrarone



The reaction tolerates a free alcohol and a TMS-protected alkyne, which were both handles for further functionalization steps. The tetracyclic ring system was constructed through a Mn(OAc)<sub>3</sub> mediated *S*-*exo*/*S*-*exo*/*S*-*exo* radical cascade cyclization, furnishing the core as a single diastereomer. Following a series of redox manipulations, the synthesis of (+)-aberrarone was completed.

#### 4.4. Ketones

**4.4.1. Overview.** Ketones are ubiquitous in natural products, bioactive molecules, and synthetic intermediates. Most synthetic procedures to assemble ketones rely on a preformed organometallic reagent, either via coupling to an activated ester (or acyl chloride),<sup>428</sup> or addition to an aldehyde, followed by oxidation of the resulting secondary alcohol.<sup>429</sup> The use of an organometallic reagent, however, limits reaction functional group tolerance and commercial availability of coupling partners. Replacing organometallic reagents with more commercially available electrophiles expands the scope of this transformation considerably.

The development of cross-electrophile approaches to ketones has been the subject of recent development, with 85% of reports in this section published in the past 10 years. This area has been previously reviewed in 2019.<sup>430</sup> This section will cover the coupling of alkyl electrophiles with acyl electrophiles. **section 3.5** covers ketone synthesis by coupling acyl electrophiles with aryl and vinyl electrophiles.

Ligands used in this section parallel common ligands used in analogous Aryl–Alkyl bond formations (Figure 30), with 96%

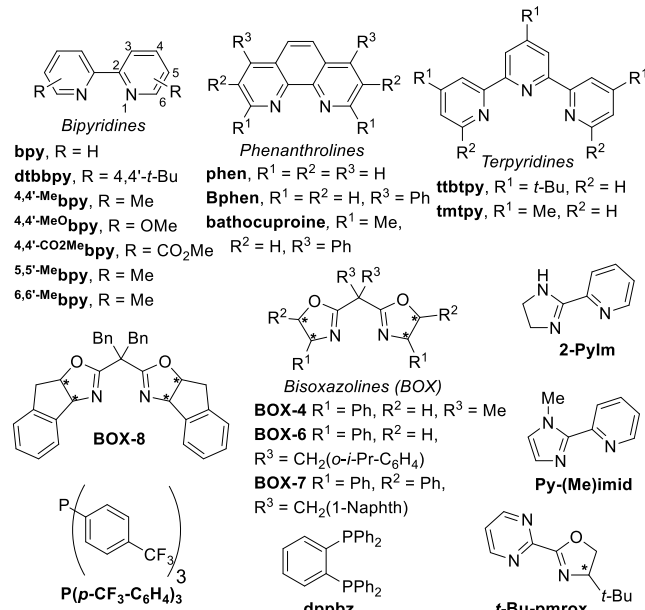
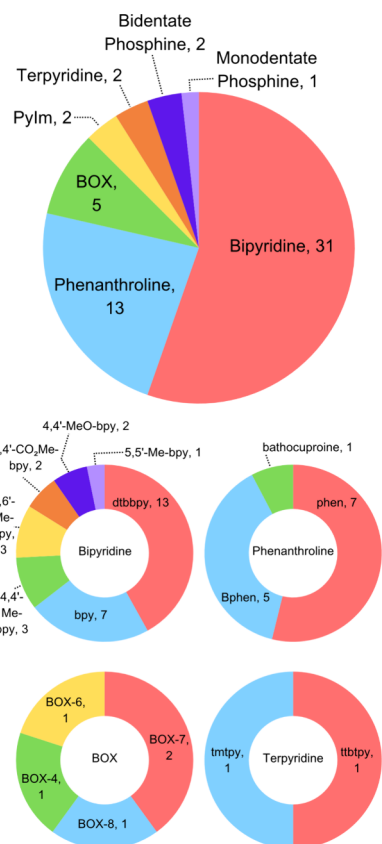


Figure 30. Ligands used in acyl–alkyl XEC reactions. \*Denotes chiral center.

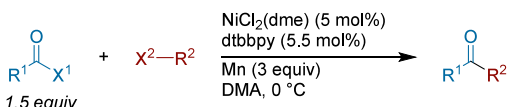
of all ligands being nitrogen heterocycles (Figure 31). The phosphine ligands used in this section are either 1) bound to a metal that is not nickel or 2) used in concert with a nitrogen ligand, further highlighting the indispensable nature of nitrogen heterocycle ligands in Ni-catalyzed XEC.

**4.4.2. Acid Halides as Electrophiles.** **4.4.2.1. XEC with Alkyl Halides.** In 2012, our group reported the coupling of alkyl acid chlorides or 2-pyridyl thioesters with alkyl iodides or benzyl chlorides (Scheme 299).<sup>431</sup> We proposed a

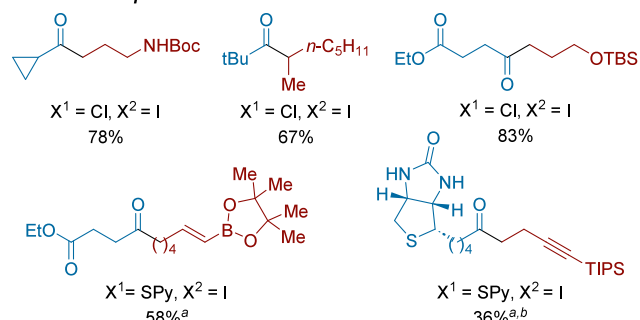


**Figure 31.** Distribution of ligands used in acyl–alkyl XEC reactions.

**Scheme 299. XEC of Alkyl Carboxylic Acid Derivatives with Alkyl Iodides or Benzyl Chlorides (2012)<sup>a</sup>**



**Selected Examples**

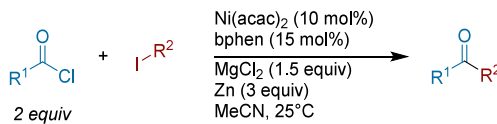


<sup>a</sup>(a) With Zn (3 equiv) instead of Mn. (b) Average of two runs.

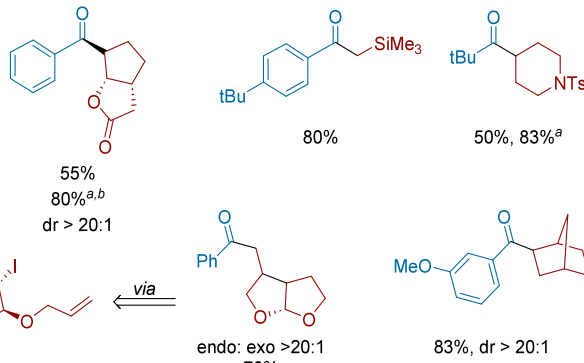
dialkylnickel(II) intermediate, formed from disproportionation of an alkynickel(II) halide complex, which then interacts with the carboxylic acid derivative to furnish the desired ketone product. Subsequent mechanistic studies suggest an alkynickel(II) intermediate coupling to an alkyl radical is more likely. In a subsequent report, these conditions were scaled up to a 98 mmol scale synthesis of ethyl 4-oxododecanoate in a 500 mL jacket reactor with minimal change in yield.<sup>432</sup>

Shortly after, Hegui Gong and Qinghua Ren reported the XEC of alkyl halides with acid chlorides (Scheme 300).<sup>433</sup> The

**Scheme 300. Ni-Catalyzed XEC of Alkyl Halides with Acid Chlorides (2012)<sup>a</sup>**



**Selected Examples**

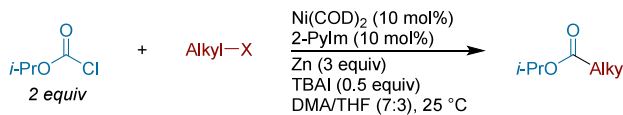


<sup>a</sup>(a) With  $\text{Ni}(\text{COD})_2$  (10 mol%). (b) With dtbbpy (10 mol%).

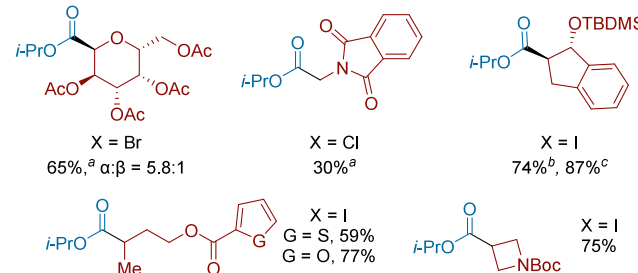
method was compatible with primary and secondary alkyl halides. On the acyl coupling partner, aryl chlorides were the most successful, but one example of a benzylic acyl chloride and pivalyl chloride coupling were shown. The authors illustrated the synthetic utility of this method by completing a 30-fold scale up of these reaction conditions with improved yields.<sup>434</sup> The presence of radical intermediates was strongly suggested by rearrangement of an allylic ether substrate. The authors conducted a competition experiment that suggested alkylzinc intermediates were not competent in the primary product-forming pathway.

In 2016, Hegui Gong and co-workers reported the coupling of alkyl halides with isopropyl chloroformate to form alkyl esters under XEC conditions (Scheme 301).<sup>435</sup> Notably, this reaction displayed a broad scope, including primary and secondary alkyl iodides, and useful levels of diastereoselectivity with cyclic alkyl halides. Functional group tolerance included

**Scheme 301. XEC of Alkyl Halides with Isopropyl Chloroformates (2016)<sup>a</sup>**



**Selected Examples**

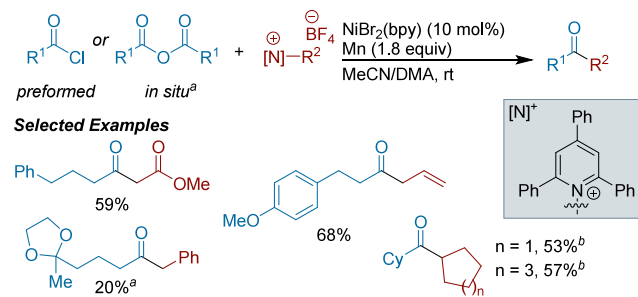


<sup>a</sup>(a) With bpy as ligand, (b) With  $i\text{-PrO}_2\text{CCl}$  (3 equiv), (c) With  $i\text{-PrO}_2\text{CCl}$  (4 equiv).

protected alcohols and amines. This method has been further extended to the three component carbonylative couplings as shown in section 4.4.6.1.

**4.4.2.2. XEC with *N*-Alkylpyridinium Salts.** The Rasappan lab reported the coupling of alkyl carboxylic acids (either via isolated acid chlorides or in situ generated acid anhydrides) with amine-derived *N*-alkylpyridinium salts to form primarily dialkyl ketones (Scheme 302).<sup>436</sup> Employing starting materials

**Scheme 302. Acylation of Pyridinium Salts by Activated Carboxylic Acids (2020)<sup>a</sup>**



<sup>a</sup>(a) In situ activation conditions = acid (1 equiv), Boc<sub>2</sub>O (1.2 equiv), MgCl<sub>2</sub> (0.33 equiv) in MeCN, followed by coupling. (b) Reduced to the corresponding alcohol with NaBH<sub>4</sub> (3 equiv).

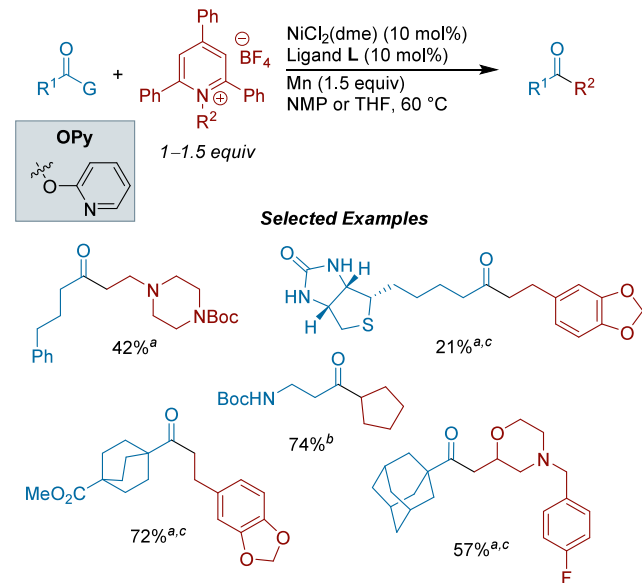
typically utilized to synthesize amide bonds offered an attractive expansion of potential coupling partners for ketone formation. Among the many tolerated functional groups were -Boc, -MOM, and other acetals. For cases where the acid chloride was difficult to purify, an in situ protocol using oxalyl chloride or thionyl chloride was demonstrated, although lower yields were observed for the coupled product.

In collaboration with the Watson group, we reported a cross-coupling strategy that utilized either preformed or in situ generated derivatives of amines (via *N*-alkylpyridinium salts) and carboxylic acids (activated as alkyl acid fluorides or 2-pyridyl esters) to form dialkyl ketones (Scheme 303).<sup>437</sup> In situ generation of the activated carboxylic acid was explored, and both acid fluorides and 2-pyridyl esters were stable enough for purification. Primary, secondary, and tertiary acid derivatives were tolerated with slight modifications to the reaction conditions, and primary and secondary *N*-alkylpyridinium salts are well tolerated. Drug fragments were successfully coupled, including amlodipine, cetirizine, and an atorvastatin intermediate.

**4.4.2.3. Other Coupling Partners.** In 2014, Kunhua Lin and Hegui Gong identified methyl tosylate (MeOTs) as a competent methyl synthon for methyl ketone synthesis from acid chlorides (Scheme 304).<sup>438</sup> The authors propose that under the optimized conditions, low concentrations of methyl iodide are maintained over the course of the reaction (generated from MeOTs and TBAI), which minimizes methyl dimerization and better matches the rates of activation between the two coupling partners. In the same report, the authors also developed distinct conditions for the XEC of alkyl halides with MeOTs (see section 6.3.3, Scheme 364).

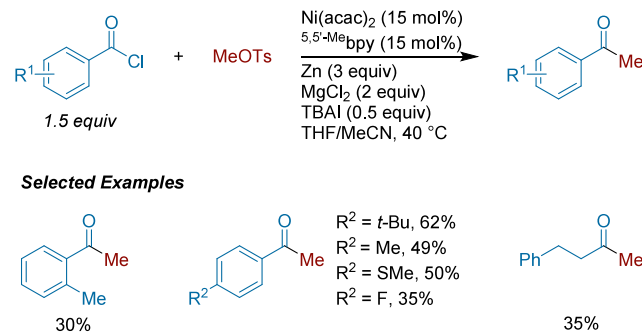
In 2018, Chuan Wang and co-workers reported a reductive electrophilic ring opening of cyclic ketone oxime esters with aryl acid chlorides that forms  $\omega$ -cyano ketones (Scheme 305).<sup>439</sup> The reaction occurs at unusually low temperatures for XEC ( $-55^{\circ}\text{C}$ ) and is an early example of C–C bond scission in XEC. The authors propose initial activation of the cyclic

**Scheme 303. XEC of Alkyl Acid Fluorides or 2-Pyridyl Esters with *N*-Alkyl Pyridinium Salts (2020)<sup>a</sup>**

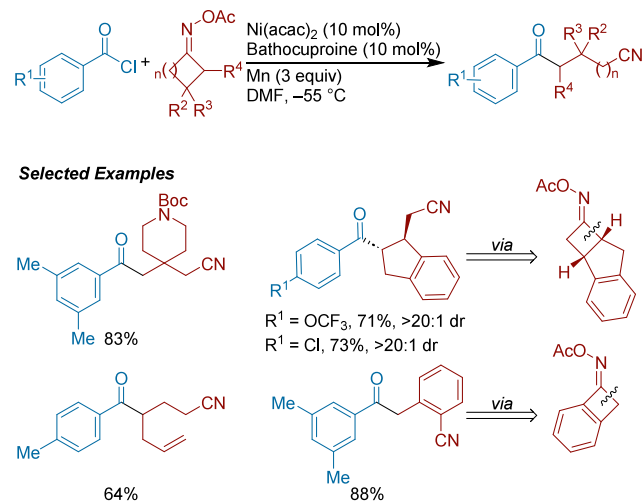


<sup>a</sup>(a) G = F, L = ttbtpy. (b) G = OPy, L = Bphen, with NiBr<sub>2</sub>(dme) as precatalyst. (c) Acid fluoride generated in situ.

**Scheme 304. Ni-Catalyzed Methylation of Acid Chlorides with Methyl Tosylate (2014)**



**Scheme 305. Ni-Catalyzed Ring Opening of Cycloketone Oxime Esters and Coupling with Aroyl Chlorides (2018)**

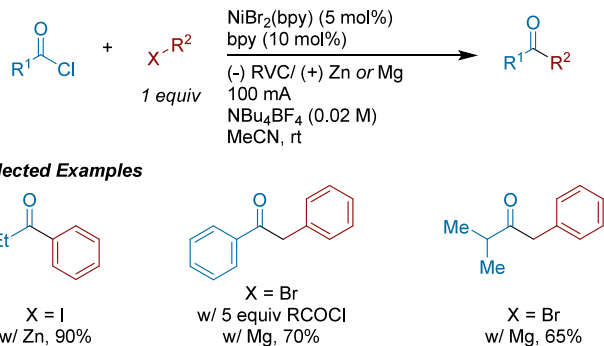


oxime ester, resulting in a caged intermediate complex consisting of an iminyl radical, which ring opens to give a C-centered radical, which then recombines with the Ni(II) complex.

#### 4.4.2.4. Electrochemical and Photochemical Approaches.

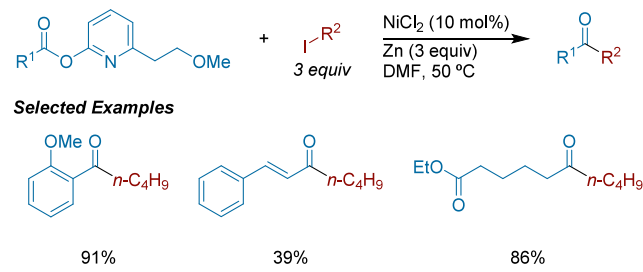
In 1989, Nédélec, Périchon and co-workers reported an electrochemical coupling of acid chlorides with benzyl, allyl, and aryl halides in an undivided cell using either a Zn or Mg rod as the sacrificial anode and a nickel bipyridine catalyst.<sup>144</sup> The authors found that Mg rod required an excess of the acid chloride for good yields, whereas the Zn rod was successful with a 1:1 ratio of starting materials (Scheme 306). The authors observed a difference in the rates of addition to the nickel center, with oxidative addition of the acid chloride being faster.

**Scheme 306. Electrochemical XEC of Acid Chlorides with Organohalides (1989)**



**4.4.3. Acid Esters as Electrophiles.** **4.4.3.1. XEC with Alkyl Halides.** In 1981, the Mukaiyama group reported the seminal synthesis of unsymmetrical ketones via nickel catalysis, coupling substituted 2-pyridyl esters with primary alkyl iodides (Scheme 307).<sup>440</sup> A variety of 2-pyridyl ester derivatives were

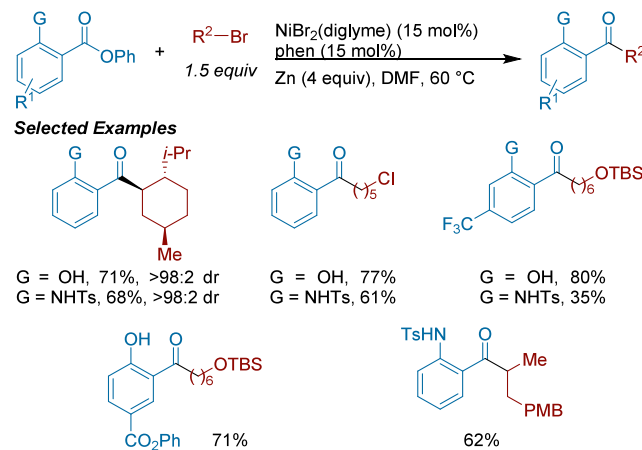
**Scheme 307. XEC of 2-(6-(2-methoxyethyl)pyridyl) carboxylates with Alkyl Iodides (1981)**



tested, however, the authors propose that the 2-methoxyethyl substituent enabled the 2-pyridyl ester to coordinate more efficiently to the nickel center. The authors reported success with a variety of esters, including aryl, vinyl, and alkyl substrates. This work represents the first example of ketone formation through XEC and showed that these conditions advantageously avoid preformation of carbon nucleophiles.

Chuan Wang and co-workers reported the cross-electrophile coupling of *ortho*-substituted benzoic acid phenyl esters with primary and secondary alkyl bromides (Scheme 308).<sup>441</sup> Phenyl esters are rarely utilized as electrophiles in cross-electrophile coupling reactions. The authors provide evidence that the 2-hydroxyl- and 2-sulfonamide functional groups on

**Scheme 308. Ni-Catalyzed XEC of Aryl Phenolic Esters with Alkyl Bromides (2020)<sup>a</sup>**

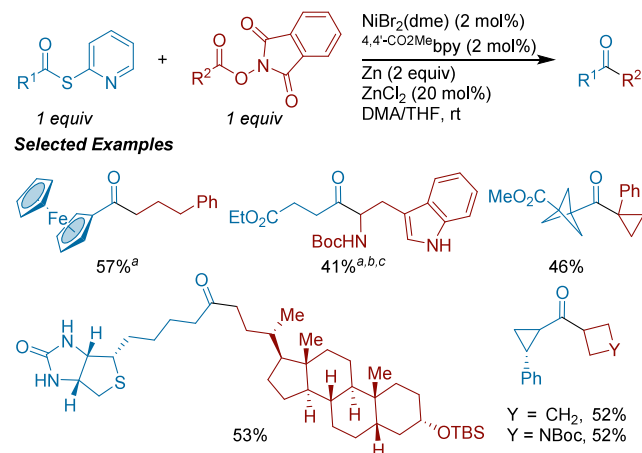


<sup>a</sup>PMB = *para*-methoxybenzyl.

the benzoic acid direct and accelerate the oxidative addition. These directing groups are also useful functional groups for further derivatization. The authors were also able to scale up the coupling with an *ortho*-hydroxy-substituted benzoic acid phenyl ester 25-fold (from 0.2 to 5 mmol) with no loss in yield.

**4.4.3.2. XEC with Alkyl NHP Esters.** In collaboration with the Gellman group, our group reported the cross-electrophile coupling of 2-pyridylthioesters (acyl donor) with alkyl *N*-hydroxypythalimide (NHP) esters (radical donor) (Scheme 309).<sup>442</sup> It was found that an electron-poor  $4,4'\text{-CO}_2\text{Me}\text{bpy}$

**Scheme 309. Ni-Catalyzed XEC of *N*-hydroxypythalimide Esters with 2-Pyridyl Thioesters (2019)<sup>a</sup>**



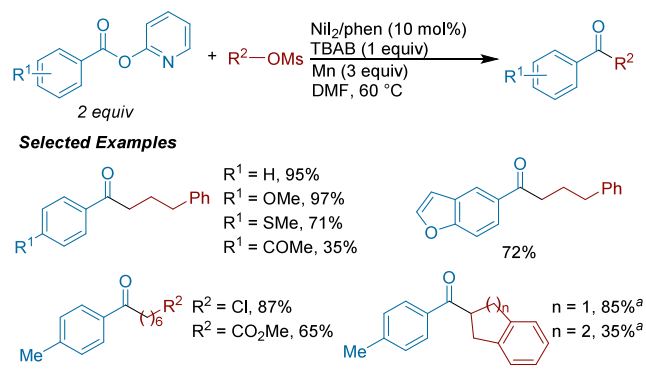
<sup>a</sup>(a) With  $\text{NiBr}_2(\text{dme})$  (10 mol%) and  $4,4'\text{-CO}_2\text{Me}\text{bpy}$  (10 mol%). (b) With tpy (2 mol%) as ligand. (c) With NHP ester (1.5 equiv).

outperformed the more commonly used electron-rich ligands. Furthermore, the consumption of the NHP ester was tuned by the inclusion of zinc salts in the reaction, and by using a mixed solvent system of 1:1 THF and DMA. In THF alone, unreacted NHP ester remained at the end of the reaction, but in DMA only, the NHP ester was consumed rapidly and resulted in lower product formation (38% yield). As an application of this method, we could selectively functionalize a

20-mer peptide fragment analogue of Exendin(9–39) (a GLP-1 receptor agonist) on solid support. L-Glutamic acid esters were incorporated into the peptide chain, and our protocol was able to selectively form ketone products at these sites.

**4.4.3.3. XEC with Alkyl Mesylates.** Zhong-Xia Wang reported the coupling of aryl 2-pyridyl esters with alkyl mesylates (via *in situ* generation of the alkyl halide) (**Scheme 310**).<sup>443</sup> Electron-rich aryl 2-pyridyl esters provided the highest

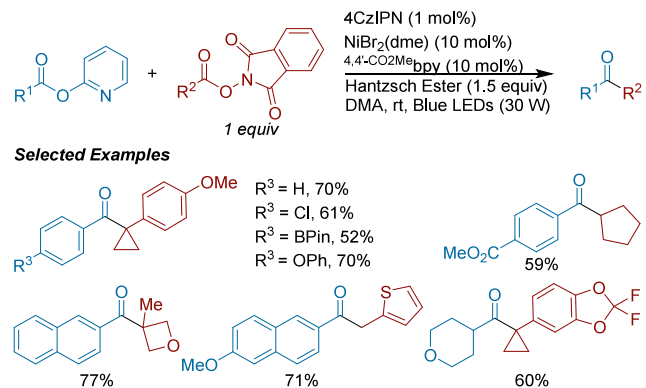
**Scheme 310. Ni-Catalyzed XEC of Aryl 2-Pyridyl Esters with Alkyl Mesylates via *in Situ* Halogenation (2023)**



yields in this report (up to 97% isolated yield), and in contrast, electron-poor aryl 2-pyridyl esters resulted in lower yields often forming unidentified side products. When coupling secondary alcohol derivatives, the authors found that extending the reaction time (from 14 to 36 h) and changing the ligand (from phen to dtbbpy) was required to increase product yield. Due to the use of NiI<sub>2</sub> and TBAB in their reaction conditions, the authors studied the effects that iodide and bromide salts had on the reaction. When replacing the alkyl mesylate with the analogous alkyl bromide or alkyl iodide, product was able to form under the optimized conditions (60% when  $X = \text{Br}$ , and 41% when  $X = \text{I}$ ), indicating that the *in situ* generation and consumption of either alkyl halide can result in product formation.

**4.4.3.4. Electrochemical and Photochemical Approaches.** A cross-electrophile coupling of 2-pyridyl esters with NHP esters to form ketones was reported by Xiaotian Qi, Weiming Yuan and co-workers through a nickel/photoredox strategy (**Scheme 311**).<sup>444</sup> The substrate scope is notably broad for both coupling partners, encompassing primary, secondary and

**Scheme 311. Photoredox-Assisted XEC of 2-Pyridyl Esters with Alkyl NHP Esters (2022)**

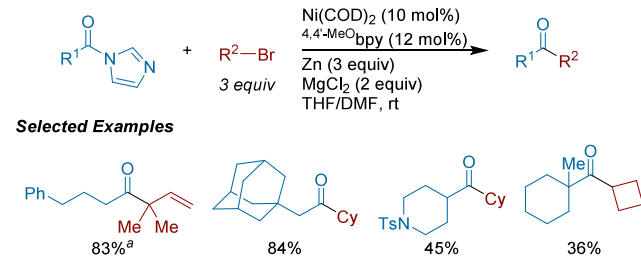


tertiary NHP esters with both aryl- and alkyl-substituted 2-pyridyl esters. A lower yielding example with a cinnamic acid-derived 2-pyridyl ester was also reported, but the authors note this substrate class is particularly susceptible to Giese addition side-products. Stoichiometric studies with an acylnickel(II) derived from the 2-pyridyl ester afforded trace product, suggesting that under these conditions, an acylnickel(II) may not be a competent intermediate. DFT calculations support these observations, and suggest a Ni(0)/Ni(I)/Ni(III) pathway could be operative.

**4.4.4. Acyl Imide Derivatives as Electrophiles.** *N*-Acyl imides and *N*-acylsulfonamides have increased stability compared to acyl chlorides, but still are activated carboxylic acids capable of oxidative addition with transition metals.<sup>445</sup> Extensive studies have been reported on their use in cross-coupling with carbon nucleophiles<sup>446–448</sup> and, more recently, carbon electrophiles.

**4.4.4.1. XEC with Alkyl Halides.** Chao Li and co-workers reported on the coupling of *N*-acylimidazoles as acyl coupling partners with alkyl and aryl bromides to form unsymmetrical ketones (**Scheme 312**).<sup>449</sup> Interestingly, when 2-cyclopropyl-1-

**Scheme 312. XEC of *N*-Acylimidazoles with Alkyl Bromides (2020)<sup>a</sup>**

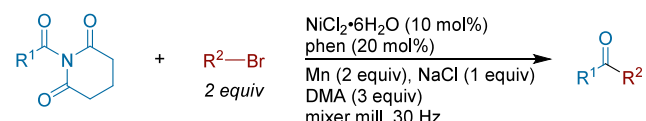


<sup>a</sup>3,3-Dimethylallyl bromide was used.

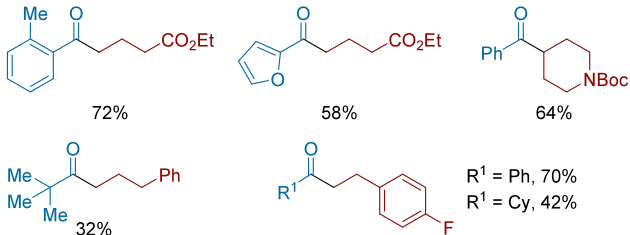
(1*H*-imidazol-1-yl)ethan-1-one was subjected to the optimized reaction conditions with alkyl and aryl bromide coupling partners, the cyclopropane ring-opened product was formed, indicating that primary and secondary *N*-acyl imidazoles engage in a carbon monoxide extrusion-recombination pathway that proceeds via a radical intermediate. This is distinct from other acyl donors in this review, which generally engage in a two-electron process. In contrast, when a tertiary *N*-acylimidazole with an  $\alpha$ -chiral stereocenter was subjected to reaction conditions, the enantiopurity was preserved, supporting a concerted oxidative addition pathway for these more hindered acyl donors. Conditions for coupling *N*-acylimidazoles with aryl bromides were also developed in this study.

The Morrill and Browne laboratories reported the XEC of *N*-acyl glutarimides with alkyl bromides under ball-milling conditions (**Scheme 313**).<sup>450</sup> Mechanical activation of metal powder reductants is well-known, and as such, is a good match for ball milling.<sup>451–453</sup> Notably, these reactions are performed under nearly neat conditions, with only 3 equiv of DMA used to assist grinding, and with no precautions to exclude air. The authors hypothesize that the addition of NaCl could assist with grinding the Mn and/or with catalyst speciation (various salts are common additives in XEC). The *N*-acylglutarimides performed better than other examined acyl donors and were synthesized from the corresponding acid chloride. Although direct insertion of manganese into the alkyl bromide was shown to be possible under ball-milling conditions, the

**Scheme 313.** Ball-Milling Enabled XEC of *N*-Acyl Glutarimides with Alkyl Bromides (2022)



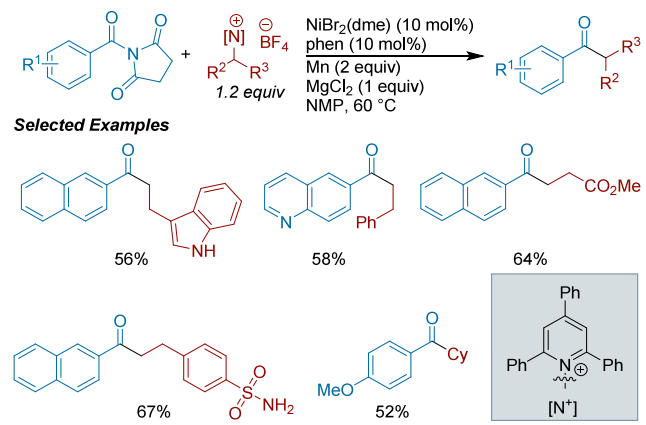
**Selected Examples**



mechanism appears to be more nuanced, as cyclopropylmethyl bromides only afforded the rearranged product from radical ring-opening.

**4.4.4.2. Other Coupling Partners.** The Matsuo lab reported the coupling of *N*-alkyl pyridinium salts with *N*-acylsuccinimides (Scheme 314).<sup>454</sup> The coupling worked best for

**Scheme 314.** Ni-Catalyzed Deaminative XEC of Alkyl Pyridinium Salts with *N*-Acylsuccinimides (2020)

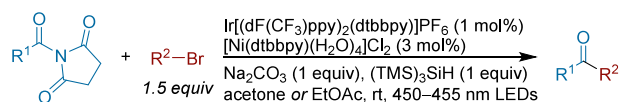


electron-rich and -neutral aryl *N*-acylsuccinamides, however, electron-poor aryls failed to couple effectively. Primary and secondary *N*-alkyl pyridiniums were both compatible under these conditions. In agreement with previous reports, the authors propose that radical generation from *N*-alkyl pyridinium salts may occur via reduction by Mn, separating the rate of activation from the nickel catalyst.<sup>282</sup>

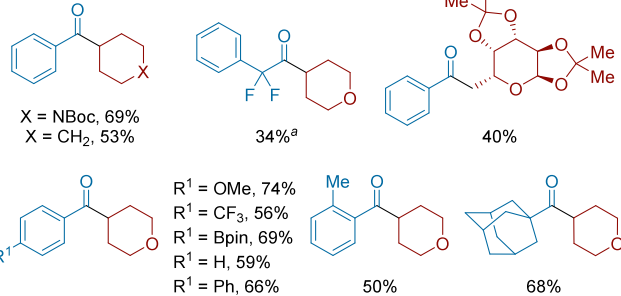
**4.4.4.3. Electrochemical and Photochemical Approaches.** The Amgoune lab reported the cross-electrophile coupling of *N*-acylsuccinimides with unactivated alkyl bromides utilizing silyl radical activation under photoredox conditions (Scheme 315).<sup>455</sup> These conditions utilize tris(trimethylsilyl)silane as the terminal reductant and halide atom transfer (XAT) agent. An equivalent of base is required to quench the HBr generated as coproduct. The iridium dye serves to both activate the supersilane reagent and reduce the nickel catalyst.

The Opatz lab developed the nickel/photochemical XEC of *N*-aroysaccharins as the acyl donor and NHP esters as the radical donor (Scheme 316).<sup>456</sup> The electron donor–acceptor complex of the Hantzsch ester with the NHP ester is directly excited by 390 nm wavelength light to generate the radical. A

**Scheme 315.** Silyl Radical Mediated XEC of *N*-Acyl Imides with Unactivated Alkyl-Bromides Under Metallaphotoredox Conditions (2020)<sup>a</sup>

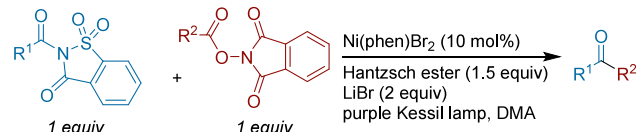


**Selected Examples**

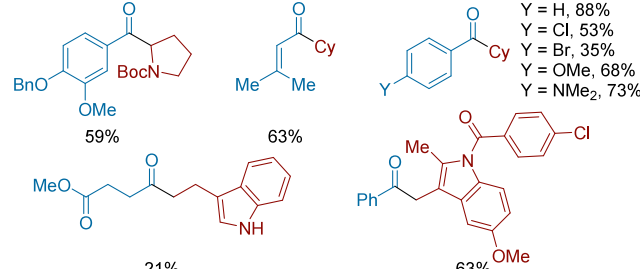


<sup>a</sup>With *N*-acyl glutarimide as the acyl donor.

**Scheme 316.** Nickel/Photochemical XEC of *N*-Acylsaccharins with NHP Esters (2021)



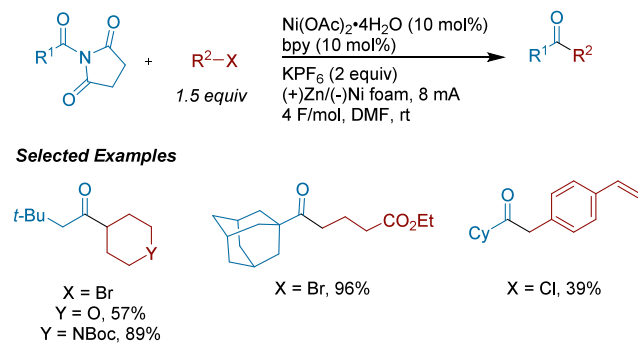
**Selected Examples**



notable advantage of this approach was a broad acyl scope—both electron-neutral to electron-rich benzoic acids as well as an  $\alpha,\beta$ -unsaturated acid and aliphatic carboxylic acids. Electron-poor benzoic acids were unsuitable, as were some more nucleophilic radicals (tertiary,  $\alpha$ -heteroatom secondary). It is notable that *N*-acylsaccharin was the only acyl donor that afforded cross-product while other more common activated amides (as well as the acyl chloride) were incompatible under these conditions.

Amgoune, Vantourout, and co-workers synthesized dialkyl ketones from the XEC reaction of *N*-acylsuccinimides with alkyl bromides or benzyl chlorides (Scheme 317).<sup>457</sup> The reactions were driven electrochemically utilizing an undivided cell with a sacrificial zinc anode. The authors synthesized and fully characterized a putative acynickel(II) intermediate, noting that the succinimidate (Su) group conferred excellent stability (1 week under  $N_2$  in solution) in comparison to the reported poor stability of the corresponding halide complexes. CV studies show that (L) $Ni^I(OAc)$  can react with both the alkyl bromide (to form a radical) and with the *N*-acyl imide (to form a transient (L) $Ni^{III}(Su)(acyl)(OAc)$  that is reduced to nickel(II)). CV studies on (L) $Ni^{II}(Su)(acyl)$  show that this species can be reduced to (L) $Ni^I(Su)(acyl)$  and this species

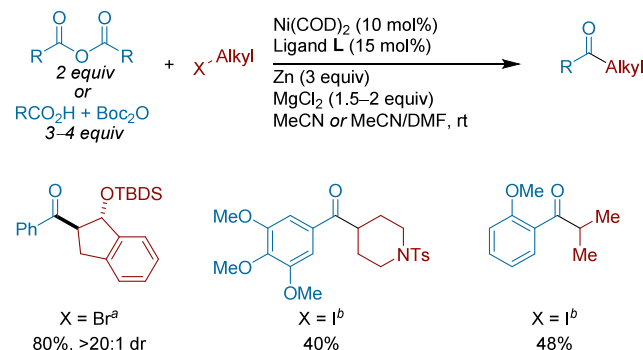
**Scheme 317. Electrochemical Cross-Electrophile Coupling of N-Acyl Imides with Alkyl Halides (2022)**



might be a source of side products as well as alkyl radical. The authors propose that (L)Ni<sup>I</sup>(OAc) is operative on cycle for the activation of both electrophiles, but conclude that (L)Ni<sup>I</sup>(Su)-acyl is not required for product formation.

**4.4.5. Mixed Anhydrides as Electrophiles.** *4.4.5.1. XEC with Alkyl Halides.* Early studies by Hegui Gong, Kunhua Lin and co-workers reported the Ni-catalyzed XEC of in situ generated mixed anhydrides (from the corresponding aryl carboxylic acid and di-*tert*-butyl dicarbonate (Boc<sub>2</sub>O)) with alkyl iodides to efficiently form unsymmetrical ketones (Scheme 318).<sup>458</sup> The authors found that MgCl<sub>2</sub> was a key

**Scheme 318. XEC of Alkyl Halides with Pre-Formed or In Situ Generated Acid Anhydrides to Form Unsymmetrical Ketones (2012)<sup>a</sup>**

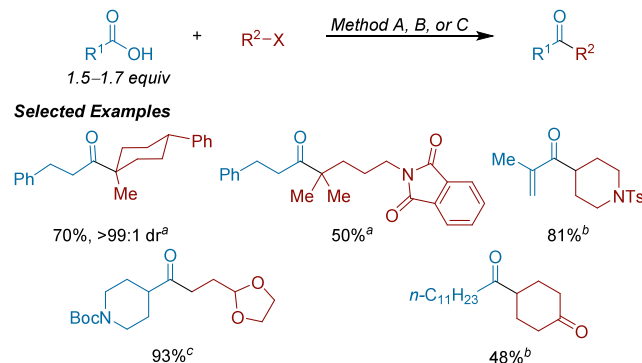


<sup>a</sup>(a) L = 4,4'-Me<sub>2</sub>bpy, (b) L = Bphen.

additive, dramatically improving yields. Primary and secondary alkyl halides were well tolerated, with cyclic secondary alkyl halides giving higher yields than acyclic ones. This work also contained studies with preformed symmetric anhydrides with alkyl iodides and bromides. This report demonstrated that in situ activation of carboxylic acids as mixed anhydrides for ketone synthesis can be an efficient alternative to other acyl donors that require preformation.

Hegui Gong and co-workers then reported the Ni-catalyzed cross-electrophile coupling of alkyl carboxylic acid derivatives with unactivated alkyl and glycosyl halides (Scheme 319).<sup>459</sup> The carboxylic acids are activated in situ as the mixed anhydride with Boc<sub>2</sub>O. Three distinct methods were developed: couplings of tertiary alkyl bromides (Method A), couplings of primary/secondary alkyl iodides (Method B) and couplings of primary/secondary bromides (Method C). In some cases, stoichiometric amounts of TBAI were required

**Scheme 319. Ni-Catalyzed XEC of In Situ-Formed Mixed Anhydrides with Alkyl Halides (2014)<sup>a</sup>**

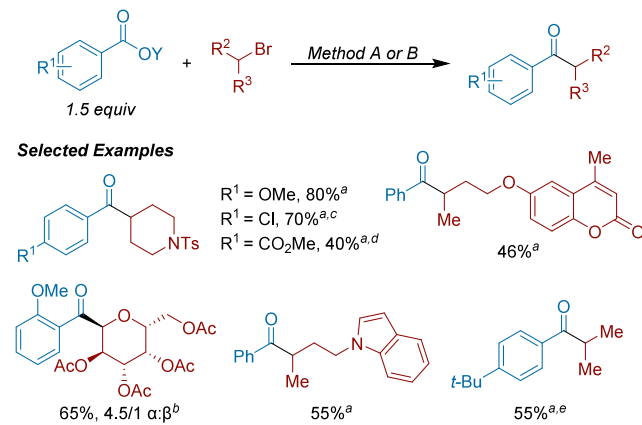


<sup>a</sup>(a) Method A: X = Br, Ni(acac)<sub>2</sub> (10 mol%), bpy (12 mol%), MgCl<sub>2</sub> (1 equiv), i-Pr<sub>2</sub>NEt (0.85 equiv), Boc<sub>2</sub>O (2 equiv), Zn (3 equiv), DMSO/DME, 30 °C. (b) Method B: X = I, Ni(acac)<sub>2</sub> (10 mol%), phen (12 mol%), Boc<sub>2</sub>O (2 equiv), Zn (3 equiv), MgCl<sub>2</sub> (1.5 equiv), MeCN/THF, 25 °C. (c) Method C: X = Br, Ni(acac)<sub>2</sub> (10 mol%), dtbbpy (12 mol%), Boc<sub>2</sub>O (2 equiv), Zn (3 equiv), MgCl<sub>2</sub> (1.5 equiv), TBAI (0.5 equiv), DMF/THF, 30 °C.

to activate primary alkyl bromides. The authors propose a radical chain mechanism, in which MgCl<sub>2</sub> accelerates reduction of the nickel(II) complexes by zinc. In addition, the authors couple glycosyl bromides with either propionic acid or the analogous anhydride, resulting in C-acyl glycosides with high  $\alpha$ -selectivity.

Hegui Gong and co-workers also utilized either preformed or in situ generated aryl acid anhydrides to couple with secondary alkyl bromides (Scheme 320).<sup>460</sup> From optimization, the authors found that a mixed solvent system of MeCN/DMF was more efficient than any single solvent system, and the primary side product was hydrodehalogenation of the alkyl bromide. This also is the first synthesis of aryl C-glycosides, in particular acyl glucosides, galactosides, and mannosides, by directly coupling glycosyl bromides with acid derivatives in an

**Scheme 320. Coupling of Aryl Carboxylic Acid Derivatives with Secondary Alkyl Bromides (2015)<sup>a</sup>**

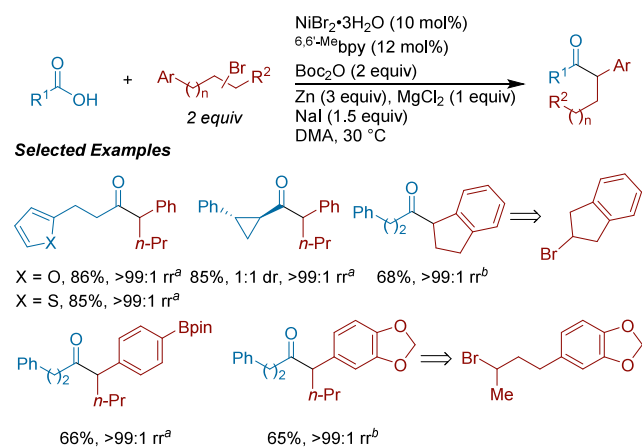


<sup>a</sup>(a) Method A: Y = H, Ni(acac)<sub>2</sub> (5 mol%), dtbbpy (7 mol%), Zn (3 equiv), MgCl<sub>2</sub> (2.5 equiv), Boc<sub>2</sub>O (3 equiv), MeCN/DMF, 25 °C. (b) Method B: Y = C(O)Ar, Ni(ClO<sub>4</sub>)<sub>2</sub>•6H<sub>2</sub>O (10 mol%), bpy (12 mol%), Zn (3 equiv), TBAI (20 mol%), MeCN/DMF, 25 °C. (c) DME/DMF as solvent. (d) Ni(acac)<sub>2</sub> (10 mol%) and dtbbpy (15 mol%) were used. (e) With alkyl iodide (2 equiv).

$\alpha$ -selective method. These methods enabled the efficient coupling of aryl acids and acid anhydrides to alkyl halides, which was previously difficult, likely due to mismatched rates of reactivity.

You Wang, Shaolin Zhu, and co-workers reported the migratory acylation of alkyl bromides with *in situ* activated alkyl carboxylic acids (Scheme 321).<sup>461</sup> The authors propose

**Scheme 321. Ni-Catalyzed Migratory Acylation of Alkyl Bromides with In Situ Activated Alkyl Carboxylic Acids (2019)<sup>a</sup>**

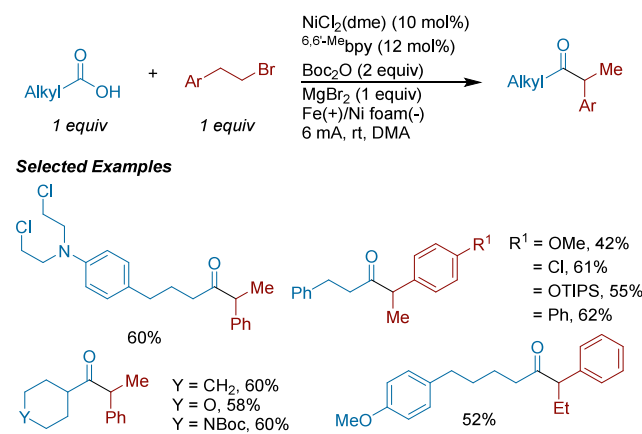


that success of this reaction may be contingent on *in situ* formation of a nickel hydride species from  $\beta$ -hydride elimination of an alkynickel species; this resulting species could then undergo chain walking before selective acyl cross-coupling. The reaction has excellent regioselectivity and allows the coupling of both terminal and internal alkyl bromides. This reaction is also highly regioconvergent, as the authors converted an isomeric mixture of three olefins to the benzylic acylation product as a single regioisomer in good yield (68% yield, >99:1 rr). Through an acylation vs arylation competition experiment, the authors obtained an approximate 5:1 ratio of acylated to arylated product, indicating the coupling of the carboxylic acid was faster than that of an aryl bromide.

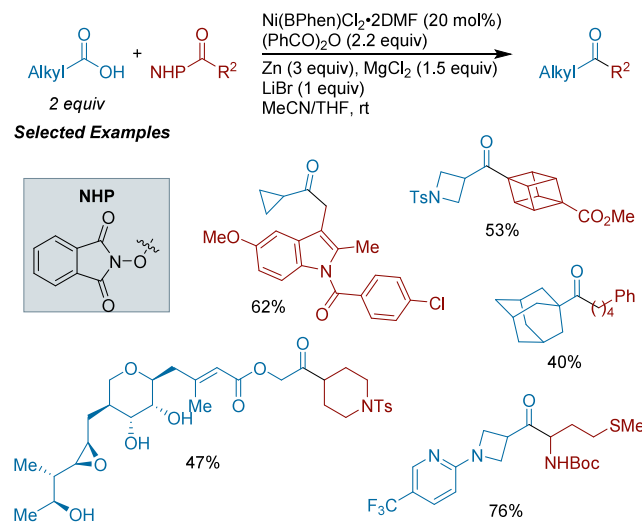
Tian-Sheng Mei, Bin Cheng, and co-workers reported an electrochemically mediated migratory cross-electrophile coupling of alkyl bromides with *in situ* activated alkyl carboxylic acids (Scheme 322).<sup>462</sup> Based on CV studies, the authors propose that the carboxylic acid undergoes oxidative addition to the nickel(0) center, followed by cathodic reduction to generate an acylnickel(I) species. After capturing the radical generated from the alkyl bromide, the resultant complex undergoes  $\beta$ -hydride elimination to an  $\eta^2$ -type intermediate, followed by reinsertion, to generate a more thermodynamically stable benzylic nickel(II) intermediate. This complex then undergoes reductive elimination to generate the desired product in high regioselectivity.

**4.4.5.2. XEC with NHP Esters.** The Baran lab, in collaboration with Pfizer, Bristol-Myers Squibb, and Enamine, reported the decarboxylative cross-electrophile coupling of NHP esters with *in situ* generated mixed anhydrides (Scheme 323).<sup>463</sup> The authors propose a radical chain mechanism, wherein the mixed anhydride coupling partner undergoes oxidative addition to the nickel(0) center, followed by  $\text{MgCl}_2$

**Scheme 322. Migratory Cross-Electrophile Coupling of In Situ Generated Alkyl Carboxylic Acid Anhydrides with Alkyl Bromides under Electrochemical Conditions (2021)**



**Scheme 323. Ni-Catalyzed Decarboxylative XEC of NHP Esters with Alkyl Carboxylic Acids (2019)**

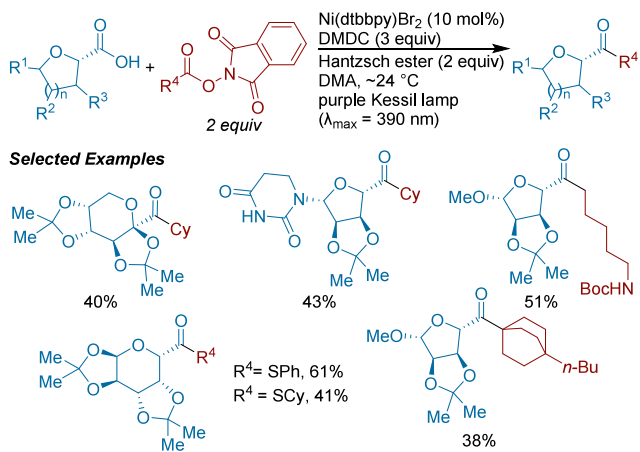


mediated anionic ligand exchange, then radical capture from the alkyl NHP ester. Through mechanistic studies, the authors propose the rate of heterogeneous electron transfer as being partially rate-determining, with positive rate dependencies on  $\text{MgCl}_2$ ,  $\text{LiBr}$ , and  $\text{Zn}$ . The scope is broad, allowing for coupling of primary, secondary, and tertiary alkyl substrates of both coupling partners.

The Molander lab utilized photoactivation of an electron donor–acceptor (EDA) complex to synthesize nonanomeric C-acyl glycosides from NHP esters with *in situ* activated pyranosyl- and furanosyl acids (Scheme 324).<sup>464</sup> The EDA complex is proposed to be formed via  $\pi$ -stacking interactions between the phthalimide fragment of the NHP ester and the Hantzsch ester photoreductant, allowing for successful coupling without an external photo- or metal reductant.

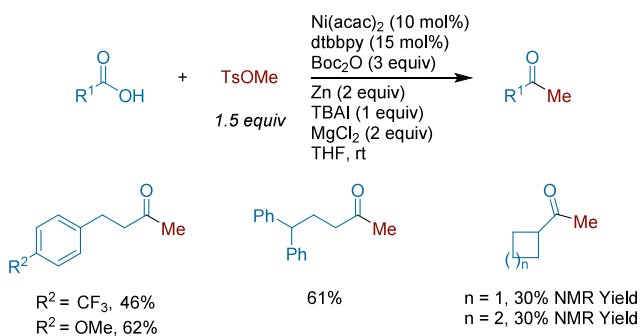
**4.4.5.3. Other Coupling Partners.** Hongyu Wang and co-workers reported the methylation of *in situ* generated alkyl acid anhydrides using  $\text{MeOTs}$  through XEC (Scheme 325).<sup>465</sup> The authors propose that the  $\text{MeOTs}$  undergoes anion exchange to either form low concentrations of  $\text{MeI}$  or  $\text{MeCl}$  in *situ*, which, in turn, participates in the catalytic reaction. This adjusts the rate of reactivity of the methyl coupling partner to better

**Scheme 324.** Formation of Non-Anomeric C-Acyl Glycosides via Photoactivation of an Electron Donor–Acceptor Complex (2022)<sup>a</sup>



<sup>a</sup>DMDC = dimethyl dicarbonate

**Scheme 325.** Ni-Catalyzed Methylation of In Situ Activated Alkyl Carboxylic Acids (2017)

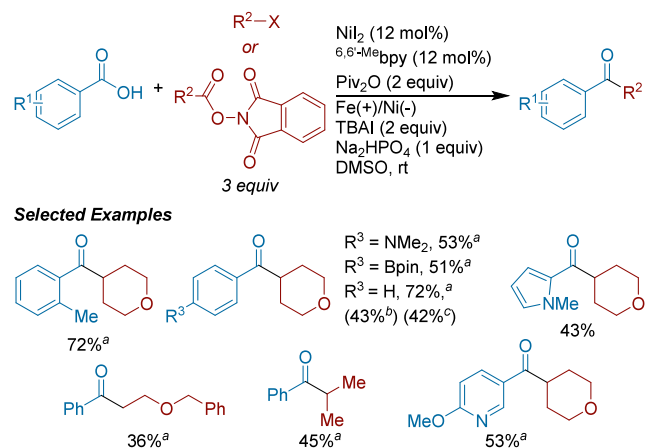


match the rate of oxidative addition of the mixed anhydride, improving the cross-selectivity. The authors found that Boc-protected amino acids are a limitation of these reaction conditions, and the authors propose that the N-alkylated compounds may complex with the catalyst, resulting in an off-cycle species.

**4.4.5.4. Electrochemical and Photochemical Methods.** Wujiong Xia, Chao Yang, and co-workers reported the electrochemical coupling of in situ activated aryl carboxylic acids with a variety of alkyl halides and NHP esters (Scheme 326).<sup>466</sup> From mechanistic experiments, the authors propose cathodic reduction of a nickel(II) species to the low-valent nickel(0) species, which can then undergo oxidative addition of the acyl coupling partner. The utilization of both organohalides and NHP esters further expands the compatibility and applicability of this protocol, given differing commercial availability of desired coupling partners. In contrast with previous reports,<sup>462</sup> no chain-walking product was observed under these conditions.

**4.4.6. XEC with Exogenous CO Source.** Formation of ketones with gaseous CO may at first seem an obvious transformation, but there are safety concerns in translation of these reactions to scale up, particularly high pressure, toxicity, flammability, as well as concerns with reliable CO incorporation. Recent publications have explored a variety of exogenous CO sources as ways of safely loading a carbonyl

**Scheme 326.** Electrochemical XEC of In Situ Activated Carboxylic Acids with Alkyl Electrophiles (2022)<sup>a</sup>



<sup>a</sup>(a) With alkyl iodide. (b) With alkyl bromide. (c) With NHP ester.

source into the reaction. These alternate pathways to CO incorporation have allowed for an even larger variety of coupling partners to be utilized in the formation of ketones.

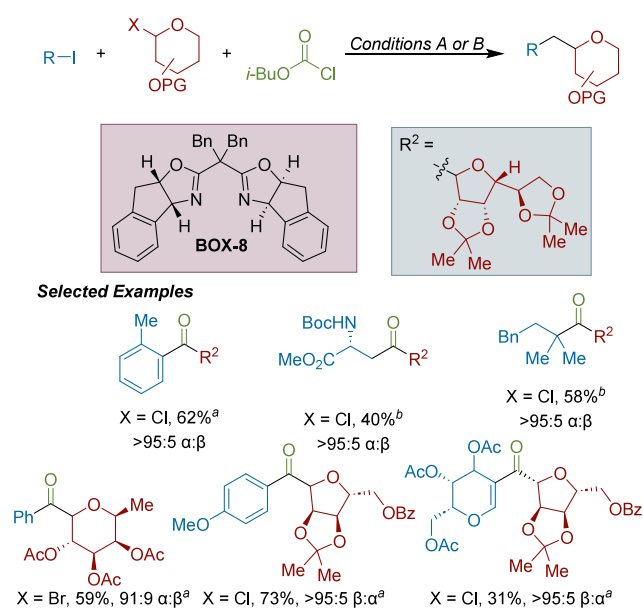
**4.4.6.1. Chloroformates as Exogenous CO Source.** Current mechanistic understanding of carbonylative couplings using chloroformates is limited. However, current DFT calculations have coalesced on chloroformates undergoing a 2-electron oxidative addition to the nickel center, followed by CO migration to form a nickel carbonyl species. What remains less understood is the comparative rate of activation of coupling partners, particularly whether aryl electrophiles or chloroformates undergo oxidative addition first.

Ming Joo Koh, Yu Lan, Shi-Jun Li, and Quanquan Wang reported the multicomponent coupling of glycosyl halides and organoiodides with isobutyl chloroformate as an exogenous CO source (Scheme 327).<sup>467</sup> The resulting C-acyl glycosides are isolated in high chemo- and diastereoselectivity. Conditions A are utilized when coupling aryl iodides and Conditions B are used when coupling alkyl iodides, providing orthogonal reactivity for coupling glycosyl halides with a vast array of coupling partners. Using DFT calculations, the authors propose that the initial oxidative addition of isobutyl chloroformate to a nickel(0) species is favored to occur first. After sequential reduction steps, organoiodides can undergo oxidative addition to the reactive nickel(0) carbonyl species, followed by 1,1-migration to generate an acylnickel(II) species.

Chen Zhu, Magnus Rueping and co-workers utilized ethyl chloroformate as a readily available source of CO in the cross-electrophile coupling of aryl iodides with alkyl bromides (Scheme 328).<sup>468</sup> DFT calculations and mechanistic studies suggest that the reaction proceeds via a sequence of oxidative additions, starting with aryl halide, then ethyl chloroformate, followed by alkyl bromide. The reaction showed high compatibility for a variety of primary alkyl bromides, and slightly modified conditions resulted in successful couplings with secondary alkyl iodides. Electron-rich aryl iodides were coupled more efficiently than their electron-deficient counterparts.

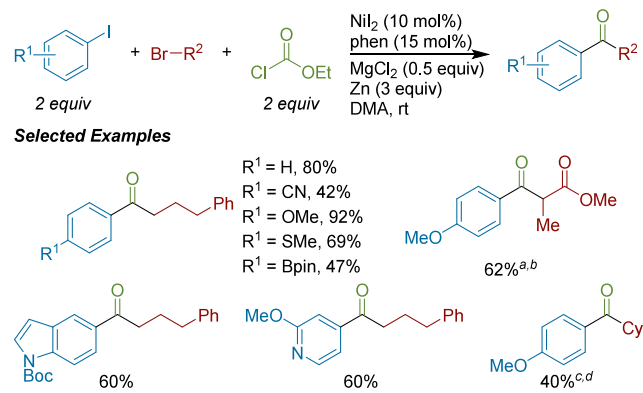
Xile Hu reported the carbonylative XEC with a variety of alkyl halides using ethyl chloroformate as a CO source to form both symmetric and unsymmetric ketones (Scheme 329).<sup>469</sup> The authors propose an oxidative addition of ethyl chloroformate, radical capture of the first alkyl coupling

**Scheme 327. Carbonylative XEC of Glycosyl Halides with Organoiodides and Isobutyl Chloroformate as a CO Source (2022)<sup>a</sup>**



<sup>a</sup>(a) Conditions A: glycosyl halide (2.0 equiv), isobutyl chloroformate (2.0 equiv), aryl iodide (1.0 equiv), NiI<sub>2</sub> (10 mol%), dtbbpy (12 mol%), Mn (3.0 equiv), TMSCl (0.5 equiv), DMA/THF, 40 °C. (b) Conditions B: glycosyl halide (1.0 equiv), isobutyl chloroformate (2.0 equiv), alkyl iodide (3.0 equiv), NiBr<sub>2</sub>(diglyme) (10 mol%), BOX-8 (12 mol%), Mn (3.0 equiv), TMSCl (0.5 equiv), DMA/THF, 40 °C.

**Scheme 328. Ni-Catalyzed XEC of Aryl Iodides with Alkyl Bromides with Ethyl Chloroformate as CO Source (2022)<sup>a</sup>**

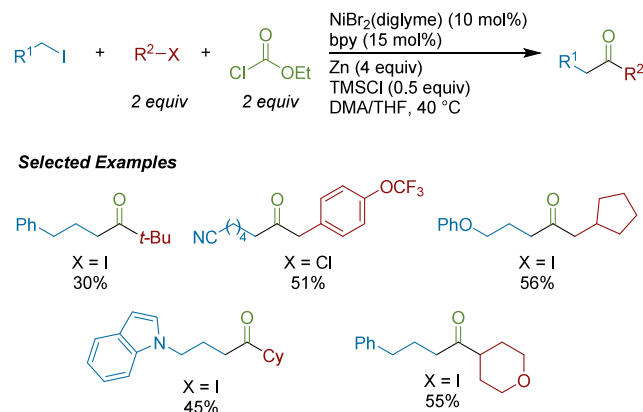


<sup>a</sup>(a) With alkyl chloride. (b) With (R)-4-(*tert*-butyl)-2-(pyrimidin-2-yl)-4,5-dihydrooxazole as ligand. (c) With alkyl iodide. (d) With Ni(COD)<sub>2</sub> (10 mol%).

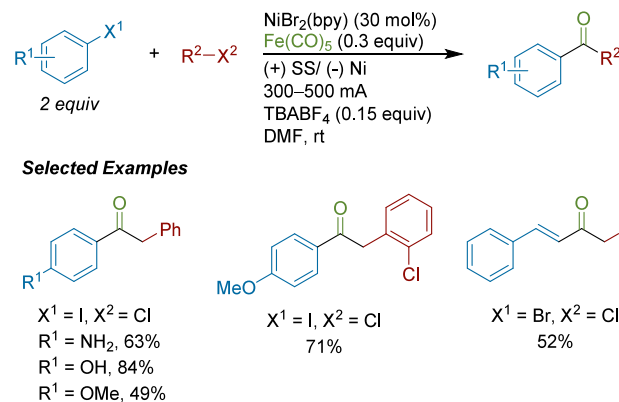
partner, then 1,1-migration to form an acylnickel species. This is followed by a second radical capture and then reductive elimination to give the desired ketone product. Interestingly, carbonylative cross-coupling was favored over carbonylative homocoupling of either alkyl substrate, even when the two alkyl substrates shared a halide class.

**4.4.6.2. Metal Carbonyls as Exogenous CO Source.** Troupel and co-workers reported an electrochemical, Ni-catalyzed carbonylative synthesis of unsymmetrical ketones by the XEC aryl halides with alkyl or benzyl halides.<sup>470</sup> By utilizing iron pentacarbonyl as the CO source (Scheme 330), the authors avoided formation of a saturated (bpy)Ni(CO)<sub>2</sub>

**Scheme 329. Carbonylative XEC of Alkyl Halides with Ethyl Chloroformate as a CO Source (2019)**



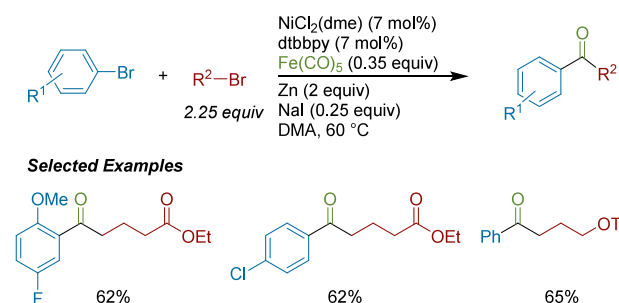
**Scheme 330. Carbonylative Electrochemical XEC of Aryl Halides with Alkyl or Benzyl Halides with Iron Pentacarbonyl as a CO Source (2001)**



complex, which was observed when an excess of CO<sub>(g)</sub> was introduced into the reaction mixture. Conversely, when the concentration of CO<sub>(g)</sub> was low, the formation of alkyl homodimer was competitive with ketone formation. Functional group tolerance was notable for this early study, which included free phenol and aniline functionality, highlighting the potential of this approach to prepare ketones.

Our group reported the Ni-catalyzed cross-electrophile coupling of aryl and alkyl bromides under carbonylative conditions utilizing iron pentacarbonyl as an exogenous CO source (Scheme 331).<sup>471</sup> The development of catalytic

**Scheme 331. Carbonylative XEC of Aryl and Alkyl Bromides with Fe(CO)<sub>5</sub> as an Exogenous CO Source (2014)**

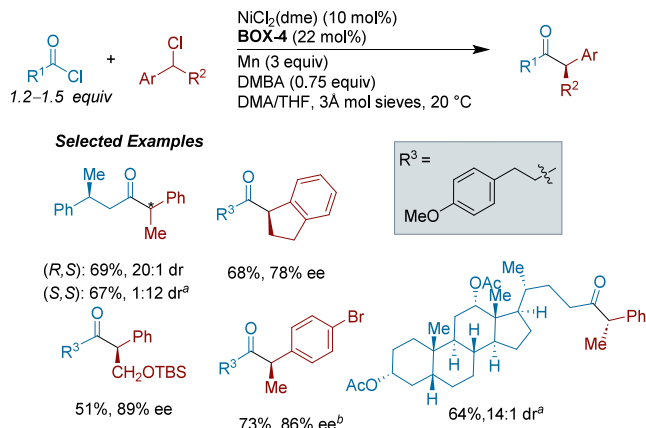


conditions was guided by stoichiometric studies of acylnickel complexes with alkyl and aryl halides. From these studies, we found that the addition of zinc to these stoichiometric reactions with alkyl halides did not improve cross-selectivity. This suggested direct reduction of an acylnickel(II) to the analogous nickel(I) complex was not a necessary step in the ketone synthesis. For the catalytic conditions, increasing the amount of alkyl bromide was needed to overcome aroylnickel(II) disproportionation to diaryl ketone side-products. Tuning the loading of iron pentacarbonyl to control the concentration of CO in solution was also important to increase the yield of carbonylated products (too much iron pentacarbonyl shuts down reactivity, however).

#### 4.4.7. Stereocontrolled XEC of Acyl-X with Alkyl-X.

Reisman and co-workers reported the first example of asymmetric XEC to prepare  $\alpha,\alpha$ -chiral ketones through the coupling of acyl chlorides with secondary benzyl chlorides (Scheme 332).<sup>472</sup> The addition of 2,6-dimethylbenzoic acid

**Scheme 332. Ni-Catalyzed Enantioconvergent XEC of Acid Chlorides with Benzyl Chlorides (2013)<sup>a</sup>**



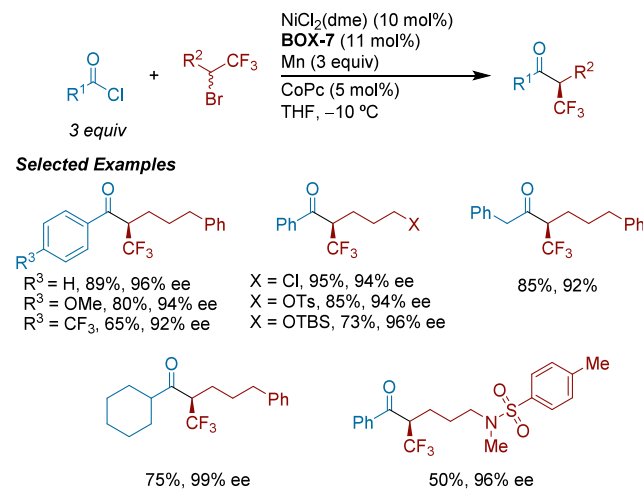
<sup>a</sup>(a) With BOX-4 (22 mol%). (b) With DMBA (1.25 equiv). DMBA = 2,6-dimethylbenzoic acid.

(DMBA) was found to decrease the amounts of homocoupled products. BOX-ligands afforded the highest enantioselectivity over other classes of chiral ligands. Benzyl chlorides were best matched in this system, as when the coupling partner was exchanged for the analogous bromide, an approximate 10-fold increase in benzyl radical dimer was observed.

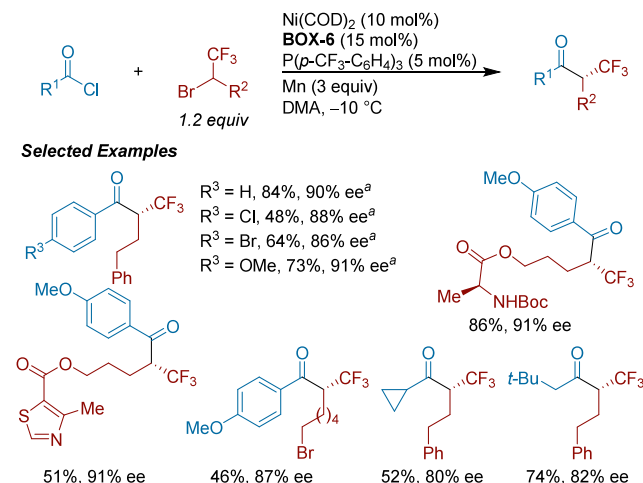
Chun Zhang, Genping Huang, and co-workers reported the enantioconvergent XEC of acyl chlorides with racemic  $\alpha$ -trifluoromethyl bromides.<sup>473</sup> In this work, the trifluoromethyl group was crucial to the success of this transformation, as changing of this group to others either resulted in no observed product, or a racemic product mixture (Scheme 333). The authors propose that cobalt phthalocyanine (CoPc) promotes the formation of a radical, in agreement with previous reports.<sup>174</sup>

Concurrently, Liang-An Chen and co-workers also developed a Ni-catalyzed XEC of acid chlorides with  $\alpha$ -CF<sub>3</sub> alkyl bromides to generate  $\alpha$ -trifluoromethylated ketones (Scheme 334).<sup>474</sup> The authors found that careful selection of an achiral monodentate phosphine coligand afforded improved enantioselectivity and coupling efficiency. Time courses showed that the phosphine ligand rapidly increased the rate of the reaction and improved product formation. The system is chemose-

**Scheme 333. Enantioconvergent XEC of Acyl Chlorides with Racemic  $\alpha$ -Trifluoromethyl Bromides (2022)**



**Scheme 334. Ni-Catalyzed Enantioselective XEC of Acid Chlorides with  $\alpha$ -Trifluoromethylated Alkyl Bromides (2022)<sup>a</sup>**



<sup>a</sup>With BOX-6 (11 mol%).

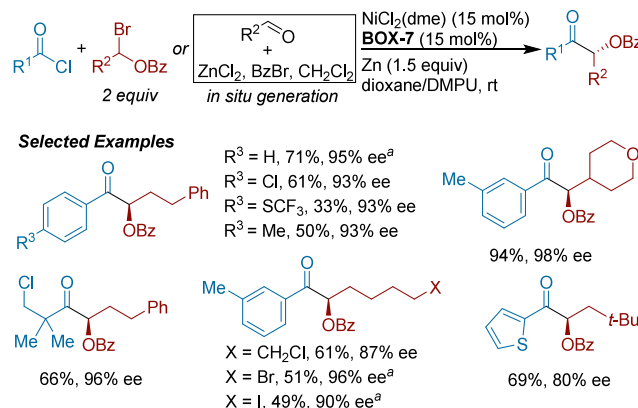
selective for  $\alpha$ -CF<sub>3</sub> secondary alkyl bromides over primary alkyl bromides.

Liang-An Chen, Qiaorong Han, and co-workers reported a Ni-catalyzed enantioselective XEC of acid chlorides with  $\alpha$ -bromobenzoates to synthesize chiral protected  $\alpha$ -hydroxy ketones (Scheme 335).<sup>475</sup> The authors observed enhanced enantioselectivities with increased steric hindrance at the bis(oxazoline) (BOX). The scope is broad, encompassing both aryl and alkyl-substituted acyl chlorides. The reaction is also chemoselective for  $\alpha$ -bromobenzoates over primary alkyl bromides and iodides. As an application of this chemistry, a series of bioactive  $\alpha$ -hydroxy ketones were efficiently prepared through this reaction. Stoichiometric experiments with chiral acylnickel(II)nickel could form product with added zinc. Taken together with other mechanistic data, the authors proposed a radical chain mechanism, contingent upon the formation of a prochiral ketyl radical, which is captured by a chiral acylnickel(II) species.

#### 4.4.8. Synthetic Applications of C(sp<sup>2</sup>)–C(sp<sup>3</sup>) Acyl–Alkyl XEC.

Kishi and co-workers have studied cross-electro-

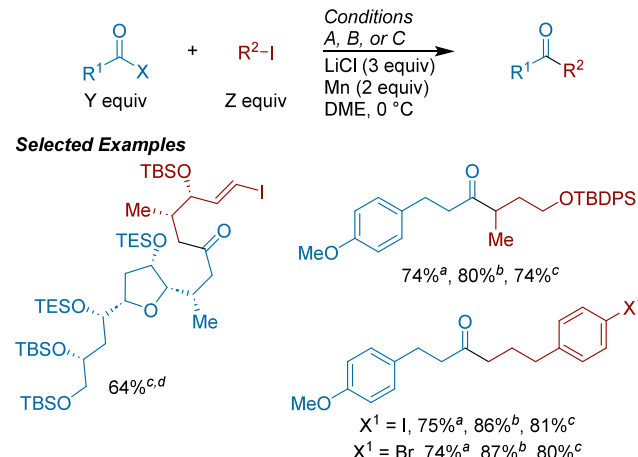
**Scheme 335.** Ni-Catalyzed XEC of  $\alpha$ -Hydroxy Ketones from Acid Chlorides and  $\alpha$ -Bromobenzoates (2022)<sup>a</sup>



<sup>a</sup>Via *in situ* generation of  $\alpha$ -oxy bromide from corresponding aldehyde.

phile coupling methods extensively in their work on the total syntheses of classes of halichondrins. Their first publication implementing these reactions saw the design of a one-pot, iron/copper-mediated coupling of alkyl iodides with alkyl acid chlorides or alkyl 2-pyridyl thioesters (Scheme 336).<sup>476</sup> By utilizing iron- and copper-based catalysts instead of nickel- or palladium-based catalysts, the reaction was selective for coupling alkyl iodides over vinyl iodides.<sup>477</sup>

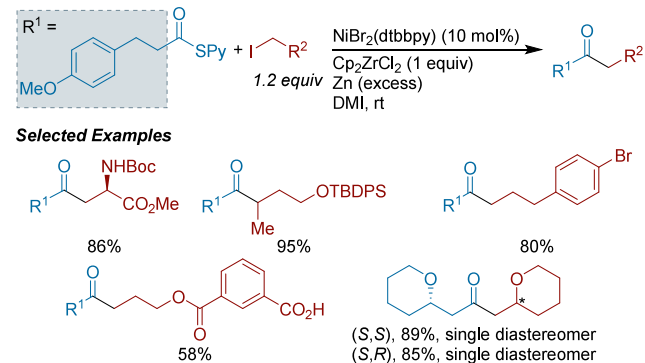
**Scheme 336.** Iron/Copper-Mediated Cross-Coupling of Alkyl Iodides and Alkyl Carboxylic Acid Derivatives (2017)<sup>a</sup>



<sup>a</sup>(a) Condition A:  $X = Cl$ ,  $Y = 3.0$ ,  $Z = 1.0$ ,  $Fe(TMHD)_3$  (10 mol%),  $CuCl_2$  (1 equiv). (b) Condition B:  $X = Cl$ ,  $Y = 1.0$ ,  $Z = 1.2$ ,  $FeBr_2(dppbz)$  (5 mol%),  $CuCl_2$  (1 equiv). (c) Condition C:  $X = 2$ -pyridyl thioester,  $Y = 1.2$ ,  $Z = 1.0$ ,  $FeBr_2(dppbz)$  (5 mol%),  $CuI$  (1 equiv),  $Cp_2ZrCl_2$  (1 equiv). (d) With  $FeBr_2(SciOPP)$  (5 mol%).

Shortly after, Kishi's lab developed a zirconium/nickel-mediated synthesis of unsymmetric alkyl ketones (Scheme 337).<sup>478</sup> In the presence of zinc reductant,  $Cp_2ZrCl_2$  accelerated coupling and suppressed side products from an  $S_N2$ -type displacement. The authors propose that  $Cp_2ZrCl_2$  assists with 1-electron activation of the alkyl iodide coupling partner, to generate an alkylzirconocene(III) complex. This complex then undergoes a transmetalation with an acylnickel

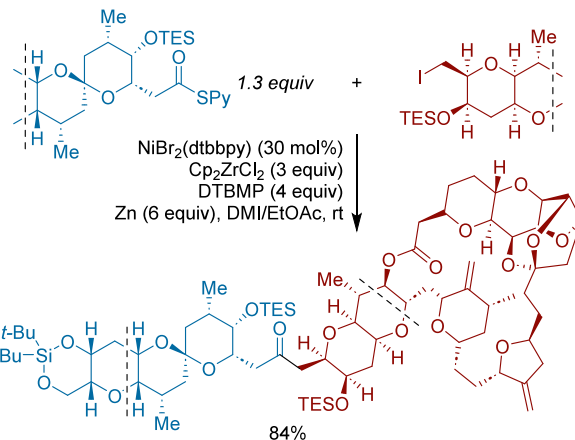
**Scheme 337.** Nickel/Zirconium Mediated Synthesis of Dialkyl Ketones from 2-Pyridyl Thioesters and Alkyl Iodides (2017)



(II) species to furnish the desired (alkyl)acylnickel(III) complex. In contrast to their previous Fe/Cu mediated ketone synthesis, these conditions were tolerant of coupling partners bearing an -OR functional group in the  $\alpha$ -position. Their scope included products isolated with perfect diastereoselectivity, providing support as a viable transformation for use in the total syntheses of the class of halichondrins.<sup>479</sup>

Submitted in tandem with this work, the Kishi's lab also reported the syntheses of nor-, homo-, and halichondrins A, B, and C.<sup>480</sup> The coupling shown in Scheme 338 was selected as

**Scheme 338.** Example Ketone Coupling using Alkyl iodide derived from Halichondrins B with Alkyl 2-Pyridyl Thioester (2017)<sup>a</sup>

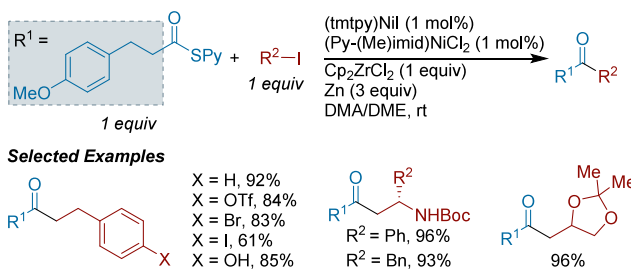


<sup>a</sup>DTBMP = 2,6-di-*tert*-butyl-4-methylpyridine

the model reaction, with 2,6-di-*tert*-butyl-4-methylpyridine (DTBMP) added to avoid partial deprotection of TES groups during the reaction. This coupling proceeded in high yield, providing motivation to proceed toward the synthesis of desired halichondrins. The desired halichondrin ketone precursors were isolated in high yields (average 85% across 9 examples).

Further studies by the Kishi lab into the nickel/zirconium-mediated coupling of alkyl 2-pyridyl thioesters and alkyl iodides found that a mixed catalyst system composed of nickel(I) and nickel(II) complexes resulted in improved yields with a 1:1 ratio of coupling partners and lower catalyst loading (Scheme 339).<sup>481</sup> The authors use modified conditions in a halichondrin synthesis, resulting in similar yields of ketone

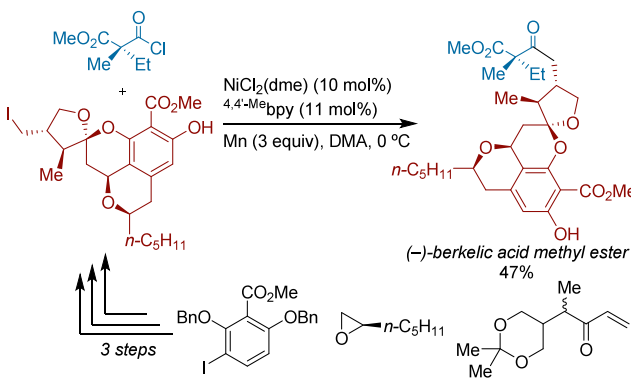
**Scheme 339.** Cross-Electrophile Coupling of Alkyl 2-Pyridyl Thioesters with Alkyl Iodides in a Two-Catalyst System (2019)



precursor to those reported in previous publications, but with a 1:1 ratio of coupling partners.

There have been several reports of the total synthesis of (−)-Berkelic Acid to date, characterized by the formation of a ketyl aldehyde and the Kiyooka aldol reaction (13 steps LLS, 2% overall yield),<sup>482</sup> Pd-catalyzed *ortho*-alkylation (11 steps LLS, 13.9% overall yield),<sup>483</sup> or a protected (10 steps LLS, 11–27% overall yield)<sup>484</sup> or protecting group-free silver-catalyzed cascade reaction (7 steps LLS, 12.5% overall yield).<sup>485,486</sup> Shuanglin Qu, Qianghui Zhou, and co-workers reported the concise synthesis of (−)-berkelic acid in eight linear steps.<sup>487</sup> A novel transformation of this total synthesis is the late-stage Ni-catalyzed cross-electrophile coupling to form the primary/tertiary unsymmetric dialkyl ketone (Scheme 340). The authors envisioned this disconnection between an

**Scheme 340.** Ni-Catalyzed Cross-Electrophile Coupling Step in the Total Synthesis of (−)-Berkelic Acid (2021)



alkyl halide and an acid chloride, and the resultant transformation proceeded in 47% yield of (−)-berkelic acid methyl ester. The mild reaction conditions ensured retention of any stereocenters previously set in the synthesis. Further work from Hong-Gang Cheng and Qianghui Zhou was able to decrease the reaction time from 10 to 5 h with no difference in yield.<sup>488</sup>

## 5. ALKYLATED ALKYNES

Currently, the cross-electrophile coupling of alkynyl electrophiles with alkyl radical precursors to generate C(sp)–C(sp<sup>3</sup>) bonds has been relatively under-explored. Several reasons could explain this situation: (1) alkyne nucleophiles are easier to access, (2) S<sub>N</sub>2 reactions of alkynyl nucleophiles with alkyl electrophiles are often high-yielding, and (3) Sonagashira coupling of terminal alkynes with alkyl electrophiles has also been reported.<sup>489</sup> Nevertheless, an XEC approach to access

these products could offer advantages, as alkynyl anions are both strong bases and nucleophiles, while alkynyl halides are straightforward to access from terminal alkynes.<sup>490–493</sup> Generally speaking, alkynyl bromides are more reactive than C(sp<sup>2</sup>)–Br species (alkynyl–Br > alkenyl–Br > aryl–Br), so the challenge remains effectively matching rates of activation of desired coupling partners. However, a number of challenges must be considered with the XEC of alkynyl electrophiles. The high reactivity of alkynyl electrophiles may hinder the overall selectivity of the reaction.<sup>494,495</sup> Second, the low steric bulk of alkynes allows for rapid transmetalation and the formation of homocoupled diynes. Lastly, alkynes can act as both radical acceptors and as ligands, leading to deleterious reactivity and/or catalyst death.<sup>496</sup>

The mechanisms invoked are typically analogous to those proposed for C(sp<sup>2</sup>)–C(sp<sup>3</sup>) XEC reactions (Figure 32), with

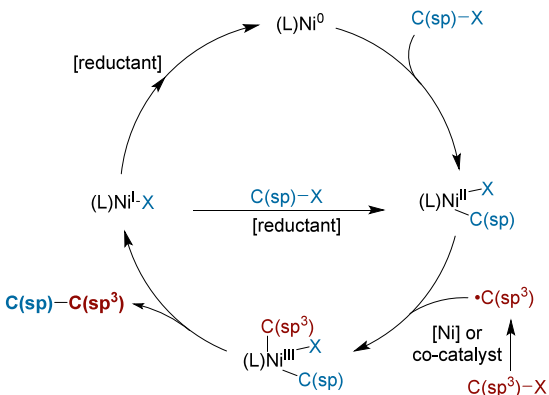


**Figure 32.** General mechanism for Ni-catalyzed cross-electrophile coupling to form C(sp)–C(sp<sup>3</sup>) bonds.

the alkynyl electrophile as the two-electron oxidative addition partner. However, mechanistic studies of these systems remain underdeveloped. For example, no alkynylnickel(II) species has been fully characterized to date.

Due to a smaller range of reports, current ligands used in C(sp)–C(sp<sup>3</sup>) reactions are limited to three bidentate nitrogen ligands, which are used in C(sp<sup>2</sup>)–C(sp<sup>3</sup>) reactions frequently (Figure 33). This is not to say that these ligands

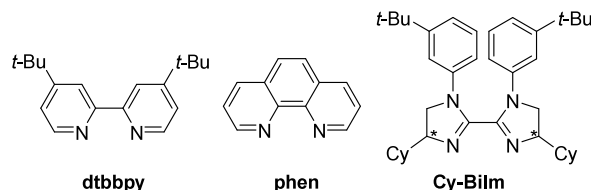
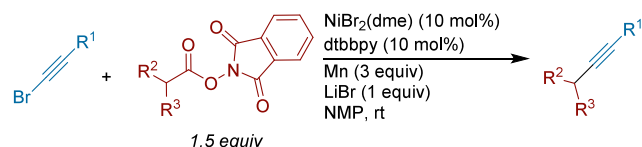


**Figure 33.** Ligands used in C(sp)–C(sp<sup>3</sup>) XEC reactions. \*Denotes chiral center.

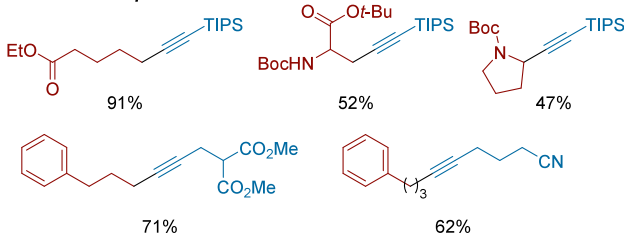
represent the full range of potential ligands in future C(sp)–C(sp<sup>3</sup>) XEC reactions; rather, it is likely that a range of ligands remain underexplored for this coupling type.

The use of alkynyl bromides in XEC was first reported in 2017 by our group, through the decarboxylative coupling of NHP esters with bromoalkynes (Scheme 341).<sup>496</sup> While initial conditions yielded primarily alkynyl homodimer (which appears to be due to transmetalation between two alkynylnickel(II) species), the addition of stoichiometric LiBr additive shut down this deleterious pathway and facilitated

**Scheme 341. Decarboxylative XEC of NHP Esters with Alkynyl Bromides (2017)**



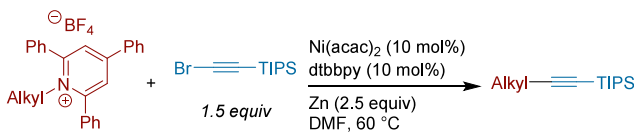
### **Selected Examples**



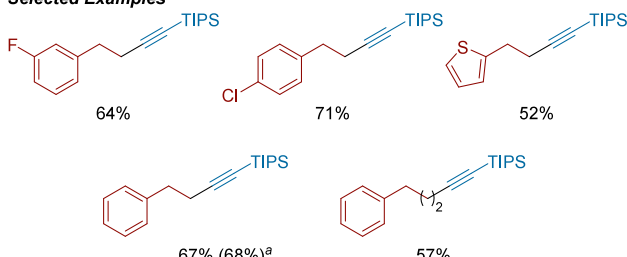
product formation. A variety of internal alkynes with good functional-group tolerance, including ketones, nitriles, secondary amides, and alkyl bromides. Running the reaction without nickel or ligand resulted in no consumption of alkynyl bromide, ruling out direct insertion of Mn into the alkynyl halide. Furthermore, studies into the possible nickel intermediates were investigated by separately reacting the two electrophiles with  $(dtbbpy)Ni^0(COD)$ . The resulting complexes were both able to form product when reacted with the complementary electrophile, indicating that an alkyl-first mechanism could be possible under these conditions. Synthetically, this approach engages alkyl carboxylic acids directly, providing a shorter sequence to alkylated alkynes compared to routes that require aldehyde intermediates.

Hong Yan, Yi Wang, Jianlin Han, and co-workers reported the cross-electrophile coupling of alkynyl bromides with *N*-alkyl pyridinium salts (**Scheme 342**).<sup>284</sup> The authors focused

**Scheme 342.** Ni-Catalyzed Deaminative XEC of Primary N-Alkyl Pyridinium Salts with Alkynyl Bromides (2019)<sup>a</sup>



### *Selected Examples*

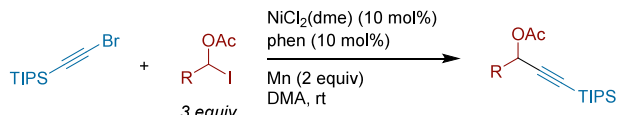


<sup>a</sup>With in situ generated N-alkylpyridinium.

on the coupling of TIPS-C≡C-Br, and they demonstrate that the *N*-alkyl pyridinium can be generated *in situ* without loss in yield. This report is part of a larger study that details the XEC of alkyl pyridinium salts with aryl, vinyl, and alkyl electrophiles to form C(sp<sup>2</sup>)—C(sp<sup>3</sup>) and C(sp<sup>3</sup>)—C(sp<sup>3</sup>) bonds, as outlined in **Schemes 166** and **369**, respectively.

Rueping, Hufeng Yue, and co-workers reported the Ni-catalyzed cross-electrophile coupling of alkynyl bromides with  $\alpha$ -acetoxy iodides to form products resembling those made through alkynyl nucleophile addition to aldehydes ([Scheme 343](#)).<sup>378</sup> These iodide substrates form a ketyl radical which can

**Scheme 343. Ni-Catalyzed XEC of  $\alpha$ -Acetoxy Iodides with Alkynyl Bromides (2022)**



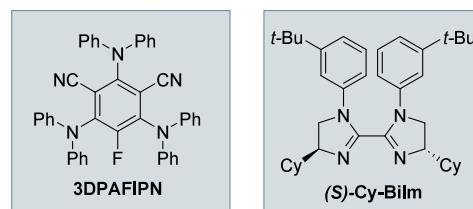
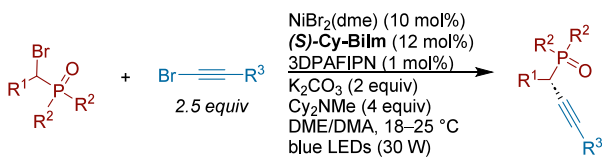
### **Selected Examples**



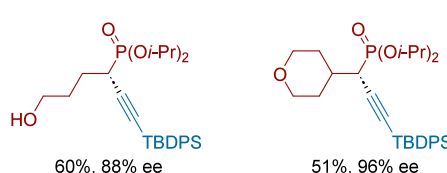
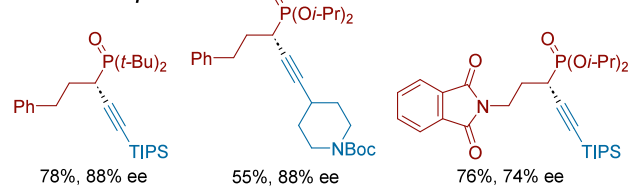
be captured by the nickel catalyst and undergo reductive elimination. This report primarily focused on the coupling of  $\alpha$ -oxy iodide substrates with aryl (see [section 4.2.3.1, Scheme 160](#)), vinyl, and acyl halide electrophiles under various approaches. Two examples of XEC on alkynyl bromides were included in this study.

Tao Xu and colleagues reported the first enantioconvergent coupling of alkynyl bromides with  $\alpha$ -bromo phosphonates to form enantioenriched  $\alpha$ -chiral phosphonates (**Scheme 344**).<sup>497</sup> This method utilized an organic photoredox cocatalyst (3DPAFIPN), as attempts to use zerovalent metal reductants (e.g., Zn, Mn) provided low yields ( $\leq 7\%$ ). Mechanistic studies

**Scheme 344. Enantioconvergent XEC of  $\alpha$ -Bromo Phosphonates with Alkynyl Bromides (2023)**



### ***Selected Examples***



are consistent with radical generation mediated by the photocatalyst instead of nickel. Overall, the method was able to engage variety of silylated, alkylated, and arylated alkyne bromides. The synthetic utility was highlighted in a gram scale synthesis (70%, 90% ee) of the model substrate, and a series of product derivatizations at the phosphorus and alkyne sites.

## 6. C(sp<sup>3</sup>)–C(sp<sup>3</sup>) Bond Formation

### 6.1. Overview

The use of two C(sp<sup>3</sup>) coupling partners to generate C(sp<sup>3</sup>)–C(sp<sup>3</sup>) bonds has not been as widely demonstrated compared to other sections within this review. The coupling of two C(sp<sup>3</sup>) electrophiles is challenging because of additional side reactions ( $\beta$ -hydride elimination) and because some of the elementary steps become more difficult or complex (oxidative addition, reductive elimination). Thus, matching the rates of radical generation, radical capture, and C(sp<sup>3</sup>) oxidative addition of alkyl halides or pseudohalides, are crucial to achieving cross-selectivity.

**6.1.1. Substrates and Organization.** In comparison to cross-electrophile coupling methods involving the formation of C(sp<sup>2</sup>)–C(sp<sup>3</sup>) bonds, more diverse and tunable radical sources, such as oxalates, pyridinium salts, N-hydroxypthalimide esters or other redox active esters, are frequently utilized in this area. Additionally, alkyl halides/pseudohalides are also attractive reagents for these transformations, as they are generally commercially available or easily prepared via robust reactions (e.g., Appel reaction of alcohols, or displacement of alkyl tosylates/mesylates by the corresponding halide). Specifically, alkyl mesylates and alkyl tosylates are usually unreactive toward nickel, allowing for controlled formation of reactive intermediates (usually via in situ exchange with halide salts). This section will discuss the use of alkyl electrophiles in both intramolecular (ring formation/contraction) and intermolecular reactions to generate allyl-, benzyl-, and alkyl–alkyl bonds.

**6.1.2. Catalysts and Ligands.** Typical ligands employed for this reaction class involve L-type ligands such as amines and phosphines, similar to those utilized in other sections of this review (Figures 34 and 35). Multidentate amine ligands have complex redox activity, enabling radical generation.<sup>181</sup> In contrast, fewer examples of alkyl radical generation exist for phosphine complexes. In comparison to amines, phosphine ligands were most successful in facilitating ring formation and polar–polar type mechanisms discussed in section 6.2, Intramolecular C(sp<sup>3</sup>)–C(sp<sup>3</sup>) XEC.

**6.1.3. Mechanisms.** In the Ni-catalyzed XEC of two alkyl electrophiles, three primary general mechanisms are proposed: (1) a mechanism with two different radicals, where the ordering and selectivity depend on both the inherent reactivity of the radicals and on the catalyst (Figure 36); (2) a mechanism involving a nonradical oxidative addition of one C(sp<sup>3</sup>) substrate (allyl, benzyl) and an alkyl radical (Figure 37); and (3) a mechanism involving only polar, nonradical steps (Figure 38).

The two-radical mechanism (Figure 36) has a central challenge of obtaining selectivity from two different radicals. However, for certain pairs of substrates, where the rate of formation of the two radicals is matched and one of the radicals is slow to self-couple, high selectivities can be achieved.<sup>112</sup> Balancing the rate of radical generation presents its own challenges and opportunities because there are a

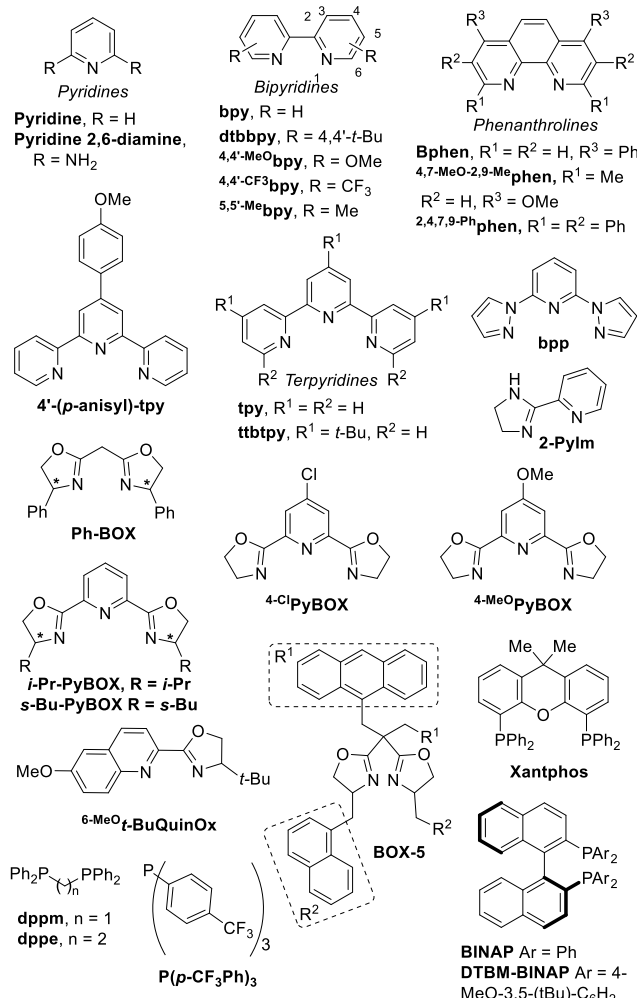


Figure 34. Ligands used in C(sp<sup>3</sup>)–C(sp<sup>3</sup>) XEC reactions. \*Denotes chiral center.

number of possibilities for radical generation: (L)Ni<sup>0</sup>, (L)Ni<sup>I</sup>X, (L)Ni<sup>I</sup>(Csp<sup>3</sup>), and even the reductant.

For allylic and benzylic electrophiles with oxygen-based leaving groups, nonradical oxidative addition to form an allylmetal or benzylmetal intermediate (Figure 37) enables a mechanistic pathway similar to that commonly invoked in C(sp<sup>2</sup>)–C(sp<sup>3</sup>) bond formation (Figure 22).<sup>309</sup>

Finally, studies on ring contraction reactions have demonstrated the possibility of a completely nonradical mechanism that proceeds by two S<sub>N</sub>2-type oxidative addition steps to yield the desired product (Figure 38).<sup>498</sup> In a few of these reactions, that use methyl Grignard reagent as the terminal reductant, undesired Kumada cross-coupling is an additional potential side reaction.

### 6.2. Intramolecular C(sp<sup>3</sup>)–C(sp<sup>3</sup>) XEC

**6.2.1. Ring-Forming Reactions.** In 2014, Hegui Gong, Qun Qian and co-workers developed an intramolecular cross-electrophile coupling strategy for the construction of 5- and 6-membered rings from the corresponding dihaloalkanes. (Scheme 34S).<sup>499</sup> The reaction was compatible with primary bromides, primary iodides, and benzylic chlorides. The formation of five- and six-membered rings was found to be most efficient, while smaller ring sizes were challenging (attributed to ring strain of the products). Additionally, attempts to form three- and four-membered rings under the

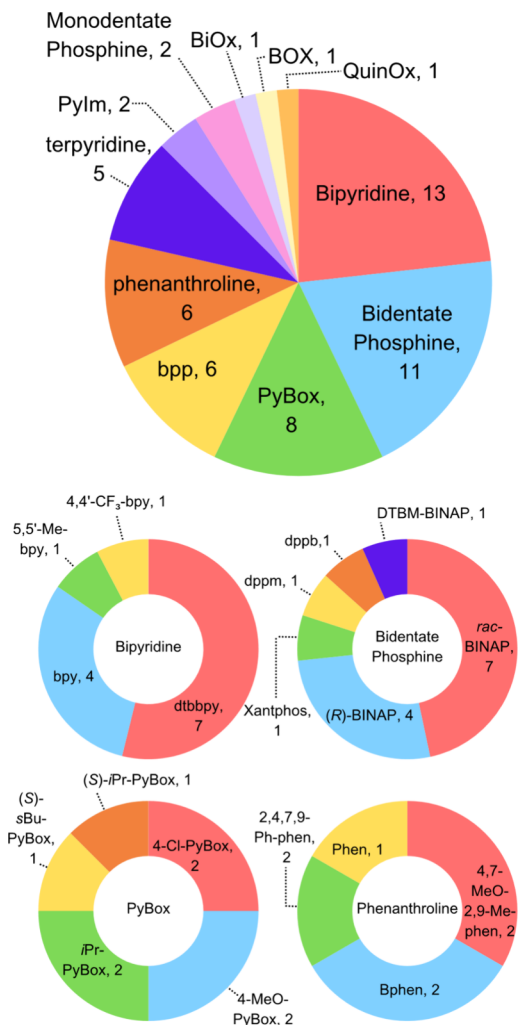


**Figure 35.** Distribution of ligands used in  $C(sp^3)-C(sp^3)$  XEC reactions.

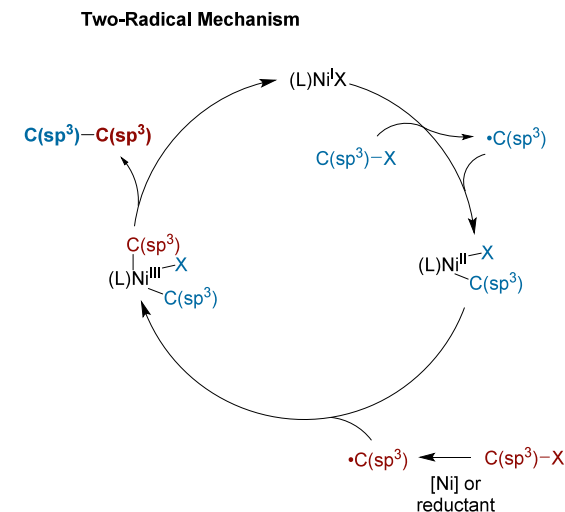


**Figure 36.** Two-radical mechanism for  $C(sp^3)-C(sp^3)$  bond formation. Alkyl radicals could be generated via low valent Ni species, reductants, or by other means.

reaction conditions resulted in oligomerization or  $\beta$ -hydride elimination side products

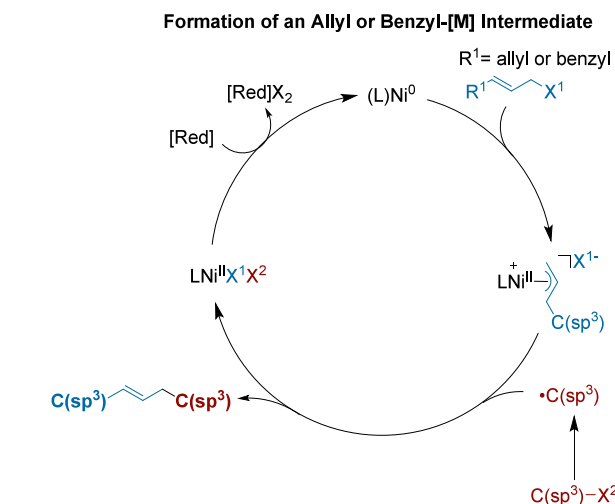


**Figure 37.** Polar/radical mechanism for  $C(sp^3)-C(sp^3)$  bond formation.

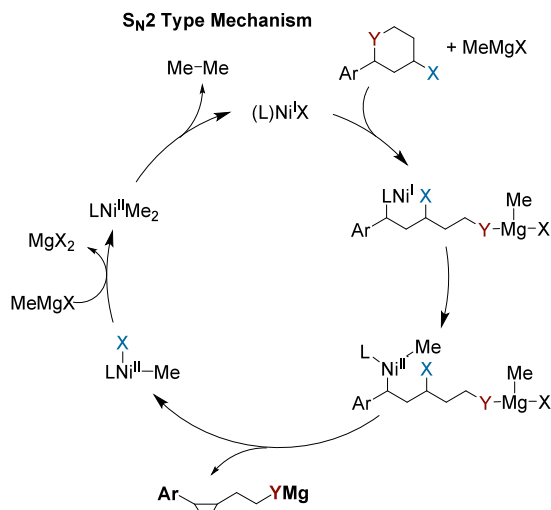
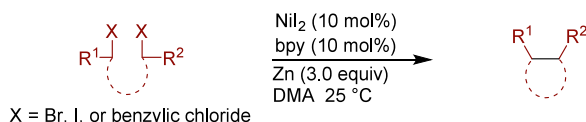


**Figure 38.**  $S_N2$ -type mechanism of a nickel(II) species to generate  $C(sp^3)-C(sp^3)$  strained ring systems.

#### Scheme 345. Intramolecular Ni-Catalyzed XEC Cyclization of Alkyl Dihalides (2014)<sup>a</sup>



#### Selected Examples

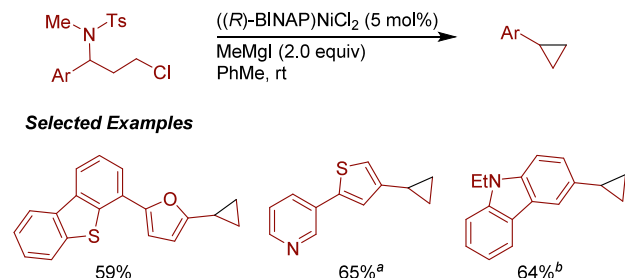


<sup>a</sup>(a)  $X = Br$ . (b)  $X = I$ . (c) With DMA/1,4-dioxane as solvent. (d)  $X = Cl$ .

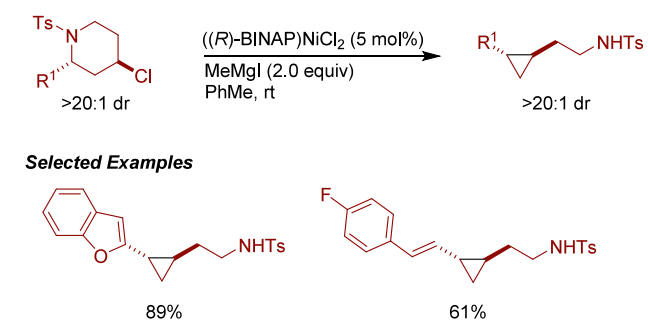
In 2020, the Jarvo and Xin Hong groups reported the Ni-catalyzed formation of cyclopropanes from the intramolecular XEC of benzylic sulfonamides with alkyl chlorides (Scheme 346).<sup>498</sup> This reaction featured the relatively rare case of a

**Scheme 346. Ni-Catalyzed XEC to Form Cyclopropanes by Intramolecular Coupling of Alkyl Sulfonamides with C–Cl Bonds (2020)<sup>a</sup>**

**Synthesis of Mono-substituted Cyclopropanes**



**Ring Contraction of *N*-Ts Piperidines**



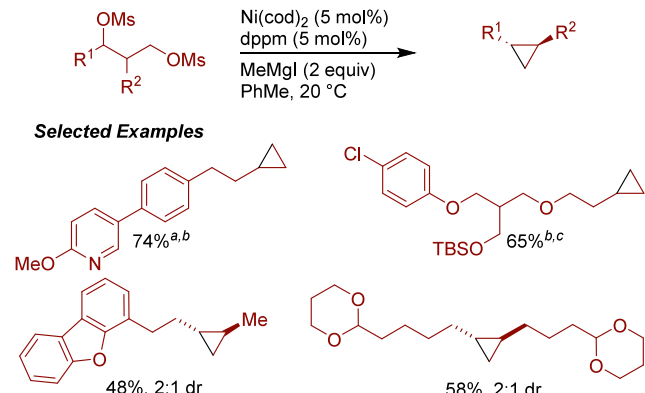
<sup>a</sup>(a) With  $\text{MgI}_2$  (1.0 equiv) added. (b) With  $\text{MgI}_2$  (1.5 equiv) added.

sulfonamide-based coupling partner in XEC. For acyclic benzylic sulfonamides, monosubstituted cyclopropanes were generated with a variety of heterocycles appended. Subjecting *N*-tosyl-4-chloropiperidines to the same reaction conditions resulted in disubstituted cyclopropanes with a pendant protected amine in excellent diastereoselectivity (>20:1 dr). DFT calculations suggest that Mg salts generated from the  $\text{MeMgI}$  reductant (and in some cases from additional  $\text{MgI}_2$  added to the reaction) activate the C–N bond for oxidative addition.

The Jarvo and Xin Hong groups then reported the Ni-catalyzed synthesis of mono- and disubstituted 1,2-cyclopropanes from 1,3-dimesylates (Scheme 347).<sup>500</sup> For branched and aryl cyclopropane substrates, dppm served as the optimal ligand, while *rac*-BINAP provided higher yields for unbranched products.  $\text{MeMgI}$  served a dual role as the reductant and as a halide exchange reagent, converting the dimesylate into the diiodide in situ. When a model diiodide was isolated and subjected to XEC conditions, the cyclopropane product was obtained in 71% yield. DFT studies suggested that the secondary carbon center is engaged by the nickel catalyst faster compared to the primary carbon center; this proposal was confirmed by competition experiments. Lastly, this method was shown to be stereoconvergent for the *trans*-isomer regardless of the stereochemistry of the starting material.

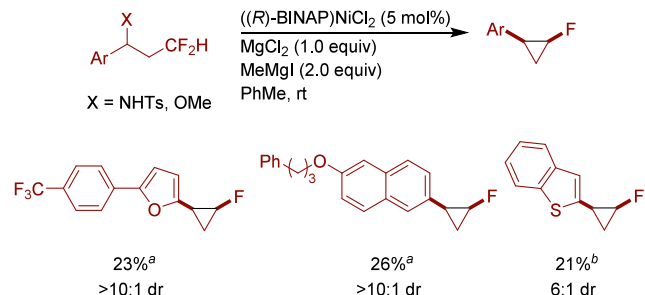
In 2021, the Jarvo group reported the Ni-catalyzed formation of fluorinated *cis*-cyclopropanes from 3,3-difluoro-1-arylsulfonamides/ethers (Scheme 348).<sup>501</sup> DFT studies suggested that *cis*-isomer of the cyclopropane product is the favored and more stable isomer due to stronger hyperconjugation interactions. Lower overall yields were attributed to the difficulty of breaking the strong C–F bond, as well as

**Scheme 347. Ni-Catalyzed XEC Synthesis of Disubstituted Cyclopropanes from 1,3-Dimesylates (2020)<sup>a</sup>**



<sup>a</sup>(a) With *rac*-BINAP (5 mol%) as ligand. (b) With  $\text{CH}_2\text{Cl}_2/\text{PhMe}$  as solvent. (c) At 0 °C.

**Scheme 348. Synthesis of *cis*-Monofluorinated Cyclopropanes by Intramolecular Ni-Catalyzed XEC with a Difluoromethyl Group (2021)<sup>a</sup>**



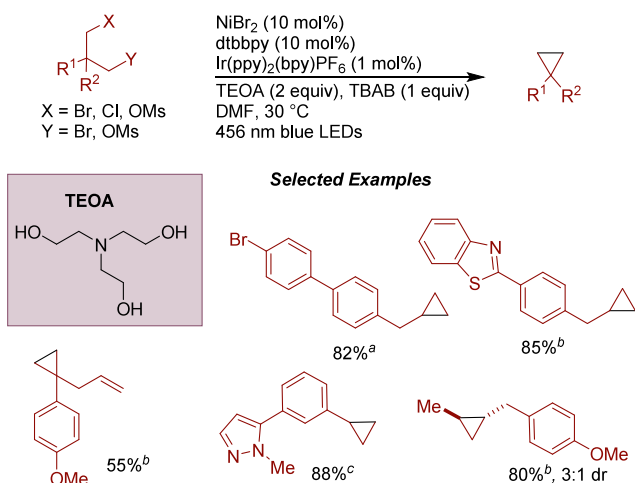
<sup>a</sup>(a) X = NHTs. (b) X = OMe.

competitive Kumada cross-coupling and  $\beta$ -hydride elimination side reactions.

Maji and co-workers reported Ni/Ir photochemical, intramolecular XEC of 1,3-alkyl dihalides to prepare functionalized cyclopropanes (Scheme 349).<sup>502</sup> The reaction showed compatibility with alkyl bromides, chlorides, and mesylate electrophiles, due to posited *in situ* formation of a common 1,3-dibromide intermediate, similar to proposals previously described by Jarvo.<sup>503</sup> The authors showed that 1,1- and 1,2-disubstituted cyclopropanes could be synthesized (the latter in 3:1 dr). One pot mesylation and ring closure of a diol was also demonstrated.

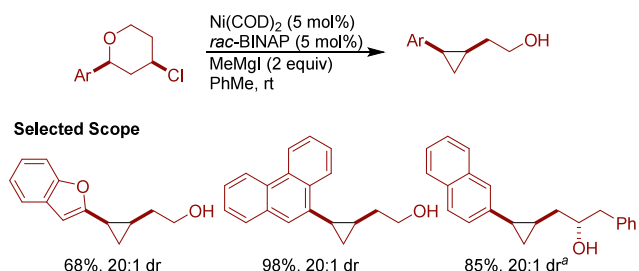
**6.2.2. Ring-Contracting Reactions.** In 2015, the Jarvo group reported a Ni-catalyzed ring contraction of tetrahydropyrans for the synthesis of *cis*-cyclopropanes (Scheme 350).<sup>504</sup> The nickel catalyst is proposed to undergo oxidative addition with the benzylic C–O bond followed by cleavage of the C–Cl bond. In contrast to reports on XEC at that time, these reactions are stereospecific: *cis*-tetrahydropyrans generate *cis*-cyclopropanes. The Grignard reagent reduces the metal center after two transmetalation steps in which a nickel(II) species then undergoes reductive elimination to release ethane, effectively turning over the catalyst. Reactions run with enantioenriched substrates showed that the reaction proceeds with net retention at the benzylic position, while the alkyl chloride reacts with net inversion. Trisubstituted

**Scheme 349. Intramolecular Ni and Ir Co-Catalyzed Photoredox XEC to Synthesize Cyclopropanes from 1,3-Di(pseudo)halides (2022)<sup>a</sup>**



<sup>a</sup>(a) With  $X$  and  $Y = \text{OMs}$ . (b) With  $X$  and  $Y = \text{Br}$  and  $\text{TBACl}$  instead of  $\text{TBABr}$ . (c) With  $X = \text{Cl}$ ,  $Y = \text{OMs}$ .

**Scheme 350. Ni-Catalyzed Formation of Disubstituted Cyclopropanes by Ring Contraction of 4-Chlorotetrahydropyrans (2015)<sup>a</sup>**

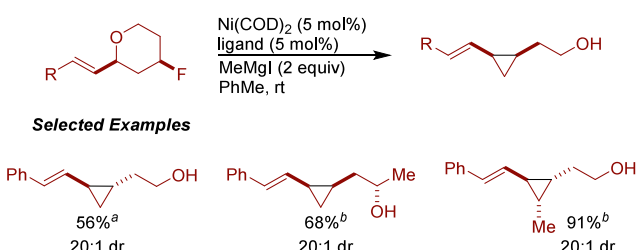


<sup>a</sup>With  $\text{MgI}_2$  (1 equiv) added.

tetrahydropyrans were also successfully obtained using this method.

The Jarvo group expanded their tetrahydropyran ring contraction strategy to include the stereospecific synthesis of vinylcyclopropanes by the cleavage of C–O and C–F bonds (Scheme 351).<sup>505</sup> As in their preceding study (Scheme 350), this XEC reaction proceeded with excellent stereospecificity. Yields could be improved by variation of the ligand between *rac*-BINAP, bpp, Xantphos, bpy, phen, and Bphen. Trisub-

**Scheme 351. Intramolecular Ring Contraction of Tetrahydropyrans via XEC of an Allylic Ether with an Alkyl Fluoride (2016)<sup>a</sup>**

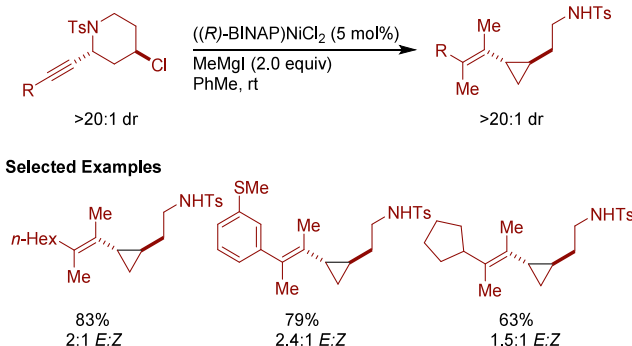


<sup>a</sup>(a) With *rac*-BINAP (5 mol%). (b) With Xantphos (5 mol%).

stituted tetrahydropyrans were shown to generate 1,2,3-trisubstituted cyclopropanes, and 2-vinyltetrahydrofurans could effectively generate hydroxymethylcyclopropanes. In a systematic follow-up study, the ability of ligands to change the reaction outcome was attributed to switching the preference of nickel between 1-electron and 2-electron pathways.<sup>506</sup>

Later studies from the Jarvo and Xin Hong groups led to the development of a novel domino reaction that combined an intramolecular stereospecific XEC with dicarbofunctionalization (Scheme 352).<sup>503</sup> The optimal conditions utilized a [(*R*)-

**Scheme 352. Ni-Catalyzed Domino XEC to Synthesize Vinylcyclopropanes (2021)**

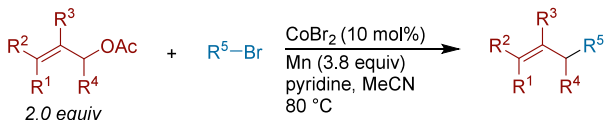


BINAP]nickel(II) precatalyst, consistent with their previous reports on XEC with alkylsulfonamides (Scheme 346). Synthetic utility was demonstrated in the derivatization of cyclopropane products into LSD1 inhibitor analogues, of which several were potent to various cancer cell lines. Stoichiometric studies were consistent with oxidative addition of the nickel catalyst into the propargylic sulfonamide to form an allenylnickel(II) species as the initiating step in the catalytic sequence. Extensive DFT calculations were used to probe the reaction mechanisms, origins of observed *E/Z* isomeric mixtures and, stereoselectivity. Ultimately, the computed free energy profiles illustrated two competing pathways at the key zwitterionic allenylnickel(II) intermediate. Transmetalation could generate an allenylnickel(II)methyl which readily undergoes  $S_{\text{N}}2'$  addition to form the *Z*-alkene-substituted cyclopropane. Alternatively, anticarbometalation to form a nickelacylcobutene could occur prior to cyclopropane formation, which leads to the *E*-alkene. The two pathways only have a 0.5 kcal/mol computed free-energy difference, accounting for the low *E/Z* selectivity. Furthermore, transition state calculations support the observation of the stereoreactive product through a double inversion mechanism ( $S_{\text{N}}2'$ -like oxidative addition followed by  $S_{\text{N}}2'$ -type addition to form the cyclopropane).

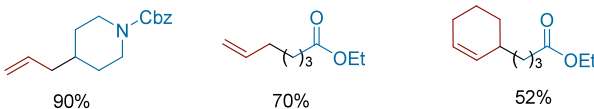
### 6.3. Intermolecular $C(sp^3)$ – $C(sp^3)$ XEC

**6.3.1. Allyl–Alkyl Bond Formation.** In 2011, Gosmini and co-workers reported a cobalt-catalyzed cross-electrophile coupling of substituted allylic acetates with primary, secondary, and tertiary alkyl bromides (Scheme 353).<sup>507</sup> The conditions were effective for the allylation of 1°, 2°, and 3° alkyl bromides. Substituted allylic acetates were also well-tolerated. Sterically hindered allylic carbonates were tolerated when paired with primary alkyl bromides but gave no product for secondary alkyl bromides. To promote efficient coupling of  $\alpha$ -halocarbonyl and benzyl chloride substrates, allylic methyl carbonates were used

**Scheme 353. Cobalt-Catalyzed XEC of Alkyl Bromides with Allylic Acetates and Carbonates (2011)**



**Selected Examples**



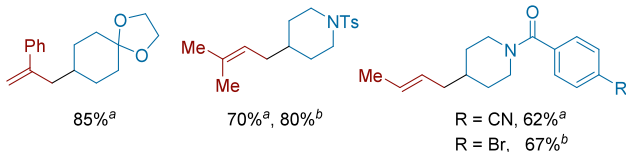
instead of allylic acetates. The reaction was generally selective for the formation of linear products over branched products.

Hegui Gong and co-workers described a Ni-catalyzed XEC of substituted allylic carbonates with secondary alkyl bromides and iodides, providing (*E*)-alkenes in good yield and regioselectivity for the linear product (Scheme 354).<sup>508</sup> A

**Scheme 354. Ni-Catalyzed XEC of Allylic Carbonates with Alkyl Bromides (2012)<sup>a</sup>**



**Selected Examples**



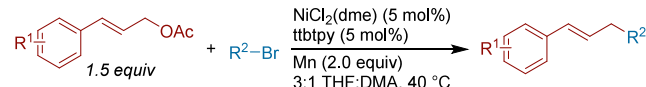
<sup>a</sup>(a) Conditions A: With X = Br, Ni(COD)<sub>2</sub> (10 mol%), tbtpy (10 mol%), Zn (3 equiv), MgCl<sub>2</sub> (1.5 equiv), DMA at 80 °C. (b) Conditions B: With X = I, Ni(COD)<sub>2</sub> (10 mol%), (S)-i-Pr-PyBOX (15 mol%), Zn (3 equiv), CuI (30 mol%), DMA at 35 °C.

CuI additive was found to improve the yield for alkyl iodide substrates, appearing to inhibit deleterious side-reactions of the alkyl iodide such as hydrodehalogenation and  $\beta$ -hydride elimination. For alkyl bromides, modified conditions with stoichiometric MgCl<sub>2</sub> as additive suppressed these byproducts.

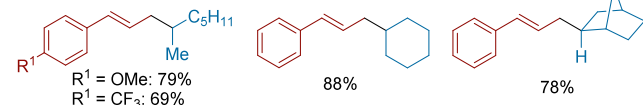
In our 2012 report detailing the Ni-catalyzed XEC of allylic acetates and aryl bromides, (see section 4.2.5.5, Scheme 194), conditions for the XEC of allylic acetates with secondary alkyl bromides were also disclosed. (Scheme 355).<sup>309</sup> Under these conditions, primary alkyl bromides were incompatible due to competing rapid dimerization by the terpyridine nickel catalyst.<sup>38</sup>

Our group reported a Ni-catalyzed XEC approach to homoallylic amines from allylic acetates and  $\alpha$ -amido sulfone precursors. (Scheme 356).<sup>509</sup> Using either Et<sub>3</sub>N (catalytic) or Cs<sub>2</sub>CO<sub>3</sub> (stoichiometric), the imines could be readily formed in situ from the  $\alpha$ -amido sulfone. The reaction was tolerant of primary and secondary alkyl substitution adjacent to the nitrogen, but tertiary and aryl substituted sulfones exhibited decreased yields. High diastereoselectivity was observed for cinnamyl acetate derivatives, and branched homoallylic amines were typically favored compared to linear products. Running the reaction with stoichiometric Ni(COD)<sub>2</sub> and dtbbpy in the

**Scheme 355. Ni-Catalyzed XEC of Alkyl Bromides with Allylic Acetates (2012)**



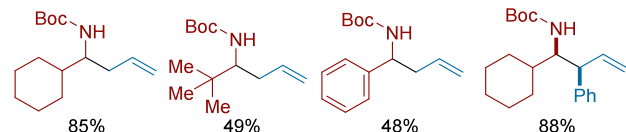
**Selected Examples**



**Scheme 356. Ni-Catalyzed XEC of  $\alpha$ -Amido Sulfones with Allylic Acetates (2015)**



**Selected Examples**

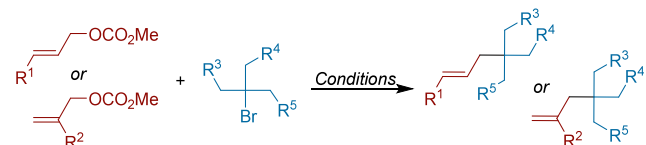


<sup>a</sup>PG = protecting group.

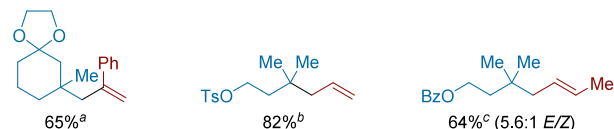
absence of Mn afforded product in 60% yield, ruling out the formation of allylmanganese intermediates.

In 2017, Hegui Gong and co-workers reported a Ni-catalyzed XEC of tertiary alkyl bromides with allylic carbonates to generate all-carbon quaternary centers (Scheme 357).<sup>510</sup>

**Scheme 357. Ni-Catalyzed XEC of Tertiary Alkyl Bromides with Allylic Carbonates (2017)<sup>a</sup>**



**Selected Examples**



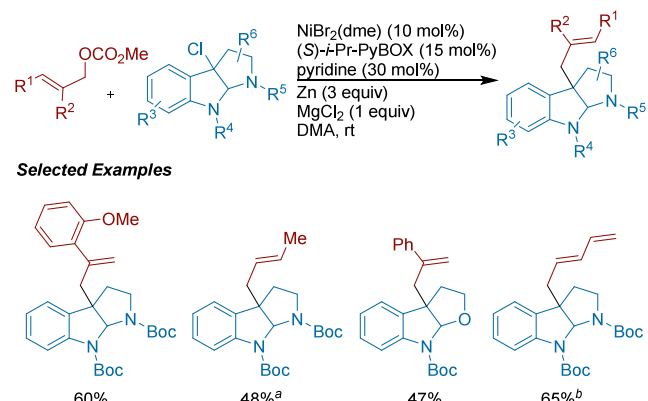
<sup>a</sup>(a) Conditions A: With NiBr<sub>2</sub>(dme) (10 mol%), (S)-i-Pr-PyBOX (15 mol%), pyridine (30 mol%), MgCl<sub>2</sub> (1 equiv), Zn (3 equiv), DMA at 25 °C. (b) Conditions B: With Ni(COD)<sub>2</sub> (10 mol%), dtbbpy (15 mol%), pyridine-2,6-diamine (30 mol%), MgCl<sub>2</sub> (1 equiv), Zn (3 equiv), DMA at 25 °C. (c) Conditions C With NiBr<sub>2</sub>(diglyme) (10 mol%), 4,7-MeO-2,9-Mephen (15 mol%), pyridine-2,6-diamine (30 mol%), MgBr<sub>2</sub> (1 equiv), Mn (3 equiv) in DMA at 25 °C.

"Conditions A" were determined to be the most general for the coupling of tertiary alkyl bromides. However, these conditions were not optimal for allylic carbonates bearing substituents at the 3-position, and the ligand system had to be swapped to a combination of dtbbpy and pyridine-2,6-diamine for improved yields. The reaction was generally selective for the linear

products, and the choice of ligand had a notable impact on regioselectivity. Changing to electron-rich and sterically hindered *4,7-MeO-2,9-Me*-phen as ligand could be used to enhance *E/Z* ratios of products with olefin geometry.

The XEC of allylic carbonates with tertiary alkyl electrophiles was extended to chloro-cyclotryptamines soon thereafter by Hegui Gong, Ken Yao, Qun Qian, and co-workers (**Scheme 358**).<sup>511</sup> This report focused on expanding the scope of their

**Scheme 358. Synthesis of Quaternary Centers from Chloro-Cyclotryptamines and Allylic Carbonates (2018)<sup>a</sup>**

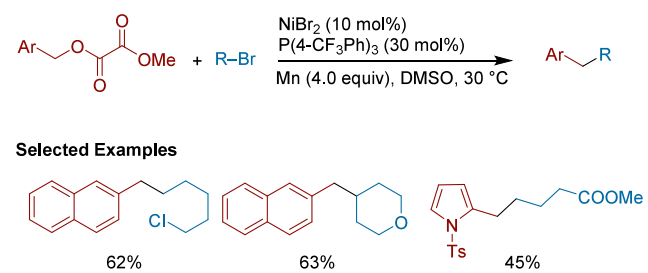


<sup>a</sup>(a) Modified Conditions: NiBr<sub>2</sub>(dme) (10 mol%), *4,7-MeO-2,9-Me*-phen (15 mol%), pyridine-2,6-diamine (30 mol%), MgBr<sub>2</sub> (1 equiv), Mn (3 equiv) in DMA at 25 °C. (b) With bromo-cyclotryptamine and *4,7-MeO-2,9-Me*-phen (15 mol%) as ligand.

previous report (**Scheme 357**). The authors additionally show modified conditions for (*E*)-pentadienyl carbonate substrates with tertiary alkyl bromides. Finally, an example of strained ring XEC was demonstrated with methyl 1-bromocyclopropane-1-carboxylate with an allylic carbonate.

**6.3.2. Benzyl–Alkyl Bond Formation.** In 2018, Xing-Zhong Shu and colleagues reported a Ni-catalyzed XEC of benzyl oxalates with primary and secondary alkyl bromides (**Scheme 359**).<sup>512</sup> An electron-poor triaryl phosphine was the

**Scheme 359. Ni-Catalyzed XEC of Primary Benzyl Oxalates with Alkyl Bromides (2018)**

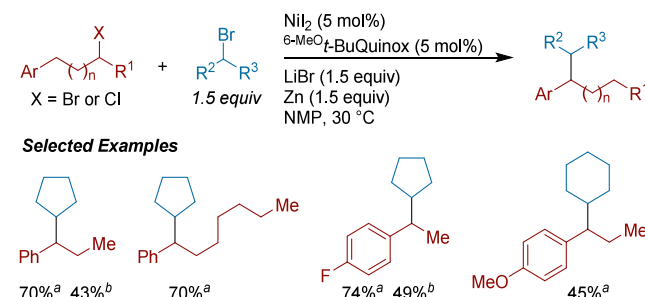


most effective ligand for this transformation, and a DMSO/DMF solvent combination helped to limit formation of benzyl alcohol side products while maintaining solubility. The scope for alkyl bromide substrates was broad, containing a variety of functional groups including phosphonate esters, amines, aldehydes, amides, borates, and free alcohols. Later mechanistic studies from Hegui Gong suggested that an oxidative addition process of primary benzylic oxalates by the nickel catalyst is possible.<sup>307</sup> They ran the reaction with stoichio-

metric Ni(COD)<sub>2</sub> and phosphine ligand with reductant omitted, which still generated ~15% of cross-coupled product.

In 2020, Guoyin Yin, Lei Zhu, and co-workers developed a Ni-catalyzed migratory XEC of primary and secondary alkyl bromides for the synthesis of alkylated benzyl products (**Scheme 360**).<sup>513</sup> It was observed that electron-donating and

**Scheme 360. Ni-Catalyzed Migratory XEC of Alkyl Halides (2020)<sup>a</sup>**

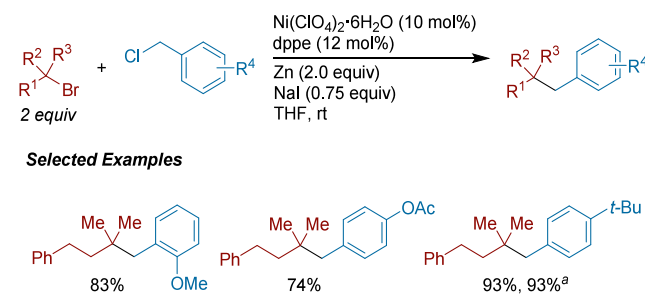


<sup>a</sup>(a) With X = Br, (b) With X = Cl

withdrawing groups on the arene were tolerated for this transformation. Primary alkyl chlorides could also be employed, albeit in lower yields. The identity of the secondary alkyl bromides was limited to carbocyclic substrates with a notable loss of yield being observed for acyclic and heterocyclic alkyl bromides. Deuterium-labeling experiments confirmed migration of the deuterium and supported chain-walking occurring in both coupling partners.

In 2021, Hegui Gong, Deli Sun, and co-workers published a method for the XEC of tertiary alkyl bromides with benzylic chlorides and chloroformates (**Scheme 361**).<sup>514</sup> Using dppe as

**Scheme 361. Ni-Catalyzed XEC of Benzyl Chlorides with Tertiary Alkyl Bromides (2021)<sup>a</sup>**

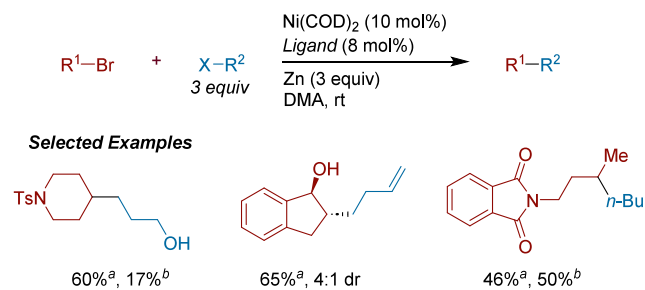


<sup>a</sup>With benzylic chloroformate instead of benzylic chloride.

a ligand, high yields were obtained for electron-rich benzyl chlorides and benzyl chloroformates, while low to moderate yields were observed for electron poor benzylic coupling partners. Both cyclic and acyclic tertiary alkyl bromides were competent substrates. A control reaction using a preformed Bn–ZnCl reagent and alkyl bromide under catalytic conditions provided only trace cross-product, ruling out a Neigishi-type mechanism.

**6.3.3. Alkyl–Alkyl Bond Formation.** In 2011, Hegui Gong and co-workers reported a Ni-catalyzed XEC between two alkyl halides (**Scheme 362**).<sup>515</sup> PyBOX ligands were more efficient than other tridentate amine ligands in promoting the differentiation of the two coupling partners over homocoupling. For benzyloxy and phenyl tethered primary alkyl halides,

**Scheme 362.** Ni-Catalyzed XEC of Alkyl Bromides with Alkyl Iodides and Bromides (2011)<sup>a</sup>

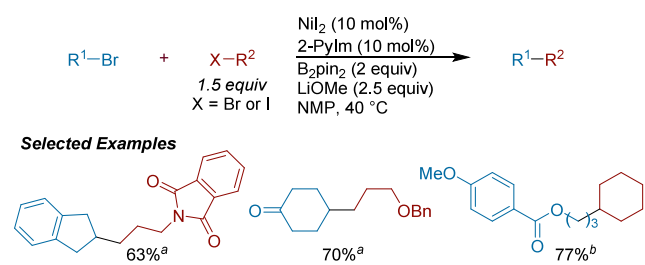


<sup>a</sup>(a) With X = Br, <sup>4-Cl</sup>PyBOX (8 mol%). (b) With X = I, (*S*)-*s*-BuPyBOX (8 mol%).

bromides were more efficient than the corresponding alkyl iodides.  $1^\circ$ - $1^\circ$ ,  $2^\circ$ - $1^\circ$ , and  $2^\circ$ - $2^\circ$   $C(sp^3)-C(sp^3)$  bond linkages were all made through this approach. In order to mitigate formation of homocoupling byproducts, an excess amount of one coupling partner (3 equiv) was typically required for good yields. At the time, mechanistic studies indicated that reactions with alkyl bromides were unlikely to proceed via *in situ* formation of organozinc species.

Two years later, Hegui Gong and colleagues reported a further advance in the Ni-catalyzed XEC of two unactivated alkyl halides (**Scheme 363**).<sup>52</sup> In contrast to heterogeneous

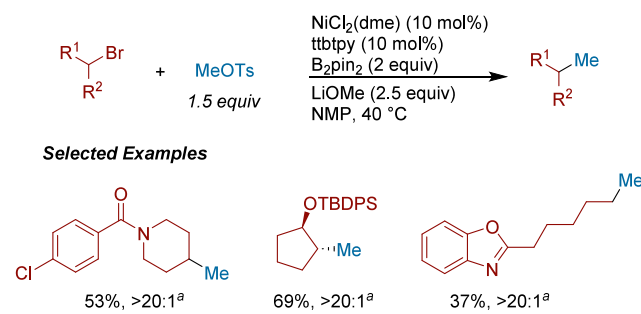
**Scheme 363.** Ni-Catalyzed XEC of Alkyl Halides Using B<sub>2</sub>pin<sub>2</sub> as Reductant (2013)<sup>a</sup>



metal powder such as Zn or Mn, bis(pinacolato)diboron ( $B_2pin_2$ ) was used as the terminal reductant, representing the first demonstration of this homogeneous reductant in Ni-catalyzed XEC. Additionally, this reductant helped improve cross-selectivity for the coupling of secondary alkyl bromides with primary alkyl bromides compared to their previous Ni/Zn catalytic conditions. (Scheme 362). The authors proposed that the selectivity originates from the Ni–Bpin intermediate, which can differentiate the two alkyl halides based on steric hindrance and reactivity. Subjecting the preformed alkyl–Bpin to reaction conditions did not result in cross-coupling, supporting that an *in situ* Suzuki process was unlikely.

In 2014, Hegui Gong, Kunhua Lin and co-workers achieved the methylation of secondary and primary alkyl bromides with MeOTs using a (ttbtpy)nickel catalyst system.<sup>438</sup> A variety of functional groups are tolerated including indoles, protected alcohols and amines, aryl chlorides, and carbonyls (**Scheme 364**). Free sulfonamides and sterically hindered primary alkyl bromides resulted in lower yields. This method was extended to the methylation of acid chlorides to form methyl ketones, under modified conditions (see section 4.4.2.3, **Scheme 304**).

**Scheme 364.** Ni-Catalyzed Methylation of Alkyl Bromides with Methyl *p*-Toluenesulfonate (2014)<sup>a</sup>

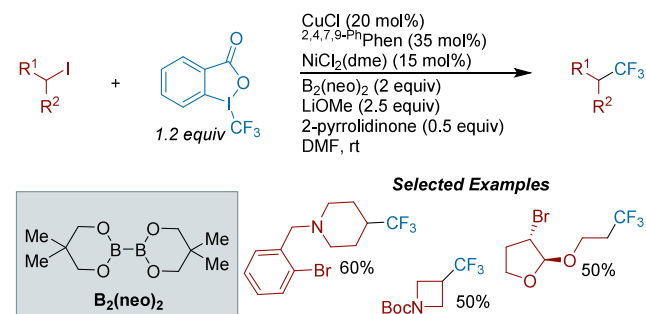


<sup>a</sup>Ratio of product to hydrodehalogenated byproduct detected by <sup>1</sup>H NMR.

The authors attribute the success of MeOTs as a methylating reagent to the slow exchange of methyl tosylate to methyl halides, maintaining a low concentration of the reactive species under the reaction conditions. Consequently, the rates of oxidative addition between the methyl and alkyl coupling partners are kinetically balanced, enabling productive reactivity. This is further backed up by the fact that replacing MeOTs with MeI led to trace yields.

In 2018, Hegui Gong and Guobin Ma reported a copper cocatalyzed trifluoromethylation of primary and secondary alkyl iodides with Togni's reagent (**Scheme 365**).<sup>516</sup> The role

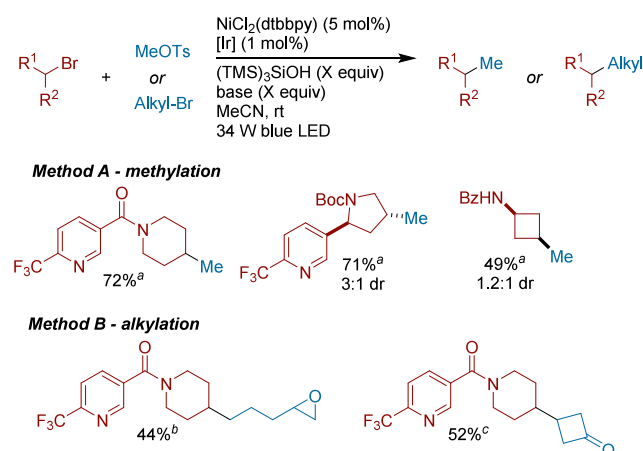
**Scheme 365. Copper-Catalyzed XEC of Alkyl Iodides with Togni's Reagent to Afford Trifluoromethylated Products (2018)**



of nickel in this reaction is to suppress alkyl borylation side reactions and bond formation is proposed to occur on copper. Running the reaction without nickel still afforded product but in lower yield. Notable functionality tolerated under these conditions are free anilines and aryl/alkyl bromides. Stoichiometric studies showed that both Cu(I)-CF<sub>3</sub> and Cu(II)-CF<sub>3</sub> reagents were not competent catalytic intermediates.

In 2018, the MacMillan group reported a Ni and Ir cocatalyzed photoredox XEC of secondary alkyl bromides with MeOTs and with other alkyl bromides (**Scheme 366**).<sup>517</sup> As in the related C(sp<sup>2</sup>)–C(sp<sup>3</sup>) coupling reactions (see section 4.2.1.2, **Scheme 126**),<sup>43</sup> a silyl radical is proposed to generate alkyl radicals by XAT. In this case, changing from a supersilane to supersilanol reagent was crucial in mitigating deleterious dehalogenation pathways from reduction by the Si–H reagent. In the methylation protocol, the TBAB additive was necessary to convert MeOTs into MeBr *in situ*. Heterocycles, strained ring systems, protected alcohols, and amides were generally tolerated under these conditions. To achieve the XEC of two

**Scheme 366.** Nickel and Iridium Metallaphotoredox XEC Alkylation of 2° Alkyl Bromides with MeOTs and Alkyl Bromides (2018)<sup>a</sup>

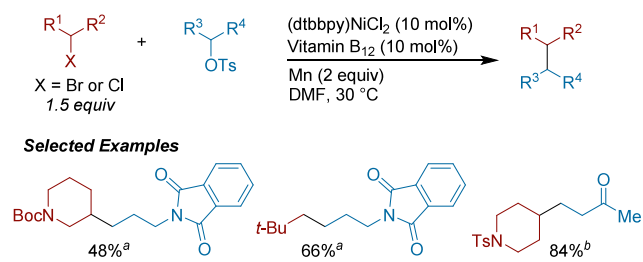


<sup>a</sup>(a) With (TMS)<sub>3</sub>SiOH (1.5 equiv), Na<sub>2</sub>CO<sub>3</sub> (2 equiv), and TBAB (2.5 equiv). (b) With (TMS)<sub>3</sub>SiOH (3 equiv) and K<sub>3</sub>PO<sub>4</sub> (3 equiv). (c) With (TMS)<sub>3</sub>SiOH (3 equiv) and Na<sub>2</sub>CO<sub>3</sub> (3 equiv).

alkyl bromides, reactions utilized an excess of one coupling partner under modified reaction conditions. The authors showcased their strategy through an iterative coupling of a molecule bearing an aryl bromide and an alkyl bromide. Regioselectivity could be controlled by selection of the supersilane reductant (XEC with aryl bromide site) or supersilanol reductant (XEC with alkyl bromide site).

In 2019, Komeyama reported the XEC of alkyl tosylates with primary and secondary alkyl halides utilizing a nickel and cobalt catalyst system (Scheme 367).<sup>518</sup> In this method,

**Scheme 367.** Nickel and Cobalt Co-Catalyzed XEC of Alkyl Halides with Alkyl Tosylates (2019)<sup>a</sup>

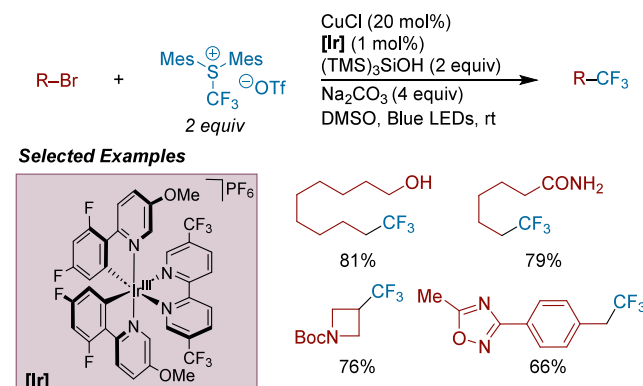


<sup>a</sup>(a) With X= Br. (b) With X = Cl and pyrazine (10 mol%).

protected amines, sulfonamides, esters, saturated heterocycles, and cyano groups were all well-tolerated. The reaction is proposed to proceed via a nucleophilic cobalt species, which is generated after Vitamin-B<sub>12</sub> is reduced by Mn. This cobalt species selectively engages the alkyl tosylate via S<sub>N</sub>2 displacement. The authors propose the product is formed following a transmetalation event between Co and Ni,<sup>174</sup> after which reduction, oxidative addition, and subsequent reductive elimination at nickel occurs.

In 2019, MacMillan and co-workers reported the copper- and iridium-catalyzed XEC of an electrophilic CF<sub>3</sub> salt with alkyl bromides in the presence of a tris(trimethylsilyl)silanol as an unusual reductant (Scheme 368).<sup>519</sup> The authors highlight radical capture and reductive elimination by the copper catalyst as product-forming steps after radical formation in the

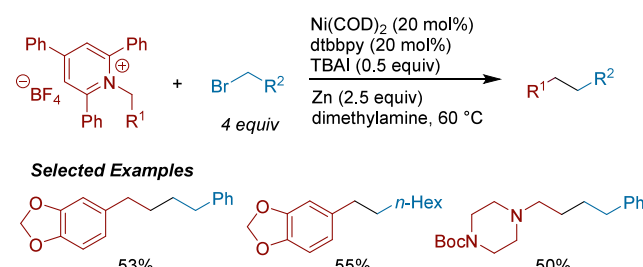
**Scheme 368.** Cu- and Ir-Catalyzed Trifluoromethylation of Alkyl Bromides with an Electrophilic CF<sub>3</sub> Source (2019)



presence of a photocatalyst. With optimized conditions, the developed method tolerated free alcohols, amides, esters, the benzyl position, and heterocycles such as pyrazoles and isoxazoles.

In 2019, Hong Yan, Yi Wang, Jianlin Han, and co-workers reported the deaminative XEC of alkylpyridinium salts with bromoalkanes (Scheme 369).<sup>284</sup> Five examples of 1°–1°

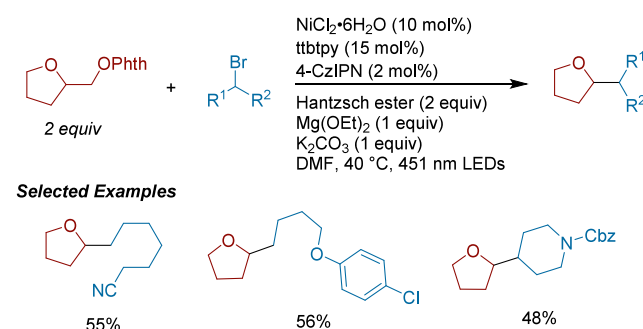
**Scheme 369.** Ni-Catalyzed XEC of N-Alkyl Pyridinium Salts with Primary Alkyl Bromides (2019)



alkyl–alkyl couplings were demonstrated. This report also details the XEC of alkylpyridinium salts with aryl, vinyl, and alkynyl electrophiles to form C(sp<sup>2</sup>)–C(sp<sup>3</sup>) and C(sp)–C(sp<sup>3</sup>) bonds, as outlined in Schemes 167 and 342, respectively.

In 2020, the Martin group reported a photoredox XEC approach to form C(sp<sup>3</sup>)–C(sp<sup>3</sup>) bonds from aliphatic alcohol feedstocks using N-alkoxyphthalimide ethers and alkyl bromides (Scheme 370).<sup>312</sup> In contrast to their C(sp<sup>2</sup>)–C(sp<sup>3</sup>) protocol (see section 4.2.5.6, Scheme 197), using a

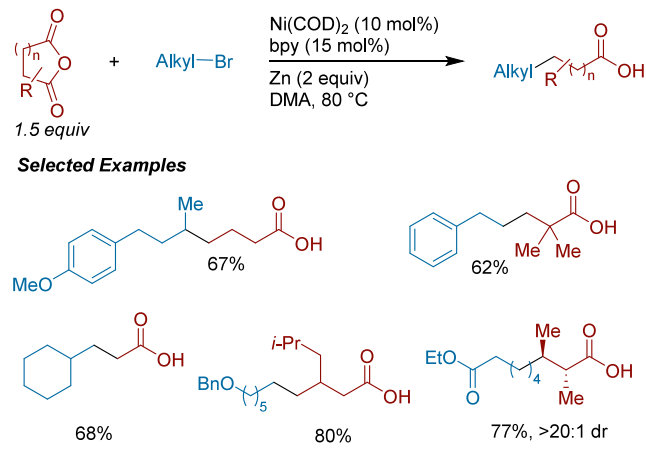
**Scheme 370.** Photoredox XEC of Alkyl Phthalimide Ethers with Alkyl Bromides (2020)



tridentate terpyridine ligand facilitated product formation in comparison to bipyridine ligands. Mechanistic probes were consistent with the formation of an oxygen centered radical on the *N*-alkoxyphthalimide ethers upon irradiation. The authors proposed that a  $\beta$ -scission event generates a carbon centered radical, which can react with a downstream alkylnickel species formed from the nickel catalyst and the alkyl bromide. This method demonstrated compatibility with primary alkyl bromides containing alkenes, free alcohols, nitriles, as well as secondary alkyl bromides.

Jianyou Mao, Walsh, and co-workers reported the decarbonylative XEC of cyclic anhydrides with alkyl bromides (Scheme 371).<sup>520</sup> The authors propose this reaction occurs via a

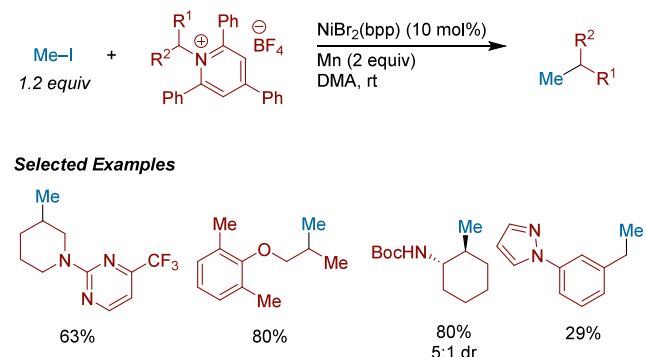
**Scheme 371. Decarbonylative XEC of Cyclic Anhydrides with Alkyl Bromides (2020)**



nonradical activation of the cyclic anhydride. Following polar oxidative addition of the cyclic anhydride compound to the nickel center, decarbonylation occurs to generate a nickel homoenolate intermediate.<sup>521</sup> Unsymmetrical anhydrides were selective for coupling at the less hindered site. Notably, the XEC with *cis*-2,3-dimethylsuccinic anhydride occurred with excellent stereospecificity.

The Watson group developed a Ni-catalyzed methylation of secondary *N*-alkylpyridiniums with methyl iodide. (Scheme 372).<sup>522</sup> This method could be utilized to methylate structurally diverse substrates containing heterocycles, including pharmaceutically relevant substrates isoxepac and ketoprofen could be methylated. A couple examples of isotopically

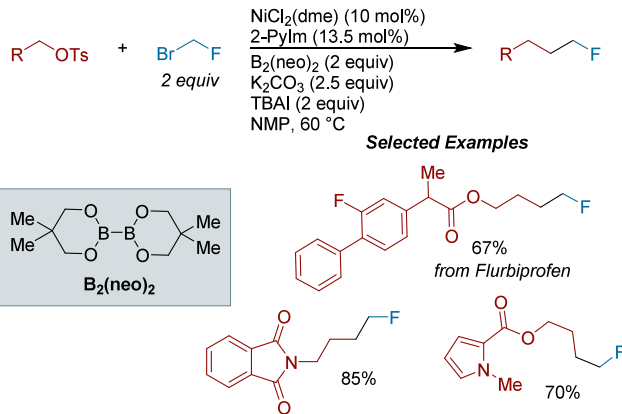
**Scheme 372. Ni-Catalyzed XEC of Secondary *N*-Alkyl Pyridinium Salts with Methyl Iodide (2021)**



labeled MeI derivatives were also demonstrated. Primary alkylpyridiniums afforded lower yields, as the slower rate of radical generation from are not well-matched with MeI.

In 2021, Xi-Sheng Wang and co-workers developed a Ni-catalyzed monofluoromethylation of alkyl tosylates with bromofluoromethane as the fluorinating reagent (Scheme 373).<sup>523</sup> This method utilized  $B_2(neo)_2$  as a homogeneous

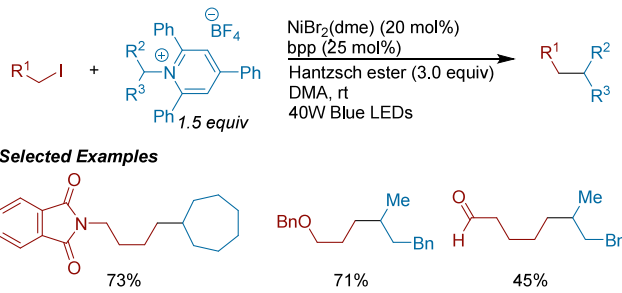
**Scheme 373. Ni-Catalyzed XEC of Alkyl Tosylates with Monofluoromethyl Bromide (2021)**



reductant. As observed by Hegui Gong with analogous systems, mechanistic experiments indicated that formation of alkylboronate intermediates was unlikely. A pyridyl-imidazoline nickel catalyst system outperformed other classes of bidentate ligands for this transformation.

In 2021, Ming Joo Koh and colleagues reported a photochemical XEC of secondary *N*-alkylpyridinium salts with primary alkyl iodides (Scheme 374).<sup>524</sup> This report also

**Scheme 374. Photochemical XEC of Secondary *N*-Alkyl Pyridinium Salts with Primary Alkyl Iodides (2021)**



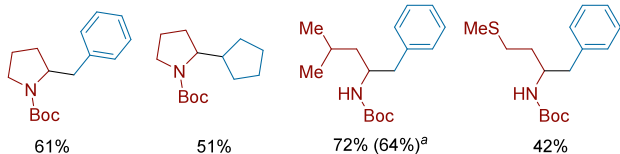
describes conditions for the  $C(sp^2)-C(sp^3)$  XEC of *N*-alkylpyridiniums with aryl bromides (see section 4.2.4.3, Scheme 174). The authors propose that the *N*-alkylpyridinium salt forms an EDA complex with the Hantzsch ester, which can be photoexcited to induce single electron transfer and fragmentation to generate an alkyl radical. The authors showed that alkyl aldehydes were better tolerated using their photochemical conditions compared to conditions using heterogeneous metallic reductants.

In 2021, the Cernak group developed a Ni-catalyzed deaminative-decarboxylative XEC for  $C(sp^3)-C(sp^3)$  bond formation from *N*-alkylpyridinium salts and NHP esters (Scheme 375).<sup>524</sup> Reaction optimization was done through a high throughput experimentation (HTE) campaign, in which

**Scheme 375. Ni-Catalyzed XEC of NHP Esters with *N*-Alkyl Pyridinium Salts (2021)<sup>a</sup>**



**Selected Examples**

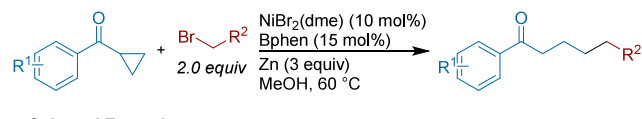


<sup>a</sup>With  $\text{NiBr}_2(\text{dme})$  (10 mol%) and  $4,4'\text{-CF}_3\text{bpy}$  (10 mol%). NHP = *N*-hydroxyphthalimide

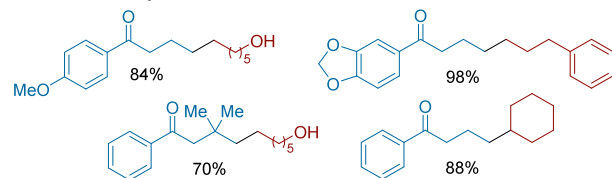
an initial hit of 22% isolated yield was iteratively and systematically optimized to 81%. Notably, the authors found that a mixed solvent system and order of reagent addition was crucial for reaction success. In addition to a traditional substrate scope, the authors ran a 96-well plate (12 NHP esters with 8 *N*-alkylpyridiniums) and found their conditions afforded product (>10% UPLC/MS conversion) in 68 of the 96 reactions. This report highlights the power of HTE to enable methodology development and the discovery of new reaction conditions.

Chuan Wang and co-workers reported conditions for the Ni-catalyzed XEC of cyclopropyl ketones with alkyl bromides (**Scheme 376**).<sup>525</sup> This reaction proceeds with excellent

**Scheme 376. Ni-Catalyzed XEC of Aryl Cyclopropyl Ketones with Alkyl Bromides (2022)**



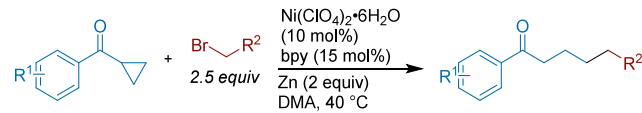
**Selected Examples**



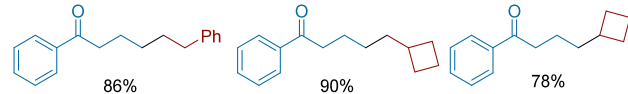
regioselectivity for the less hindered site. This provides complementary products to those generated from radical initiated ring-opening of cyclopropyl ketones, which favor functionalization at the more substituted site. Deuteration studies support the formation of enolizable intermediates, consistent with a nickel oxidative cycloaddition step with the cyclopropyl ketone coupling partner.

Concurrently in 2022, Jianyou Mao, Walsh and co-workers developed a Ni-catalyzed C–C bond activation of cyclopropyl ketones and coupled them to primary and secondary alkyl bromides (**Scheme 377**).<sup>526</sup> The authors proposed that the reaction proceeds through a six membered nickelacycle intermediate, which is formed after oxidative addition and ring-opening of the cyclopropyl phenyl ketone. Control experiments ruled out the formation of organozinc intermediates.

**Scheme 377. C–C Bond Activation XEC of Cyclopropyl Ketones with Alkyl Bromides (2022)**

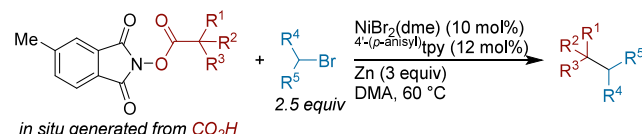


**Selected Examples**

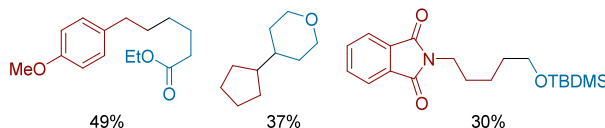


Our group reported a method for the Ni-catalyzed  $\text{C}(\text{sp}^3)\text{–C}(\text{sp}^3)$  XEC of unactivated alkyl bromides with *in situ* generated NHP esters (**Scheme 378**).<sup>527</sup> Electron rich NHP

**Scheme 378. Ni-Catalyzed XEC of Alkyl Bromides with In Situ Generated NHP Esters (2022)**



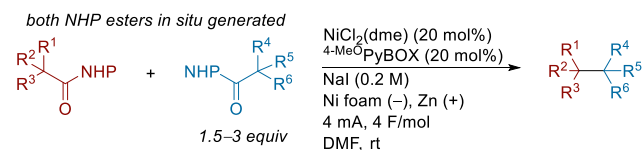
**Selected Examples**



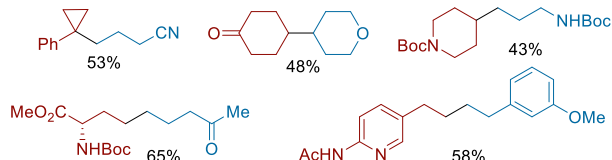
esters gave higher yields compared to electron poor esters, which favored decarboxylative dimerization as the major side reaction. The reaction conditions require an excess of alkyl bromide, but the desired products can be separated from alkyl bromide side products. While the focus of the scope was on 1°–1° alkyl linkages, examples of more hindered 2° and 3° coupling partners were demonstrated in lower yield. In addition, alkyl iodides and benzyl chlorides were also successfully implemented in the coupling with NHP esters in comparable yield.

Baran and co-workers reported a Ni-catalyzed doubly decarboxylative cross-electrophile coupling of alkyl carboxylic acids driven electrochemically in an undivided cell (**Scheme 379**).<sup>528</sup> Both acids could be activated *in situ* to the NHP ester prior to cross-coupling without a solvent swap. An excess of

**Scheme 379. Ni-Catalyzed Doubly-Decarboxylative XEC Driven by Electrochemistry (2022)**



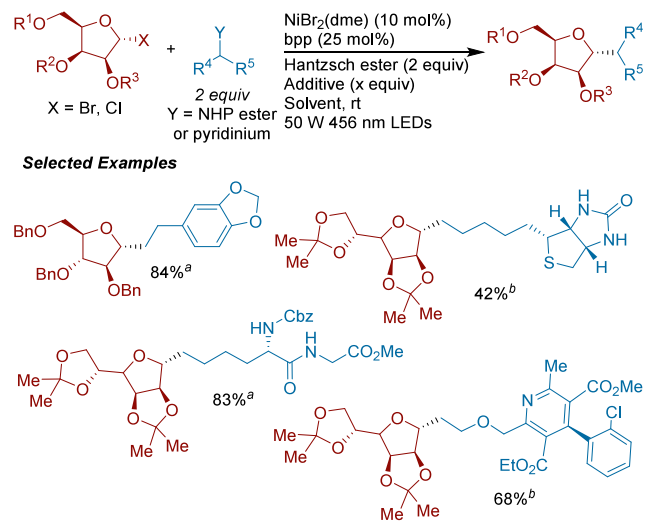
**Selected Examples**



one of the acids (1.5 to 3 equiv, generally the less expensive coupling partner) was needed to avoid competitive homodimerization products arising from both acids. Various combinations of  $1^\circ$ – $1^\circ$ ,  $1^\circ$ – $2^\circ$ ,  $2^\circ$ – $2^\circ$ , and  $1^\circ$ – $3^\circ$  couplings were all compatible in this method. The authors highlighted the synthetic utility of this approach by decreasing the step-count to the synthesis of known intermediates previously made through 2-electron disconnections. Radical clock experiments performed with cyclopropylmethyl- and 5-hexenyl-NHP esters unambiguously confirmed that both coupling partners form alkyl radicals.

Ming Joo Koh and Quanquan Wang reported the synthesis of C-glycosides via the Ni-catalyzed XEC of glycosyl halides with redox active amine and carboxylic acid derivatives (Scheme 380).<sup>529</sup> Hantzsch ester was used to form a

**Scheme 380. Photoinduced XEC of Glycosyl Halides with NHP Esters or N-Alkyl Pyridiniums (2022)<sup>a</sup>**

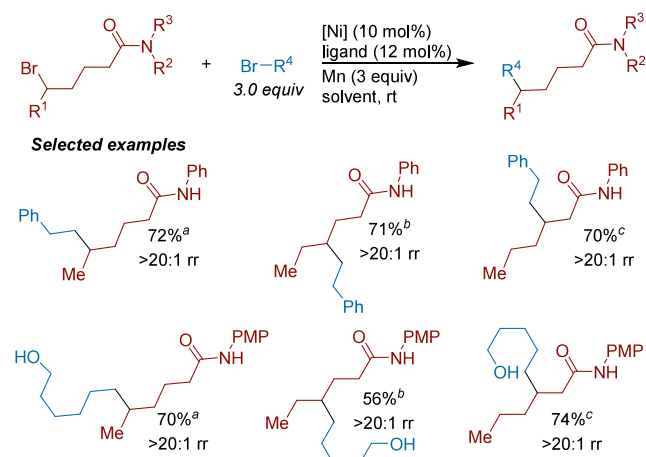


<sup>a</sup>(a) With  $X = \text{Cl}$ ,  $N$ -alkylpyridinium (2 equiv),  $\text{Et}_3\text{N}$  (3 equiv), and DMA. (b) With  $X = \text{Br}$ , NHP ester (2 equiv),  $\text{LiI}$  (2 equiv), and DMA/MTBE (1:1).

photoinduced EDA complex with either the NHP ester or pyridinium salt, promoting alkyl radical generation. UV-vis absorption studies illustrated the crucial role of additives in generating the EDA complex. The scope of the reaction was broad, showing compatibility with short peptides and other protected sugars. Radical-clock and radical trapping experiments supported the formation of alkyl radicals from both coupling partners.

In 2023, Wei Shu and co-workers developed a ligand-controlled regiodivergent XEC of secondary alkyl bromides with primary and secondary alkyl bromides (Scheme 381).<sup>530</sup> Three sets of conditions were reported, where different degrees of chain-walking across the  $\delta$ -bromoamide substrate are promoted by choice of ligand. Accordingly, a variety of remote couplings to the  $\beta$ -,  $\gamma$ -, and  $\delta$ -positions of these alkyl amides was achieved in excellent regioselectivity. Longer chain bromoamides and  $\delta$ -bromoketones also exhibited this ligand-controlled regiodivergency. Outside of ligand-selection, there also appeared to be a solvent effect on regioselectivity, as protic solvent mixtures seemed to promote chain-walking, while aprotic solvents favored coupling at the original C–Br site.

**Scheme 381. Ni-Catalyzed Regioselective XEC of  $\delta$ -Bromoamides (2023)<sup>a</sup>**

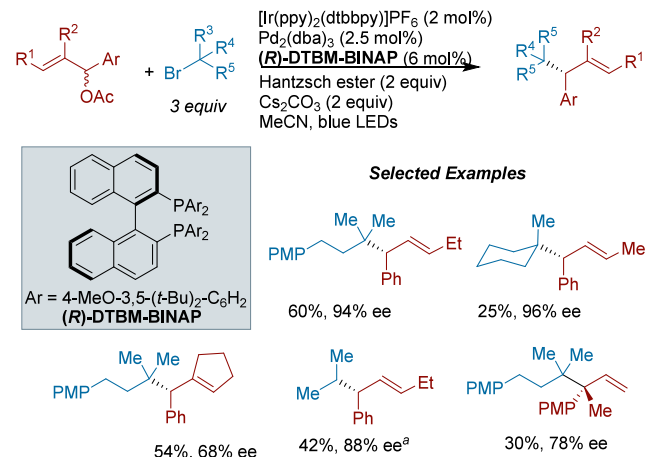


<sup>a</sup>(a) Conditions A: [Ni] =  $\text{NiBr}_2(\text{dme})$ , ligand =  ${}^4\text{Cl}^-\text{PyBOX}$ , and DMA. (b) Conditions B: [Ni] =  $\text{NiCl}_2 \bullet 6\text{H}_2\text{O}$ , ligand =  ${}^{5,5'}\text{-Me}^-\text{bpy}$ , and MeOH/TFE. (c) Conditions C: [Ni] =  $\text{NiBr}_2(\text{dme})$ , ligand =  $\text{BOX-S}$ , and MeOH. PMP = *para*-methoxyphenyl.

#### 6.4. Enantioselective C(sp<sup>3</sup>)–C(sp<sup>3</sup>) XEC

Shouyun Yu and Hong-Hao Zhang reported the enantioselective photochemical, Pd-catalyzed XEC of allylic acetates with secondary and tertiary alkyl bromides (Scheme 382).<sup>531</sup>

**Scheme 382. Enantioselective Pd and Ir Co-Catalyzed Photochemical XEC of Allylic Acetates with Alkyl Bromides (2023)<sup>a</sup>**

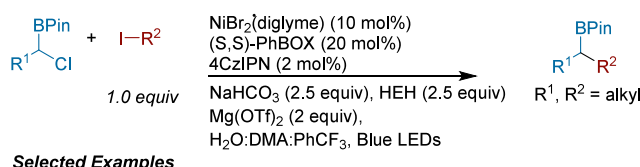


<sup>a</sup>PMP = *para*-methoxyphenyl. (a) At 0 °C.

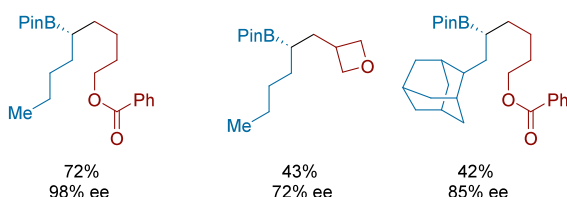
This method furnished products that contained adjacent tertiary and quaternary carbon centers, with a stereocenter set at the tertiary carbon. Using Hantzsch ester as a terminal reductant and a chiral phosphine ligand, the authors were able to couple a range of disubstituted allylic acetates with high enantio- and regioselectivity. In addition to tertiary alkyl bromides, secondary alkyl bromides could also be coupled, albeit in lower yield. Mechanistic experiments suggest that this reaction proceeds by an allylpalladium intermediate and an alkyl radical, but the authors acknowledged an excited state palladium pathway is also possible.

In 2023, Tao Xu and co-workers developed a Ni-catalyzed enantioconvergent XEC of alkyl iodides with alkyl  $\alpha$ -chloroboronates (Scheme 383).<sup>532</sup> The addition of water

**Scheme 383.** Ni-Catalyzed Enantioconvergent XEC of  $\alpha$ -Chloroboronates with Alkyl Iodides (2023)



**Selected Examples**

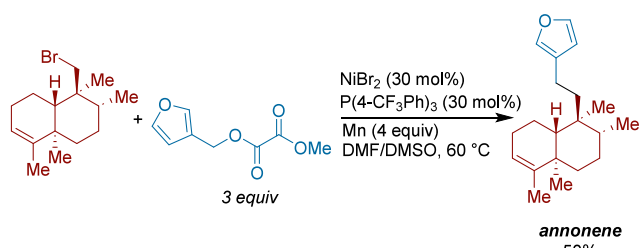


helped increase yields, possibly by improving solubility of the inorganic base. Employing a chiral BOX ligand ensured high enantioselectivity. The authors showcased their method by synthesizing a key chiral intermediate in the total synthesis of Calonectin A2 in a single XEC step, which had only been reported in several steps in previous total syntheses.

### 6.5. Synthetic Applications of C(sp<sup>3</sup>)–C(sp<sup>3</sup>) XEC

Ming Yang and co-workers utilized XEC conditions in their modular total syntheses of *trans*-clerodane and sesquiterpene hydroquinone natural products, adopting conditions first reported by Shu<sup>512</sup> (Scheme 384).<sup>533</sup> The authors used XEC

**Scheme 384.** XEC in the Total Synthesis of Annonene (2022)



in the final step of the synthesis of annonene to join together an alkyl bromide with a heterobenzyl oxalate fragment. A subsequent oxidation step affords the related natural product PL-3.

## 7. DIFUNCTIONALIZATION OF ALKENES AND ALKYNES WITH TWO ELECTROPHILES

### 7.1. Alkene Difunctionalization

Cross-electrophile difunctionalization of alkenes with transition metal catalysts represents an efficient strategy to construct complex carbon skeletons through multicomponent coupling. The major challenge of this approach is avoiding the many possible side products (e.g., unproductive pairwise couplings). While several successful difunctionalization strategies have been developed using palladium catalysts, the general ease and favorability of  $\beta$ -hydride elimination from palladium(II) intermediates remains a challenge. In contrast,

the 3d transition metals have two advantages as these metals can access oxidation states, electronic configurations, and geometries that can slow  $\beta$ -hydride elimination.<sup>534–536</sup> These differences in reactivity, in conjunction with the ability of nickel catalysts to generate and capture organic radicals, has enabled a diversification of alkene difunctionalization methodology beyond the capability of palladium.<sup>537</sup> Indeed, we found that nickel is the main metal utilized for transformations discussed in this chapter.

Owing to these advantages, the repository of inter- and intramolecular alkene difunctionalization reactions has expanded to include transformations such as diarylation, enantioselective dialkylation, and regioselective three-component coupling reactions utilizing both activated and unactivated alkenes. Furthermore, the development of such transformations has placed reductive difunctionalization as an increasingly utilized tool in total synthesis.<sup>538</sup>

In this section we describe transition metal-mediated inter- and intramolecular difunctionalization of alkenes using two  $\sigma$ -electrophiles. Stereoselective variants of these transformations are highlighted. We also discuss total syntheses that apply these alkene difunctionalization strategies. Additions in which two of the coupling partners are  $\pi$ -electrophiles, such as a carbonyl or another alkene, will not be discussed even if they are net reductive (e.g., additions to fluoroalkenes with subsequent  $\beta$ -F elimination). Outstanding challenges to this area include formation of rings with >5–6 atoms using cyclization methods and developing enantioselective variants of cyclization reactions with tethered C(sp<sup>3</sup>) electrophiles. Furthermore, the application of photochemical and electrochemical technologies in this area remains somewhat limited.

Mechanisms for alkene difunctionalization generally proceed analogously to the conventional two-component cross-electrophile coupling (Figure 22). The alkene insertion generally occurs from either radical addition to an alkene (inter- or intramolecular, Figure 39) or migratory insertion of an aryl or alkynickel bond into an alkene (Figure 40, most commonly intermolecular).

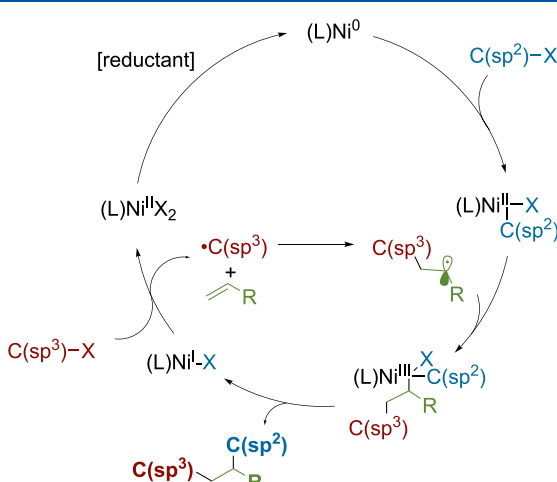


**Figure 39.** General intermolecular alkene difunctionalization mechanism. While oxidative addition at Ni<sup>0</sup> is depicted, oxidative addition from Ni<sup>I</sup> followed by sequential reduction to form the same Ni<sup>II</sup> complex is also possible.<sup>535</sup> Radical generation (red) is depicted as originating from a low valent Ni species; however, radicals (aryl or alkyl) could be generated by other mechanisms.

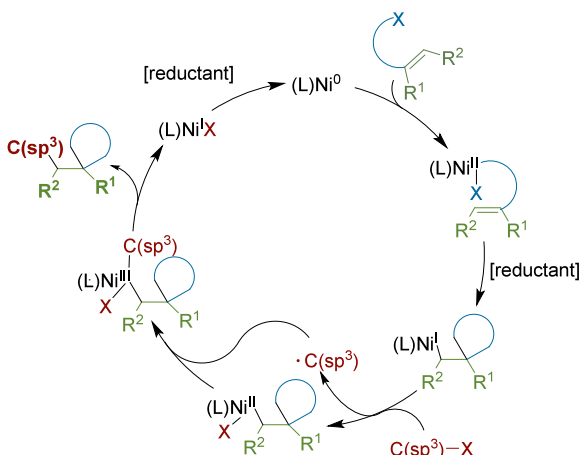


**Figure 40.** General intramolecular alkene difunctionalization mechanism. While oxidative addition at  $\text{Ni}^0$  is depicted, oxidative addition from  $\text{Ni}^{\text{I}}$  followed by reduction to form the same  $\text{Ni}^{\text{I}}$  complex is also possible. Additionally, migratory insertion can occur from either a  $\text{Ni}^{\text{I}}$  or  $\text{Ni}^{\text{II}}$  species.<sup>539</sup>

For radical addition, general strategies have been developed to ensure success (Figure 39). The intramolecular reaction is quite general as long as the ring closure involves a 5- or 6-membered ring and the thermochemistry for the ring closure is favorable. The intermolecular reaction can be challenging if both the first radical and the second radical (formed after addition to alkene) have similar reactivity with the nickel catalyst. The formation of the two-component product can be avoided if (1) the first-formed radical will not couple under the conditions (e.g., tertiary radicals require different catalysts than primary and secondary)<sup>540</sup> or sometimes, (2) an excess of an electron poor acceptor alkene is used.

Migratory insertion into alkenes can provide a straightforward way to access metal– $\text{C}(\text{sp}^3)$  intermediates that can (1) react directly with another electrophilic coupling partner, or (2) undergo reduction to afford a low valent metal intermediate primed for oxidative addition. For the inter- and intramolecular reactions, migratory insertion strategies have been used in directing group-mediated reactions, providing a method toward regiocontrol that is otherwise inaccessible.<sup>541</sup> For intramolecular reactions, chiral catalysts can facilitate construction of stereogenic centers through enantio- or diastereo-determining migratory insertion, which has been demonstrated using both internal and terminal alkenes.<sup>542</sup> Tuning alkene reactivity in intramolecular reactions, especially for internal alkenes, can be used to mitigate formation of Heck and/or direct coupling byproducts.<sup>543–545</sup>

Due to the added complexity inherent to three-component couplings, the ligands utilized in this section are quite diverse (Figure 41, Figure 42). While bipyridine ligands are still the most utilized (20%), a sizable portion of reports use no exogenous ligand and rely on either 8-aminoquinoline (AQ) or quinolinamide (QA) as a directing group. In addition, bioxazoline (BiOX) and pyridyl oxazoline (PyOX) ligands represent a much larger portion of ligands used in this section due to an increased proportion of enantioselective reactions. Finally, more  $P,N$ -ligands are used in this section, particularly phosphinoxazoline (PHOX) and phosphinoferrocenyloxazoline (PhosFerrox); this ligand type is only seen in this review when adding electrophiles across a  $\pi$ -system (see Alkyne Difunctionalization, section 7.2, and C–Si, section 8.1).

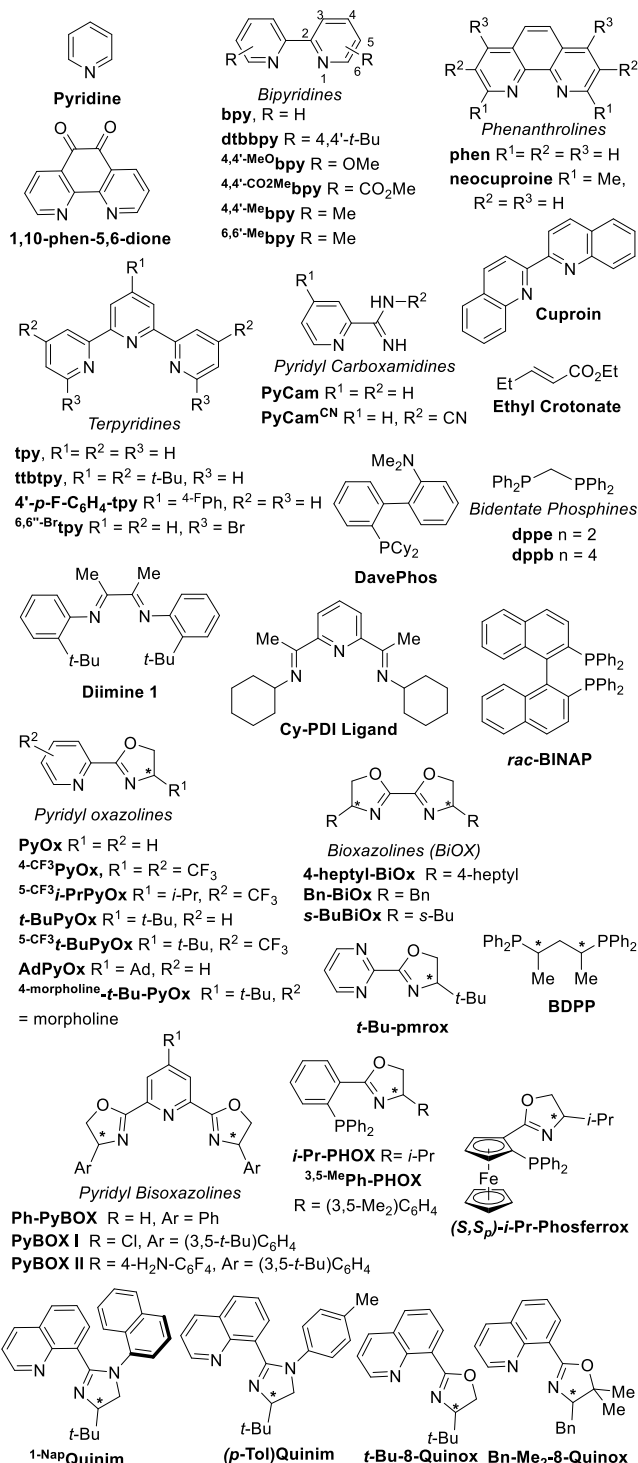


**Figure 41.** Structure of ligands used in the cross-electrophile difunctionalization of alkenes. \*Denotes chiral center.

**7.1.1. Intermolecular, Three-Component Difunctionalizations.** The reactions in this section involve three reactants (two  $\sigma$ -electrophiles and one alkene) and result in a product with two new C–C bonds. A few C–X bond forming reactions are also discussed.

**7.1.1.1. Addition of  $C(\text{sp}^2)$  and  $C(\text{sp}^3)$  Electrophiles Across Alkenes.** In 2017, the Nevada group reported an intermolecular alkene dicarbofunctionalization of tertiary alkyl iodides and aryl iodides across a variety of alkenes (Scheme 38S).<sup>546</sup>

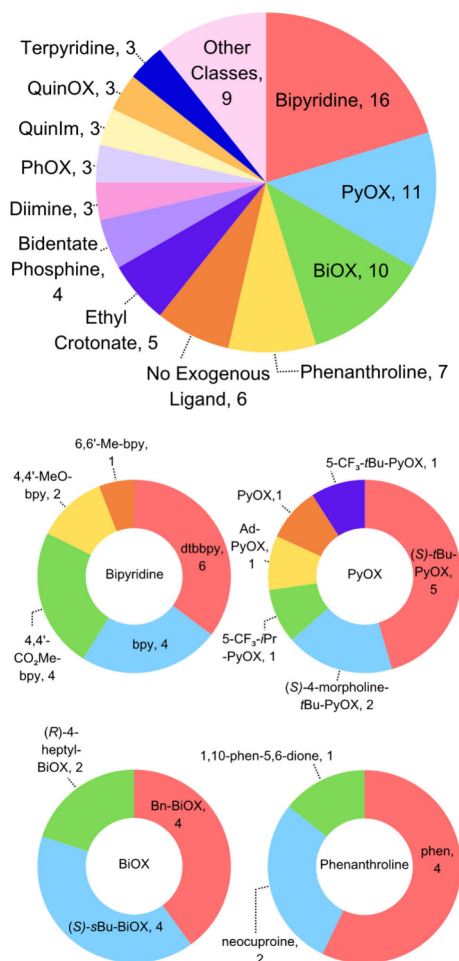
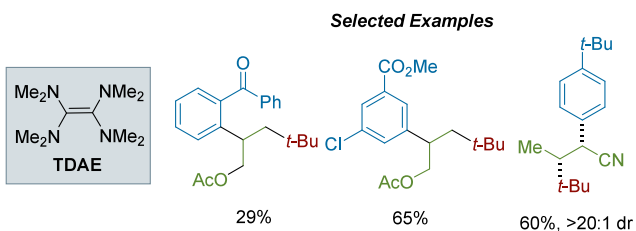
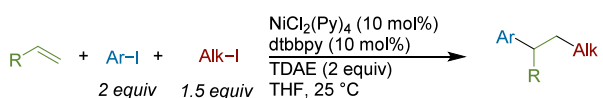


**Figure 42.** Distribution of ligand-types used in the cross-electrophile difunctionalization of alkenes.

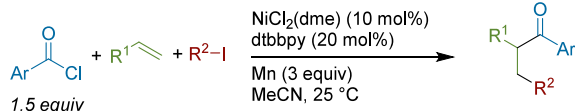
**Scheme 385. Ni-Catalyzed Cross-Electrophile Dicarbofunctionalization of Alkenes with Tertiary Alkyl Iodides and Aryl Iodides (2017)**



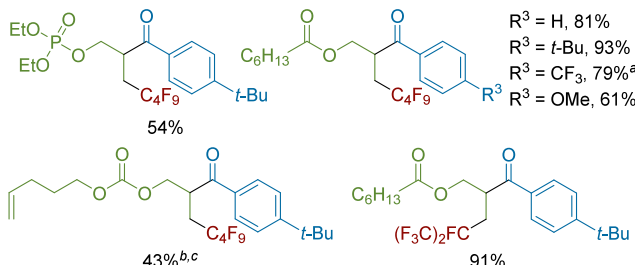
Tetrakis(dimethylamino)ethylene (TDAE) was superior to metal powder reductants. The conditions did not activate C(sp<sup>2</sup>)–Br and C(sp<sup>2</sup>)–Cl bonds. Both electron-rich and electron-poor alkenes could be utilized; specifically, crotononitrile afforded radical addition products with high diastereoselectivity. A number of mechanistic experiments, including stoichiometric studies, were consistent with formation of an arynickel(II) complex and addition of the tertiary radical to the alkene (Figure 39). Further control experiments ruled out the formation of a secondary alkyl iodide intermediate.

Lingling Chu and colleagues developed a three-component carboacylation of alkenes with acid chlorides and fluoroalkyl iodides to synthesize β-fluoroalkyl ketones (Scheme 386).<sup>547</sup> A

**Scheme 386. Ni-Catalyzed Carboacylation of Alkenes with Benzoyl Chlorides and Perfluoroalkyl Iodides (2018)<sup>a</sup>**



**Selected Examples**

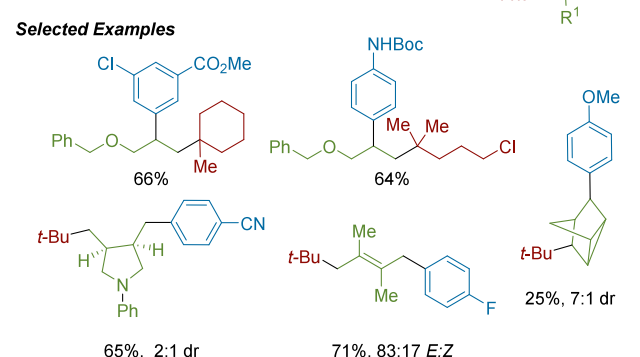
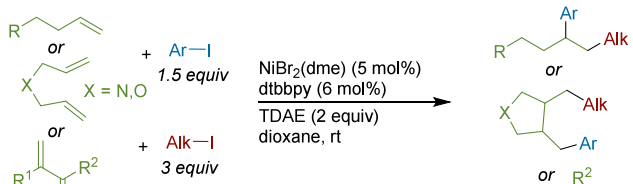


<sup>a</sup>(a) With Zn (3 equiv) at 40 °C. (b) With alkene (2 equiv) in 4:1 MeCN/DME.

range of electronics were tolerated on the benzoic acid chloride, and alkenes with a variety of weakly coordinating functional groups were competent coupling partners. In reactions of more complex substrates with multiple alkenes, chemoselectivity for the alkene proximal to the coordinating group was observed.

The reliance on functionalized alkenes in their 2017 report motivated the Nevado group to target simple terminal alkenes and dienes in a follow-up report (Scheme 387).<sup>548</sup> High regioselectivity and excellent chemoselectivity was observed. Additionally, 1,1,1,1-di-en-ynes, trienes, and dienes could be selectively functionalized under the optimized conditions. In

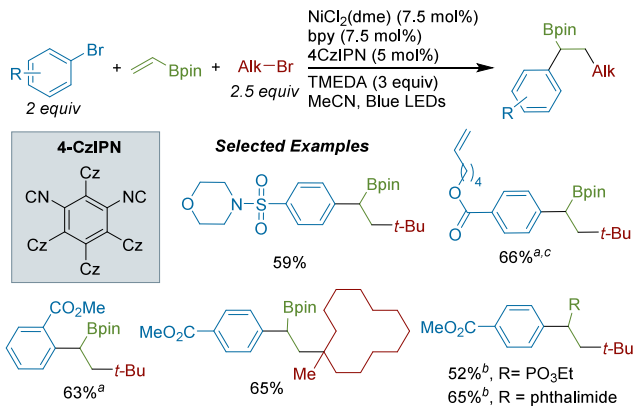
**Scheme 387. Ni-Catalyzed Cross-Electrophile Dicarbofunctionalization of Alkenes, Trienes, and Di-ynes with Tertiary Alkyl and Aryl Iodides (2019)**



contrast to their 2017 report, DFT analysis revealed that radical generation by a nickel(I) iodide species was thermodynamically unfavorable. However, activation of the alkyl iodide with different nickel species was probed, and results revealed that low valent nickel species could consistently activate the alkyl halide, while nickel(II) species could not. While the exact speciation of the nickel catalyst throughout this catalytic cycle remains unclear, stoichiometric studies with arylnickel(II) complexes with TDAE provide support for the reduction of these complexes in this reaction.

Martin and co-workers developed a cross-electrophile difunctionalization method that added tertiary alkyl bromides and bromoarenes across vinyl boronates (Scheme 388).<sup>549</sup> The

**Scheme 388. Ni-Catalyzed Photochemical 1,2-Dicarbofunctionalization of Vinyl Boronates with Tertiary Alkyl and Aryl Bromides (2020)<sup>a</sup>**



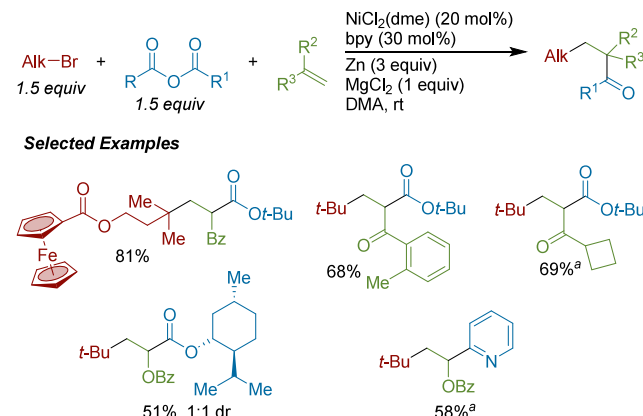
<sup>a</sup>(a) Yield of product after treatment with NaBO<sub>3</sub>. (b) With 4,4'-MeO<sub>2</sub>bipy (7.5 mol%). (c) With Ni(COD)<sub>2</sub> (7.5 mol%) and 4,4'-MeO<sub>2</sub>bipy (7.5 mol%).

difunctionalized product was afforded in high yields, with no evidence of competitive Suzuki–Miyaura or Heck-type side reactivity. Although only tertiary alkyl bromides were effective, the scope of aryl coupling partner was broad, and several other vinyl derivatives could be used. Stoichiometric experiments with an arylnickel(II) complex showed that TMEDA was required for product formation. Photoluminescence quenching studies supported a reductive quenching photocatalytic cycle.

In 2020, Chuan Wang and co-workers disclosed conditions for the arylacylation of alkenes with anhydrides and tertiary alkyl bromides (Scheme 389).<sup>550</sup> Primary and secondary alkyl bromides and iodides were unsuitable substrates, as they underwent direct cross-coupling with benzoic acid anhydride. Stoichiometric studies using Ni(COD)<sub>2</sub> revealed that nickel(0) favors an irreversible oxidative addition with benzoic anhydride over the alkyl bromide. Additionally, a reaction performed in absence of the nickel catalyst promoted the hydroalkylation side reaction. Moreover, MgCl<sub>2</sub> was required for this reaction. Thus, a mechanism relying on the synergy of nickel, zinc, and MgCl<sub>2</sub> was proposed: a radical generated by either a nickel species or zinc was proposed to undergo a Giese-type addition to the alkene. Afterward, this Giese-adduct could be captured by an acylnickel(II) species, which furnishes the final product following reductive elimination (as in Figure 39).

Ming Joo Koh and co-workers reported a substrate directing-group approach to achieve regioselective alkene

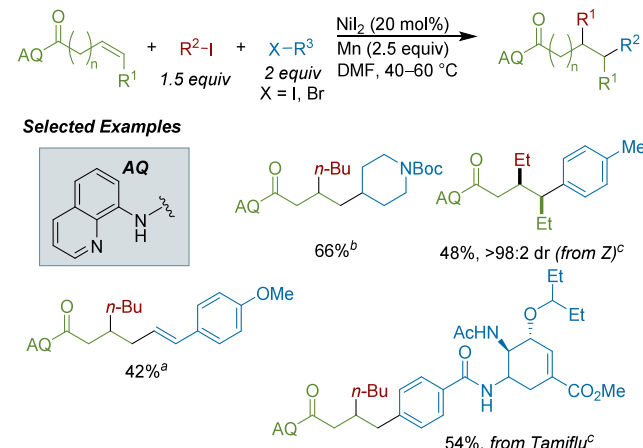
**Scheme 389. Ni-Catalyzed Alkylacetylation of Alkenes with Anhydrides and Tertiary Alkyl Bromides (2020)<sup>a</sup>**



<sup>a</sup>With Zn (4 equiv), MgCl<sub>2</sub> (2 equiv), and 4 Å molecular sieves.

arylation, (Scheme 390).<sup>551</sup> Although a directing group adds additional steps for introduction and removal, these

**Scheme 390. Ni-Catalyzed Aminoquinoline-Directed Dicarbofunctionalization of Alkenes with Alkyl Halides and Vinyl and Aryl Halides (2020)<sup>a</sup>**

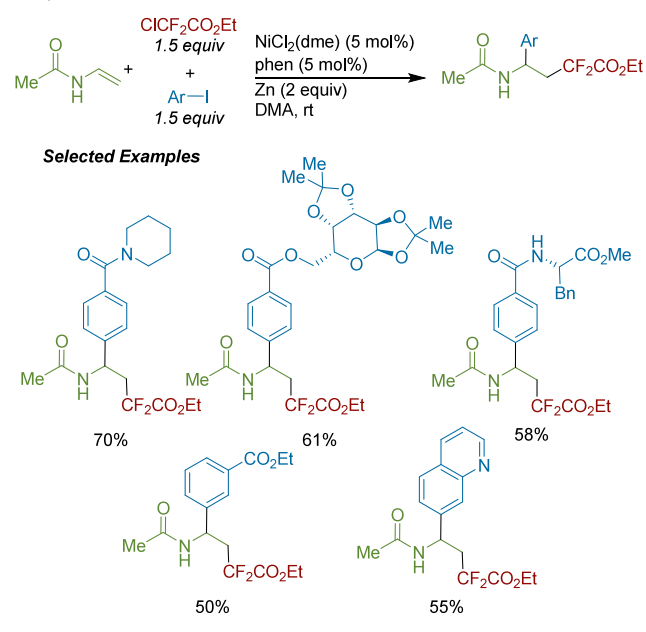


<sup>a</sup>(a) With R<sup>3</sup>-X = vinyl bromide. (b) With R<sup>3</sup>-X = alkyl iodide. (c) With R<sup>3</sup>-X = aryl iodide.

conditions were compatible with primary alkyl iodides and provided reversed regioselectivity compared to nondirected reactions.<sup>548</sup> Of the β-γ unsaturated amide directing group auxiliaries evaluated, 8-aminoquinoline (AQ) provided the highest yield with the desired regioselectivity. Shortened synthetic routes for three separate complex small molecules illustrated the synthetic utility of this method. The results of mechanistic studies were consistent with initial oxidative addition of the aryl halide and turnover-limiting alkyl halide activation.

Xingang Zhang and co-workers developed a three component difunctionalization strategy to synthesize α,α-difluoro-γ-amino acids (Scheme 391).<sup>552</sup> The reaction adds an aryl iodide and α,α-difluoroacetate across vinyl acetamide. Compared to the brominated reagent, the less reactive chloro(difluoro)acetate reagent suppressed hydrodehalogenation side products. Functional group compatibility was high, highlighted by amino acid and carbohydrate-containing aryl

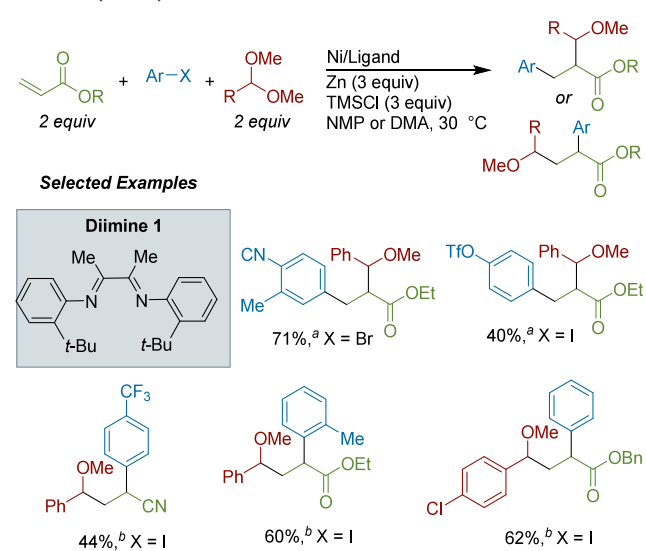
**Scheme 391.** Ni-Catalyzed Synthesis of  $\alpha,\alpha$ -Difluoro- $\gamma$ -Amino Acids via Aryldifluoroacetylation of *N*-Vinylacetamides (2021)



iodides. A gram scale modification of a synthetic peptide highlighted the synthetic utility of this method.

In 2022, a three-component arylalkylation reaction of alkenes was reported by Guoyin Yin, Lei Zhu, and co-workers. The authors observed that the regiochemical outcome of the reaction could be ligand-controlled (Scheme 392).<sup>553</sup> The more sterically hindered diamine ligand resulted in  $\beta$ -arylation, while the less hindered bipyridine ligand resulted in  $\alpha$ -arylation. Ultimately, the authors hypothesize that ligand choice biases olefin migratory insertion: the diamine ligand facilitates insertion into a arylnickel(II) species, while a

**Scheme 392.** Ni-Catalyzed Regiodivergent Difunctionalization of Acrylates with Aryl Halides and Acetals (2022)<sup>a</sup>

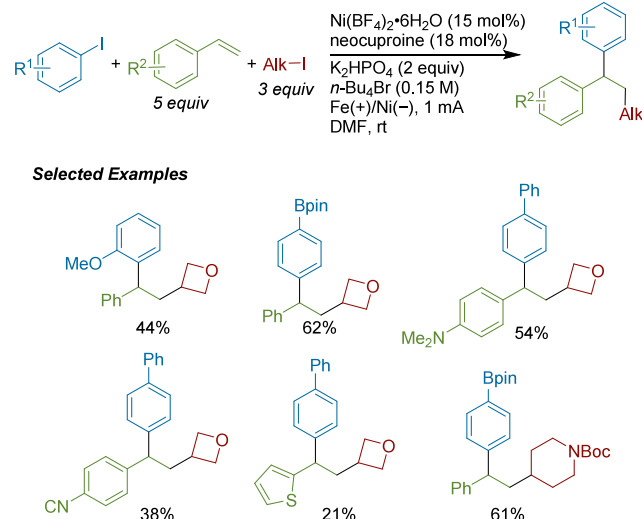


<sup>a</sup>(a) With  $\text{NiCl}_2(\text{Py})_4$  (5 mol%), Diimine 1 (5 mol%) in DMA. (b) With  $(4,4'\text{-MeO}\text{bpy})\text{NiCl}_2$  (7.5 mol%) in NMP.

bipyridine ligand facilitates insertion into a nickel(II) alkyl species. Both electron-rich and electron-deficient aryl iodides afforded the products in high yields, and some aryl bromides and aryl triflates were also compatible. Generally, the electronics of either coupling partner had little impact on the regioselectivity outcome. In addition to acrylates, acrylonitrile could be used as the alkene partner.

Later in 2022, an electrosynthetic approach to the arylalkylation of styrenes was reported by Chao Yang, Wujong Xia, and co-workers (Scheme 393).<sup>554</sup> The reaction proceeds

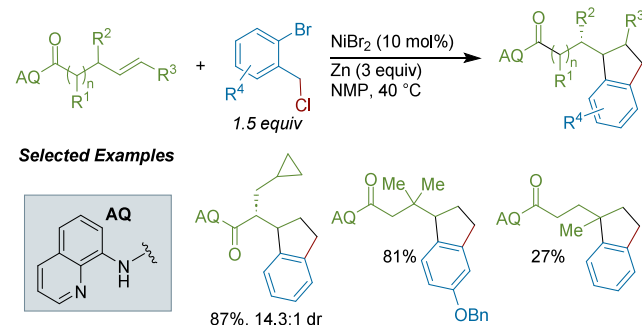
**Scheme 393.** Ni-Catalyzed Electrochemical Arylalkylation of Styrenes with Aryl Halides and Alkyl Iodides (2022)



under a constant current of 1 mA in an undivided cell with a sacrificial iron anode. Electron-poor iodoarenes bearing *para*-, *meta*-, and *ortho*-substitution provided high yields, while electron-rich iodoarenes provided lower yields. Additionally, a variety of sterically and electronically diverse styrenes were well-tolerated. Compared to previous reports that required tertiary or perfluoroalkyl halides, this method worked favorably with secondary alkyl iodides. EPR studies verified the intermediacy of a secondary alkyl radical species forming in the reaction.

An alkene annulation reaction with 2'-bromobenzyllic chlorides to afford indanes was reported by Lianhui Wang, Si-Hai Wu, and co-workers (Scheme 394).<sup>555</sup> The reaction is substrate-directed by an 8-aminoquinoline (AQ) group and no

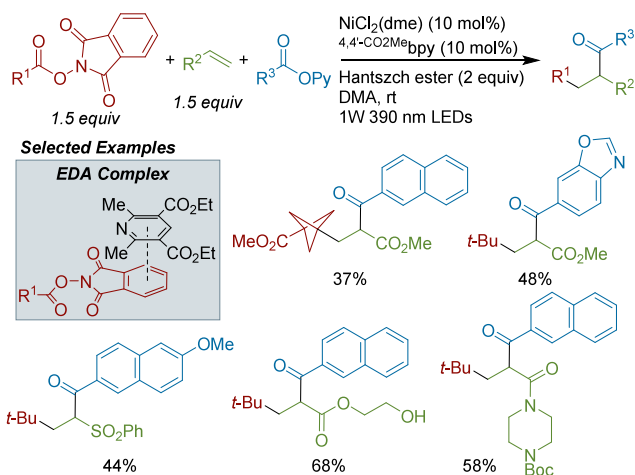
**Scheme 394.** Ni-Catalyzed Directed Annulation of Alkenes with *ortho*-Bromobenzyl Chlorides (2022)



additional ligand is required for the nickel catalyst. While this method worked most efficiently for terminal alkenes, decreasing the chain length of the alkenylamides showed no detrimental effect on yield and regioselectivity. One example of a 2,2-disubstituted alkene was coupled, albeit in lower yield.

Weiming Yuan and co-workers reported a photochemical Ni-catalyzed alkylacetylation of electron-deficient alkenes (**Scheme 395**).<sup>556</sup> Their strategy relied on the in situ formation

**Scheme 395. Ni-Catalyzed Alkylacetylation of Alkenes Promoted by a Photoactive Electron Donor–Acceptor Complex (2022)**

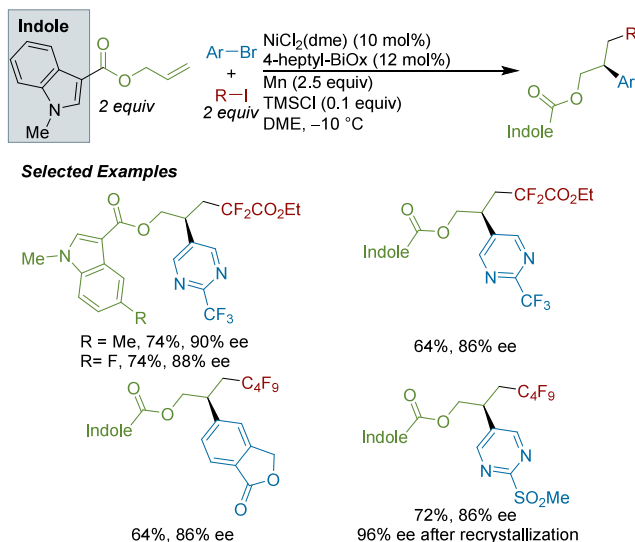


of a photoactive electron donor–acceptor (EDA) complex of the *N*-hydroxypthalimide ester with Hantzsch ester that can be directly excited by 390 nm light. Electron-poor ligands provided increased yields, with 4,4'-CO<sub>2</sub>Me-bpy providing the highest yield. Only NHP esters that formed tertiary radicals were effective, as primary and secondary radicals formed the two-component coupling products. A variety of acceptor alkenes were compatible.

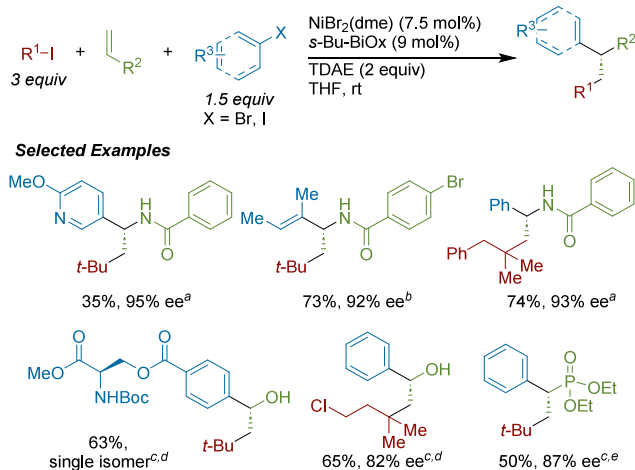
**7.1.1.2. Stereocontrolled Addition of C(sp<sup>2</sup>) and C(sp<sup>3</sup>) Electrophiles Across Alkenes.** Building upon their work in racemic three-component coupling reactions, Lingling Chu and co-workers developed an enantioselective three-component coupling of unactivated terminal olefins with aryl bromides and perfluoroalkyl iodides (**Scheme 396**).<sup>557</sup> A variety of electron deficient 5-bromopyrimidines, pyridines, and quinolines could be coupled. A range of perfluoroalkyl and tertiary alkyl iodides could be coupled. The indole-3-carboxylate moiety was critical in maintaining high enantioselectivity. Substitution on the indole moiety often resulted in a decrease in enantioselectivity, while removal of this directing group entirely led to low yields and poor levels of stereocontrol.

Shortly after their initial reports, the Nevada group designed an nickel asymmetric intermolecular dicarbofunctionalization reaction of vinyl amides (**Scheme 397**).<sup>558</sup> BiOx ligands proved superior compared to PyBOX or PyOx ligands, and the authors utilized DFT calculations to develop a stereochemical model for this transformation. A wide variety of iodoarenes and heterocycles provided good yields. An increase in catalyst loading allowed expansion of the scope to include vinyl bromides (in place of aryl iodides) as well as vinyl boronates and vinyl phosphonates.

**Scheme 396. Ni-Catalyzed Enantioselective Fluoroalkylation of Allyl Alcohol Derivatives (2020)**



**Scheme 397. Ni-Catalyzed Enantioselective Arylalkylation of Vinyl Amides, Boronates, and Phosphonates (2020)<sup>a</sup>**

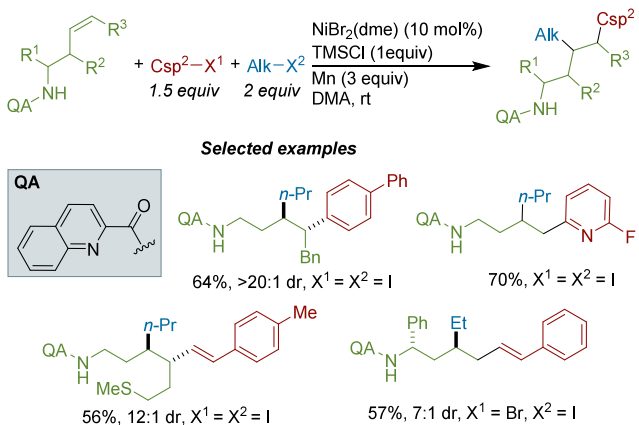


<sup>a</sup>(a) With X = I. (b) With X = Br. (c) With precomplexed [(S)-s-Bu<sub>2</sub>-BiOx]NiBr<sub>2</sub> (10 mol%) and LiBF<sub>4</sub> (1 equiv). (d) With vinyl boronate and yield is after treatment with NaBO<sub>3</sub>•4H<sub>2</sub>O. (e) With vinyl phosphonate.

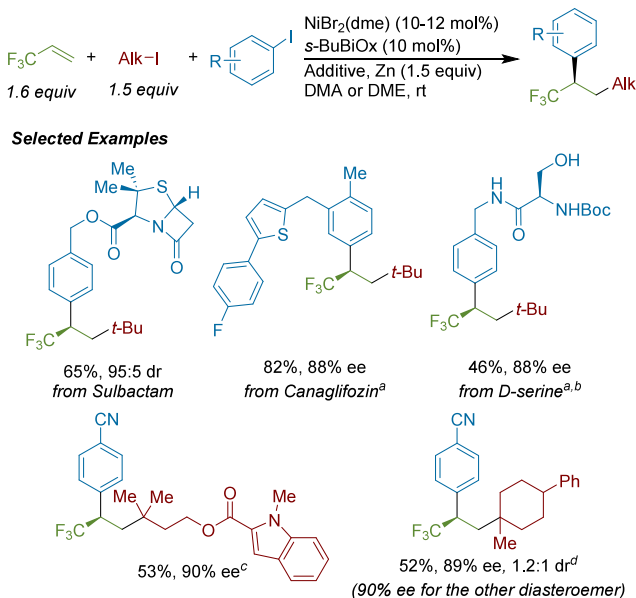
In 2021, Chao Wang and co-workers reported a directed arylalkylation of homoallylic amines with diastereocontrol of both 1,2 and 1,3 stereocenters (**Scheme 398**).<sup>559</sup> Of the variety of 3-butenamine compounds bearing different directing groups, quinolinamide (QA) was the most effective in minimizing side reactions. Aryl iodides bearing various *ortho*-, *meta*-, and *para*-functionalities were well-tolerated, as well as heteroaryl iodides, aryl bromides, and vinyl bromides. Primary and secondary alkyl iodides afforded high yields, but tertiary alkyl iodides were not compatible. The reaction is stereospecific: changing olefin geometry resulted in the formation of a different diastereomer.

The low cost of 3,3,3-trifluoropropene motivated Xingang Zhang and co-workers to explore its enantioselective arylalkylation in 2022 (**Scheme 399**).<sup>560</sup> Reactions with chiral BiOx ligands provided the highest enantioselectivity, with s-Bu<sub>2</sub>-BiOx performing the best. Overall, reactions with electron-

**Scheme 398. Ni-Catalyzed Quinolinamide-Directed Diastereoselective Difunctionalization of Alkenes with Aryl or Vinyl Halides and Alkyl Halides (2021)**



**Scheme 399. Ni-Catalyzed Enantioselective Dicarbofunctionalization of 3,3,3-trifluoropropene (2022)<sup>a</sup>**

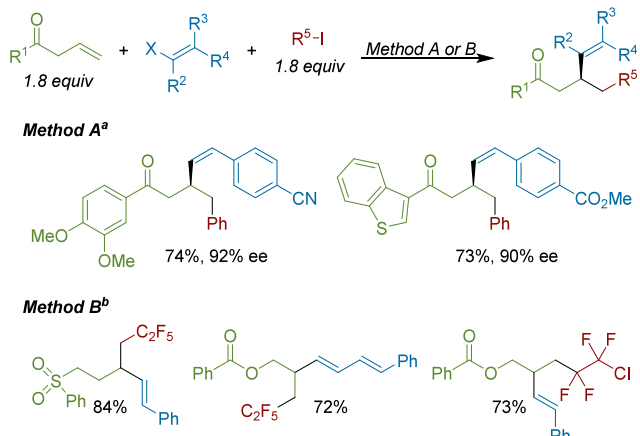


<sup>a</sup>(a) With NaI (0.5 equiv). (b) With NiBr<sub>2</sub>(dme) (13 mol%) and (S)-s-Bu-BiOx (13 mol%). (c) With FeCl<sub>3</sub> (0.25 equiv). (d) With FeBr<sub>2</sub> (0.25 equiv).

deficient aryl iodides (including heteroaryl iodides) gave higher yields than electron-rich aryl iodides. The broad scope required the authors to map out a number of additive effects, including iron, sodium, and calcium halide salts. Experiments supplied evidence for two different radical intermediates.

Leveraging the reactivity of five-membered nickel metallacycles, Lingling Chu and co-workers developed an enantioselective fluoroalkylalkenylation of  $\beta,\gamma$ -unsaturated ketones (Scheme 400).<sup>561</sup> The addition of benzoic acid decreased the amount of byproduct arising from the two-component XEC. The coordinating ability of the ketone and chelate ring size were important for enantioselectivity, with electron-rich  $\beta,\gamma$ -unsaturated ketones consistently providing >90% ee. A variety of alkenyl iodides and perfluoroalkyl iodides were compatible. In this study, the authors also further developed

**Scheme 400. Alkylalkenylation of Alkenes via Carbonyl-Directed Nickel XEC (2022)<sup>a</sup>**

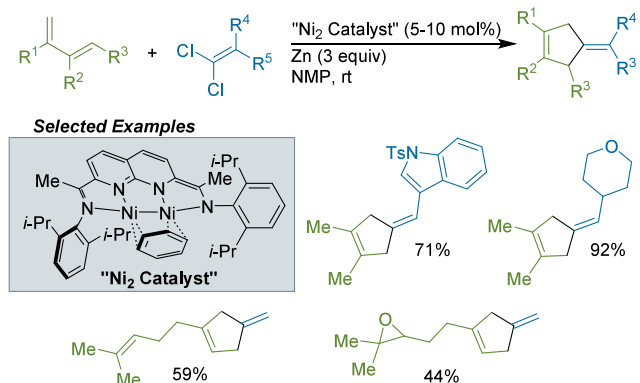


<sup>a</sup>Method A: With X = I, Ni(COD)<sub>2</sub> (10 mol%), s-Bu-BiOx (12 mol %), PhCO<sub>2</sub>H (0.6 equiv), Mn (2.5 equiv), and DME at –30 °C. Method B: With X = Br, NiCl<sub>2</sub>(dme) (10 mol%), Bn-BiOx (12 mol%), Mn (2.5 equiv), and diglyme at rt.

couplings with other directing groups to form racemic products using two C(sp<sup>2</sup>) electrophiles; the products are also shown in Scheme 400.

**7.1.1.3. Difunctionalization with C(sp<sup>2</sup>)/C(sp<sup>2</sup>) and C(sp)/C(sp) Electrophiles.** A [4 + 1] cycloaddition method was disclosed by the Uyeda group using dinickel catalysis, providing direct access to polysubstituted cyclopentenes from 1,3-dienes, which are difficult to engage through traditional pericyclic reactivity (Scheme 401).<sup>562</sup> Using a sterically bulky

**Scheme 401. Ni-Catalyzed [4 + 1] Cycloadditions of Dienes with Dichlorovinylidene Electrophiles (2019)**

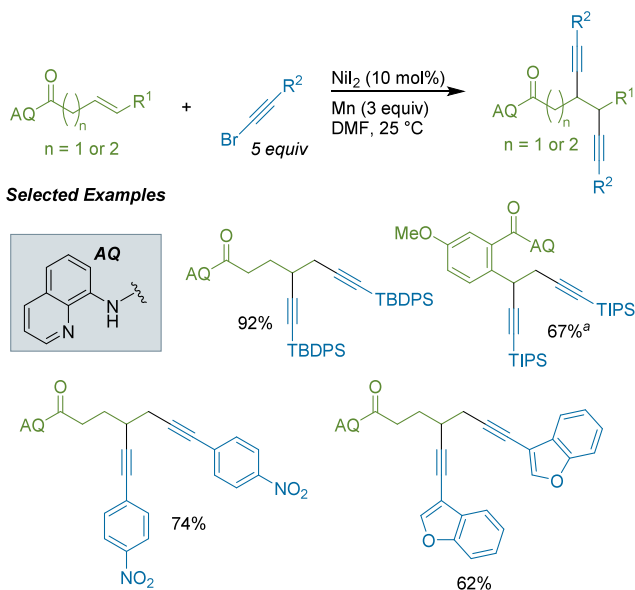


dinuclear nickel catalyst they previously developed for methylenecyclopropanation,<sup>563</sup> methylenecyclopentenes were successfully synthesized with minimal isomerization. A variety of substituted cycloalkenes could be accessed with control of alkene geometry. No rearranged product from a vinylcyclopropane intermediate was observed under the reaction conditions, suggesting that a mechanism proceeding through [2 + 1] cycloaddition followed by a cyclopropane rearrangement was not operative. DFT models highlighted the unique ability of the dinickel catalyst to stabilize both  $\pi$  systems during the C–C bond forming reductive elimination step.

A directing group strategy enabled Aijun Lin, Hequan Yao, and co-workers to achieve alkene dialkylation by (Scheme

402).<sup>564</sup> 8-Aminoquinone gave superior reactivity compared to other directing groups. A range of bromoalkynes bearing bulky

**Scheme 402.** Ni-Catalyzed 1,2-Dialkylation of Alkenes Using an 8-Aminoquinoline Directing Group (2019)<sup>a</sup>



<sup>a</sup>With Zn (3 equiv) at 40 °C.

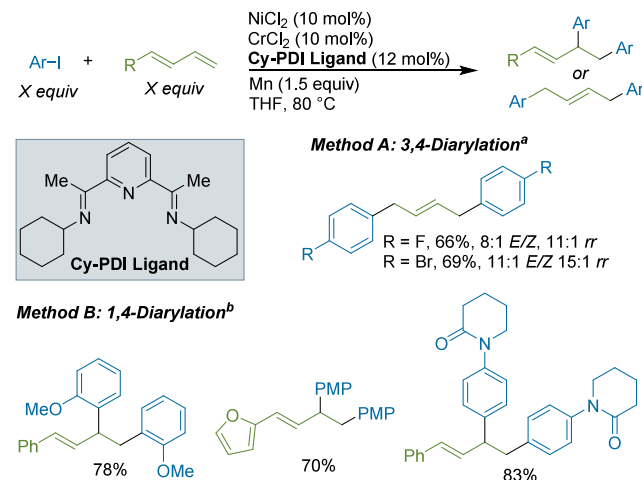
silyl protecting groups were well tolerated. Electron neutral and electron rich aryl-substituted bromoalkynes were well tolerated, and both mono- and disubstituted alkenes, as well as internal and terminal alkenes could be employed. Notably, this was a rare case where an aromatic nitro group was tolerated under XEC conditions.

In 2022, Qing-An Chen and co-workers developed a divergent regio- and stereoselective diarylation of dienes using Ni/Cr cocatalysis that did not require the formation of a polar metal alkoxide (e.g., Cr–O) as a thermodynamic driving force (Scheme 403).<sup>565,566</sup> Compared to bipyridine ligands, tridentate pyridine-2,6-diimine (PDI) ligands improved the yield and *E/Z* ratio of the products. The 1,3-diarylation reaction was tolerant of electronically and sterically diverse iodoarenes. Using modified reaction conditions, the feedstock chemical 1,3-butadiene could be functionalized to afford 1,4-diarylated products. Subjecting a 1:1 mixture of *E/Z* isomers led to stereoconvergence to the (*E*)-product, while other mechanistic probes supported Cr-mediated formation of aryl radicals. EPR studies suggested CrCl<sub>2</sub> could regenerate PDI-ligated Ni(I) species under these conditions.

The Giri group reported the Ni-catalyzed  $\beta,\delta$ -dialkenylation of  $\gamma,\delta$ -unsaturated nitriles with alkenyl triflates as the electrophile (Scheme 404).<sup>40</sup> These conditions do not require a strong directing group auxiliary used in other reports, but rather rely on nitrile substitution on the alkene. In contrast to metal powder reducing agents, the authors found that 3-phenylpropyl zinc bromide the best performing. Additive effects were also notable: zinc chloride was proposed to activate the alkenyl triflate, while KPF<sub>6</sub> was proposed to ensure a sufficient concentration of cationic nickel species.

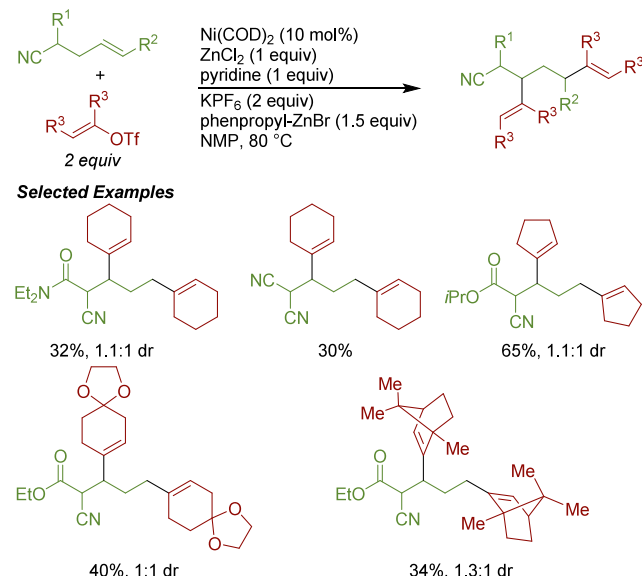
**7.1.1.4. Stereocontrolled Difunctionalization with C(sp<sup>2</sup>) and C(sp) Electrophiles.** In order to access chiral  $\alpha,\alpha,\beta$ -triarylated ethane motifs, the Diao group developed the enantioselective diarylation of styrenes with aryl and heteroaryl

**Scheme 403.** Nickel- and Chromium-Catalyzed Regioselective Diarylation of Dienes (2022)<sup>a</sup>



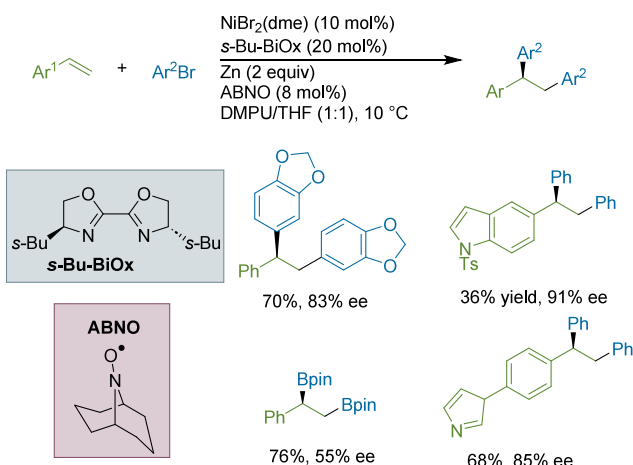
<sup>a</sup>Method A: aryl iodide (2.2 equiv), diene (1 equiv), conditions as in the Scheme. Method B: With aryl iodide (1 equiv), diene (3 equiv), NiCl<sub>2</sub> (10 mol%), PDI-Ligand (12 mol%), CrCl<sub>2</sub> (20 mol%), (PhO)<sub>2</sub>PO<sub>H</sub> (7.5 mol%), and MeCN at 80 °C. PMP = *para*-methoxyphenyl.

**Scheme 404.** Ni-Catalyzed Regioselective  $\beta,\delta$ -Dialkenylation of  $\gamma,\delta$ -Unsaturated Nitriles with Vinyl Triflates (2023)



bromides (Scheme 405).<sup>567</sup> Sterically hindered BiOx ligands provided the highest enantioselectivity, while other *N*-ligands resulted in low conversion of starting material. The use of 9-azabicyclo[3.3.1]nonane *N*-oxyl radical (ABNO) was essential and unusual in XEC reactions. Multivariate analysis determined that the percent buried volume of the *N*-oxyl radical additive was the dominant effect on enantioselectivity, with sterically unhindered *N*-oxyl radicals providing low enantioselectivities. In addition to the effect seen with differential Ni/ABNO stoichiometry, these correlations give evidence toward ABNO serving as an auxiliary ligand. Observed inhibition of the reaction by excess ABNO, as well

**Scheme 405.** Ni-Catalyzed Enantioselective Diarylation of Styrenes with Aryl Bromides (2019)



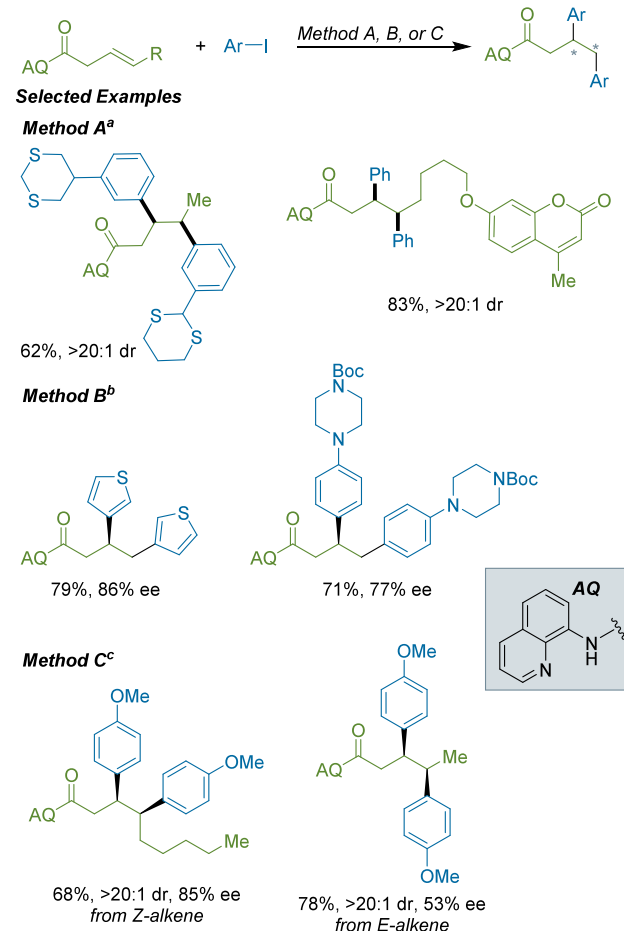
as benzylic dimer formation, lent evidence for an on-cycle benzylic radical intermediate.

Liang-An Chen, Liangliang Song, and co-workers reported a diastereoselective and enantioselective directed diarylation of  $\beta,\gamma$ -unsaturated AQ amides (Scheme 406).<sup>568</sup> Both *E*- and *Z*-internal alkenes were well tolerated, as well as a variety of electronically and sterically diverse heteroaryl iodides. High *syn*-diastereoselectivity for *E*-alkene substrates was attributed to the formation of a cationic nickel species that could strongly coordinate the alkene. Building on this logic, two different cationic nickel catalyst systems, along with PHOX ligands, were utilized to achieve enantioselective diarylation for internal or terminal alkenes. Salt additives  $\text{CaF}_2$  and KF were essential to achieve high yields, possibly functioning as halide scavenging agents to facilitate regeneration of cationic arylnickel species. In addition to ligand choice, *Z*-alkene geometry was crucial for high enantioselectivity.

**7.1.1.5. Addition of  $C(sp^3)$  Electrophiles Across Alkenes.** Ming Joo Koh, Yu Lan, and colleagues also utilized the AQ directing group to achieve vicinal dialkylation of  $\beta,\gamma$ -unsaturated amides with *N*-hydroxyphthalimide (NHP) esters and alkyl iodides in high regioselectivity (Scheme 407).<sup>569</sup> The NHP ester coupling partner demonstrated broad scope: benzylic, primary, secondary, and tertiary alkyl groups were all tolerated (although benzylic 1° provided the highest yield). Meanwhile, productive yields were observed for primary alkyl iodides only. The alkene was almost exclusively unfunctionalized  $\beta,\gamma$ -unsaturated AQ amide, although examples of more substituted alkenes exhibited high diastereocontrol. The authors undertook extensive DFT studies that suggested: 1) the NHP ester reacts with  $[\text{Ni}^0]$  faster than the primary alkyl iodide; 2) the alkyl iodide reacts faster with  $[\text{Ni}^1]$  than the NHP ester; and 3) the regioselectivity likely arises from the migratory insertion of the initially formed alkynickel intermediate.

Wei Shu reported the dialylation of *N*-aryl 3,4-butenamides with two different alkyl bromides differentiated by their adjacent functional groups (Scheme 408).<sup>570</sup> The primary alkyl bromide was well-matched with the  $\alpha$ -bromoacetonitrile. The authors reported a two-step mechanism in which initial atom-transfer radical addition of the  $\alpha$ -bromoacetonitrile forms a 3-bromobutenaamide intermediate (up to 80% yield during the reaction) followed by  $C(sp^3)-C(sp^3)$  XEC.

**Scheme 406.** Ni-Catalyzed Directed Asymmetric 1,2-Diarylation of  $\beta,\gamma$ -Unsaturated Aminoquinone Amides (2023)<sup>a</sup>

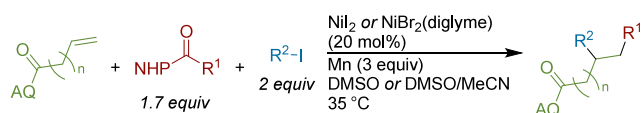


<sup>a</sup>(a) Method A: With aryl iodide (3 equiv),  $\text{Ni}(\text{OTf})_2$  (5 mol%),  $\text{Mn}$  (3 equiv), and DMF at 50 °C. (b) Method B: With aryl iodide (6 equiv),  $\text{Ni}(\text{ClO}_4)_2 \bullet 6\text{H}_2\text{O}$  (20 mol%), (S)-*I*-Pr-PHOX (25 mol%),  $\text{Mn}$  (4 equiv), KF (0.5 equiv), and DMPU at 30 °C. Method C: With aryl iodide (4 equiv),  $\text{Ni}(\text{BF}_4)_2 \bullet 6\text{H}_2\text{O}$  (20 mol%), (S)-*s*-Bu-PHOX (25 mol%),  $\text{CaF}_2$  (1 equiv),  $\text{Mn}$  (4 equiv), and DMF at 30 °C.

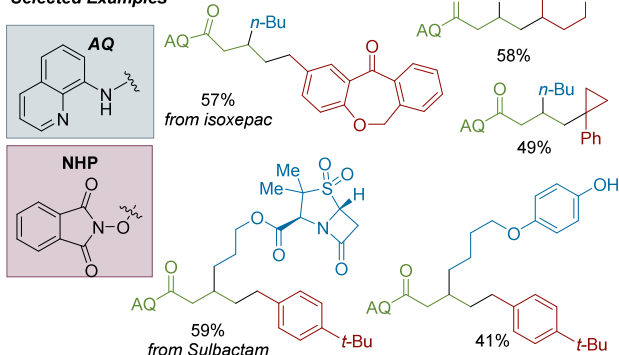
**7.1.1.6. C–X Bond Formation Across Alkenes.** Beginning in 2011, our group published a series of reports detailing the 1,4-addition of organic halides and chlorosilanes to  $\alpha,\beta$ -unsaturated ketones.<sup>571</sup> Although these reactions resemble a conjugate addition with trapping of the enolate by a chlorosilane, the mechanism is a catalytic version of chemistry reported by MacKenzie<sup>572</sup> where  $\text{Ni}^0$  reacts with chlorosilane and enone to form an O-silylated allylnickel intermediate. These reagents have rich reactivity with a variety of organic halides. Coupling with secondary and tertiary alkyl bromides worked best with a catalyst composed of nickel and ttbtipy (Scheme 409), but primary alkyl bromides led to alkyl dimer products. Selective coupling with primary alkyl bromides required changing to the more hindered  $6,6''\text{-Br}_2\text{tpy}$  and a different solvent (Scheme 410).<sup>573</sup>

This reactivity could be extended to the three-component coupling with aryl halides and chlorosilanes (Scheme 411). Where the previously used terpyridine ligand gave low conversion, producing mostly silylated allyl dimer byproducts, a systematic study of bidentate pyridine ligands revealed that

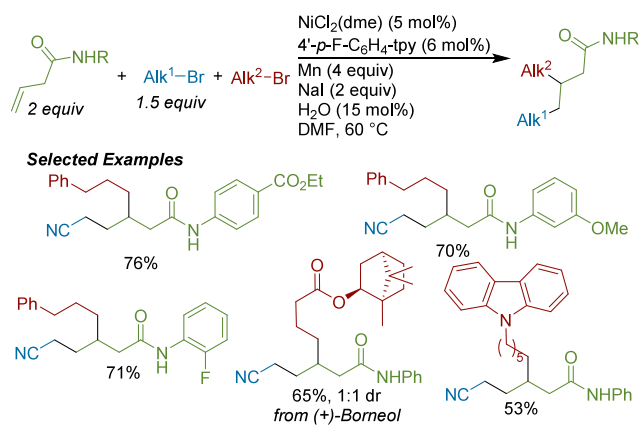
**Scheme 407.** Ni-Catalyzed Dialkylation of  $\beta,\gamma$ -Unsaturated Aminoquinone Amides with Alkyl Halides and NHP Esters (2020)



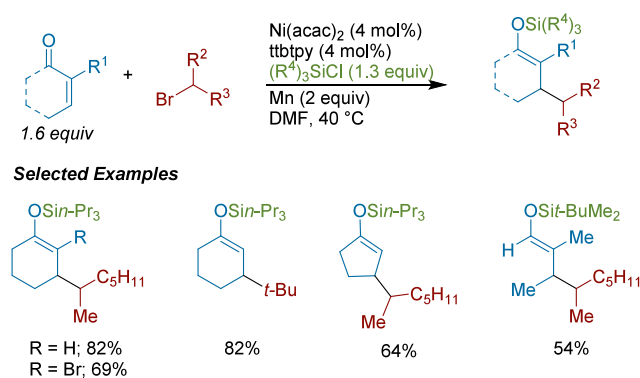
**Selected Examples**



**Scheme 408.** Ni-Catalyzed Dialkylation of *N*-Aryl 3,4-Butenamides with 1° Alkyl Bromides and  $\alpha$ -Bromoacetonitrile (2022)

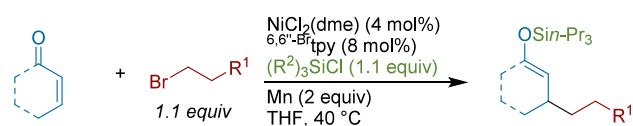


**Scheme 409.** Ni-Catalyzed 1,4-Addition of Alkyl Bromides and Chlorosilanes to  $\alpha,\beta$ -Unsaturated Ketones (2011)

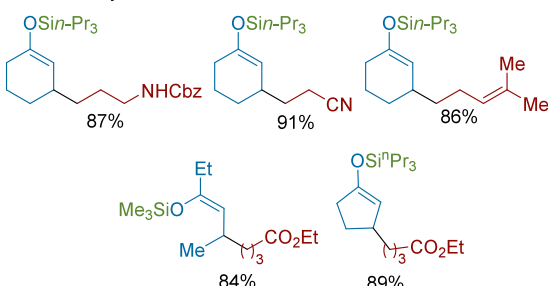


neocuproine afforded the highest yield and cross-selectivity (except with hindered aryl halides and acyclic *E*-enones, which worked best with less hindered bpy ligands). A variety of  $\alpha,\beta$ -unsaturated cyclic and linear ketones and aldehydes performed well, and electron poor aryl bromides coupled in the highest

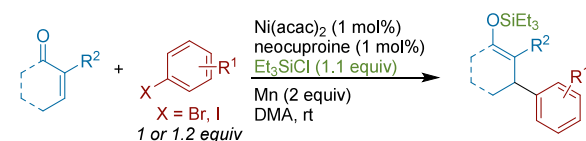
**Scheme 410.** Ni-Catalyzed 1,4-Addition of 1° Alkyl Bromides and Chlorosilanes to  $\alpha,\beta$ -Unsaturated Ketones (2017)



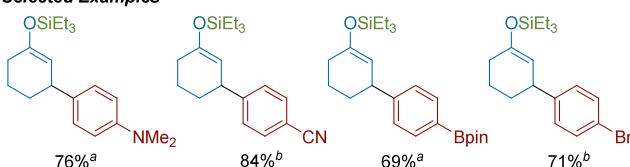
**Selected Examples**



**Scheme 411.** Ni-Catalyzed 1,4-Addition of Aryl Halides and Chlorosilanes to  $\alpha,\beta$ -Unsaturated Ketones (2013)<sup>a</sup>



**Selected Examples**



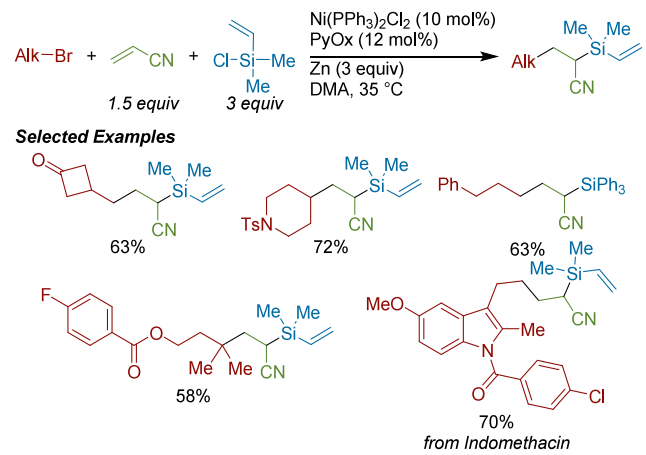
<sup>a</sup>(a) With X = I, (b) With X = Br.

yields. Notably, high-oxidation state functional groups, including sulfone and sulfur pentafluoride products could be obtained in high yield, and aryl halides that were sensitive to hydrolysis could be used. Mechanistic experiments provided concrete evidence for an enone-first mechanism that proceeded through an allynickel(II) intermediate.

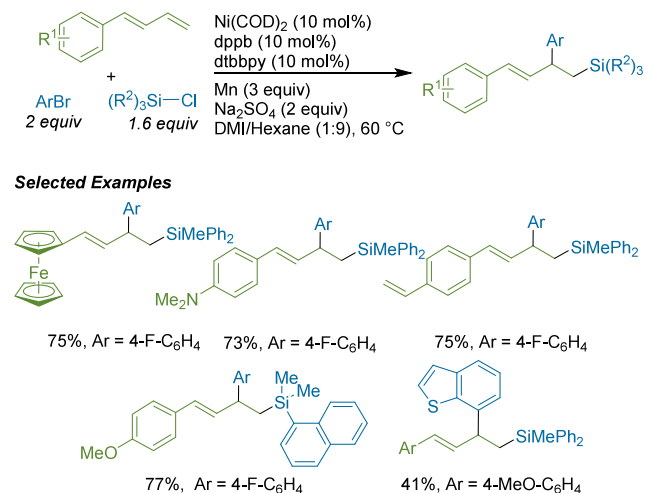
Xuan Zhang reported the cross-electrophile carbosilylation of an acrylonitrile in 2022 (Scheme 412).<sup>575</sup> The PyOx ligand (along with PPh<sub>3</sub> brought in by the precatalyst) was essential for overall reaction success. A wide range of primary, secondary, and tertiary alkyl bromides were tolerated. While chlorodimethylvinylsilane was the best performing silane, good yields could also be obtained with Ph<sub>3</sub>SiCl and Me<sub>3</sub>SiCl. As a synthetic application, the authors utilized this method to increase the hydrophobicity on the surface of silicon-based glass materials using modified reaction conditions.

One year later, Xing-Zhong Shu and co-workers reported the 1,2-carbosilylation of 1-aryl-1,3-butadienes with aryl bromides and chlorosilanes (Scheme 413).<sup>576</sup> Optimal conditions used a 1:1:1 ratio of nickel/dppb/dbbipy, which suggested serial ligand catalysis or the presence of two catalyst species. The authors found that bisphosphine ligands with either shorter or more rigid backbones led to sluggish arylation and larger distribution of silyl-protonation side products, while monodentate phosphate ligands gave no yield. The improvement in yield provided by electron-rich bidentate nitrogenous ligands was attributed to promotion of the silylation step. Both mono

**Scheme 412.** Ni-Catalyzed Carbosilylation of Acrylonitrile with Alkyl Bromides and Chlorosilanes (2022)



**Scheme 413.** Ni-Catalyzed 1,2-Carbosilylation of 1-Aryl-1,3-Butadienes with Aryl Bromides and Chlorosilanes (2023)



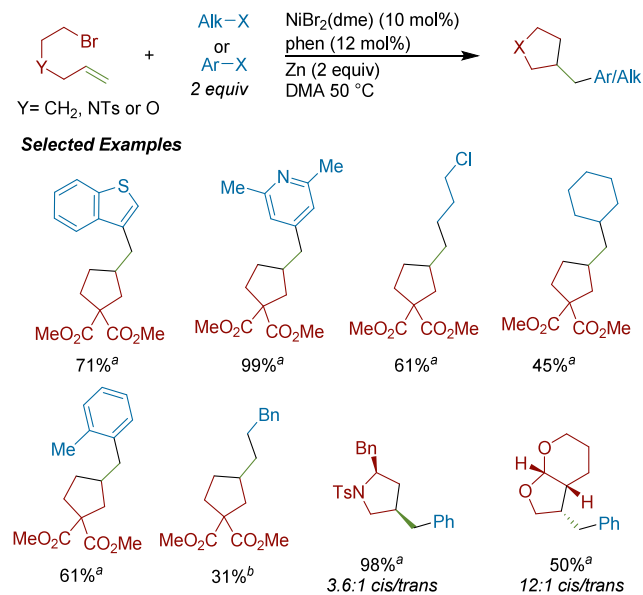
and diaryl chlorosilanes exhibited high yields, among many other diverse silyl groups. Studies supported the formation of  $\pi$ -allylnickel intermediate species.

**7.1.2. Cyclizations.** The reactions in this section mostly involve two reactants: one alkene-tethered electrophile and a separate electrophilic coupling partner and result in cyclized products via the formation of two new C–C bonds. Additionally, a few C–X bond forming cyclizations are discussed.

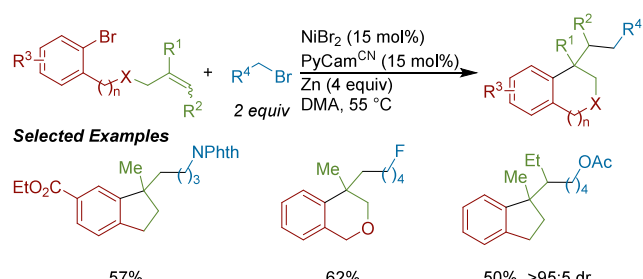
**7.1.2.1. Cyclizations with  $C(sp^2)$  and  $C(sp^3)$  Electrophiles.** While radical cyclization reactions had previously been used as a mechanistic probe,<sup>577</sup> it was not until 2018 that this reaction was optimized and turned into a useful transformation by Diao and co-workers (**Scheme 414**).<sup>578</sup> Successful substrates required some bias to accelerate cyclization or else direct cross-coupling with the aryl bromide competed (as for simple, unsubstituted chains). This reaction was insensitive to the electronics and sterics of the aryl bromides and provided high yields for a variety of heterocycles. For substrates containing initial stereocenters, moderate to good diastereoselectivity was observed.

Soon thereafter, Chuan Wang developed a cyclization and arylation of aryl bromide-tethered alkenes with alkyl halides (**Scheme 415**).<sup>579</sup> Bromides were the best-performing electro-

**Scheme 414.** Ni-Catalyzed Intramolecular Radical Cascade Cyclization and Arylation to Form Five-Membered Rings (2018)



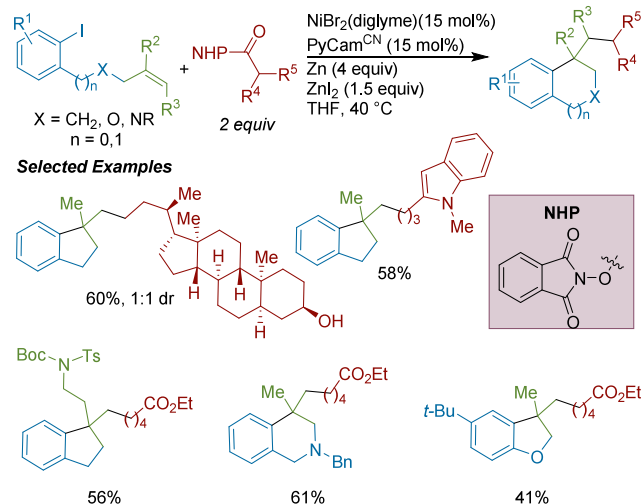
**Scheme 415.** Ni-Catalyzed Cyclization and Alkylation with Alkyl Bromides to form Benzene-Fused Carbocycles and Heterocycles (2019)



phile for both reaction partners, as the iodide analogues resulted in high levels of reductive Heck side products. In comparison to PyCam<sup>CN</sup>, other pyridine-based ligands performed poorly. Various disubstituted and  $\alpha,\alpha,\beta$ -trisubstituted alkenes reacted with high diastereocontrol, suggesting that radical addition across the alkene was not an operative mechanistic step. Instead, the authors proposed an “aryl-first” mechanism followed by cyclative migratory insertion and C–C bond formation. In addition to indane cores, tetrahydroisoquinoline, isochroman, and indoline derivatives were obtained.

Chuan Wang and co-workers then developed modified conditions that replaced the alkyl bromide coupling partner in their previous report (**Scheme 415**) with an NHP ester (**Scheme 416**).<sup>580</sup> PyCam<sup>CN</sup> was again found to be optimal for this transformation. In this case, alkene-tethered iodoarenes were reactive, whereas bromoarenes were unreactive. The authors observed that amide solvent afforded cross-coupling of the iodoarene with the NHP ester instead of the desired product. Coupling with secondary alkyl NHP esters proceeded readily, but tertiary and benzylic NHP esters were not tolerated. Geminal disubstituted and  $\alpha,\alpha,\beta$ -trisubstituted alkenes were also successful coupling partners under these conditions, and heterocyclic indolines and dihydropyranofurans could be used. While lower yielding, an asymmetric variation of

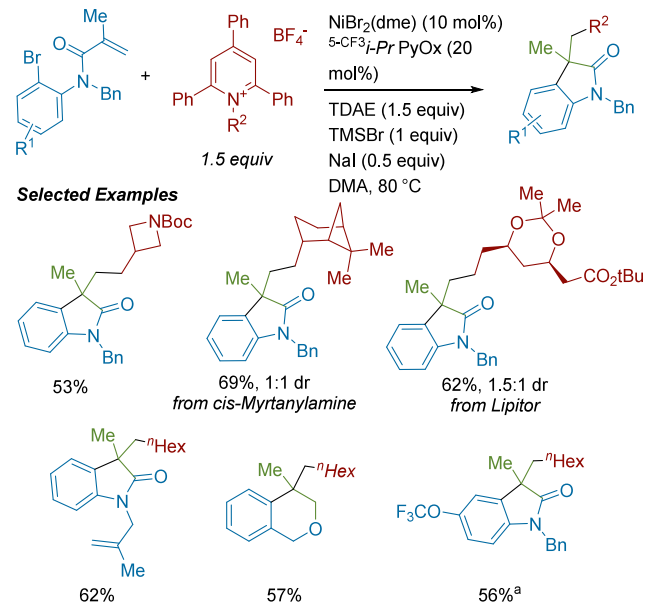
**Scheme 416. Ni-Catalyzed Cyclization and Alkylation with NHP Esters to Form Benzene-Fused Carbocycles and Heterocycles (2019)**



the model substrate pair was demonstrated. Employing Bn-BiOx as the chiral ligand afforded the product in 89% ee.

Liang Gong, Haibin Liu, Yu-Long Li, and co-workers reported a cyclization and alkylation of aryl bromide–tethered methacrylamides with *N*-alkylpyridinium salts (Scheme 417).<sup>581</sup> A catalyst system containing NiBr<sub>2</sub>(dme) and PyOx

**Scheme 417. Ni-Catalyzed Cyclization and Alkylation with *N*-Alkylpyridinium Salts to form Benzene-Fused Carbocycles and Heterocycles (2022)<sup>a</sup>**



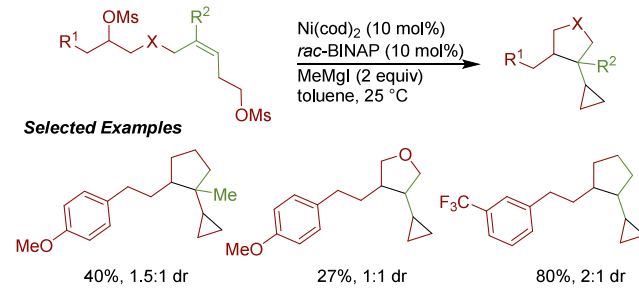
<sup>a</sup>With aryl iodide.

as a ligand provided the highest yields, and TDAE was a superior reductant to both Zn and Mn. Notably, sterically hindered primary alkylamine derivatives afforded high yields, while secondary amines required slight modification of the pyridinium backbone to achieve high yield. For some alkene-tethered aryl bromides, a different PyOx ligand was necessary to achieve full consumption. Benzene-annulated cyclic

compounds including dihydrobenzofurans and dihydroisoquinolines could be synthesized.

In 2022, the Jarvo group disclosed a method to prepare cyclopropyl substituted cyclopentanes and tetrahydrofurans by the double cyclization of the dimesylate of 1,3-dihydroxy-alk-3-enes (Scheme 418).<sup>582</sup> The authors observed that both di- and

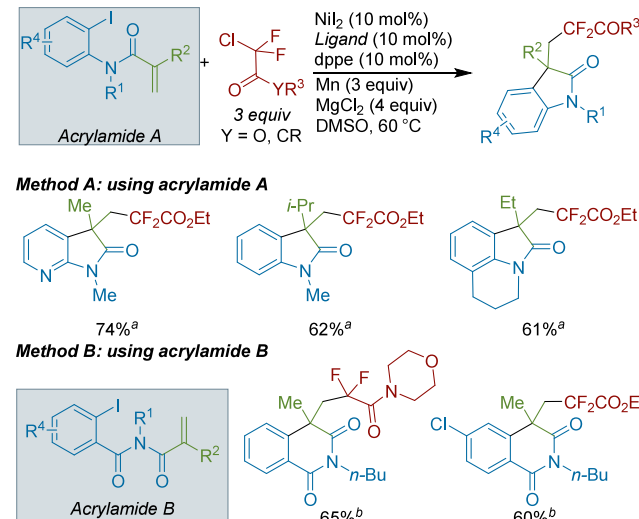
**Scheme 418. Synthesis of Vicinal Cyclopropane and Cyclopentane Rings by Double Cyclization of an Alkene Dimesylate (2022)**



trisubstituted alkenes could be used as substrates, with the latter forming vicinal quaternary and tertiary all-carbon centers. Both *E*- and *Z*-dimesylate compounds afforded the same major diastereomer under the optimized conditions, consistent with a mechanism involving radical *exo*-trig cyclization over migratory insertion. Further control experiments suggested that the dimesylate is converted into the diiodide before coupling. Meanwhile, competition studies illustrated that *S*-*exo*-trig radical cyclization occurs at the secondary electrophilic center.

Dechun Huang, Fei Ji, and co-workers reported on a related cyclization and alkylation reaction with  $\alpha$ -chloro- $\alpha,\alpha$ -difluoroacetates and ketones (Scheme 419).<sup>583</sup> The optimized conditions featured a dual-ligand catalyst system composed of both dppe and a bipyridine ligand. Both oxindoles and isoquinoline-1,3-diones could be synthesized under similar conditions.

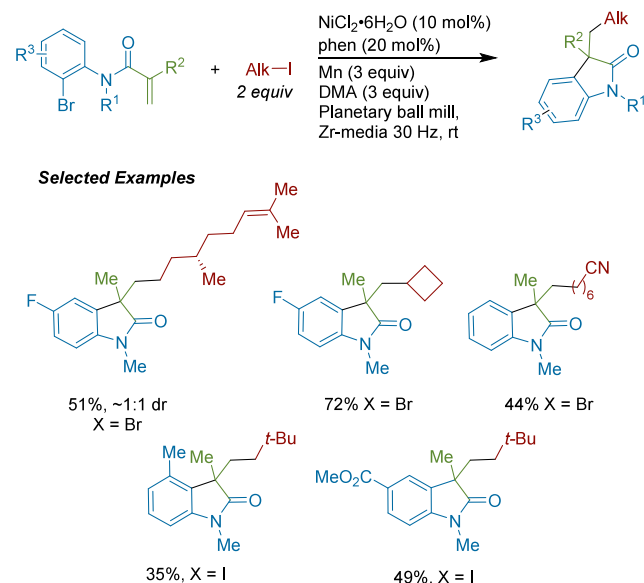
**Scheme 419. Ni-Catalyzed Cyclization and Alkylation to Form Difluorocarbonyl-Functionalized Oxindoles and Isoquinoline-1,2-diones (2023)**



<sup>a</sup>(a) With  $^{4,4'}\text{-CO}_2\text{Me}$ bpy as ligand. (b) With  $^{4,4'}\text{-MeO}$ bpy as ligand.

In 2023, Morrill and Browne developed mechanochemical conditions for the cyclization and alkylation of aryl bromide-tethered alkenes with alkyl iodides to form oxindoles (**Scheme 420**).<sup>584</sup> Compared to typical XEC reactions with metal

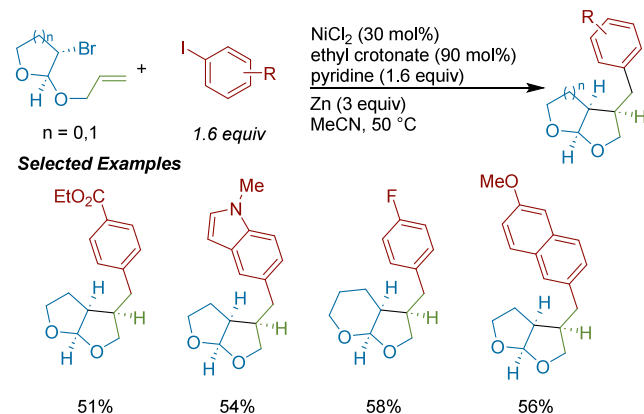
**Scheme 420.** Ni-Catalyzed Mechanochemical Cyclization and Alkylation with Alkyl Iodides to Form Oxindoles (2023)



powders, mechanochemistry offers a few key advantages: shorter reaction times than their solution phase counterparts, and less solvent use owing to liquid-assisted grinding. The reaction proceeded in a steel ball milling machine at room temperature, affording oxindole products of comparable complexity to solution-based methods.<sup>580</sup> A preliminary result of a chiral oxindole obtained in moderate yield and enantioselectivity using  $t\text{-BuPyOx}$  highlighted the viability of mechanochemistry for enantioselective nickel catalysis.

**7.1.2.2. Stereocontrolled Cyclizations with  $C(sp^2)$  and  $C(sp^3)$  Electrophiles.** In 2012, Yu Peng and co-workers developed a Ni-catalyzed stereoselective cyclization of  $\beta$ -bromo acetals with aryl iodide (**Scheme 421**).<sup>205</sup> Pyridine and a  $\pi$ -ligand are added to generate the catalyst in situ. Both methyl acrylate and ethyl crotonate are common, but ethyl

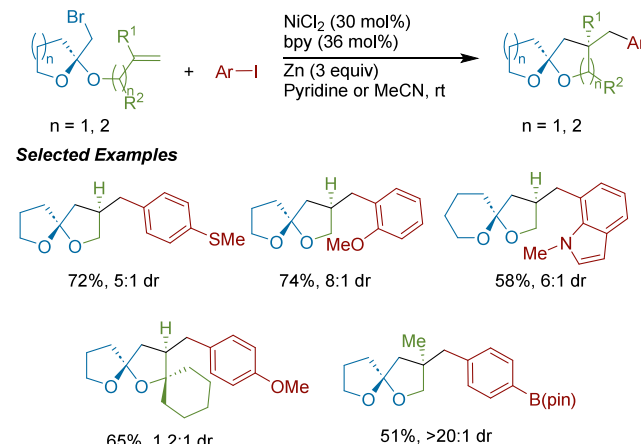
**Scheme 421.** Ni-Catalyzed Stereoselective Cyclization and Arylation of  $\beta$ -Bromo Acetals with Aryl Iodides (2012)



crotonate was chosen, as methyl acrylate could hinder cross-productivity by acting as a Michael acceptor. Initial studies determined that  $\beta$ -bromo acetals had a much higher conversion rate than aryl iodides, and all of the aryl iodide coupling partner must be added before the  $\beta$ -bromo acetal is introduced. Aryl iodides bearing electron-donating and -withdrawing groups were tolerated with good *endo*-diastereoselectivity.

An early example of a difunctionalization/cyclization reaction that afforded stereo-enriched products was also disclosed by Yu Peng and co-workers in 2014, in which 6-*exo*-trig cyclization and bis-spiroketalization onto ketal-tethered alkenes afforded [5,6]-spiroketals (**Scheme 422**).<sup>585</sup>

**Scheme 422.** Ni-Catalyzed Stereocontrolled Synthesis of Spiroketsals by Intramolecular Radical Cascade Cyclization and Coupling with Aryl Iodides (2014)

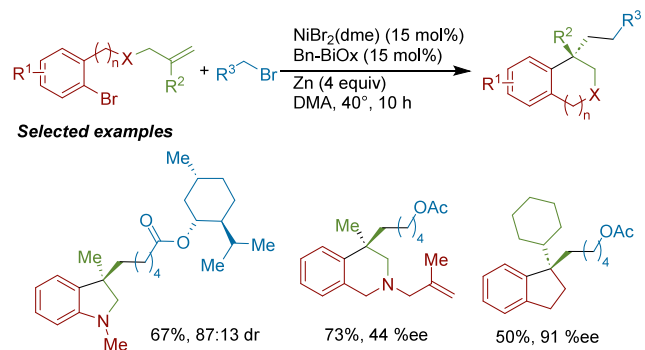


Using a relatively high catalyst loading, the intramolecular radical cascade cyclization-coupling of various functionalized aryl iodides could be achieved. The substrate scope is broad, affording a large number of complex spiroketals with good diastereoselectivity. In the proposed mechanism, the authors hypothesize that the anomeric effect forces a pseudochair conformation of the radical ketal tethered species formed by halogen atom abstraction. A 5- or 6-exo trig stereoselective radical cyclization could afford the observed stereochemical outcome.

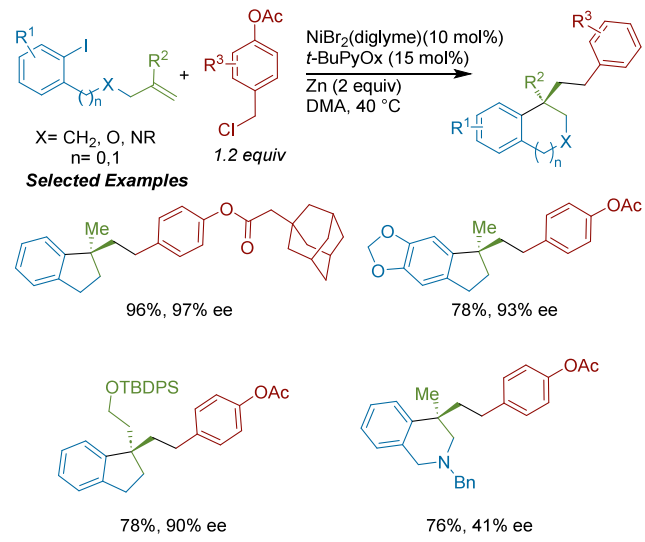
Chuan Wang and co-workers reported modified intramolecular radical cascade cyclization conditions that afforded enantioenriched products (**Scheme 423**).<sup>586</sup> Systematic examination of chiral phosphine and oxazoline-based ligands identified BnBiOx as the optimal ligand. High yields and enantioselectivities were achieved with disubstituted olefins, while monosubstituted olefins only gave large amounts of reductive Heck side product. Stoichiometric investigations of potential organonickel intermediates showed the wrong stereoisomer was obtained in the absence of Zn reductant, which is suggestive of migratory insertion by nickel(I). Ultimately, they concluded that migratory insertion was likely enantiodetermining.

In the above (**Scheme 423**) report, benzyl electrophiles were not compatible due to their propensity to undergo homodimerization. Motivated by this challenge, Chuan Wang and colleagues developed conditions to engage this common substrate class in their enantioselective intramolecular radical cascade cyclization and coupling (**Scheme 424**).<sup>587</sup> To match

**Scheme 423.** Ni-Catalyzed Enantioselective Cyclization and Alkylation with Alkyl Bromides to form Benzene-Fused Carbocycles and Heterocycles (2019)



**Scheme 424.** Ni-Catalyzed Enantioselective Cyclization and Benzylation to form Benzene-Fused Carbocycles and Heterocycles (2020)

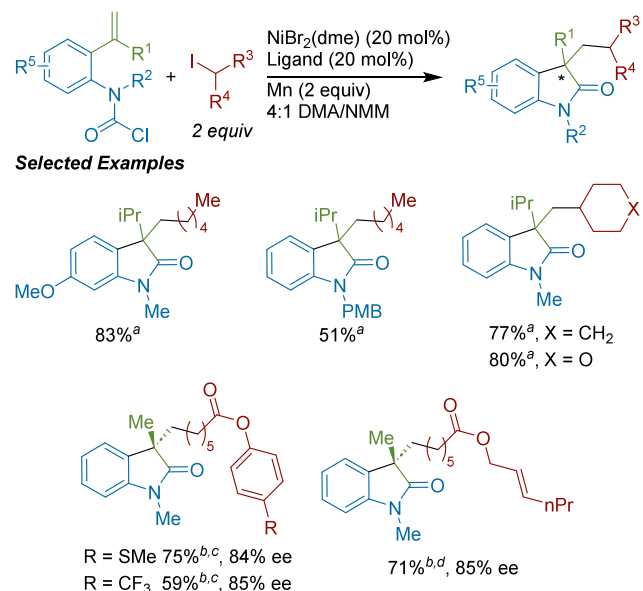


the higher reactivity of benzyl chlorides, the authors utilized more reactive aryl iodides. A PyOx ligand provided the best yields and enantiocontrol. For both the iodoarene partner and the benzyl chloride partner, electronically diverse functionalities could be tolerated, but secondary benzylic chlorides were not competent substrates. The authors proposed migratory insertion at a nickel(II) species rather than at nickel(I), but still proposed that migratory insertion was enantiodetermining.

In 2020, Chuan Wang and colleagues developed the first enantioselective carboacylation alkylation reaction (Scheme 425).<sup>588</sup> The racemic reaction progressed with *rac*-*t*-Bu-PyOx as a ligand and Mn as a reductant in a polar solvent mixture. In this report, switching to a more electron-rich morpholine-substituted *t*-Bu-PyOx ligand improved enantioselectivity (up to 88% ee). Both primary and secondary alkyl iodides as well as benzyl chlorides were well tolerated. Analogous to their previous arylalkylation reactions (Schemes 423 and 424), the authors proposed an enantiodetermining migratory insertion step.

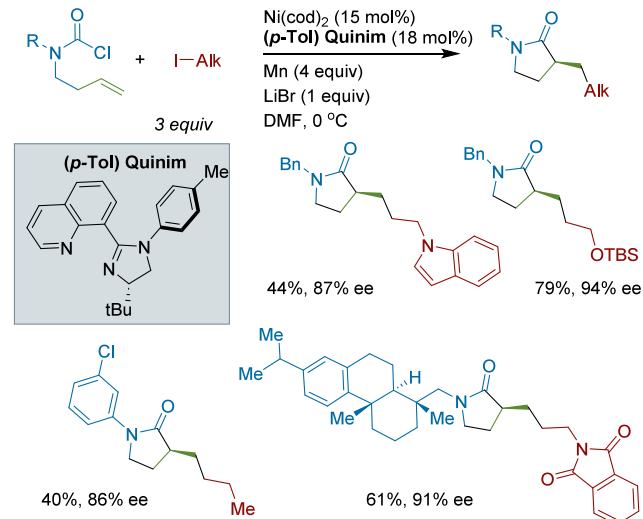
Motivated by the challenges of using internal alkenes in similar cyclization reactions, Jingping Qu, Yifeng Chen and colleagues developed a highly diastereo- and enantioselective

**Scheme 425.** Ni-Catalyzed Enantioselective Cyclization and Alkylation to Form Oxindoles (2020)<sup>a</sup>



<sup>a</sup>(a) With *rac*-*t*-Bu-PyOx as ligand at 0 °C. (b) With 4-morpholine (*S*)-*t*-Bu-PyOx as ligand. (c) At 10 °C. (d) At rt.

**Scheme 426.** Ni-Catalyzed Enantioselective Reductive Alkyl-Carbamoylation of Internal Alkenes (2020)

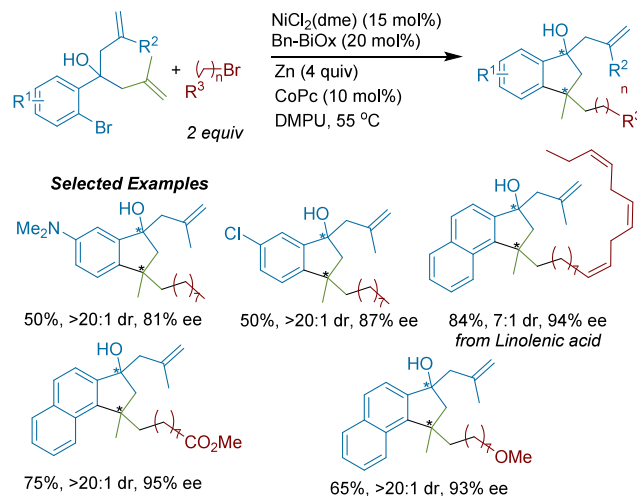


carbamoylation protocol that afforded pyrrolidinones bearing vicinal stereocenters (Scheme 426).<sup>589</sup> The electron-rich *t*-BuQuinim ligand provided higher enantioselectivity than the initially investigated Quinox ligand class. However, all Quinim ligands provided superior stereoinduction compared to commercially available PHOX or BiOx ligands. In addition to the PMB protecting group, other benzyl and alkyl protecting groups were well tolerated. Diverse tethered arenes could be coupled, including heteroaromatic compounds. High diastereeocontrol was also achieved, even when both trans and cis alkene isomers were used, indicating that alkene configuration did not impede stereochemical outcome. Importantly, the

same ligand scaffold permitted 1,1-disubstituted alkenes to be used as coupling partners, furnishing substrates with primary, secondary, and cyclic alkyl functionalities. Synthetic applications were demonstrated, affording  $\gamma$ -amino acids, among other synthetically useful intermediates. Through extensive DFT analysis of the two possible enantiomers formed by nickel(I) migratory insertion, the authors proposed that enantioinduction arises from a favorable orientation of the carbonyl group away from the *tert*-butyl group of the ligand.

Qi-Lin Zhou reported on the enantioselective desymmetrization/alkylation of 4-hydroxy-4-(2-bromophenyl)-1,6-dienes to form enantioenriched indanol products with two stereocenters (**Scheme 427**).<sup>590,591</sup> Evaluation of a series of chiral

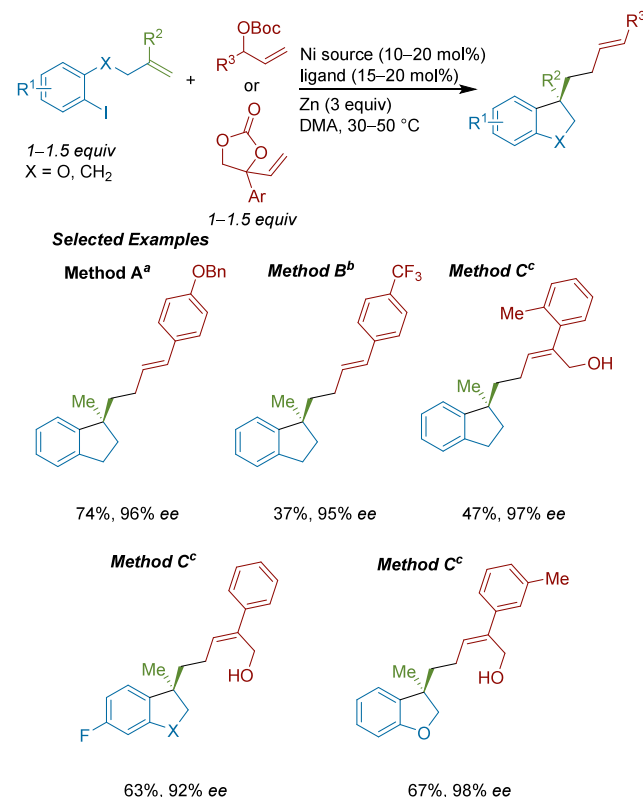
### Scheme 427. Nickel and Cobalt-Catalyzed Enantioselective Desymmetrization of 1,6-Dienes by Arylalkylation (2021)



oxazoline ligands revealed that Bn-BiOx provided the highest enantioinduction. Additionally, a catalytic amount of Co(Pc) significantly improved the yield and enantioselectivity.<sup>50,174</sup> Studies that interrupted the coupling reaction with deuteration by D<sub>2</sub>O suggested that [Ni<sup>I</sup>] is necessary for migratory insertion (a pattern among these reactions).

In 2021, Chuan Wang and colleagues reported a Ni-catalyzed reductive allylation of unactivated alkenes where both acyclic allyl carbonates and cyclic vinyl ethylene carbonates were engaged as coupling partners (**Scheme 428**).<sup>592</sup> Initial investigations revealed that PyOx ligands gave complete regio- and stereoselectivity compared to BiOx ligands. Acetates were tested in place of carbonates, but the cross-product was found to be the major reaction pathway. Utilizing NiCl<sub>2</sub> as the nickel source afforded the allylation product. However, the nickel source was changed to NiBr<sub>2</sub>(dme) when using electron poor aryl substrates. Electron-donating and -withdrawing substituents were well tolerated, but primary and secondary alkyl-substituted allylic carbonates formed no product. The authors expanded the scope to include vinyl ethylene carbonates, which afforded chiral allylic alcohols with high enantioselectivity. The authors propose the mechanism goes through a facially selective intramolecular migratory insertion step to determine the enantioselectivity. However, they acknowledge that the initial oxidative addition of the aryl iodide could also be facially selective.

### Scheme 428. Ni-Catalyzed Allylation of Unactivated Alkenes (2021)<sup>a</sup>



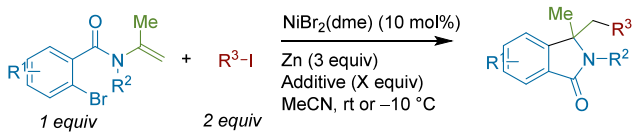
<sup>a</sup>(a) Method A: With alkene (1 equiv), allylic carbonate (1.5 equiv), NiCl<sub>2</sub> (20 mol%), and *t*-Bu-PyOx (20 mol%) at 50 °C. (b) Method B: With alkene (1 equiv), allylic carbonate (1.5 equiv), NiBr<sub>2</sub>(dme) (10 mol%), and *t*-Bu-PyOx (15 mol%) at 40 °C. (c) Method C: With alkene (1.5 equiv), allylic carbonate (1 equiv), NiI<sub>2</sub> (15 mol%), and 4-morpholine-*t*-Bu-PyOx (20 mol%) at 30 °C.

In 2021, Yifeng Chen and co-workers developed conditions for the racemic and enantioselective synthesis of 3,3-dialkylated isoindolinones (**Scheme 429**).<sup>593</sup> The racemic protocol was compatible with a wide range of functionalities; notably, the reaction exhibited good chemoselectivity as Br and Cl-substituted aryl enamides provided good yields. For the enantioselective reaction, reactions with Bn-BiOx provided the highest yield and enantioselectivity. Additionally, lower temperatures and halide salt additives significantly increased conversion. Although the scope was primarily primary alkyl iodides, isopropyl iodide and phenyl iodide provided lower yields of product with high ee.

Later, Yifeng Chen and co-workers reported the enantioselective cyclization desymmetrization and alkylation of 4-(N-carbamoyl)-1,6-dienes with alkyl iodides to form 1,5-disubstituted  $\gamma$ -lactams (**Scheme 430**).<sup>594</sup> The pyrrolidinones were formed with excellent enantio- and diastereoselectivity. Chiral Quinox ligands that have a wider bite angle performed better than PyOx and BiOx ligands. When exchanging the alkyl iodide for the analogous alkyl bromide, the ee and the reaction yields dropped significantly; however, stoichiometric equivalents of LiBr were added to further improve the yield and ee value.

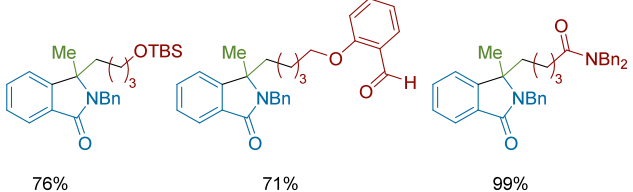
Yifeng Chen and colleagues then collaborated with the Houk group to develop a cyclative acylalkylation of internal alkenes that formed chiral pyrrolidinones with vicinal stereo-

**Scheme 429.** Ni-Catalyzed Synthesis of 3,3-Dialkyl Isoindolines by Cyclative Arylalkylation (2021)<sup>a</sup>

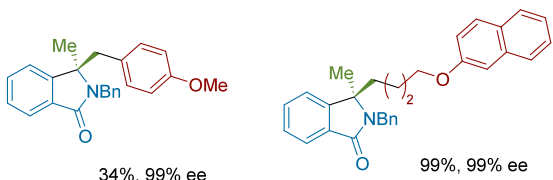


**Selected Examples**

**Method A**

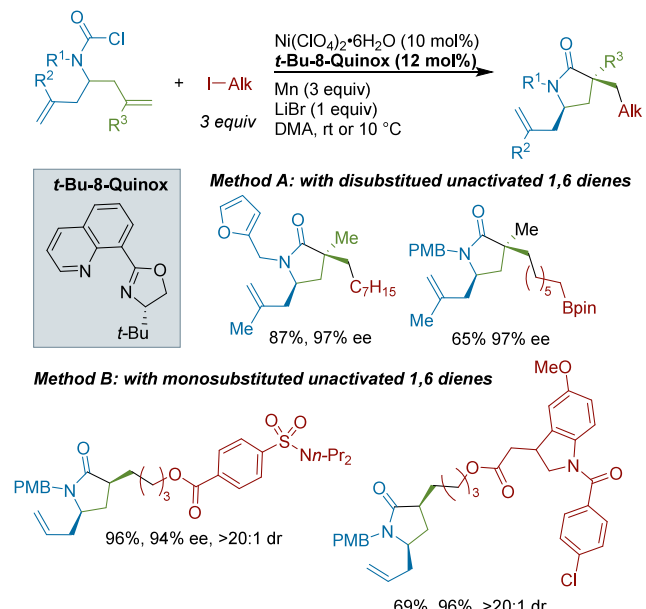


**Method B**



<sup>a</sup>Method A: With phen (15 mol%) at rt. Method B: With Bn-BiOx (20 mol%), LiBr (1.5 equiv) at -10 °C.

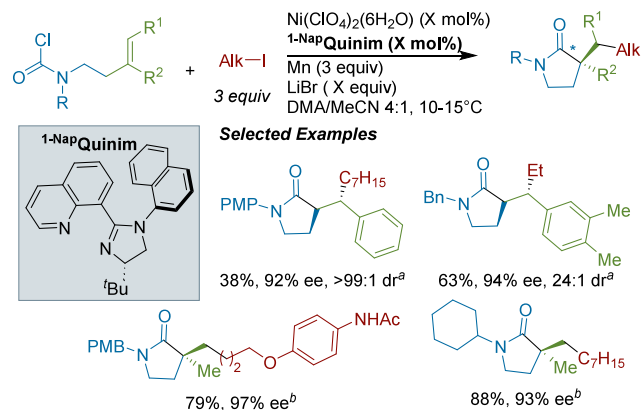
**Scheme 430.** Ni-Catalyzed Enantioselective Desymmetrizing Dicarbofunctionalization of Unactivated Alkenes (2022)<sup>a</sup>



<sup>a</sup>Method A at rt, Method B at 10 °C.

genic centers (Scheme 431).<sup>539</sup> Using a modified Quinim ligand (<sup>1-Nap</sup>Quinim) under modified conditions, the authors were able to couple alkenes bearing both 1,1- and 1,2-disubstitution patterns. Based upon extensive DFT studies, the authors propose the enantiodetermining migratory insertion happens from [Ni<sup>I</sup>] rather than [Ni<sup>II</sup>]. Although both barriers are low, only the [Ni<sup>I</sup>] pathway has a lower barrier, and it predicted an enantioselectivity consistent with experimental

**Scheme 431.** Ni-Catalyzed Enantioselective Cyclative Carbamoylation/Alkylation Synthesis of Scalemic Pyrrolidinones with Vicinal Stereogenic Centers (2022)<sup>a</sup>

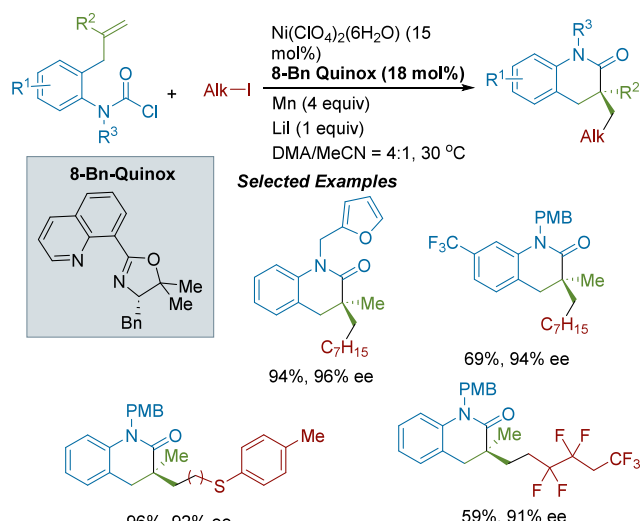


<sup>a</sup>(a) With alkyl iodide (2 equiv), Ni (20 mol%), ligand (24 mol%), and KI (1 equiv) at 15 °C. (b) With alkyl iodide (3 equiv), Ni (15 mol%), ligand (18 mol%), 1 equiv LiBr at 10 °C.

data. Additionally, the authors determined that, for [Ni<sup>II</sup>], the migratory insertion is faster on the singlet energy surface than the triplet energy surface. As migratory insertion is a common step in many reactions in this section, these results are especially notable. Finally, calculations were used to probe the sense of induction and origin of enantioselectivity.

Continuing their studies of enantioselective cyclative carbamoylation/alkylation, Yifeng Chen and colleagues published approaches to substituted piperidinones (not shown) and 3,4-dihydro-2-quinolones (Scheme 432).<sup>595</sup> Minimal

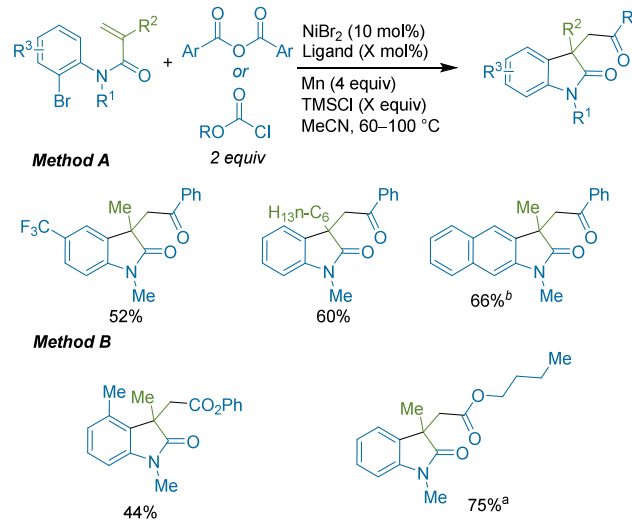
**Scheme 432.** Ni-Catalyzed Enantioselective Carbamoylation/Alkylation Synthesis of Six-Membered Lactams (2022)



success with Quinim ligands prompted the authors to screen a set of derivatized Quinox ligands, with C5-dimethylated Quinox affording the highest yield and enantioselectivity. Only primary alkyl iodides could be used, but the carbamoyl coupling partner could have various substitution on both the arene and nitrogen. The mechanistic hypothesis was similar to that of the authors' previous reports. (Scheme 431).<sup>539</sup>

**7.1.2.3. Cyclizations with Two  $C(sp^2)$  Electrophiles.** Wangqing Kong and co-workers reported on the cyclative arylacetylation of acrylamides to form 2-oxindoles (Scheme 433).<sup>596</sup> The authors developed conditions for cyclative

**Scheme 433. Ni-Catalyzed Cyclative Arylacylation to Form Substituted Oxindoles (2022)<sup>a</sup>**



<sup>a</sup>Method A: With anhydride, 1,10-phen-5,6-dione (20 mol%), 2 equiv  $K_3PO_4$  at 60 °C. Method B: with chloroformate, bpy (20 mol%) at 100 °C. (a) With 0.4 mmol chloroformate. (b) With aryl triflate.

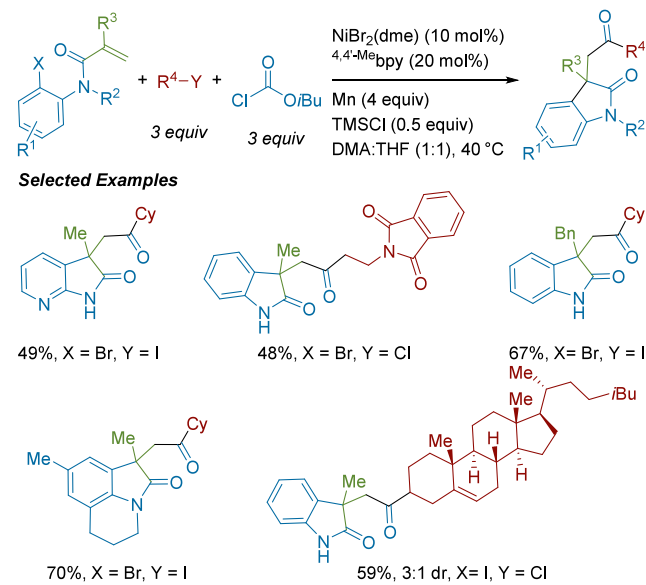
coupling with both symmetric benzoic acid anhydrides and chloroformates. In both cases, ligand choice was crucial, MeCN helped reduce reductive Heck side products, and TBAB improved conversion. The authors proposed mechanism is hypothesized to go through a  $\sigma$ -alkynickel(II) species.

In 2019, Wangqing Kong and co-workers developed a complementary carbonylative approach to the same oxindole products using alkyl halides and isobutyl chloroformate as a CO source instead of activated carboxylic acids (Scheme 434).<sup>597</sup> The reaction was proposed to proceed via a cyclization, carbonylation, and then radical capture/reductive elimination. Notably, various heterocycles including azaoxindole and quinolin-2-one could be constructed using this method. Both primary and secondary alkyl iodides could be used. Control experiments provided evidence for Ni-catalyzed decarbonylation from isobutyl chloroformate.

Aiwen Lei, Wangqing Kong, and co-workers developed a cyclative arylalkenylation to form oxindoles with tethered alkenes (Scheme 435).<sup>598</sup> The racemic variant of this reaction utilized the electron poor 4,4'-CO<sub>2</sub>Me<sup>bipy</sup> as ligand and afforded diverse oxindole products as well as tricyclic indolines and azaindolines. Several key changes—including choice of chiral ligand, a less potent reductant, and lower temperature—rendered the reaction enantioselective. A comparable scope to the racemic reaction was achieved: electronically differentiated aryl halides could be tolerated, and different geminal substituted alkenes could be coupled with minimal loss of enantioenrichment. Finally, concise total syntheses of (+)-physostigmine and (+)-physovenine were completed to demonstrate synthetic utility of this method.

**7.1.2.4. Stereocontrolled Cyclizations with Two  $C(sp^2)$  Electrophiles.** An enantioselective cyclative arylalkenylation to form 3,3-disubstituted dihydrobenzofurans was reported by

**Scheme 434. Ni-Catalyzed Cyclative Carbonylative Arylacylation of Alkenes Affording Carbonyl-Containing Oxindoles (2019)**



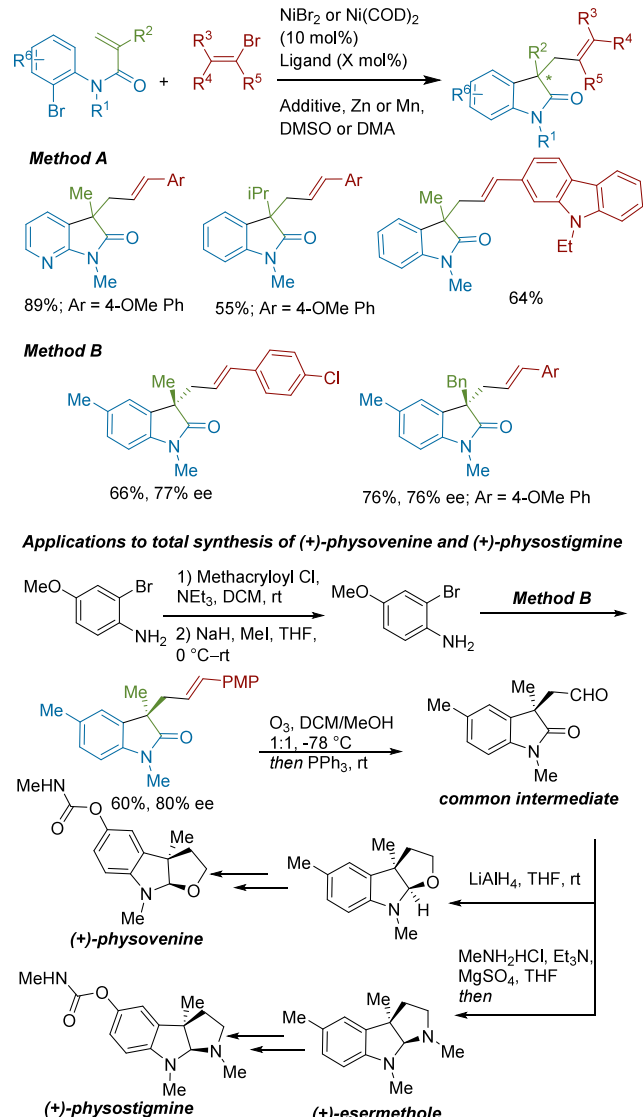
Xing-Zhong Shu and co-workers in 2019 (Scheme 436).<sup>599</sup>

Proceeding at room temperature with equimolar amounts of starting materials, the reaction had best success with the (*S*)-3-*t*-BuPyOx ligand; additionally, THF as a cosolvent helped reduce formation of homocoupled cyclization byproducts. Numerous cyclic and heterocyclic alkanyl triflates ranging from 5- to 8-membered rings could be coupled to give highly enantioenriched products in good yields. The aryl-iodide tethered alkene could have substitution on the aryl ring at the *para*- and *meta* positions, but not the position *ortho* to the iodide. Adjustment of the solvent mixture enabled the authors to extend this reaction to the synthesis of disubstituted indolines and electron-rich indanes.

Enantioselective cyclative diarylation was published by Wangqing Kong and co-workers a few years later (Scheme 437).<sup>186,600</sup> The cyclization substrate, an aryl bromide containing a pendant N-protected methacrylamide, was coupled efficiently to aryl bromides using a catalyst containing the *i*-Pr-Phosferrox ligand (a P,N-ligand). Unusually, two reductant systems were used together ( $K_3PO_4/B_2pin_2$  and Zn). The scope for both coupling partners was broad. No evidence of an arylzinc intermediate was found, as the reaction proceeded well with TDAE. A postcyclization alkynickel complex was partially characterized and demonstrated to react with bromobenzene or an arylnickel(II) complex to form product. For this reason, the authors were unable to determine if arylation occurs from a second oxidative addition step or from transmetalation between two nickel(II) centers.

In 2021, Xing-Zhong Shu and co-workers reported an enantioselective cyclative divinylation to form 3,3-dialkyl-4-methylene-pyrrolidines (Scheme 438).<sup>601</sup> The failure of conventional chiral ligands prompted the authors to explore Pmrox ligands. Ultimately, using a *t*-BuPmrox ligand while running the reaction at higher dilution and lower temperatures afforded the desired cyclized products in high yield and enantioselectivity. The alkene scope was broad, with styrenyl bromides and both cyclic and acyclic vinyl triflates affording high yields. For reactions with groups larger than methyl at  $R^1$ ,

**Scheme 435. Ni-Catalyzed Enantioselective Cyclative Arylalkenylation and Application to the Synthesis of (+)-Physovenine and (+)-Physostigmine (2019)<sup>a</sup>**

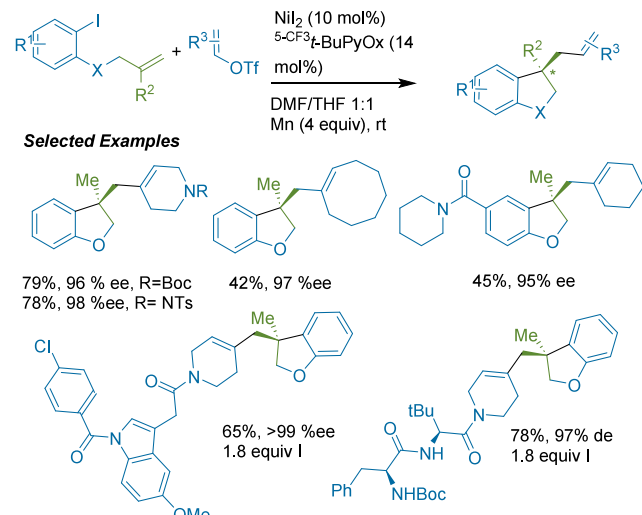


<sup>a</sup>Method A: With NiBr<sub>2</sub> (10 mol%), 4,4'-CO<sub>2</sub>MeBpy (20 mol%), 4 equiv MgCl<sub>2</sub>, 3 equiv Mn in DMSO at 60 °C. Method B: With Ni(COD)<sub>2</sub> (10 mol%), (S)-Bn-BiOx (20 mol%), 3 equiv Zn in DMA at rt.

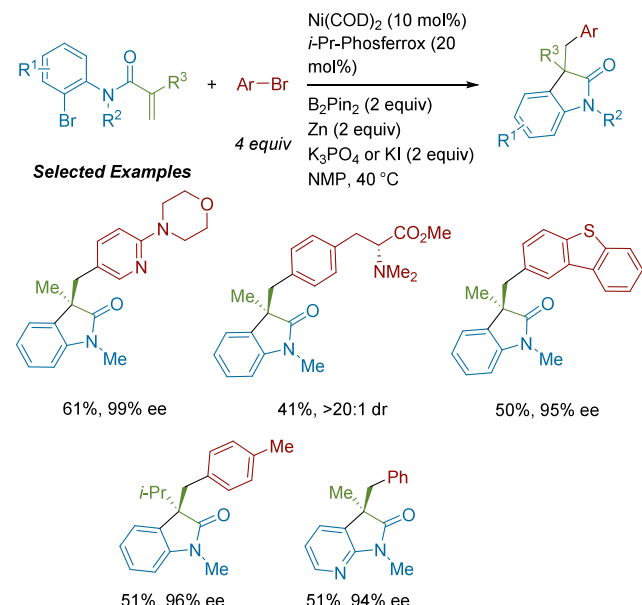
AgBF<sub>4</sub> and Na<sub>2</sub>SO<sub>4</sub> were essential to achieve higher yields. This method could also be applied to the synthesis of methylene tetrahydrofurans. Control experiments suggested a reaction pathway proceeding through sequential oxidative addition at nickel, wherein a nickel(II) species facilitates an enantiodetermining migratory insertion before a second oxidative addition to the vinyl bromide occurs.

Chuan Wang and co-workers reported a cyclative arylacetylation to form indoline, indane, and dihydrobenzofurans with all-carbon quaternary centers (Scheme 439).<sup>602</sup> Of the electrophilic acylating reagents evaluated, a pyridyl ester allowed the highest yield and enantioselectivity with *t*-Bu-PyOx ligand. Although not part of this review, the authors also developed arylcarbamoylation using isocyanates. Similar to their other reports, the authors propose a mechanism involving facially selective arylnickelation from [Ni<sup>I</sup>].

**Scheme 436. Ni-Catalyzed Enantioselective Cyclative Arylalkenylation to Form Dihydrobenzofurans (2019)**



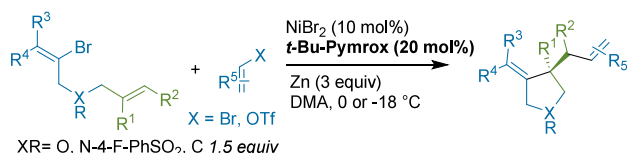
**Scheme 437. Ni-Catalyzed Enantioselective Reductive Diarylation of Activated Alkenes by Domino Cyclization/Cross-coupling (2018)**



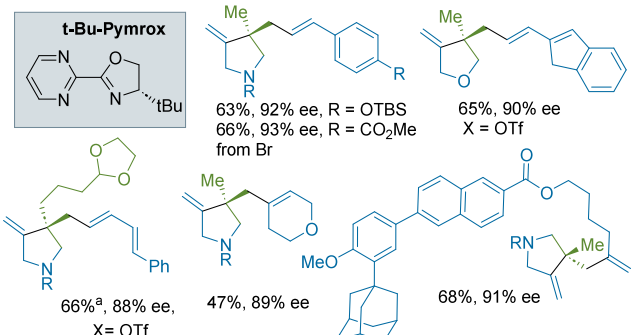
Later, Xiangqing Wu, and Yifeng Chen found that the 8-Quinox ligand class could be applied to the enantioselective synthesis of oxindoles by cyclative carbamoylation/alkylation (Scheme 440).<sup>603</sup> The catalyst system of *t*-Bu-8-Quinox and Ni(ClO<sub>4</sub>)<sub>2</sub>•6H<sub>2</sub>O was optimal. The closely related Quinim ligands (imidazoline vs oxazole) were ineffective.

**7.1.2.5. Cyclizations Using C(sp<sup>2</sup>) and C(sp) Electrophiles.** In 2021 Wangqiang Kong and co-workers reported a cyclative arylcyanation to form the familiar oxindole core with cyanomethyl substitution at the 3 position (Scheme 441).<sup>604</sup> The electrophilic *N*-cyano *N*-phenyl-*p*-toluenesulfonamide is considered less toxic than nucleophilic cyanating agents,<sup>605</sup> providing an advantage to this approach. Interestingly, for this nonenantioselective method, a chiral tridentate ligand, (*R*)-Ph-PyBOX, was optimal. However, two enantioselective examples were demonstrated using a DuanPhos derivative provided 73%

**Scheme 438. Ni-Catalyzed Enantioselective Cyclative Divinylation to form Methylene Pyrrolidines and Tetrahydrofurans (2021)<sup>a</sup>**

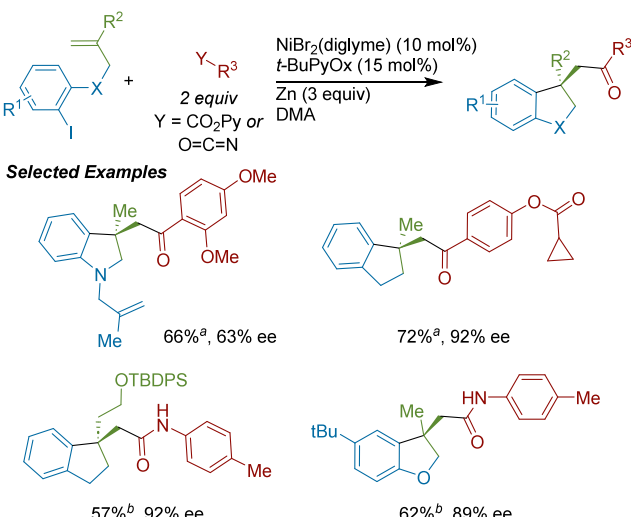


**Selected Examples**



<sup>a</sup>With AgBF<sub>4</sub> (0.6 equiv), Na<sub>2</sub>SO<sub>4</sub> (2 equiv) in 1:1 DMA/THF

**Scheme 439. Ni-Catalyzed Enantioselective Cyclative Arylation to Form Indoline, Indane, and Dihydrobenzofurans (2022)<sup>a</sup>**

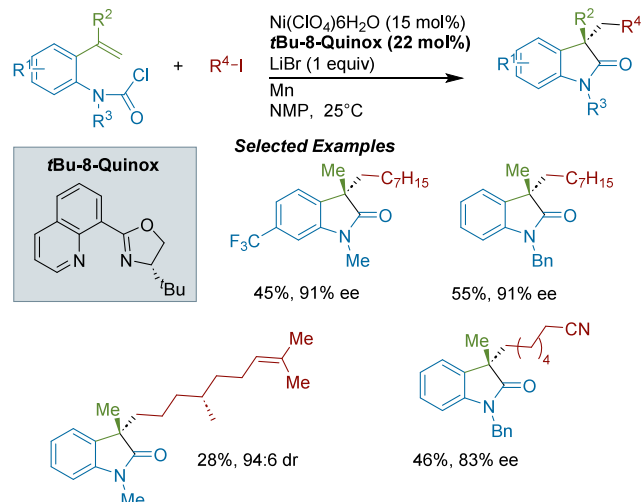


<sup>a</sup>(a) With Y = CO<sub>2</sub>Py at 60 °C. (b) With Y = O=C=N and NEt<sub>3</sub> (1 equiv) at 30 °C.

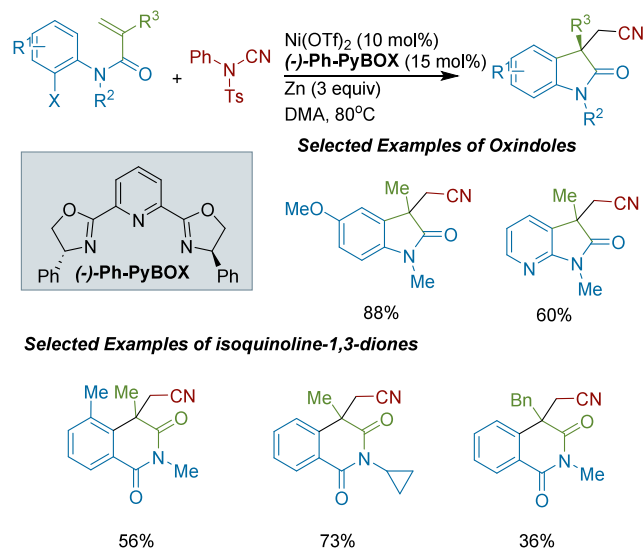
and 82% ee, respectively. After completing the synthesis of several structurally diverse oxindoles, the authors applied this method to the synthesis of isoquinoline-1,3-diones. In contrast to the method for oxindole synthesis, the reaction outcome for isoindolines was directly impacted by electronic variation of the alkene-tethered aryl bromide, but sterically differentiated arenes were tolerated. The utility of this method was showcased in an enantioselective formal synthesis of clinical Alzheimer's drug (+)-physostigmine. Mechanistic studies were consistent with cyanation by oxidative addition of an alkynickel(I) species to an N–CN bond.

Another cyanation strategy was disclosed by Kaiwu Dong and colleagues in 2022 using 2-methyl-2-phenyl malononitrile as a cyanating reagent (Scheme 442).<sup>606</sup> As in the Kong report

**Scheme 440. Ni-Catalyzed Enantioselective Cyclative Carbamoylation/Alkylation to form Oxindoles (2022)**



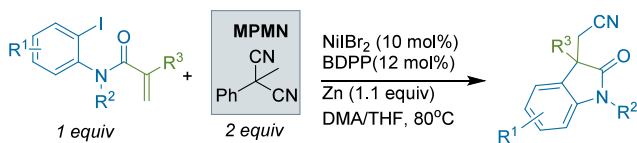
**Scheme 441. Ni-Catalyzed Cyclative Arylcyanation to form Oxindoles (2021)**



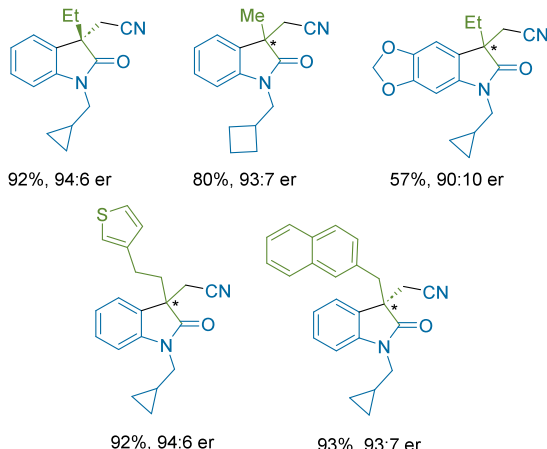
(Scheme 439), a chiral bisphosphine ((S,S)-BDPP) was optimal. Stepwise mechanistic experiments were consistent with a mechanism involving 1,2-migratory insertion and  $\beta$ -carbon elimination for cyano group transfer to nickel. DFT-modeling of potential reaction intermediates indicated that a stabilizing agnostic (BDPP)Ni<sup>0</sup>C–H during oxidative addition likely contributed the most to the observed enantioselectivity. This counterintuitive enantiodetermining step (as opposed to migratory insertion) was proposed previously by Kozlowski and Desrosiers for an enantioselective Mizoroki–Heck reaction.<sup>607</sup>

**7.1.2.6. C–X Bond Forming Cyclizations.** Chuan Wang and colleagues reported a cyclative iminoacylation to form pyrrolines (Scheme 443).<sup>608</sup> The sterically encumbered cuproin was the optimal ligand for this transformation. The cyclization substrate was an alkene-tethered oxime benzoyl or pivaloyl ester. Both complex aromatic oxime esters and simple oxime esters lacking geminal disubstitution were used; notably, monosubstituted alkenes prone to  $\beta$ -hydride elimination were also competent substrates. An assessment of acylation partners

**Scheme 442.** Ni-Catalyzed Enantioselective Cyclative Arylcyanation to Form Oxindoles (2022)



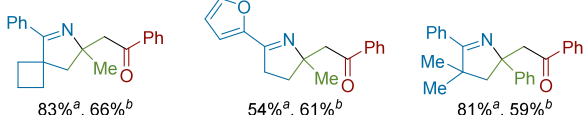
**Selected Examples**



**Scheme 443.** Ni-Catalyzed Cyclative Iminoacylation to form Substituted Pyrrolines (2018)<sup>a</sup>



**Selected Examples**



<sup>a</sup>(a) With X = OBz. (b) With X = Cl.

revealed anhydrides could also be used; moreover, in situ generation of an anhydride from carboxylic acid was possible. Control experiments argued against iminyl radical formation.

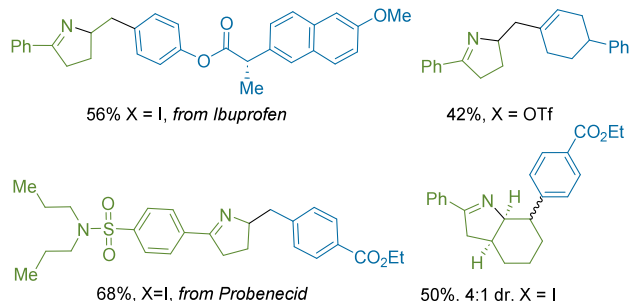
Xingjie Zhang and Guisheng Zhang reported a cyclative iminoarylation protocol in 2023 (Scheme 444).<sup>609</sup> A synergistic additive effect was observed with both MgBr<sub>2</sub> and LiBr. The authors proposed that this combination of salts helped to facilitate reduction by Mn by increasing the ionic strength of the solvent. Oxime esters bearing spirocyclic, heteroaromatic, and alkenyl functionalities were well tolerated; however, internal alkenes could not be used in this method. In addition to arylation, vinylation was also achieved. The authors conducted studies that suggested initial formation of halogenated pyrrolines was followed by cross-electrophile coupling with the aryl halide. The authors could not rule out the formation of an organomanganese reagent during the reaction.

You Wang, Shaolin Zhu, and co-workers reported the enantioselective coupling of alkene-tethered aryl iodides with O-benzoyl-hydroxylamines to form  $\beta$ -chiral amines with an aryl-substituted quaternary carbon center (Scheme 445).<sup>610</sup> These conditions offer excellent complementary reactivity to previously reported palladium- and copper-catalyzed 1,2-

**Scheme 444.** Ni-Catalyzed Cyclative Iminoarylation to Form Substituted Pyrrolines (2023)<sup>a</sup>

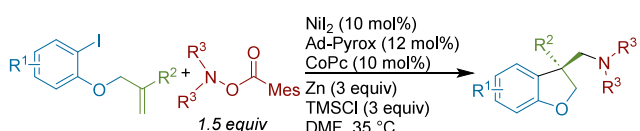


**Selected Examples**

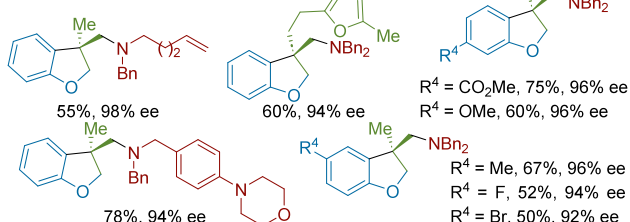


<sup>a</sup>TFM<sup>Bz</sup> = 3,5-bis(trifluoromethyl)benzoyl

**Scheme 445.** Nickel- and Cobalt-Catalyzed Enantioselective Coupling of Alkene-Tethered Aryl Iodides with O-Benzoyl-hydroxylamines to Form Dihydrobenzofurans (2020)



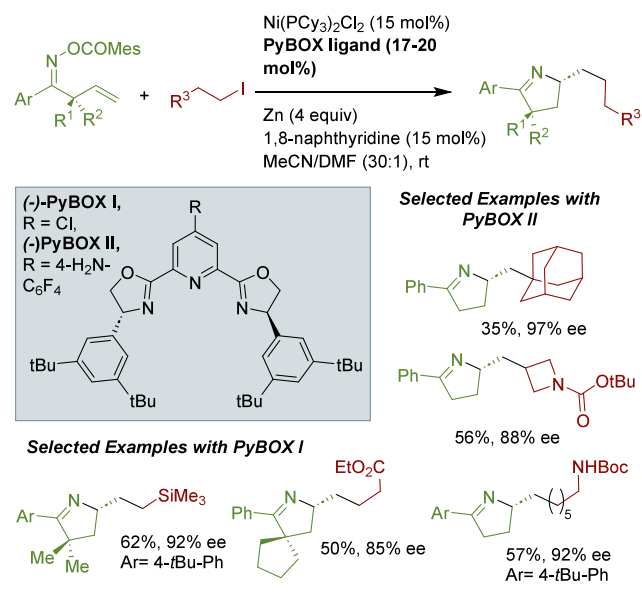
**Selected Examples**



carboaminations, which tend to be used to form  $\alpha$ -chiral amines.<sup>50,174</sup> The optimal catalyst system is a combination of a nickel PyOx catalyst with a cobalt phthalocyanine cocatalyst.<sup>50,174</sup> The authors report that more sterically hindered groups at the alkene ( $R^2$ ) resulted in decreases to enantioselectivity and yields. Mechanistic studies led the authors to propose that cyclization occurs via cyclative migratory insertion of the initial arylnickel(II) species into the tethered alkene.

Xing-Zhong Shu and co-workers reported on an asymmetric cyclative iminoalkylation reaction of alkene-tethered oxime esters in 2022 (Scheme 446).<sup>611</sup> The optimal catalyst mixture contained both PCy<sub>3</sub> and a PyBOX ligand; the authors proposed PCy<sub>3</sub> stabilizes an alkynickel(II) intermediate. Additionally, 1,8-naphthyridine helped inhibit the formation of the reduced cyclization side product. The authors observed that the leaving group on the oxime ester had a direct impact on both yield and enantioenrichment. Slight alteration of the PyBOX ligand backbone from an electron-poor to electron-rich moiety enabled coupling with secondary and tertiary alkyl iodides in moderate yield and high enantioselectivity. The authors proposed a mechanism wherein the oxime ester is first

**Scheme 446.** Ni-Catalyzed Enantioselective Cyclative Iminoalkylation of Alkene-Tethered Oxime Esters with Alkyl Iodides to Form Enantioenriched Pyrrolines (2022)



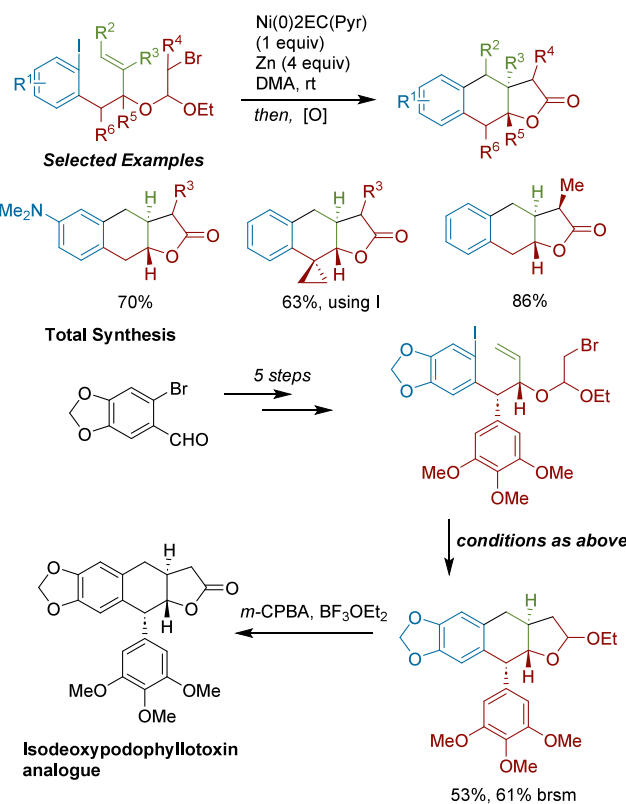
activated and cyclized before coupling with the alkyl iodide occurs.

**7.1.3. Synthetic Applications of Cross-Electrophile Difunctionalizations.** Yu Peng and co-workers disclosed a series of total syntheses of compounds bearing a *trans*-tetrahydronaphtho[2,3-*b*]furan core using a double cyclization strategy (Scheme 447).<sup>612</sup> In their initial 2016 report, a cascade reaction of an aryl-tethered  $\beta$ -bromo acetal was accomplished using a stoichiometric amount of a (ethylcrotonate)<sub>2</sub>Ni<sup>0</sup>(Py) complex; upon oxidation, the lactone products could be furnished in high yield and good diastereoselectivity, even for substrates bearing vicinal stereocenters. This method was applied to the total synthesis of a novel isodeoxypodophyllotoxin analogue bearing three contiguous stereocenters.

An extension of the intramolecular Ni-catalyzed reductive cyclization was demonstrated by the same group in 2017 (Scheme 448).<sup>613</sup> Using conditions developed in a prior report, the synthesis of *cis*-tetrahydro(2*H*)-inden[1,2-*b*]furan, a core of a strigolactone analogue was completed. The reaction proceeded stereoselectively to afford the tricyclic ABC ring system. Bidentate nitrogen ligands provided a higher yield than ethyl crotonate. Where previous methods had afforded both trans and cis stereoisomers for a similar cyclization, exclusively cis products were observed. Preliminary DFT studies suggested favorable pseudohalf-chair conformation of the alkyl radical intermediate is responsible for this outcome.

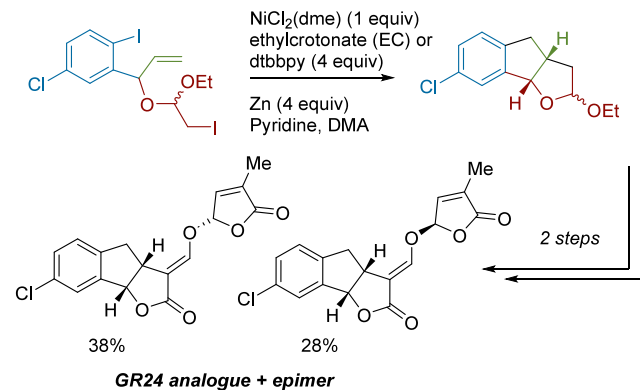
Soon thereafter, Yu Peng and colleagues elaborated on the podophyllotoxin scaffold and reported the stereoselective synthesis of eight podophyllotoxin congeners (Scheme 449).<sup>614–616</sup> Starting from commercially available 6-bromoperonal, five steps (carried out at gram scale) afforded the key  $\beta$ -bromo acetal cyclization substrates. Modified conditions from their previous report produced the *cis* and *trans*-tetrahydronaphtho[2,3-*c*]furan isomers with excellent stereocontrol. Through a series of oxidative transformations, a total of eight podophylum members were synthesized from these intermediates. Overall, this approach showcased the divergent

**Scheme 447.** Stereoselective Synthesis of Tetrahydronaphtho[2,3-*b*]furans Enabled by Nickel Mediated Cyclative Arylalkylation (2016)



**Scheme 448.** Synthesis of a New Aromatic Strigolactone Analogue by Ni-Catalyzed Cyclative Arylalkylation (2017)

*Synthesis Towards a new bioactive strigolactone analogue, GR24*

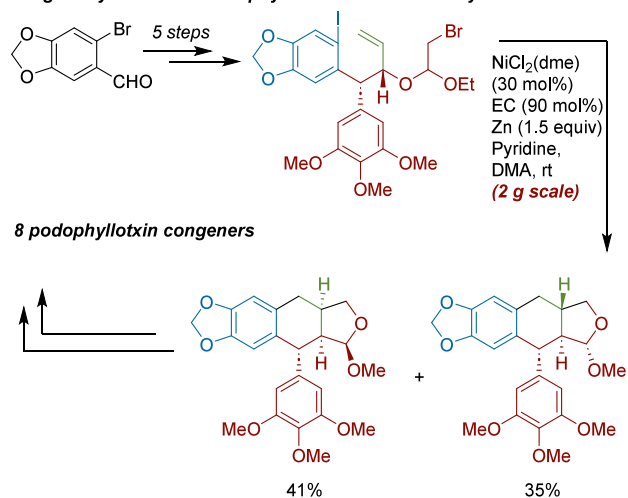


qualities of this synthesis, enabled by the Ni-catalyzed cyclization step.

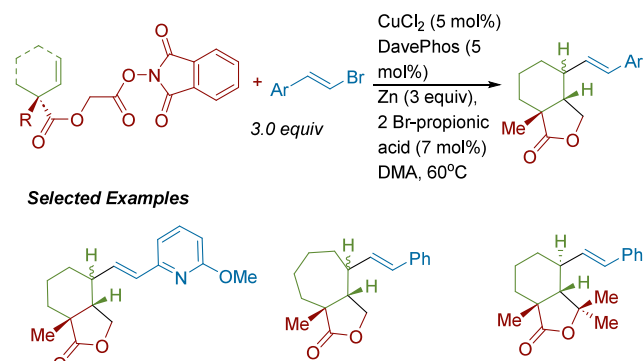
Chao Li and colleagues reported the first total syntheses of spiro-lactone *ent*-karanooids including longirabdiol, longirabdalactone, and effusin using XEC alkene difunctionalization (Scheme 450).<sup>617</sup> Key to the success of this method was a copper-catalyzed tandem decarboxylative cyclization/alkenylation of a tethered alkene. Activation of a cyclic carboxylic acid intermediate with *N*-hydroxyphthalimide afforded a redox active ester substrate that was primed for *S*-*exo*-trig cyclization via reductive decarboxylation. Compared to a nickel catalyst

**Scheme 449. Divergent Syntheses of Natural Podophyllotoxin and Congeners Using Ni-Catalyzed Cyclative Arylalkylation (2021)**

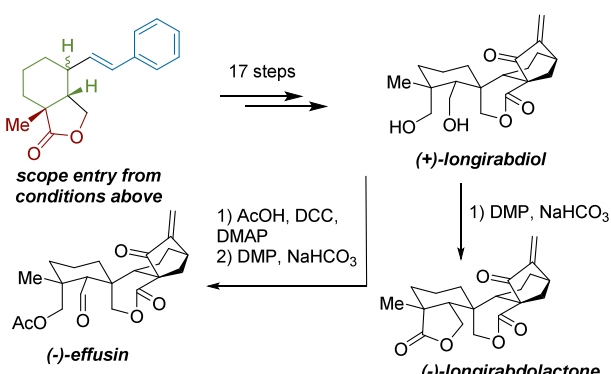
Divergent Syntheses of Podophyllotoxin-Related Family Members



**Scheme 450. Ni-Catalyzed Cyclative Alkylalkenylation for the Total Syntheses of (+)-Longirabdiol, (-)-Longirabdolactone, and (-)-Effusin (2019)**



Completed Synthesis of Longirabdiol, Longirabdolactone, and Effusin

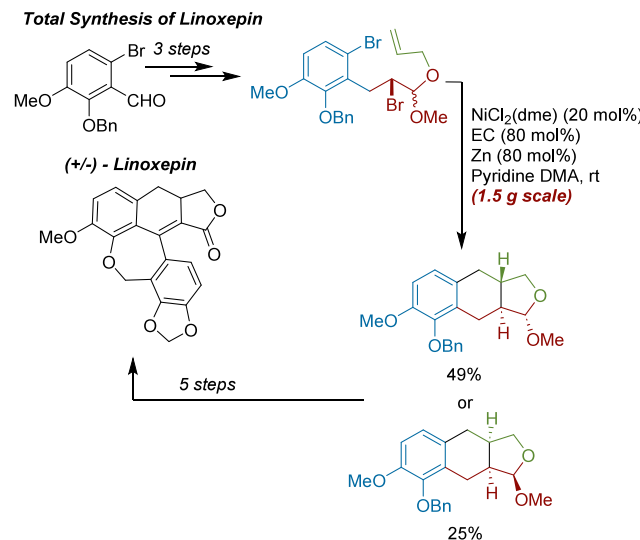


system (which provided a 34% yield with 3.2:1 dr), the combination of CuCl<sub>2</sub> and DavePhos furnished the desired products in 60% yield and 4.2:1 dr. Structurally diverse lactone systems could be synthesized using electronically differentiated styrenyl bromides; notably, quaternary centers could be forged at both the site of cyclization and alkenylation. Subsequent transformations afford (+)-longirabdiol, and further derivatization of this compound realized the syntheses of two additional

natural products. This exciting result is a rare example of a copper-catalyzed XEC reaction that could perhaps be developed further.

Yu Peng and co-workers further extended their expertise in intramolecular difunctionalization to the total synthesis of linoxepin in 2022 (Scheme 451). Here, a cyclative

**Scheme 451. Total Synthesis of Linoxepin Facilitated by Ni-Catalyzed Cyclative Arylalkylation**



arylalkylation efficiently formed the ABC tricyclic ring system in one step from a simple linear precursor. An ethylcrotonate-ligated nickel complex was again utilized as the catalyst. Acetal oxidation afforded the desired ABC tricyclic core. Following a short sequence of oxidation and C–C bond forming reactions, the synthesis of linoxepin was completed. To showcase potential divergency of the Ni-catalyzed step, several D-ring modified linoxepins were prepared from the tricyclic intermediates of the nickel step.

## 7.2. Alkyne Difunctionalization

The difunctionalization of alkynes via XEC is currently more limited than the difunctionalization of alkenes (section 7.1). This can be attributed to added challenges from (1) the propensity of terminal alkynes to undergo deleterious side reactivity with nickel such as cyclotrimerization, (2) control of E/Z selectivity of the resultant alkene can be difficult, and (3) most developed methods in this area cannot easily engage internal alkynes. In these reactions, it is often proposed that an alkyl radical adds across the alkyne, forming the corresponding vinyl radical.<sup>618</sup> This vinyl radical is then engaged in a second nickel-mediated functionalization step with the other coupling partner (Figure 43). Mechanistic understanding in this area is still underdeveloped, and more complex mechanisms could be relevant depending on coupling partners and reaction conditions.

Owing to a diversity of mechanistic outcomes, alkyne difunctionalization reactions utilize a broad range of ligands (Figure 44). The ligands reported in this section are also utilized in alkene difunctionalization (see Figure 41), which could offer insight into ligand scaffolds worth exploring in future alkyne difunctionalizations.

### 7.2.1. Intermolecular, Three-Component Difunctionalization of Alkynes

Yu Zhao, Ming Joo Koh, and co-

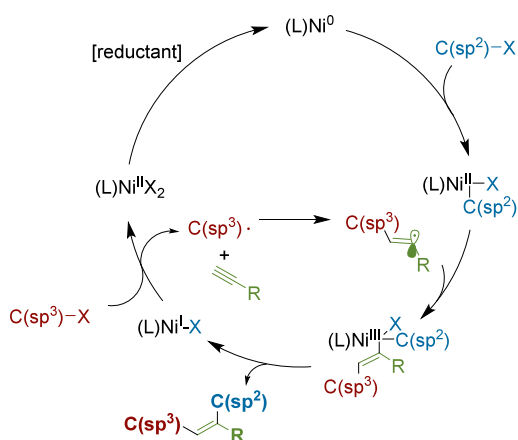


**Figure 43.** Mechanism of alkyne difunctionalization with one  $C(sp^2)-X$  and one  $C(sp^3)-X$  coupling partner. Depending on the coupling partners, the mechanistic details of this cycle can change (e.g., in systems with two  $C(sp^3)-X$  coupling partners).

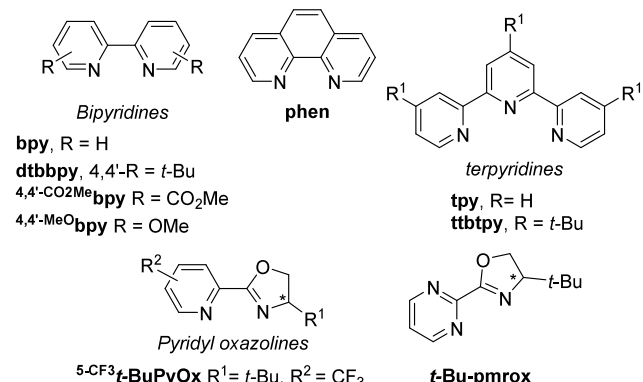


**Figure 44.** Ligands used in cross-electrophile alkyne difunctionalization reactions. \*Denotes chiral centers.

workers developed a Ni-catalyzed three-component coupling of alkynyl bromides and *N*-hydroxyphthalimide (NHP) esters with terminal alkynes (**Scheme 452**).<sup>619</sup> In addition to deriving from a more commercially abundant substrate pool, NHP esters have been shown to be well-matched for XEC reactions with alkynyl bromides. The addition of LiBr helped increase yields further and lower the formation of diyne.<sup>496</sup> Replacing the NHP ester with an alkyl iodide only afforded cyclo-trimerization byproducts and homodimerization of the alkynyl bromide. The method was compatible with primary, secondary, and tertiary alkyl NHP esters as well as both aryl and alkyl functionalized alkynyl bromides. However, internal alkynes were not tolerated with these methods. High regioselectivity and stereoselectivity for *E*-alkene products was observed.

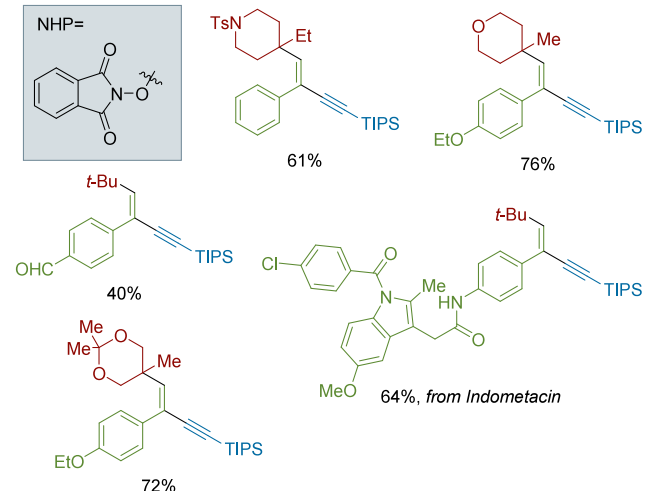
Maiti reported a Ni-catalyzed three-component coupling of alkynes with aryl iodides and tertiary alkyl iodides (**Scheme 453**).<sup>620</sup> The reaction was found to exclusively form the *anti*-alkylarylation product without the need for a directing group. The reaction was most successful with electron-poor aryl iodides. Radical trapping experiments with triethylphosphite confirmed the presence of vinyl radical intermediates. Stoichiometric reactions supported arylnickel(II) being competent intermediates.

Wei Shu and colleagues developed a Ni-catalyzed, regio- and stereoselective approach to trisubstituted alkenes from the

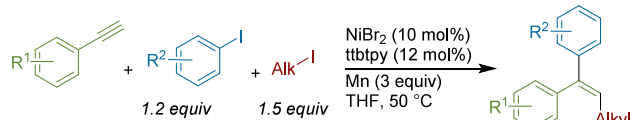
**Scheme 452. Ni-Catalyzed Three-Component Alkylalkynylation of Alkynyl Bromides, *N*-Hydroxyphthalimide (NHP) Esters, and Alkynes (2021)**



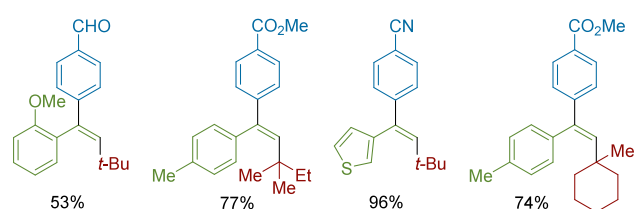
**Selected Examples**



**Scheme 453. Ni-Catalyzed Three-Component Coupling of Alkynes with Aryl Halides and Tertiary Alkyl Halides (2021)**



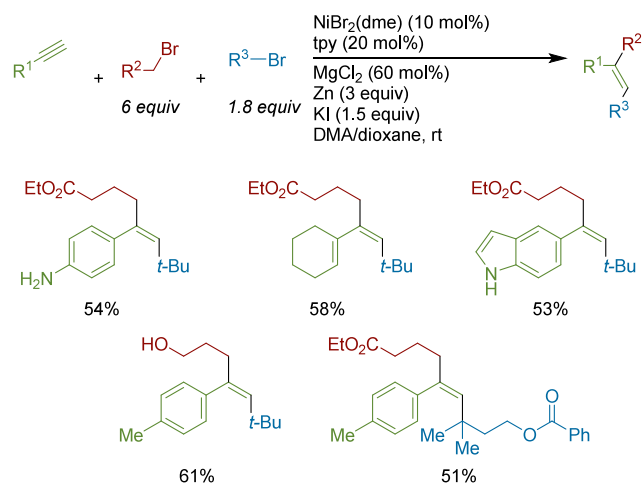
**Selected Examples**



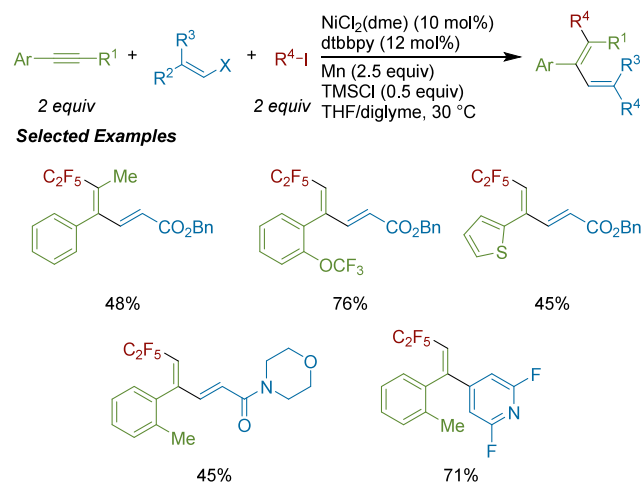
coupling of two different alkyl bromides with a terminal alkyne (**Scheme 454**).<sup>621</sup> This method was most efficient when one of the alkyl radical precursors was a primary alkyl bromide used in large excess and the other was a tertiary alkyl bromide. When a secondary alkyl bromide was used in place of the tertiary alkyl bromide coupling partner, no product was formed. Notably, free anilines and alcohols were well tolerated. Running the reaction in the absence of the primary alkyl bromide afforded radical addition products consistent with the formation of vinyl radical intermediates.

Lingling Chu and co-workers developed a nickel catalyzed three-component coupling of alkynes with alkenyl iodides and perfluoroalkyl iodides to generate fluoroalkyl 1,3-dienes (**Scheme 455**).<sup>622</sup> It was discovered that alkynes with an *ortho*-substituted aryl group performed best in these conditions, owing to the added hindrance slowing down undesired cyclotrimerization. Notably, a single example of an internal

**Scheme 454. Ni-Catalyzed Dialkylation of Alkynes with Primary and Tertiary Alkyl Bromides (2022)**



**Scheme 455. Three-Component Coupling of Alkynes with Alkenyl Halides and Fluoroalkyl Halides (2022)**

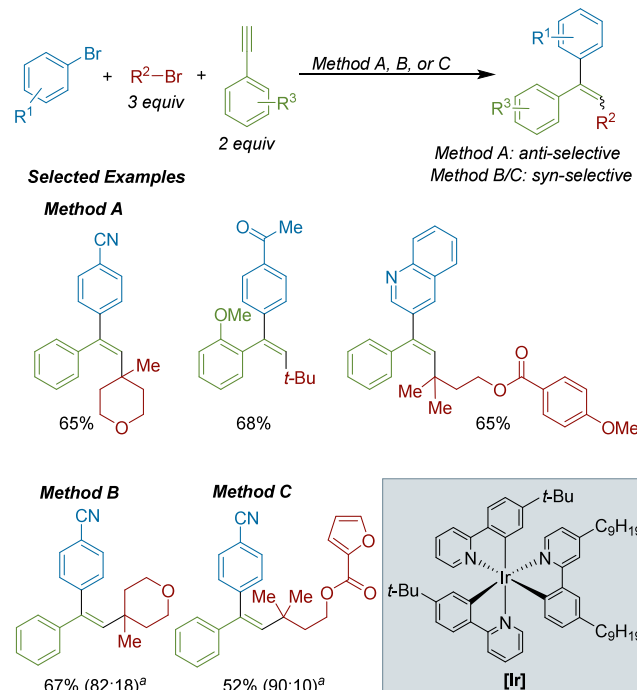


alkyne was shown, which are generally more limited in this type of coupling. Regio- and stereoselectivity was generally high across the substrate scope.

Huifeng Yue and Rueping developed a Ni-catalyzed, three-component, stereodivergent synthesis of trisubstituted alkenes, where the *E/Z* selectivity of the product could be governed by the mode of catalysis (**Scheme 456**).<sup>623</sup> Their electrochemical conditions (Method A) favored the *anti*-products while their photochemical conditions (Method B) favored the *syn*-products. *Syn*-selectivity was also achieved under photoelectrochemical conditions (Method C) with higher energy light (390 nm) and removal of the iridium photocatalyst. Observed olefin selectivity outcomes were attributed to energy-transfer-mediated *E* to *Z* isomerization under photochemical conditions. Nitriles, free phenols, and sulfonamides were compatible in all three protocols.

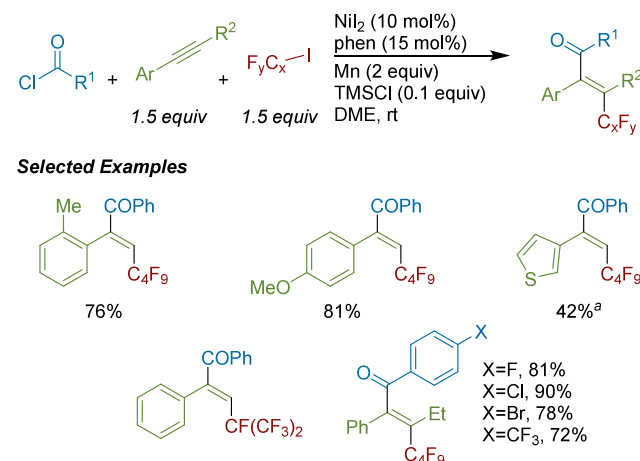
Hai-Yong Tu, Xiao-Hong Zhang and co-workers developed a Ni-catalyzed, three-component coupling of terminal alkynes with fluoroalkyl halides and acyl chlorides to form fluoroalkylated enones ([Scheme 457](#)).<sup>624</sup> Both primary and secondary fluoroalkyl halides were utilized, and the terminal aryl alkynes could tolerate a variety of substitutions, including *ortho*-sterics. In general, aroyl chlorides provided high yields, and one

**Scheme 456.** Ni-Catalyzed, Stereodivergent Synthesis of Trisubstituted Alkenes by Different Approaches (2022)<sup>a</sup>



<sup>a</sup>Method A: With aryl bromide (1 equiv), alkyne (2 equiv), alkyl bromide (3 equiv), NiBr<sub>2</sub>(<sup>4,4'-MeO</sup>bpy) (10 mol%), TMEDA (3 equiv), *n*-Bu<sub>4</sub>NBr (2 equiv), DMA, 4 mA, (+) graphite, (-) nickel foam. Method B: With alkyne (1 equiv), aryl bromide (2 equiv), alkyl bromide (3 equiv), [Ir] (1 mol%), NiBr<sub>2</sub>(<sup>4,4'MeO</sup>bpy) (10 mol%), PMDTA (3 equiv), LiCl (3 equiv), DMA, 440 nm blue LEDs. Method C: With aryl bromide (1 equiv), alkyne (2 equiv), alkyl bromide (3 equiv), NiBr<sub>2</sub>(<sup>4,4'MeO</sup>bpy) (10 mol%), TEMDA (3 equiv), *n*-Bu<sub>4</sub>NBr (2 equiv), DMA, 4 mA, (+)graphite, (-)nickel foam, 2 × 390 nm purple LEDs. (a) Reported as (%syn:%anti). PMDTA = *N,N,N',N''-pentamethyldiethylenetriamine*.

**Scheme 457. Three-Component Fluoroalkylation of Alkynes with Fluoroalkyl Halides and Acyl Chlorides (2022)<sup>a</sup>**



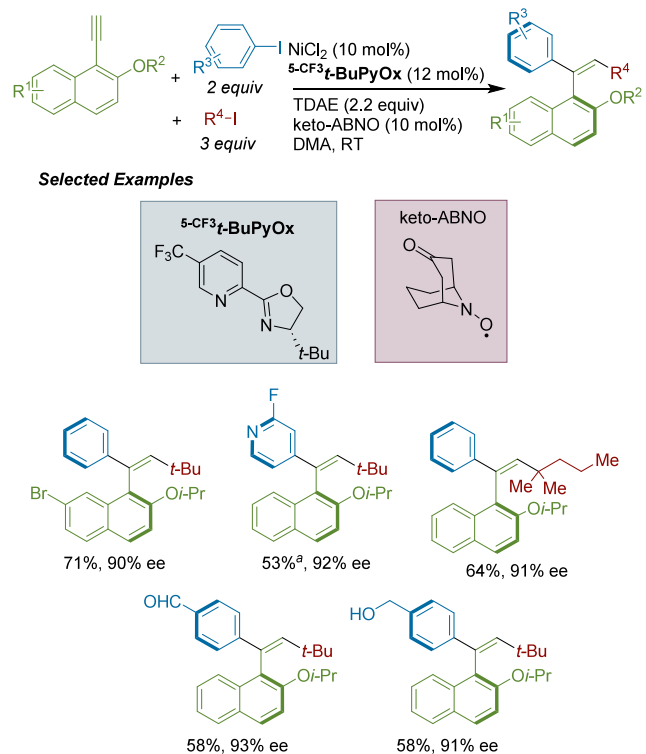
<sup>a</sup>At 60 °C.

example of pivaloyl chloride was demonstrated. A control experiment without acyl chloride present afforded products

consistent with vinyl radical intermediates forming in the reaction.

Shu-Yu Zhang and co-workers developed an enantioselective Ni-catalyzed reaction between an aryl acetylene, an aryl iodide, and a tertiary alkyl iodide to form axially chiral styrenes (Scheme 458).<sup>625</sup> The addition of keto-ABNO was found to

**Scheme 458. Ni-Catalyzed Asymmetric Three-Component Coupling to Form Enantioenriched Axially Chiral Styrenes (2022)<sup>a</sup>**



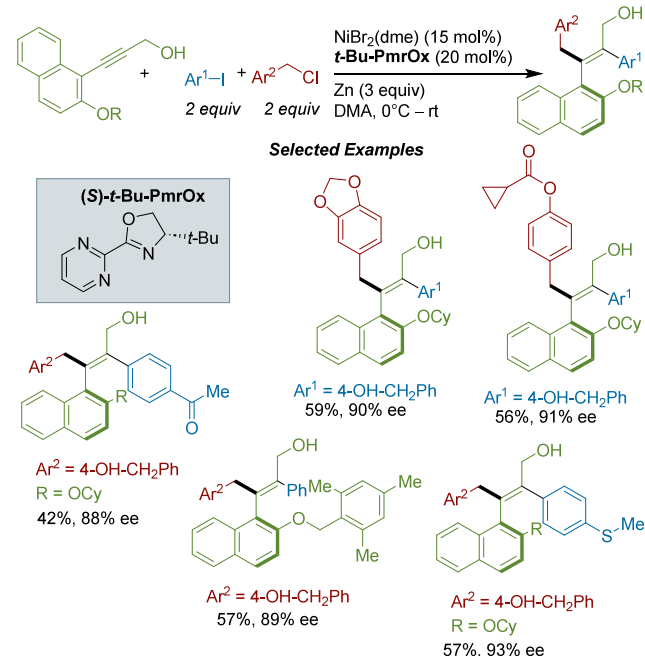
<sup>a</sup>With aryl bromide instead of aryl iodide

improve the enantioselectivity of the reaction and may act as an additional ligand on nickel. On the aryl iodide, both electron-donating and -withdrawing groups were tolerated, but only tertiary alkyl iodides could be used. DFT calculations supported the observed enantioselectivity, which arises from a steric clash between the allene intermediate and the aryl group on nickel. This chemistry was applied to the synthesis of a new axially chiral phosphine ligand that provided high enantioselectivity in a model asymmetric allylation reaction.

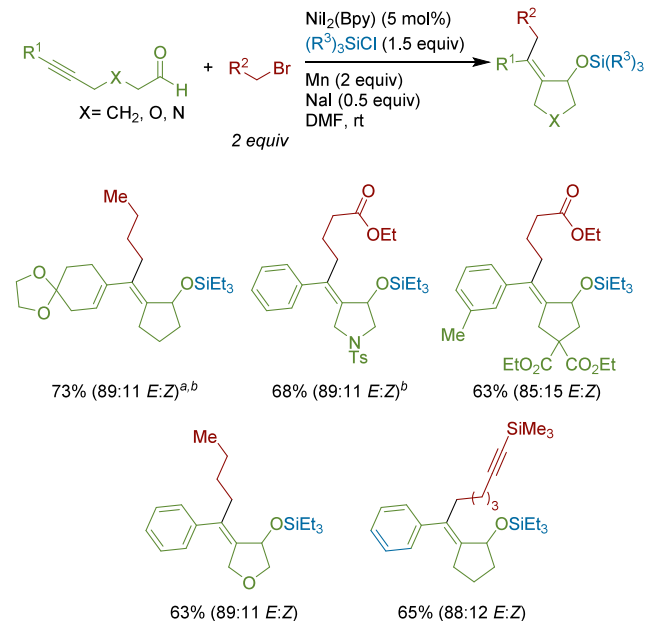
Chuan Wang and co-workers developed the atroposelective coupling of 1-naphthyl propargyl alcohols with aryl iodides and benzyl chlorides to form *E*-tetrasubstituted alkenes (Scheme 459).<sup>626</sup> The aryl iodide and benzylic chloride coupling partners could bear electronically donating or withdrawing groups at both the *ortho*- and *para*-positions. Stoichiometric studies with Ni(COD)<sub>2</sub> showed that zinc reductant was required for enantioselectivity, due to advantageous ZnI<sub>2</sub> forming in the reaction. This was further supported by an experiment showing how increased amounts of ZnI<sub>2</sub> could enhance enantioselectivity from 0% ee (no ZnI<sub>2</sub> added) to 71% ee (2.4 equiv ZnI<sub>2</sub> added).

**7.2.2. Cyclization Reactions.** The Montgomery lab developed a tandem cyclization/cross-electrophile coupling system to generate tetrasubstituted alkenes (Scheme 460).

**Scheme 459. *E*-Selective Synthesis of Tetrasubstituted Alkenes (2023)**



**Scheme 460. Ni-Catalyzed, Tandem Metallacycle Formation and XEC of Ynals with Alkyl Bromides to Form Tetrasubstituted Alkenes (2018)<sup>a</sup>**



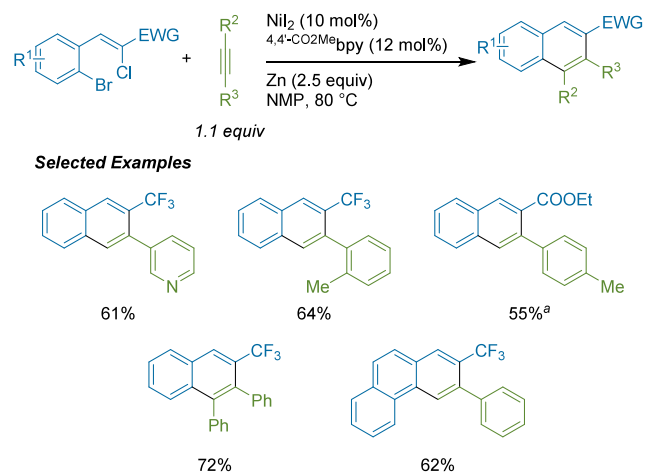
<sup>a</sup>(a) *n*-Bu<sub>4</sub>NI used in place of NaI. (b) With NiI<sub>2</sub>(bpy) (2 mol%).

This system takes advantage of known alkyne-aldehyde oxidative cyclizations onto nickel centers,<sup>628</sup> and the metallacycle is further functionalized via radical addition across the alkene. Formally, the first step of the catalytic cycle is an oxidative cyclization event, wherein a stable nickelacycle is formed in the presence of SiEt<sub>3</sub>. This nickelacycle is then able to capture an alkyl radical generated from another nickel center and undergo reductive elimination to form the tetrasubstituted alkene. Studies showed that in more concentrated reactions,

primary alkyl bromides favored the *E*-isomer. However, secondary alkyl bromides favored the *Z*-isomer, and this selectivity could further be enhanced by diluting the reaction further. Alkynes tethered to alkyl bromide coupling partners were found to be unreactive in this system, suggestive of the alkyne being critical for selective cyclizations/cross-coupling.

Most cyclization methods in this section utilize two different electrophiles, one of which has a tethered alkyne. In contrast, Hai-Yong Tu, Xing-Guo Zhang, and co-workers, developed a cyclization reaction based upon coupling a 1,4-dielectrophile with an alkyne (Scheme 461).<sup>629</sup> This approach enabled the

**Scheme 461. Ni-Catalyzed Formation of Substituted Naphthalenes by Cyclization of a 1,4-Dielectrophile with an Alkyne (2022)<sup>a</sup>**



formation of substituted naphthalenes from the coupling of terminal or symmetric alkynes and substituted styrenes. Although the desired product could be formed without an  $\alpha$ -electron-withdrawing group on the vinyl chloride, the reaction was most effective with either a  $-CF_3$  or  $-CO_2Et$  functional group at that site.

## 8. CARBON–HETEROATOM XEC

**Overview:** C–C bond formations dominate the field of XEC, perhaps because most heteroatoms are natural nucleophiles and C–X cross-coupling is well-developed.<sup>630–633</sup> On the other hand, a number of heteroatom electrophiles are either commonly available or offer other advantages, especially with heavier elements (Si, P, S) and nitrogen ( $-N_3$ ,  $-NO_2$ ,  $-NHOAc$ ). The diversity makes it more difficult to generalize much further (Figure 45). Indeed, the diversity of mechanisms led us to discuss them in the corresponding subsection.

### 8.1. Group 14 (Si/Ge)

**8.1.1. C–Si Bond Forming Reactions.** The XEC of chlorosilanes is a relatively new area, with the first report coming from Xing-Zhong Shu's group in 2020.<sup>634</sup> As with carbon nucleophiles, organosilicon nucleophiles can be challenging to prepare. Unlike C–X bonds, the high Si–X bond strengths exhibited by halogenated silicon reagents (e.g., 113 kcal/mol for  $Me_3SiCl$ )<sup>635</sup> can render them more challenging to activate. Unlike C–H bonds, Si–H bonds are easily activated, and hydrosilylation of  $\pi$ -bonds is a well-developed approach to Si–C bond formation.<sup>636–638</sup> Oxidative

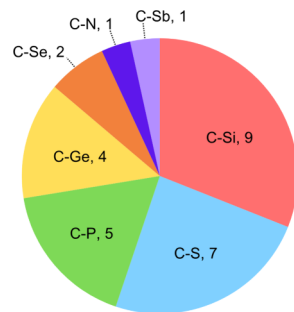


**Figure 45.** Distribution of heteroatoms in C–X XEC reactions.

addition of Si–X bonds is less developed than C–X bonds, but vinyl chlorosilanes seem to be especially reactive.<sup>639</sup>

While C–Si XEC reaction development is still in its infancy, several ligands have already been identified. Again, nitrogen ligands predominate and phosphines have only been reported as part of mixed-ligand systems (Figure 46, Figure 47).

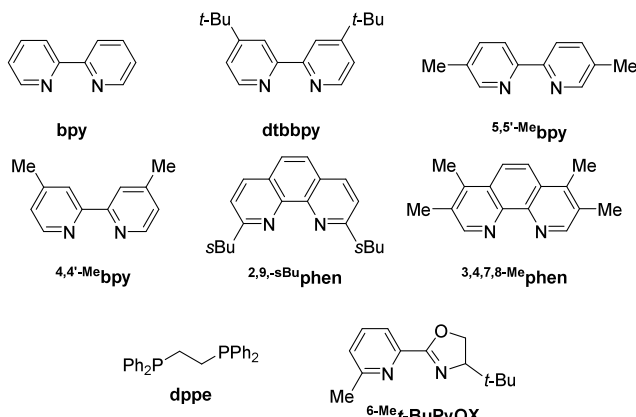


**Figure 46.** Ligands used in C–Si bond-forming XEC reactions.

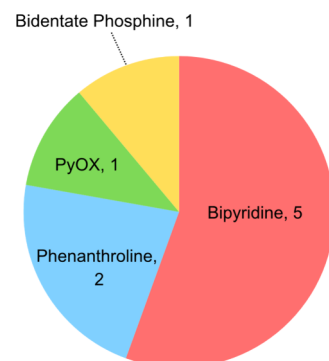


**Figure 47.** Distribution of ligands used in C–Si XEC reactions.

Proposed mechanisms generally fall into two categories (Figure 48): 1) sequential oxidative addition of C–X and Si–X, and 2) oxidative addition of Si–X followed by radical capture.

Mechanism A, with sequential oxidative addition of the aryl (pseudo)halide, followed by the chlorosilane, was supported by work done in Xing-Zhong Shu's first report of XEC with vinyl chlorosilanes.<sup>634</sup>

Mechanism B is most analogous to the mechanisms described for  $C(sp^2)$ – $C(sp^3)$  XEC reactions (see Figure 22). While the mechanism of oxidative addition for Si–Cl bonds to

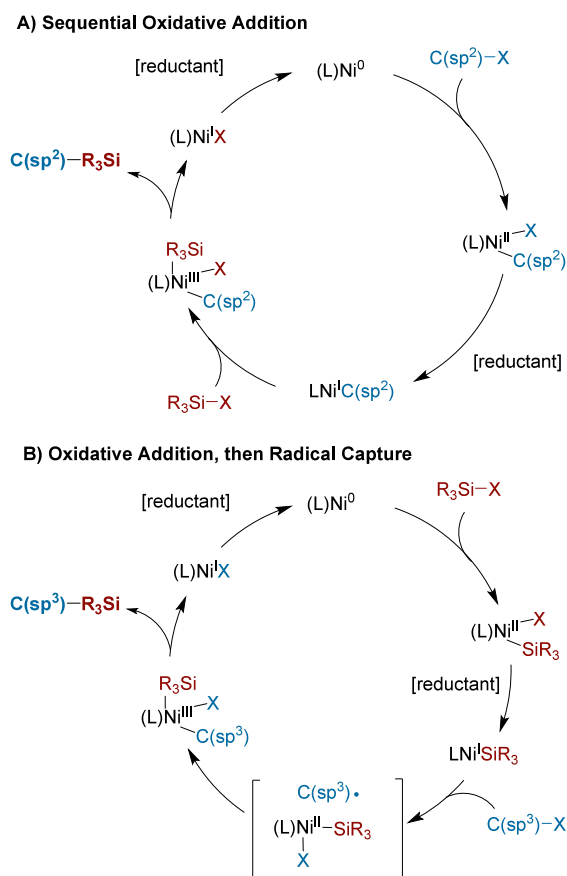
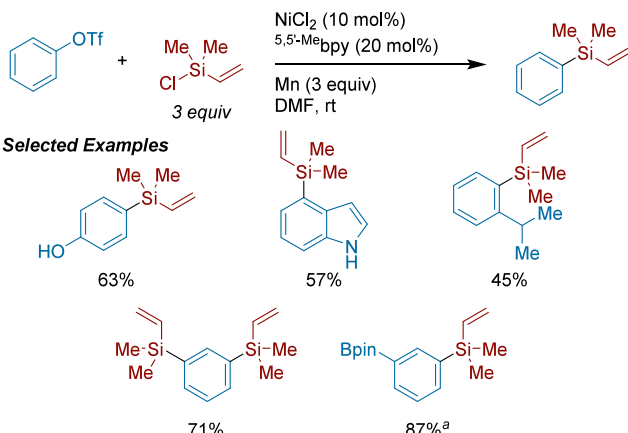


**Figure 48.** Proposed mechanisms for the XEC of silane electrophiles with carbon electrophiles.

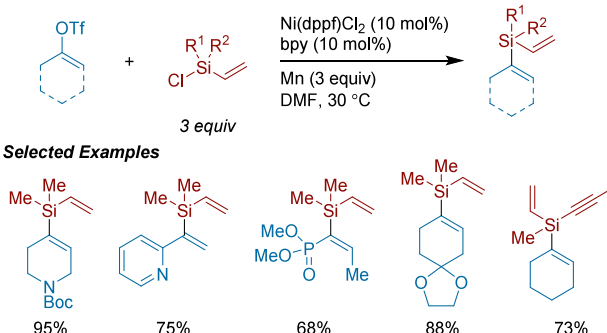
nickel remains unclear, initial formation of an  $(L)Ni^{II}(Si)(Cl)$  intermediate is reasonable and an  $Si^\bullet$  intermediate might be expected to participate in XAT side-reactions.<sup>640</sup> Evidence is available for alkyl radical formation and in the coupling of alkyl bromides with chlorosilanes. Data from Chun Zhang's group supports a mechanism analogous to  $C(sp^2)-C(sp^3)$  couplings of aryl halides with alkyl radicals (ring opening of bromomethylcyclopropane).<sup>160,641</sup>

Xing-Zhong Shu and co-workers reported the first XEC with silane-based electrophiles, successfully coupling vinyl chlorosilanes with aryl triflates (**Scheme 462**).<sup>634</sup> Vinylchlorosilanes outperformed TMSCl, TBSCl, and other common chlorosilane reagents, as their ability to coordinate to the nickel center helped improve cross-selectivity. Functional group tolerance was broad, encompassing free alcohols, phenols, and indoles. Additionally, select aryl bromides and iodides could be engaged. In conjunction with other mechanistic probes, the stoichiometric reaction with an arynickel(II) intermediate only proceeded in the presence of Mn, suggesting that an arynickel(I) species reacts with the vinylchlorosilane (**Figure 48A**). The resulting substituted organosilane products were further derivatized in downstream Hiyama cross-coupling reactions, demonstrating the synthetic utility of this method.

In the same report, the coupling of cyclic and acyclic vinyl triflates was achieved using a modified catalyst system composed of both phosphine and nitrogenous ligands (**Scheme 463**).<sup>634</sup> Tri- and tetrasubstituted vinyl triflates were tolerated, with *E*-isomers coupling in high yield and with complete

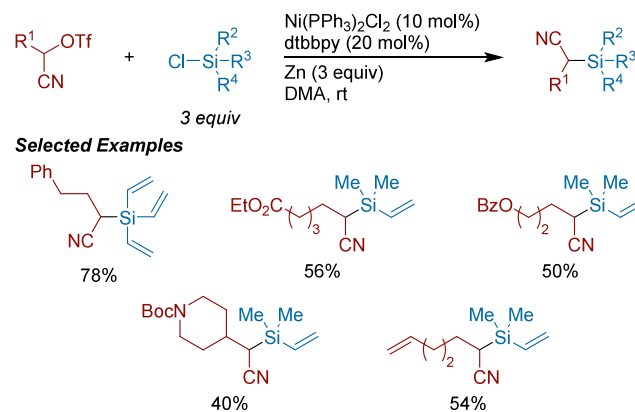
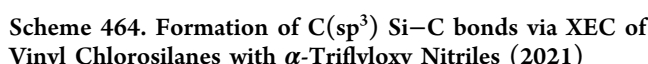


<sup>a</sup>With vinylchlorosilane (6 equiv)



stereoretention. This method enabled the facile synthesis of valuable benzocyclobutene monomers in two steps.

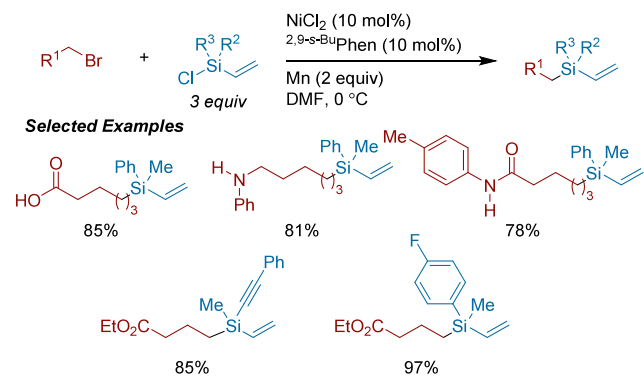
The Oestreich group demonstrated the XEC of activated alkyl coupling partners with chlorosilanes to form C(sp<sup>3</sup>)–Si bonds (**Scheme 464**).<sup>640</sup> Using a combination of dtbbpy and PPh<sub>3</sub> ligands, the  $\alpha$ -triflyloxy nitriles could be activated and efficiently coupled. In contrast to Xing-Zhong Shu's reports, trialkylchlorosilanes were moderately reactive under these conditions. Radical trapping and radical clocks were both consistent with nonradical activation of the  $\alpha$ -triflyloxy nitriles.



in line with the mechanism described in Figure 48A. The catalyst was much faster to react with Si–Cl bonds than C–Br and C–Cl bonds, allowing organic bromides and chlorides to be tolerated. In addition to aryl halides, esters, protected alcohols, and secondary amines were also tolerated in the reaction.

Complementary to prior studies, Xing-Zhong Shu and co-workers developed a method to engage unactivated alkyl bromides in the coupling with vinyl chlorosilanes (Scheme 465).<sup>642</sup> A sterically hindered phenanthroline ligand improved

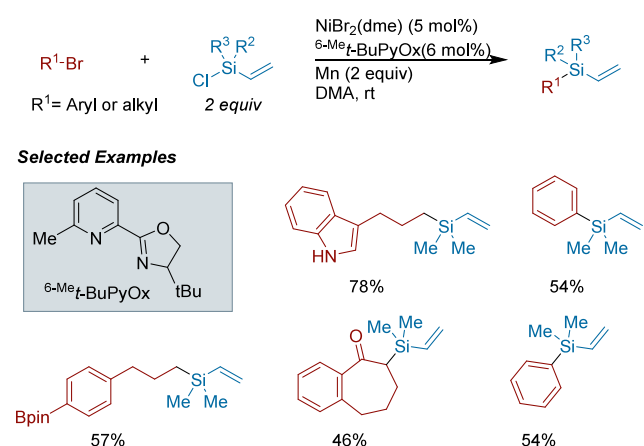
**Scheme 465. Cross-Coupling of Primary, Unactivated Alkyl Bromides with Vinyl Chlorosilanes (2021)**



reaction efficiency. Only primary alkyl bromides could be utilized, but they could bear a variety of unprotected, acidic functional groups. Alkynyl, cyclopropyl, and monoarylated functionalized chlorosilanes were suitable coupling partners. Competition experiments supported the alkyl bromide reacting first with nickel. One of the resulting vinylsilane products was used in a downstream Ir-catalyzed reaction to modify the hydrophobicity of a glass substrate, highlighting a material science-based application of this method.

Concurrently, Chun Zhang and colleagues also developed a cross-coupling of vinyl chlorosilanes with unactivated alkyl bromides (Scheme 466).<sup>641</sup> Racemic  $^{6\text{-Me}}t\text{-BuPyOx}$  outperformed other bidentate and tridentate nitrogenous ligands assessed. Both primary and secondary alkyl bromides could be utilized, and one aryl bromide, bromobenzene, was coupled successfully. Aryl and alkyl functional groups on the vinyl

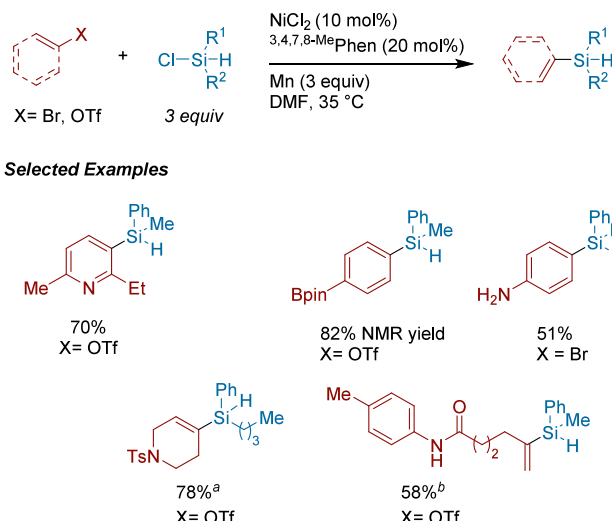
**Scheme 466. Cross-Electrophile Coupling of Unactivated Alkyl Bromides with Vinyl Chlorosilanes (2021)**



chlorosilanes did not hinder reactivity. Control experiments suggested a mechanism analogous to Figure 48B.

In an effort to expand past vinylsilyl coupling partners, Xing-Zhong Shu and co-workers coupled chlorohydrosilanes with aryl bromides, aryl triflates, and cyclic alkenyl triflates (Scheme 467).<sup>643</sup> For the aryl bromide and triflate system use of

**Scheme 467. Cross-Coupling of Chlorohydrosilanes with Aryl and Alkenyl Bromides and Triflates (2022)<sup>a</sup>**



<sup>a</sup>(a) With  $\text{Ni}(\text{OTf})_2$  (10 mol%), bpy (15 mol%), and Mn (2 equiv).

<sup>b</sup>(b) With  $\text{Ni}(\text{dppe})\text{Cl}_2$  (10 mol%),  $^{4,4\text{-Me}}\text{bpy}$  (15 mol%) and Mn (2 equiv) at 0 °C.

electron-rich  $^{3,4,7,8\text{-Me}}\text{phen}$  ligand was essential to obtaining high yields. Aryl triflates or bromides with electron-withdrawing or -donating groups were all cross-coupled, and primary amines, phenols, and ketal and THP protecting groups were well tolerated. A modified catalyst system enabled the coupling of vinyl triflates with chlorohydrosilanes. Kinetic experiments supported the intermediacy of an arynickel(II) intermediate, and further stoichiometric experiments indicated that this species is likely reduced to a nickel(I) before reacting with the hydrochlorosilane (Figure 48A).

**8.1.2. C–Ge Bond Forming Reactions.** XEC of chlorogermaines is less developed than the hydrogermylation of alkenes and the reaction of preformed organometallic reagents with chlorogermaines.<sup>644,645</sup> While well-established, these methods require prefunctionalization of either the germanium reagent or the corresponding alkyl/alkenyl fragment. Previously reported cross-couplings of organogermaines required the formation of  $\text{R}_3\text{GeZnCl}\cdot 2\text{LiCl}$  or utilized Grignard reagents as coupling partners.<sup>646</sup> Taken together, the development of more direct couplings of chlorogermaines would be advantageous. Thus far, each report of C–Ge XEC has utilized a different ligand (Figure 49). Ligand types, along with coupling partner identity, will continue to grow as new reactions in this area develop. The proposed mechanisms are analogous to one of the C–Si XEC mechanisms (Figure 48A): initial oxidative addition of the carbon electrophile, reduction to a Ni(I) intermediate, oxidative addition of the chlorogermaine, and reductive elimination.

Xing-Zhong Shu and colleagues developed the first XEC of chlorogermaines with aryl and vinyl (pseudo)halides (Scheme 468).<sup>647</sup> The substrate scope of the transformation is broad, in

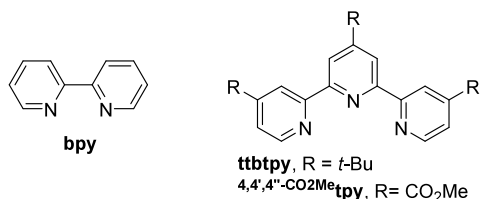
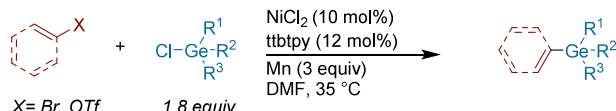
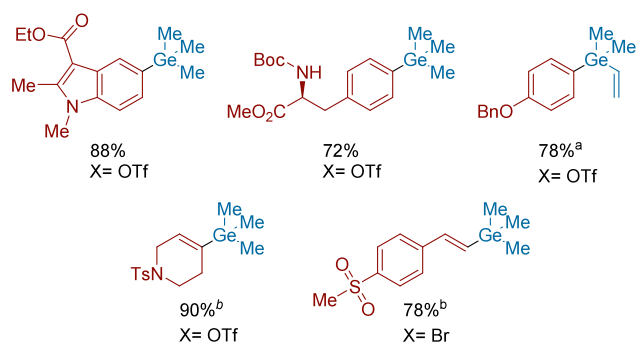


Figure 49. Ligands used in C–Ge bond-forming XEC reactions.

**Scheme 468. Ni-Catalyzed XEC of Chlorogermanes with Aryl and Vinyl (Pseudo)halides (2021)<sup>a</sup>****Selected Examples**

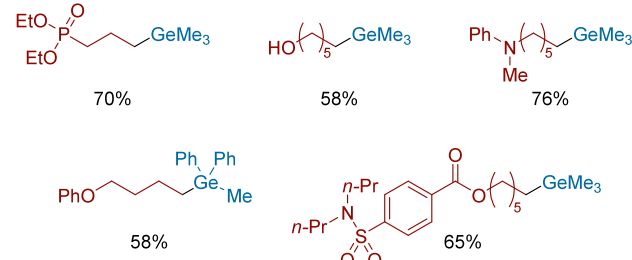
<sup>a</sup>(a) With dtbbpy (12 mol%) as ligand. (b) With <sup>4,4',4''</sup>-CO<sub>2</sub>Me tpy (12 mol%) as ligand, Ge–Cl (1.5 equiv), and DMF at 30 °C.

analogy to their previous work with C–Si XEC (see section 8.1.1, Scheme 462 and Scheme 463),<sup>634</sup> tolerating functionality such as organotin, organoboron, organosilicon, and a free phenol. A series of variably substituted tertiary chlorogermanes could be coupled, except for Ph<sub>3</sub>GeCl. In the presence of various Michael acceptors, no germanyl adducts were detected; moreover, radical cyclization probes resulted in uncyclized products. An arylnickel(II) complex was prepared, and with the addition of chlorogermane in the presence of manganese, cross-coupled product was formed; when manganese was omitted, no product was observed. Taken together, these data supported the hypothesis that a reduced arylnickel(II) species was potentially responsible for the oxidative addition of chlorogermane onto the nickel center.

Soon thereafter, Xing-Zhong Shu and colleagues introduced alkyl bromides as efficient coupling partners to form C(sp<sup>3</sup>)–Ge bonds through XEC (Scheme 469).<sup>648</sup> In contrast to their preceding studies (Scheme 468), bipyridine ligands performed superior to terpyridine ligands. Increased selectivity for the cross-coupled product was achieved at lower temperatures. While these conditions were specific for primary alkyl bromides, good functional group tolerance was observed (nitriles, aldehydes, phosphodiesters, and free alcohols). Additionally, the method was used to modify biologically active molecules such as D-biotin. Stochiometric studies supported the alkyl bromide reacting first with nickel(0)

**8.2. Group 15 (N/P/Sb)**

Pnictogen electrophiles such as chlorophosphines and azides are commonly utilized in organic synthesis with appropriate

**Scheme 469. Ni-Catalyzed XEC of Chlorogermanes with Primary Alkyl Bromides (2022)****Selected Examples**

carbon nucleophiles.<sup>649,650</sup> This area would benefit from a wider array of carbon electrophiles as well as improved functional group compatibility.

**8.2.1. C–N Coupling.** An area which has remained relatively less explored in the field of XEC has been the development of reactions of N-electrophiles to form C–N bonds. This stems in part from the fact that amines are among the most abundant functional groups and are excellent nucleophiles for C–N bond-forming reactions. There are also relatively fewer formal N-electrophiles. However, azides and nitro species offer advantages over free amines and are easy to access. There are only a few reports, so the list of catalysts is expected to grow in the future (Figure 50).

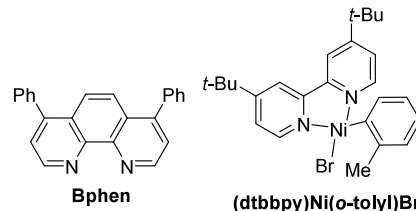
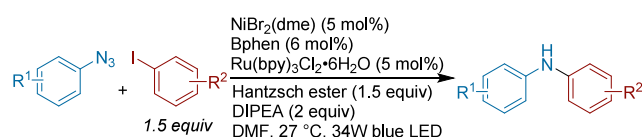


Figure 50. Ligands and precatalysts used in C–N bond forming XEC reactions.

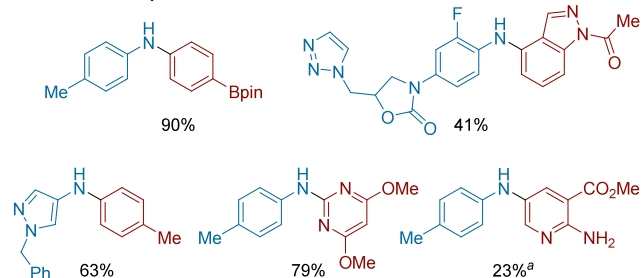
Konev, McTeague and Johannes at AstraZeneca reported the formation of diarylamines through a metallaphotoredox-catalyzed coupling of aryl iodides with arylazides (Scheme 470).<sup>651</sup> Interestingly, unprotected anilines were tolerated, allowing for selective N-arylation. Competition studies between aryl azides and an analogous aniline revealed that (1) the azide-derived product was reacted preferentially, and (2) the aniline was also able to form product, indicating that the photochemical conditions could potentially oxidize any aniline species generated in situ, leading to product formation. The authors propose that N-coordination of the azide to the nickel center enables the single-electron transfer, extrusion of N<sub>2</sub>, and protonation of the nitrogen to form the amine product. The reaction was compatible with a number of heterocyclic azides and heteroaryl halides, while tolerating Bpin, ester, and sulfonamide functional groups.

Dong Xue and co-workers developed a photochemical, Ni-catalyzed C–N coupling of nitroarenes and aryl halides to form diarylamines through the use of a preformed (o-tolyl)Ni<sup>II</sup>–Br precatalyst (Scheme 471).<sup>652</sup> Previous reductive

**Scheme 470.** Preparation of Diarylamines via Nickel/Photoredox XEC of Aryl Azides with Aryl (Pseudo)Halides (2018)<sup>a</sup>

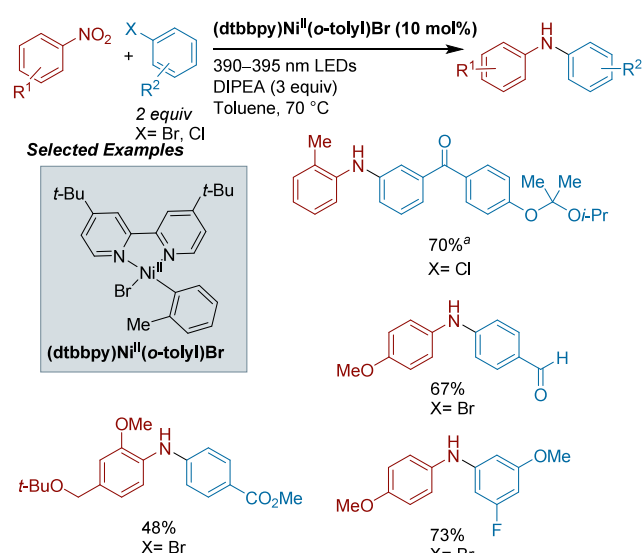


**Selected Examples**



<sup>a</sup>With aryl bromide

**Scheme 471.** Photochemical, Ni-Catalyzed C–N Coupling of Nitroarenes with Aryl Halides to Form Diarylamines (2021)<sup>a</sup>



<sup>a</sup>With (dtbbpy)Ni<sup>II</sup>(o-tolyl)Br (15 mol%)

methods of forming diarylamines from nitroarenes required the use of boronic acids as nucleophilic coupling partners,<sup>653</sup> but this method enables the cross-coupling of the two electrophiles without the need for reduction of the nitroarene or activation of the aryl halide. The complex proposed mechanism involves reduction of the nitroarene to a nitrosoarene that is proposed to react with an arylradical intermediate and a further reduction of the hydroxylamine. While this is borderline between XEC and formal XEC, we elected to include it as an example of an exciting direction for the field.

**8.2.2. C–P Coupling.** Translation of XEC chemistry to the synthesis of C–P bonds has been achieved in many contexts, perhaps arising from the stability and convenience of chlorophosphines and the challenge of using phosphide nucleophiles (Figure 51). Indeed, many C–P XEC reactions were reported in the 1990s, predating the majority of analogous C–C bond-forming XECs. At the time of writing

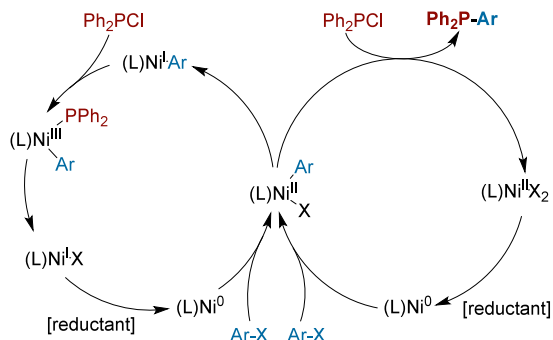


**Figure 51.** Proposed mechanisms for the XEC of aryl (pseudo)halides with chlorophosphines.

this review, a definitive mechanism for the cross-coupling between chlorophosphines and aryl or alkyl (pseudo)halides has not been agreed upon, but mechanistic work done by Budnikova has shed some light on the electrochemically driven reactions.<sup>654</sup> It is understood that a (bpy)Ni<sup>II</sup>(X<sub>2</sub>) species is reduced at the cathode and undergoes oxidative addition with the aryl halide to generate an (aryl)Ni<sup>II</sup>(bpy)(X) species. From this intermediate, it is believed that there are two plausible mechanisms for product formation: 1) intermediate reduction of the (aryl)Ni<sup>II</sup>(bpy)(X) to (aryl)Ni<sup>I</sup>(bpy) allowing for oxidative addition of the chlorodiphenylphosphine to generate a (Ph<sub>2</sub>P)(aryl)Ni<sup>III</sup>(bpy)(X), from which reductive elimination of the aryl and phosphine yields product, or 2) chlorodiphenylphosphine reacts directly with the Ni<sup>II</sup> intermediate via transmetalation, wherein (bpy)Ni<sup>II</sup>(X<sub>2</sub>) is regenerated and Ar-PPh<sub>2</sub> is formed. The plausible mechanisms are shown in Figure 51 and the relevant ligands are shown in Figure 52.

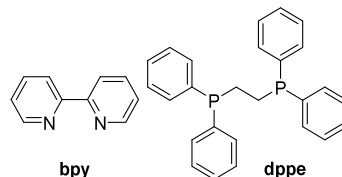
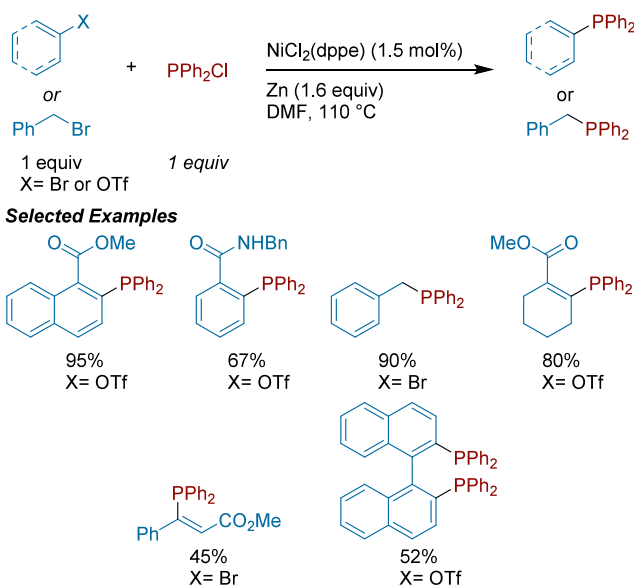


**Figure 52.** Ligands used in C–P XEC coupling reactions

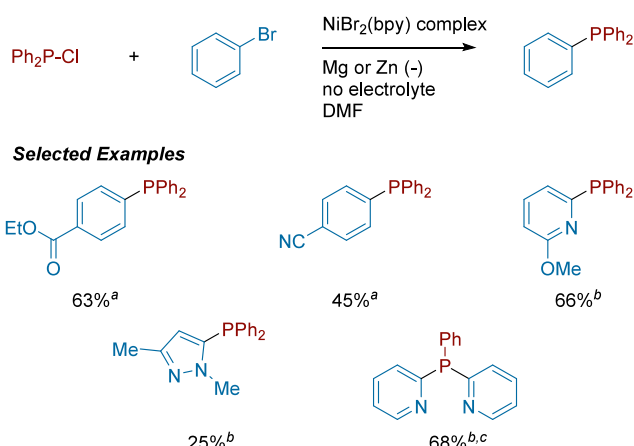
In 1997, Laneman and co-workers developed an efficient synthesis of tertiary phosphines via a Ni-catalyzed XEC of chlorodiphenylphosphine with benzylic halides, aryl halides, vinylic halides, and aryl sulfonates (Scheme 472).<sup>655</sup> Ortho-sterics were well tolerated for aryl substrates, and apart from free carboxylic acids, carbonyl containing moieties were coupled in productive yields. In general, triflate substrates afforded higher yields, as bromides resulted in large quantities of hydrodehalogenated byproducts. The synthetic utility of this method was illustrated in the preparation of (S)-BINAP without erosion of axial chirality.

Budnikova and co-workers developed an electrochemical method of forming tertiary phosphines via an electrochemically reduced Ni(bpy) complex (Scheme 473).<sup>656</sup> The reactions were run in an undivided cell, with a magnesium anode used for electron-rich aryl bromides, and a zinc anode used for electron-deficient ones. It was proposed that the reaction proceeds through a sequential oxidative addition mechanism, in which the aryl bromide reacts with the nickel center first followed by uptake of the chlorophosphine. A (bpy)Ni<sup>0</sup>(o-tolyl) complex was synthesized electrochemically, and with

**Scheme 472.** XEC of Chlorodiphenylphosphine with Aryl Halides and Sulfonates to form Tertiary Phosphines (1997)



**Scheme 473.** Electrochemical Coupling of (Hetero) Aryl Bromides with Phosphorus Chloride to Form Tertiary Phosphines (1999)<sup>a</sup>

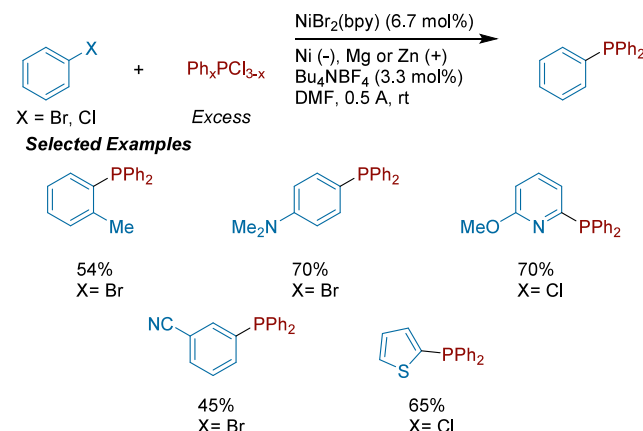


<sup>a</sup>(a) Zn anode was used. (b) Mg anode was used. (c) PhPCl<sub>2</sub> was the starting material.

addition of chlorodiphenylphosphine, diphenyl-*o*-tolylphosphine and its oxide were isolated. In the reaction of the preformed nickel diphenylphosphide complex, the addition of aryl bromide resulted in no product formation. The reported protocol could tolerate esters, nitriles, protected phenols, and efficiently coupled heteroaryl bromides.

Nédélec developed an electrochemical approach to access tertiary phosphines from aryl halides and phenyldichlorophosphine or diphenylchlorophosphine (Scheme 474).<sup>657</sup> Both aryl bromides and heteroaryl chlorides were able to couple efficiently. In order to achieve the highest yields, the aryl bromide was added portionwise until a steady concentration of tertiary phosphine was detected via GC.).<sup>657</sup> Both aryl bromides and heteroaryl chlorides were able to couple efficiently. In order to achieve the highest yields, the aryl halide was added portion-wise to the reaction mixture until a steady concentration of tertiary phosphine was detected via

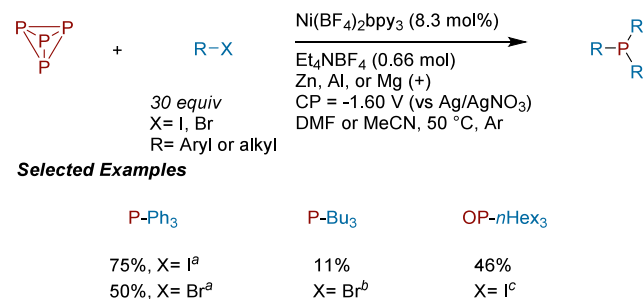
**Scheme 474.** Ni-Catalyzed, Electrochemical XEC of Mono- and Dichlorophenylphosphines with Aryl Halides (1999)



GC. The authors found that a magnesium anode was necessary to engage electron-neutral and electron-rich aryl halides, while electron-deficient aryl halides necessitated a zinc anode. When PCl<sub>3</sub> was subjected to the reaction conditions, only a minimal amount of PPh<sub>3</sub> was generated at the start of electrolysis. It was hypothesized that the PCl<sub>3</sub> was much quicker to react with the zerovalent nickel species compared to aryl halides, resulting in inefficient coupling.

Budnikova and co-workers further developed electrochemical conditions to functionalize white phosphorus (P<sub>4</sub>) with both aryl and alkyl halides (Scheme 475).<sup>658,659</sup> Selective

**Scheme 475.** Ni-Catalyzed, Electrochemical XEC of Alkyl and Aryl Halides with White Phosphorus (2002)<sup>a</sup>

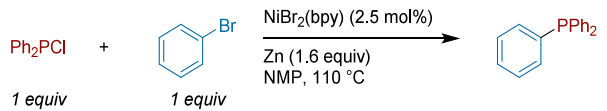


<sup>a</sup>(a) Zn anode was used in DMF. (b) Mg anode was used in DMF. (c) Al anode was used in MeCN, oxide formation likely occurs during isolation.

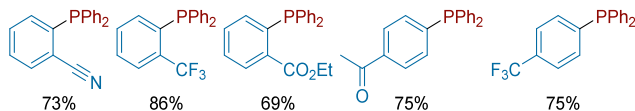
formation of the tertiary phosphine or its oxide could be controlled by the choice of anode or solvent. Mechanistic investigations illustrated that both Ni<sup>II</sup> and Ni<sup>0</sup> species could coordinate with P<sub>4</sub>, with the latter forming more stable complexes. However, under the reaction conditions, the authors propose that Ni<sup>0</sup> initially reacts with the aryl or alkyl halide, and the oxidized nickel species is what enables the formation of the tertiary phosphines.

Le Gall published a follow up on Nédélec's electrochemical work with heterogeneous metallic reductants toward the synthesis of tertiary phosphines (Scheme 476).<sup>660</sup> With zinc as the terminal reductant, the reaction proceeded efficiently in NMP at higher temperatures (110 °C). Notably, these XEC conditions could tolerate functional groups (such as ketones) that might not tolerate the use of carbon or phosphorus

**Scheme 476. Formation of Triarylphosphines via the XEC of Chlorodiphenylphosphine with Aryl Bromides (2003)**



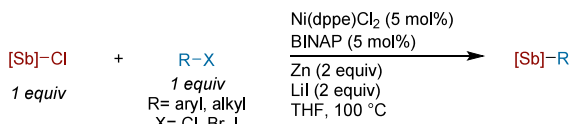
**Selected Examples**



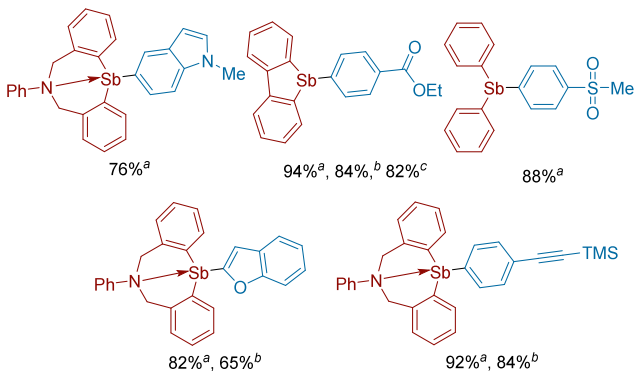
nucleophiles. However, the substituent position and electronics proved to have a major influence on the reaction profile. In the case of trifluoromethyl-bromobenzene, the *meta*- and *para*-versions coupled efficiently (86% and 75% yield, respectively), but the *ortho*-substituted version only resulted in a 30% yield. Additionally, aryl halides with electron-donating groups, such as *para*-methoxy, could easily form the corresponding tertiary phosphine oxide.

Wai-Yeung Wong, Shuang-Feng Yin, Nobuaki Kambe, Renhua Qiu and colleagues reported the Ni-catalyzed XEC of bench stable chlorostibines with aryl halides (Scheme 477).<sup>661</sup> A mixed phosphine ligand system of dppe and BINAP

**Scheme 477. Ni-Catalyzed Cross-Electrophile Coupling of Chlorostibines with Aryl and Alkyl Halides (2022)<sup>a</sup>**



**Selected Examples**



<sup>a</sup>(a) With X = I, (b) With X = Br, (c) With X = Cl.

was utilized, and LiI boosted reaction efficiency. Electronically diverse aryl iodides and bromides, as well as activated aryl chlorides were all competent coupling partners. Only primary alkyl bromides and iodides could be utilized, as secondary alkyl halides gave no yield. Stibines functionalized with natural product and pharmaceutical cores could be obtained in high yields. The resulting stibine products were further functionalized in high chemoselectivity in a downstream palladium cross coupling sequence, affording valuable bi- and triarylated motifs. Ultimately, the authors propose three potential mechanisms, one of which is analogous to the sequential oxidative addition (Figure 21A). However, stoichiometric studies indicated that in situ generated distibine intermediates could be competent reaction partners. Thus, the authors

propose that diverging cross coupling mechanisms involving a key transmetalation event between Ni(II) species with distibines could also be invoked.

**8.3. Group 16 (S/Se)**

The development of new methodologies to form carbon–chalcogen bonds has been focused on two major points; first, the development of new thiolating agents which are less nucleophilic in nature than those previously reported using thiols and disulfides, and second, the synthesis of effective and odorless reagents to form said carbon–chalcogen bonds. Although RS<sup>−</sup> and RSe<sup>−</sup> are excellent nucleophiles, RS• and RSe• are easily accessible and complementary. As shown by some of the reports below, the parallel selenylation is often accessible using the same conditions and similar activating reagents that are used in the thiolation protocols. Interestingly, these new reagents are not limited to being redox active, but in some instances, have been proposed to form sulfur radicals to engage in productive cross-coupling.

Mechanistic experiments done by Shun-Yi Wang and Shun-Jun Ji's groups showed that in the presence of a nickel catalyst and a metal powder reductant, sulfur and selenium sulfate groups can dimerize to form disulfides. When the nickel was removed, manganese powder alone could not activate the reagents, indicating that these S/Se–sulfate groups are likely redox active. As such, it is proposed that these groups (and other redox active groups), when reacted with an alkyl radical precursor, undergo an oxidative addition/radical capture mechanism (Figure 53).<sup>662</sup> The reports in this section point

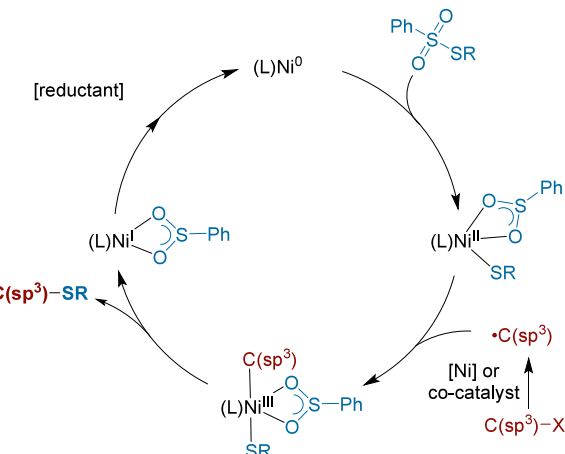


**Figure 53.** Thiolation of aryl halides via a thiosulfonate or analogous redox active group.

to bipyridine and phenanthroline-based ligands being the best for C–S coupling reactions, but there is room to discover catalyst and ligand combinations that could introduce more secondary and tertiary radical precursors into the C–S coupling regime (Figure 54).

Included in their report of the Ni-catalyzed C–S coupling of aryl iodides and thiols, Yu Peng and co-workers investigated thioacetates as stable surrogates for intramolecular C–S coupling with aryl iodides to form saturated heterocycles (Scheme 478).<sup>663</sup> While this method displayed a small scope, the reaction could be run at gram scale at lower catalyst loading, (5 mol% NiCl<sub>2</sub> at 1 mmol scale vs 10 mol% NiCl<sub>2</sub> at 2.4 g scale) highlighting the practical advantages of this method.

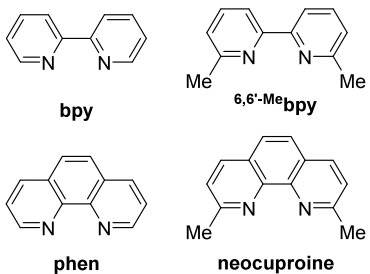
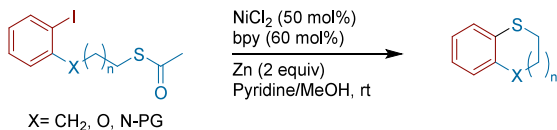
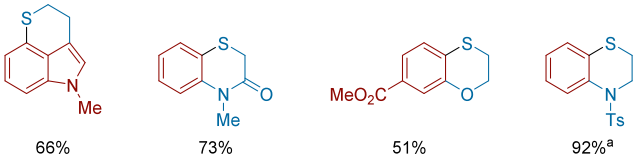


**Figure 54.** Ligands used in C–S and C–Se bond forming XEC reactions.

**Scheme 478. Nickel-Mediated, Intramolecular C–S Coupling of Thioacetates with Aryl Iodides (2013)<sup>a</sup>**



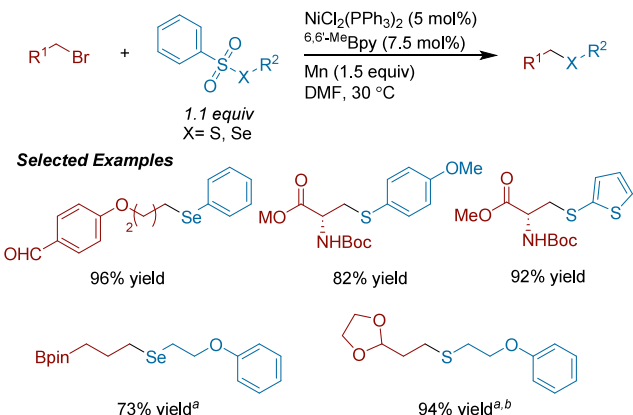
**Selected Examples**



<sup>a</sup>NiCl<sub>2</sub> (10 mol%), bpy (20 mol%), Zn (0.5 equiv), run at 2.4 g scale.

The Shun-Yi Wang and Shun-Jun Ji groups developed a Ni-catalyzed, thiolation and selenylation of unactivated alkyl bromides, by using thio- and selenosulfonates as redox active electrophiles (**Scheme 479**).<sup>662</sup> Bipyridine ligands with flanking

**Scheme 479. Ni-Catalyzed Thiolation and Selenylation of Unactivated Alkyl Bromides (2018)<sup>a</sup>**



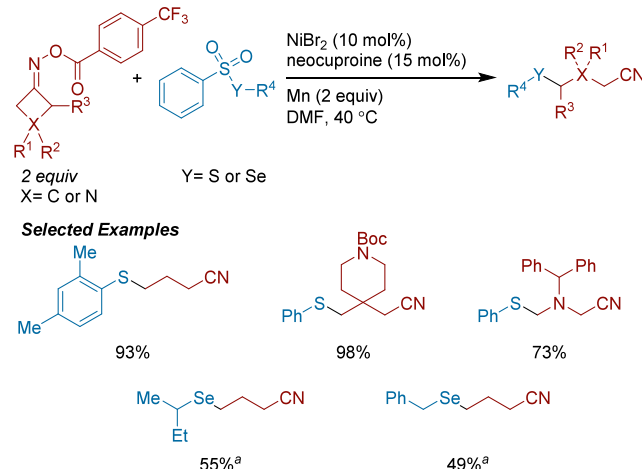
<sup>a</sup>(a) With Alkyl-Br (1.1 equiv), benzenesulfonoselenoates (1 equiv), NiBr<sub>2</sub> (5 mol%), neocuproine (7.5 mol%), Mn (1.5 equiv), DMF. (b) DMF/MeCN (2:3 v/v) was used instead of DMF.

6,6'-methyl groups resulted in the highest yield. The reaction proved to be chemoselective, with alcohols, aldehydes, and alkyl borates tolerated by the system. Selenylation was achievable with similar conditions as the thiolation protocol.

Shortly after, Shun-Yi Wang and Shun-Jun Ji published the Ni-catalyzed ring opening and cross-coupling of cyclobutanone oxime esters with thio- and selenylthiosulfonates to form

C(sp<sup>3</sup>)–S and C(sp<sup>3</sup>)–Se bonds (**Scheme 480**).<sup>664</sup> The cyclobutanone O-acyl oxime is proposed to be reduced via

**Scheme 480. Ni-Catalyzed Thiolation and Selenylation of Cyclobutanone Oxime Esters with Thiosulfonates or Seleniumsulfonates (2019)<sup>a</sup>**

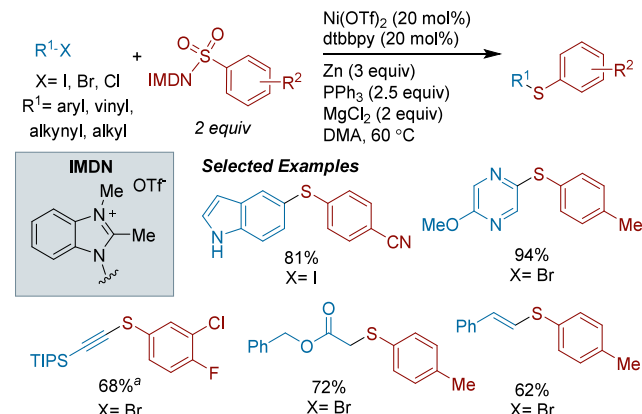


<sup>a</sup>At 60 °C.

SET to generate an N-centered radical that undergoes  $\beta$ -scission to form a  $\gamma$ -cyanoalkyl radical. This can then be captured by the nickel thiolate intermediate and undergo reductive elimination to form the rearranged sulfide product.

Yi Wang and co-workers reported the use of redox active benzimidazolium sulfonamides as convenient thiolating reagents in the XEC with alkyl, vinyl, aryl, and alkynyl halides, to form C–S bonds (**Scheme 481**).<sup>665</sup> The reagents are made

**Scheme 481. XEC of Redox Active Benzimidazolium Sulfonamides with Alkyl, Vinyl, Alkynyl, And Aryl Halides (2020)<sup>a</sup>**



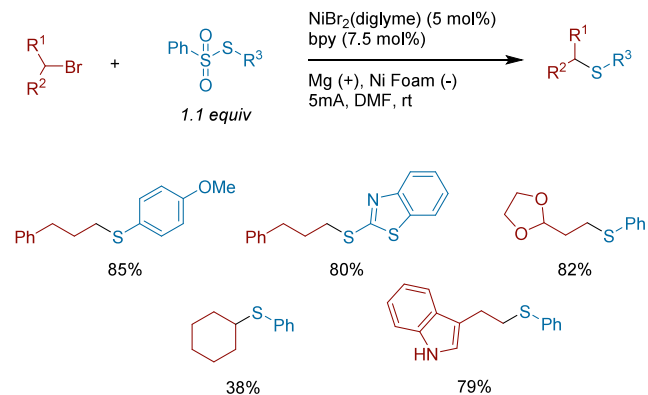
<sup>a</sup>With 4-(trifluoromethyl)pyridine (20 mol%) as ligand in THF.

in one step from sulfonyl chlorides, benzimidazole, and methyl triflate. These salts are reduced by PPh<sub>3</sub> to generate an R-S-[N<sup>+</sup>] sulfonamide that forms an S-centered radical, which is then captured by the nickel catalyst. The use of this benzimidazolium sulfonamide avoids the formation of disulfide side-products, which is common from the direct reduction of sulfonyl chloride. The method can form C(sp<sup>2</sup>)–S, C(sp<sup>3</sup>)–S, and C(sp<sup>3</sup>)–S bonds with very little modification to the

optimized reaction conditions. The reaction is tolerant of esters, alkyl Bpin, and terminal alkenes.

The Ackermann group drove the XEC of alkyl bromides with thiosulfonates with electrochemistry (**Scheme 482**).<sup>666</sup>

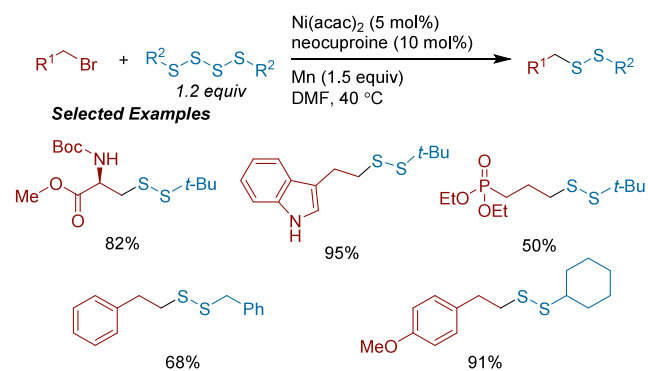
**Scheme 482.** Ni-Catalyzed, Electrochemical Thiolation by the XEC of Alkyl Bromides with Thiosulfonates to Form C(sp<sup>3</sup>)–S Bonds (2021)



The reaction was run with a magnesium anode and nickel foam cathode under constant current conditions. The reaction was run in a commercial electrochemical instrument with only slightly diminished yields. Aryl, benzylic, and secondary thiosulfonates were all able to couple efficiently, with no obvious electronic preference of the substitution on the aryls. However, except for one secondary alkyl bromide example, alkyl bromide coupling partners were limited to primary alkyl bromides.

Shun-Yi Wang and Lutz Ackermann developed a method for accessing unsymmetrical disulfides via the cross-coupling of tetrasulfides with primary alkyl bromides (**Scheme 483**).<sup>667</sup>

**Scheme 483.** Formation of Unsymmetrical Disulfides via the Ni-Catalyzed XEC of Alkyl Bromides with Alkyl and Aryl Tetrasulfides (2022)



The tetrasulfides are proposed to regioselectively generate an ( $\text{R}^1\text{-S}_3\text{Ni(S--R}^2\text{)}$ ) oxidative addition complex (**Figure 55**). This complex is able to capture alkyl radicals, forming a trisulfide intermediate ( $\text{R}^1\text{-S}_3\text{-R}^2$ ) upon reductive elimination from the nickel center. The trisulfide is proposed to be redox active as well, forming a new ( $\text{R}^1\text{-S}_2\text{Ni(S--R}^2\text{)}$ ) oxidative addition complex on the nickel. XRD characterizations determined that the formation of  $\text{S}_8$  and other sulfur polyanions resulted when a sulfur atom was extruded by the nickel center. Following the extrusion of the sulfur atom, the disulfide

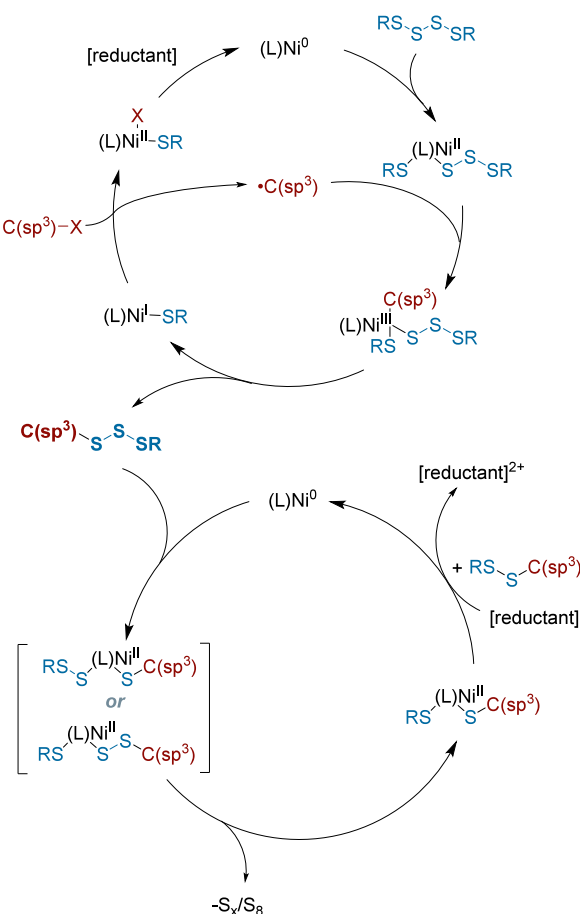


**Figure 55.** Mechanism for the formation of unsymmetrical disulfides via the cross-coupling of tetrasulfides with alkyl radicals

product is formed by reductive elimination from the nickel. The formation of a redox active, trisulfide species was supported via Raman frequency measurements of a synthesized trisulfide reagent subjected to standard reactions conditions. Raman frequencies for the trisulfide disappeared over time, and signals for the disulfide product appeared, indicating that the trisulfide intermediate was most likely consumed during the course of the reaction. The protocol was compatible with free  $-\text{OH}$ ,  $-\text{NH}$ , and phosphoester functional groups.

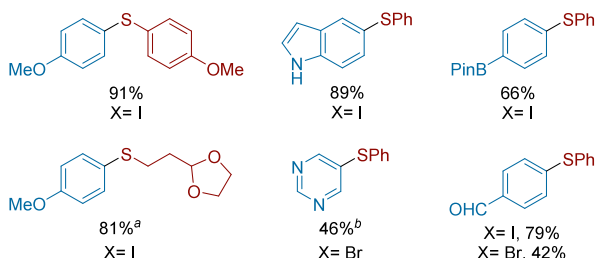
Xinxin Shao and colleagues developed a new electrophilic sulfur reagent, *N*-thiophthalimides, for XEC with aryl halides (**Scheme 484**).<sup>668</sup> These reagents are formed via the combination of an *N*-(chlorosulfonyl)phthalimide intermediate, and an organozinc reagent, resulting in the alkyl or aryl *N*-thiophthalimide reagent. This approach reports an attractive catalyst loading of only 0.5 mol%, which is relatively low for XEC reactions of any type. With respect to the *N*-thiophthalimide starting material, functional groups were limited to those that could tolerate organozinc intermediates, but the cross-coupling protocol itself tolerated aldehydes, esters, and pinacol boranes.

Xinxin Shao and Ying Bai reported that *N*-sulfanylsuccinamides could be used in place of *N*-sulfanylphthalimides under nearly the same conditions (**Scheme 484** vs **Scheme 485**).<sup>669</sup> The reaction primarily utilized aryl iodides, but in some cases, aryl bromides could be utilized. Aldehydes, aryl Bpin, and free  $-\text{NH}$  heterocycles were tolerated with the protocol.

**Scheme 484.** Ni-Catalyzed XEC of Aryl, Vinyl, and Alkynal Halides with *N*-Thiophthalimides (2022)<sup>a</sup>

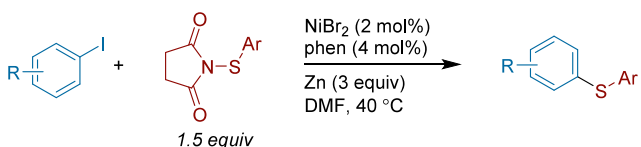


**Selected Examples**

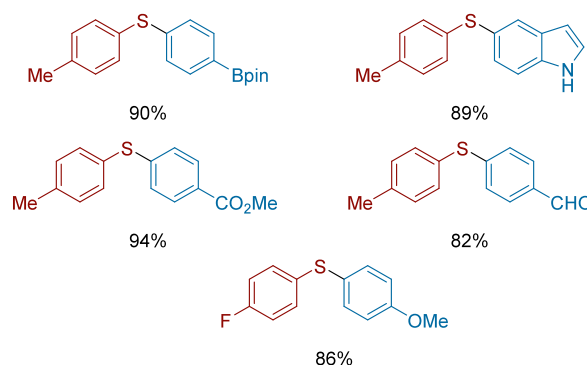


<sup>a</sup>(a) With 2 equiv *N*-thiophthalimide,  $\text{NiCl}_2(\text{PPh}_3)_2$  (5 mol%), phen (10 mol%), 3 equiv Zn in DMF at 120 °C. (b) *N*-Thiophthalimide (1.2 equiv),  $\text{NiBr}_2$  (2.5 mol%), phen (5 mol%), 2 equiv NaI, 3 equiv Zn in DMF at 80 °C.

**Scheme 485.** Ni-Catalyzed XEC of Organo-Iodides With *N*-Thioimidates to Generate C(sp<sup>2</sup>)–S Bonds (2023)



**Selected Examples**



## 9. OUTLOOK AND CHALLENGES FOR THE FIELD

### 9.1. Scope and Selectivity

While avoiding the synthesis of carbon nucleophiles increases the functional group tolerance of XEC reactions, there are still limitations in what electrophiles can be successfully coupled. For example, functional groups that are easily reduced, such as nitro groups or azides, are often not tolerated. In addition, coupling partners that can undergo ring opening, such as isoxazoles, represent general challenges in the field.<sup>670</sup>

In contrast to conventional cross-coupling, where one coupling partner favors oxidative addition and the other transmetalation, XEC can suffer from poor cross-selectivity. First, even in cases where differential activation is robust (e.g., polar oxidative addition of aryl halides vs radical activation of alkyl halides), high selectivity is contingent on successfully matching rates of activation of both coupling partners. In

practice this means that coupling electrophiles of very different reactivity is difficult (e.g., aryl chlorides with alkyl iodides). Methods to match the reactivity of the larger substrate pools are still required (e.g., denitrative coupling of amines with aryl chlorides). In general, coupling partners that are slower to react, such as organochlorides, are underreported as competent coupling partners, compared to more reactive organobromides and -iodides, despite higher commercial availability.

Another selectivity challenge occurs when the electrophiles react in the same way by the same mechanism. In this case, cross-selectivity is not possible. If the electrophiles have similar rates of reactivity, statistical mixtures are observed; if their reactivity is very different, then primarily homodimers are observed. While this can be addressed by manipulating concentrations of reagents (excess of one partner and/or slow addition), a more general approach is the development of catalysts or combinations of catalysts that enable mechanistic differentiation of the substrates (e.g., aryl tosylates and aryl triflates can be differentiated by Pd and Ni multimetallic catalysis).<sup>20</sup> Another approach well-suited to C(sp<sup>3</sup>)–C(sp<sup>3</sup>) bond formation is utilizing the different reactivities of two radical intermediates to engender cross-selectivity. As formulated in the “persistent radical effect”: as long as one radical is slow to self-couple compared to cross-coupling and both radicals are generated at about the same rate, this can result in high selectivity.<sup>112</sup> Metals can assist with this “sorting” process by stabilizing one of the radical intermediates and assisting in the bond-forming steps.<sup>52,112,671</sup> While exciting progress has been made using these strategies, more advances in this area are needed.

Few XEC methods have focused upon coupling reactions to form highly sterically hindered bonds. This problem is especially challenging for XEC because hindered substrates are slower to activate, adding the problems of matching reactivity to those of the bond-forming step.

However, with all of these challenges, it is important to note that many XEC reactions have been reported with nearly perfect cross-selectivity and high yields, even with a 1:1 ratio of starting materials. In addition, stepwise stoichiometric reactions of arylnickel(II)<sup>672,673</sup> and alkynickel(II)<sup>674</sup> complexes demonstrate that high yields in the radical-capture and bond-forming steps should be possible in nearly all cases. We recently reported on a new nonradical method to access alkynickel(II) intermediates that should provide new approaches to cross-selective C(sp<sup>3</sup>)–C(sp<sup>3</sup>) reactions.<sup>675</sup> It is our view that, with sufficient further study and understanding, XEC reactions can be as cross-selective as the best cross-couplings of nucleophiles with electrophiles.

### 9.2. Ligand Design and Discovery

While there has been progress in ligand design in recent years, ligand choice remains limited to a relatively small range of privileged classes (see Figures 6, 7, and 8). The discovery of the pyridyl-2-carboxamidine structure (e.g., PyCam, BpyCam, and PyBCam) and its broad success offers promise for future ligand discovery.<sup>32</sup> More recently, work into Di(2-picoly)amines (DPAs) shows promise as a robust class for further XEC reactions.<sup>234</sup> Ongoing computational studies in our group and others will undoubtedly introduce a broader range of ligand classes compatible with XEC reactions of interest.<sup>161,676</sup> In general, the field would benefit from efforts in mechanism-guided ligand design, such as the recent dumbbell ligands of Sawamura.<sup>230</sup>

### 9.3. Reductants, Photochemistry, and Electrochemistry

The most common reductants used in XEC are metal powders, most frequently Zn<sup>0</sup> or Mn<sup>0</sup>, which are inexpensive, easy to handle and store. However, with translation to larger scale (>100 g), there are concerns regarding disposal of resulting metal salts.<sup>34,677</sup> In addition, heterogeneous reductants on larger scale can exhibit mass-transfer limitations, which can result in irreproducible kinetics.<sup>47,678,679</sup> Variations in the form of the heterogeneous reductant (e.g., zinc powder vs zinc flake) can result in differing rates of reactivity which can be difficult to predict. The variability in metal powders is complicated because characterization usually requires testing them out in the reaction of interest. In addition, translation of heterogeneous reactions to smaller scale (e.g., HTE reaction setups) often requires additional technologies, such as ChemBeads, to allow for reproducible dosing and efficient stirring.<sup>115,226,227</sup>

Organic reductants offer an attractive alternative to heterogeneous reductants because of easier dosing and scaling. While the most developed, the use of tetrakis(amino)ethylenes has been limited to high prices (TDAE is \$6170/mol while Zn is \$7/mol and Mn is \$12/mol from Sigma-Aldrich) or a lack of commercial availability. The use of bis(pinacolato)diboron (B<sub>2</sub>pin<sub>2</sub>) with added base is lower cost (B<sub>2</sub>pin<sub>2</sub> is \$670/mol) and is promising for the XEC of alkyl and aryl halides.<sup>52–54</sup> Further study of these two systems, simplified syntheses of tetrakis(amino)ethylenes, as well as the discovery of novel homogeneous reductants, are all promising future directions. Despite these current issues, the advantages of homogeneous reactions make it is easy to see a near future when homogeneous reductant prices and availability have improved to the point where they will be the default choice in XEC.

Photochemical applications of XEC bypass the need for stoichiometric amounts of metal reductants yet often still involve the use of expensive Ir photocatalysts.<sup>680</sup> While Ir is unlikely to become more abundant, research in organic and main-group alternatives (e.g., 4-CzIPN,<sup>681</sup> benzophenones,<sup>253</sup> semiconductor QDs<sup>682</sup>) has recently gained momentum. Given the growing confidence of organic chemists in utilizing photochemistry on both large and small scale, the ability to tune reactivity with light intensity and wavelength, and the affinity of photochemistry for radical generation process, it is also easy to envision a future where photochemically driven XEC is among the first strategies researchers choose to try.

Finally, electrochemistry is a natural fit for XEC because the reduction and oxidation reactions are separated in space, especially when a divided cell is used. Like photochemistry, electrochemistry offers many ways to tune the reaction (voltage, electrode materials, cell design) and can be adapted to flow chemistry. While early work has relied on sacrificial anodes (still generating metal salt waste), even this approach has advantages in the ability to tune reduction potential and avoid handling metal powders (and using plates and rods instead). Further, the reductive XEC chemistry can, in theory, be combined with nearly any oxidative reaction.<sup>683</sup> XEC driven by simple oxidation processes perfected in fuel cells (H<sub>2</sub> oxidation to generate protons, water oxidation to generate O<sub>2</sub>) would produce benign side products.<sup>684</sup> Finally, electro-organic synthesis on large scale offers the opportunity to decarbonize large-scale chemical synthesis.

### 9.4. Stereocontrol

Enantioconvergent XEC has seen the most development and already offers an attractive alternative to the use of carbon

nucleophiles.<sup>685</sup> The palette of racemic electrophiles compatible with enantioconvergent XEC remains more limited than for enantioconvergent cross-coupling, and more work is needed. This is especially the case in ligand design, and a better understanding of the mechanisms of these reactions is needed.

Enantiospecific cross-electrophile coupling complements enantioconvergent couplings by converting easily accessible enantioenriched molecules into challenging ones.<sup>686</sup> This area is scarcely developed, perhaps because most XEC reactions of alkyl electrophiles proceed by alkyl radicals that are a better fit for enantioconvergent coupling. Promising results with allylic and benzylic alcohols should be further investigated, but additional mechanistic strategies are needed in this area.

Finally, derivatization of chiral pool materials by XEC has already proven exciting, even at this early stage. Peripheral derivatization of amino acids to make various unnatural amino acids and deoxygenative coupling of sugars are two examples.<sup>270,287</sup> Natural products are usually more oxidized than petrochemical feedstocks. Compared to deoxygenation approaches, deoxygenative C–C bond formation offers new ways to utilize these abundant feedstocks without throwing away their stereochemical information.

### 9.5. Mechanistic Understanding

While there are a variety of coupling types reported, the field has largely coalesced on a few mechanisms that share characteristics steps: (1) C(sp<sup>2</sup>) electrophiles are activated via a nonradical mechanism to form an (L)Ni<sup>II</sup> species, and the C(sp<sup>3</sup>) electrophiles are converted to an alkyl radical intermediate. (2) The alkyl species interacts with the (L)Ni<sup>II</sup> species to form a proposed (L)Ni<sup>III</sup> species that rapidly undergoes reductive elimination to furnish the desired cross-product. (3) The Ni catalyst is rapidly reduced by an external reductant to turn over the catalytic cycle. The mechanistic understanding is most developed in the area of C(sp<sup>2</sup>)–C(sp<sup>3</sup>) bond formation, but even here many key aspects are not well understood. These details will matter immensely to perfecting XEC chemistry and enabling the coupling of recalcitrant or complex electrophiles.

The understanding of C(sp<sup>3</sup>)–C(sp<sup>3</sup>) XEC mechanisms remains underdeveloped compared to C(sp<sup>2</sup>)–C(sp<sup>3</sup>) XEC, owing to challenges in isolating and studying alkylmetal intermediates, the wide differences in reactivity observed depending on substitution (e.g., 1°, 2°, 3°), and the influence of adjacent functional groups (e.g., allylic, benzylic,  $\alpha$ -carbonyl). Further, all but the most trivial of C(sp<sup>3</sup>)–C(sp<sup>3</sup>) bond-forming reactions must account for stereochemical control, which is also a challenge for XEC in general. It is our view that a host of strategies will be required to address these many different requirements, but that the field is poised for rapid growth.

### 9.6. No More Nucleophiles?

Cross-electrophile coupling is now a formidable force in the field of organic chemistry, experiencing near exponential growth over the past decade, and it will undoubtedly continue to expand in the future. For certain types of bond formations, XEC is already supplanting cross-coupling approaches.<sup>249</sup> With this review as a springboard, we expect that these limitations will be addressed by the global XEC community in due course, further advancing the field.

## 9.7. Ask Your Own Questions About the Field

While writing this review, we collected a variety of data from our references into a spreadsheet in order to organize such a large project. This ended up amounting to about 69 000 data points. While we did not have the resources to extract a high level of detail (such as substrates or all details of conditions), we have already found this data set to be of enormous value for answering questions about XEC chemistry. The plots throughout the review were all generated with relatively little further effort from this spreadsheet. We have included this data set as Supporting Information with the hope that other researchers find it useful and fun. We only ask that when you use this data in a paper that you reference this review as the source.

## ASSOCIATED CONTENT

### SI Supporting Information

The Supporting Information is available free of charge at <https://pubs.acs.org/doi/10.1021/acs.chemrev.4c00524>.

Chemical structures (PDF)

Data set (XLSX)

## AUTHOR INFORMATION

### Corresponding Author

Daniel J. Weix – Department of Chemistry, University of Wisconsin–Madison, Madison, Wisconsin 53706, United States;  [orcid.org/0000-0002-9552-3378](https://orcid.org/0000-0002-9552-3378); Email: [dweix@wisc.edu](mailto:dweix@wisc.edu)

### Authors

Lauren E. Ehehalt – Department of Chemistry, University of Wisconsin–Madison, Madison, Wisconsin 53706, United States;  [orcid.org/0000-0003-4267-214X](https://orcid.org/0000-0003-4267-214X)

Omar M. Beleh – Department of Chemistry, University of Wisconsin–Madison, Madison, Wisconsin 53706, United States;  [orcid.org/0000-0001-8927-5382](https://orcid.org/0000-0001-8927-5382)

Isabella C. Priest – Department of Chemistry, University of Wisconsin–Madison, Madison, Wisconsin 53706, United States;  [orcid.org/0000-0002-3265-6907](https://orcid.org/0000-0002-3265-6907)

Julianne M. Mouat – Department of Chemistry, University of Wisconsin–Madison, Madison, Wisconsin 53706, United States;  [orcid.org/0000-0002-3976-3676](https://orcid.org/0000-0002-3976-3676)

Alyssa K. Olszewski – Department of Chemistry, University of Wisconsin–Madison, Madison, Wisconsin 53706, United States;  [orcid.org/0000-0002-3707-5423](https://orcid.org/0000-0002-3707-5423)

Benjamin N. Ahern – Department of Chemistry, University of Wisconsin–Madison, Madison, Wisconsin 53706, United States

Alexandro R. Cruz – Department of Chemistry, University of Wisconsin–Madison, Madison, Wisconsin 53706, United States;  [orcid.org/0000-0003-2296-3329](https://orcid.org/0000-0003-2296-3329)

Benjamin K. Chi – Department of Chemistry, University of Wisconsin–Madison, Madison, Wisconsin 53706, United States;  [orcid.org/0000-0001-5672-9827](https://orcid.org/0000-0001-5672-9827)

Anthony J. Castro – Department of Chemistry, University of Wisconsin–Madison, Madison, Wisconsin 53706, United States

Kai Kang – Department of Chemistry, University of Wisconsin–Madison, Madison, Wisconsin 53706, United States

Jiang Wang – Department of Chemistry, University of Wisconsin–Madison, Madison, Wisconsin 53706, United States

Complete contact information is available at:  
<https://pubs.acs.org/10.1021/acs.chemrev.4c00524>

### Author Contributions

<sup>‡</sup>L.E.E. and O.M.B. contributed equally.

### Notes

The authors declare no competing financial interest.

### Biographies

Lauren E. Ehehalt is from Clinton Township, Michigan, and received her A.B. degree in chemistry from Princeton University in 2020, where she conducted undergraduate research with Professor Paul Chirik. During her undergraduate program, Lauren was also a visiting research fellow in the lab of Professor Stephen Thomas at the University of Edinburgh, in Edinburgh, Scotland, UK. Lauren is currently a Ph.D. candidate at University of Wisconsin–Madison in the lab of Professor Daniel Weix, and she is an NSF Graduate Research Fellow. Her research explores decarbonylative cross-electrophile coupling reactions to form C–C bonds.

Omar M. Beleh is from Ann Arbor, Michigan. He received his B.S. in biochemistry in 2015 from the University of Michigan, where he did research with Dr. Matthew B. Soellner. Omar also did a Drug Discovery internship at Lycera, a biopharmaceutical company that develops treatments for autoimmune diseases and cancer. He then completed his Ph.D. in organic chemistry in 2021 in the lab of Professor Scott J. Miller at Yale University working on atroposelective catalysis. Omar then joined the group of Professor Daniel J. Weix in 2022 as an NIH NRSA Postdoctoral Research Fellow where he has developed cross-electrophile coupling approaches to prepare enones and olefins from carboxylic acids.

Isabella C. Priest was born into a military family and mainly grew up in Spring Branch, Texas, and Ramstein, Germany. She received her B.S. in chemistry with a minor in mathematics from Texas A&M University in 2022, completing undergraduate research under the guidance of Prof. John Gladysz. Isabella then moved to the University of Wisconsin–Madison where she conducted graduate research within the group of Prof. Daniel J. Weix and obtained her M.S. in chemistry in 2024. Currently, she is the assistant laboratory manager for the STEM laboratories at the University of North Texas–Dallas.

Julianna M. Mouat is from Abilene, Texas. She received her B.S. degree in chemistry with a minor in art history from Southwestern University in 2021, where she conducted research with Prof. Michael Gesinski. Julianna is currently a Ph.D. candidate at the University of Wisconsin–Madison in the lab of Prof. Daniel J. Weix, where she is developing C(sp<sup>2</sup>)–C(sp<sup>3</sup>) and C(sp<sup>3</sup>)–C(sp<sup>3</sup>) nickel-catalyzed cross-electrophile coupling reactions.

Alyssa K. Olszewski is from Kankakee, Illinois. She received her B.A. in chemistry in 2021 from Northwestern University, where she conducted research with Prof. Omar Farha. Alyssa is currently a Ph.D. candidate at the University of Wisconsin–Madison in the lab of Prof. Daniel J. Weix, where she is an NSF Graduate Research Fellow. Her research focuses on ligand and catalyst design for new nickel-catalyzed cross-electrophile coupling reactions.

Benjamin N. Ahern is from Acton, Massachusetts. He received his B.S. degree in biochemistry and molecular biology from Dickinson College in 2020, where he conducted research with Prof. David Kushner and Dr. Jason Gavenonis. Before joining the Weix Lab, he

also conducted research with Prof. David Fairlie (University of Queensland) and at Goldfinch Bio, Angiex, Fogpharma, and Relay Therapeutics (Cambridge, MA). Ben is currently a graduate student at the University of Wisconsin–Madison in the lab of Prof. Daniel J. Weix, where he is conducting research on C(sp<sup>2</sup>)–C(sp<sup>3</sup>) nickel-catalyzed cross-electrophile coupling reactions.

Alexandro R. Cruz was raised in Wilmington, California. He received his B.A. in chemistry with a minor in history from Kalamazoo College in 2021, where he conducted research with Prof. Jeffrey Bartz. Alexandro is currently a Ph.D. candidate and at the University of Wisconsin–Madison in the lab of Prof. Daniel J. Weix, and a trainee in the university's Chemical–Biology Interface (CBI) Training Program. His research focuses on adapting cross-electrophile coupling methods for use in DNA-Encoded Libraries syntheses, and developing new cross-electrophile coupling reactions using homogeneous reductants.

Benjamin K. Chi was raised in Kingsville, Texas. He received his B.S. degree in chemistry with a minor in math in 2019 from Texas A&M University–Kingsville, where he conducted research with Prof. Jason N. Abrams. Ben is currently a Ph.D. candidate at the University of Wisconsin–Madison in the lab of Prof. Daniel J. Weix. His research is broadly on medicinally relevant cross-electrophile coupling reactions, including work on strained-rings, difluoromethylation, and diastereoselective methods.

Anthony J. Castro is from San Diego, California, and obtained his B.S. degree in chemistry from UC Irvine. He conducted research with Professor Elizabeth R. Jarvo to develop nickel-catalyzed cross-electrophile coupling reactions for the formation of cyclopropanes. He then obtained his M.S. degree in chemistry at California State University, Los Angeles, where he applied metal–organic frameworks for the degradation of nerve agent simulants under Professor Yangyang Liu. Currently, he is a graduate student at the University of Wisconsin, Madison, in Professor Daniel J. Weix's group developing cross-electrophile coupling reactions for C(sp<sup>2</sup>)–C(sp<sup>2</sup>) and C(sp<sup>2</sup>)–C(sp<sup>3</sup>) bond formation.

Kai Kang is from Rizhao, China, and earned his bachelor's degree in 2012 from China Pharmaceutical University and completed his Ph.D. in organic chemistry at the Shanghai Institute of Organic Chemistry in 2017. His doctoral research centered on organofluorine chemistry and the reductive elimination mechanisms of gold(III) complexes. In 2018, he joined the Weix research group as a postdoctoral researcher, where he explored cross-electrophile coupling methodologies to construct C(sp<sup>2</sup>)–C(sp<sup>2</sup>) and C(sp<sup>3</sup>)–C(sp<sup>3</sup>) bonds. Since 2022, he has been a medicinal chemist at Acerand Therapeutics (Shanghai), where his work focuses on the design and synthesis of small-molecule anticancer agents.

Jiang Wang was born in Lanzhou, China, and obtained his B.S. degree in chemistry from Lanzhou University in 2010 where he conducted undergraduate research with Prof. Yong-ming Liang. He moved to United States to continue his Ph.D. work with Prof. Nan Zheng at the University of Arkansas and developed photoredox catalyzed functionalization of cyclopropylamines and cyclobutylamines. Upon obtaining his Ph.D. in 2017, he joined Prof. Daniel J. Weix's lab in UW–Madison as a postdoc where he developed several cross-electrophile coupling methodologies for ketone synthesis, as well as decarbonylative C(sp<sup>2</sup>)–C(sp<sup>3</sup>) bond formation reactions. In 2021, he started as a process chemist at Eli Lilly & Co. in Indianapolis to support early and late phase development efforts.

Daniel J. Weix was raised in Oak Creek, WI and obtained his BA in Chemistry from Columbia University in 2000, where he conducted undergraduate research with Prof. Jung-Ja Kim (at the Medical

College of Wisconsin), Prof. Nicholas Turro (Columbia), and Prof. Thomas Katz (Columbia). Dan completed his PhD studies at UC Berkeley with Prof. Jonathan Ellman on the synthesis and chemistry of *tert*-butane sulfonamide. Following postdoctoral studies at Yale and UIUC with John Hartwig on Ir-catalyzed allylic substitution chemistry, Dan started his independent career at the University of Rochester in 2008. At both Rochester and the UW–Madison (2017–), the Weix group has focused on the development of new concepts and strategies for practical organic synthesis, including cross-electrophile coupling, multimetallic catalysis, radicals in organometallic reactions, and the use of semiconductor QDs in photoredox catalysis. This work has been recognized and supported by a mixture of academic and industrial awards and support.

## ACKNOWLEDGMENTS

This work was supported by the NIH (R01GM097243 to D.J.W., F32GM146357 to O.M.B., and T32GM152341 for A.R.C.), the NSF (DGE-2137424 to A.K.O. and L.E.E., CHE-2154698 to D.J.W.), and the University of Wisconsin–Madison. We thank Mareena Franke (Gilead) and Gray Cicmanec (UW–Madison) for helpful comments on drafts of this review.

## ABBREVIATIONS

1° = primary
2,6-lutidine = 2,6-dimethylpyridine
2° = secondary
3° = tertiary
ABNO = 9-azabicyclo[3.3.1]nonane N-oxyl
acac = acetylacetone
Anisyl = CH <sub>3</sub> OC <sub>6</sub> H <sub>4</sub>
B <sub>2</sub> Pin <sub>2</sub> = bis(pinacolato) diboron
Barton's Base = 2- <i>tert</i> -butyl-1,1,3,3-tetramethylguanidine, BTMG
BCP = bicyclo[1.1.1]pentane
Bn = benzyl (R–CH <sub>2</sub> –C <sub>6</sub> H <sub>5</sub> )
Boc = <i>tert</i> -butyloxycarbonyl (R–C(O)-OC(CH <sub>3</sub> ) <sub>3</sub> )
Bpin = boronic pinacol ester
Bz = benzoyl (R–C(O)–C <sub>6</sub> H <sub>5</sub> )
BzTFM = 3,5-bis(trifluoromethyl)benzoyl
CCE = constant current electrolysis
CEBO = 2-chloro-3-ethylbenzo[d]oxazol-3-iium
CEC = cross-electrophile coupling
Co(PC) = cobalt phthalocyanin
COD = 1,5-cyclooctadiene
collidine = 2,4,6-trimethylpyridine
COSTA = continuous processing utilizing an oscillatory flow with static mixing
Cp = cyclopentadienyl
CSTR = continuous stirred tank reactor
CV = cyclic voltammetry
DABCÖ = 1,4-diazabicyclo[2.2.2]octane, triethylenediamine
dba = dibenzylideneacetone
DCM = dichloromethane
DEL = DNA Encoded Library
DFT = density functional theory
diglyme = bis(2-methoxyethyl) ether
DIPEA = diisopropylethylamine
DMA = dimethylacetamide
DMAP = 4-dimethylaminopyridine
DMBA = dimethylbenzoic acid

DME = dimethoxyethane  
DMF = dimethylformamide  
DMI = 1,3-dimethyl-2-imidazolidinone  
DMO = dimethyl oxalate  
DMP = Dess–Martin periodinane  
DMPU = *N,N'*-dimethylpropyleneurea  
DMSO = dimethyl sulfoxide  
DPPBA = diphenylphosphinobenzoic acid  
dr = diastereomeric ratio  
EC = ethyl crotonate  
Echem = electrochemistry  
EDA = electron donor–acceptor  
ee = enantiomeric excess  
equiv = equivalent  
er = enantiomeric ratio  
F = Faraday  
Hantzsch ester = 1,4-dihydro-2,6-dimethyl-3,5-pyridinedi-carboxylic acid diethyl ester  
HAT = hydrogen atom transfer  
HATU = hexafluorophosphate azabenzotriazole tetramethyl uronium  
HMPA = hexamethylphosphoramide  
HTE = high-throughput experimentation  
IPAc = isopropyl acetate  
KetoABNO = 9-azabicyclo[3.3.1]nonan-3-one-9-oxyl  
LLS = longest linear sequence  
M = molar  
mA = milliampere  
MS = molecular sieves  
MVR = multivariate linear regression  
NBO = nonbonding orbital  
NEP = *N*-ethylpyrrolidinone  
NHAc = R-NH-C(O)-CH<sub>3</sub>  
NHC = *N*-heterocyclic carbene  
NHP = *N*-hydroxyphthalimide  
nm = nanometer  
NMP = *N*-methyl-2-pyrrolidone  
NTs = *p*-toluenesulfonamides  
OAc = R-O-C(O)-CH<sub>3</sub>  
OMs = mesylate (methanesulfonate) R-O-S(O)<sub>2</sub>-CH<sub>3</sub>  
OTf = triflate (trifluoromethanesulfonate), R-O-S(O)<sub>2</sub>-CF<sub>3</sub>  
OTs = tosylate (toluenesulfonate), R-O-S(O)<sub>2</sub>-C<sub>6</sub>H<sub>4</sub>-CH<sub>3</sub>  
PEG = polyethylene glycol  
PITU = *N*-hydroxyphthalimide tetramethyluronium hexa-fluorophosphate  
Piv = pivaloyl, R-C(O)-C(CH<sub>3</sub>)<sub>3</sub>  
POP = triphenylphosphonium anhydride trifluoromethane-sulfonate  
PROTACs = proteolysis targeting chimeras  
QD = quantum dot  
RCY = radiochemical yield  
rpm = rotations per minute  
rr = regioisomeric ratio  
rt = room temperature  
RVC = reticulated vitreous carbon  
SET = single electron transfer  
TBAB = tetrabutylammonium bromide (nBu<sub>4</sub>NBr)  
TBABF<sub>4</sub> = tetrabutylammonium tetrafluoroborate (nBu<sub>4</sub>NBF<sub>4</sub>)  
TBAC = tetrabutylammonium chloride (nBu<sub>4</sub>NCl)  
TBAI = tetrabutylammonium iodide (nBu<sub>4</sub>NI)  
TBAPF<sub>6</sub> = tetrabutylammonium hexafluorophosphate (nBu<sub>4</sub>NPF<sub>6</sub>)

TBDMS = *tert*-butyldimethylsilyl  
TBDPS = *tert*-butyldiphenylsilyl  
TBS = *tert*-butyldimethylsilyl  
TDAE = tetrakis(dimethylamino)ethylene  
TEA = triethylamine (Et<sub>3</sub>N)  
TEOA = triethanolamine (N(CH<sub>2</sub>CH<sub>2</sub>OH)<sub>3</sub>)  
TES = triethylsilyl  
TFA = trifluoroacetic acid  
TFE = 2,2,2-trifluoroethanol  
TFP = tris(2-furyl)phosphine  
THF = tetrahydrofuran  
TIPS = triisopropylsilyl  
TMEDA = tetramethylethylenediamine  
TMS = trimethylsilyl  
Togni's reagent = 1-trifluoromethyl-1,2-benziodoxol-3(1*H*)-one  
V = volt  
VB<sub>12</sub> = vitamin B-12  
W = watt  
XAT = halide atom transfer  
XEC = cross-electrophile coupling

## REFERENCES

- (1) Dugger, R. W.; Ragan, J. A.; Ripin, D. H. B. Survey of GMP Bulk Reactions Run in a Research Facility between 1985 and 2002. *Org. Process Res. Dev.* **2005**, *9*, 253–258.
- (2) Slagt, V. F.; de Vries, A. H. M.; de Vries, J. G.; Kellogg, R. M. Practical Aspects of Carbon–Carbon Cross-Coupling Reactions Using Heteroarenes. *Org. Process Res. Dev.* **2010**, *14*, 30–47.
- (3) Roughley, S. D.; Jordan, A. M. The Medicinal Chemist's Toolbox: An Analysis of Reactions Used in the Pursuit of Drug Candidates. *J. Med. Chem.* **2011**, *54*, 3451–3479.
- (4) Magano, J.; Dunetz, J. R. Large-Scale Applications of Transition Metal-Catalyzed Couplings for the Synthesis of Pharmaceuticals. *Chem. Rev.* **2011**, *111*, 2177–2250.
- (5) Busacca, C. A.; Fandrick, D. R.; Song, J. J.; Senanayake, C. H. The Growing Impact of Catalysis in the Pharmaceutical Industry. *Adv. Synth. Catal.* **2011**, *353*, 1825–1864.
- (6) Nadin, A.; Hattotuwagama, C.; Churcher, I. Lead-Oriented Synthesis: A New Opportunity for Synthetic Chemistry. *Angew. Chem., Int. Ed.* **2012**, *51*, 1114–1122.
- (7) Schneider, N.; Lowe, D. M.; Sayle, R. A.; Tarselli, M. A.; Landrum, G. A. Big Data from Pharmaceutical Patents: A Computational Analysis of Medicinal Chemists' Bread and Butter. *J. Med. Chem.* **2016**, *59*, 4385–4402.
- (8) Bostrom, J.; Brown, D. G.; Young, R. J.; Keseru, G. M. Expanding the medicinal chemistry synthetic toolbox. *Nat. Rev. Drug. Discovery* **2018**, *17*, 709–727.
- (9) Carey, J. S.; Laffan, D.; Thomson, C.; Williams, M. T. Analysis of the Reactions Used for the Preparation of Drug Candidate Molecules. *Org. Biomol. Chem.* **2006**, *4*, 2337–2347.
- (10) Laird, T. What Type of Reactions Do Process Chemists Use on Scale? *Org. Process Res. Dev.* **2006**, *10*, 851–852.
- (11) Cooper, T. W.; Campbell, I. B.; Macdonald, S. J. Factors Determining the Selection of Organic Reactions by Medicinal Chemists and the Use of These Reactions in Arrays (Small Focused Libraries). *Angew. Chem., Int. Ed.* **2010**, *49*, 8082–8091.
- (12) Brown, D. G.; Bostrom, J. Analysis of Past and Present Synthetic Methodologies on Medicinal Chemistry: Where Have All the New Reactions Gone? *J. Med. Chem.* **2016**, *59*, 4443–4458.
- (13) The Nobel Prize in Chemistry 2010 (accessed 2024-09-18).
- (14) Davies, H. M.; Morton, D. Recent Advances in C–H Functionalization. *J. Org. Chem.* **2016**, *81*, 343–350.
- (15) We elected to use XEC because it appeared to not be in active use in any area of chemistry. CEC is in use for Cation Exchange Capacity, Capillary Electrophoresis, and in electrochemistry for a reaction that has chemical/electrochemical/chemical steps. As

- "X" is often used for crossings, we thought XEC would ultimately be beneficial for the field in locating papers and delineating it from related cross-coupling reactions.
- (16) Krasovskiy, A.; Duplais, C.; Lipshutz, B. H. Zn-Mediated, Pd-Catalyzed Cross-Couplings in Water at Room Temperature Without Prior Formation of Organozinc Reagents. *J. Am. Chem. Soc.* **2009**, *131*, 15592–15593.
- (17) Zhang, W.; Lu, L.; Zhang, W.; Wang, Y.; Ware, S. D.; Mondragon, J.; Rein, J.; Strotman, N.; Lehnher, D.; See, K. A.; et al. Electrochemically driven cross-electrophile coupling of alkyl halides. *Nature* **2022**, *604*, 292–297.
- (18) Guan, W.; Lu, L.; Jiang, Q.; Gittens, A. F.; Wang, Y.; Novaes, L. F. T.; Klausen, R. S.; Lin, S. An Electrochemical Strategy to Synthesize Disilanes and Oligosilanes from Chlorosilanes. *Angew. Chem., Int. Ed.* **2023**, *62*, No. e202303592.
- (19) Lu, L.; Wang, Y.; Zhang, W.; Zhang, W.; See, K. A.; Lin, S. Three-Component Cross-Electrophile Coupling: Regioselective Electrochemical Dialkylation of Alkenes. *J. Am. Chem. Soc.* **2023**, *145*, 22298–22304.
- (20) Kang, K.; Huang, L.; Weix, D. J. Sulfonate Versus Sulfonate: Nickel and Palladium Multimetallic Cross-Electrophile Coupling of Aryl Triflates with Aryl Tosylates. *J. Am. Chem. Soc.* **2020**, *142*, 10634–10640.
- (21) Wurtz, A. Ueber Eine Neue Klasse Organischer Radicale. *Ann. Chem. Pharm.* **1855**, *96*, 364–375.
- (22) Tollen, B.; Fittig, R. Ueber die Synthese der Kohlenwasserstoffe der Benzolreihe. *Liebigs Ann. Chem.* **1864**, *131*, 303–323.
- (23) Lewis, H. F.; Hendricks, R.; Yohe, G. R. The Wurtz Reaction. Factors Involved in the Preparation of Octane. *J. Am. Chem. Soc.* **1928**, *50*, 1993–1998.
- (24) Semmelhack, M. F.; Helquist, P. M.; Jones, L. D. Synthesis with Zerovalent Nickel - Coupling of Aryl Halides with Bis(1,5-Cyclooctadiene)Nickel(0). *J. Am. Chem. Soc.* **1971**, *93*, 5908–5910.
- (25) Kende, A. S.; Liebeskind, L. S.; Braitsch, D. M. Generation of a Solvated Zerovalent Nickel Reagent. *Biaryl formation. Tetrahedron Lett.* **1975**, *16*, 3375–3378.
- (26) Zembayashi, M.; Tamao, K.; Yoshida, J.-i.; Kumada, M. Nickel-Phosphine Complex-Catalyzed Homo Coupling of Aryl Halides in the Presence of Zinc Powder. *Tetrahedron Lett.* **1977**, *18*, 4089–4091.
- (27) Inaba, S.; Matsumoto, H.; Rieke, R. D. Metallic Nickel as a Reagent for the Coupling of Aromatic and Benzylic Halides. *Tetrahedron Lett.* **1982**, *23*, 4215–4216.
- (28) Chaussard, J.; Folest, J. C.; Nédélec, J. Y.; Périchon, J.; Sible, S.; Troupel, M. Use of Sacrificial Anodes in Electrochemical Functionalization of Organic Halides. *Synthesis* **1990**, *1990*, 369–381.
- (29) Hassan, J.; Sévignon, M.; Gozzi, C.; Schulz, E.; Lemaire, M. Aryl-Aryl Bond Formation One Century After the Discovery of the Ullmann Reaction. *Chem. Rev.* **2002**, *102*, 1359–1470.
- (30) Jutand, A. Contribution of Electrochemistry to Organometallic Catalysis. *Chem. Rev.* **2008**, *108*, 2300–2347.
- (31) Clevenger, A. L.; Stolley, R. M.; Aderibigbe, J.; Louie, J. Trends in the Usage of Bidentate Phosphines as Ligands in Nickel Catalysis. *Chem. Rev.* **2020**, *120*, 6124–6196.
- (32) Hansen, E. C.; Pedro, D. J.; Wotal, A. C.; Gower, N. J.; Nelson, J. D.; Caron, S.; Weix, D. J. New Ligands for Nickel Catalysis from Diverse Pharmaceutical Heterocycle Libraries. *Nat. Chem.* **2016**, *8*, 1126–1130.
- (33) Hansen, E. C.; Li, C.; Yang, S.; Pedro, D.; Weix, D. J. Coupling of Challenging Heteroaryl Halides with Alkyl Halides via Nickel-Catalyzed Cross-Electrophile Coupling. *J. Org. Chem.* **2017**, *82*, 7085–7092.
- (34) Anka-Lufford, L. L.; Huihui, K. M.; Gower, N. J.; Ackerman, L. K.; Weix, D. J. Nickel-Catalyzed Cross-Electrophile Coupling with Organic Reductants in Non-Amide Solvents. *Chem. - Eur. J.* **2016**, *22*, 11564–11567.
- (35) Alder, C. M.; Hayler, J. D.; Henderson, R. K.; Redman, A. M.; Shukla, L.; Shuster, L. E.; Sneddon, H. F. Updating and Further Expanding GSK's Solvent Sustainability Guide. *Green. Chem.* **2016**, *18*, 3879–3890.
- (36) Delgado, P.; Glass, R. J.; Geraci, G.; Duvadie, R.; Majumdar, D.; Robinson, R. I.; Elmaarouf, I.; Mikus, M.; Tan, K. L. Use of Green Solvents in Metallaphotoredox Cross-Electrophile Coupling Reactions Utilizing a Lipophilic Modified Dual Ir/Ni Catalyst System. *J. Org. Chem.* **2021**, *86*, 17428–17436.
- (37) Liu, J.; Ye, Y.; Sessler, J. L.; Gong, H. Cross-Electrophile Couplings of Activated and Sterically Hindered Halides and Alcohol Derivatives. *Acc. Chem. Res.* **2020**, *53*, 1833–1845.
- (38) Prinsell, M. R.; Everson, D. A.; Weix, D. J. Nickel-Catalyzed, Sodium Iodide-Promoted Reductive Dimerization of Alkyl Halides, Alkyl Pseudohalides, and Allylic Acetates. *Chem. Commun.* **2010**, *46*, 5743–5745.
- (39) Zackasee, J. L. S.; Al Zubaydi, S.; Truesdell, B. L.; Sevov, C. S. Synergistic Catalyst-Mediator Pairings for Electroreductive Cross-Electrophile Coupling Reactions. *ACS Catal.* **2022**, *12*, 1161–1166.
- (40) Wickham, L. M.; Dhungana, R. K.; Giri, R. Ni-Catalyzed Regioselective Reductive 1,3-Dialkenylation of Alkenes. *ACS Omega* **2023**, *8*, 1060–1066.
- (41) Everson, D. A.; Jones, B. A.; Weix, D. J. Replacing Conventional Carbon Nucleophiles with Electrophiles: Nickel-Catalyzed Reductive Alkylation of Aryl Bromides and Chlorides. *J. Am. Chem. Soc.* **2012**, *134*, 6146–6159.
- (42) Turro, R. F.; Wahlman, J. L. H.; Tong, Z. J.; Chen, X.; Yang, M.; Chen, E. P.; Hong, X.; Hadt, R. G.; Houk, K. N.; Yang, Y. F.; et al. Mechanistic Investigation of Ni-Catalyzed Reductive Cross-Coupling of Alkenyl and Benzyl Electrophiles. *J. Am. Chem. Soc.* **2023**, *145*, 14705–14715.
- (43) Zhang, P.; Le, C. C.; MacMillan, D. W. Silyl Radical Activation of Alkyl Halides in Metallaphotoredox Catalysis: A Unique Pathway for Cross-Electrophile Coupling. *J. Am. Chem. Soc.* **2016**, *138*, 8084–8087.
- (44) Everson, D. A.; Shrestha, R.; Weix, D. J. Nickel-Catalyzed Reductive Cross-Coupling of Aryl Halides with Alkyl Halides. *J. Am. Chem. Soc.* **2010**, *132*, 920–921.
- (45) Wang, X.; Wang, S.; Xue, W.; Gong, H. Nickel-Catalyzed Reductive Coupling of Aryl Bromides with Tertiary Alkyl Halides. *J. Am. Chem. Soc.* **2015**, *137*, 11562–11565.
- (46) Beutner, G. L.; Simmons, E. M.; Ayers, S.; Bemis, C. Y.; Goldfogel, M. J.; Joe, C. L.; Marshall, J.; Wisniewski, S. R. A Process Chemistry Benchmark for  $sp^2$ – $sp^3$  Cross Couplings. *J. Org. Chem.* **2021**, *86*, 10380–10396.
- (47) Nimmagadda, K.; Korapati, S.; Dasgupta, D.; Malik, N. A.; Vinodini, A.; Gangu, A. S.; Kalidindi, S.; Maity, P.; Bondigela, S. S.; Venu, A.; et al. Development and Execution of an Ni(II)-Catalyzed Reductive Cross-Coupling of Substituted 2-Chloropyridine and Ethyl 3-Chloropropanoate. *Org. Process Res. Dev.* **2020**, *24*, 1141–1148.
- (48) Lovato, K.; Fier, P. S.; Maloney, K. M. The Application of Modern Reactions in Large-Scale Synthesis. *Nat. Rev. Chem.* **2021**, *5*, 546–563.
- (49) Perkins, R. J.; Hughes, A. J.; Weix, D. J.; Hansen, E. C. Metal-Reductant-Free Electrochemical Nickel-Catalyzed Couplings of Aryl and Alkyl Bromides in Acetonitrile. *Org. Process Res. Dev.* **2019**, *23*, 1746–1751.
- (50) Charboneau, D. J.; Barth, E. L.; Hazari, N.; Uehling, M. R.; Zultanski, S. L. A Widely Applicable Dual Catalytic System for Cross-Electrophile Coupling Enabled by Mechanistic Studies. *ACS Catal.* **2020**, *10*, 12642–12656.
- (51) Charboneau, D. J.; Huang, H.; Barth, E. L.; Germe, C. C.; Hazari, N.; Mercado, B. Q.; Uehling, M. R.; Zultanski, S. L. Tunable and Practical Homogeneous Organic Reductants for Cross-Electrophile Coupling. *J. Am. Chem. Soc.* **2021**, *143*, 21024–21036.
- (52) Xu, H. L.; Zhao, C. L.; Qian, Q.; Deng, W.; Gong, H. G. Nickel-Catalyzed Cross-Coupling of Unactivated Alkyl Halides Using Bis(pinacolato)diboron as Reductant. *Chem. Sci.* **2013**, *4*, 4022–4029.
- (53) Sun, D.; Gong, Y.; Wu, Y.; Chen, Y.; Gong, H. Bis(pinacolato)-diboron-Enabled Ni-Catalyzed Reductive Arylation/Vinylation of Alkyl Electrophiles. *Adv. Sci.* **2024**, *11*, No. 2404301.
- (54) Zhang, Y.; Du, P.; Ji, Y.; Wang, S.; Zhu, Y.; Liu, Z.; He, Y.; Peng, Q.; Feng, Z. Catalytic Cross-Electrophile Coupling of Aryl

- Chlorides with Unactivated Alkyl Chlorides: The synergy of Iron and Li. *Chem.* **2023**, *9*, 3623–3636.
- (55) Franke, M. C.; Weix, D. J. Recent Advances in Electrochemical, Ni-Catalyzed C–C Bond Formation. *Isr. J. Chem.* **2024**, *64*, No. e202300089.
- (56) Kammer, L. M.; Badir, S. O.; Hu, R. M.; Molander, G. A. Photoactive Electron Donor-Acceptor Complex Platform for Ni-Mediated C(sp<sup>3</sup>)–C(sp<sup>2</sup>) Bond Formation. *Chem. Sci.* **2021**, *12*, 5450–5457.
- (57) Cardinale, L.; Beutner, G. L.; Bemis, C. Y.; Weix, D. J.; Stahl, S. S. Non-Innocent Role of Sacrificial Anodes in Electrochemical Nickel-Catalyzed C(sp<sup>2</sup>)–C(sp<sup>3</sup>) Cross-Electrophile Coupling *ChemRxiv* 2024, 2024-78n0x.
- (58) Ackerman-Biegasiewicz, L. K. G.; Kariofillis, S. K.; Weix, D. J. Multimetallic-Catalyzed C–C Bond-Forming Reactions: From Serendipity to Strategy. *J. Am. Chem. Soc.* **2023**, *145*, 6596–6614.
- (59) Pérez-Temprano, M. H.; Casares, J. A.; Espinet, P. Bimetallic Catalysis using Transition and Group 11 Metals: An Emerging Tool for C–C Coupling and Other Reactions. *Chem. - Eur. J.* **2012**, *18*, 1864–1884.
- (60) Fanta, P. E. The Ullmann Synthesis of Biaryls. *Synthesis* **1974**, *1974*, 9–21.
- (61) Fanta, P. E. The Ullmann Synthesis of Biaryls. *Chem. Rev.* **1946**, *38*, 139–196.
- (62) Fanta, P. E. The Ullmann Synthesis of Biaryls, 1945–1963. *Chem. Rev.* **1964**, *64*, 613–632.
- (63) Semmelhack, M. F.; Helquist, P.; Jones, L. D.; Keller, L.; Mendelson, L.; Ryono, L. S.; Gorzynski Smith, J.; Stauffer, R. D. Reaction of Aryl and Vinyl Halides with Zerovalent Nickel-Preparative Aspects and the Synthesis of Alnusone. *J. Am. Chem. Soc.* **1981**, *103*, 6460–6471.
- (64) Kende, A. S.; Liebeskind, L. S.; Braitsch, D. M. In Situ Generation of a Solvated Zerovalent Nickel Reagent. *Biaryl Formation. Tetrahedron Lett.* **1975**, *16*, 3375–3378.
- (65) Jennings, P. W.; Pillsbury, D. G.; Hall, J. L.; Brice, V. T. Carbon-Carbon Bond Formation Via Organometallic Electrochemistry. *J. Org. Chem.* **1976**, *41*, 719–722.
- (66) Colon, I.; Kelsey, D. R. Coupling of Aryl Chlorides by Nickel and Reducing Metals. *J. Org. Chem.* **1986**, *51*, 2627–2637.
- (67) Shimizu, N.; Kitamura, T.; Watanabe, K.; Yamaguchi, T.; Shigyo, H.; Ohta, T. A Simple and Efficient Synthesis of 2-, 3-, or 4-(2-nitrophenyl)pyridine Derivatives via Palladium Catalyzed Ullmann Cross-Coupling Reaction. *Tetrahedron Lett.* **1993**, *34*, 3421–3424.
- (68) Nelson, T. D.; Crouch, R. D. Cu, Ni, and Pd Mediated Homocoupling Reactions in Biaryl Syntheses: The Ullmann Reaction. In *Organic Reactions*; Wiley, 2004; pp 265–555.
- (69) Goshchaev, M.; Otroshchenko, O. S.; Sadykov, A. S. The Ullmann Reaction. *Russ. Chem. Rev.* **1972**, *41*, 1046–1059.
- (70) Panda, S.; Coffin, A.; Nguyen, Q. N.; Tantillo, D. J.; Ready, J. M. Synthesis and Utility of Dihydropyridine Boronic Esters. *Angew. Chem., Int. Ed.* **2016**, *55*, 2205–2209.
- (71) Tian, X.; Kaur, J.; Yakubov, S.; Barham, J. P. α-Amino Radical Halogen Atom Transfer Agents for Metallaphotoredox-Catalyzed Cross-Electrophile Couplings of Distinct Organic Halides. *ChemSusChem* **2022**, *15*, No. e202200906.
- (72) Cao, Z.-C.; Luo, Q.-Y.; Shi, Z.-J. Practical Cross-Coupling between O-Based Electrophiles and Aryl Bromides via Ni Catalysis. *Org. Lett.* **2016**, *18*, 5978–5981.
- (73) Zhang, C.; Ma, N. N.; Yu, Z. L.; Shen, C. A. J.; Zhou, X. C.; Chu, X. Q.; Rao, W. D.; Shen, Z. L. Palladium-Catalyzed Direct Reductive Cross-Coupling of Aryltrimethylammonium Salts with Aryl Bromides. *Org. Chem. Front.* **2021**, *8*, 4865–4870.
- (74) Ma, N. N.; Ren, J. A.; Liu, X.; Chu, X. Q.; Rao, W.; Shen, Z. L. Nickel-Catalyzed Direct Cross-Coupling of Aryl Sulfonium Salt with Aryl Bromide. *Org. Lett.* **2022**, *24*, 1953–1957.
- (75) Li, W. X.; Yang, B. W.; Ying, X.; Zhang, Z. W.; Chu, X. Q.; Zhou, X.; Ma, M.; Shen, Z. L. Nickel-Catalyzed Direct Cross-Coupling of Diaryl Sulfoxide with Aryl Bromide. *J. Org. Chem.* **2022**, *87*, 11899–11908.
- (76) Miao, W.; Ni, C.; Xiao, P.; Jia, R.; Zhang, W.; Hu, J. Nickel-Catalyzed Reductive 2-Pyridination of Aryl Iodides with Difluoromethyl 2-Pyridyl Sulfone. *Org. Lett.* **2021**, *23*, 711–715.
- (77) Arriola, D. J.; Carnahan, E. M.; Hustad, P. D.; Kuhlman, R. L.; Wenzel, T. T. Catalytic Production of Olefin Block Copolymers via Chain Shutting Polymerization. *Science* **2006**, *312*, 714–719.
- (78) Tsou, T. T.; Kochi, J. K. Mechanism of Biaryl Synthesis with Nickel-Complexes. *J. Am. Chem. Soc.* **1979**, *101*, 7547–7560.
- (79) Bajo, S.; Laidlaw, G.; Kennedy, A. R.; Sproules, S.; Nelson, D. J. Oxidative Addition of Aryl Electrophiles to a Prototypical Nickel(0) Complex: Mechanism and Structure/Reactivity Relationships. *Organometallics* **2017**, *36*, 1662–1672.
- (80) Yamamoto, T.; Wakabayashi, S.; Osakada, K. Mechanism of C–C Coupling Reactions of Aromatic Halides, Promoted by Ni(cod)<sub>2</sub> in the Presence of 2,2'-Bipyridine and PPh<sub>3</sub>, to Give Biaryls. *J. Organomet. Chem.* **1992**, *428*, 223–237.
- (81) Luo, J.; Davenport, M. T.; Carter, A.; Ess, D. H.; Liu, T. L. Mechanistic Studies of Ni-Catalyzed Electrochemical Homo-Coupling Reactions of Aryl Halides. *Faraday Discuss.* **2023**, *247*, 136–146.
- (82) Amatore, C.; Jutand, A.; Mottier, L. Mechanism of Nickel-Catalysed Electron Transfer Activation of Aromatic Halides: Part 1. Biphenyl Electrosynthesis from Bromobenzene. *J. Electroanal. Chem.* **1991**, *306*, 125–140.
- (83) Gosmini, C.; Lasry, S.; Nedelec, J. Y.; Perichon, J. Electrochemical Cross-Coupling Between 2-Halopyridines and Aryl or Heteroaryl Halides Catalysed by Nickel-2,2'-Bipyridine Complexes. *Tetrahedron* **1998**, *54*, 1289–1298.
- (84) Gosmini, C.; Nédélec, J. Y.; Périchon, J. Electrochemical Cross-Coupling Between Functionalized Aryl Halides and 2-Chloropyrimidine or 2-Chloropyrazine Catalyzed by Nickel 2,2'-Bipyridine Complex. *Tetrahedron Lett.* **2000**, *41*, 201–203.
- (85) Gosmini, C.; Nédélec, J. Y.; Périchon, J. Electrosynthesis of Functionalized 2-Arylpyridines from Functionalized Aryl and Pyridine Halides Catalyzed by Nickel Bromide 2,2'-Bipyridine Complex. *Tetrahedron Lett.* **2000**, *41*, 5039–5042.
- (86) Sengmany, S.; Léonel, E.; Polissaint, F.; Nédélec, J. Y.; Pipelier, M.; Thobie-Gautier, C.; Dubreuil, D. Preparation of Functionalized Aryl- and Heteroarylpyridazines by Nickel-Catalyzed Electrochemical Cross-Coupling Reactions. *J. Org. Chem.* **2007**, *72*, 5631–5636.
- (87) Gosmini, C.; Bassene-Ernst, C.; Durandetti, M. Synthesis of Functionalized 2-Arylpyridines from 2-Halopyridines and Various Aryl Halides via a Nickel Catalysis. *Tetrahedron* **2009**, *65*, 6141–6146.
- (88) Sengmany, S.; Le Gall, E.; Léonel, E. An Electrochemical Synthesis of Functionalized Arylpyrimidines from 4-Amino-6-Chloropyrimidines and Aryl Halides. *Molecules* **2011**, *16*, 5550–5560.
- (89) Oliveira, J. L.; Silva, M. J.; Florencio, T.; Urgin, K.; Sengmany, S.; Léonel, E.; Nédélec, J. Y.; Navarro, M. Electrochemical Coupling of Mono and Dihalopyridines Catalyzed by Nickel Complex in Undivided Cell. *Tetrahedron* **2012**, *68*, 2383–2390.
- (90) Sengmany, S.; Vitu-Thiebaud, A.; Le Gall, E.; Condon, S.; Léonel, E.; Thobie-Gautier, C.; Pipelier, M.; Lebreton, J.; Dubreuil, D. An Electrochemical Nickel-Catalyzed Arylation of 3-Amino-6-Chloropyridazines. *J. Org. Chem.* **2013**, *78*, 370–379.
- (91) Sengmany, S.; Sitter, M.; Léonel, E.; Le Gall, E.; Loirand, G.; Martens, T.; Dubreuil, D.; Dilasser, F.; Rousselle, M.; Sauzeau, V.; et al. Synthesis and Biological Evaluation of 3-Amino-, 3-Alkoxy- and 3-Aryloxy-6-(Hetero)arylpyridazines as Potent Antitumor Agents. *Bioorg. Med. Chem. Lett.* **2019**, *29*, 755–760.
- (92) Lin, K.; Qian, Q.; Zang, Z.; Wang, S.; Chen, Y.; Gong, H. Nickel-Catalyzed Reductive Cross-Coupling of Aryl Halides. *Synlett* **2013**, *24*, 619–624.
- (93) Liao, L. Y.; Kong, X. R.; Duan, X. F. Reductive Couplings of 2-Halopyridines without External Ligand: Phosphine-Free Nickel-Catalyzed Synthesis of Symmetrical and Unsymmetrical 2,2'-Bipyridines. *J. Org. Chem.* **2014**, *79*, 777–782.
- (94) Sengmany, S.; Vasseur, S.; Lajnef, A.; Le Gall, E.; Léonel, E. Beneficial Effects of Electrochemistry in Cross-Coupling Reactions: Electroreductive Synthesis of 4-Aryl- or 4-Heteroaryl-6-Pyrrolypyrimidines. *Eur. J. Org. Chem.* **2016**, *2016*, 4865–4871.

- (95) Dewanj, A.; Bulow, R. F.; Rueping, M. Photoredox/Nickel Dual-Catalyzed Reductive Cross Coupling of Aryl Halides Using an Organic Reducing Agent. *Org. Lett.* **2020**, *22*, 1611–1617.
- (96) Zuo, Z.; Ahneman, D. T.; Chu, L.; Terrett, J. A.; Doyle, A. G.; MacMillan, D. W. Merging Photoredox with Nickel Catalysis: Coupling of  $\alpha$ -Carboxyl  $sp^3$ -Carbons with Aryl Halides. *Science* **2014**, *345*, 437–440.
- (97) Mirabi, B.; Marchese, A. D.; Lautens, M. Nickel-Catalyzed Reductive Cross-Coupling of Heteroaryl Chlorides and Aryl Chlorides. *ACS Catal.* **2021**, *11*, 12785–12793.
- (98) Nohira, I.; Chatani, N. Nickel-Catalyzed Cross-Electrophile Coupling between  $C(sp^2)$ -F and  $C(sp^2)$ -Cl Bonds by the Reaction of *ortho*-Fluoro-Aromatic Amides with Aryl Chlorides. *ACS Catal.* **2021**, *11*, 4644–4649.
- (99) Li, Z. M.; Shuai, B.; Ma, C.; Fang, P.; Mei, T. S. Nickel-Catalyzed Electroreductive Syntheses of Triphenylenes Using *ortho*-Dihalobenzene-Derived Benzyne. *Chin. J. Chem.* **2022**, *40*, 2335–2344.
- (100) Hassan, J.; Hathroubi, C.; Gozzi, C.; Lemaire, M. Synthesis of Unsymmetrical Biaryls via Palladium-Catalyzed Coupling Reaction of Aryl Halides. *Tetrahedron Lett.* **2000**, *41*, 8791–8794.
- (101) Hassan, J.; Hathroubi, C.; Gozzi, C.; Lemaire, M. Preparation of Unsymmetrical Biaryls via Palladium-Catalyzed Coupling Reaction of Aryl Halides. *Tetrahedron* **2001**, *57*, 7845–7855.
- (102) Wang, L.; Zhang, Y.; Liu, L.; Wang, Y. Palladium-Catalyzed Homocoupling and Cross-Coupling reactions of Aryl Halides in Poly(ethylene glycol). *J. Org. Chem.* **2006**, *71*, 1284–1287.
- (103) Qin, J.; Zhu, S.; Chu, L. Dual Photoredox/Palladium-Catalyzed Cross-Electrophile Couplings of Polyfluoroarenes with Aryl Halides and Triflates. *Organometallics* **2021**, *40*, 2246–2252.
- (104) Wu, T.; Zhang, Y.; Fu, Y.; Liu, F.; Tang, J.; Liu, P.; Toste, F.; Ye, B. Zirconium-Redox-Shuttled Cross-Electrophile Coupling of Aromatic and Heteroaromatic Halides. *Chem.* **2021**, *7*, 1963–1974.
- (105) Le Gall, E.; Gosmini, C.; Nédélec, J.-Y.; Périchon, J. Cobalt-Catalyzed Electrochemical Cross-Coupling of Functionalized Phenyl Halides with 4-Chloroquinoline Derivatives. *Tetrahedron Lett.* **2001**, *42*, 267–269.
- (106) Gomes, P.; Fillon, H.; Gosmini, C.; Labbé, E.; Périchon, J. Synthesis of Unsymmetrical Biaryls by Electroreductive Cobalt-Catalyzed Cross-Coupling of Aryl Halides. *Tetrahedron* **2002**, *58*, 8417–8424.
- (107) Amatore, M.; Gosmini, C. Efficient Cobalt-Catalyzed Formation of Unsymmetrical Biaryl Compounds and its Application in the Synthesis of a Sartan Intermediate. *Angew. Chem., Int. Ed.* **2008**, *47*, 2089–2092.
- (108) Schwartz, L. A.; Spielmann, K.; Swyka, R. A.; Xiang, M.; Krische, M. J. Formate-Mediated Cross-Electrophile Reductive Coupling of Aryl Iodides and Bromopyridines. *Isr. J. Chem.* **2021**, *61*, 298–301.
- (109) Ackerman, L. K. G.; Lovell, M. M.; Weix, D. J. Multimetallic Catalysed Cross-Coupling of Aryl Bromides with Aryl Triflates. *Nature* **2015**, *524*, 454–457.
- (110) Gong, C. Y.; Huo, C. D.; Wang, X. C.; Quan, Z. J. Nickel-Catalyzed Cross-Electrophile Coupling of Aryl Bromides with Pyrimidin-2-yl Tosylates. *Chin. J. Chem.* **2017**, *35*, 1366–1370.
- (111) Lv, L.; Qiu, Z.; Li, J.; Liu, M.; Li, C. J.  $N_2H_4$  as Traceless Mediator for Homo- and Cross-Aryl Coupling. *Nat. Commun.* **2018**, *9*, 4739.
- (112) Leifert, D.; Studer, A. The Persistent Radical Effect in Organic Synthesis. *Angew. Chem., Int. Ed.* **2020**, *59*, 74–108.
- (113) Huang, L.; Ackerman, L. K. G.; Kang, K.; Parsons, A. M.; Weix, D. J. LiCl-Accelerated Multimetallic Cross-Coupling of Aryl Chlorides with Aryl Triflates. *J. Am. Chem. Soc.* **2019**, *141*, 10978–10983.
- (114) Xiong, B.; Li, Y.; Wei, Y.; Kramer, S.; Lian, Z. Dual Nickel-/Palladium-Catalyzed Reductive Cross-Coupling Reactions between Two Phenol Derivatives. *Org. Lett.* **2020**, *22*, 6334–6338.
- (115) Kang, K.; Loud, N. L.; DiBenedetto, T. A.; Weix, D. J. A General, Multimetallic Cross-Ullmann Biheteroaryl Synthesis from Heteroaryl Halides and Heteroaryl Triflates. *J. Am. Chem. Soc.* **2021**, *143*, 21484–21491.
- (116) Su, Z.-M.; Twilton, J.; Hoyt, C. B.; Wang, F.; Stanley, L.; Mayes, H. B.; Kang, K.; Weix, D. J.; Beckham, G. T.; Stahl, S. S. Ni- and Ni/Pd-Catalyzed Reductive Coupling of Lignin-Derived Aromatics to Access Biobased Plasticizers. *ACS Cent. Sci.* **2023**, *9*, 159–165.
- (117) Zhang, G. F.; Luo, X. F.; Guan, C. F.; Cui, Y.; Ding, C. R. Pd/Ni Co-catalyzed Selective Cross-Coupling of Aryl Bromides and Aryl Fluorosulfonates at Room Temperature. *Eur. J. Org. Chem.* **2023**, *26*, No. e202300114.
- (118) Huang, X.; Tang, L.; Song, Z.; Jiang, S.; Liu, X.; Ma, M.; Chen, B.; Ma, Y. Nickel-Catalyzed Desulfonylative Reductive Cross-Coupling of Aryl Sulfones with Aryl Bromides. *Org. Lett.* **2023**, *25*, 1198–1203.
- (119) Manna, K.; Jana, R. Palladium-Catalyzed Cross-Electrophile Coupling between Aryl Diazonium Salt and Aryl Iodide/Diaryliodonium Salt in  $H_2O$ -EtOH. *Org. Lett.* **2023**, *25*, 341–346.
- (120) Dorval, C.; Tricoire, M.; Begouin, J.-M.; Gandon, V.; Gosmini, C. Cobalt-Catalyzed  $C(sp^2)$ -CN Bond Activation: Cross-Electrophile Coupling for Biaryl Formation and Mechanistic Insight. *ACS Catal.* **2020**, *10*, 12819–12827.
- (121) Song, Z.; Huang, X.; Jiang, S.; He, C.; Tang, L.; Ni, Q.; Ma, M.; Chen, B.; Ma, Y.  $C(sp^2)$ - $C(sp^2)$  Reductive Cross-Coupling of Triarylphosphines with Aryl Halides by Palladium/Nickel Co-catalysis. *Org. Lett.* **2022**, *24*, 5573–5578.
- (122) Peng, Y. F.; Isshiki, R.; Muto, K.; Yamaguchi, J. Decarbonylative Reductive Coupling of Aromatic Esters by Nickel and Palladium Catalyst. *Chem. Lett.* **2022**, *51*, 749–753.
- (123) Tang, J.; Liu, L. L.; Yang, S.; Cong, X.; Luo, M.; Zeng, X. Chemoselective Cross-Coupling between Two Different and Unactivated  $C(aryl)-O$  Bonds Enabled by Chromium Catalysis. *J. Am. Chem. Soc.* **2020**, *142*, 7715–7720.
- (124) Tang, J.; Fan, F.; Cong, X.; Luo, M.; Zeng, X. Reductive Cross-Coupling between Unactivated  $C(aryl)-N$  and  $C(aryl)-O$  Bonds by Chromium Catalysis Using a Bipyriddy Ligand. *J. Am. Chem. Soc.* **2020**, *142*, 12834–12840.
- (125) Fan, F.; Zhao, L. X.; Luo, M. M.; Zeng, X. M. Chromium-Catalyzed Selective Cross-Electrophile Coupling between Unactivated  $C(aryl)-F$  and  $C(aryl)-O$  Bonds. *Organometallics* **2022**, *41*, 561–568.
- (126) Cannes, C.; Condon, S.; Durandetti, M.; Périchon, J.; Nédélec, J. Y. Nickel-Catalyzed Electrochemical Couplings of Vinyl Halides: Synthetic and Stereochemical Aspects. *J. Org. Chem.* **2000**, *65*, 4575–4583.
- (127) Liu, J.; Ren, Q.; Zhang, X.; Gong, H. Preparation of Vinyl Arenes by Nickel-Catalyzed Reductive Coupling of Aryl Halides with Vinyl Bromides. *Angew. Chem., Int. Ed.* **2016**, *55*, 15544–15548.
- (128) Xiong, B. J.; Wang, T.; Sun, H. T.; Li, Y.; Kramer, S.; Cheng, G. J.; Lian, Z. Nickel-Catalyzed Cross-Electrophile Coupling Reactions for the Synthesis of *gem*-Difluorovinyl Arenes. *ACS Catal.* **2020**, *10*, 13616–13623.
- (129) Li, Y. Q.; Yin, G. Y. Bathocuproine-Enabled Nickel-Catalyzed Selective Ullmann Cross-Coupling of Two  $sp^2$ -Hybridized Organo-halides. *Synlett* **2021**, *32*, 1657–1661.
- (130) Ma, X. H.; Vo, Y.; Banwell, M. G.; Willis, A. C. Total Synthesis of Marinoquinoline A Using a Palladium(0)-Catalyzed Ullmann Cross-Coupling Reaction. *Asian J. Org. Chem.* **2012**, *1*, 160–165.
- (131) Khan, F.; Dlugosch, M.; Liu, X.; Khan, M.; Banwell, M. G.; Ward, J. S.; Carr, P. D. Palladium-Catalyzed Ullmann Cross-Coupling of  $\beta$ -Iodoenones and  $\beta$ -Iodoacrylates with *o*-Halonitroarenes or *o*-Iodobenzonitriles and Reductive Cyclization of the Resulting Products To Give Diverse Heterocyclic Systems. *Org. Lett.* **2018**, *20*, 2770–2773.
- (132) Tan, S.; Lan, P.; Banwell, M. G.; White, L. V. Practical, Multigram Preparation of Synthetically Useful, Enantiomerically Pure Building-Blocks from Quinic Acid. *Synopen* **2022**, *06*, 306–311.

- (133) Moncomble, A.; Le Floch, P.; Lledos, A.; Gosmini, C. Cobalt-Catalyzed Vinylation of Aromatic Halides Using  $\beta$ -Halostyrene: Experimental and DFT Studies. *J. Org. Chem.* **2012**, *77*, 5056–5062.
- (134) Bassler, D. P.; Alwali, A.; Spence, L.; Beale, O.; Beng, T. K. Cobalt-Catalyzed Arylation and Alkenylation of  $\alpha$ -Bromo Eneformamides and Enecarbamates by Cross-Coupling with Organic Bromides: Application to the Synthesis of Functionalized Piperidines and Azepanes. *J. Organomet. Chem.* **2015**, *780*, 6–12.
- (135) Xiong, B. J.; Li, Y.; Zhang, J. Y.; Liu, J. J.; Zhang, X. M.; Lian, Z. Cross-Electrophile Coupling between Aryl/Vinyl Triflates and Vinyl Tosylates for the Synthesis of *gem*-Difluoroalkenes via Ni/Pd Cooperative Catalysis. *Adv. Synth. Catal.* **2022**, *364*, 1009–1015.
- (136) Su, M.; Huang, X.; Lei, C.; Jin, J. Nickel-Catalyzed Reductive Cross-Coupling of Aryl Bromides with Vinyl Acetate in Dimethyl Isosorbide as a Sustainable Solvent. *Org. Lett.* **2022**, *24*, 354–358.
- (137) Gomes, P.; Gosmini, C.; Périchon, J. Cobalt-Catalyzed Electrochemical Vinylation of Aryl Halides using Vinylic Acetates. *Tetrahedron* **2003**, *59*, 2999–3002.
- (138) Amatore, M.; Gosmini, C.; Périchon, J. Cobalt-Catalyzed Vinylation of Functionalized aryl Halides with Vinyl Acetates. *Eur. J. Org. Chem.* **2005**, *2005*, 989–992.
- (139) Sha, Y.; Liu, J.; Wang, L.; Liang, D.; Wu, D.; Gong, H. Nickel-Catalyzed Reductive 1,3-Diene Formation from the Cross-Coupling of Vinyl Bromides. *Org. Biomol. Chem.* **2021**, *19*, 4887–4890.
- (140) Xu, G.-L.; Liu, C.-Y.; Pang, X.; Liu, X.-Y.; Shu, X.-Z. Nickel-Catalyzed Cross-Electrophile Vinyl–Vinyl Coupling: An Approach to Structurally Versatile Dienylboronates. *CCS Chemistry* **2022**, *4*, 864–871.
- (141) Li, X.; Li, Y.; Shan, W.; Wang, Z.; Liu, R.; Zhang, Z.; Li, X.; Shi, D. Nickel-Catalyzed Stereoselective Reductive Cross-Coupling of *gem*-Difluoroalkenes with Alkenyl Electrophiles. *Chem. Commun.* **2023**, *59*, 6893–6896.
- (142) Beng, T. K.; Sincavage, K.; Silaire, A. W.; Alwali, A.; Bassler, D. P.; Spence, L. E.; Beale, O. Direct Access to Functionalized Benzotropones, Azepanes, and Piperidines by Reductive Cross-Coupling of  $\alpha$ -Bromo Enones with  $\alpha$ -Bromo Enamides. *Org. Biomol. Chem.* **2015**, *13*, 5349–5353.
- (143) Olivares, A. M.; Weix, D. J. Multimetallic Ni- and Pd-Catalyzed Cross-Electrophile Coupling To Form Highly Substituted 1,3-Dienes. *J. Am. Chem. Soc.* **2018**, *140*, 2446–2449.
- (144) Marzouk, H.; Rollin, Y.; Folest, J. C.; Nédélec, J. Y.; Périchon, J. Electrochemical Synthesis of Ketones from Acid-Chlorides and Alkyl and Aryl Halides Catalyzed by Nickel-Complexes. *J. Organomet. Chem.* **1989**, *369*, C47–C50.
- (145) Pan, F. F.; Guo, P.; Li, C. L.; Su, P.; Shu, X. Z. Enones from Acid Fluorides and Vinyl Triflates by Reductive Nickel Catalysis. *Org. Lett.* **2019**, *21*, 3701–3705.
- (146) Wu, F. P.; Yuan, Y.; Liu, J.; Wu, X. F. Pd/Cu-Catalyzed Defluorinative Carbonylative Coupling of Aryl Iodides and *gem*-Difluoroalkenes: Efficient Synthesis of  $\alpha$ -Fluorochalcones. *Angew. Chem., Int. Ed.* **2021**, *60*, 8818–8822.
- (147) Chen, G.; Zhou, R. X.; Zhang, X. M.; Xiao, X.; Kramer, S.; Cheng, G. J.; Lian, Z. Carbonylative Cross-Electrophile Coupling between Aryl Bromides and Aryl Triflates Enabled by Palladium and Rhodium Cooperative Catalysis and CO as Reductant. *ACS Catal.* **2022**, *12*, 14582–14591.
- (148) Ni, S.; Zhang, W.; Mei, H.; Han, J.; Pan, Y. Ni-Catalyzed Reductive Cross-Coupling of Amides with Aryl Iodide Electrophiles via C–N Bond Activation. *Org. Lett.* **2017**, *19*, 2536–2539.
- (149) Lin, T.; Mi, J.; Song, L.; Gan, J.; Luo, P.; Mao, J.; Walsh, P. J. Nickel-Catalyzed Desymmetrizing Cross-Electrophile Coupling of Cyclic *meso*-Anhydrides. *Org. Lett.* **2018**, *20*, 1191–1194.
- (150) Zhu, Z.; Gong, Y.; Tong, W.; Xue, W.; Gong, H. Ni-Catalyzed Cross-Electrophile Coupling of Aryl Triflates with Thiocarbonates via C–O/C–O Bond Cleavage. *Org. Lett.* **2021**, *23*, 2158–2163.
- (151) Ruzi, R.; Liu, K.; Zhu, C.; Xie, J. Upgrading Ketone Synthesis Direct from Carboxylic Acids and Organohalides. *Nat. Commun.* **2020**, *11*, 3312.
- (152) Li, Y.; Shao, Q.; He, H.; Zhu, C.; Xue, X. S.; Xie, J. Highly Selective Synthesis of All-Carbon Tetrasubstituted Alkenes by Deoxygenative Alkenylation of Carboxylic Acids. *Nat. Commun.* **2022**, *13*, 10.
- (153) Isshiki, R.; Inayama, N.; Muto, K.; Yamaguchi, J. Ester Transfer Reaction of Aromatic Esters with Haloarenes and Arenols by a Nickel Catalyst. *ACS Catal.* **2020**, *10*, 3490–3494.
- (154) Chen, T. Y.; Wu, Y. K.; Han, P. L.; Gao, J. Q.; Wu, Y. Q.; Zhao, J. B.; Liang, H. T.; Liu, Y. S.; Liu, Y. Nickel-Catalyzed Ring Expansion of Cyclobutanones towards Indanones. *Helv. Chim. Acta* **2022**, *105*, No. e202100184.
- (155) Sakata, K.; Wang, Y.; Urabe, D.; Inoue, M. Synthesis of the Tetracyclic Structure of Batrachotoxin Enabled by Bridgehead Radical Coupling and Pd/Ni-Promoted Ullmann Reaction. *Org. Lett.* **2018**, *20*, 130–133.
- (156) Wright, A. C.; Stoltz, B. M. Enantioselective Construction of the Tricyclic Core of Curcusones A–D via a Cross-Electrophile Coupling Approach. *Chem. Sci.* **2019**, *10*, 10562–10565.
- (157) Liu, X.; Carr, P.; Gardiner, M. G.; Banwell, M. G.; Elbanna, A. H.; Khalil, Z. G.; Capon, R. J. Levoglucosanone and Its Pseudoenantiomer iso-Levoglucosanone as Scaffolds for Drug Discovery and Development. *ACS Omega* **2020**, *5*, 13926–13939.
- (158) Bolte, B.; Bryan, C. S.; Sharp, P. P.; Sayyahi, S.; Rihouey, C.; Kendrick, A.; Lan, P.; Banwell, M. G.; Jackson, C. J.; Fraser, N. J.; et al. Total Syntheses of the 3H-Pyrrolo[2,3-c]quinolone-Containing Alkaloids Marinoquinolines A–F, K, and Aplidiopsamine A Using a Palladium-Catalyzed Ullmann Cross-Coupling/Reductive Cyclization Pathway. *J. Org. Chem.* **2020**, *85*, 650–663.
- (159) Banwell, M. G.; White, L. V.; Ye, S. Y. Formal Total Syntheses of (+)- and (−)-Aspidophytine from a Common, Homochiral Precursor. *J. Org. Chem.* **2022**, *87*, 14407–14421.
- (160) Biswas, S.; Weix, D. J. Mechanism and Selectivity in Nickel-Catalyzed Cross-Electrophile Coupling of Aryl Halides with Alkyl Halides. *J. Am. Chem. Soc.* **2013**, *135*, 16192–16197.
- (161) Akana, M. E.; Tcyruikov, S.; Akana-Schneider, B. D.; Reyes, G. P.; Monfette, S.; Sigman, M. S.; Hansen, E. C.; Weix, D. J. Computational Methods Enable the Prediction of Improved Catalysts for Nickel-Catalyzed Cross-Electrophile Coupling. *J. Am. Chem. Soc.* **2024**, *146*, 3043–3051.
- (162) Cagan, D. A.; Bim, D.; McNicholas, B. J.; Kazmierczak, N. P.; Oyala, P. H.; Hadt, R. G. Photogenerated Ni(I)–Bipyridine Halide Complexes: Structure–Function Relationships for Competitive C-(sp<sup>2</sup>)–Cl Oxidative Addition and Dimerization Reactivity Pathways. *Inorg. Chem.* **2023**, *62*, 9538–9551.
- (163) Till, N. A.; Oh, S.; MacMillan, D. W. C.; Bird, M. J. The Application of Pulse Radiolysis to the Study of Ni(I) Intermediates in Ni-Catalyzed Cross-Coupling Reactions. *J. Am. Chem. Soc.* **2021**, *143*, 9332–9337.
- (164) Ting, S. I.; Williams, W. L.; Doyle, A. G. Oxidative Addition of Aryl Halides to a Ni(I)-Bipyridine Complex. *J. Am. Chem. Soc.* **2022**, *144*, 5575–5582.
- (165) Ren, Q. H.; Zhang, D. T.; Zheng, L. DFT Studies on the Mechanisms of Enantioselective Ni-Catalyzed Reductive Coupling Reactions to Form 1,1-Diarylalkanes. *J. Organomet. Chem.* **2021**, *952*, No. 122042.
- (166) Greaves, M. E.; Ronson, T. O.; Maseras, F.; Nelson, D. J. The Effect of Added Ligands on the Reactions of [Ni(COD)(dpff)] with Alkyl Halides: Halide Abstraction May Be Reversible. *Organometallics* **2021**, *40*, 1997–2007.
- (167) Diccianni, J. B.; Katigbak, J.; Hu, C.; Diao, T. Mechanistic Characterization of (Xantphos)Ni(I)-Mediated Alkyl Bromide Activation: Oxidative Addition, Electron Transfer, or Halogen-Atom Abstraction. *J. Am. Chem. Soc.* **2019**, *141*, 1788–1796.
- (168) Greaves, M. E.; Johnson Humphrey, E. L. B.; Nelson, D. J. Reactions of nickel(0) with organochlorides, organobromides, and organoiodides: mechanisms and structure/reactivity relationships. *Catal. Sci. Technol.* **2021**, *11*, 2980–2996.
- (169) Hartwig, J. F. *Organotransition Metal Chemistry: from Bonding to Catalysis*; University Science Books, 2010.

- (170) Ju, L.; Lin, Q.; LiBretto, N. J.; Wagner, C. L.; Hu, C. T.; Miller, J. T.; Diao, T. Reactivity of (bi-Oxazoline)organonickel Complexes and Revision of a Catalytic Mechanism. *J. Am. Chem. Soc.* **2021**, *143*, 14458–14463.
- (171) Bour, J. R.; Camasso, N. M.; Meucci, E. A.; Kampf, J. W.; Canty, A. J.; Sanford, M. S. Carbon-Carbon Bond-Forming Reductive Elimination from Isolated Nickel(III) Complexes. *J. Am. Chem. Soc.* **2016**, *138*, 16105–16111.
- (172) Lin, Q.; Spielvogel, E. H.; Diao, T. N. Carbon-centered radical capture at nickel(II) complexes: Spectroscopic evidence, rates, and selectivity. *Chem.* **2023**, *9*, 1295–1308.
- (173) Mohadjer Beromi, M.; Brudvig, G. W.; Hazari, N.; Lant, H. M. C.; Mercado, B. Q. Synthesis and Reactivity of Paramagnetic Nickel Polypyridyl Complexes Relevant to  $C(sp^2)-C(sp^3)$  Coupling Reactions. *Angew. Chem., Int. Ed.* **2019**, *58*, 6094–6098.
- (174) Ackerman, L. K. G.; Anka-Lufford, L. L.; Naodovic, M.; Weix, D. J. Cobalt Co-Catalysis for Cross-Electrophile Coupling: Diarylmethanes from Benzyl Mesylates and Aryl Halides. *Chem. Sci.* **2015**, *6*, 1115–1119.
- (175) Suga, T.; Ukaji, Y. Nickel-Catalyzed Cross-Electrophile Coupling between Benzyl Alcohols and Aryl Halides Assisted by Titanium Co-reductant. *Org. Lett.* **2018**, *20*, 7846–7850.
- (176) Lin, Q.; Fu, Y.; Liu, P.; Diao, T. Monovalent Nickel-Mediated Radical Formation: A Concerted Halogen-Atom Dissociation Pathway Determined by Electroanalytical Studies. *J. Am. Chem. Soc.* **2021**, *143*, 14196–14206.
- (177) Ren, Q. H.; Jiang, F.; Gong, H. G. DFT Study of the Single Electron Transfer Mechanisms in Ni-Catalyzed Reductive Cross-Coupling of Aryl Bromide and Alkyl Bromide. *J. Organomet. Chem.* **2014**, *770*, 130–135.
- (178) Ying, X.; Li, Y.; Li, L.; Li, C. Nickel-Catalyzed C—I-Selective  $C(sp^2)-C(sp^3)$  Cross-Electrophile Coupling of Bromo(iodo)arenes with Alkyl Bromides. *Angew. Chem., Int. Ed.* **2023**, *62*, No. e202304177.
- (179) Gutierrez, O.; Tellis, J. C.; Primer, D. N.; Molander, G. A.; Kozlowski, M. C. Nickel-Catalyzed Cross-Coupling of Photoredox-Generated Radicals: Uncovering a General Manifold for Stereoconvergence in Nickel-Catalyzed Cross-Couplings. *J. Am. Chem. Soc.* **2015**, *137*, 4896–4899.
- (180) Diccianni, J. B.; Diao, T. N. Mechanisms of Nickel-Catalyzed Cross-Coupling Reactions. *Trends Chem.* **2019**, *1*, 830–844.
- (181) Dawson, G. A.; Spielvogel, E. H.; Diao, T. Nickel-Catalyzed Radical Mechanisms: Informing Cross-Coupling for Synthesizing Non-Canonical Biomolecules. *Acc. Chem. Res.* **2023**, *56*, 3640–3653.
- (182) Yamamoto, T.; Kohara, T.; Yamamoto, A. Preparation and Properties of Monoalkynickel(II) Complexes Having a Phenoxy, Benzenethiolato, Oximato,  $\beta$ -Diketonato, or Halo Ligand. *Bull. Chem. Soc. Jpn.* **1981**, *54*, 2010–2016.
- (183) Yamamoto, T.; Kohara, T.; Osakada, K.; Yamamoto, A. Reactions of Dialkynickel(II) Complexes  $NiR_2L_2$  with Alkyl (or Aryl) Halides, R'COY (Y = Cl, Br, OPh, OCOPh), and CS<sub>2</sub>. *Bull. Chem. Soc. Jpn.* **1983**, *56*, 2147–2153.
- (184) Hegedus, L. S.; Miller, L. L. Reaction of  $\pi$ -allylnickel Bromide Complexes with Organic Halides. Stereochemistry and Mechanism. *J. Am. Chem. Soc.* **1975**, *97*, 459–460.
- (185) Hegedus, L. S.; Thompson, D. H. P. The Reactions of Organic Halides with ( $\pi$ -allyl)nickel Halide Complexes: A Mechanistic Study. *J. Am. Chem. Soc.* **1985**, *107*, 5663–5669.
- (186) Wang, K.; Ding, Z.; Zhou, Z.; Kong, W. Ni-Catalyzed Enantioselective Reductive Diarylation of Activated Alkenes by Domino Cyclization/Cross-Coupling. *J. Am. Chem. Soc.* **2018**, *140*, 12364–12368.
- (187) Xu, S.; Ping, Y. Y.; Li, W.; Guo, H. Y.; Su, Y. Y.; Li, Z. Y.; Wang, M. Y.; Kong, W. Q. Enantioselective  $C(sp^3)-H$  Functionalization of Oxacycles via Photo-HAT/Nickel Dual Catalysis. *J. Am. Chem. Soc.* **2023**, *145*, 5231–5241.
- (188) Griller, D.; Ingold, K. U. Persistent Carbon-Centered Radicals. *Acc. Chem. Res.* **1976**, *9*, 13–19.
- (189) Ben-Tal, Y.; Lloyd-Jones, G. C. Kinetics of a Ni/Ir-Photocatalyzed Coupling of ArBr with RBr: Intermediacy of ArNi(II)(L)Br and Rate/Selectivity Factors. *J. Am. Chem. Soc.* **2022**, *144*, 15372–15382.
- (190) Zhang, X.; MacMillan, D. W. C. Alcohols as Latent Coupling Fragments for Metallaphotoredox Catalysis: sp<sup>3</sup>–sp<sup>2</sup> Cross-Coupling of Oxalates with Aryl Halides. *J. Am. Chem. Soc.* **2016**, *138*, 13862–13865.
- (191) Jacobi von Wangelin, A.; Czaplik, W.; Mayer, M. Direct Cobalt-Catalyzed Cross-Coupling Between Aryl and Alkyl Halides. *Synlett* **2009**, *2009*, 2931–2934.
- (192) Duplais, C.; Krasovskiy, A.; Wattberg, A.; Lipshutz, B. H. Cross-Couplings Between Benzylic and Aryl Halides "On Water": Synthesis of Diarylmethanes. *Chem. Commun.* **2010**, *46*, 562–564.
- (193) Krasovskiy, A.; Duplais, C.; Lipshutz, B. H. Stereoselective Negishi-Like Couplings Between Alkenyl and Alkyl Halides in Water at Room Temperature. *Org. Lett.* **2010**, *12*, 4742–4744.
- (194) Duplais, C.; Krasovskiy, A.; Lipshutz, B. H. Organozinc Chemistry Enabled by Micellar Catalysis. Palladium-Catalyzed Cross-Couplings between Alkyl and Aryl Bromides in Water at Room Temperature. *Organometallics* **2011**, *30*, 6090–6097.
- (195) Krasovskaya, V.; Krasovskiy, A.; Bhattacharjya, A.; Lipshutz, B. H. "On Water" sp<sup>3</sup>-sp<sup>2</sup> Cross-Couplings Between Benzylic and Alkenyl Halides. *Chem. Commun.* **2011**, *47*, 5717–5719.
- (196) Krasovskaya, V.; Krasovskiy, A.; Lipshutz, B. H. Synthesis of Unsymmetrical Arylheteroarylmethanes by Direct "On Water" Cross-Coupling Between Benzylic and Heteroaromatic Halides. *Chem. - Asian J.* **2011**, *6*, 1974–1976.
- (197) Krasovskiy, A.; Thomé, I.; Graff, J.; Krasovskaya, V.; Konopelski, P.; Duplais, C.; Lipshutz, B. H. Cross-Couplings of Alkyl Halides with Heteroaromatic Halides, in Water at Room Temperature. *Tetrahedron Lett.* **2011**, *52*, 2203–2205.
- (198) Lipshutz, B. H.; Ghorai, S.; Abela, A. R.; Moser, R.; Nishikata, T.; Duplais, C.; Krasovskiy, A.; Gaston, R. D.; Gadwood, R. C. TPGS-750-M: A Second-Generation Amphiphile for Metal-Catalyzed Cross-Couplings in Water at Room Temperature. *J. Org. Chem.* **2011**, *76*, 4379–4391.
- (199) Klumphu, P.; Lipshutz, B. H. Nok": A Phytosterol-Based Amphiphile Enabling Transition-Metal-Catalyzed Couplings in Water at Room Temperature. *J. Org. Chem.* **2014**, *79*, 888–900.
- (200) Bhattacharjya, A.; Klumphu, P.; Lipshutz, B. H. Kumada-Grignard-Type Biaryl Couplings on Water. *Nat. Commun.* **2015**, *6*, 7401.
- (201) Bhone, V. R.; O'Neill, B. T.; Buchwald, S. L. An Improved System for the Aqueous Lipshutz-Negishi Cross-Coupling of Alkyl Halides with Aryl Electrophiles. *Angew. Chem., Int. Ed.* **2016**, *55*, 1849–1853.
- (202) Czaplik, W. M.; Mayer, M.; Jacobi von Wangelin, A. Domino Iron Catalysis: Direct Aryl-Alkyl Cross-Coupling. *Angew. Chem., Int. Ed.* **2009**, *48*, 607–610.
- (203) Amatore, M.; Gosmini, C. Direct Method for Carbon-Carbon Bond Formation: The Functional Group Tolerant Cobalt-Catalyzed Alkylation of Aryl Halides. *Chem. - Eur. J.* **2010**, *16*, 5848–5852.
- (204) Wang, S.; Qian, Q.; Gong, H. Nickel-Catalyzed Reductive Coupling of Aryl Halides with Secondary Alkyl Bromides and Allylic Acetate. *Org. Lett.* **2012**, *14*, 3352–3355.
- (205) Yan, C.-S.; Peng, Y.; Xu, X.-B.; Wang, Y.-W. Nickel-Mediated Inter- and Intramolecular Reductive Cross-Coupling of Unactivated Alkyl Bromides and Aryl Iodides at Room Temperature. *Chem. - Eur. J.* **2012**, *18*, 6039–6048.
- (206) Everson, D. A.; George, D. T.; Weix, D. J. Nickel-Catalyzed Cross-Coupling of Aryl Halides with Alkyl Halides: Ethyl 4-(4-(4-methylphenylsulfonamido)-phenyl)butanoate. *Org. Synth.* **2013**, *90*, 200–214.
- (207) Liu, X. G.; Yang, Z. L.; Li, Y. M.; Yang, F.; Feng, L.; Wang, N. Z.; Ma, D. B.; Chang, K. J.; Shen, Y. H. A Practical Nickel-Catalyzed Reductive Alkylation of Amidophenyl Bromides. *Tetrahedron* **2014**, *70*, 9522–9529.

- (208) Molander, G. A.; Traister, K. M.; O'Neill, B. T. Reductive Cross-Coupling of Nonaromatic, Heterocyclic Bromides with Aryl and Heteroaryl Bromides. *J. Org. Chem.* **2014**, *79*, 5771–5780.
- (209) Liu, H. Y.; Liang, Z. Y.; Qian, Q.; Lin, K. H. Nickel-Catalyzed Reductive Alkylation of Halogenated Pyridines with Secondary Alkyl Bromides. *Synth. Commun.* **2014**, *44*, 2999–3007.
- (210) Everson, D. A.; Buonomo, J. A.; Weix, D. J. Nickel-Catalyzed Cross-Electrophile Coupling of 2-Chloropyridines with Alkyl Bromides. *Synlett* **2014**, *25*, 233–238.
- (211) Liu, H.; Wei, J.; Qiao, Z.; Fu, Y.; Jiang, X. Palladium-catalyzed intramolecular reductive cross-coupling of  $Csp^2$ – $Csp^3$  bond formation. *Chem. - Eur. J.* **2014**, *20*, 8308–8313.
- (212) Breitenfeld, J.; Vechorkin, O.; Corminboeuf, C.; Scopelliti, R.; Hu, X. Why Are  $(NN_2)$ Ni Pincer Complexes Active for Alkyl–Alkyl Coupling:  $\beta$ -H Elimination Is Kinetically Accessible but Thermodynamically Uphill. *Organometallics* **2010**, *29*, 3686–3689.
- (213) Li, X.; Feng, Z.; Jiang, Z. X.; Zhang, X. Nickel-Catalyzed Reductive Cross-Coupling of (Hetero)Aryl Iodides with Fluorinated Secondary Alkyl Bromides. *Org. Lett.* **2015**, *17*, 5570–5573.
- (214) Durandetti, M.; Périchon, J. Iron-Catalyzed Reformatsky-Type Reactions. *Synthesis* **2006**, *2006*, 1542–1548.
- (215) Chen, F.; Chen, K.; Zhang, Y.; He, Y.; Wang, Y. M.; Zhu, S. Remote Migratory Cross-Electrophile Coupling and Olefin Hydroarylation Reactions Enabled by in Situ Generation of Ni–H. *J. Am. Chem. Soc.* **2017**, *139*, 13929–13935.
- (216) He, Y.; Cai, Y.; Zhu, S. Mild and Regioselective Benzylic C–H Functionalization: Ni-Catalyzed Reductive Arylation of Remote and Proximal Olefins. *J. Am. Chem. Soc.* **2017**, *139*, 1061–1064.
- (217) Peng, L.; Li, Y. Q.; Li, Y. Y.; Wang, W.; Pang, H. L.; Yin, G. Y. Ligand-Controlled Nickel-Catalyzed Reductive Relay Cross-Coupling of Alkyl Bromides and Aryl Bromides. *ACS Catal.* **2018**, *8*, 310–313.
- (218) Sun, S. Z.; Martin, R. Nickel-Catalyzed Umpolung Arylation of Ambiphilic  $\alpha$ -Bromoalkyl Boronic Esters. *Angew. Chem., Int. Ed.* **2018**, *57*, 3622–3625.
- (219) Wang, X.; Ma, G.; Peng, Y.; Pitsch, C. E.; Moll, B. J.; Ly, T. D.; Wang, X.; Gong, H. Ni-Catalyzed Reductive Coupling of Electron-Rich Aryl Iodides with Tertiary Alkyl Halides. *J. Am. Chem. Soc.* **2018**, *140*, 14490–14497.
- (220) Liu, J.; Gong, H. Stereoselective Preparation of  $\alpha$ -C-Vinyl/Aryl Glycosides via Nickel-Catalyzed Reductive Coupling of Glycosyl Halides with Vinyl and Aryl Halides. *Org. Lett.* **2018**, *20*, 7991–7995.
- (221) Liu, J.; Lei, C.; Gong, H. Nickel-Catalyzed Reductive Coupling of Glucosyl Halides with Aryl/Vinyl Halides Enabling  $\beta$ -Selective Preparation of C-Aryl/Vinyl Glucosides. *Sci. China Chem.* **2019**, *62*, 1492–1496.
- (222) Mennie, K. M.; Vara, B. A.; Levi, S. M. Reductive  $sp^3$ – $sp^2$  Coupling Reactions Enable Late-Stage Modification of Pharmaceuticals. *Org. Lett.* **2020**, *22*, 556–559.
- (223) Biswas, S.; Qu, B.; Desrosiers, J. N.; Choi, Y.; Haddad, N.; Yee, N. K.; Song, J. J.; Senanayake, C. H. Nickel-Catalyzed Cross-Electrophile Reductive Couplings of Neopentyl Bromides with Aryl Bromides. *J. Org. Chem.* **2020**, *85*, 8214–8220.
- (224) Hofstra, J. L.; Cherney, A. H.; Ordner, C. M.; Reisman, S. E. Synthesis of Enantioenriched Allylic Silanes via Nickel-Catalyzed Reductive Cross-Coupling. *J. Am. Chem. Soc.* **2018**, *140*, 139–142.
- (225) Sun, Y. R.; Liu, J. D.; Lin, Q.; Yao, K.; Tong, W. Q.; Qian, Q. Facile Preparation of Aryl C-Glycosides by Nickel-Catalyzed Reductive Coupling of Glycosyl Halides with Aryl Halides. *Chin. J. Org. Chem.* **2021**, *41*, 1551–1562.
- (226) Aguirre, A. L.; Loud, N. L.; Johnson, K. A.; Weix, D. J.; Wang, Y. ChemBead Enabled High-Throughput Cross-Electrophile Coupling Reveals a New Complementary Ligand. *Chem. - Eur. J.* **2021**, *27*, 12981–12986.
- (227) Tu, N. P.; Dombrowski, A. W.; Goshu, G. M.; Vasudevan, A.; Djuric, S. W.; Wang, Y. High-Throughput Reaction Screening with Nanomoles of Solid Reagents Coated on Glass Beads. *Angew. Chem., Int. Ed.* **2019**, *58*, 7987–7991.
- (228) Impastato, A. C.; Brown, J. T. C.; Wang, Y.; Tu, N. P. Readily Accessible High-Throughput Experimentation: A General Protocol for the Preparation of ChemBeads and EnzyBeads. *ACS Med. Chem. Lett.* **2023**, *14*, 514–520.
- (229) Gao, N. X.; Li, Y. S.; Cao, G. R.; Teng, D. W. Nickel-Catalyzed Cross-Electrophile Coupling of Aryl Bromides and Cyclic Secondary Alkyl Bromides with Spiro-Bidentate-PyOx Ligands. *New J. Chem.* **2021**, *45*, 16477–16481.
- (230) Kim, Y.; Iwai, T.; Fujii, S.; Ueno, K.; Sawamura, M. Dumbbell-Shaped 2,2'-Bipyridines: Controlled Metal Monochelation and Application to Ni-Catalyzed Cross-Couplings. *Chem. - Eur. J.* **2021**, *27*, 2289–2293.
- (231) Tang, S.; Xu, Z. H.; Liu, T.; Wang, S. W.; Yu, J.; Liu, J.; Hong, Y.; Chen, S. L.; He, J.; Li, J. H. Radical 1,4-Aryl Migration Enabled Remote Cross-Electrophile Coupling of  $\alpha$ -Amino- $\beta$ -Bromo Acid Esters with Aryl Bromides. *Angew. Chem., Int. Ed.* **2021**, *60*, 21360–21367.
- (232) Jones, A. C.; Nicholson, W. I.; Leitch, J. A.; Browne, D. L. A Ball-Milling-Enabled Cross-Electrophile Coupling. *Org. Lett.* **2021**, *23*, 6337–6341.
- (233) Wu, S. S.; Shi, W. J.; Zou, G. Mechanical Metal Activation for Ni-Catalyzed, Mn-Mediated Cross-Electrophile Coupling Between Aryl and Alkyl Bromides. *New J. Chem.* **2021**, *45*, 11269–11274.
- (234) Rago, A. J.; Vasilopoulos, A.; Dombrowski, A. W.; Wang, Y. Di(2-picoly)amines as Modular and Robust Ligands for Nickel-Catalyzed  $C(sp^2)$ – $C(sp^3)$  Cross-Electrophile Coupling. *Org. Lett.* **2022**, *24*, 8487–8492.
- (235) Gao, N.; Li, Y.; Teng, D. Nickel-Catalysed Cross-Electrophile Coupling of Aryl Bromides and Primary Alkyl Bromides. *RSC Adv.* **2022**, *12*, 3569–3572.
- (236) Xi, L. L.; Du, L. T.; Shi, Z. Z. Nickel-catalyzed reductive cross-coupling of polyfluoroarenes with alkyl electrophiles by site-selective C–F bond activation. *Chin. Chem. Lett.* **2022**, *33*, 4287–4292.
- (237) Lin, Q.; Gong, H.; Wu, F. Ni-Catalyzed Reductive Coupling of Heteroaryl Bromides with Tertiary Alkyl Halides. *Org. Lett.* **2022**, *24*, 8996–9000.
- (238) Han, D.; Sun, J.; Jin, J. Picolinamide Ligands: Nickel-Catalyzed Reductive Cross-Coupling of Aryl Bromides with Bromocyclopropane and Beyond. *Chem. - Asian J.* **2023**, *18*, No. e202201132.
- (239) Folest, J. C.; Périchon, J.; Fauvarque, J. F.; Jutand, A. Synthèse électrochimique d'esters arylacétiques et arylpropioniques via des complexes du nickel. *J. Organomet. Chem.* **1988**, *342*, 259–261.
- (240) Perkins, R. J.; Pedro, D. J.; Hansen, E. C. Electrochemical Nickel Catalysis for  $sp^2$ – $sp^3$  Cross-Electrophile Coupling Reactions of Unactivated Alkyl Halides. *Org. Lett.* **2017**, *19*, 3755–3758.
- (241) Franke, M. C.; Longley, V. R.; Rafiee, M.; Stahl, S. S.; Hansen, E. C.; Weix, D. J. Zinc-Free, Scalable Reductive Cross-Electrophile Coupling Driven by Electrochemistry in an Undivided Cell. *ACS Catal.* **2022**, *12*, 12617–12626.
- (242) Jiao, K.-J.; Liu, D.; Ma, H. X.; Qiu, H.; Fang, P.; Mei, T.-S. Nickel-Catalyzed Electrochemical Reductive Relay Cross-Coupling of Alkyl Halides to Aryl Halides. *Angew. Chem., Int. Ed.* **2020**, *59*, 6520–6524.
- (243) Truesdell, B. L.; Hamby, T. B.; Sevov, C. S. General  $C(sp^2)$ – $C(sp^3)$  Cross-Electrophile Coupling Reactions Enabled by Overcharge Protection of Homogeneous Electrocatalysts. *J. Am. Chem. Soc.* **2020**, *142*, 5884–5893.
- (244) Hamby, T. B.; LaLama, M. J.; Sevov, C. S. Controlling Ni Redox States by Dynamic Ligand Exchange for Electroreductive  $Csp^3$ – $Csp^2$  Coupling. *Science* **2022**, *376*, 410–416.
- (245) Montero Bastidas, J. R.; L'Heureux, S.; Liu, W.; Lee, K.; El Marrouni, A. High-Throughput Photo- and Electrochemical  $sp^2$ – $sp^3$  Cross-Electrophile Coupling to Access Novel Tedizolid Analogs. *ACS Med. Chem. Lett.* **2023**, *14*, 666–671.
- (246) Duan, Z.; Li, W.; Lei, A. Nickel-Catalyzed Reductive Cross-Coupling of Aryl Bromides with Alkyl Bromides:  $Et_3N$  as the Terminal Reductant. *Org. Lett.* **2016**, *18*, 4012–4015.
- (247) Paul, A.; Smith, M. D.; Vannucci, A. K. Photoredox-Assisted Reductive Cross-Coupling: Mechanistic Insight into Catalytic Aryl-Alkyl Cross-Couplings. *J. Org. Chem.* **2017**, *82*, 1996–2003.

- (248) Pomberger, A.; Mo, Y. M.; Nandiwale, K. Y.; Schultz, V. L.; Duvadie, R.; Robinson, R. I.; Altinoglu, E. I.; Jensen, K. F. A Continuous Stirred-Tank Reactor (CSTR) Cascade for Handling Solid-Containing Photochemical Reactions. *Org. Process Res. Dev.* **2019**, *23*, 2699–2706.
- (249) Dombrowski, A. W.; Gesmundo, N. J.; Aguirre, A. L.; Sarris, K. A.; Young, J. M.; Bogdan, A. R.; Martin, M. C.; Gedeon, S.; Wang, Y. Expanding the Medicinal Chemist Toolbox: Comparing Seven  $C(sp^2)$ - $C(sp^3)$  Cross-Coupling Methods by Library Synthesis. *ACS Med. Chem. Lett.* **2020**, *11*, 597–604.
- (250) Debrouwer, W.; Kimpe, W.; Dangreau, R.; Huvaere, K.; Gemoets, H. P. L.; Mottaghi, M.; Kuhn, S.; Van Aken, K. Ir/Ni Photoredox Dual Catalysis with Heterogeneous Base Enabled by an Oscillatory Plug Flow Photoreactor. *Org. Process Res. Dev.* **2020**, *24*, 2319–2325.
- (251) Kolmel, D. K.; Ratnayake, A. S.; Flanagan, M. E. Photoredox Cross-Electrophile Coupling in DNA-Encoded Chemistry. *Biochem. Biophys. Res. Commun.* **2020**, *533*, 201–208.
- (252) Perkins, J. J.; Shurtleff, V. W.; Johnson, A. M.; El Marrouni, A. Synthesis of C6-Substituted Purine Nucleoside Analogues via Late-Stage Photoredox/Nickel Dual Catalytic Cross-Coupling. *ACS Med. Chem. Lett.* **2021**, *12*, 662–666.
- (253) Luridiana, A.; Mazzarella, D.; Capaldo, L.; Rincon, J. A.; Garcia-Losada, P.; Mateos, C.; Frederick, M. O.; Nuno, M.; Jan Buma, W.; Noel, T. The Merger of Benzophenone HAT Photocatalysis and Silyl Radical-Induced XAT Enables Both Nickel-Catalyzed Cross-Electrophile Coupling and 1,2-Dicarbofunctionalization of Olefins. *ACS Catal.* **2022**, *12*, 11216–11225.
- (254) Steiner, A.; Krieger, J.; Jones, R.; Bose, D.; Wang, Y. P.; Eggenweiler, H. M.; Williams, J. D.; Kappe, C. O. Photoredox  $Csp^3$ - $Csp^2$  Reductive Cross-Couplings of Cereblon Ligands for PROTAC Linker Exploration in Batch and Flow. *ChemCatChem.* **2022**, *14*, No. e202201184.
- (255) Garry, O. L.; Heilmann, M.; Chen, J.; Liang, Y.; Zhang, X.; Ma, X.; Yeung, C. S.; Bennett, D. J.; MacMillan, D. W. C. Rapid Access to 2-Substituted Bicyclo[1.1.1]pentanes. *J. Am. Chem. Soc.* **2023**, *145*, 3092–3100.
- (256) Ma, Y.; Cammarata, J.; Cornella, J. Ni-Catalyzed Reductive Liebeskind-Srogl Alkylation of Heterocycles. *J. Am. Chem. Soc.* **2019**, *141*, 1918–1922.
- (257) Chen, Q.; You, J.; Tian, T.; Li, Z.; Kashihara, M.; Mori, H.; Nishihara, Y. Nickel-Catalyzed Decarbonylative Reductive Alkylation of Aroyl Fluorides with Alkyl Bromides. *Org. Lett.* **2022**, *24*, 9259–9263.
- (258) Wang, F.; Tong, Y.; Zou, G. Nickel-Catalyzed, Manganese-Assisted Denitrogenative Cross-Electrophile-Coupling of Benzotriazinones with Alkyl Halides for *ortho*-Alkylated Benzamides. *Org. Lett.* **2022**, *24*, 5741–5745.
- (259) Durandetti, M.; Gosmini, C.; Périchon, J. Ni-Catalyzed Activation of  $\alpha$ -Chloroesters: a Simple Method for the Synthesis of  $\alpha$ -Arylesters and  $\beta$ -Hydroxyesters. *Tetrahedron* **2007**, *63*, 1146–1153.
- (260) Pal, S.; Chowdhury, S.; Rozwadowski, E.; Auffrant, A.; Gosmini, C. Cobalt-Catalyzed Reductive Cross-Coupling Between Benzyl Chlorides and Aryl Halides. *Adv. Synth. Catal.* **2016**, *358*, 2431–2435.
- (261) Kuroboshi, M.; Tanaka, M.; Kishimoto, S.; Goto, K.; Mochizuki, M.; Tanaka, H. Tetrakis(dimethylamino)ethylene (TDAE) as a Potent Organic Electron Source: Alkenylation of Aldehydes Using an Ni/Cr/TDAE Redox System. *Tetrahedron Lett.* **2000**, *41*, 81–84.
- (262) Zhang, Q. C.; Wang, X.; Qian, Q.; Gong, H. G. Nickel-Catalyzed Reductive Cross-Coupling of Benzyl Halides with Aryl Halides. *Synthesis* **2016**, *48*, 2829–2836.
- (263) Kim, S.; Goldfogel, M. J.; Gilbert, M. M.; Weix, D. J. Nickel-Catalyzed Cross-Electrophile Coupling of Aryl Chlorides with Primary Alkyl Chlorides. *J. Am. Chem. Soc.* **2020**, *142*, 9902–9907.
- (264) Wu, Z.; Jiang, H.; Zhang, Y. Pd-catalyzed Cross-Electrophile Coupling/C–H Alkylation Reaction Enabled by a Mediator Generated via  $C(sp^3)$ -H Activation. *Chem. Sci.* **2021**, *12*, 8531–8536.
- (265) Durandetti, M.; Sibille, S.; Nédélec, J.-Y.; Périchon, J. A Novel Method of Arylation of  $\alpha$ -Chloroketones. *Synth. Commun.* **1994**, *24*, 145–151.
- (266) Durandetti, M.; Nédélec, J. Y.; Périchon, J. Nickel-Catalyzed Direct Electrochemical Cross-Coupling between Aryl Halides and Activated Alkyl Halides. *J. Org. Chem.* **1996**, *61*, 1748–1755.
- (267) Chen, T. Q.; MacMillan, D. W. C. A Metallaphotoredox Strategy for the Cross-Electrophile Coupling of  $\alpha$ -Chloro Carbonyls with Aryl Halides. *Angew. Chem., Int. Ed.* **2019**, *58*, 14584–14588.
- (268) Brill, Z. G.; Ritts, C. B.; Mansoor, U. F.; Sciammetta, N. Continuous Flow Enables Metallaphotoredox Catalysis in a Medicinal Chemistry Setting: Accelerated Optimization and Library Execution of a Reductive Coupling between Benzylic Chlorides and Aryl Bromides. *Org. Lett.* **2020**, *22*, 410–416.
- (269) Xu, W.; Zheng, P.; Xu, T. Dual Nickel- and Photoredox-Catalyzed Reductive Cross-Coupling of Aryl Halides with Dichloromethane via a Radical Process. *Org. Lett.* **2020**, *22*, 8643–8647.
- (270) Wei, Y.; Lam, J.; Diao, T. Synthesis of C-Acyl Furanosides via the Cross-Coupling of Glycosyl Esters with Carboxylic Acids. *Chem. Sci.* **2021**, *12*, 11414–11419.
- (271) Mou, Z. D.; Wang, J. X.; Zhang, X.; Niu, D. W. Stereoselective Preparation of C-Aryl Glycosides via Visible-Light-Induced Nickel-Catalyzed Reductive Cross-Coupling of Glycosyl Chlorides and Aryl Bromides. *Adv. Synth. Catal.* **2021**, *363*, 3025–3029.
- (272) Lu, X.; Yi, J.; Zhang, Z. Q.; Dai, J. J.; Liu, J. H.; Xiao, B.; Fu, Y.; Liu, L. Expedient Synthesis of Chiral  $\alpha$ -Amino Acids through Nickel-Catalyzed Reductive Cross-Coupling. *Chem. - Eur. J.* **2014**, *20*, 15339–15343.
- (273) Molander, G. A.; Wisniewski, S. R.; Traister, K. M. Reductive Cross-Coupling of 3-Bromo-2,1-Borazonaphthalenes with Alkyl Iodides. *Org. Lett.* **2014**, *16*, 3692–3695.
- (274) Hu, L.; Liu, X.; Liao, X. Nickel-Catalyzed Methylation of Aryl Halides with Deuterated Methyl Iodide. *Angew. Chem., Int. Ed.* **2016**, *55*, 9743–9747.
- (275) Ariyaratna, J. P.; Wu, F.; Colombo, S. K.; Hillary, C. M.; Li, W. Aerobic Catalytic Features in Photoredox- and Copper-Catalyzed Iodolactonization Reactions. *Org. Lett.* **2018**, *20*, 6462–6466.
- (276) Ishida, N.; Masuda, Y.; Sun, F. Z.; Kamae, Y.; Murakami, M. A Strained Vicinal Diol as a Reductant for Coupling of Organyl Halides. *Chem. Lett.* **2019**, *48*, 1042–1045.
- (277) Ye, N.; Wu, B.; Zhao, K.; Ge, X.; Zheng, Y.; Shen, X.; Shi, L.; Cortes-Clerget, M.; Regnier, M. L.; Parmentier, M.; et al. Micelle Enabled  $C(sp^2)$ - $C(sp^3)$  Cross-Electrophile Coupling in Water via Synergistic Nickel and Copper Catalysis. *Chem. Commun.* **2021**, *57*, 7629–7632.
- (278) Zhu, C.; Lee, S. C.; Chen, H.; Yue, H.; Rueping, M. Reductive Cross-Coupling of  $\alpha$ -Oxy Halides Enabled by Thermal Catalysis, Photocatalysis, Electrocatalysis, or Mechanochemistry. *Angew. Chem., Int. Ed.* **2022**, *61*, No. e202204212.
- (279) Sumida, Y.; Sumida, T.; Hosoya, T. Nickel-Catalyzed Reductive Cross-Coupling of Aryl Triflates and Nonaflates with Alkyl Iodides. *Synthesis* **2017**, *49*, 3590–3601.
- (280) Yedase, G. S.; Jha, A. K.; Yatham, V. R. Visible-Light Enabled  $C(sp^3)$ - $C(sp^2)$  Cross-Electrophile Coupling via Synergistic Halogen-Atom Transfer (XAT) and Nickel Catalysis. *J. Org. Chem.* **2022**, *87*, 5442–5450.
- (281) Constantin, T.; Zanini, M.; Regni, A.; Sheikh, N. S.; Julia, F.; Leonori, D. Aminoalkyl Radicals as Halogen-Atom Transfer Agents for Activation of Alkyl and Aryl halides. *Science* **2020**, *367*, 1021–1026.
- (282) Liao, J.; Basch, C. H.; Hoerrner, M. E.; Talley, M. R.; Boscoe, B. P.; Tucker, J. W.; Garnsey, M. R.; Watson, M. P. Deaminative Reductive Cross-Electrophile Couplings of Alkylpyridinium Salts and Aryl Bromides. *Org. Lett.* **2019**, *21*, 2941–2946.
- (283) Martin-Montero, R.; Yatham, V. R.; Yin, H.; Davies, J.; Martin, R. Ni-Catalyzed Reductive Deaminative Arylation at  $sp^3$  Carbon Centers. *Org. Lett.* **2019**, *21*, 2947–2951.

- (284) Ni, S.; Li, C. X.; Mao, Y.; Han, J.; Wang, Y.; Yan, H.; Pan, Y. Ni-Catalyzed Deaminative Cross-Electrophile Coupling of Katritzky Salts with Halides via C–N Bond Activation. *Sci. Adv.* **2019**, *5*, No. eaaw9516.
- (285) Yi, J.; Badir, S. O.; Kammer, L. M.; Ribagorda, M.; Molander, G. A. Deaminative Reductive Arylation Enabled by Nickel/Photo-redox Dual Catalysis. *Org. Lett.* **2019**, *21*, 3346–3351.
- (286) Yue, H.; Zhu, C.; Shen, L.; Geng, Q.; Hock, K. J.; Yuan, T.; Cavallo, L.; Rueping, M. Nickel-Catalyzed C–N Bond Activation: Activated Primary Amines as Alkylating Reagents in Reductive Cross-Coupling. *Chem. Sci.* **2019**, *10*, 4430–4435.
- (287) Twitty, J. C.; Hong, Y.; Garcia, B.; Tsang, S.; Liao, J.; Schultz, D. M.; Hanisak, J.; Zultanski, S. L.; Dion, A.; Kalyani, D.; et al. Diversifying Amino Acids and Peptides via Deaminative Reductive Cross-Couplings Leveraging High-Throughput Experimentation. *J. Am. Chem. Soc.* **2023**, *145*, 5684–5695.
- (288) Wang, J.; Ehehalt, L. E.; Huang, Z.; Belehr, O. M.; Guzei, I. A.; Weix, D. J. Formation of C(sp<sup>2</sup>)–C(sp<sup>3</sup>) Bonds Instead of Amide C–N Bonds from Carboxylic Acid and Amine Substrate Pools by Decarbonylative Cross-Electrophile Coupling. *J. Am. Chem. Soc.* **2023**, *145*, 9951–9958.
- (289) Douthwaite, J. L.; Zhao, R.; Shim, E.; Mahjour, B.; Zimmerman, P. M.; Cernak, T. Formal Cross-Coupling of Amines and Carboxylic Acids to Form sp<sup>3</sup>–sp<sup>2</sup> Carbon–Carbon Bonds. *J. Am. Chem. Soc.* **2023**, *145*, 10930–10937.
- (290) He, R. D.; Li, C. L.; Pan, Q. Q.; Guo, P.; Liu, X. Y.; Shu, X. Z. Reductive Coupling between C–N and C–O Electrophiles. *J. Am. Chem. Soc.* **2019**, *141*, 12481–12486.
- (291) Yang, T.; Wei, Y.; Koh, M. J. Photoinduced Nickel-Catalyzed Deaminative Cross-Electrophile Coupling for C(sp<sup>2</sup>)–C(sp<sup>3</sup>) and C(sp<sup>3</sup>)–C(sp<sup>3</sup>) Bond Formation. *ACS Catal.* **2021**, *11*, 6519–6525.
- (292) Yang, G.; Wang, Y.; Qiu, Y. Electroreductive Cross-Electrophile Coupling of Aziridines and Aryl Bromides. *Chem. - Eur. J.* **2023**, *29*, No. e202300959.
- (293) Jia, X. G.; Guo, P.; Duan, J.; Shu, X. Z. Dual Nickel and Lewis Acid Catalysis for Cross-Electrophile Coupling: the Allylation of Aryl Halides with Allylic Alcohols. *Chem. Sci.* **2018**, *9*, 640–645.
- (294) Li, Z.; Sun, W.; Wang, X.; Li, L.; Zhang, Y.; Li, C. Electrochemically Enabled, Nickel-Catalyzed Dehydroxylative Cross-Coupling of Alcohols with Aryl Halides. *J. Am. Chem. Soc.* **2021**, *143*, 3536–3543.
- (295) Yu, H.; Wang, Z. X. Nickel-Catalyzed Cross-Electrophile Coupling of Aryl Chlorides with Allylic Alcohols. *Org. Biomol. Chem.* **2021**, *19*, 9723–9731.
- (296) Lin, Q.; Ma, G. B.; Gong, H. Ni-Catalyzed Formal Cross-Electrophile Coupling of Alcohols with Aryl Halides. *ACS Catal.* **2021**, *11*, 14102–14109.
- (297) Chi, B. K.; Widness, J. K.; Gilbert, M. M.; Salgueiro, D. C.; Garcia, K. J.; Weix, D. J. In-Situ Bromination Enables Formal Cross-Electrophile Coupling of Alcohols with Aryl and Alkenyl Halides. *ACS Catal.* **2022**, *12*, 580–586.
- (298) Guo, P.; Wang, K.; Jin, W. J.; Xie, H.; Qi, L.; Liu, X. Y.; Shu, X. Z. Dynamic Kinetic Cross-Electrophile Arylation of Benzyl Alcohols by Nickel Catalysis. *J. Am. Chem. Soc.* **2021**, *143*, 513–523.
- (299) Wang, H.; Yang, M.; Wang, Y.; Man, X.; Lu, X.; Mou, Z.; Luo, Y.; Liang, H. Nickel-Catalyzed Reductive C(sp<sup>2</sup>)–C(sp<sup>3</sup>) Cross Coupling Using Phosphonium Salts. *Org. Lett.* **2021**, *23*, 8183–8188.
- (300) Molander, G. A.; Traister, K. M.; O'Neill, B. T. Engaging Nonaromatic, Heterocyclic Tosylates in Reductive Cross-Coupling with Aryl and Heteroaryl Bromides. *J. Org. Chem.* **2015**, *80*, 2907–2911.
- (301) Komeyama, K.; Ohata, R.; Kiguchi, S.; Osaka, I. Highly Nucleophilic Vitamin B<sub>12</sub>-Assisted Nickel-Catalysed Reductive Coupling of Aryl Halides and Non-Activated Alkyl Tosylates. *Chem. Commun.* **2017**, *53*, 6401–6404.
- (302) Wang, J.; Zhao, J.; Gong, H. Nickel-Catalyzed Methylation of Aryl Halides/Tosylates with Methyl Tosylate. *Chem. Commun.* **2017**, *53*, 10180–10183.
- (303) Reddy, B. R. P.; Chowdhury, S.; Auffrant, A.; Gosmini, C. Cobalt-Catalyzed Formation of Functionalized Diarylmethanes from Benzylmesylates and Aryl Halides. *Adv. Synth. Catal.* **2018**, *360*, 3026–3029.
- (304) Dumas, A.; Garsi, J. B.; Poissonnet, G.; Hanessian, S. Ni-Catalyzed Reductive and Merged Photocatalytic Cross-Coupling Reactions toward sp<sup>3</sup>/sp<sup>2</sup>-Functionalized Isoquinolones: Creating Diversity at C-6 and C-7 to Address Bioactive Analogues. *ACS Omega* **2020**, *5*, 27591–27606.
- (305) Zhao, Y.; Weix, D. J. Nickel-Catalyzed Regiodivergent Opening of Epoxides with Aryl Halides: Co-Catalysis Controls Regioselectivity. *J. Am. Chem. Soc.* **2014**, *136*, 48–51.
- (306) Parasram, M.; Shields, B. J.; Ahmad, O.; Knauber, T.; Doyle, A. G. Regioselective Cross-Electrophile Coupling of Epoxides and (Hetero)aryl Iodides via Ni/Ti/Photoredox Catalysis. *ACS Catal.* **2020**, *10*, 5821–5827.
- (307) Ye, Y.; Chen, H.; Sessler, J. L.; Gong, H. Zn-Mediated Fragmentation of Tertiary Alkyl Oxalates Enabling Formation of Alkylated and Arylated Quaternary Carbon Centers. *J. Am. Chem. Soc.* **2019**, *141*, 820–824.
- (308) Gao, M.; Sun, D.; Gong, H. Ni-Catalyzed Reductive C–O Bond Arylation of Oxalates Derived from  $\alpha$ -Hydroxy Esters with Aryl Halides. *Org. Lett.* **2019**, *21*, 1645–1648.
- (309) Anka-Lufford, L. L.; Prinsell, M. R.; Weix, D. J. Selective Cross-Coupling of Organic Halides with Allylic Acetates. *J. Org. Chem.* **2012**, *77*, 9989–10000.
- (310) Cui, X.; Wang, S.; Zhang, Y.; Deng, W.; Qian, Q.; Gong, H. Nickel-Catalyzed Reductive Allylation of Aryl Bromides with Allylic Acetates. *Org. Biomol. Chem.* **2013**, *11*, 3094–3097.
- (311) Arendt, K. M.; Doyle, A. G. Dialkyl Ether Formation by Nickel-Catalyzed Cross-Coupling of Acetals and Aryl Iodides. *Angew. Chem., Int. Ed.* **2015**, *54*, 9876–9880.
- (312) Cong, F.; Lv, X. Y.; Day, C. S.; Martin, R. Dual Catalytic Strategy for Forging sp<sup>2</sup>–sp<sup>3</sup> and sp<sup>3</sup>–sp<sup>3</sup> Architectures via  $\beta$ -Scission of Aliphatic Alcohol Derivatives. *J. Am. Chem. Soc.* **2020**, *142*, 20594–20599.
- (313) Lombardi, L.; Cerveri, A.; Giovanelli, R.; Castineira Reis, M.; Silva Lopez, C.; Bertuzzi, G.; Bandini, M. Direct Synthesis of  $\alpha$ -Aryl- $\alpha$ -Trifluoromethyl Alcohols via Nickel Catalyzed Cross-Electrophile Coupling. *Angew. Chem., Int. Ed.* **2022**, *61*, No. e202211732.
- (314) Konev, M. O.; Hanna, L. E.; Jarvo, E. R. Intra- and Intermolecular Nickel-Catalyzed Reductive Cross-Electrophile Coupling Reactions of Benzylic Esters with Aryl Halides. *Angew. Chem., Int. Ed.* **2016**, *55*, 6730–6733.
- (315) Li, Y. X.; Wang, Z.; Li, L. Y.; Tian, X. Y.; Shao, F.; Li, C. Chemoselective and Diastereoselective Synthesis of C-Aryl Nucleoside Analogues by Nickel-Catalyzed Cross-Coupling of Furanosyl Acetates with Aryl Iodides. *Angew. Chem., Int. Ed.* **2022**, *61*, No. e20211039.
- (316) Pratsch, G.; Lackner, G. L.; Overman, L. E. Constructing Quaternary Carbons from N-(Acyloxy)phthalimide Precursors of Tertiary Radicals Using Visible-Light Photocatalysis. *J. Org. Chem.* **2015**, *80*, 6025–6036.
- (317) Okada, K.; Okamoto, K.; Oda, M. A New and Practical Method of Decarboxylation - Photosensitized Decarboxylation of N-Acyloxyphthalimides Via Electron-Transfer Mechanism. *J. Am. Chem. Soc.* **1988**, *110*, 8736–8738.
- (318) Cornella, J.; Edwards, J. T.; Qin, T.; Kawamura, S.; Wang, J.; Pan, C. M.; Gianatassio, R.; Schmidt, M.; Eastgate, M. D.; Baran, P. S. Practical Ni-Catalyzed Aryl-Alkyl Cross-Coupling of Secondary Redox-Active Esters. *J. Am. Chem. Soc.* **2016**, *138*, 2174–2177.
- (319) Huihui, K. M.; Caputo, J. A.; Melchor, Z.; Olivares, A. M.; Spiewak, A. M.; Johnson, K. A.; DiBenedetto, T. A.; Kim, S.; Ackerman, L. K. G.; Weix, D. J. Decarboxylative Cross-Electrophile Coupling of N-Hydroxypythalimide Esters with Aryl Iodides. *J. Am. Chem. Soc.* **2016**, *138*, 5016–5019.
- (320) Koyanagi, T.; Herath, A.; Chong, A.; Ratnikov, M.; Valiere, A.; Chang, J.; Molteni, V.; Loren, J. One-Pot Electrochemical Nickel-

- Catalyzed Decarboxylative  $sp^2$ – $sp^3$  Cross-Coupling. *Org. Lett.* **2019**, *21*, 816–820.
- (321) Watanabe, E.; Chen, Y.; May, O.; Ley, S. V. A Practical Method for Continuous Production of  $sp^3$ -Rich Compounds from (Hetero)Aryl Halides and Redox-Active Esters. *Chem. - Eur. J.* **2020**, *26*, 186–191.
- (322) Behnke, N. E.; Sales, Z. S.; Li, M.; Herrmann, A. T. Dual Photoredox/Nickel-Promoted Alkylation of Heteroaryl Halides with Redox-Active Esters. *J. Org. Chem.* **2021**, *86*, 12945–12955.
- (323) Brewster, J. T., 2nd; Randall, S. D.; Kowalski, J.; Cruz, C.; Shoemaker, R.; Tarlton, E.; Hinklin, R. J. A Decarboxylative Cross-Coupling Platform To Access 2-Heteroaryl Azetidines: Building Blocks with Application in Medicinal Chemistry. *Org. Lett.* **2022**, *24*, 9123–9129.
- (324) Gabbey, A. L.; Michel, N. W. M.; Hughes, J. M. E.; Campeau, L. C.; Rousseaux, S. A. L. Synthesis of  $\alpha$ -Aryl Secondary Amides via Nickel-Catalyzed Reductive Coupling of Redox-Active Esters. *Org. Lett.* **2022**, *24*, 3173–3178.
- (325) Salgueiro, D. C.; Chi, B. K.; Guzei, I. A.; Garcia-Reynaga, P.; Weix, D. J. Control of Redox-Active Ester Reactivity Enables a General Cross-Electrophile Approach to Access Arylated Strained Rings. *Angew. Chem., Int. Ed.* **2022**, *61*, No. e202205673.
- (326) West, M. S.; Gabbey, A. L.; Huestis, M. P.; Rousseaux, S. A. L. Ni-Catalyzed Reductive Cross-Coupling of Cyclopropylamines and Other Strained Ring NHP Esters with (Hetero)Aryl Halides. *Org. Lett.* **2022**, *24*, 8441–8446.
- (327) Palkowitz, M. D.; Laudadio, G.; Kolb, S.; Choi, J.; Oderinde, M. S.; Ewing, T. E.; Bolduc, P. N.; Chen, T.; Zhang, H.; Cheng, P. T. W.; et al. Overcoming Limitations in Decarboxylative Arylation via Ag-Ni Electrocatalysis. *J. Am. Chem. Soc.* **2022**, *144*, 17709–17720.
- (328) Chen, H.; Hu, L.; Ji, W. Z.; Yao, L. C.; Liao, X. B. Nickel-Catalyzed Decarboxylative Alkylation of Aryl Iodides with Anhydrides. *ACS Catal.* **2018**, *8*, 10479–10485.
- (329) Du, W.; Luo, Q.; Wei, Z.; Wang, X.; Ni, C.; Hu, J. Switching from 2-Pyridination to Difluoromethylation: Ligand-Enabled Nickel-Catalyzed Reductive Difluoromethylation of Aryl Iodides with Difluoromethyl 2-Pyridyl Sulfone. *Sci. China Chem.* **2023**, *66*, 2785–2790.
- (330) Chi, B. K.; Gavin, S. J.; Ahern, B. N.; Peperni, N.; Monfette, S.; Weix, D. Sulfone Electrophiles in Cross-Electrophile Coupling: Nickel-Catalyzed Difluoromethylation of Aryl Bromides. *ACS Catal.* **2024**, *14*, 11087–11100.
- (331) Bacauanu, V.; Cardinal, S.; Yamauchi, M.; Kondo, M.; Fernandez, D. F.; Remy, R.; MacMillan, D. W. C. Metallaphotoredox Difluoromethylation of Aryl Bromides. *Angew. Chem., Int. Ed.* **2018**, *57*, 12543–12548.
- (332) He, X.; Gao, X.; Zhang, X. G. Nickel-Catalyzed Difluoroalkylation of (Hetero)Aryl Bromides with Unactivated 1-Bromo-1,1-difluoroalkanes. *Chin. J. Chem.* **2018**, *36*, 1059–1062.
- (333) Yin, H.; Sheng, J.; Zhang, K. F.; Zhang, Z. Q.; Bian, K. J.; Wang, X. S. Nickel-Catalyzed Monofluoromethylation of (Hetero)aryl Bromides via Reductive Cross-Coupling. *Chem. Commun.* **2019**, *55*, 7635–7638.
- (334) Gao, X.; He, X.; Zhang, X. G. Nickel-Catalyzed Difluoromethylation of (Hetero)Aryl Bromides with  $BrCF_2H$ . *Chin. J. Org. Chem.* **2019**, *39*, 215–222.
- (335) Sheng, J.; Ni, H. Q.; Zhang, H. R.; Zhang, K. F.; Wang, Y. N.; Wang, X. S. Nickel-Catalyzed Reductive Cross-Coupling of Aryl Halides with Monofluoroalkyl Halides for Late-Stage Monofluoroalkylation. *Angew. Chem., Int. Ed.* **2018**, *57*, 7634–7639.
- (336) Li, H.; Sheng, J.; Liao, G. X.; Wu, B. B.; Ni, H. Q.; Li, Y.; Wang, X. S. Nickel-Catalyzed Direct Trifluoroethylation of Aryl Iodides with 1,1,1-Trifluoro-2-Iodoethane via Reductive Coupling. *Adv. Synth. Catal.* **2020**, *362*, 5363–5367.
- (337) Yang, Y.; Luo, G.; Li, Y.; Tong, X.; He, M.; Zeng, H.; Jiang, Y.; Liu, Y.; Zheng, Y. Nickel-Catalyzed Reductive Coupling for Transforming Unactivated Aryl Electrophiles into  $\beta$ -Fluoroethylenes. *Chem. - Asian J.* **2020**, *15*, 156–162.
- (338) Xu, C.; Guo, W. H.; He, X.; Guo, Y. L.; Zhang, X. Y.; Zhang, X. Difluoromethylation of (Hetero)aryl Chlorides with Chlorodifluoromethane Catalyzed by Nickel. *Nat. Commun.* **2018**, *9*, 1170.
- (339) Li, X.; Gao, X.; He, C. Y.; Zhang, X. Using Chlorotrifluoroethane for Trifluoroethylation of (Hetero)aryl Bromides and Chlorides via Nickel Catalysis. *Org. Lett.* **2021**, *23*, 1400–1405.
- (340) Diao, Z.; Feng, Y.; Zhang, J.; Wang, X.; Li, H.; Ding, C.; Zhou, Z.; Li, X. Nickel-Catalyzed Reductive Cross-Coupling of (Hetero)aryl Halides with 2-Chloro-1,1-difluoroethane: Facile Access to 2,2-Difluoroethylated Aromatics. *Asian J. Org. Chem.* **2022**, *11*, No. e202200169.
- (341) Zhang, D.; Gao, X.; Min, Q. Q.; Gu, Y.; Berthon, G.; Zhang, X. Coupling of Heteroaryl Halides with Chlorodifluoroacetamides and Chlorodifluoroacetate by Nickel Catalysis. *Chem. - Eur. J.* **2022**, *28*, No. e202200642.
- (342) Hughes, J. M. E.; Fier, P. S. Desulfonylative Arylation of Redox-Active Alkyl Sulfones with Aryl Bromides. *Org. Lett.* **2019**, *21*, 5650–5654.
- (343) Fu, X.; Ran, T.; Zhou, Y.; Liu, J. Electroreductive Nickel-Catalyzed Allylation of Aryl Chlorides. *J. Org. Chem.* **2023**, *88*, 6132–6139.
- (344) Li, C.; Ling, L.; Luo, Z.; Wang, S.; Zhang, X.; Zeng, X. Deoxygenative Cross-Coupling of C(aryl)=O and C(amide)=O Electrophiles Enabled by Chromium Catalysis Using Bipyridine Ligand. *ACS Catal.* **2023**, *13*, 3120–3130.
- (345) Wang, W.; Yao, K.; Wu, F. Nickel-Catalyzed Reductive Cross-Coupling of Benzylic Sulfonium Salts with Aryl Iodides. *Synlett* **2022**, *33*, 361–366.
- (346) Hsu, C. M.; Lee, S. C.; Tsai, H. E.; Tsao, Y. T.; Chan, C. L.; Minoza, S.; Tsai, Z. N.; Li, L. Y.; Liao, H. H. Desulfurative Ni-Catalyzed Reductive Cross-Coupling of Benzyl Mercaptans/Mercaptoacetates with Aryl Halides. *J. Org. Chem.* **2022**, *87*, 3799–3803.
- (347) Durandetti, M.; Périchon, J.; Nédélec, J. Y. Asymmetric Induction in the Electrochemical Cross-Coupling of Aryl Halides with  $\alpha$ -Chloropropionic Acid Derivatives Catalyzed by Nickel Complexes. *J. Org. Chem.* **1997**, *62*, 7914–7915.
- (348) Kadunce, N. T.; Reisman, S. E. Nickel-Catalyzed Asymmetric Reductive Cross-Coupling between Heteroaryl Iodides and  $\alpha$ -Chloronitriles. *J. Am. Chem. Soc.* **2015**, *137*, 10480–10483.
- (349) Poremba, K. E.; Kadunce, N. T.; Suzuki, N.; Cherney, A. H.; Reisman, S. E. Nickel-Catalyzed Asymmetric Reductive Cross-Coupling To Access 1,1-Diarylkhanes. *J. Am. Chem. Soc.* **2017**, *139*, 5684–5687.
- (350) Guan, H.; Zhang, Q.; Walsh, P. J.; Mao, J. Nickel/Photoredox-Catalyzed Asymmetric Reductive Cross-Coupling of Racemic  $\alpha$ -Chloro Esters with Aryl Iodides. *Angew. Chem., Int. Ed.* **2020**, *59*, 5172–5177.
- (351) DeLano, T. J.; Dibrell, S. E.; Lacker, C. R.; Pancoast, A. R.; Poremba, K. E.; Cleary, L.; Sigman, M. S.; Reisman, S. E. Nickel-Catalyzed Asymmetric Reductive Cross-Coupling of  $\alpha$ -Chloroesters with (Hetero)aryl Iodides. *Chem. Sci.* **2021**, *12*, 7758–7762.
- (352) Sun, D. L.; Ma, G. B.; Zhao, X. L.; Lei, C. H.; Gong, H. G. Nickel-Catalyzed Asymmetric Reductive Arylation of  $\alpha$ -Chlorosulfones with Aryl Halides. *Chem. Sci.* **2021**, *12*, 5253–5258.
- (353) Sun, D.; Tao, X.; Ma, G.; Wang, J.; Chen, Y. Asymmetric Synthesis of Aryl/Vinyl Alkyl Carbinol Esters via Ni-Catalyzed Reductive Arylation/Vinylation of 1-Chloro-1-Alkanol Esters. *Chem. Sci.* **2022**, *13*, 8365–8370.
- (354) Liu, D.; Liu, Z.; Wang, Z.; Ma, C.; Herbert, S.; Schirok, H.; Mei, T. Paired Electrolysis-Enabled Nickel-Catalyzed Enantioselective Reductive Cross-Coupling Between  $\alpha$ -Chloroesters and Aryl Bromides. *Nat. Commun.* **2022**, *13*, 7318.
- (355) Ding, D.; Dong, H.; Wang, C. Nickel-Catalyzed Asymmetric Domino Ring Opening/Cross-Coupling Reaction of Cyclobutanones via a Reductive Strategy. *iScience* **2020**, *23*, No. 101017.
- (356) Trost, B. M.; Van Vranken, D. L. Asymmetric Transition Metal-Catalyzed Allylic Alkylation. *Chem. Rev.* **1996**, *96*, 395–422.
- (357) Song, X. D.; Guo, M. M.; Xu, S.; Shen, C. A. J.; Zhou, X. C.; Chu, X. Q.; Ma, M. T.; Shen, Z. L. Nickel-Catalyzed Diaster-

- eoselective Reductive Cross-Coupling of Disubstituted Cycloalkyl Iodides with Aryl Iodides. *Org. Lett.* **2021**, *23*, 5118–5122.
- (358) Woods, B. P.; Orlandi, M.; Huang, C. Y.; Sigman, M. S.; Doyle, A. G. Nickel-Catalyzed Enantioselective Reductive Cross-Coupling of Styrenyl Aziridines. *J. Am. Chem. Soc.* **2017**, *139*, 5688–5691.
- (359) Zhao, Y.; Weix, D. J. Enantioselective Cross-Coupling of *meso*-Epoxides with Aryl Halides. *J. Am. Chem. Soc.* **2015**, *137*, 3237–3240.
- (360) Banerjee, A.; Yamamoto, H. Nickel Catalyzed Regio-, Diastereo-, and Enantioselective Cross-Coupling of 3,4-Epoxyalcohol with Aryl Iodides. *Org. Lett.* **2017**, *19*, 4363–4366.
- (361) Wang, C.; Yamamoto, H. Nickel-Catalyzed Regio- and Enantioselective Aminolysis of 3,4-Epoxy Alcohols. *J. Am. Chem. Soc.* **2015**, *137*, 4308–4311.
- (362) Lau, S. H.; Borden, M. A.; Steiman, T. J.; Wang, L. S.; Parasram, M.; Doyle, A. G. Ni/Photoredox-Catalyzed Enantioselective Cross-Electrophile Coupling of Styrene Oxides with Aryl Iodides. *J. Am. Chem. Soc.* **2021**, *143*, 15873–15881.
- (363) Min, Y.; Sheng, J.; Yu, J. L.; Ni, S. X.; Ma, G.; Gong, H.; Wang, X. S. Diverse Synthesis of Chiral Trifluoromethylated Alkanes via Nickel-Catalyzed Asymmetric Reductive Cross-Coupling Fluoroalkylation. *Angew. Chem., Int. Ed.* **2021**, *60*, 9947–9952.
- (364) Zhou, P.; Li, X.; Wang, D.; Xu, T. Dual Nickel- and Photoredox-Catalyzed Reductive Cross-Coupling to Access Chiral Trifluoromethylated Alkanes. *Org. Lett.* **2021**, *23*, 4683–4687.
- (365) Wang, D.; Xu, T. A Pivotal Role of Chloride Ion on Nickel-Catalyzed Enantioselective Reductive Cross-Coupling to Perfluoroalkylated Boronate Esters. *ACS Catal.* **2021**, *11*, 12469–12475.
- (366) Fakhouri, L.; Cook, C. D.; Al-Huniti, M. H.; Console-Bram, L. M.; Hurst, D. P.; Spano, M. B. S.; Nasrallah, D. J.; Caron, M. G.; Barak, L. S.; Reggio, P. H.; et al. Design, Synthesis and Biological Evaluation of GPR55 Agonists. *Bioorg. Med. Chem.* **2017**, *25*, 4355–4367.
- (367) Menger, M.; Lentz, D.; Christmann, M. Synthesis of (+)-Vitepyrroloid A and (+)-Vitepyrroloid B by Late-Stage Ni-Catalyzed C(sp<sup>2</sup>)-C(sp<sup>3</sup>) Cross-Electrophile Coupling. *J. Org. Chem.* **2018**, *83*, 6793–6797.
- (368) Luo, L.; Zhai, X. Y.; Wang, Y. W.; Peng, Y.; Gong, H. Divergent Total Syntheses of C3 a-C7' Linked Diketopiperazine Alkaloids (+)-Asperazine and (+)-Pestalazine A Enabled by a Ni-Catalyzed Reductive Coupling of Tertiary Alkyl Chloride. *Chem. - Eur. J.* **2019**, *25*, 989–992.
- (369) Girvin, Z. C.; Andrews, M. K.; Liu, X.; Gellman, S. H. Foldamer-Templated Catalysis of Macrocycle Formation. *Science* **2019**, *366*, 1528–1531.
- (370) Chen, T. G.; Mele, L.; Jentzer, O.; Delbrayelle, D.; Echeverria, P. G.; Vantourout, J. C.; Baran, P. S. Convergent Synthesis of (*R*)-Silodosin via Decarboxylative Cross-Coupling. *Tetrahedron Lett.* **2021**, *79*, 153290.
- (371) Yan, P.-C.; Zhang, X.-Y.; Hu, X.-W.; Zhang, B.; Zhang, X.-D.; Zhao, M.; Che, D.-Q.; Li, Y.-Q.; Zhou, Q.-L. First Asymmetric Synthesis of Silodosin Through Catalytic Hydrogenation by Using Ir-SIPHOX Catalysts. *Tetrahedron Lett.* **2013**, *S4*, 1449–1451.
- (372) Barve, I. J.; Chen, L.-H.; Wei, P. C. P.; Hung, J.-T.; Sun, C.-M. Enantioselective Synthesis of (-)-(R)-Silodosin by Ultrasound-Assisted Diastereomeric Crystallization. *Tetrahedron* **2013**, *69*, 2834–2843.
- (373) Calogero, F.; Allegrini, P.; Attolino, E.; Passarella, D. Synthesis of Silodosin by Copper-Catalysed C–C Arylation. *Eur. J. Org. Chem.* **2015**, *2015*, 6011–6016.
- (374) Simon, R. C.; Sattler, J. H.; Farnberger, J. E.; Fuchs, C. S.; Richter, N.; Zepeck, F.; Kroutil, W. Enzymatic asymmetric synthesis of the silodosin amine intermediate. *Tetrahedron: Asymmetry* **2014**, *25*, 284–288.
- (375) Pipal, R. W.; Stout, K. T.; Musacchio, P. Z.; Ren, S.; Graham, T. J. A.; Verhoog, S.; Gantert, L.; Lohith, T. G.; Schmitz, A.; Lee, H. S.; et al. Metallaphotoredox Aryl and Alkyl Radiomethylation for PET Ligand Discovery. *Nature* **2021**, *589*, 542–547.
- (376) Pang, X.; Peng, X. J.; Shu, X. Z. Reductive Cross-Coupling of Vinyl Electrophiles. *Synthesis* **2020**, *S2*, 3751–3763.
- (377) Xiong, B. J.; Chen, X. M.; Liu, J. J.; Zhang, X. M.; Xia, Y.; Lian, Z. Stereoselective gem-Difluorovinylation of gem-Difluorinated Cyclopropanes Enabled by Ni/Pd Cooperative Catalysis. *ACS Catal.* **2021**, *11*, 11960–11965.
- (378) He, X.; Liu, J.; Chen, G.; Xiong, B.; Xiao, X.; Chen, L.; Zhang, X.; Dong, L.; Ma, X.; Lian, Z. Nickel-Catalyzed Cross-Electrophile Coupling Reactions between Allylic Acetates and *gem*-Difluorovinyl Tosylate. *Org. Lett.* **2022**, *24*, 3538–3543.
- (379) Ye, Y.; Chen, H.; Yao, K.; Gong, H. Iron-Catalyzed Reductive Vinylation of Tertiary Alkyl Oxalates with Activated Vinyl Halides. *Org. Lett.* **2020**, *22*, 2070–2075.
- (380) Xie, H.; Wang, S.; Wang, Y. Q.; Guo, P.; Shu, X. Z. Ti-Catalyzed Reductive Dehydroxylative Vinylation of Tertiary Alcohols. *ACS Catal.* **2022**, *12*, 1018–1023.
- (381) Jiang, Y.; Wang, Q. Q.; Zhang, X. L.; Koh, M. J. Synthesis of C-Glycosides by Ti-Catalyzed Stereoselective Glycosyl Radical Functionalization. *Chem.* **2021**, *7*, 3377–3392.
- (382) Condon, S.; Nédélec, J. Y. Overview on Nickel-Catalyzed Electrochemical Conjugate Addition of Organic Halides on Electron-Deficient Olefins. *Synthesis* **2004**, 3070–3078.
- (383) Johnson, K. A.; Biswas, S.; Weix, D. J. Cross-Electrophile Coupling of Vinyl Halides with Alkyl Halides. *Chem. - Eur. J.* **2016**, *22*, 7399–7402.
- (384) Qiu, C.; Yao, K.; Zhang, X.; Gong, H. Ni-Catalyzed Reductive Coupling of  $\alpha$ -Halocarbonyl Derivatives with Vinyl Bromides. *Org. Biomol. Chem.* **2016**, *14*, 11332–11335.
- (385) Gu, J.; Qiu, C. B.; Lu, W. B.; Qian, Q.; Lin, K. H.; Gong, H. G. Nickel-Catalyzed Reductive Cross-Coupling of Vinyl Bromides with Unactivated Alkyl Halides. *Synthesis* **2017**, *49*, 1867–1873.
- (386) Cai, Y.; Benischke, A. D.; Knochel, P.; Gosmini, C. Cobalt-Catalyzed Reductive Cross-Coupling Between Styryl and Benzyl Halides. *Chem. - Eur. J.* **2017**, *23*, 250–253.
- (387) Suga, T.; Takahashi, Y.; Ukaji, Y. One-Shot Radical Cross Coupling Between Benzyl Alcohols and Alkenyl Halides Using Ni/Ti/Mn System. *Adv. Synth. Catal.* **2020**, *362*, 5622–5626.
- (388) Harwood, S. J.; Palkowitz, M. D.; Gannett, C. N.; Perez, P.; Yao, Z.; Sun, L.; Abruna, H. D.; Anderson, S. L.; Baran, P. S. Modular Terpene Synthesis Enabled by Mild Electrochemical Couplings. *Science* **2022**, *375*, 745–752.
- (389) Ye, C.; Tong, W. Q.; Wu, F. Nickel-Catalyzed Reductive Cross-Coupling of Oxalates Derived from  $\alpha$ -Hydroxy Carbonyls with Vinyl Bromides. *Synthesis* **2022**, *S4*, 2251–2257.
- (390) Ye, Y.; Qi, X.; Xu, B.; Lin, Y.; Xiang, H.; Zou, L.; Ye, X. Y.; Xie, T. Nickel-Catalyzed Cross-Electrophile Allylation of Vinyl Bromides and the Modification of Anti-Tumour Natural Medicine  $\beta$ -Elemene. *Chem. Sci.* **2022**, *13*, 6959–6966.
- (391) Wang, Q.; Sun, Q.; Jiang, Y.; Zhang, H.; Yu, L.; Tian, C.; Chen, G.; Koh, M. J. Nickel-Catalyzed Reductive Coupling of Glucosyl Halides with Aryl/Vinyl Halides Enabling  $\beta$ -Selective Preparation of C-Aryl/Vinyl Glucosides. *Nat. Synth.* **2022**, *1*, 235–244.
- (392) Liu, X. G.; Yang, Q.; Liu, D. Y.; Liu, J.; Tan, D. H.; Ruan, Y. J.; Wang, P. F.; Wang, X. L.; Wang, H. Nickel-Catalyzed Reductive Decarboxylative/Deaminative Glycosylation of Activated Aliphatic Acids and Primary Amines. *Org. Lett.* **2023**, *25*, 5022–5026.
- (393) An, J. L.; Zhou, X.; Zhang, Y. F.; Ye, Z. F.; Guo, Q. Y.; Song, H.; Song, Z. L.; Liu, X. Y.; Qin, Y. Carboxylic Acid-Assisted Sterically Demanding Reductive Cross-Coupling Between Cycloalkenyl and Alkyl Bromides. *Org. Chem. Front.* **2023**, *10*, 1897–1902.
- (394) Zhou, Q. Q.; Dusel, S. J. S.; Lu, L. Q.; Konig, B.; Xiao, W. J. Alkenylation of Unactivated Alkyl Bromides Through Visible Light Photocatalysis. *Chem. Commun.* **2019**, *55*, 107–110.
- (395) Yu, W.; Chen, L.; Tao, J.; Wang, T.; Fu, J. Dual Nickel- and Photoredox-Catalyzed Reductive Cross-Coupling of Aryl Vinyl Halides and Unactivated Tertiary Alkyl Bromides. *Chem. Commun.* **2019**, *55*, 5918–5921.

- (396) Garbacz, M.; Stecko, S. The Synthesis of Chiral Allyl Carbamates via Merger of Photoredox and Nickel Catalysis. *Adv. Synth. Catal.* **2020**, *362*, 3213–3222.
- (397) Garbacz, M.; Stecko, S. Synthesis of Chiral Branched Allylamines Through Dual Photoredox/Nickel Catalysis. *Org. Biomol. Chem.* **2021**, *19*, 8578–8585.
- (398) Lu, X.; Wang, Y.; Zhang, B.; Pi, J. J.; Wang, X. X.; Gong, T. J.; Xiao, B.; Fu, Y. Nickel-Catalyzed Defluorinative Reductive Cross-Coupling of *gem*-Difluoroalkenes with Unactivated Secondary and Tertiary Alkyl Halides. *J. Am. Chem. Soc.* **2017**, *139*, 12632–12637.
- (399) Yu, L.; Tang, M. L.; Si, C. M.; Meng, Z.; Liang, Y.; Han, J.; Sun, X. Zinc-Mediated Decarboxylative Alkylation of *gem*-difluoroalkenes. *Org. Lett.* **2018**, *20*, 4579–4583.
- (400) Zhou, L.; Zhu, C.; Bi, P.; Feng, C. Ni-Catalyzed Migratory Fluoro-Alkenylation of Unactivated Alkyl Bromides with *gem*-Difluoroalkenes. *Chem. Sci.* **2019**, *10*, 1144–1149.
- (401) Chen, H.; Sun, S.; Liao, X. Nickel-Catalyzed Decarboxylative Alkenylation of Anhydrides with Vinyl Triflates or Halides. *Org. Lett.* **2019**, *21*, 3625–3630.
- (402) Pang, X. B.; He, R. D.; Shu, X. Z. Construction of C-C Bond via C-N and C-O Cleavage. *Synlett* **2020**, *31*, 635–640.
- (403) Duan, J.; Du, Y. F.; Pang, X.; Shu, X. Z. Ni-Catalyzed Cross-Electrophile Coupling Between Vinyl/Aryl and Alkyl Sulfonates: Synthesis of Cycloalkenes and Modification of Peptides. *Chem. Sci.* **2019**, *10*, 8706–8712.
- (404) Qiao, J. B.; Zhao, Z. Z.; Zhang, Y. Q.; Yin, K.; Tian, Z. X.; Shu, X. Z. Allylboronates from Vinyl Triflates and  $\alpha$ -Chloroboronates by Reductive Nickel Catalysis. *Org. Lett.* **2020**, *22*, 5085–5089.
- (405) He, R. D.; Bai, Y.; Han, G. Y.; Zhao, Z. Z.; Pang, X.; Pan, X.; Liu, X. Y.; Shu, X. Z. Reductive Alkylation of Alkenyl Acetates with Alkyl Bromides by Nickel Catalysis. *Angew. Chem., Int. Ed.* **2022**, *61*, No. e202114556.
- (406) Su, L.; Ma, G.; Song, Y.; Gong, H. Nickel-Catalyzed Reductive Vinylation of Chloro-hexahydropyrroloindoline Derivatives with Vinyl Triflates. *Org. Lett.* **2021**, *23*, 2493–2497.
- (407) Tao, X.; Chen, Y.; Guo, J.; Wang, X.; Gong, H. Preparation of  $\alpha$ -Amino Acids via Ni-Catalyzed Reductive Vinylation and Arylation of  $\alpha$ -Pivaloyloxy Glycine. *Chem. Sci.* **2021**, *12*, 220–226.
- (408) Tao, X. H.; Ma, G. B.; Song, Y. H.; Chen, Y. R.; Qian, Q.; Sun, D. L.; Gong, H. G. Alkenylation and Arylation of Peptides via Ni-Catalyzed Reductive Coupling of  $\alpha$ -C-Tosyl Peptides with C(sp<sup>2</sup>) Triflates/Halides. *Org. Lett.* **2021**, *23*, 7418–7422.
- (409) Tao, X.; Yao, K.; Xue, W. Ni-Catalyzed cross-Electrophile Coupling of  $\alpha$ -Hydroxy Carbonyl Compound-Derived Oxalates with Vinyl Triflates. *Tetrahedron Lett.* **2021**, *73*, No. 153129.
- (410) Song, F.; Wang, F.; Guo, L.; Feng, X.; Zhang, Y.; Chu, L. Visible-Light-Enabled Stereodivergent Synthesis of E- and Z-Configured 1,4-Dienes by Photoredox/Nickel Dual Catalysis. *Angew. Chem., Int. Ed.* **2020**, *59*, 177–181.
- (411) Singh, K.; Staig, S. J.; Weaver, J. D. Facile Synthesis of Z-Alkenes via Uphill Catalysis. *J. Am. Chem. Soc.* **2014**, *136*, 5275–5278.
- (412) Cherney, A. H.; Reisman, S. E. Nickel-Catalyzed Asymmetric Reductive Cross-Coupling Between Vinyl and Benzyl Electrophiles. *J. Am. Chem. Soc.* **2014**, *136*, 14365–14368.
- (413) Suzuki, N.; Hofstra, J. L.; Poremba, K. E.; Reisman, S. E. Nickel-Catalyzed Enantioselective Cross-Coupling of N-Hydroxyphthalimide Esters with Vinyl Bromides. *Org. Lett.* **2017**, *19*, 2150–2153.
- (414) DeLano, T. J.; Reisman, S. E. Enantioselective Electro-reductive Coupling of Alkenyl and Benzyl Halides via Nickel Catalysis. *ACS Catal.* **2019**, *9*, 6751–6754.
- (415) Zhu, Z.; Lin, L.; Xiao, J.; Shi, Z. Nickel-Catalyzed Stereo- and Enantioselective Cross-Coupling of *gem*-Difluoroalkenes with Carbon Electrophiles by C–F Bond Activation. *Angew. Chem., Int. Ed.* **2022**, *61*, No. e202113209.
- (416) Geng, J.; Sun, D.; Song, Y.; Tong, W.; Wu, F. Ni-Catalyzed Asymmetric Reductive Alkenylation of  $\alpha$ -Chlorosulfones with Vinyl Bromides. *Org. Lett.* **2022**, *24*, 1807–1811.
- (417) Jin, R. X.; Wu, B. B.; Bian, K. J.; Yu, J. L.; Dai, J. C.; Zuo, Y. W.; Zhang, Y. F.; Wang, X. S. Asymmetric Construction of Allylicstereogenic Carbon Center Featuring a Trifluoromethyl Group via Enantioselective Reductive Fluoroalkylation. *Nat. Commun.* **2022**, *13*, 7035.
- (418) Li, T.; Cheng, X.; Lu, J.; Wang, H.; Fang, Q.; Lu, Z. Enantioselective Reductive Cross-Coupling of Aryl/Alkenyl Bromides with Benzylic Chlorides via Photoredox/Biimidazoline Nickel Dual Catalysis. *Chin. J. Chem.* **2022**, *40*, 1033–1038.
- (419) Lu, Q.; Guan, H.; Wang, Y. E.; Xiong, D.; Lin, T.; Xue, F.; Mao, J. Nickel/Photoredox-Catalyzed Enantioselective Reductive Cross-Coupling between Vinyl Bromides and Benzyl Chlorides. *J. Org. Chem.* **2022**, *87*, 8048–8058.
- (420) Hu, X.; Cheng-Sanchez, I.; Cuesta-Galisteo, S.; Nevado, C. Nickel-Catalyzed Enantioselective Electrochemical Reductive Cross-Coupling of Aryl Aziridines with Alkenyl Bromides. *J. Am. Chem. Soc.* **2023**, *145*, 6270–6279.
- (421) Ma, W. Y.; Han, G. Y.; Kang, S.; Pang, X.; Liu, X. Y.; Shu, X. Z. Cobalt-Catalyzed Enantiospecific Dynamic Kinetic Cross-Electrophile Vinylation of Allylic Alcohols with Vinyl Triflates. *J. Am. Chem. Soc.* **2021**, *143*, 15930–15935.
- (422) Fegheh-Hassanpour, Y.; Arif, T.; Sintim, H. O.; Al Mamari, H. H.; Hodgson, D. M. Synthesis of (–)-6,7-Dideoxsqualenol HS by Carbonyl Ylide Cycloaddition-Rearrangement and Cross-electrophile Coupling. *Org. Lett.* **2017**, *19*, 3540–3543.
- (423) Boeckman, R. K., Jr.; Pero, J. E.; Boehmle, D. J. Toward the Development of a General Chiral Auxiliary. Enantioselective Alkylation and a New Catalytic Asymmetric Addition of Silyloxyfurans: Application to a Total Synthesis of (–)-Rasfonin. *J. Am. Chem. Soc.* **2006**, *128*, 11032–11033.
- (424) Boeckman, R. K., Jr.; Niziol, J. M.; Biegasiewicz, K. F. Scalable Synthesis of (–)-Rasfonin Enabled by a Convergent Enantioselective  $\alpha$ -Hydroxymethylation Strategy. *Org. Lett.* **2018**, *20*, 5062–5065.
- (425) McGeough, C. P.; Strom, A. E.; Jamison, T. F. Ni-Catalyzed Cross-Electrophile Coupling for the Synthesis of Skipped Polyenes. *Org. Lett.* **2019**, *21*, 3606–3609.
- (426) Yan, B. C.; Zhou, M.; Li, J.; Li, X. N.; He, S. J.; Zuo, J. P.; Sun, H. D.; Li, A.; Puno, P. T. (–)-Isoscopariusin A, a Naturally Occurring Immunosuppressive Meroterpenoid: Structure Elucidation and Scalable Chemical Synthesis. *Angew. Chem., Int. Ed.* **2021**, *60*, 12859–12867.
- (427) Wang, Y.; Su, Y.; Jia, Y. Total Synthesis of (+)-Aberrarone. *J. Am. Chem. Soc.* **2023**, *145*, 9459–9463.
- (428) Dieter, R. K. Reaction of Acyl Chlorides with Organometallic Reagents: A Banquet Table of Metals for Ketone Synthesis. *Tetrahedron* **1999**, *55*, 4177–4236.
- (429) Lawrence, N. J. Aldehydes and Ketones. *J. Chem. Soc., Perkin Trans.* **1998**, *1*, 1739–1750.
- (430) Goldfogel, M. J.; Huang, L.; Weix, D. J. *Cross-Electrophile Coupling: Principles and New Reactions*; Wiley, 2020.
- (431) Wotal, A. C.; Weix, D. J. Synthesis of Functionalized Dialkyl Ketones from Carboxylic Acid Derivatives and Alkyl Halides. *Org. Lett.* **2012**, *14*, 1476–1479.
- (432) Wotal, A. C.; Batesky, D. C.; Weix, D. J. Nickel-Catalyzed Synthesis of Ketones from Alkyl Halides and Acid Chlorides: Preparation of Ethyl 4-Oxododecanoate. *Org. Synth.* **2016**, *93*, 50–62.
- (433) Wu, F.; Lu, W.; Qian, Q.; Ren, Q.; Gong, H. Ketone Formation via Mild Nickel-Catalyzed Reductive Coupling of Alkyl Halides with Aryl Acid Chlorides. *Org. Lett.* **2012**, *14*, 3044–3047.
- (434) Lu, W. B.; Liang, Z. Y.; Zhang, Y. W.; Wu, F.; Qian, Q.; Gong, H. G. Gram-Scale Ketone Synthesis by Direct Reductive Coupling of Alkyl Iodides with Acid Chlorides. *Synthesis* **2013**, *45*, 2234–2240.
- (435) Zheng, M.; Xue, W.; Xue, T.; Gong, H. Ester Formation via Nickel-Catalyzed Reductive Coupling of Alkyl Halides with Chloroformates. *Org. Lett.* **2016**, *18*, 6152–6155.
- (436) Pulikottil, F. T.; Pillai, R.; Suku, R. V.; Rasappan, R. Nickel-Catalyzed Cross-Coupling of Alkyl Carboxylic Acid Derivatives with Pyridinium Salts via C–N Bond Cleavage. *Org. Lett.* **2020**, *22*, 2902–2907.

- (437) Wang, J.; Hoerrner, M. E.; Watson, M. P.; Weix, D. J. Nickel-Catalyzed Synthesis of Dialkyl Ketones from the Coupling of *N*-Alkyl Pyridinium Salts with Activated Carboxylic Acids. *Angew. Chem., Int. Ed.* **2020**, *59*, 13484–13489.
- (438) Liang, Z.; Xue, W.; Lin, K.; Gong, H. Nickel-Catalyzed Reductive Methylation of Alkyl Halides and Acid Chlorides with Methyl p-Tosylate. *Org. Lett.* **2014**, *16*, 5620–5623.
- (439) Ding, D.; Wang, C. Nickel-Catalyzed Reductive Electrophilic Ring Opening of Cycloketone Oxime Esters with Aroyl Chlorides. *ACS Catal.* **2018**, *8*, 11324–11329.
- (440) Onaka, M.; Matsuoka, Y.; Mukaiyama, T. A Convenient Method for the Direct Preparation of Ketones from 2-(6-(2-Methoxyethyl)Pyridyl) Carboxylates and Alkyl Iodides by Use of Zinc Dust and a Catalytic Amount of Nickel Dichloride. *Chem. Lett.* **1981**, *10*, 531–534.
- (441) Yang, F.; Ding, D.; Wang, C. Nickel-Catalyzed Directed Cross-Electrophile Coupling of Phenolic Esters with Alkyl Bromides. *Org. Lett.* **2020**, *22*, 9203–9209.
- (442) Wang, J.; Cary, B. P.; Beyer, P. D.; Gellman, S. H.; Weix, D. J. Ketones from Nickel-Catalyzed Decarboxylative, Non-Symmetric Cross-Electrophile Coupling of Carboxylic Acid Esters. *Angew. Chem., Int. Ed.* **2019**, *58*, 12081–12085.
- (443) Yu, H.; Wang, Z. X. Nickel-Catalyzed Reductive Coupling of Arylcarboxylic Acid 2-Pyridyl Esters with Alkyl Methanesulfonates: Access to Alkyl Aryl Ketones. *Org. Biomol. Chem.* **2023**, *21*, 3423–3431.
- (444) Xi, X.; Luo, Y.; Li, W.; Xu, M.; Zhao, H.; Chen, Y.; Zheng, S.; Qi, X.; Yuan, W. From Esters to Ketones via a Photoredox-Assisted Reductive Acyl Cross-Coupling Strategy. *Angew. Chem., Int. Ed.* **2022**, *61*, No. e202114731.
- (445) Pace, V.; Holzer, W.; Meng, G.; Shi, S.; Lalancette, R.; Szostak, R.; Szostak, M. Structures of Highly Twisted Amides Relevant to Amide N–C Cross-Coupling: Evidence for Ground-State Amide Destabilization. *Chem. - Eur. J.* **2016**, *22*, 14494–14498.
- (446) Meng, G.; Shi, S.; Szostak, M. Cross-Coupling of Amides by N–C Bond Activation. *Synlett* **2016**, *27*, 2530–2540.
- (447) Liu, C.; Szostak, M. Twisted Amides: From Obscurity to Broadly Useful Transition-Metal-Catalyzed Reactions by N–C Amide Bond Activation. *Chem. - Eur. J.* **2017**, *23*, 7157–7173.
- (448) Meng, G.; Szostak, M. N-Acyl-Glutaramides: Privileged Scaffolds in Amide N–C Bond Cross-Coupling. *Eur. J. Org. Chem.* **2018**, *2018*, 2352–2365.
- (449) Zhuo, J. M.; Zhang, Y.; Li, Z. J.; Li, C. Nickel-Catalyzed Direct Acylation of Aryl and Alkyl Bromides with Acylimidazoles. *ACS Catal.* **2020**, *10*, 3895–3903.
- (450) Jones, A. C.; Williams, M. T. J.; Morrill, L. C.; Browne, D. L. Mechanical Activation of Zero-Valent Metal Reductants for Nickel-Catalyzed Cross-Electrophile Coupling. *ACS Catal.* **2022**, *12*, 13681–13689.
- (451) Cao, Q.; Stark, R. T.; Fallis, I. A.; Browne, D. L. A Ball-Milling-Enabled Reformatsky Reaction. *ChemSusChem* **2019**, *12*, 2554–2557.
- (452) Yin, J.; Stark, R. T.; Fallis, I. A.; Browne, D. L. A Mechanochemical Zinc-Mediated Barbier-Type Allylation Reaction under Ball-Milling Conditions. *J. Org. Chem.* **2020**, *85*, 2347–2354.
- (453) Cao, Q.; Howard, J. L.; Wheatley, E.; Browne, D. L. Mechanochemical Activation of Zinc and Application to Negishi Cross-Coupling. *Angew. Chem., Int. Ed.* **2018**, *57*, 11339–11343.
- (454) Yu, C. G.; Matsuo, Y. Nickel-Catalyzed Deaminative Acylation of Activated Aliphatic Amines with Aromatic Amides via C–N Bond Activation. *Org. Lett.* **2020**, *22*, 950–955.
- (455) Kerackian, T.; Reina, A.; Bouyssi, D.; Monteiro, N.; Amgoune, A. Silyl Radical Mediated Cross-Electrophile Coupling of *N*-Acylimides with Alkyl Bromides under Photoredox/Nickel Dual Catalysis. *Org. Lett.* **2020**, *22*, 2240–2245.
- (456) Brauer, J.; Quraishi, E.; Kammer, L. M.; Opatz, T. Nickel-Mediated Photoreductive Cross Coupling of Carboxylic Acid Derivatives for Ketone Synthesis. *Chem. - Eur. J.* **2021**, *27*, 18168–18174.
- (457) Kerackian, T.; Bouyssi, D.; Pilet, G.; Medebielle, M.; Monteiro, N.; Vantourout, J. C.; Amgoune, A. Nickel-Catalyzed Electro-Reductive Cross-Coupling of Aliphatic *N*-Acyl Imides with Alkyl Halides as a Strategy for Dialkyl Ketone Synthesis: Scope and Mechanistic Investigations. *ACS Catal.* **2022**, *12*, 12315–12325.
- (458) Yin, H.; Zhao, C.; You, H.; Lin, K.; Gong, H. Mild Ketone Formation via Ni-Catalyzed Reductive Coupling of Unactivated Alkyl Halides with Acid Anhydrides. *Chem. Commun.* **2012**, *48*, 7034–7036.
- (459) Zhao, C.; Jia, X.; Wang, X.; Gong, H. Ni-Catalyzed Reductive Coupling of Alkyl Acids with Unactivated Tertiary Alkyl and Glycosyl Halides. *J. Am. Chem. Soc.* **2014**, *136*, 17645–17651.
- (460) Jia, X.; Zhang, X.; Qian, Q.; Gong, H. Alkyl-Aryl Ketone Synthesis via Nickel-Catalyzed Reductive Coupling of Alkyl Halides with Aryl Acids and Anhydrides. *Chem. Commun.* **2015**, *51*, 10302–10305.
- (461) He, J.; Song, P. H.; Xu, X. F.; Zhu, S. L.; Wang, Y. Migratory Reductive Acylation between Alkyl Halides or Alkenes and Alkyl Carboxylic Acids by Nickel Catalysis. *ACS Catal.* **2019**, *9*, 3253–3259.
- (462) Jiao, K.-J.; Ma, C.; Liu, D.; Qiu, H.; Cheng, B.; Mei, T.-S. Nickel-Catalyzed Electrochemical Reductive Relay Cross-Coupling of Alkyl Halides with Alkyl Carboxylic Acids. *Org. Chem. Front.* **2021**, *8*, 6603–6608.
- (463) Ni, S.; Padial, N. M.; Kingston, C.; Vantourout, J. C.; Schmitt, D. C.; Edwards, J. T.; Kruszyk, M. M.; Merchant, R. R.; Mykhailiuk, P. K.; Sanchez, B. B.; et al. A Radical Approach to Anionic Chemistry: Synthesis of Ketones, Alcohols, and Amines. *J. Am. Chem. Soc.* **2019**, *141*, 6726–6739.
- (464) Escolano, M.; Cabrera-Afonso, M. J.; Ribagorda, M.; Badir, S. O.; Molander, G. A. Nickel-Mediated Synthesis of Non-Anomeric C-Acyl Glycosides through Electron Donor-Acceptor Complex Photoactivation. *J. Org. Chem.* **2022**, *87*, 4981–4990.
- (465) Gu, J.; Liu, J. D.; Sun, Y. R.; Wang, H. Y. Nickel-Catalyzed Reductive Methylation of Alkyl Acid with Methyl p-Tosylate. *Chin. J. Org. Chem.* **2017**, *37*, 1830–1834.
- (466) Zhou, X.; Guo, L.; Zhang, H. X.; Xia, R. Y.; Yang, C.; Xia, W. J. Nickel-Catalyzed Reductive Acylation of Carboxylic Acids with Alkyl Halides and N-Hydroxyphthalimide Esters Enabled by Electrochemical Process. *Adv. Synth. Catal.* **2022**, *364*, 1526–1531.
- (467) Jiang, Y.; Yang, K.; Wei, Y.; Wang, Q.; Li, S. J.; Lan, Y.; Koh, M. J. Catalytic Multicomponent Synthesis of C-Acyl Glycosides by Consecutive Cross-Electrophile Couplings. *Angew. Chem., Int. Ed.* **2022**, *61*, No. e202211043.
- (468) Chen, H.; Yue, H.; Zhu, C.; Rueping, M. Reactivity in Nickel-Catalyzed Multi-component Sequential Reductive Cross-Coupling Reactions. *Angew. Chem., Int. Ed.* **2022**, *61*, No. e202204144.
- (469) Shi, R.; Hu, X. From Alkyl Halides to Ketones: Nickel-Catalyzed Reductive Carbonylation Utilizing Ethyl Chloroformate as the Carbonyl Source. *Angew. Chem., Int. Ed.* **2019**, *58*, 7454–7458.
- (470) Dolhem, E.; Barhdadi, R.; Folest, J. C.; Nédelec, J. Y.; Troupel, M. Nickel Catalysed Electrosynthesis of Ketones from Organic Halides and Iron Pentacarbonyl: Part 2:: Unsymmetrical Ketones. *Tetrahedron* **2001**, *57*, 525–529.
- (471) Wotal, A. C.; Ribson, R. D.; Weix, D. J. Stoichiometric Reactions of Acylnickel(II) Complexes with Electrophiles and the Catalytic Synthesis of Ketones. *Organometallics* **2014**, *33*, 5874–5881.
- (472) Cherney, A. H.; Kadunce, N. T.; Reisman, S. E. Catalytic Asymmetric Reductive Acyl Cross-Coupling: Synthesis of Enantioenriched Acyclic  $\alpha,\alpha$ -Disubstituted Ketones. *J. Am. Chem. Soc.* **2013**, *135*, 7442–7445.
- (473) Wu, J.; Wu, H.; Liu, X.; Zhang, Y.; Huang, G.; Zhang, C. Nickel-Catalyzed Cross-Coupling of Acyl Chloride with Racemic  $\alpha$ -Trifluoromethyl Bromide to Access Chiral  $\alpha$ -Trifluoromethyl Ketones. *Org. Lett.* **2022**, *24*, 4322–4327.
- (474) Lin, D.; Chen, Y.; Dong, Z.; Pei, P.; Ji, H.; Tai, L.; Chen, L. General and Modular Access to Enantioenriched  $\alpha$ -Trifluoromethyl Ketones via Nickel-Catalyzed Reductive Trifluoroalkylation. *CCS Chemistry* **2023**, *5*, 1386–1397.

- (475) Ji, H.; Lin, D.; Tai, L.; Li, X.; Shi, Y.; Han, Q.; Chen, L. A. Nickel-Catalyzed Enantioselective Coupling of Acid Chlorides with  $\alpha$ -Bromobenzoates: An Asymmetric Acyloin Synthesis. *J. Am. Chem. Soc.* **2022**, *144*, 23019–23029.
- (476) Kumar, V. P.; Babu, V. S.; Yahata, K.; Kishi, Y. Fe/Cu-Mediated One-Pot Ketone Synthesis. *Org. Lett.* **2017**, *19*, 2766–2769.
- (477) Kishi, Y.; Yahata, K.; Kumar, V. P.; Vaddela, S. B. Fe/Cu-Mediated Ketone Synthesis. US PatentUS WO2019009956-A1, 2019.
- (478) Ai, Y.; Ye, N.; Wang, Q.; Yahata, K.; Kishi, Y. Zirconium/Nickel-Mediated One-Pot Ketone Synthesis. *Angew. Chem., Int. Ed.* **2017**, *56*, 10791–10795.
- (479) Fukuyama, T.; Kishi, Y.; Ai, Y.; Ye, N.; Wang, Q.; Yahata, K.; Iso, K.; Naini, S. R.; Yamashita, S.; Lee, J.; et al. Synthesis of Halichondrins. World PatentWO2019010363-A1 WO2019010363-A8, 2019.
- (480) Yahata, K.; Ye, N.; Ai, Y.; Iso, K.; Kishi, Y. Unified, Efficient, and Scalable Synthesis of Halichondrins: Zirconium/Nickel-Mediated One-Pot Ketone Synthesis as the Final Coupling Reaction. *Angew. Chem., Int. Ed.* **2017**, *56*, 10796–10800.
- (481) Umehara, A.; Kishi, Y. Further Studies on Ni/Zr-mediated One-pot Ketone Synthesis: Use of a Mixture of Ni-I- and Ni-II-catalysts Greatly Improves the Molar Ratio of Coupling Partners. *Chem. Lett.* **2019**, *48*, 947–950.
- (482) Wu, X.; Zhou, J.; Snider, B. B. Synthesis of (−)-Berkelic Acid. *Angew. Chem., Int. Ed.* **2009**, *48*, 1283–1286.
- (483) Wang, H.-H.; Wang, X.-D.; Cao, F.; Gao, W.-W.; Ma, S.-M.; Li, Z.; Deng, X.-M.; Shi, T.; Wang, Z. Application of Palladium-Catalyzed Aryl C–H Alkylation in Total Synthesis of (−)-Berkelic Acid. *Org. Chem. Front.* **2021**, *8*, 82–86.
- (484) Bender, C. F.; Yoshimoto, F. K.; Paradise, C. L.; De Brabander, J. K. A Concise Synthesis of Berkelic Acid Inspired by Combining the Natural Products Spicifernin and Pulvilloric Acid. *J. Am. Chem. Soc.* **2009**, *131*, 11350–11352.
- (485) Fananas, F. J.; Mendoza, A.; Arto, T.; Temelli, B.; Rodriguez, F. Scalable Total Synthesis of (−)-Berkelic Acid by using a Protecting-Group-Free Strategy. *Angew. Chem., Int. Ed.* **2012**, *51*, 4930–4939.
- (486) Arto, T.; de Santa-María, I. S.; Chiara, M. D.; Fañanás, F. J.; Rodríguez, F. Berkelic Acid: Straightforward Analogue Synthesis and Studies of Activity Against Selected Cancer Cell Lines. *Eur. J. Org. Chem.* **2016**, *2016*, 5876–5880.
- (487) Cheng, H. G.; Yang, Z.; Chen, R.; Cao, L.; Tong, W. Y.; Wei, Q.; Wang, Q.; Wu, C.; Qu, S.; Zhou, Q. A Concise Total Synthesis of (−)-Berkelic Acid. *Angew. Chem., Int. Ed.* **2021**, *60*, 5141–5146.
- (488) Yang, Z. J.; Cheng, H. G.; Chen, R. M.; Cao, L. M.; Wei, Q.; Wang, Q. Q.; Zhou, Q. H. Eight-Step Asymmetric Synthesis of (−)-Berkelic Acid. *Synthesis* **2022**, *54*, 4691–4702.
- (489) Eckhardt, M.; Fu, G. C. The First Applications of Carbene Ligands in Cross-Couplings of Alkyl Electrophiles: Sonogashira Reactions of Unactivated Alkyl Bromides and Iodides. *J. Am. Chem. Soc.* **2003**, *125*, 13642–13643.
- (490) Hofmeister, H.; Annen, K.; Laurent, H.; Wiechert, R. A Novel Entry to  $17\alpha$ -Bromo- and  $17\alpha$ -Iodoethynyl Steroids. *Angew. Chem., Int. Ed.* **1984**, *23*, 727–729.
- (491) Brandsma, L.; Verkruissse, H. D. Practical and Safe Procedures for the Preparation of the Lower Homologues of Bromoacetylene. *Synthesis* **1990**, *1990*, 984–985.
- (492) Brand, J. P.; Waser, J. Electrophilic Alkylation: The Dark Side of Acetylene Chemistry. *Chem. Soc. Rev.* **2012**, *41*, 4165–4179.
- (493) Wu, W.; Jiang, H. Haloalkynes: A Powerful and Versatile Building Block in Organic Synthesis. *Acc. Chem. Res.* **2014**, *47*, 2483–2504.
- (494) Thaler, T.; Guo, L.-N.; Mayer, P.; Knochel, P. Highly Diastereoselective  $C(sp^3)$ – $C(sp)$  Cross-Coupling Reactions between 1,3- and 1,4-Substituted Cyclohexylzinc Reagents and Bromoalkynes through Remote Stereocontrol. *Angew. Chem., Int. Ed.* **2011**, *50*, 2174–2177.
- (495) Corpet, M.; Bai, X.-Z.; Gosmini, C. Cobalt-Catalyzed Cross-Coupling of Organozinc Halides with Bromoalkynes. *Adv. Synth. Catal.* **2014**, *356*, 2937–2942.
- (496) Huang, L.; Olivares, A. M.; Weix, D. J. Reductive Decarboxylative Alkylation of N-Hydroxyphthalimide Esters with Bromoalkynes. *Angew. Chem., Int. Ed.* **2017**, *56*, 11901–11905.
- (497) Wang, H.; Wu, X.; Xu, T. Enantioconvergent Reductive  $C(sp)$ – $C(sp^3)$  Cross-Coupling to Access Chiral  $\alpha$ -Alkynyl Phosphonates Under Dual Nickel/Photoredox Catalysis. *Angew. Chem., Int. Ed.* **2023**, *62*, No. e202218299.
- (498) Lucas, E. L.; Hewitt, K. A.; Chen, P. P.; Castro, A. J.; Hong, X.; Jarvo, E. R. Engaging Sulfonamides: Intramolecular Cross-Electrophile Coupling Reaction of Sulfonamides with Alkyl Chlorides. *J. Org. Chem.* **2020**, *85*, 1775–1793.
- (499) Xue, W.; Xu, H.; Liang, Z.; Qian, Q.; Gong, H. Nickel-Catalyzed Reductive Cyclization of Alkyl Dihalides. *Org. Lett.* **2014**, *16*, 4984–4987.
- (500) Sanford, A. B.; Thane, T. A.; McGinnis, T. M.; Chen, P. P.; Hong, X.; Jarvo, E. R. Nickel-Catalyzed Alkyl-Alkyl Cross-Electrophile Coupling Reaction of 1,3-Dimesylates for the Synthesis of Alkylcyclopropanes. *J. Am. Chem. Soc.* **2020**, *142*, 5017–5023.
- (501) Lucas, E. L.; McGinnis, T. M.; Castro, A. J.; Jarvo, E. R. Nickel-Catalyzed Cross-Electrophile Coupling of the Difluoromethyl Group for Fluorinated Cyclopropane Synthesis. *Synlett* **2021**, *32*, 1525–1530.
- (502) Jana, S. K.; Maiti, M.; Dey, P.; Maji, B. Photoredox/Nickel Dual Catalysis Enables the Synthesis of Alkyl Cyclopropanes via  $C(sp^3)$ – $C(sp^3)$  Cross Electrophile Coupling of Unactivated Alkyl Electrophiles. *Org. Lett.* **2022**, *24*, 1298–1302.
- (503) Hewitt, K. A.; Xie, P. P.; Thane, T. A.; Hirbawi, N.; Zhang, S. Q.; Matus, A. C.; Lucas, E. L.; Hong, X.; Jarvo, E. R. Nickel-Catalyzed Domino Cross-Electrophile Coupling Dicarbofunctionalization Reaction To Afford Vinylcyclopropanes. *ACS Catal.* **2021**, *11*, 14369–14380.
- (504) Tollefson, E. J.; Erickson, L. W.; Jarvo, E. R. Stereospecific Intramolecular Reductive Cross-Electrophile Coupling Reactions for Cyclopropane Synthesis. *J. Am. Chem. Soc.* **2015**, *137*, 9760–9763.
- (505) Erickson, L. W.; Lucas, E. L.; Tollefson, E. J.; Jarvo, E. R. Nickel-Catalyzed Cross-Electrophile Coupling of Alkyl Fluorides: Stereospecific Synthesis of Vinylcyclopropanes. *J. Am. Chem. Soc.* **2016**, *138*, 14006–14011.
- (506) Thane, T. A.; Jarvo, E. R. Ligand-Based Control of Nickel Catalysts: Switching Chemoselectivity from One-Electron to Two-Electron Pathways in Competing Reactions of 4-Halotetrahydropyrans. *Org. Lett.* **2022**, *24*, 5003–5008.
- (507) Qian, X.; Auffrant, A.; Felouat, A.; Gosmini, C. Cobalt-Catalyzed Reductive Allylation of Alkyl Halides with Allylic Acetates or Carbonates. *Angew. Chem., Int. Ed.* **2011**, *50*, 10402–10405.
- (508) Dai, Y.; Wu, F.; Zang, Z.; You, H.; Gong, H. Ni-Catalyzed Reductive Allylation of Unactivated Alkyl Halides with Allylic Carbonates. *Chem. - Eur. J.* **2012**, *18*, 808–812.
- (509) Caputo, J. A.; Naodovic, M.; Weix, D. J. Nickel-Catalyzed Allylation of  $\alpha$ -Amido Sulfones To Form Protected Homoallylic Amines. *Synlett* **2015**, *26*, 323–326.
- (510) Chen, H.; Jia, X.; Yu, Y.; Qian, Q.; Gong, H. Nickel-Catalyzed Reductive Allylation of Tertiary Alkyl Halides with Allylic Carbonates. *Angew. Chem., Int. Ed.* **2017**, *56*, 13103–13106.
- (511) Yu, Y.; Chen, H.; Qian, Q.; Yao, K.; Gong, H. An Extension of Nickel-Catalyzed Reductive Coupling between Tertiary Alkyl Halides with Allylic Carbonates. *Tetrahedron* **2018**, *74*, 5651–5658.
- (512) Yan, X. B.; Li, C. L.; Jin, W. J.; Guo, P.; Shu, X. Z. Reductive Coupling of Benzyl Oxalates with Highly Functionalized Alkyl Bromides by Nickel Catalysis. *Chem. Sci.* **2018**, *9*, 4529–4534.
- (513) Li, Y.; Li, Y.; Peng, L.; Wu, D.; Zhu, L.; Yin, G. Nickel-Catalyzed Migratory Alkyl-Alkyl Cross-Coupling Reaction. *Chem. Sci.* **2020**, *11*, 10461–10464.
- (514) Wang, J.; Gong, Y.; Sun, D.; Gong, H. Nickel-Catalyzed Reductive Benzylation of Tertiary Alkyl Halides with Benzyl

- Chlorides and Chloroformates. *Org. Chem. Front.* **2021**, *8*, 2944–2948.
- (515) Yu, X.; Yang, T.; Wang, S.; Xu, H.; Gong, H. Nickel-Catalyzed Reductive Cross-Coupling of Unactivated Alkyl Halides. *Org. Lett.* **2011**, *13*, 2138–2141.
- (516) Chen, Y.; Ma, G.; Gong, H. Copper-Catalyzed Reductive Trifluoromethylation of Alkyl Iodides with Togni's Reagent. *Org. Lett.* **2018**, *20*, 4677–4680.
- (517) Smith, R. T.; Zhang, X.; Rincon, J. A.; Agejas, J.; Mateos, C.; Barberis, M.; Garcia-Cerrada, S.; de Frutos, O.; MacMillan, D. W. C. Metallaphotoredox-Catalyzed Cross-Electrophile C(sp<sup>3</sup>)–C(sp<sup>3</sup>) Coupling of Aliphatic Bromides. *J. Am. Chem. Soc.* **2018**, *140*, 17433–17438.
- (518) Komeyama, K.; Michiyuki, T.; Osaka, I. Nickel/Cobalt-Catalyzed C(sp<sup>3</sup>)–C(sp<sup>3</sup>) Cross-Coupling of Alkyl Halides with Alkyl Tosylates. *ACS Catal.* **2019**, *9*, 9285–9291.
- (519) Kornfilt, D. J. P.; MacMillan, D. W. C. Copper-Catalyzed Trifluoromethylation of Alkyl Bromides. *J. Am. Chem. Soc.* **2019**, *141*, 6853–6858.
- (520) Lin, T.; Gu, Y.; Qian, P.; Guan, H.; Walsh, P. J.; Mao, J. Nickel-Catalyzed Reductive Coupling of Homoenolates and their Higher Homologues with Unactivated Alkyl Bromides. *Nat. Commun.* **2020**, *11*, 5638.
- (521) O'Brien, E. M.; Bercot, E. A.; Rovis, T. Decarbonylative Cross-Coupling of Cyclic Anhydrides: Introducing Stereochemistry at an sp<sup>3</sup> Carbon in the Cross-Coupling Event. *J. Am. Chem. Soc.* **2003**, *125*, 10498–10499.
- (522) Bercher, O. P.; Plunkett, S.; Mortimer, T. E.; Watson, M. P. Deaminative Reductive Methylation of Alkylpyridinium Salts. *Org. Lett.* **2021**, *23*, 7059–7063.
- (523) Cui, R.; Sheng, J.; Wu, B. B.; Hu, D. D.; Zheng, H. Q.; Wang, X. S. Nickel-Catalyzed Reductive Monofluoroalkylation of Alkyl Tosylate with Bromofluoromethane to Primary Alkyl Fluoride. *Chem. Commun.* **2021**, *57*, 9084–9087.
- (524) Zhang, Z.; Cernak, T. The Formal Cross-Coupling of Amines and Carboxylic Acids to Form sp<sup>3</sup>–sp<sup>3</sup> Carbon–Carbon Bonds. *Angew. Chem., Int. Ed.* **2021**, *60*, 27293–27298.
- (525) Yuan, B.; Ding, D. C.; Wang, C. Nickel-Catalyzed Regioselective Reductive Ring Opening of Aryl Cyclopropyl Ketones with Alkyl Bromides. *ACS Catal.* **2022**, *12*, 4261–4267.
- (526) Cui, N.; Lin, T.; Wang, Y. E.; Wu, J.; Han, Y.; Xu, X.; Xue, F.; Xiong, D.; Walsh, P. J.; Mao, J. Nickel-Catalyzed Reductive Coupling of  $\gamma$ -Metalated Ketones with Unactivated Alkyl Bromides. *Org. Lett.* **2022**, *24*, 3987–3992.
- (527) Kang, K.; Weix, D. J. Nickel-Catalyzed C(sp<sup>3</sup>)–C(sp<sup>3</sup>) Cross-Electrophile Coupling of In Situ Generated NHP Esters with Unactivated Alkyl Bromides. *Org. Lett.* **2022**, *24*, 2853–2857.
- (528) Zhang, B.; Gao, Y.; Hioki, Y.; Oderinde, M. S.; Qiao, J. X.; Rodriguez, K. X.; Zhang, H. J.; Kawamata, Y.; Baran, P. S. Ni-Electrocatalytic C(sp<sup>3</sup>)–C(sp<sup>3</sup>) Doubly Decarboxylative Coupling. *Nature* **2022**, *606*, 313–318.
- (529) Wei, Y.; Wang, Q.; Koh, M. J. A Photoinduced, Nickel-Catalyzed Reaction for the Stereoselective Assembly of C-Linked Glycosides and Glycopeptides. *Angew. Chem., Int. Ed.* **2023**, *62*, No. e202214247.
- (530) Zhao, W. T.; Meng, H.; Lin, J. N.; Shu, W. Ligand-Controlled Nickel-Catalyzed Regiodivergent Cross-Electrophile Alkyl-Alkyl Couplings of Alkyl Halides. *Angew. Chem., Int. Ed.* **2023**, *62*, No. e202215779.
- (531) Tang, S.; Zhang, H. H.; Yu, S. Enantioselective Reductive Allylic Alkylation Enabled by Dual Photoredox/Palladium Catalysis. *Chem. Commun.* **2023**, *59*, 1153–1156.
- (532) Zhou, J.; Wang, D.; Xu, W.; Hu, Z.; Xu, T. Enantioselective C(sp<sup>3</sup>)–(Csp<sup>3</sup>) Reductive Cross-Electrophile Coupling of Unactivated Alkyl Halides with  $\alpha$ -Chloroboronates via Dual Nickel/Photoredox Catalysis. *J. Am. Chem. Soc.* **2023**, *145*, 2081–2087.
- (533) Zhu, W.; Yin, Q.; Lou, Z.; Yang, M. Modular Total Syntheses of trans-Clerodanes and Sesquiterpene (Hydro)quinones via Tail-to-Head Cyclization and Reductive Coupling Strategies. *Nat. Commun.* **2022**, *13*, 6633.
- (534) Diccianni, J.; Lin, Q.; Diao, T. Mechanisms of Nickel-Catalyzed Coupling Reactions and Applications in Alkene Functionalization. *Acc. Chem. Res.* **2020**, *53*, 906–919.
- (535) Lin, Q.; Diao, T. Mechanism of Ni-Catalyzed Reductive 1,2-Dicarbofunctionalization of Alkenes. *J. Am. Chem. Soc.* **2019**, *141*, 17937–17948.
- (536) Leatherman, M. D.; Svejda, S. A.; Johnson, L. K.; Brookhart, M. Mechanistic Studies of Nickel(II) Alkyl Agostic Cations and Alkyl Ethylene Complexes: Investigations of Chain Propagation and Isomerization in ( $\alpha$ -diimine)Ni(II)-Catalyzed Ethylene Polymerization. *J. Am. Chem. Soc.* **2003**, *125*, 3068–3081.
- (537) Qi, X.; Diao, T. Nickel-Catalyzed Dicarbofunctionalization of Alkenes. *ACS Catal.* **2020**, *10*, 8542–8556.
- (538) Cao, J. S.; Zeng, J.; Xiao, J.; Wang, X. H.; Wang, Y. W.; Peng, Y. Total Synthesis of Linoxepin Facilitated by a Ni-catalyzed Tandem Reductive Cyclization. *Chem. Commun.* **2022**, *58*, 7273–7276.
- (539) Wu, X.; Turlik, A.; Luan, B.; He, F.; Qu, J.; Houk, K. N.; Chen, Y. Nickel-Catalyzed Enantioselective Reductive Alkyl-Carbamoylation of Internal Alkenes. *Angew. Chem., Int. Ed.* **2022**, *61*, No. e202207536.
- (540) Yuan, M.; Song, Z.; Badir, S. O.; Molander, G. A.; Gutierrez, O. On the Nature of C(sp<sup>3</sup>)–C(sp<sup>2</sup>) Bond Formation in Nickel-Catalyzed Tertiary Radical Cross-Couplings: A Case Study of Ni/Photoredox Catalytic Cross-Coupling of Alkyl Radicals and Aryl Halides. *J. Am. Chem. Soc.* **2020**, *142*, 7225–7234.
- (541) Lin, C.; Shen, L. Recent Progress in Transition Metal-Catalyzed Regioselective Functionalization of Unactivated Alkenes/Alkynes Assisted by Bidentate Directing Groups. *ChemCatChem.* **2019**, *11*, 961–968.
- (542) Ping, Y. Y.; Kong, W. Q. Ni-Catalyzed Reductive Difunctionalization of Alkenes. *Synthesis* **2020**, *52*, 979–992.
- (543) Medina, J. M.; Moreno, J.; Racine, S.; Du, S.; Garg, N. K. Mizoroki-Heck Cyclizations of Amide Derivatives for the Introduction of Quaternary Centers. *Angew. Chem., Int. Ed.* **2017**, *56*, 6567–6571.
- (544) Bhakta, S.; Ghosh, T. Emerging Nickel Catalysis in Heck Reactions: Recent Developments. *Adv. Synth. Catal.* **2020**, *362*, 5257–5274.
- (545) Desrosiers, J. N.; Hie, L.; Biswas, S.; Zatolochnaya, O. V.; Rodriguez, S.; Lee, H.; Grinberg, N.; Haddad, N.; Yee, N. K.; Garg, N. K.; et al. Construction of Quaternary Stereocenters by Nickel-Catalyzed Heck Cyclization Reactions. *Angew. Chem., Int. Ed.* **2016**, *55*, 11921–11924.
- (546) Garcia-Dominguez, A.; Li, Z.; Nevado, C. Nickel-Catalyzed Reductive Dicarbofunctionalization of Alkenes. *J. Am. Chem. Soc.* **2017**, *139*, 6835–6838.
- (547) Zhao, X.; Tu, H. Y.; Guo, L.; Zhu, S.; Qing, F. L.; Chu, L. Intermolecular Selective Carboacylation of Alkenes via Nickel-Catalyzed Reductive Radical Relay. *Nat. Commun.* **2018**, *9*, 3488.
- (548) Shu, W.; Garcia-Dominguez, A.; Quiros, M. T.; Mondal, R.; Cardenas, D. J.; Nevado, C. Ni-Catalyzed Reductive Dicarbofunctionalization of Nonactivated Alkenes: Scope and Mechanistic Insights. *J. Am. Chem. Soc.* **2019**, *141*, 13812–13821.
- (549) Sun, S. Z.; Duan, Y.; Mega, R. S.; Somerville, R. J.; Martin, R. Site-Selective 1,2-Dicarbofunctionalization of Vinyl Boronates through Dual Catalysis. *Angew. Chem., Int. Ed.* **2020**, *59*, 4370–4374.
- (550) Wang, L.; Wang, C. Nickel-Catalyzed Three-Component Reductive Alkylacylation of Electron-Deficient Activated Alkenes. *Org. Lett.* **2020**, *22*, 8829–8835.
- (551) Yang, T.; Chen, X. Z.; Rao, W. D.; Koh, M. J. Broadly Applicable Directed Catalytic Reductive Difunctionalization of Alkenyl Carbonyl Compounds. *Chem.* **2020**, *6*, 738–751.
- (552) Zhang, X.; Zhao, Q.-W.; Yang, Z.-F.; Fu, X.-P. Access to  $\alpha,\alpha$ -Difluoro- $\gamma$ -Amino Acids by Nickel-Catalyzed Reductive Arylidfluorocetylation of N-Vinylacetamide. *Synlett* **2021**, *32*, 1565–1569.

- (553) Belal, M.; Li, Z. Q.; Zhu, L.; Yin, G. Y. Catalyst-Controlled Regiodivergent 1,2-Difunctionalization of Alkenes with Two Carbon-Based Electrophiles. *Sci. China Chem.* **2022**, *65*, 514–520.
- (554) Hu, P.; Guo, L.; Zhao, L.; Yang, C.; Xia, W. Nickel-Catalyzed Reductive Dicarbofunctionalization of Vinylarenes Enabled by Electrochemical Process. *Org. Lett.* **2022**, *24*, 7583–7588.
- (555) Wang, H.; Huang, H.; Gong, C.; Diao, Y.; Chen, J.; Wu, S. H.; Wang, L. Nickel-Catalyzed Chemo- and Regioselective Benzylarylation of Unactivated Alkenes with *o*-Bromobenzyl Chlorides. *Org. Lett.* **2022**, *24*, 328–333.
- (556) Xi, X.; Chen, Y.; Yuan, W. Nickel-Catalyzed Three-Component Alkylacylation of Alkenes Enabled by a Photoactive Electron Donor-Acceptor Complex. *Org. Lett.* **2022**, *24*, 3938–3943.
- (557) Tu, H. Y.; Wang, F.; Huo, L.; Li, Y.; Zhu, S.; Zhao, X.; Li, H.; Qing, F. L.; Chu, L. Enantioselective Three-Component Fluoroalkylarylation of Unactivated Olefins through Nickel-Catalyzed Cross-Electrophile Coupling. *J. Am. Chem. Soc.* **2020**, *142*, 9604–9611.
- (558) Wei, X.; Shu, W.; Garcia-Dominguez, A.; Merino, E.; Nevado, C. Asymmetric Ni-Catalyzed Radical Relayed Reductive Coupling. *J. Am. Chem. Soc.* **2020**, *142*, 13515–13522.
- (559) Zhao, L.; Meng, X.; Zou, Y.; Zhao, J.; Wang, L.; Zhang, L.; Wang, C. Directed Nickel-Catalyzed Diastereoselective Reductive Difunctionalization of Alkenyl Amines. *Org. Lett.* **2021**, *23*, 8516–8521.
- (560) Li, Y.-Z.; Rao, N.; An, L.; Wan, X.-L.; Zhang, Y.; Zhang, X. Enantioselective Nickel-Catalyzed Dicarbofunctionalization of 3,3,3-Trifluoropropene. *Nat. Commun.* **2022**, *13*, 5539.
- (561) Wang, F.; Pan, S. W.; Zhu, S. Q.; Chu, L. L. Selective Three-Component Reductive Alkylation of Unbiased Alkenes via Carbonyl-Directed Nickel Catalysis. *ACS Catal.* **2022**, *12*, 9779–9789.
- (562) Zhou, Y.-Y.; Uyeda, C. Catalytic Reductive [4 + 1]-Cycloadditions of Vinylidenes and Dienes. *Science* **2019**, *363*, 857–862.
- (563) Pal, S.; Zhou, Y. Y.; Uyeda, C. Catalytic Reductive Vinylidene Transfer Reactions. *J. Am. Chem. Soc.* **2017**, *139*, 11686–11689.
- (564) Pan, R.; Shi, C.; Zhang, D.; Tian, Y.; Guo, S.; Yao, H.; Lin, A. Nickel-Catalyzed Reductive 1,2-Dialkynylation of Alkenes Bearing an 8-Aminoquinoline Directing Group. *Org. Lett.* **2019**, *21*, 8915–8920.
- (565) Zhang, W.-S.; Ji, D.-W.; Li, Y.; Zhang, X.-X.; Zhao, C.-Y.; Hu, Y.-C.; Chen, Q.-A. Regio- and Stereoselective Diarylation of 1,3-Dienes via Ni/Cr Cocatalysis. *ACS Catal.* **2022**, *12*, 2158–2165.
- (566) Fürstner, A.; Shi, N. Nozaki–Hiyama–Kishi Reactions Catalytic in Chromium. *J. Am. Chem. Soc.* **1996**, *118*, 12349–12357.
- (567) Anthony, D.; Lin, Q.; Baudet, J.; Diao, T. Nickel-Catalyzed Asymmetric Reductive Diarylation of Vinylarenes. *Angew. Chem., Int. Ed.* **2019**, *58*, 3198.
- (568) Dong, Z.; Tang, Q.; Xu, C.; Chen, L.; Ji, H.; Zhou, S.; Song, L.; Chen, L. A. Directed Asymmetric Nickel-Catalyzed Reductive 1,2-Diarylation of Electronically Unactivated Alkenes. *Angew. Chem., Int. Ed.* **2023**, *62*, No. e202218286.
- (569) Yang, T.; Jiang, Y.; Luo, Y.; Lim, J. J. H.; Lan, Y.; Koh, M. J. Chemoselective Union of Olefins, Organohalides, and Redox-Active Esters Enables Regioselective Alkene Dialkylation. *J. Am. Chem. Soc.* **2020**, *142*, 21410–21419.
- (570) Zhang, J. X.; Shu, W. Ni-Catalyzed Reductive 1,2-Cross-Dialkylation of Unactivated Alkenes with Two Alkyl Bromides. *Org. Lett.* **2022**, *24*, 3844–3849.
- (571) Shrestha, R.; Weix, D. J. Reductive Conjugate Addition of Haloalkanes to Enones To Form Silyl Enol Ethers. *Org. Lett.* **2011**, *13*, 2766–2769.
- (572) Johnson, J. R.; Tully, P. S.; Mackenzie, P. B.; Sabat, M. A Practical Reversed-Polarity Alternative to Organocuprate Conjugate Addition Chemistry - Halocarbon Coupling Reactions of Enal-Derived and Enone-Derived Allylnickel Reagents. *J. Am. Chem. Soc.* **1991**, *113*, 6172–6177.
- (573) Huihui, K. M.; Shrestha, R.; Weix, D. J. Nickel-Catalyzed Reductive Conjugate Addition of Primary Alkyl Bromides to Enones To Form Silyl Enol Ethers. *Org. Lett.* **2017**, *19*, 340–343.
- (574) Shrestha, R.; Dorn, S. C.; Weix, D. J. Nickel-Catalyzed Reductive Conjugate Addition to Enones via Allylnickel Intermediates. *J. Am. Chem. Soc.* **2013**, *135*, 751–762.
- (575) Sun, J.; Zhou, Y.; Gu, R.; Li, X.; Liu, A.; Zhang, X. Regioselective Ni-Catalyzed Reductive Alkylsilylation of Acrylonitrile with Unactivated Alkyl Bromides and Chlorosilanes. *Nat. Commun.* **2022**, *13*, 7093.
- (576) Pan, Q. Q.; Qi, L.; Pang, X.; Shu, X. Z. Nickel-Catalyzed Cross-Electrophile 1,2-Silyl-Arylation of 1,3-Dienes with Chlorosilanes and Aryl Bromides. *Angew. Chem., Int. Ed.* **2023**, *62*, No. e202215703.
- (577) Griller, D.; Ingold, K. U. Free-Radical Clocks. *Acc. Chem. Res.* **1980**, *13*, 317–323.
- (578) Kuang, Y.; Wang, X.; Anthony, D.; Diao, T. Ni-Catalyzed Two-Component Reductive Dicarbofunctionalization of Alkenes via Radical Cyclization. *Chem. Commun.* **2018**, *54*, 2558–2561.
- (579) Jin, Y.; Wang, C. Ni-Catalysed Reductive Arylalkylation of Unactivated Alkenes. *Chem. Sci.* **2019**, *10*, 1780–1785.
- (580) Jin, Y.; Yang, H.; Wang, C. Nickel-Catalyzed Reductive Arylalkylation via a Migratory Insertion/Decarboxylative Cross-Coupling Cascade. *Org. Lett.* **2019**, *21*, 7602–7608.
- (581) Yang, J.; Yang, L.; Gu, J.; Shuai, L.; Wang, H.; Ouyang, Q.; Li, Y. L.; Liu, H.; Gong, L. Nickel-Catalyzed Reductive Cascade Arylalkylation of Alkenes with Alkylpyridinium Salts. *Org. Lett.* **2022**, *24*, 2376–2380.
- (582) Hewitt, K. A.; Herbert, C. A.; Jarvo, E. R. Synthesis of Vicinal Carbocycles by Intramolecular Nickel-Catalyzed Conjunctive Cross-Electrophile Coupling Reaction. *Org. Lett.* **2022**, *24*, 6093–6098.
- (583) Sha, X.; Fang, Y.; Nie, T.; Qin, S.; Yang, Y.; Huang, D.; Ji, F. Nickel-Catalyzed Reductive Dicarbofunctionalizations of Alkenes for the Synthesis of Difluorocarbonyl Oxindoles and Isoquinoline-1,3-diones. *J. Org. Chem.* **2023**, *88*, 4995–5006.
- (584) Williams, M. T. J.; Morrill, L. C.; Browne, D. L. Nickel-Catalyzed Intramolecular Alkene Difunctionalization by Ball-Milling. *Adv. Synth. Catal.* **2023**, *365*, 1477–1484.
- (585) Peng, Y.; Xu, X. B.; Xiao, J.; Wang, Y. W. Nickel-Mediated Stereocontrolled Synthesis of Spiroketal via Tandem Cyclization-Coupling of  $\beta$ -Bromo Ketals and Aryl Iodides. *Chem. Commun.* **2014**, *50*, 472–474.
- (586) Jin, Y.; Wang, C. Nickel-Catalyzed Asymmetric Reductive Arylalkylation of Unactivated Alkenes. *Angew. Chem., Int. Ed.* **2019**, *58*, 6722–6726.
- (587) Jin, Y.; Yang, H.; Wang, C. Nickel-Catalyzed Asymmetric Reductive Arylbenzylation of Unactivated Alkenes. *Org. Lett.* **2020**, *22*, 2724–2729.
- (588) Lan, Y.; Wang, C. Nickel-Catalyzed Enantioselective Reductive Carbo-Acylation of Alkenes. *Commun. Chem.* **2020**, *3*, 45.
- (589) Wu, X.; Qu, J.; Chen, Y. Quinim: A New Ligand Scaffold Enables Nickel-Catalyzed Enantioselective Synthesis of  $\alpha$ -Alkylated  $\gamma$ -Lactam. *J. Am. Chem. Soc.* **2020**, *142*, 15654–15660.
- (590) Zhao, T. Y.; Xiao, L. J.; Zhou, Q. L. Nickel-Catalyzed Desymmetric Reductive Cyclization/Coupling of 1,6-Dienes: An Enantioselective Approach to Chiral Tertiary Alcohol. *Angew. Chem., Int. Ed.* **2022**, *61*, No. e202115702.
- (591) Wu, X. Q.; Shrestha, M.; Chen, Y. F. Asymmetric Synthesis of  $\alpha$ -Alkylated  $\gamma$ -Lactam via Nickel/8-Quinim-Catalyzed Reductive Alkyl-Carbamoylation of Unactivated Alkene. *Synlett* **2021**, *32*, 955–961.
- (592) Lin, Z.; Jin, Y.; Hu, W.; Wang, C. Nickel-Catalyzed Asymmetric Reductive Aryl-Allylation of Unactivated Alkenes. *Chem. Sci.* **2021**, *12*, 6712–6718.
- (593) Fang, K.; Huang, W.; Shan, C.; Qu, J.; Chen, Y. Synthesis of 3,3-Dialkyl-Substituted Isoindolinones Enabled by Nickel-Catalyzed Reductive Dicarbofunctionalization of Enamides. *Org. Lett.* **2021**, *23*, 5523–5527.
- (594) Wu, X.; Luan, B.; Zhao, W.; He, F.; Wu, X. Y.; Qu, J.; Chen, Y. Catalytic Desymmetric Dicarbofunctionalization of Unactivated Alkenes. *Angew. Chem., Int. Ed.* **2022**, *61*, No. e20211598.

- (595) Zhang, C.; Wu, X.; Xia, T.; Qu, J.; Chen, Y. Ni-Catalyzed Carbamoylation of Unactivated Alkenes for Stereoselective Construction of Six-Membered Lactams. *Nat. Commun.* **2022**, *13*, 5964.
- (596) Ding, Z.; Kong, W. Synthesis of Carbonyl-Containing Oxindoles via Ni-Catalyzed Reductive Aryl-Acylation and Aryl-Esterification of Alkenes. *Molecules* **2022**, *27*, 5899.
- (597) Xu, S.; Wang, K.; Kong, W. Ni-Catalyzed Reductive Arylacylation of Alkenes toward Carbonyl-Containing Oxindoles. *Org. Lett.* **2019**, *21*, 7498–7503.
- (598) Li, Y.; Ding, Z.; Lei, A.; Kong, W. Ni-Catalyzed Enantioselective Reductive Aryl-Alkenylation of Alkenes: Application to the Synthesis of (+)-Physovenine and (+)-Phystostigmine. *Org. Chem. Front.* **2019**, *6*, 3305–3309.
- (599) Tian, Z. X.; Qiao, J. B.; Xu, G. L.; Pang, X.; Qi, L.; Ma, W. Y.; Zhao, Z. Z.; Duan, J.; Du, Y. F.; Su, P.; et al. Highly Enantioselective Cross-Electrophile Aryl-Alkenylation of Unactivated Alkenes. *J. Am. Chem. Soc.* **2019**, *141*, 7637–7643.
- (600) Wang, K.; Kong, W. Q. Enantioselective Reductive Diarylation of Alkenes by Ni-Catalyzed Domino Heck Cyclization/Cross Coupling. *Synlett* **2019**, *30*, 1008–1014.
- (601) Qiao, J. B.; Zhang, Y. Q.; Yao, Q. W.; Zhao, Z. Z.; Peng, X.; Shu, X. Z. Enantioselective Reductive Divinylation of Unactivated Alkenes by Nickel-Catalyzed Cyclization Coupling Reaction. *J. Am. Chem. Soc.* **2021**, *143*, 12961–12967.
- (602) Jin, Y. X.; Fan, P.; Wang, C. Nickel-Catalyzed Reductive Asymmetric Aryl-Acylation and Aryl-Carbamoylation of Unactivated Alkenes. *CCS Chemistry* **2022**, *4*, 1510–1518.
- (603) Luan, B.; Tang, Z.; Wu, X.; Chen, Y. 8-Quinolinyl Oxazoline: Ligand Exploration in Enantioselective Ni-Catalyzed Reductive Carbamoyl-Alkylation of Alkene to Access the Chiral Oxindoles. *Synlett* **2022**, *33*, 1847–1852.
- (604) Li, H.; Chen, J.; Dong, J.; Kong, W. Ni-Catalyzed Reductive Arylcyanation of Alkenes. *Org. Lett.* **2021**, *23*, 6466–6470.
- (605) Nauth, A. M.; Opatz, T. Non-Toxic Cyanide Sources and Cyanating Agents. *Org. Biomol. Chem.* **2019**, *17*, 11–23.
- (606) Wang, G.; Shen, C.; Ren, X.; Dong, K. Ni-Catalyzed Enantioselective Reductive Arylcyanation/cyclization of *N*-(2-Iodo-Aryl) Acrylamide. *Chem. Commun.* **2022**, *58*, 1135–1138.
- (607) Desrosiers, J.-N.; Wen, J.; Tcyrulnikov, S.; Biswas, S.; Qu, B.; Hie, L.; Kuroski, D.; Wu, L.; Grinberg, N.; Haddad, N.; et al. Enantioselective Nickel-Catalyzed Mizoroki–Heck Cyclizations To Generate Quaternary Stereocenters. *Org. Lett.* **2017**, *19*, 3338–3341.
- (608) Wang, L.; Wang, C. Ni-Catalyzed 1,2-Iminoacylation of Alkenes via a Reductive Strategy. *Org. Chem. Front.* **2018**, *5*, 3476–3482.
- (609) Qi, D.; Zhang, X.; Wang, X.; Liu, X.; Zhang, Z.; Shi, L.; Zhang, G. Nickel-Catalyzed Reductive Iminoarylation of Oxime Ester-Tethered Alkenes: Rapid Entrance to Diverse Functionalized Pyrrolines. *Org. Lett.* **2023**, *25*, 1126–1130.
- (610) He, J.; Xue, Y.; Han, B.; Zhang, C.; Wang, Y.; Zhu, S. Nickel-Catalyzed Asymmetric Reductive 1,2-Carboamination of Unactivated Alkenes. *Angew. Chem., Int. Ed.* **2020**, *59*, 2328–2332.
- (611) Jia, X. G.; Yao, Q. W.; Shu, X. Z. Enantioselective Reductive *N*-Cyclization-Alkylation Reaction of Alkene-Tethered Oxime Esters and Alkyl Iodides by Nickel Catalysis. *J. Am. Chem. Soc.* **2022**, *144*, 13461–13467.
- (612) Peng, Y.; Xiao, J.; Xu, X. B.; Duan, S. M.; Ren, L.; Shao, Y. L.; Wang, Y. W. Stereospecific Synthesis of Tetrahydronaphtho[2,3-b]furans Enabled by a Nickel-Promoted Tandem Reductive Cyclization. *Org. Lett.* **2016**, *18*, 5170–5173.
- (613) Xiao, J.; Wang, Y. W.; Peng, Y. Nickel-Promoted Reductive Cyclization Cascade: A Short Synthesis of a New Aromatic Strigolactone Analogue. *Synthesis* **2017**, *49*, 3576–3581.
- (614) Xiao, J.; Cong, X. W.; Yang, G. Z.; Wang, Y. W.; Peng, Y. Divergent Asymmetric Syntheses of Podophyllotoxin and Related Family Members via Stereoselective Reductive Ni-Catalysis. *Org. Lett.* **2018**, *20*, 1651–1654.
- (615) Xiao, J.; Wang, Y. W.; Qiu, Z. P.; Peng, Y. Ni-Catalyzed Intramolecular Reductive 1,2-Dicarbofunctionalization of Alkene:
- Facile Access to Podophyllum Lignans Core. *Synlett* **2021**, *32*, 1662–1664.
- (616) Xiao, J.; Cong, X. W.; Yang, G. Z.; Wang, Y. W.; Peng, Y. Stereoselective synthesis of a Podophyllum Lignan Core by Intramolecular Reductive Nickel-Catalysis. *Chem. Commun.* **2018**, *54*, 2040–2043.
- (617) Zhang, J.; Li, Z.; Zhuo, J.; Cui, Y.; Han, T.; Li, C. Tandem Decarboxylative Cyclization/Alkenylation Strategy for Total Syntheses of (+)-Longirabdiol, (-)-Longirabdolactone, and (-)-Effusin. *J. Am. Chem. Soc.* **2019**, *141*, 8372–8380.
- (618) Liu, Z. Q. *Science of Synthesis: Free Radicals: Fundamentals and Applications in Organic Synthesis*; Thieme Chemistry, 2020.
- (619) Jiang, Y.; Pan, J. T.; Yang, T.; Zhao, Y.; Koh, M. J. Nickel-Catalyzed Site- and Stereoselective Reductive Alkylalkynylation of Alkynes. *Chem.* **2021**, *7*, 993–1005.
- (620) Maiti, S.; Rhlee, J. H. Reductive Ni-Catalysis for Stereoselective Carboarylation of Terminal Aryl Alkynes. *Chem. Commun.* **2021**, *57*, 11346–11349.
- (621) Zhan, Y. Z.; Meng, H.; Shu, W. Rapid Access to *t*-Butylalkylated Olefins Enabled by Ni-catalyzed Intermolecular Regio- and *trans*-Selective Cross-Electrophile *t*-Butylalkylation of Alkynes. *Chem. Sci.* **2022**, *13*, 4930–4935.
- (622) Dai, Y. B.; Wang, F.; Zhu, S. Q.; Chu, L. L. Selective Ni-Catalyzed Cross-Electrophile Coupling of Alkynes, Fluoroalkyl Halides, and Vinyl Halides. *Chin. Chem. Lett.* **2022**, *33*, 4074–4078.
- (623) Zhu, C.; Yue, H.; Rueping, M. Nickel-Catalyzed Multi-component Stereodivergent Synthesis of Olefins Enabled by Electrochemistry, Photocatalysis and Photo-Electrochemistry. *Nat. Commun.* **2022**, *13*, 3240.
- (624) Zhang, Z.-Z.; Lei, J.-J.; Zhang, X.-H.; Zhang, X.-G.; Tu, H.-Y. Ni-Catalyzed Reductive Fluoroalkylation of Alkynes for the Stereoselective Synthesis of Fluoroalkylated Enones. *Org. Lett.* **2022**, *24*, 6192–6196.
- (625) Li, Q. Z.; Li, Z. H.; Kang, J. C.; Ding, T. M.; Zhang, S. Y. Ni-Catalyzed, Enantioselective Three-Component Radical Relayed Reductive Coupling of Alkynes: Synthesis of Axially Chiral Styrenes. *Chem. Catal.* **2022**, *2*, 3185–3195.
- (626) Lin, Z. Y.; Hu, W. T.; Zhang, L. C.; Wang, C. Nickel-Catalyzed Asymmetric Cross-Electrophile *trans*-Aryl- Benzylation of  $\alpha$ -Naphthyl Propargylic Alcohols. *ACS Catal.* **2023**, *13*, 6795–6803.
- (627) Shimkin, K. W.; Montgomery, J. Synthesis of Tetrasubstituted Alkenes by Tandem Metallacycle Formation/Cross-Electrophile Coupling. *J. Am. Chem. Soc.* **2018**, *140*, 7074–7078.
- (628) Tang, X.-Q.; Montgomery, J. Nickel-Catalyzed Preparation of Bicyclic Heterocycles: Total Synthesis of (+)-Allopumiliotoxin 267A, (+)-Allopumiliotoxin 339A, and (+)-Allopumiliotoxin 339B. *J. Am. Chem. Soc.* **2000**, *122*, 6950–6954.
- (629) Zeng, M. Q.; Feng, K. X.; Hu, B. L.; Tu, H. Y.; Zhang, X. G. Ni-Catalyzed Reductive Arylalkenylation of Alkynes for the Selective Synthesis of Polysubstituted Naphthalenes. *Org. Lett.* **2022**, *24*, 5386–5390.
- (630) Ruiz-Castillo, P.; Buchwald, S. L. Applications of Palladium-Catalyzed C–N Cross-Coupling Reactions. *Chem. Rev.* **2016**, *116*, 12564–12649.
- (631) Lin, H.; Sun, D. Recent Synthetic Developments and Applications of the Ullmann Reaction. A Review. *Org. Prep. Proced. Int.* **2013**, *45*, 341–394.
- (632) Korch, K. M.; Watson, D. A. Cross-Coupling of Heteroatomic Electrophiles. *Chem. Rev.* **2019**, *119*, 8192–8228.
- (633) Dorel, R.; Grugel, C. P.; Haydl, A. M. The Buchwald–Hartwig Amination After 25 Years. *Angew. Chem., Int. Ed.* **2019**, *58*, 17118–17129.
- (634) Duan, J.; Wang, K.; Xu, G. L.; Kang, S.; Qi, L.; Liu, X. Y.; Shu, X. Z. Cross-Electrophile C(sp<sup>2</sup>)-Si Coupling of Vinyl Chlorosilanes. *Angew. Chem., Int. Ed.* **2020**, *59*, 23083–23088.
- (635) Walsh, R. Bond Dissociation Energy Values in Silicon-Containing Compounds and Some of their Implications. *Acc. Chem. Res.* **1981**, *14*, 246–252.

- (636) Obligacion, J. V.; Chirik, P. J. Earth-Abundant Transition Metal Catalysts for Alkene Hydrosilylation and Hydroboration. *Nat. Chem. Rev.* **2018**, *2*, 15–34.
- (637) de Almeida, L. D.; Wang, H.; Junge, K.; Cui, X.; Beller, M. Recent Advances in Catalytic Hydrosilylations: Developments beyond Traditional Platinum Catalysts. *Angew. Chem., Int. Ed.* **2021**, *60*, 550–565.
- (638) Hiyama, T.; Oestreich, M. *Organosilicon Chemistry: Novel Approaches and Reactions*; Wiley-VCH: Weinheim, 2019.
- (639) Bähr, S.; Xue, W. C.; Oestreich, M. C(sp<sup>3</sup>)—Si Cross-Coupling. *ACS Catal.* **2019**, *9*, 16–24.
- (640) Zhang, L.; Oestreich, M. Nickel-Catalyzed, Reductive C(sp<sup>3</sup>)—Si Cross-Coupling of  $\alpha$ -Cyano Alkyl Electrophiles and Chlorosilanes. *Angew. Chem., Int. Ed.* **2021**, *60*, 18587–18590.
- (641) Xing, M.; Cui, H.; Zhang, C. Nickel-Catalyzed Reductive Cross-Coupling of Alkyl Bromides and Chlorosilanes. *Org. Lett.* **2021**, *23*, 7645–7649.
- (642) Duan, J.; Wang, Y.; Qi, L.; Guo, P.; Pang, X.; Shu, X. Z. Nickel-Catalyzed Cross-Electrophile C(sp<sup>3</sup>)—Si Coupling of Unactivated Alkyl Bromides with Vinyl Chlorosilanes. *Org. Lett.* **2021**, *23*, 7855–7859.
- (643) Zhao, Z. Z.; Pang, X.; Wei, X. X.; Liu, X. Y.; Shu, X. Z. Nickel-Catalyzed Reductive C(sp<sup>2</sup>)—Si Coupling of Chlorohydrosilanes via Si—Cl Cleavage. *Angew. Chem., Int. Ed.* **2022**, *61*, No. e202200215.
- (644) Nanjo, M.; Oda, T.; Mochida, K. Preparation and Structural Characterization of Trimethylsilyl-Substituted Germylzinc Halides, (Me<sub>3</sub>Si)<sub>3</sub>GeZnX (X = Cl, Br, and I) and Silylzinc Chloride, R(Me<sub>3</sub>Si)<sub>2</sub>SiZnCl (R = SiMe<sub>3</sub> and Ph). *J. Organomet. Chem.* **2003**, *672*, 100–108.
- (645) Wolfsberger, W. Hydrogermylierungsreaktionen. *J. Prakt. Chem./Chem-Ztg.* **1992**, *334*, 453–464.
- (646) Xue, W.; Mao, W.; Zhang, L.; Oestreich, M. Mechanistic Dichotomy of Magnesium- and Zinc-Based Germanium Nucleophiles in the C(sp<sup>3</sup>)—Ge Cross-Coupling with Alkyl Electrophiles. *Angew. Chem., Int. Ed.* **2019**, *58*, 6440–6443.
- (647) Su, P. F.; Wang, K.; Peng, X.; Pang, X.; Guo, P.; Shu, X. Z. Nickel-Catalyzed Reductive C—Ge Coupling of Aryl/Alkenyl Electrophiles with Chlorogermanes. *Angew. Chem., Int. Ed.* **2021**, *60*, 26571–26576.
- (648) Guo, P.; Pang, X.; Wang, K.; Su, P. F.; Pan, Q. Q.; Han, G. Y.; Shen, Q.; Zhao, Z. Z.; Zhang, W.; Shu, X. Z. Nickel-Catalyzed Reductive C(sp<sup>3</sup>)—Ge Coupling of Alkyl Bromides with Chlorogermanes. *Org. Lett.* **2022**, *24*, 1802–1806.
- (649) Huang, D.; Yan, G. Recent Advances in Reactions of Azides. *Adv. Synth. Catal.* **2017**, *359*, 1600–1619.
- (650) Wauters, I.; Debrouwer, W.; Stevens, C. V. Preparation of phosphines through C—P bond formation. *Beilstein J. Org. Chem.* **2014**, *10*, 1064–1096.
- (651) Konev, M. O.; McTeague, T. A.; Johannes, J. W. Nickel-Catalyzed Photoredox-Mediated Cross-Coupling of Aryl Electrophiles and Aryl Azides. *ACS Catal.* **2018**, *8*, 9120–9124.
- (652) Li, G.; Yang, L.; Liu, J.-J.; Zhang, W.; Cao, R.; Wang, C.; Zhang, Z.; Xiao, J.; Xue, D. Light-Promoted C—N Coupling of Aryl Halides with Nitroarenes. *Angew. Chem., Int. Ed.* **2021**, *60*, 5230–5234.
- (653) Nykaza, T. V.; Cooper, J. C.; Li, G.; Mahieu, N.; Ramirez, A.; Luzung, M. R.; Radosevich, A. T. Intermolecular Reductive C—N Cross Coupling of Nitroarenes and Boronic Acids by P<sup>III</sup>/P<sup>V</sup>=O Catalysis. *J. Am. Chem. Soc.* **2018**, *140*, 15200–15205.
- (654) Budnikova, Y. H.; Perichon, J.; Yakhvarov, D. G.; Kargin, Y. M.; Sinyashin, O. G. Highly Reactive  $\sigma$ -Organonickel Complexes in Electrocatalytic Processes. *J. Organomet. Chem.* **2001**, *630*, 185–192.
- (655) Ager, D. J.; Laneman, S. A. Convenient and Direct Preparation of Tertiary Phosphines via Nickel-Catalysed Cross-Coupling. *Chem. Commun.* **1997**, 2359–2360.
- (656) Budnikova, Y. G.; Kargin, Y. M.; Sinyashin, O. G. Electrosynthesis of Mixed Tertiary Phosphines Catalysed by Nickel Complexes. *Mendeleev Commun.* **1999**, *9*, 193–194.
- (657) Budnikova, Y.; Kargin, Y.; Nédélec, J.-Y.; Périchon, J. Nickel-Catalysed Electrochemical Coupling Between Mono- or Di-Chlorophenylphosphines and Aryl or Heteroaryl Halides. *J. Organomet. Chem.* **1999**, *575*, 63–66.
- (658) Yakhvarov, D. G.; Budnikova, Y. H.; Tazeev, D. I.; Sinyashin, O. G. The Influence of the Sacrificial Anode Nature on the Mechanism of Electrochemical Arylation and Alkylation of White Phosphorus. *Russ. Chem. Bull.* **2002**, *51*, 2059–2064.
- (659) Budnikova, Y. H.; Yakhvarov, D. G.; Sinyashin, O. G. Electrocatalytic Eco-Efficient Functionalization of White Phosphorus. *J. Organomet. Chem.* **2005**, *690*, 2416–2425.
- (660) Le Gall, E.; Troupel, M.; Nédélec, J.-Y. Nickel-Catalyzed Reductive Coupling of Chlorodiphenylphosphine with Aryl Bromides into Functionalized Triarylphosphines. *Tetrahedron* **2003**, *59*, 7497–7500.
- (661) Zhang, D. J.; Tang, T.; Zhang, Z.; Le, L. Y.; Xu, Z.; Lu, H.; Tong, Z.; Zeng, D. S.; Wong, W. Y.; Yin, S. F.; et al. Nickel- and Palladium-Catalyzed Cross-Coupling of Stibines with Organic Halides: Site-Selective Sequential Reactions with Polyhalogenated Arenes. *ACS Catal.* **2022**, *12*, 854–867.
- (662) Fang, Y.; Rogge, T.; Ackermann, L.; Wang, S. Y.; Ji, S. J. Nickel-Catalyzed Reductive Thiolation and Selenylation of Unactivated Alkyl Bromides. *Nat. Commun.* **2018**, *9*, 2240.
- (663) Xu, X.-B.; Liu, J.; Zhang, J.-J.; Wang, Y.-W.; Peng, Y. Nickel-Mediated Inter- and Intramolecular C—S Coupling of Thiols and Thioacetates with Aryl Iodides at Room Temperature. *Org. Lett.* **2013**, *15*, 550–553.
- (664) Li, J.; Wang, S. Y.; Ji, S. J. Nickel-Catalyzed Thiolation and Selenylation of Cycloketone Oxime Esters with Thiosulfonate or Seleniumsulfonate. *J. Org. Chem.* **2019**, *84*, 16147–16156.
- (665) Zhang, W.; Huang, M.; Zou, Z.; Wu, Z.; Ni, S.; Kong, L.; Zheng, Y.; Wang, Y.; Pan, Y. Redox-Active Benzimidazolium Sulfonamides as Cationic Thiolating Reagents for Reductive Cross-Coupling of Organic Halides. *Chem. Sci.* **2021**, *12*, 2509–2514.
- (666) Ang, N. W. J.; Ackermann, L. Electroreductive Nickel-Catalyzed Thiolation: Efficient Cross-Electrophile Coupling for C—S Formation. *Chem. - Eur. J.* **2021**, *27*, 4883–4887.
- (667) Wang, F.; Chen, Y.; Rao, W.; Ackermann, L.; Wang, S. Y. Efficient Preparation of Unsymmetrical Disulfides by Nickel-Catalyzed Reductive Coupling Strategy. *Nat. Commun.* **2022**, *13*, 2588.
- (668) Liu, Y.; Xu, Y. N.; Zhang, Y.; Gao, W. C.; Shao, X. X. "Thiol-Free Synthesized" and Sustainable Thiolating Synthons for Nickel-Catalyzed Reductive Assembly of Sulfides with High Efficiency. *Org. Chem. Front.* **2022**, *9*, 6490–6497.
- (669) Xu, Y.; Liu, Y.; Zhang, Y.; Yang, K.; Wang, Y.; Peng, J.; Shao, X.; Bai, Y. Nonbasic Synthesis of Thioethers via Nickel-Catalyzed Reductive Thiolation Utilizing NBS-Like N-Thioimides as Electrophilic Sulfur Donors. *J. Org. Chem.* **2023**, *88*, 2773–2783.
- (670) Bogdos, M. K.; Muller, P.; Morandi, B. Structural Evidence for Aromatic Heterocycle N—O Bond Activation via Oxidative Addition. *Organometallics* **2023**, *42*, 211.
- (671) Tsymbal, A. V.; Bizzini, L. D.; MacMillan, D. W. C. Nickel Catalysis via S<sub>H</sub>2 Homolytic Substitution: The Double Decarboxylative Cross-Coupling of Aliphatic Acids. *J. Am. Chem. Soc.* **2022**, *144*, 21278–21286.
- (672) Odena, C.; Santiago, T. G.; Linares, M. L.; Castellanos-Blanco, N.; McGuire, R. T.; Chaves-Arquero, B.; Alonso, J. M.; Dieguez-Vazquez, A.; Tan, E.; Alcazar, J.; et al. Late-Stage C(sp<sup>2</sup>)—C(sp<sup>3</sup>) Diversification via Nickel Oxidative Addition Complexes. *J. Am. Chem. Soc.* **2024**, *146*, 21264–21270.
- (673) Dinh, L. P.; Starbuck, H. F.; Hamby, T. B.; LaLama, M. J.; He, C. Q.; Kalyani, D.; Sevov, C. S. Persistent Organonickel Complexes as General Platforms for Csp<sup>2</sup>—Csp<sup>3</sup> Coupling Reactions. *Nat. Chem.* **2024**, *16*, 1515–1522.
- (674) Al Zubaydi, S.; Waske, S.; Akyildiz, V.; Starbuck, H. F.; Majumder, M.; Moore, C. E.; Kalyani, D.; Sevov, C. S. Reductive Alkyl-Alkyl Coupling from Isolable Nickel-Alkyl Complexes. *Nature* **2024**, *634*, 585.

- (675) Huang, Z.; Akana, M. E.; Sanders, K. M.; Weix, D. J. A Decarbonylative Approach to Alkylnickel Intermediates and C(sp<sup>3</sup>)—C(sp<sup>3</sup>) Bond Formation. *Science* **2024**, *385*, 1331–1337.
- (676) Tcyrulnikov, S.; Hubbell, A. K.; Pedro, D.; Reyes, G. P.; Monfette, S.; Weix, D. J.; Hansen, E. C. Computationally Guided Ligand Discovery from Compound Libraries and Discovery of a New Class of Ligands for Ni-Catalyzed Cross-Electrophile Coupling of Challenging Quinoline Halides. *J. Am. Chem. Soc.* **2024**, *146*, 6947–6954.
- (677) Acemoglu, M.; Baenziger, M.; Krell, C.; Marterer, W. Experiences with Negishi Couplings on Technical Scale in Early Development. In *Transition Metal-Catalyzed Couplings in Process Chemistry: Case Studies from the Pharmaceutical Industry*; Magano, J., Dunetz, J. R., Eds.; Wiley-VCH, 2013; pp 15–23.
- (678) Yin, J.; Maguire, C. K.; Yasuda, N.; Brunskill, A. P. J.; Klapars, A. Impact of Lead Impurities in Zinc Dust on the Selective Reduction of a Dibromoimidazole Derivative. *Org. Process Res. Dev.* **2017**, *21*, 94–97.
- (679) Takai, K.; Kakiuchi, T.; Utimoto, K. A Dramatic Effect of a Catalytic Amount of Lead on the Simmons-Smith Reaction and Formation of Alkylzinc Compounds from Iodoalkanes. Reactivity of Zinc Metal: Activation and Deactivation. *J. Org. Chem.* **1994**, *59*, 2671–2673.
- (680) Yi, L.; Ji, T.; Chen, K.-Q.; Chen, X.-Y.; Rueping, M. Nickel-Catalyzed Reductive Cross-Couplings: New Opportunities for Carbon–Carbon Bond Formations through Photochemistry and Electrochemistry. *CCS Chemistry* **2022**, *4*, 9–30.
- (681) Uoyama, H.; Goushi, K.; Shizu, K.; Nomura, H.; Adachi, C. Highly Efficient Organic Light-Emitting Diodes from Delayed Fluorescence. *Nature* **2012**, *492*, 234–238.
- (682) Mouat, J. M.; Widness, J. K.; Enny, D. G.; Meidenbauer, M. T.; Awan, F.; Krauss, T. D.; Weix, D. J. CdS Quantum Dots for Metallaphotoredox-Enabled Cross-Electrophile Coupling of Aryl Halides with Alkyl Halides. *ACS Catal.* **2023**, *13*, 9018–9024.
- (683) Klein, M.; Waldvogel, S. R. Counter Electrode Reactions—Important Stumbling Blocks on the Way to a Working Electro-organic Synthesis. *Angew. Chem., Int. Ed.* **2022**, *61*, No. e202204140.
- (684) Twilton, J.; Johnson, M. R.; Sidana, V.; Franke, M. C.; Bottecchia, C.; Lehnher, D.; Lévesque, F.; Knapp, S. M. M.; Wang, L.; Gerken, J. B.; et al. Quinone-Mediated Hydrogen Anode for Non-Aqueous Reductive Electrosynthesis. *Nature* **2023**, *623*, 71–76.
- (685) Poremba, K. E.; Dibrell, S. E.; Reisman, S. E. Nickel-Catalyzed Enantioselective Reductive Cross-Coupling Reactions. *ACS Catal.* **2020**, *10*, 8237–8246.
- (686) Lucas, E. L.; Jarvo, E. R. Stereospecific and Stereoconvergent Cross-Couplings Between Alkyl Electrophiles. *Nat. Rev. Chem.* **2017**, *1*, No. 0065.